

DECLARATION

I, John Alexander King, declare that this thesis was composed by myself, and the work described was carried out by myself except for the instances detailed in the text and acknowledgements.

signed

ACKNOWLEDGMENTS

The author wishes to express his sincere thanks to the following:

Dr. A. A. Smith of the Edinburgh School of Agriculture, Soil Science Department, for his constant guidance and supervision throughout this work, and valuable advice during the preparation of this thesis.

Dr. D. G. Potts of the Forestry Commission for his help and guidance throughout the work, and for allowing me to use temperature, rainfall and relative humidity data from the Poltairs experiment (Section 6) which was conducted by him and staff of the Forestry Commission.

Dr. R. P. Courts of the Forestry Commission for advice and facilities, when carrying out the work described in Section 11.

Dr. B. G. Hall of the Scottish Institute of Agricultural Engineering for advice when measuring gaseous diffusion through soil cores (Section 3), and to the Agricultural Research Council, Leamington Laboratory, for the use of instrument for the gas diffusion measurements.

The Forestry Commission for providing the sites and research facilities, their research staff at Poltairs Forest for assistance in the collection of samples and data, and staff at the Northern Research Station.

Thesis submitted for the Degree of Doctor of Philosophy in the Faculty of Science, Department of Agriculture.

UNIVERSITY OF EDINBURGH

1982



ACKNOWLEDGEMENTS

The author wishes to express his sincere thanks to the following:

Dr.K.A. Smith of the Edinburgh School of Agriculture, Soil Science Department, for his constant guidance and supervision throughout this work, and valuable advice during the preparation of this thesis.

Dr.D.G. Pyatt of the Forestry Commission for his help and guidance throughout the work, and for allowing me to use temperature, rainfall and matric potential data from the Falstone experiment (Section 6) which was conducted by him and staff of the Forestry Commission.

Dr.M.P. Coutts of the Forestry Commission for advice and facilities, when conducting the root growth experiment in Section 11.

Dr.B.C. Ball of the Scottish Institute of Agricultural Engineering for advice when measuring gaseous diffusion through peat cores (Section 9), and to the Agricultural Research Council, Letcombe Laboratory, for the use of equipment for the gas diffusion measurements.

The Forestry Commission for providing the sites and research facilities, their research staff at Falstone forest for assistance in the collection of samples and data, and staff at the Northern Research Station for help with some analyses, and statistical advice.

The Edinburgh School of Agriculture for providing space and research facilities and to all members of staff of the Soil Science Department for helpful discussion and assistance.

Mrs. Gail Chilton for typing this thesis.

The Natural Environment Research Council for funding the project in the form of a Research Studentship.

ABSTRACT

AERATION OF UPLAND SOILS UNDER AFFORESTATION

The relationships between soil aeration and other physical properties of two upland soils prone to waterlogging, a peaty gley in the Kielder forest region of Northumberland (Falstone forest) and a deep peat in Eddleston forest of the Borders region of Scotland, were investigated.

The investigations examined the soil atmosphere composition, moisture potential, depth to water table, temperature and rainfall/throughfall throughout 1978 and 1979 at Falstone, and during 1979 at Eddleston. Measurements were made under stands of Picea sitchensis and Pinus contorta, and neighbouring areas of the original vegetation. Samples removed from the soil pore space were analysed for oxygen and carbon dioxide concentrations by gas chromatography.

Oxygen concentrations in the soil were found to be greater under the tree species than the unplanted areas, at all depths, during the moisture deficit period. During the moisture deficit period the soil dried to a greater depth under the trees, and to lower matric potentials above the water table. The oxygen concentrations were found to be near atmospheric ($0.21 \text{ m}^3 \text{ m}^{-3}$) when the matric potential fell below -5 kPa , and could be as low as $0.01 \text{ m}^3 \text{ m}^{-3}$, or even zero, at higher potentials. The oxygen concentrations were also found to decrease, and carbon dioxide concentrations increase, with increasing depth under all species corresponding to increasing matric potential. Statistical analysis revealed a small but significant improvement in aeration under Pinus contorta over Picea sitchensis on both soil types. It was also revealed that lower oxygen concentrations and higher carbon dioxide concentrations could be expected for matric potentials above about

-5kPa, when soil temperatures were at their maximum (about 10°C). These trends were observed in both soils and during both years of study.

The moisture release characteristics, bulk density and pore volume fraction of the soils were also measured, and increasing oxygen concentrations over a range of matric potentials from 0 to -10kPa found to correlate with an increase in gas filled pore volume.

Gaseous diffusion through peat cores was measured over a range of 0 to -10kPa matric potential and the equation $D/D_0 = 0.65 \epsilon_g^{2.16}$ found to describe the increase in diffusivity (D/D_0) with gas filled pore space (ϵ_g).

The respiration rate of peat cores was found to vary randomly over a range of gas filled pore volume fractions (from 0 to about 0.4) but increase with increasing temperature from 5°C to 30°C, having a Q_{10} of about 3.

An investigation into root growth rate of Pinus contorta and Picea sitchensis cuttings grown in a range of carbon dioxide concentrations (0.01, 0.06, 0.12 and 0.18 $\text{m}^3 \text{m}^{-3}$), showed no reduction in growth rate when oxygen concentrations were 0.21 $\text{m}^3 \text{m}^{-3}$, but growth ceased when oxygen concentrations were 0.01 $\text{m}^3 \text{m}^{-3}$ and the carbon dioxide concentration greater than this value.

CONTENTS

	<u>Page</u>
ACKNOWLEDGEMENTS	i
ABSTRACT	ii
CONTENTS	iv
 1. REVIEW	
1.1 Diffusion of gases in soil	1
1.2 Respiration in soil	11
1.3 Chemical and electrochemical transformations in a waterlogged soil	22
1.4 Plant responses and tolerance to waterlogging	29
1.5 Windthrow and the aeration status of soils	34
 2. FIELD EXPERIMENTS	
2.1 Aims of field experiments	42
2.2 Faltone:experimental plan	44
2.3 Eddleston :experimental plan	49
 3. METHOD OF MEASURING SOIL AERATION	
3.1 Review of available techniques	54
3.2 Sampling and analysis of the soil pore space	
3.2.1 Sampling	57
3.2.2 Analysis of gas samples	62
3.2.3 Analysis of water samples	67
 4. SOIL PHYSICAL PROPERTIES - FALSTONE	
4.1 Methods	
4.1.1 Bulk density	75
4.1.2. Stone content and stone density	77
4.1.3 Fine earth density and true particle density	78
4.1.4 Particle size distribution and organic matter content	79
4.1.5 Moisture release data	81
4.2 Results	
4.2.1 Profile description	85
4.2.2 Bulk density	87
4.2.3 Organic matter content	91
4.2.4 Particle size distribution	94
4.2.5 Pore space and moisture release characteristics	96
4.3 Conclusions	
 5. PHYSICAL PROPERTIES OF PEAT AT EDDLESTON	
5.1 Methods	
5.1.1 Bulk density and true density	109
5.1.2 Fibre content of peat	110
5.1.3 Moisture release characteristics	111
5.2 Results	
5.2.1 Bulk density and true density	112
5.2.2 Fibre content	115
5.2.3 Moisture release characteristics of peat	120
5.3 Conclusions	140

6. FALSTONE FIELD EXPERIMENTS

6.1	Moisture regime	
6.1.1	1978 Data	143
6.1.2	1979 Data	158
6.2	Temperature regime	169
6.3	Soil atmosphere	
6.3.1	1978 Data	175
6.3.2	1979 Data	191
6.4	Conclusions	202

7. EDDLESTON FIELD EXPERIMENTS

7.1	Moisture regime	213
7.2	Temperature regime	219
7.3	Soil atmosphere	224
7.4	Conclusions	242

8. RESPIRATION IN PEAT CORES

8.1	Aims	252
8.2	Methods	252
8.3	Results	259
8.3.1	Variation of respiration rate with moisture potential	259
8.3.2	Variation of respiration rate with temperature	265
8.4	Conclusions	271

9. GASEOUS DIFFUSION THROUGH PEAT CORES

9.1	Aims	273
9.2	Methods	273
9.3	Results	281
9.4	Conclusions	288

10. THE VARIATION OF FIELD OXYGEN AND CARBON DIOXIDE CONCENTRATIONS WITH MOISTURE CONTENT AND TEMPERATURE 292

11. GROWTH OF CONIFER ROOTS UNDER VARIOUS CARBON DIOXIDE CONCENTRATIONS

11.1	Aims	318
11.2	Methods	318
11.3	Results	320
11.4	Conclusions	328

12. GENERAL SUMMARY 331

BIBLIOGRAPHY 335

Appendix 1 346

Appendix 2 349

Appendix 3 366

Appendix 4 367

Appendix 5 371

1. REVIEW

1.1 DIFFUSION OF GASES IN SOIL

The first process in soil to be affected by waterlogging is gaseous movement and exchange. The constant removal of oxygen from soil by respiration necessitates an equally constant means of supply, if aerobic respiration is to be maintained. The two physical processes available for this replenishment from the ambient atmosphere are (a) mass-flow down a pressure gradient, and (b) diffusion down a concentration gradient. Of these, diffusion has long been considered the more important, and can occur through both the soil and plant root systems.

The basic mathematical model of diffusion has become known as Fick's first law of diffusion:

$$F = -D \frac{dc}{dl} \quad \dots (1)$$

where F is the diffusive flux or rate of transfer of gas per unit cross section, dc is the change in concentration and dl the distance over which the concentration decreases.

The diffusion coefficient, D , for a gas diffusing through a porous medium such as soil, will be lower than that for a gas diffusing through free air (D_0), a fact first recognised by Buckingham (1904). He proposed that D was a function of the gas-filled pore volume fraction (ϵ_g), with the relationship

$$\frac{D}{D_0} \propto \epsilon_g^2 \quad \dots (2)$$

Penman (1940a) improved upon this by not only taking into account the pore volume fraction, but also the tortuous nature of the pores. If the length of a mass of soil is l with a cross-sectional area A , then the effective lengths and cross-sectional area, are l_e and $A\epsilon_g$ respectively, and

$$\frac{dq}{dt} = \frac{D_0}{\beta} A\epsilon_g \frac{p_1 - p_2}{l_e} \quad \dots (3)$$

where dq is the change of the amount of gas, dt the change in time, p_1 and p_2 are the partial pressures distance l apart,

and β is a mathematical constant.

$$\text{or } D = D_o \epsilon_g \frac{1}{l_e} \quad \dots (4)$$

Penman showed that $D/D_o = 0.66 \epsilon_g$ for pore fractions lower than about 0.6 (Fig. 1.1). This relationship was derived by measuring the diffusion of carbon disulphide and acetone through various dry solids, but was subsequently found to hold for carbon dioxide also (Penman, 1940b).

Blake and Page (1948) found that diffusion approached zero well above zero pore volume fraction in some soils. They attributed this to water films blocking the pores, as the diffusion of oxygen is 10^4 times slower through water than through air, and to the existence of "blind alleys". The effective pore space for gaseous diffusion is therefore less than the gas filled pore space.

Taylor (1949) showed the "effective diffusion distance" to decline as the water content in sand and powdered glass mixtures was varied from low to high tensions, falling sharply between 2 and 3 kPa water tension, and then remaining steady. His value for D/D_o still corresponded closely with $0.66 \epsilon_g$, as did other experimental values derived at this time, e.g. $D/D_o = 0.6 \epsilon_g$ (van Bavel, 1952a).

In 1959 Marshall related permeability to the size distribution of pores:

$$a = \epsilon_g^{0.5} \sqrt{\frac{n-1}{n} \frac{(r_1^2 + 3r_2^2 + \dots + (2n-1)r_n^2)}{r_1^2 + r_2^2 + \dots + r_n^2}} \quad \dots (5)$$

where a = fraction of ϵ_g through which gas can diffuse freely

n = number of pore size classes

r = radii of pores (in size classes 1.....n).

This relationship took into account the three dimensional connections of the gas filled pore space. Marshall suggested that Penman's constant of 0.66 should be replaced by $\epsilon_g^{0.5}$, as the effects of pore size can be

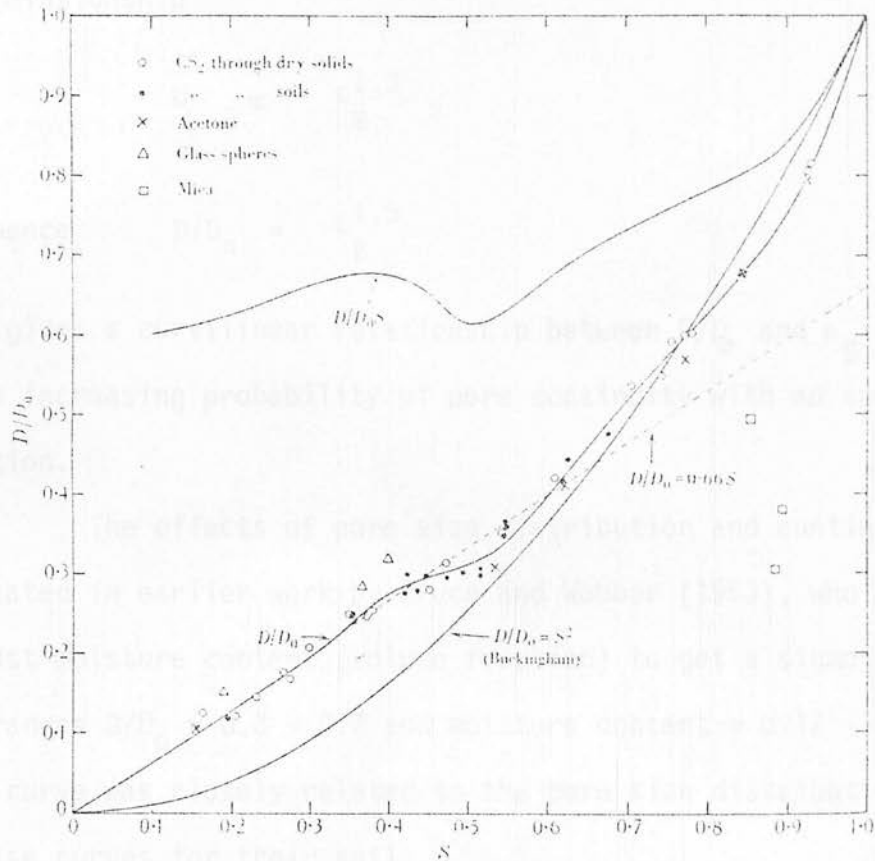


Fig. 1.1 The dependence of coefficient of diffusion (D) on the pore volume fraction (s) (s corresponds to ϵ_g in the text) as derived by Penman (1940a).

neglected for diffusion. This gives

$$D/D_o = \epsilon_g^{1.5} \quad \dots (6)$$

Millington (1959) reworked this equation, taking into account the probability of continuity of pores in adjacent planes, to obtain the relationship

$$D \propto \epsilon_g^{1.3}$$

and hence
$$D/D_o = \epsilon_g^{1.3} \quad \dots (7)$$

This gives a curvilinear relationship between D/D_o and ϵ_g (Fig. 1.2) due to an increasing probability of pore continuity with an increasing pore fraction.

The effects of pore size distribution and continuity were indicated in earlier work by Bruce and Webber (1953), who plotted D/D_o against moisture content (volume fraction) to get a sigmoid curve within the ranges $D/D_o = 0.3 - 0.7$ and moisture content = $0.17 - 0.25 \text{ m}^3 \text{ m}^{-3}$. This curve was closely related to the pore size distribution and moisture release curves for their soil:

The generally lower data points that Gradwell (1960) obtained for undisturbed soil cores (Fig. 1.3) when compared to theoretical lines for straight pores and spherical particulate packings (De Vries, 1950), are probably due mainly to tortuosity factors not being taken into account. If the curves from Millington in Fig. 1.2 are compared to Fig. 1.3, then a close agreement can be seen between $D/D_o = n^2(\epsilon_g^{4/3}/m^2)$ and Gradwell's data points at low gas filled pore volume fractions.

Currie (1960b) introduced another factor into the discussion, that of pore and particle shape. Experiments he performed, using a non-steady state method of measurement (Currie, 1960a), on over 20 dry granular packing materials, showed that many materials (especially

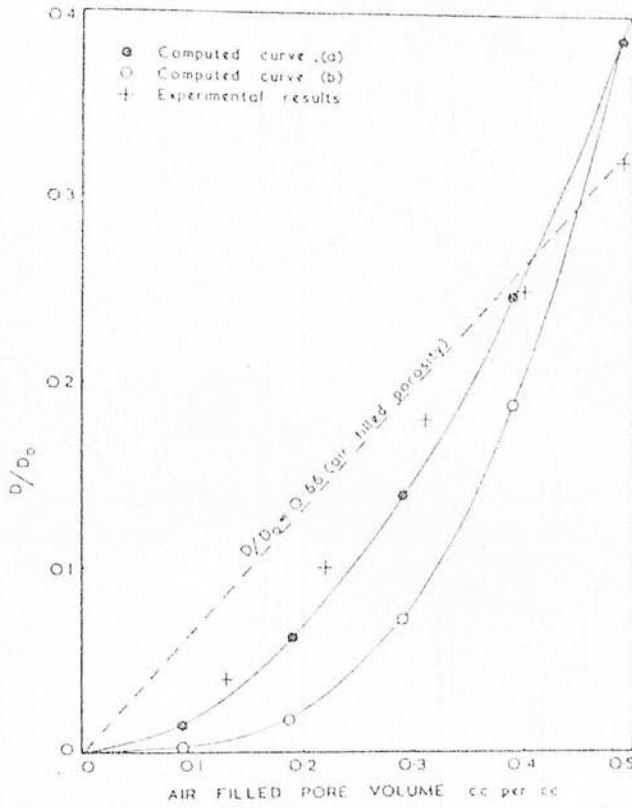


Fig. 1.2 Relationship between coefficient of diffusion (D) and air filled pore volume (ϵ_g) for experimental results (from Taylor, 1949) and computed curves (a) $D/D_0 = n^2 (\epsilon^{1.33}/m^2)$ and (b) $D/D_0 = n^2 (\epsilon_g^{1.33}/m^2)$. Where ϵ is the total pore volume made up of m equal -volume components of which n are drained. From Millington, 1959.

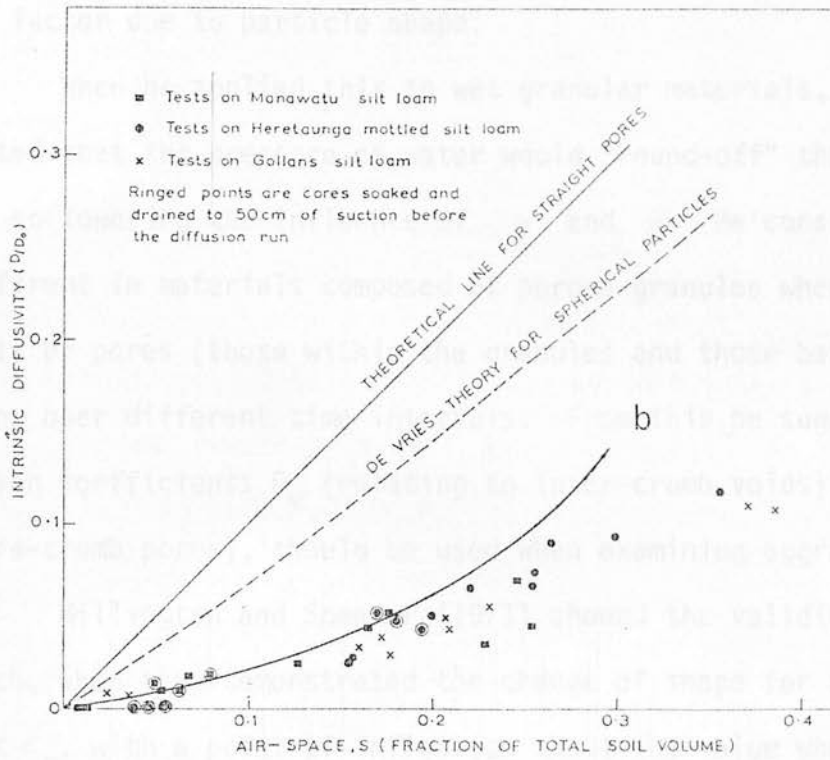


Fig. 1.3 Relationship between diffusivity (D/D_0) and air filled pore volume fraction (s) (s corresponds to ϵ_g in the text) for undisturbed samples of pasture topsoil. From Gradwell, 1960. The curve (b) from Fig. 1.2 has been superimposed.

those with a pore volume fraction of 0.8 - 1.0) did not fit the Penman equation $D/D_0 = 0.66 \epsilon_g$. He suggested that for dry granular materials, a better general equation was,

$$D/D_0 = \gamma \epsilon_g^\mu \quad \dots (8)$$

where γ lies between 0.8 and 1 and varies with the pore fraction, and μ is a factor due to particle shape.

When he applied this to wet granular materials, Currie (1961a) suggested that the presence of water would "round-off" the shape of the pores, so lowering the influence of γ and μ . He considered this to be different in materials composed of porous granules where there were two sets of pores (those within the granules and those between them), draining over different time intervals. From this he suggested that two diffusion coefficients D_v (relating to inter-crumbs voids) and D_c (relating to intra-crumbs pores), should be used when examining aggregated media.

Millington and Shearer (1971) showed the validity of this approach, when they demonstrated the change of shape for a graph of D/D_0 against ϵ_g , with a point of inflection about the value when drainage of inter-crumbs voids ceased, and that of intra-crumbs pores commenced (Fig. 1.4).

The previously mentioned attempts to describe quantitatively the diffusion of gases through soil have generally omitted one important aspect that separates soil from inert porous media. This is the consumption of oxygen and the evolution of carbon dioxide throughout the medium, due to respiration.

Van Bavel (1951) recognised this when he derived the equation

$$\frac{dc}{dt} = -D \frac{d^2c}{dL^2} + \beta a \quad \dots (9)$$

where a is a term relating to any "activity" whereby gases are absorbed or released in the soil, and β is a constant dependent upon temperature (t) and pore fraction. In this paper he went on to develop

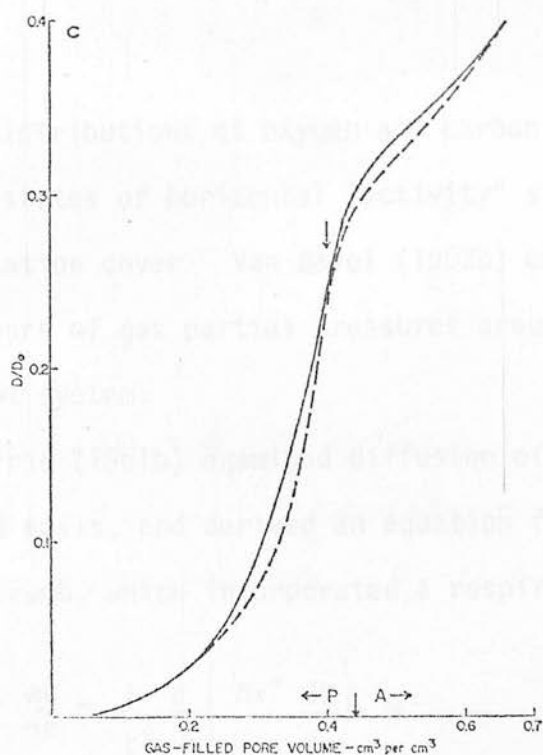


Fig. 1.4 Relationship between diffusivity (D/D_0) and gas filled pore volume fraction of soil aggregates, with the inter-aggregate (P) and intra-aggregate (A) pore volumes indicated. From Millington and Shearer, 1971.

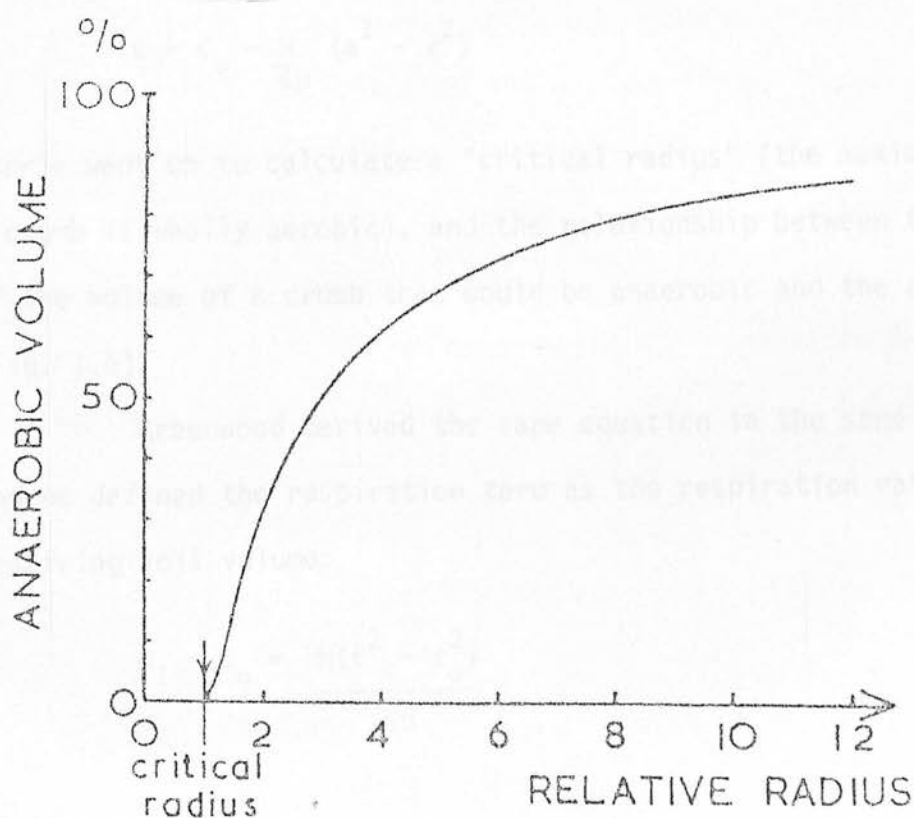


Fig. 1.5 The effect of crumb radius on the anaerobic volume of soil crumbs. From Currie (1961.)

theoretical distributions of oxygen and carbon dioxide down a profile with various states of horizontal "activity" stratification and a uniform vegetation cover. Van Bavel (1952b) employed similar techniques to plot contours of gas partial pressures around a single hemispherical (assumed) root system.

Currie (1961b) examined diffusion of oxygen and carbon dioxide in aggregated soils, and derived an equation for diffusion of oxygen into a spherical crumb, which incorporated a respiration term:

$$\epsilon_g \frac{dC}{dt} = \frac{1}{r^2} \frac{d}{dr} \left(Dr^2 \frac{dC}{dt} \right) + M \quad \dots (10)$$

where M is the respiration term (negative for oxygen absorption, positive for carbon dioxide evolution) for an isotropic concentric shell of radius r . Integration of Equation (9) gave a relationship between the concentration C of oxygen at radius r in a soil crumb of radius ' a ', and a surface oxygen concentration of C_a ,

$$C = C_a - \frac{M}{6D} (a^2 - r^2) \quad \dots (11)$$

Currie went on to calculate a "critical radius" (the maximum at which a crumb is wholly aerobic), and the relationship between the fraction of the volume of a crumb that would be anaerobic and the crumb radius (Fig. 1.5).

Greenwood derived the same equation in the same year (1961), and he defined the respiration term as the respiration rate per unit of respiring soil volume:

$$C_1 - C_o = \frac{M(r^2 - r_o^2)}{6D} \quad \dots (12)$$

Where, C_1 corresponds to C in Equation (11)

$$\begin{array}{ccccccc} C_o & " & " & C_a & " & " & " \\ r & " & " & r & " & " & " \\ r_o & " & " & a & " & " & " \end{array}$$

Equations (11) and (12) apply to perfect spheres, but soil crumbs are irregularly shaped. Greenwood (1963) suggested that irregularly shaped crumbs with volume V_2 and surface area A could be approximated to a sphere with radius r_1 , according to the equation

$$r_1 = 3V_2/A \quad \dots (13)$$

He then substituted $3V_2/A$ for r_o in Equation (12), to give:

$$6DC_1 = Mr_1^2 f(V_1/V_2) \quad \dots (14)$$

which defines the volume of aggregates that are anaerobic when the concentration of oxygen at their boundary is C_1 .

When measuring oxygen concentrations in partially saturated columns of soil crumbs Greenwood and Goodman (1967) found a better agreement between predicted and measured values of D when they took into account the solubility of oxygen in aqueous solution. This can be incorporated into the diffusion equation for water saturated crumbs, to give a maximum radius r without having an oxygen-free centre under a partial pressure P and oxygen uptake of M .

$$r = \sqrt{\frac{6DSP}{M}} \quad \dots (15)$$

where S is the solubility coefficient of oxygen in water (Greenwood, 1975).

When reviewing soil aeration, Smith (1977) contributed further by considering the size distribution of soil aggregates found in field soils. He took data of Gardner (1956) and Russell and Tamhane (1940), which illustrated that sieved size distributions (weight fractions) were log-normally distributed, and derived the fraction ' v_r ' of the total

volume which occurred as aggregates of radius r .

$$V_r = \frac{1}{\sigma_r \sqrt{2\pi}} \exp \left[-\frac{(\log r - \log \mu)^2}{2\sigma^2} \right] \quad \dots (16)$$

In Equation (16) μ is the mean radius, and σ^2 the variance of the distribution. Combining this with equations that give the fraction of an individual aggregate that is anaerobic, he was able to calculate the fraction ϕ of the total aggregate volume which is anaerobic (Smith, 1980):

$$\phi = \frac{1}{\sigma \sqrt{2\pi}} \int_{r_c}^{\infty} r_o^3 \exp \left[-\frac{(\log r - \log \mu)^2}{2\sigma^2} \right] dr \quad \dots (17)$$

where r_o is the radius of the anaerobic zone, and r_c is the radius of the largest aggregate that is wholly aerobic. If equation (17) is combined with Equations (11) or (12) then curves can be derived showing the relationship between ϕ and inter-aggregate oxygen concentrations, at different values of D (Fig. 1.6).

The discussion and equations above indicate the main physical properties of soil that govern the diffusion of gases through it, and hence its ability to maintain aerobic conditions. They also demonstrate that the ultimate aeration status is a balance between the supply of oxygen and the biological activities that act as a sink for it, and also as a source of carbon dioxide. This biological activity is now discussed in Section 1.2.

1.2 RESPIRATION IN SOIL

Respiratory demand for oxygen is considered to have two sources in the soil, i.e. microorganisms and plant root systems.

Respiration can be either aerobic or anaerobic according to conditions and microbial species present. Of the two, aerobic breakdown

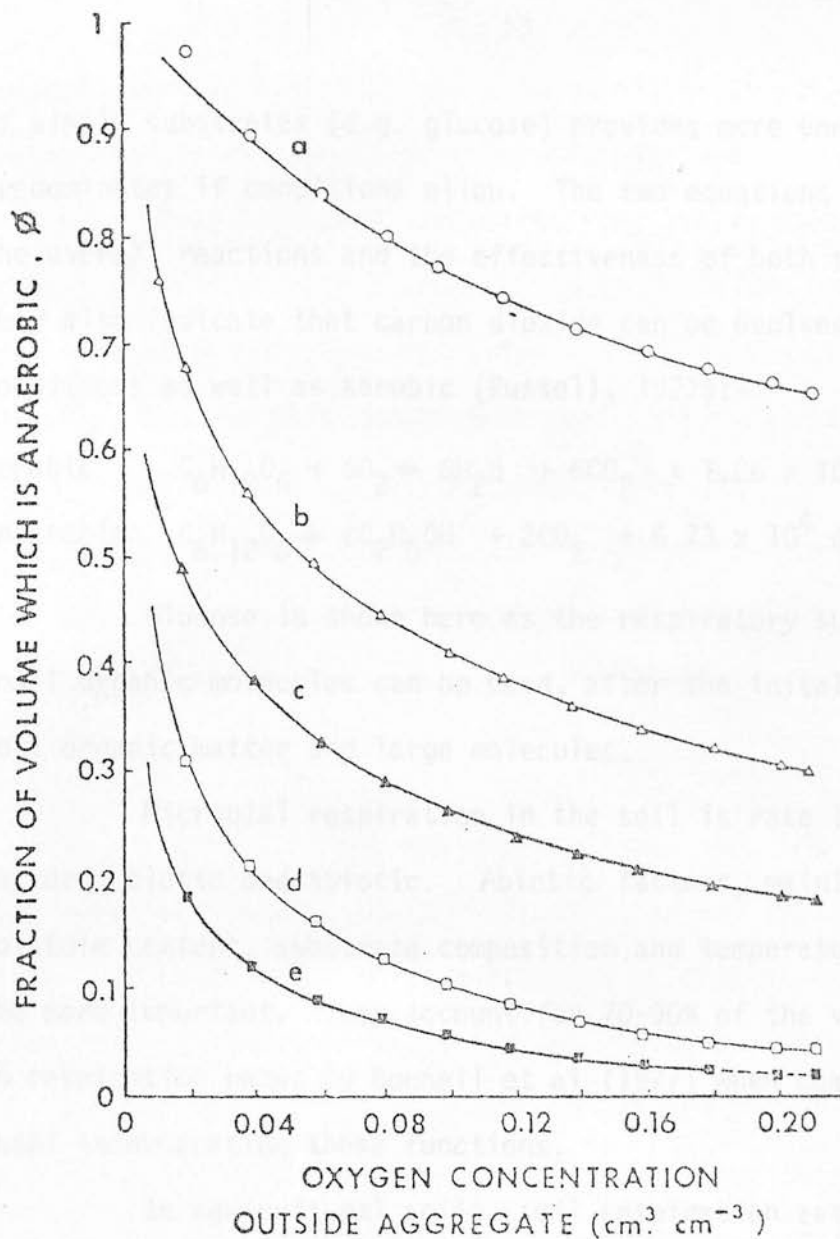


Fig.1.6 Relationship between the fraction of the total aggregate volume which is anaerobic (ϕ) and the oxygen concentration, outside the aggregate, for the conditions;

a : $D_a = 10^{-6} \text{ cm}^2 \text{ s}^{-1}$; $\log_{10} \mu = 0.7$

b : $D_a = 10^{-5} \text{ cm}^2 \text{ s}^{-1}$; $\log_{10} \mu = 0.7$

c : $D_a = 10^{-5} \text{ cm}^2 \text{ s}^{-1}$; $\log_{10} \mu = -0.3$

d : $D_a = 10^{-4} \text{ cm}^2 \text{ s}^{-1}$; $\log_{10} \mu = 0.7$

e : $D_a = 10^{-4} \text{ cm}^2 \text{ s}^{-1}$; $\log_{10} \mu = -0.3$

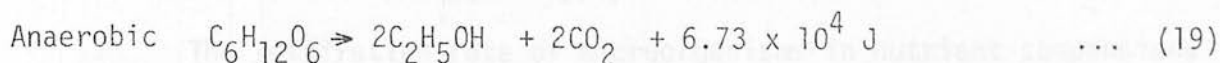
Where D_a is the diffusion coefficient within aggregates,

μ is the mean radius of aggregates, the oxygen consumption

rate is $2 \times 10^{-7} \text{ cm}^3 \text{ cm}^{-3} \text{ s}^{-1}$ and the variance of the

aggregate distribution is 1. From Smith, 1980.

of simple substrates (e.g. glucose) provides more energy, and predominates if conditions allow. The two equations below demonstrate the overall reactions and the effectiveness of both respiration paths. They also indicate that carbon dioxide can be evolved under anaerobic conditions as well as aerobic (Russell, 1977):-



Glucose is shown here as the respiratory substrate, but other small organic molecules can be used, after the initial degradation of soil organic matter and large molecules.

Microbial respiration in the soil is rate limited by several factors, biotic and abiotic. Abiotic factors, mainly oxygen supply, moisture content, substrate composition and temperature, are by far the more important. They account for 70-90% of the variability observed in respiration rates by Bunnell et al (1977) when compared against a model incorporating these functions.

In agricultural soils, soil respiration rates (as shown by carbon dioxide evolution) increased with additions of fresh organic matter, though the percentages of the additions decomposed in a given time period were similar, and therefore somewhat independent of the amount added (Jenkinson, 1977). There is also evidence that addition of organic matter can increase the decomposition of soil organic matter already present, though this effect is small and doubted by some workers (see Russell, 1973 page 277).

In a natural or forest soil profile, without manure additions of organic matter over a short period, the effect of the change of organic

NB The energy evolved in Equations (18) and (19) is defined as only that gained via ATP synthesis, and so biologically useful.

matter quantity with depth down the profile can still be seen. Near the surface there will be large quantities derived from litter decomposition, while at depth in mineral subsoils, very little will be present. The amounts (and degree of decomposition in which the organic matter exists) will vary with soil type and climatic conditions, but will not fluctuate rapidly, and the main constraints upon soil respiration will therefore be moisture content and oxygen supply.

The respiration rate of microorganisms in nutrient suspensions has been shown to follow the Michaelis-Menten relationship for substrate concentrations against time (Longmuir, 1954), giving the relationship,

$$\frac{-dC}{dt} = \frac{kC}{K_m + C} \quad \dots \quad (20)$$

Where k is the maximum reaction rate, and K_m is the concentration of substance for $k/2$. Greenwood (1961) argued that if K_m is small compared to C (concentration), then providing C is greater than that for zero respiration, dC/dt can be considered constant. This gave a constant M for the rate of soil respiration per unit of respiring volume, assuming a uniform distribution of organisms. Greenwood included this constant in the diffusion equation (12), which he used to calculate the respiration rate of saturated soil crumbs under different oxygen concentrations. He found that appreciable inhibition of respiration did not occur unless oxygen concentrations fell to values about $3 \times 10^{-9} \text{ mol m}^{-3}$ ($\cong 0.015 \text{ m}^3 \text{ m}^{-3}$ in the gas phase). This explains the rapid decline in dissolved oxygen concentrations found by Scott and Evans (1955) in saturated soil, and is comparable with values of K_m found in pure cultures of various microorganisms by Longmuir (1954) ($1 \times 10^{-16} \text{ mol m}^{-3}$ to $1 \times 10^{-3} \text{ mol m}^{-3}$).

These conclusions were supported by further experiments involving the measurements of respiration rates in moulded soil spheres (Greenwood and Goodman, 1964), and held true for mixtures of microorganisms and over a wide range of soil types.

Data from other workers may at first suggest inhibition at higher concentrations of oxygen ($0.02 - 0.05 \text{ m}^3 \text{ m}^{-3}$ in the gas phase), especially when obtained from bulked soil samples or undisturbed soil cores (Parr and Reuszer, 1959; Howeler and Bouldin, 1971). However, it is clear from their experiments that the respiring microsites were in saturated regions away from the applied gas treatment, and were having to rely on oxygen diffusing from gaseous regions in the soil. These sites may therefore have been at lower oxygen concentrations than those nominally supplied.

The relationship between diffusion and moisture content results in the inhibition of the overall respiration of soil at high moisture contents, by reducing the volume which is aerobic. It must be remembered though, that under very dry conditions corresponding roughly to the "wilting-point", carbon dioxide evolution from soil and plant litter is drastically reduced (Wiant, 1967b). Miller and Johnson (1964) found that carbon dioxide evolution increased with increasing moisture tension from 0 to 15-50 kPa and from there on gradually decreased to minimal levels at higher tensions. They concluded that maximum microbial respiration would take place at the lowest tension where aeration is not limiting but at higher tensions it would be reduced, due to the effects of drying at the cellular level.

Yamaguchi et al (1967) arrived at a similar conclusion to explain carbon dioxide and oxygen levels in incubated soil columns, but also proposed the possibility of release of dissolved carbon dioxide upon drying by the reaction



Greenwood (1970) investigated the distribution of carbon dioxide in the aqueous phase of water saturated soil spheres and agar shapes. He found that while oxygen concentrations fell by $0.05 - 0.15 \text{ m}^3 \text{ m}^{-3}$ over

distances of 2-4 mm, the concentration of carbon dioxide increased by less than $0.003 \text{ m}^3 \text{ m}^{-3}$. He concluded that in soil containing no oxygen-free zones the concentration of carbon dioxide in the aqueous phase will not be more than $0.01 \text{ m}^3 \text{ m}^{-3}$ greater than in the gas phase.

Macauley and Griffen (1969) showed that high carbon dioxide concentrations had a limiting effect on the growth of certain soil fungi isolated from some Australian soils. However, the effect was small and occurred at concentrations above $0.1 \text{ m}^3 \text{ m}^{-3}$, so it is unlikely that this could be a significant effect in aerobic soils, in view of Greenwood's observations.

Another parameter often used to characterise soil respiration is the "Respiratory Quotient" (RQ), which is the amount of carbon dioxide evolved per unit of oxygen consumed. Ideally $\text{RQ}=1$ for aerobic respiration where one molecule of oxygen gives rise to one molecule of carbon dioxide, but can rise above 1 in anaerobic soil (Rixon and Bridge, 1968), and for certain substrates (alcohols and amino acids) can be less than 1 in pure microbial cultures (Brock, 1970).

Rixon and Bridge (1968) measured the RQ of several sieved soil samples over a range of matric water potentials (0 to 100 kPa), and found that the transition from above unity to about 1 occurred at moisture potentials that gave an increase in the gas-filled pore fraction from about 0.1 to 0.6-0.7 (Fig. 1.7).

Bridge and Rixon (1976) again employed the same approach on undisturbed field cores, and obtained similar results, showing RQ's greater than 1 at gas filled pore fractions less than 0.1 (Fig. 1.8). Their plot of oxygen uptake against air-filled pore fractions gives maxima at values just higher than the critical air filled pore fraction for the onset of anaerobic respiration. This supports the earlier statement that maximum aerobic soil respiration takes place at the highest moisture content which is non-limiting to aeration. As would

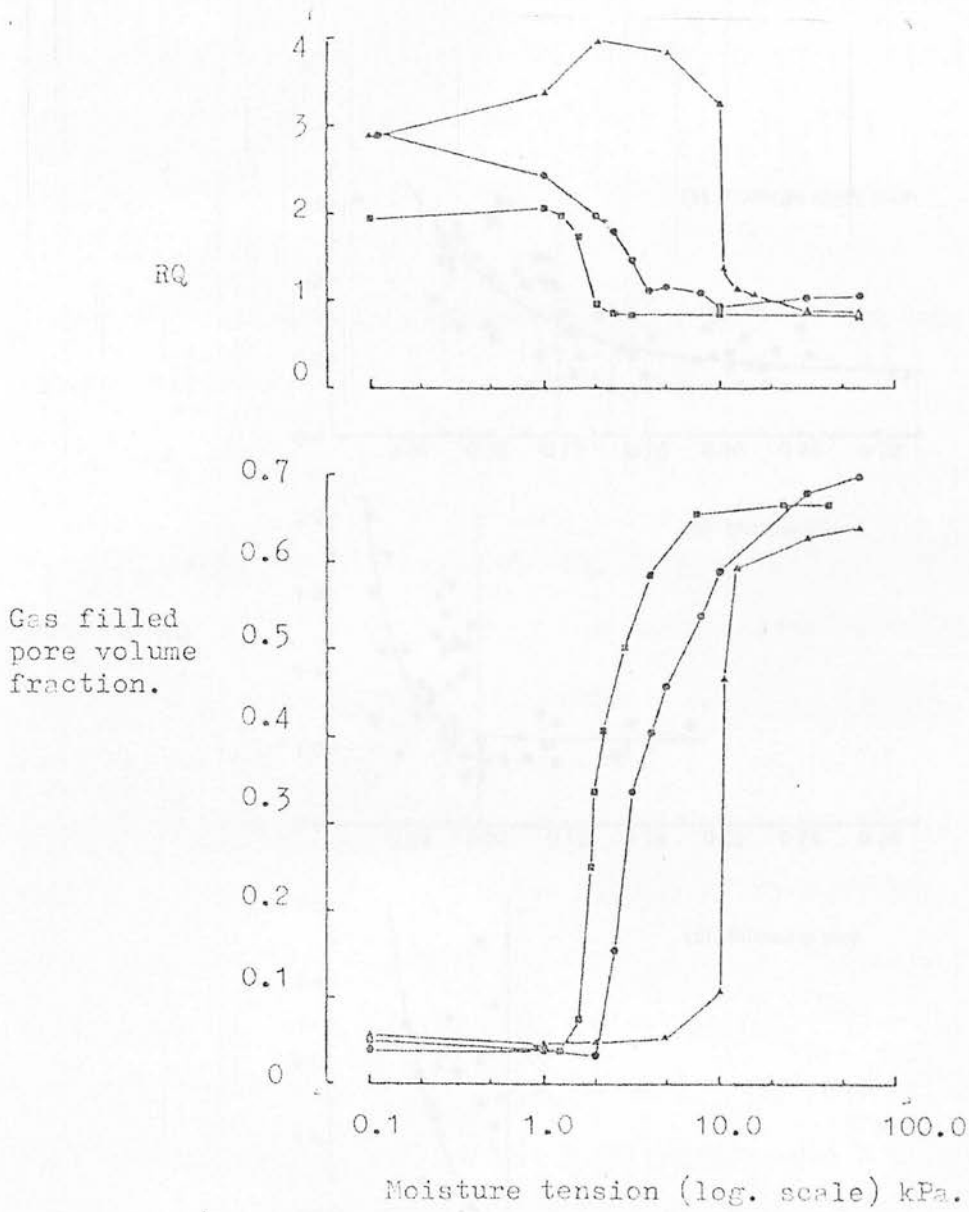


Fig. 1.7 Relationship between respiratory quotient (RQ), moisture tension and gas filled volume fraction for a sandy loam, clay loam and a clay soil. ■ - Conargo sandy loam; ● - Mundiwa clay loam; ▲ - Riverina clay. From Rixon and Bridge (1968).

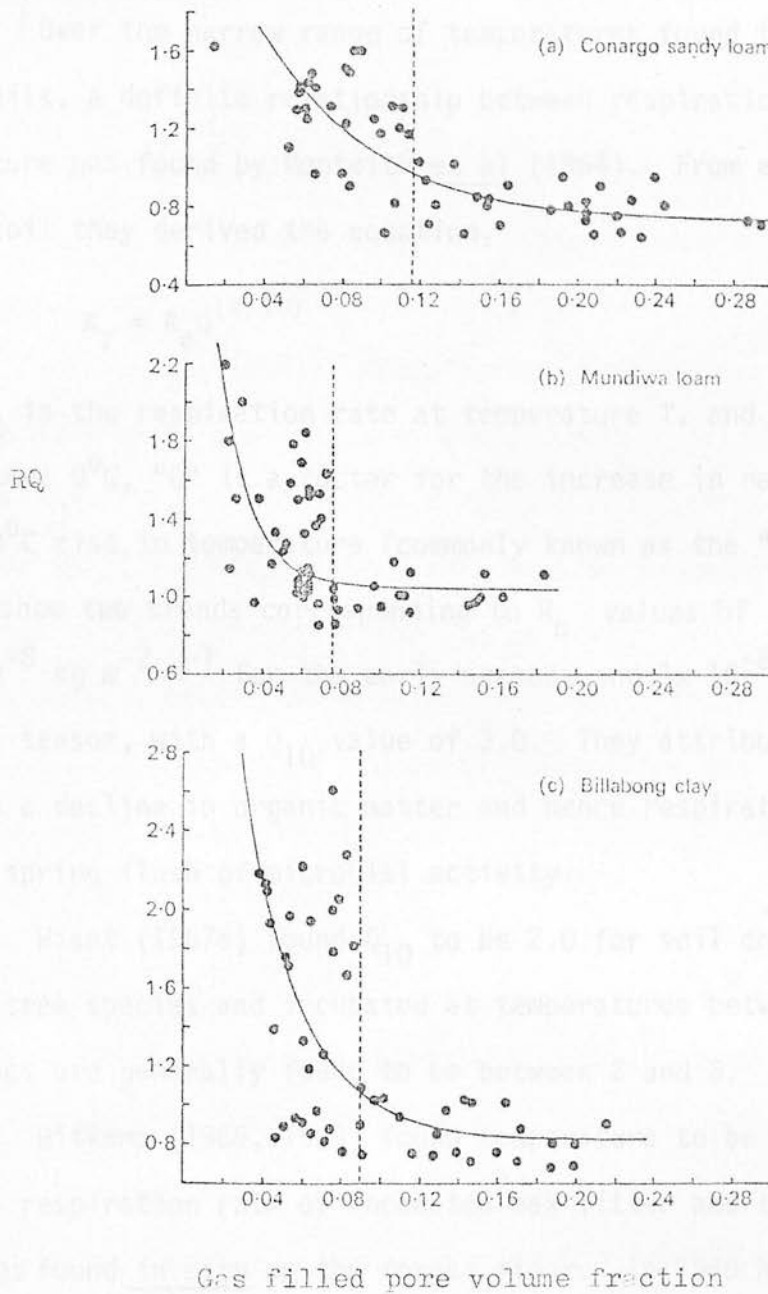


Fig. 1.8 Relationship between respiratory quotient and gas filled pore volume fraction. From Bridge and Rixon, 1976.

be expected for a metabolic process, respiration is highly dependent upon temperature and different microorganisms show various optimum temperature ranges for maximum efficiency.

Over the narrow range of temperatures found in temperate field soils, a definite relationship between respiration rate and temperature was found by Monteith et al (1964). From experiments on a bare soil they derived the equation,

$$R_T = R_0 Q^{(T/10)} \quad \dots (22)$$

Where R_T is the respiration rate at temperature T , and R_0 that at temperature 0°C , " Q " is a factor for the increase in respiration rate for a 10°C rise in temperature (commonly known as the " Q_{10} "). Their results show two trends corresponding to R_0 values of $1.4 \times 10^{-8} \text{ kg m}^{-2} \text{ s}^{-1}$ for the early season, and $1 \times 10^{-8} \text{ kg m}^{-2} \text{ s}^{-1}$ for late season, with a Q_{10} value of 3.0. They attributed the difference in R_0 to a decline in organic matter and hence respiratory substrate, after a spring flush of microbial activity.

Wiant (1967a) found Q_{10} to be 2.0 for soil collected under various tree species and incubated at temperatures between 20 and 30°C , and values are generally found to be between 2 and 3.

Witkamp (1966, 1969) found temperature to be highly correlated with the respiration rate of incubated oak litter and this correlated with rates found in situ on the forest floor. In 1969 he showed that the evolution of carbon dioxide from forest litter followed a daily cycle that paralleled the daily temperature cycle. Also, Witkamp and Frank (1969) suggested that high production of carbon dioxide in the litter layer during the afternoon resulted in downward diffusion of carbon dioxide into lower horizons. This carbon dioxide was evolved later as a pre-dawn flush due to thermal convection (Witkamp, 1969).

The rate of formation of other ^aanerobic products (such as

ethylene) is also greatly affected by temperature. Smith and Dowdell (1974), examining ethylene levels in field conditions for two clay soils, found an apparent Q_{10} of 66 over the range 5-11°C. They argued that the normal rise due to increasing metabolic activity was compounded by increased depletion of oxygen and hence increasing volumes of ethylene-producing anaerobic zones.

Another possible interaction between temperature and moisture content was investigated in semi-arid steppe grassland by Wildung et al (1975). Taken independently, water content and temperature did not correlate well with carbon dioxide evolution but soil water content did correlate significantly ($P < 0.01$) with soil respiration when temperatures were above 15°C, and the relative influence of water content on respiration rate varied with temperature.

Bunnell et al (1977) developed a model incorporating several abiotic influences governing microbial respiration and substrate weight loss. The model was of the form

$$R_{tM} = \left(\frac{M}{a_1 + M} \right) \left(\frac{a_2}{a_2 + M} \right) a_3 a_4^{(t-10)/10} \quad \dots \quad (23)$$

Where, R_{tM} = respiration rate at temperature t and moisture content M .

a_1 = moisture content at which activity is half its optimal value.

a_2 = moisture content at which gaseous exchange is half its optimal value.

a_3 = respiration rate that would occur at 10°C if neither moisture nor oxygen were limiting.

a_4 = Q_{10}

This model was used to simulate respiration rates which were compared with measured values from an aspen forest floor (Fig. 1.9).

The other major source of respiratory demand in the soil, i.e. plant roots, is discussed in Section 1.4, together with mechanisms by which some plants tolerate waterlogged conditions.

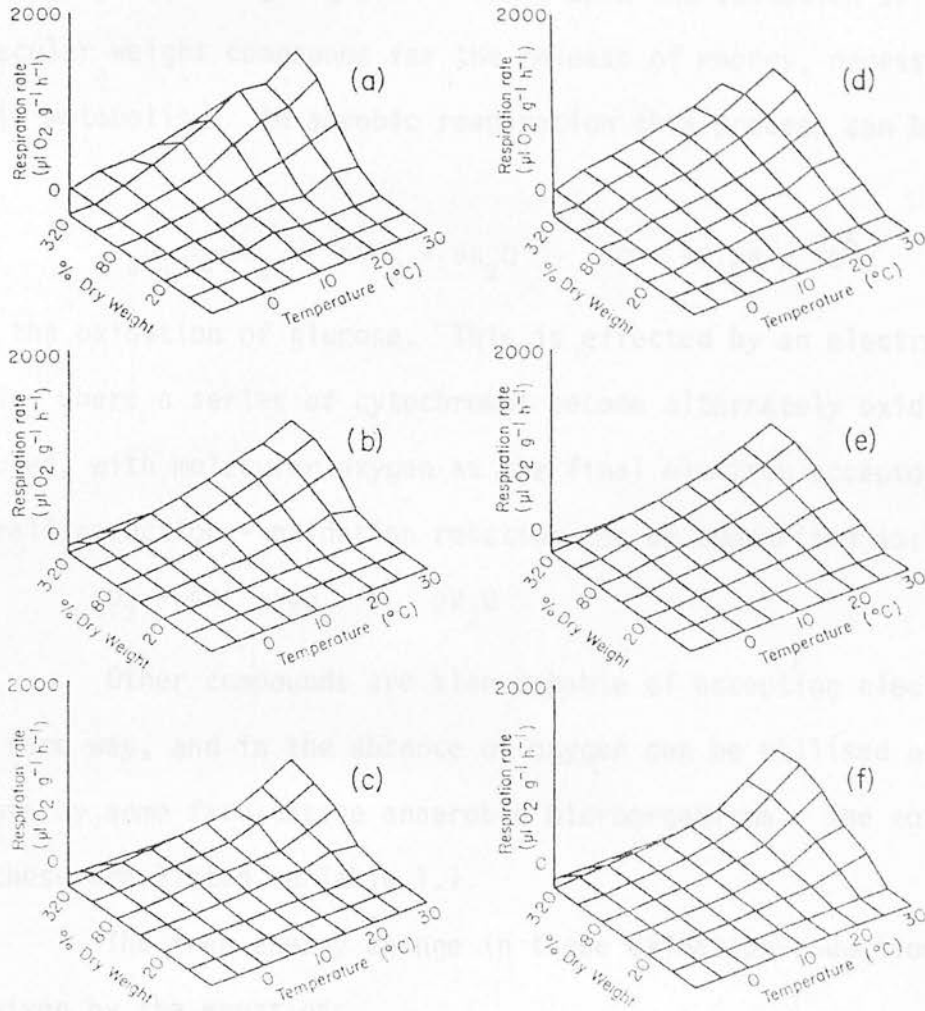
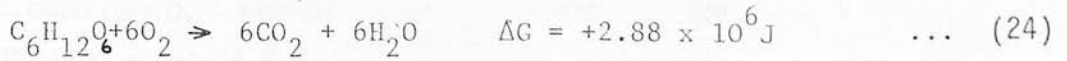


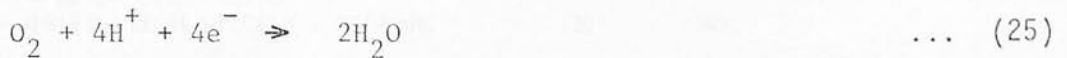
Fig. 1.9 Measured rates of microbial respiration for the litter (a), fermentation (b) and humus layers (c) of aspen (*Populus tremuloides*) forest floor, and simulated rates for the same layers (d, e and f respectively) using Equation (23) in the text. From Bunnell et al, 1977.

1.3 CHEMICAL AND ELECTROCHEMICAL TRANSFORMATIONS IN A WATERLOGGED SOIL

All living organisms depend upon the oxidation of high molecular weight compounds for the release of energy, necessary for their metabolism. In aerobic respiration this process can be generalised as:



for the oxidation of glucose. This is effected by an electron transfer chain, where a series of cytochromes become alternately oxidised and reduced, with molecular oxygen as the final electron acceptor. The overall reduction - oxidation reaction can be summarised as:



Other compounds are also capable of accepting electrons in the same way, and in the absence of oxygen can be utilised as oxidising agents by some facultative anaerobic microorganisms. The more important of these are listed in Table 1.1.

The free energy change in these oxidation-reduction equations is given by the equation:

$$\Delta G = \Delta G^0 + RT \ln \frac{(Red)}{(Oxid)} \quad \dots (26)$$

where ΔG = free energy change

ΔG^0 = free energy change when activities are 1

(Red) = Activity of reduced form

(Oxid) = Activity of oxidised form

R = the gas constant

T = temperature (K)

But the free energy change is also given by:

$$\Delta G = -n EF \quad \dots (27)$$

Table 1.1 The major oxidation-reduction systems in the soil with their "redox" potentials. From Russell, 1977, 1972, 1977.

System	Oxidation-reduction potential in mV, 25°C	
	At pH 5	At pH 7
$O_2 + 4H^+ + 4e^- = 2H_2O$ $E_h = 1.23 + 0.0148 \log P(O_2) - 0.059 \text{ pH}$	930	820
$NO_3^- + 2H^+ + 2e^- = NO_2^- + H_2O$ $E_h = 0.83 - 0.0295 \log NO_2^-/NO_3^- - 0.059 \text{ pH}$	530	420
$MnO_2 + 4H^+ + 2e^- = Mn^{2+} + 2H_2O$ $E_h = 1.23 - 0.0295 \log Mn^{2+} - 0.119 \text{ pH}$	640	410
$Fe(OH)_3 + 3H^+ + e^- = Fe^{2+} + 3H_2O$ $E_h = 1.06 - 0.059 \log Fe^{2+} - 0.177 \text{ pH}$	170	-180
$SO_4^{2-} + 10H^+ + 8e^- = H_2S + 4H_2O$ $E_h = 0.30 - 0.0074 \log H_2S/SO_4^{2-} - 0.074 \text{ pH}$	-70	-220
$CO_2 + 8H^+ + 8e^- = CH_4 + 2H_2O$ $E_h = 0.17 - 0.059 \log P(CH_4)/P(CO_2) - 0.059 \text{ pH}$	-120	-240
$2H^+ + 2e^- = H_2$ $E_h = 0.00 - 0.059 \text{ pH}$	-295	-413

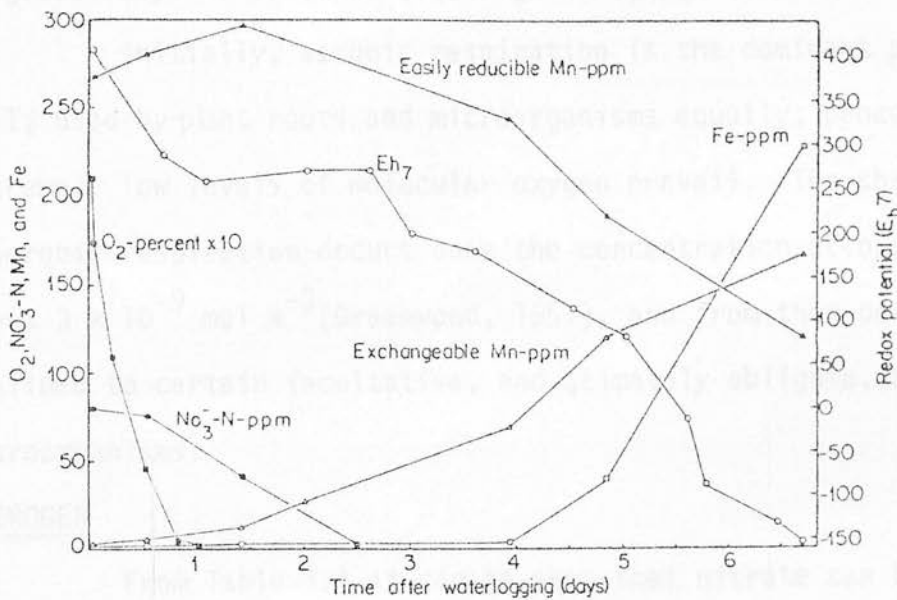


Fig. 1.10 Changes in the major redox systems and potential of a silty clay after waterlogging. From Patrick and Turner, 1968.

where E = voltage of the reaction

F = Faraday constant

Substituting this relationship for ΔG in Equation (26) converts it to a voltage equation:

$$E_h = E_o + \frac{RT}{nF} \ln \frac{(\text{Oxid})}{(\text{Red})} \quad \dots (28)$$

where E_h denotes that E is measured against the standard hydrogen electrode. Equations (26)-(28) have been taken from Ponnamperna (1972).

The major reduction-oxidation (or "Redox") systems in the soil, together with their redox potentials at standard pHs, are listed in Table 1.1.

This series of decreasing redox potentials corresponds closely with the sequence of changes in electron acceptor used in soil respiration, as the soil changes from an aerobic system to an anaerobic one, and becomes progressively more reduced (see Fig. 1.10).

Initially, aerobic respiration is the dominant process in the soil, used by plant roots and microorganisms equally, proceeding until extremely low levels of molecular oxygen prevail. The change to anaerobic respiration occurs once the concentration of oxygen falls below about $3 \times 10^{-9} \text{ mol m}^{-3}$ (Greenwood, 1961), and from then on respiration is confined to certain facultative, and ultimately obligate, anaerobic microorganisms.

NITROGEN

From Table 1.1 it can be seen that nitrate can be used as an electron acceptor under reduced conditions, forming nitrite and water:



This is a faculty of many bacteria, but some can proceed further, forming gaseous reduction products such as nitrous oxide (N_2O) and molecular nitrogen (N_2), which constitutes a net loss of nitrogen from the soil. This process, termed denitrification (Nicholas, 1963), only

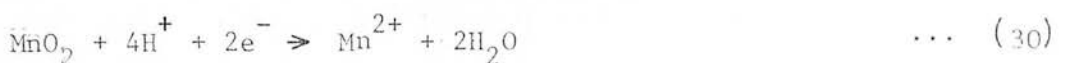
occurs in soils depleted of oxygen. Greenwood (1962) found that nitrate reduction only takes place once the oxygen concentration in solution falls below about $4 \times 10^{-9} \text{ mol m}^{-3}$, which agrees fairly closely with the estimated concentration at which aerobic respiration ceases.

Denitrifying bacteria need a substrate to supply H^+ ions and electrons for nitrate reduction, and so the process is dependent upon the availability of organic matter in the soil (Bremner and Shaw, 1958). It is also temperature dependent to a certain extent, but the rate is essentially the same between temperatures of 15 and 30°C (Bremner and Shaw, 1958; Cho and Ponnamperna, 1971). It is only very low temperatures near 0°C that retard denitrification significantly. Therefore denitrification may be minimal in mineral subsoils, and slow during winter but increasing in the spring (Dowdell and Smith, 1974). However it can occur even in well aerated topsoils, within localised sites such as the centre of crumbs or peds that may be waterlogged (Burford and Millington, 1968; Burford and Stefanson, 1973).

Another feature due to the lack of oxygen is that mineralisation of organic nitrogen cannot proceed to nitrate and nitrite. There is therefore an initial build up of ammonium $-\text{N}$, and this is the form available to plants growing in waterlogged soils. Some ammonia may be lost by volatilisation under alkaline conditions (Russell, 1973).

MANGANESE AND IRON

Table 1.1 indicates that manganese (IV) is the next redox system to become reduced after nitrate, but because soils usually contain more iron than manganese, it is usually iron hydroxides that dominate the redox system. Even so, the presence of manganese dioxide will delay the reduction of iron (III) compounds. The reductions take the form:

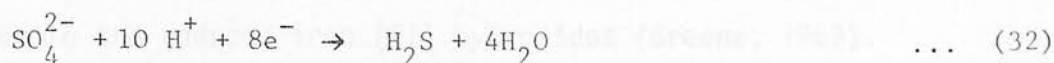


and $\text{Fe}(\text{OH})_3 + 3\text{H}^+ + \text{e}^- \Rightarrow \text{Fe}^{2+} + 3\text{H}_2\text{O}$... (31)
 giving the Mn^{2+} and Fe^{2+} forms.

Although both elements are necessary in small amounts as plant micronutrients, both are toxic in high concentrations. This has important consequences for the response of crops in waterlogged agricultural soils, and for species distribution in natural ecosystems, e.g. the distribution of Erica tetralix and E. cinerea, where E. tetralix is more tolerant of high iron concentrations (Jones and Etherington, 1970; Jones, 1971).

SULPHUR

The next system to become reduced after iron (III) is sulphate, which is reduced to sulphide:



It is mainly bacteria of the genus Desulphovibrio that carry out this reaction, and are responsible for the formation of localised iron and hydrogen sulphides which occur in bogs and other waterlogged soils.

Free soluble sulphides (S^{2-} , HS^- , H_2S) are highly toxic to plants, poisoning many enzyme systems, but are probably prevented from reaching toxic concentrations in many soils by being precipitated out as iron sulphide by the Fe^{2+} ions already present (Connell and Patrick, 1968).

PHOSPHORUS

The main transformation of phosphorus after waterlogging is an increase in availability of the orthophosphate ion in both acidic and alkaline soils. In acidic soils this is accomplished by (a) release of sorbed P from Fe(III) hydroxides when the iron is reduced to Fe(II), (b) release on the hydrolysis of iron and aluminium phosphates, and (c) release from anion exchange sites on clay particles etc. Process (a) is a direct result of reducing conditions, while (b) and (c) are due to a

rise in pH brought about by the reduced conditions.

In alkaline soils any increase in available P is brought about by the decrease in pH, making hydroxylapatite more soluble (Ponnamperuma, 1972).

pH CHANGES

Ponnamperuma (1972) demonstrated that the pH of a number of soils tended towards neutrality after several weeks submergence; this applied to both originally acidic and alkaline soils.

The initial fall in pH of most soils, and the continued fall in alkaline soils, is probably due to an increase in the concentration of CO_2 dissolving to form carbonic acid (Ponnamperuma et al, 1966). The rise in pH of acidic soils is due to the conversion of inert iron (III) sesquioxide to the reduced iron (II) hydroxides (Greene, 1963).

ORGANIC COMPOUNDS

Of the wide range of organic compounds that derive from anaerobic microbial respiration, only ethylene, and certain carboxylic acids, regularly occur in amounts that are likely to have significant physiological effects on root growth.

ETHYLENE

Ethylene is a naturally occurring growth regulator produced by many plant tissues and has a wide range of effects. It promotes senescence, germination and adventitious rooting, but inhibits other systems such as stem and root elongation (Russell, 1977).

This substance is evolved before the soil has become completely anoxic, but only after the oxygen concentration in the soil gas phase has fallen below about $0.02 \text{ m}^3 \text{ m}^{-3}$ (Smith and Restall, 1971). Other soil factors controlling the evolution of ethylene are the quantity and type of organic matter (Goodlass and Smith, 1978a), soil moisture content (when considering unsaturated soils), and temperature (Smith and Dowdell, 1974). Other suggestions that it is

limited by nitrate levels, have been shown to be only partially true (Goodlass and Smith, 1978b).

The reduction in the rate of root elongation caused by ethylene was examined by Smith and Robertson (1971) for rice, barley and rye varieties. Rice was less affected than the mesophytic cereals, which suffered reductions in their rate of root elongation between 20 and 40% at only $1 \times 10^{-6} \text{ m}^3 \text{ m}^{-3}$ of ethylene in the gas phase. Field studies have indicated that concentrations can rise to higher levels than this ($5 \times 10^{-6} - 1 \times 10^{-5} \text{ m}^3 \text{ m}^{-3}$) during periods of high rainfall in heavy arable soils (Dowdell et al, 1972). It seems therefore that ethylene could play an important part in plant damage during waterlogging.

OTHER ORGANIC COMPOUNDS

Ethylene is not the only gaseous hydrocarbon evolved from the reduction of soil organic matter. Methane, ethane, propane, n- and isobutane, propylene and butene-1 are also evolved (Smith and Restall, 1971), but only in the initial stages of waterlogging, and are probably of little physiological consequence.

Apart from gaseous hydrocarbons, a whole range of fatty and hydroxy acids can also be produced, some being reduced further to gaseous end products. The principal organic acids produced are, acetic, propionic, butyric, lactic, valeric, fumaric, malic and succinic, and their total concentration can reach $1 \times 10^{-5} \text{ mol m}^{-3}$ in waterlogged soil with a liberal supply of organic matter (Russell, 1973). Some of these acids are toxic at very low concentrations, e.g. n- and isobutyric acid at $1 \times 10^{-7} \text{ mol m}^{-3}$, but others in dilute solution actually promote growth, e.g. $1 \times 10^{-7} \text{ mol m}^{-3}$ lactic, malic or succinic acids (Wang, et al, 1967).

Generally, they contribute to the unfavourable conditions for plant growth found in waterlogged soil, but are not themselves a very major factor.

1.4 PLANT RESPONSES AND TOLERANCE TO WATERLOGGING

Anaerobic conditions created by waterlogging affect plant growth, directly by restricting root respiration, and indirectly by nutrient restriction and the production of phytotoxins (Cannell, 1977). An anaerobic root environment causes severe effects in the shoots of susceptible dicotyledons, causing leaf epinasty and disruption of hormonal balance very rapidly in tomatoes (Jackson and Campbell, 1975), and reducing leaf expansion in tobacco, eventually leading to wilting and death (Williamson and Splinter, 1969).

This last observation is consistent with the general view that water uptake and transport through a flooded root system is reduced (Kramer, 1951), and the effect can be seen in woody species susceptible to waterlogging, giving reduced transpiration and apparent photosynthesis in apple trees (Childers and White, 1942). However, replacing the soil air with nitrogen had little effect on Pinus strobus seedlings (Keller, 1972), and flooding for a month produced little response in Pinus taeda (Kramer, 1951). This merely demonstrates that tree species are as varied in their tolerance to waterlogging as herbaceous species.

The most immediate effect of waterlogging is to limit root respiration. Lemon and Wiegand (1962) looked in some detail at the oxygen requirement of roots. Using an equation for the radial diffusion of oxygen into the root derived by Lemon (1962):

$$C_R - C_C = \frac{Q r^2}{4 D_r S} \quad \dots \quad (33)$$

where C_R = oxygen concentration at root surface

C_C = oxygen concentration at root centre

r = radius of root

Q = rate of oxygen uptake

D_r = diffusion coefficient through root

S = solubility coefficient of oxygen in water.

they could predict critical oxygen levels at the root surface for roots of various thickness and respiratory demand. Thick or highly active roots were calculated to be more susceptible to low oxygen concentrations. The respiratory activity of a root increases with increasing temperature or when encountering a resistance to penetration (Eavis and Payne, 1969), which itself induces root thickening. Reduced respiration chiefly manifests itself as a reduction in root elongation. A survey of 51 sets of data by Greenwood (1971) indicated that a rather low gas phase oxygen concentration of $0.06 \text{ m}^3 \text{ m}^{-3}$ was necessary to reduce elongation to 70% of its maximum rate, and in some cases elongation was unaffected until concentrations of $0.02 \text{ m}^3 \text{ m}^{-3}$ were reached. These quoted oxygen concentrations relate to the gas phase and to experiments conducted at high temperatures (about 24°C), so at lower field temperatures and in an aqueous solution, greater inhibitory effects cannot be ruled out. Work by Letey and Stolzy (1967) shows how an increase in the thickness of the water film around a root limits its oxygen supply at various soil pore fractions. Assuming the air-filled pores contain an oxygen concentration of $0.21 \text{ m}^3 \text{ m}^{-3}$ a film 0.08 mm thick is sufficient to be limiting at a pore volume fraction of 0.2, and one of 0.35 mm is limiting at a pore volume fraction of 0.5.

Although most work of this nature has been conducted on herbaceous species, Leyton and Rousseau (1957) also demonstrated reduced respiration rates in response to low oxygen regimes for excised root tips of several coniferous species. Boggie (1974) demonstrated reduced root growth for Pinus contorta and Picea sitchensis in response to lowered oxygen concentrations in nutrient solution. The increase in root weights was severely restricted once oxygen concentrations were below $0.1 \text{ m}^3 \text{ m}^{-3}$ (equivalent gas phase) for P.sitchensis, but not until about $0.05 \text{ m}^3 \text{ m}^{-3}$ (equivalent gas phase) was reached for P. contorta. This seemingly

greater tolerance of P. contorta over P. sitchensis, is also shown by Coutts and Philipson (1978a). They found that a greater proportion of P. contorta root tips and bases survived a flooding treatment than those of P. sitchensis. The roots of seedlings were submerged for 28 days at 6 or 15⁰ C. The lower temperature treatment gave better survival rates of root tips for both species (60% of P. contorta and 10% of P. sitchensis). Dormant roots of both species survived waterlogging, suggesting that the stage of plant development is important to their response. Letey et al (1962) demonstrated that the developing root systems of cotton, sunflower and green bean seedlings were vulnerable to an anaerobic environment. Lees (1972) showed a similar vulnerability of P. sitchensis seedlings. The seedlings were planted on a peat slope where the depth of the water table ranged from 0 to 1.20m. Roots did not emerge from the seedling containers unless the water table was deeper than 0.50 - 0.60m, and where aeration was sufficient (the oxygen diffusion rate was $6.6 \times 10^{-9} \text{ kg m}^{-2} \text{ s}^{-1}$).

Lack of oxygen is not the only problem in a waterlogged environment, and there is usually an increase in carbon dioxide concentration. Various studies have shown that this has to rise considerably to have any toxic effect in the presence of atmospheric oxygen (concentration $0.21 \text{ m}^3 \text{ m}^{-3}$), i.e. to $0.08 \text{ m}^3 \text{ m}^{-3}$ for cotton (Tackett and Pearson, 1964), $0.1 \text{ m}^3 \text{ m}^{-3}$ for maize, $0.2 \text{ m}^3 \text{ m}^{-3}$ for soyabean (Hammond, et al, 1955) and $0.45 \text{ m}^3 \text{ m}^{-3}$ for willow (Bergman, 1959). In swamp species such as swamp tupelo (Nigra sylvatica) root growth was not retarded at 0.02 or $0.1 \text{ m}^3 \text{ m}^{-3}$ carbon dioxide concentration even when the oxygen concentration was only $0.01 \text{ m}^3 \text{ m}^{-3}$, needing $0.31 \text{ m}^3 \text{ m}^{-3}$ of carbon dioxide before any effect (Hook et al, 1971). However in a non-hydrophilic species, "sweetgum", seedlings only survived 15 days in a carbon dioxide concentration of $0.1 \text{ m}^3 \text{ m}^{-3}$. From this it seems that high carbon dioxide concentrations will not be

damaging unless accompanied by a large oxygen deficit. Harris and Van Bavel (1957), working on tobacco, came to the conclusion that general plant metabolism was not affected until the carbon dioxide concentration rose above the oxygen concentration.

Possibly the most successful adaptation to waterlogging, shown in a wide range of plants, is the development of intercellular air spaces (aerenchyma) in the root and stem tissue, so creating an internal gas diffusion pathway. This is a widespread phenomenon in herbaceous wetland species (Spartina, Teal and Kanwisher, 1966; Molinia and Eriophorum, Armstrong, 1964), and is also observed in some crop plants, e.g. barley and rice (Barber et al, 1962) and also tree species (Coutts and Armstrong, 1976).

The amount of oxygen transported from the atmosphere to respiring roots can be a highly significant proportion of that respired by the roots. Luxmoore et al (1970 a, b, c, d) constructed a model of oxygen diffusion through a plant root system, and showed that the oxygen transported in this way could be between 34% and 42% of that required by maize roots, and all of that required by rice. They also noted that rice could exhibit a net oxygen loss to the soil, a phenomenon also observed by Armstrong (1971 a and b) following his previous observations of it in bog plants (1964) and some woody species (1968). Armstrong and Read (1972) measured the oxygen flux from the seedling root systems of several pine and spruce species (Pinus contorta, P. sylvestris, P. nigra, Picea abies and P. sitchensis), noting that the rate was increased when the shoots were transferred from air to pure oxygen, and that the rate from pines was much greater than from spruce.

Philipson and Coutts (1978) noted that Pinus contorta will transport (and effuse) oxygen down its roots for greater distances than Picea sitchensis, and that seedling roots of the former species will transport oxygen over 0.3m if allowed to grow into a water table.

It seems certain that internal oxygen diffusion is responsible for the ability of P. contorta to tolerate an anaerobic root environment, as Coutts and Philipson (1978b) demonstrated that when allowed to grow into an anaerobic zone, its roots developed large continuous air spaces within the stele. They also observed a decline in root extension with depth, which is also consistent with the hypothesis of oxygen diffusing down the root, with respiration and radial loss depleting it over greater distances.

We have already seen in Section 1.3 how possibly physiologically active compounds may be produced in the soil in waterlogged conditions, but it should also be noted that certain plants may also produce these compounds endogenously. Ethylene is not only a product of soil microorganisms but is also produced by tomato plants upon waterlogging (Jackson and Campbell, 1975b) and many other plant tissues (Russell, 1977). Hydrogen cyanide, which destroys the respiratory cytochrome system, may also be produced (Greenwood, 1975). A more common response is the production of ethanol by glycolysis during anaerobic respiration. An adaptation to this, seen in many flood-tolerant species, is an alternative biochemical pathway producing non-toxic lactic, malic and shikimic acids instead (McManmon and Crawford, 1971). The ability to limit ethanol production is also seen in P. contorta, which produces less than P. sitchensis at the base of the trunk after flooding (Crawford and Baines, 1977). Germinating seeds also show this response to anaerobic conditions (Crawford, 1977).

Sanderson and Armstrong (1978) compared the effects of various soil phytotoxins on P. contorta and P. sitchensis, with those due to anoxia, and also measured their typical concentrations in the field. They came to the conclusion that most toxins (with the possible exception of Fe(II) compounds) rarely reached lethal concentrations in the soil they studied, and that the chief cause of root death in P. sitchensis was

anoxia itself.

1.5 WINDTHROW AND THE AERATION STATUS OF SOILS

In the previous section it was indicated how low oxygen concentrations could limit root elongation and penetration. Field observations of rooting depth and soil oxygen status tend to show a good correlation between the two. Wiersum (1960) found that as the oxygen diffusion rate decreased with depth down a "polder" soil, then so did the root density of Phragmites communis. Where the reed had been fertilized, and as a consequence of better growth had lowered the water table further, then rooting occurred to a greater depth.

The depth of rooting takes on a special significance in plantation forests, because these may be susceptible to windthrow, i.e. the uprooting and toppling of trees in high winds. The occurrence of windthrow depends on many factors in addition to the speed of the wind. The degree of thinning, the crown form and whether the canopy is also laden with snow are examples of such factors, but a major component is the strength of root anchorage in the soil (Day, 1949).

The strength of the anchorage depends upon the shape of the root system and its depth (Day, 1949, 1963). A restriction on the root system may be imposed by disease (Day, 1953), but more commonly by site characteristics. The development of shallow root systems in Picea sitchensis due to soil limitations is discussed by Day (1963) and more extensively by Fraser and Gardiner (1967).

The depth and spread of the root system partially determines the turning moment required to overturn a tree (Fraser and Gardiner, 1967). From this Fraser (1965), was able to devise predictions for the heights of tree which would be blown over by winds of different speed on various soil types (Fig. 1.11). A survey in Newcastleton forest in southern Scotland (Pyatt, 1966), over five soil types (defined by

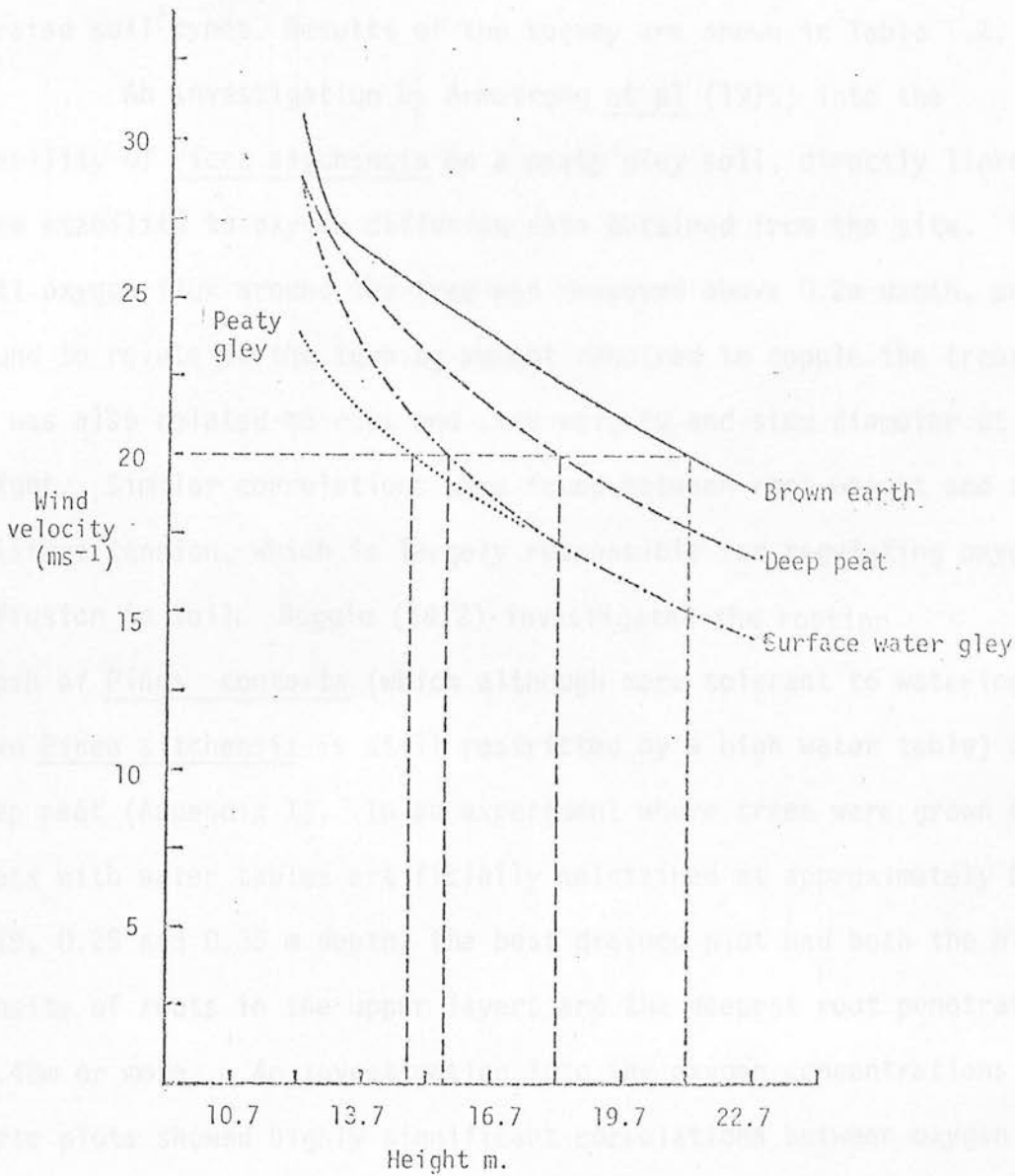


Fig. 1.11 Curves showing the relationship between critical velocity and tree size, for trees on different soil types. From Fraser, 1965.

Pyatt, 1970 and in Appendix 1), indicated that the incidence of windthrow was related to the size and shape of the root systems, and occurred predominantly on the poorly drained, and hence badly aerated soil types. Results of the survey are shown in Table 1.2.

An investigation by Armstrong et al (1976) into the stability of Picea sitchensis on a peaty gley soil, directly linked tree stability to oxygen diffusion data obtained from the site. The soil oxygen flux around the tree was measured above 0.2m depth, and found to relate to the turning moment required to topple the trees. It was also related to root and stem weights and stem diameter at breast height. Similar correlations were found between root weight and soil moisture tension, which is largely responsible for regulating oxygen diffusion in soil. Boggie (1972) investigated the rooting depth of Pinus contorta (which although more tolerant to waterlogging than Picea sitchensis is still restricted by a high water table) on a deep peat (Appendix 1). In an experiment where trees were grown on five plots with water tables artificially maintained at approximately 0, 0.11, 0.19, 0.25 and 0.35 m depth, the best drained plot had both the highest density of roots in the upper layers and the deepest root penetration (0.40m or more). An investigation into the oxygen concentrations of these plots showed highly significant correlations between oxygen concentrations and root weights per unit volume of peat (Boggie, 1977). It also showed that the fluctuations of oxygen concentrations within the profile were seasonal. The highest concentrations and greatest depths of good aeration occurred between July and September for the plots with a high water table, and in winter (November and December) for the deepest drained plot, though this was generally well aerated throughout the year.

The seasonal fluctuations of soil oxygen and carbon dioxide concentrations have been recognised since 1915, when Russell and Appleyard

Table 1.2 The extent of windthrow in Newcastleton forest, related to soil types and rooting characteristics. From Pyatt, 1966.

Soil types	Area of soil type (ha)	Mean rooting depth (m)	Mean rooting spread (m)	Percentage of area with complete windthrow
Brown earths	152.6	1.12	2.06	Negligible
Iron pan soils	244.1	0.66	2.21	Negligible
Surface-water gleys	512.6	0.51	2.59	5.8
Peaty gleys	1502.8	0.43	2.97	2.1
Deep peat	598.8	0.51	3.20	Negligible

carried out the first detailed investigation of the soil atmosphere. Their investigation showed maximum oxygen concentrations during the summer months, though all their oxygen values were in the range $0.19 - 0.2 \text{ m}^3 \text{ m}^{-3}$, as only surface soil air was sampled. The carbon dioxide concentrations also showed a seasonal trend, with a distinct maximum in April or May.

This seasonal trend has been observed more recently under forest plantations. Hu and Linnartz (1972) observed lower oxygen values during winter and early spring and high values during the summer. This was observed in both well and poorly drained sites in a Louisiana loamy soil, afforested with Pinus taeda, and became more noticeable at greater depths, as the surface layers were practically at atmospheric oxygen concentrations throughout the year. They also demonstrated that a reduction in oxygen concentrations occurred when it rained, and that the concentrations generally decreased with depth, ranging from $0.2 \text{ m}^3 \text{ m}^{-3}$ at the surface to about $0.05 \text{ m}^3 \text{ m}^{-3}$ at 1.2m. The extent of this range varied with time of year and water table depth, but the trend was consistent over all sites.

Flühler (1973) found that oxygen concentrations in the top 1m of soil under Abies alba (on Riss Moraine in Switzerland), rarely fell below $0.15 \text{ m}^3 \text{ m}^{-3}$, except during the winter months (November-April). During this period the top 0.5m remained at about $0.18 - 0.21 \text{ m}^3 \text{ m}^{-3}$, but below this there was a rapid decrease to about $0.06 \text{ m}^3 \text{ m}^{-3}$, or less down to 1m. This decrease in oxygen concentration with depth was also noticed by Smith (1976, 1977) when investigating soil aeration under Picea sitchensis. Samples were taken from four soil types (brown earth, iron-pan soil, surface-water gley and peaty gley) in Newcastleton forest in southern Scotland (which was also the site of other work already mentioned). The brown earth remained well aerated at all depths sampled (0.20, 0.35 and 0.50m) throughout the year, but the poorly drained gleys

experienced periods of poor aeration when the oxygen concentration was lower than $0.05 \text{ m}^3 \text{ m}^{-3}$. These periods lasted longer at greater depths. At 0.2m the period of worst aeration ran from May to August, with oxygen concentrations being higher ($0.1\text{-}0.2 \text{ m}^3 \text{ m}^{-3}$) from August to October. At first this seems a contradiction to the contention that the oxygen concentration rises with an increasing moisture deficit, but May-August is also a period of relatively high soil temperatures, and it seems that the consequent effect on soil respiration is greater than that of increasing moisture deficit on oxygen diffusion rate through the soil.

This idea is supported by evidence of Cooper (1975) from a tropical soil in western Kenya. He noticed that the peak oxygen deficit at depths of 0.15, 0.45 and 0.90m occurred from May to July under grass, but was absent from a bare fallow plot. However, the maximum deficit (oxygen concentrations of about $0.15 \text{ m}^3 \text{ m}^{-3}$), and others observed under maize, occurred after periods of heavy rain, and were probably due to a combination of high respiration rates coinciding with a temporary restriction of soil gas diffusion.

As the duration and timing of rainfall have a noticeable short-term effect on field oxygen concentrations, one would expect soils with a low hydraulic conductivity to suffer frequent periods of oxygen deficit. This was found in an arable clay soil (Evesham series) under winter wheat (Dowdell *et al*, 1979), oxygen concentrations falling to $0.1 \text{ m}^3 \text{ m}^{-3}$ at 0.15m depth and below $0.05 \text{ m}^3 \text{ m}^{-3}$ at 0.60m in one summer, and even lower in the following, generally wetter, year. These workers examined oxygen concentrations over two cultivation regimes of ploughing and direct-drilling, and noticed a small, but significant, improvement in aeration under direct drilling (shown by the frequency of sampling points above $0.1 \text{ m}^3 \text{ m}^{-3}$). They attributed this to a better developed system of large continuous pores being maintained in the direct drilled

plots, but which may have been destroyed in the ploughed plot.

It is the low proportion of large pores (diameter $>60\ \mu\text{m}$ which release water at less than 5 kPa tension), and hence the low hydraulic conductivity, of surface-water gleys that make them so liable to waterlogging for long periods (Thomasson and Bullock, 1975). In the forest region around Newcastleton, soils with waterlogging problems cover 95% of the area (Pyatt, 1966). In a more detailed examination of these soils types (Pyatt et al, 1979), it was found that the surface-water gleys and peaty gleys had a shallow water table for 6-8 months of the year, falling to 0.7 -1.0m during the summer. The downward percolation of water is impeded by fine-textured clayey subsoil derived from a uniform glacial till overlying carboniferous sediments, with only a moderate slope. Apart from subsurface runoff, the only appreciable mode of water removal from the soil is evapotranspiration during the summer months. Table 1.3 shows the deficit period compared with the predicted evapotranspiration figures (both potential and actual) and annual rainfall. As the soil temperature could still be about 10°C at the end of the deficit period, even at 0.6m depth (Pyatt et al, 1979), the problems for roots which are still growing when faced with a rising water table, become apparent.

Table 1. 3 Rainfall and predicted evapotranspiration (mm) for
Newcastleton forest. From Pyatt et al, 1979.

Year	Rainfall in year	Deficit period (predicted)	PPED	PAED	ID	TD
1974	1332	21 Mar-4 Sept	335	312	109	203
1975	1234	14 May-7 Sept	310	279	98	181
1976	1133	22 Jun-7 Oct	239	204	71	133

PPED = predicted potential evapotranspiration during the deficit period.

PAED = predicted actual evapotranspiration during the deficit period (which equals the rainfall during the period).

ID = predicted interception loss (35 percent rainfall) during deficit period

TD = predicted transpiration (strict sense) during deficit period.

2. FIELD EXPERIMENTS

2.1 AIMS OF FIELD EXPERIMENTS

Most of the land now available to the Forestry Commission for planting is in the upland regions of Britain. Plantations in certain of these regions are particularly liable to windthrow, due to their high degree of exposure and, very often, poor soil type (see Section 1.5). One such region, which spans the border between southern Scotland and northern England, was planted predominantly with Picea abies (Norway spruce) and Picea sitchensis (Sitka spruce) mainly during the period 1940-1960. Large areas are now suffering windthrow, causing the economic rotation in this area to be typically 30-35 years, instead of the preferred 50-55 years .

The soils in this area are derived from a glacial till or boulder clay overlying Carboniferous sediments, giving rise predominantly to surface-water gleys and peaty gleys (Pyatt, 1966) (Appendix I). Trees grown on these soils are shallow-rooted; this is presumed to be because of lack of aeration. Until recently little was known of the water regime under the crops on these soils, or of the relationship between the water regime and the occurrence and duration of anaerobic conditions.

The moisture regime of peaty gleys and surface-water gleys in this region has been studied under Picea sitchensis (Pyatt et al, 1979); together with a concurrent investigation of the soil aeration in the same sites (Pyatt and Smith, in press). The aeration regime and development of anaerobic conditions in these soils proved to be complex, with poorly aerated periods during midsummer when root respiration was at a maximum, though the soil was at its driest.

The effects of other species, in particular Pinus contorta, have not been studied. The ability of Pinus contorta to tolerate wetter conditions than Picea sitchensis may prove beneficial on these soils, as it may create drier soil conditions, and promote better development of soil structure.

An experiment was therefore laid out on a peaty gley soil in the Falstone forest of Northumberland, to examine the soil moisture and aeration regimes under Picea sitchensis, Pinus contorta and uncropped grassland.

Another problem soil type in upland areas is deep peat, the physical nature of which changes radically upon afforestation. Peat forms in regions of high rainfall, poor drainage and low temperatures, where the breakdown of organic matter is severely retarded by waterlogging. Plant remains (typically sedges and Sphagnum mosses) therefore accumulate in a partially humified form to give extensive deposits of organic soil (peat). For the same reason that lead to their formation, areas of open peat are waterlogged to the surface for long periods of the year, but upon afforestation the transpiring tree crop produces intensive drying in the summer months. The drying causes progressive shrinkage in the peat, which, if the peat is strongly humified, may be irreversible (Binns, 1959).

It was noticed that under Pinus contorta drying was sufficient to produce large cracks in the peat, which were slow to close upon re-wetting (Pyatt, 1976). It was considered that this cracking may give rise to a semi-permanent improvement in the aeration of the peat, producing greater mineralisation and ultimately an improved soil for forestry.

An experiment was laid out on a deep peat in the Eddleston block of Glentress forest south of Edinburgh, to study the same relationship between water regime and aeration under cropped and open

areas that were being examined at Falstone.

The experiment on the peaty gley soil will from now on be referred to as "Falstone" after its forest name, and that on the deep peat similarly termed "Eddleston".

2.2 FALSTONE: EXPERIMENTAL PLAN

The experiment was laid out over an area of Falstone forest that was originally a species trial planted in 1951-1953. This area (O.S. grid ref. NY755921 and NY752922, Sheet 80, 1:50000 series) was chosen by the staff of the Forestry Commission Northern Research Station for an investigation into the water relationships under, and drying potential of, several species. As part of this investigation, equipment for sampling the soil atmosphere was installed in selected sites, to measure the oxygen and carbon dioxide concentrations down the profile. It is data from these sites that constitute the Falstone experiment in this work, and only the layout of these sites is described here. Other factors examined in the main Forestry Commission experiment were the relationship between rainfall, interception and estimated transpiration, the increase in stem diameter over the season, and nitrogen mineralisation rates in the peat layer. The main experiment extended the examination of soil moisture regimes into blocks of Scots pine, hybrid larch, grand fir and silver birch, but these were not monitored for soil aeration changes.

The experiment was laid out in 1977 and consisted of 12 sites spread over 2 main areas that were approximately 0.5 km distant from each other. The surrounding and separating land was all afforested, except for small areas along forest rides and streams. The elevation of the site was about 210 m with only a moderate slope.

The two main areas chosen coincided with two cultivation regimes commonly employed at the time of planting. In one area (NY 755921)

the trees were planted in 1951 by a turf planting method. The ground was ploughed at 4.5m spacing and then turfs were cut from the ridge and spread at a 1.5m x 1.5m spacing. This area will be referred to as the "turfed area". In the other area (NY 752922) the ground was ploughed with a Cuthbertson single mouldboard plough at 1.5m spacing, the trees being planted at a spacing of 1.5m along the rows. This area will be referred to as the "ploughed area". Species plots in both areas were 45m square.

In each area, 2 sites were selected in each of 2 species plots. The species chosen were those of most interest for commercial forestry in wetland regions: Picea sitchensis and Pinus contorta. Two more sites were selected in plots which had been planted with hardwood species which did not survive, and hence had remained under the original grassland vegetation, which was dominated by Molinia caerulea (Purple moor-grass).

The sites were numbered from 1 to 12 and the numbers assigned to each site are given in Table 2.1. Their positions relative to each other are given in Fig. 2.1.

The measurements made at each site, and the equipment used, were as follows:

1. Depth to water table

Auger holes 50mm diameter were lined with perforated plastic tubing to a depth of 1.2m, leaving 50mm protruding above the surface, plugged with a plastic cap. Two were installed at each site.

2. Soil water potential

Sets of tensiometers ("Lark" type supplied by Soil Moisture Equipment Corp., Santa Barbara, California, U.S.A.) were installed at each site, with one at each of 5 depths: 0.15, 0.30, 0.60, 0.90 and 1.2m.

Table 2.1 Site numbers assigned to species and cultivation regimes
in the Falstone experiment

Cultivation regime	Species					
	Molinia caerulea		Picea sitchensis		Pinus contorta	
			Replicate			
	1	2	1	2	1	2
Ploughed	1	2	3	4	5	6
Turf planted	7	8	9	10	11	12

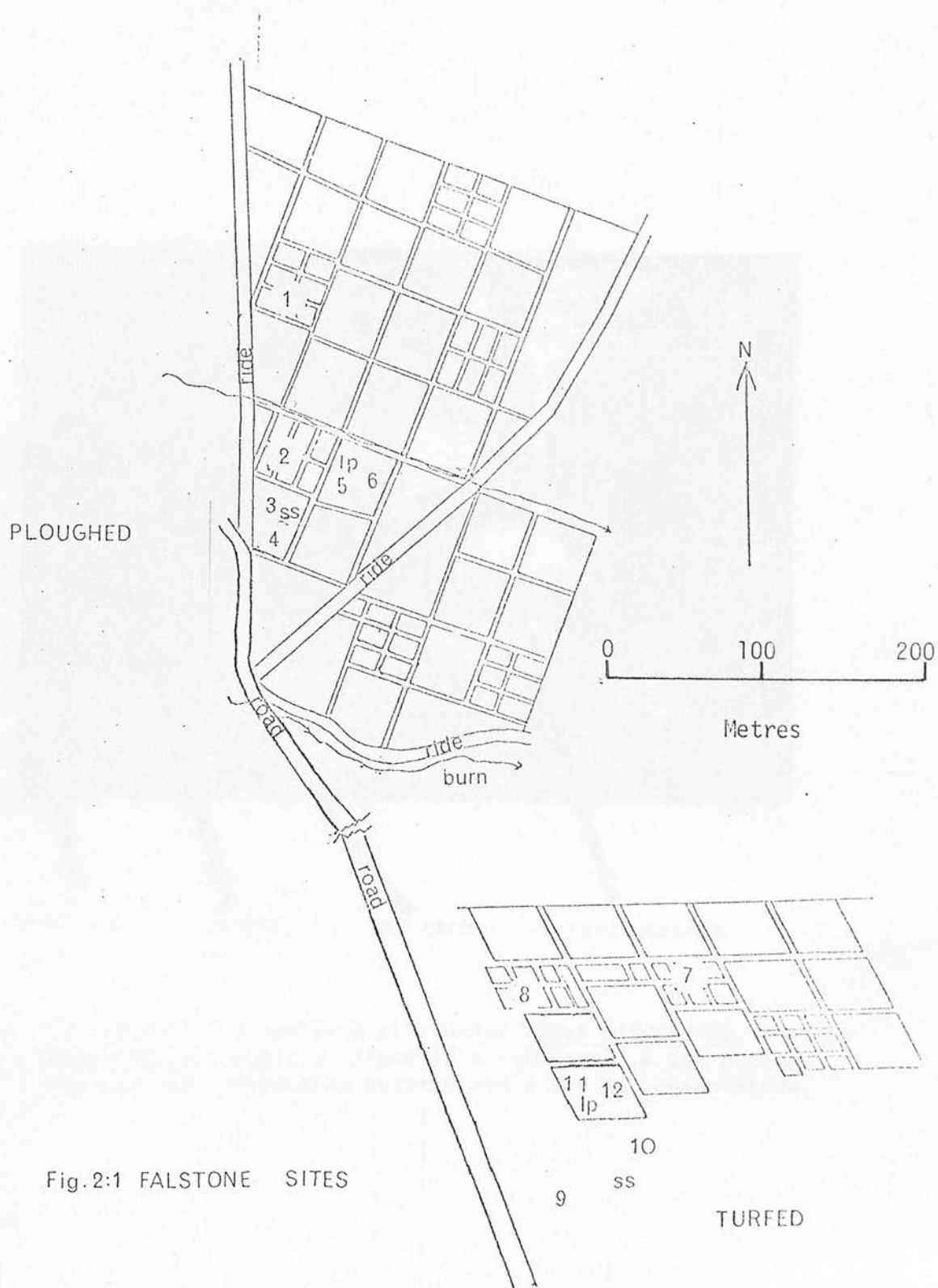
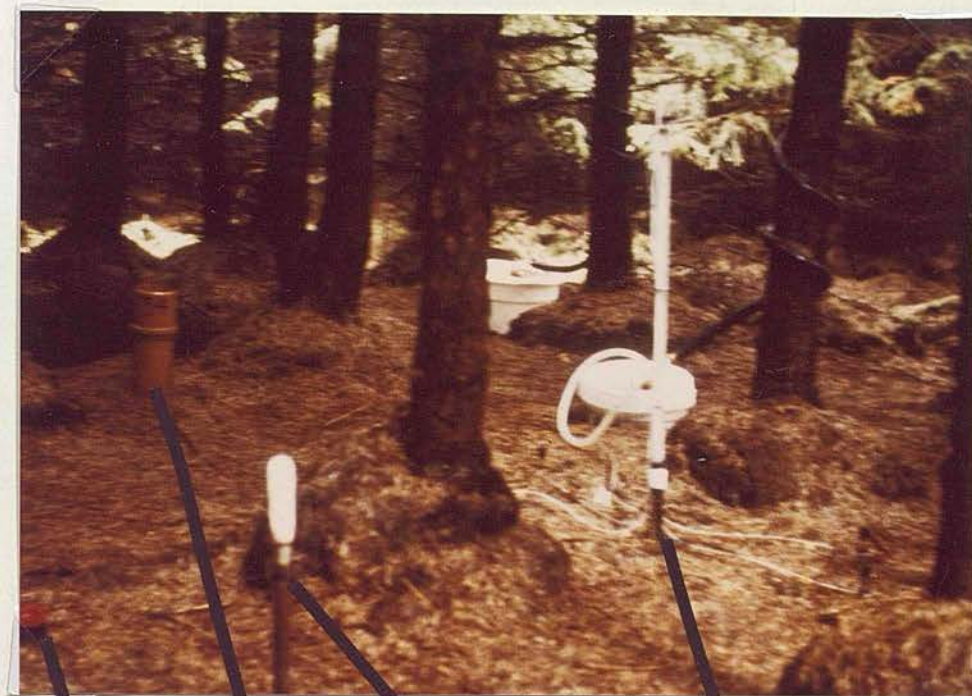


Fig.2:1 FALSTONE SITES



dipwell

raingauge

gas probe

tensiometers

Plate 2.1 The layout of a sampling site under Picea sitchensis, showing from left to right; a dipwell, a raingauge, a gas probe, two stemflow collecting buckets and a set of tensiometers.

3. Rainfall, throughfall and stemflow

Four plastic raingauges were installed in sites 1, 2, 7 and 8 to obtain rainfall data from the open non-forested areas. Also, 6 gauges were distributed randomly in each of sites 3, 4, 5, 6, 9, 10, 11 and 12, totalling 24 gauges under each species to give throughfall data. Stemflow was collected from the trunk, by cut rubber tubing wrapped around the trunk in a spiral fashion, eventually leading into a collecting bucket. Three trees in each of sites 3, 4, 5, 6, 9, 10, 11 and 12, were selected for stemflow measurements.

4. Soil aeration

Four gas probes (described in Section 3) were installed randomly in each site, with one at each of 4 depths: 0.15, 0.30, 0.60 and 0.90m. Thus a total of 48 probes were installed over the whole experiment.

5. Soil temperature

Thermistors were installed at depths of 0.05, 0.10, 0.20, 0.40 and 0.60 m in sites 2, 4, 6, 7, 10 and 12.

A typical site layout (site 11) is shown in Plate 2.1.

All measurements were made at weekly intervals by Forestry Commission research staff based at Kielder Forest. Readings of the instruments were always made at about the same time of day. All ^{variables} parameters except soil aeration were measured continuously during 1978 and 1979. Soil aeration was measured during periods approximating to the growing seasons of 1978 and 1979; in 1978 this was for 27 weeks from 26.4.78 to 25.10.78, and in 1979 for 23 weeks from 25.4.79 to 26.9.79. During these periods soil gas samples were collected in the field by the Forestry Commission staff, and then dispatched to the Edinburgh School of Agriculture, for analysis by the author.

During 1978, readings were taken from all sites, but due to partial windthrow in sites 11 and 12 during the winter of 1978 (Plate 2.2)



Plate 2.2 Windthrow damage in a Pinus contorta site, showing the uprooted root system.

and a discovered marked difference in site drainage characteristics in this turfed area, sites 7, 8, 9, 10, 11 and 12 were discontinued for 1979.

In addition to these weekly measurements, other physical properties were measured on bulk soil samples and in situ. Bulk density measurements were made in situ in each soil horizon, by gamma-ray densitometry (see Section 4). Bulk soil samples were taken from sites 8, 9 and 12 in September 1978, and from sites 2, 4 and 5 in April 1979; these bulk samples were subsequently dried and analysed for stone content, stone and fine earth densities, and particle size distribution.

Undisturbed soil cores were also taken from depths of 0.15, 0.30 and 0.60 m at sites 2, 4 and 5 in December 1979, to obtain water release data.

2.3 EDDLESTON: EXPERIMENTAL PLAN

The experiment was laid out in plots of trees on 7.5 ha of peatland that serves as a demonstration area for peatland afforestation techniques, species and provenance trials, and other allied experimental demonstrations. None of these demonstration plots are replicated and so only one plot of each species was available for use.

The area (O.S. grid ref. NT 234541, sheet 66 1:50 000 series) was a raised peat bog, with oligotrophic pseudofibrous peat 3-7m deep, overlying boulder clay at an elevation of about 285 m. The plots were approximately 20m square with a 1m deep drain surrounding each. All were ploughed to 0.60 m depth with a single mouldboard plough, at spacings of 1.8m. In the cropped plots, trees were planted in the plough ridges at 1.8m spacings during 1967.

Four sites were chosen for study; one in the virgin peat

(termed OV), one in an area that had been ploughed but left unplanted (termed OP), and one each in plots of Pinus contorta (termed LP, for lodgepole pine) and Picea sitchensis (termed SS, for Sitka spruce). The positions of the sites relative to each other are shown in Fig.2.2.

The LP, SS and OP sites differed from the OV site only in that they had been ploughed, and had received an initial addition of fertilizer ($150\text{kg ha}^{-1}\text{N}$, $100\text{kg ha}^{-1}\text{K}$ and $100\text{kg ha}^{-1}\text{P}$) at the time of planting.

A preliminary investigation into the depth to the water table in these sites had shown that the maximum depths could be up to 1m, in sites LP and SS, but only about 0.5m in site OP, and 0.3m in site OV. For this reason it was considered less profitable to make measurements at the same depths in each site, than to vary the intervals from site to site according to the expected maximum depth to the water table (using the equipment available).

The measurements made and experimental methods were similar to those made at Falstone and were as follows:-

1. Depth to water table

Plastic borehole tubing was installed to a depth of 1.2m in the same manner as at Falstone. Two were installed in sites OP, SS and LP, and three in site OV.

2. Soil water potential

Sets of tensiometers (the same as used at Falstone) were installed according to Table 2.2.

3. Soil aeration

Gas probes were installed in all sites in the pattern shown in Table 2.2.

4. Soil temperature

Thermistors were installed at the depths shown in Table 2.2.

5. Rainfall

Four plastic gauges were installed, 3 in the OV site and 1 in the OP site. Throughfall was not measured, as the small area and patchy

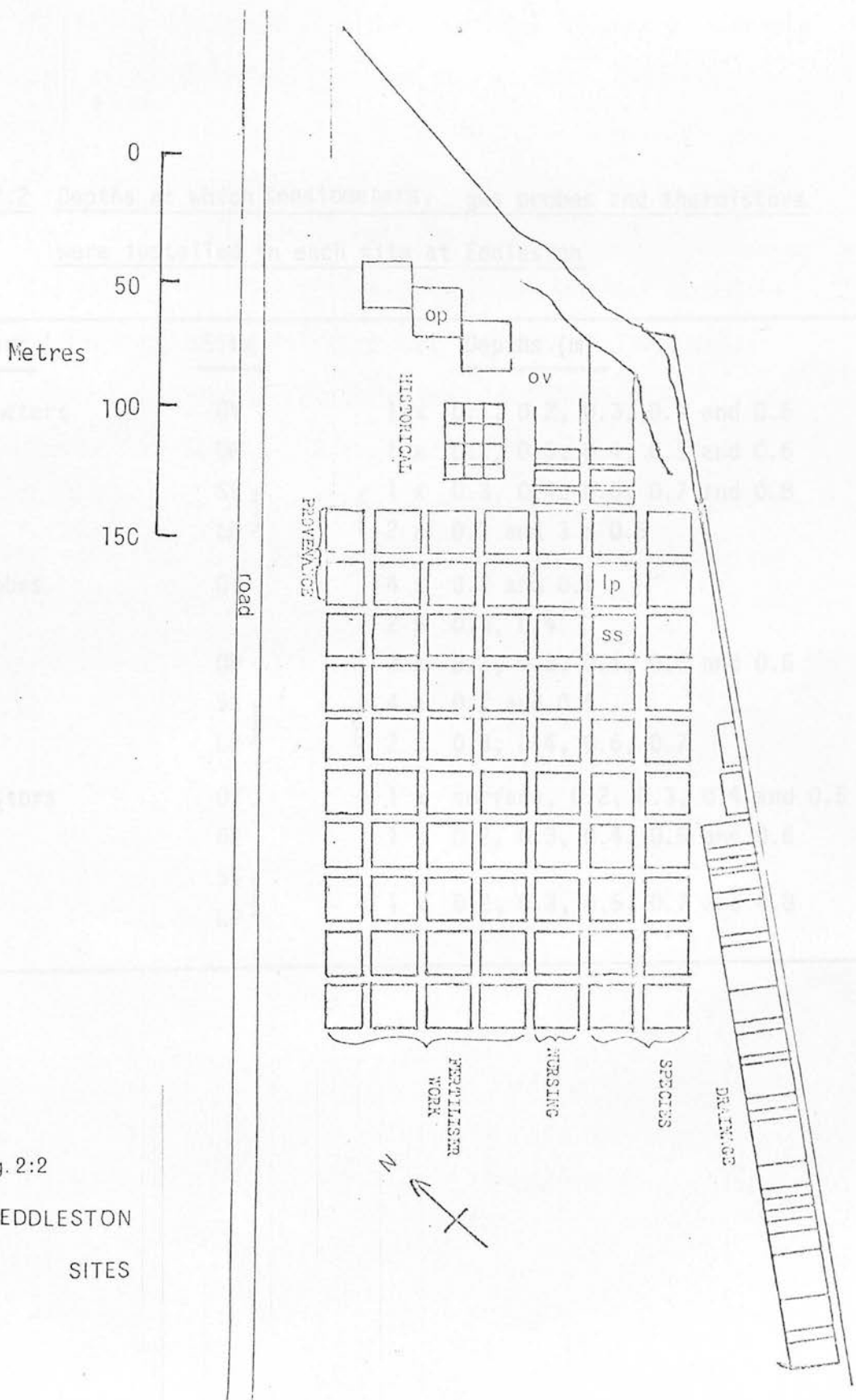


Fig. 2:2

EDDLESTON
SITES



Table 2.2 Depths at which tensiometers, gas probes and thermistors were installed in each site at Eddleston

<u>Equipment</u>	<u>Site</u>	<u>Depths (m)</u>
Tensiometers	OV	1 x 0.1, 0.2, 0.3, 0.4 and 0.5
	OP	1 x 0.2, 0.3, 0.4, 0.5 and 0.6
	SS } {	1 x 0.3, 0.4, 0.6, 0.7 and 0.8
	LP } {	2 x 0.2 and 3 x 0.5
Gas probes	OV	4 x 0.2 and 0.5
		2 x 0.3, 0.4
	OP	2 x 0.2, 0.3, 0.4, 0.5 and 0.6
	SS } {	4 x 0.2 and 0.5
	LP } {	2 x 0.3, 0.4, 0.6, 0.7
Thermistors	OV	1 x surface, 0.2, 0.3, 0.4 and 0.5
	OP	1 x 0.2, 0.3, 0.4, 0.5 and 0.6
	SS } {	
	LP } {	1 x 0.2, 0.3, 0.5, 0.7 and 0.8

nature of the crop canopy would make it unreliable.

All measurements and samplings were made at weekly intervals by the author at approximately the same time of day. Soil aeration measurements were made between 3.5.79 and 20.9.79, at weekly intervals but then fortnightly until 15.11.79. The other measurements were continued on a weekly basis until 20.12.79.

Undisturbed cores were taken from all four sites at depths of 0.2, 0.4 and 0.6m during February 1980 for water release data, bulk density and respiration rate measurements. Undisturbed cores were also taken from depths of 0.15, 0.25, 0.45 and 0.75m from all four sites to determine the peat fibre content and size distribution. Other cores were taken only from the OP site at 0.45m depth for the gaseous diffusion experiment described in Section 9.

The second alternative mentioned above, the technique usually employed by the majority of workers was the polarographic method using a platinum micro-electrode. This electrode was derived from the more general polarographic system employing the dropping mercury electrode (described by Colloff and Lingard, 1962). It was found to be suitable for the measurement of dissolved oxygen in solution, and found early biological applications in determining oxygen in photosynthesising leaves (Blinks and Shaw, 1930) and respiring animal tissue (Davies and Brink, 1942). It was incorporated into soil studies by Lemon and Erickson (1952).

The general principle upon which the platinum electrode system is based is the reduction of oxygen at the surface of the electrode. A potential difference is applied between the platinum electrode and a reference electrode, and a current flows only when oxygen is reduced, according to the equation:



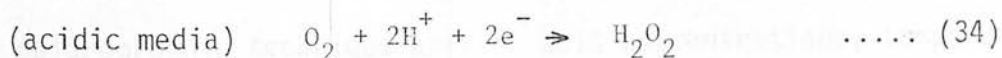
3. METHOD OF MEASURING SOIL AERATION

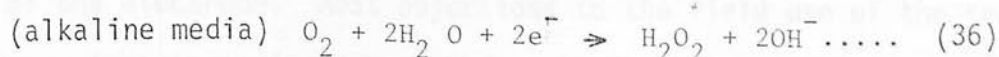
3.1 REVIEW OF AVAILABLE TECHNIQUES

Attempts to determine the extent to which the soil is oxygenated have centred ^{on} around two experimental approaches. These are: 1) methods that attempt to measure the oxygen and/or carbon dioxide concentrations in the soil, and 2) methods that attempt to measure the rate at which oxygen diffuses to a site within the soil. A third alternative also exists, which is to derive a value from another measured parameter which is dependent on the degree of aeration, eg. Redox potentials.

The most common approach taken by previous workers has been the second alternative mentioned above. The technique usually employed by the majority of workers was the polarographic method using a platinum micro-electrode. This electrode was derived from the more general polarographic system employing the dropping mercury electrode (described by Koltoff and Lingane, 1952). It was found to be suitable for the measurement of dissolved oxygen in solution, and found early biological applications in determining oxygen in photosynthesising leaves (Blinks and Skow, 1938) and respiring animal tissue (Davies and Brink, 1942). It was introduced into soil studies by Lemon and Ericksen (1952).

The general principle upon which the platinum electrode system is based is the reduction of oxygen at the surface of the electrode. A potential difference is applied between the platinum electrode and a reference electrode, and a current flows only when oxygen is reduced, according to the equations:





(from Koltoff and Lingane, 1952).

As the voltage is increased the current first increases, then reaches a plateau and remains fairly constant over a range of potentials (Armstrong, 1967; Poel, 1960 a). In this region, therefore, the current varies only according to the supply of oxygen to the platinum electrode, and can thus be used to indicate the rate of oxygen diffusing to the electrode. The position of this plateau is different for different media and is shifted by such characteristics as pH and even oxygen availability itself (Armstrong, 1967).

So far, the platinum electrode method has been considered as being used in a two-phase, solid - water system, where it is reasonably reliable and works well, if the chemical characteristics of the solution are known. However, if it is used to characterise a natural soil in the field (as it has been by Poel, 1960b; and Armstrong et al, 1976) then it is operating in a three-phase solid-water-air medium. The problems that this creates were illustrated by Birkle et al (1964), who demonstrated that the potential voltage applied becomes critical when comparing oxygen diffusion rates from different investigations. The chief problem, for in situ soil use, is that to work efficiently the electrode must be wetted completely, and the variations caused by varying moisture contents of the media were also discussed by the same authors.

Other factors affecting the readings obtained using this polarographic technique are: - salt concentrations, temperature, pH,

oxygen concentrations, the time to equilibration, poisoning and size of the electrode. Most objections to the field use of the technique were lucidly reviewed by McIntyre (1970).

Previous experience in the use of these electrode systems, by the staff at the Northern Research Station of the Forestry Commission (Pyatt, unpublished), confirmed the suspicions of their somewhat inconsistent characteristics and their limited life and practicability in field use. This problem, plus the fact that they can only measure the oxygen diffusion rate in a totally waterlogged soil, make them unsuitable for regular sampling at the same site throughout the growing season.

A novel attempt to avoid some of these problems was employed by Boggie (1977), who buried tubes incorporating a gas permeable membrane containing deaerated water in a peat soil, until they were in equilibrium with the soil oxygen concentrations (in both water and air). These were periodically removed to measure the oxygen diffusion rate in the water, in the usual manner. This procedure is impracticable in a peaty gley soil especially at depths of 0.6 or 0.9m, because it requires too much disturbance of the soil profile, and also has the major limitation that only oxygen can be measured. For a balanced appreciation of soil aeration, some account must be taken of the levels of carbon dioxide in the soil, and this is not possible with a platinum micro-electrode.

The third alternative approach mentioned, invariably involves the Redox system of the soil, either by an electrochemical system, or by measuring the concentrations of the reduction products of the series of ionic redox reactions that occur. The latter method would not be quantitative for oxygen concentrations as it could only be used over that part of the range below the point at which oxygen is theoretically totally reduced. The electrochemical system would suffer the same disadvantage

as the platinum micro-electrode and, oxygen being the first component reduced, only part of the range could be used (about 0.8 - 0.3 V corrected to a solution of pH 7, Ponnampetuma, 1972).

For these reasons the measurement of soil oxygen in this project employed the first method mentioned, i.e. that of measuring the oxygen concentration of a removed sample, whether soil air or water.

There are two major difficulties associated with the measurement of soil oxygen concentrations by sampling the content of the pore space, namely: (1) the reliable removal of a soil air (or water) sample from a point within the profile, and (2) its subsequent analysis to give an accurate measurement of its constituents. The means by which various workers have attempted to overcome these problems has been extensively reviewed by Smith (1977) (who also devised the final system chosen here).

Samples can be removed from the soil either instantaneously, by pushing in a sampling device such as that used by Tackett (1968), or from a permanently buried chamber in the soil (Burford and Millington, 1968; Tackett, 1968; Dowdell et al, 1972). Of the sampling wells described in the literature, that of Dowdell et al (1972), seemed the best design and had given satisfactory performance in previous work in similar upland soils (Smith, 1977) as well as the lowland arable soils for which it was designed (Dowdell et al, 1972).

The subsequent analysis of samples obtained from these devices may be satisfactorily carried out by gas chromatography.

3.2 SAMPLING AND ANALYSIS OF THE SOIL PORE SPACE

3.2.1 SAMPLING

The device (referred to as a "gas probe") used is shown in Fig. 3.1. The sample cup is made of sintered bronze with pores of 5 μ m, through which air and water but not soil particles can enter freely. The

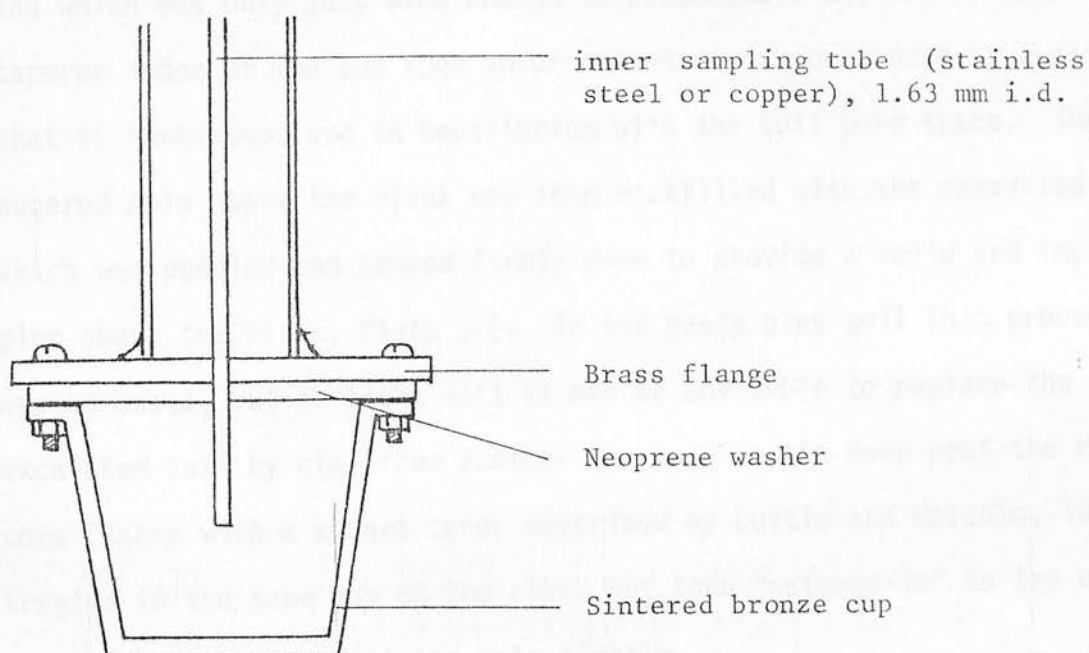
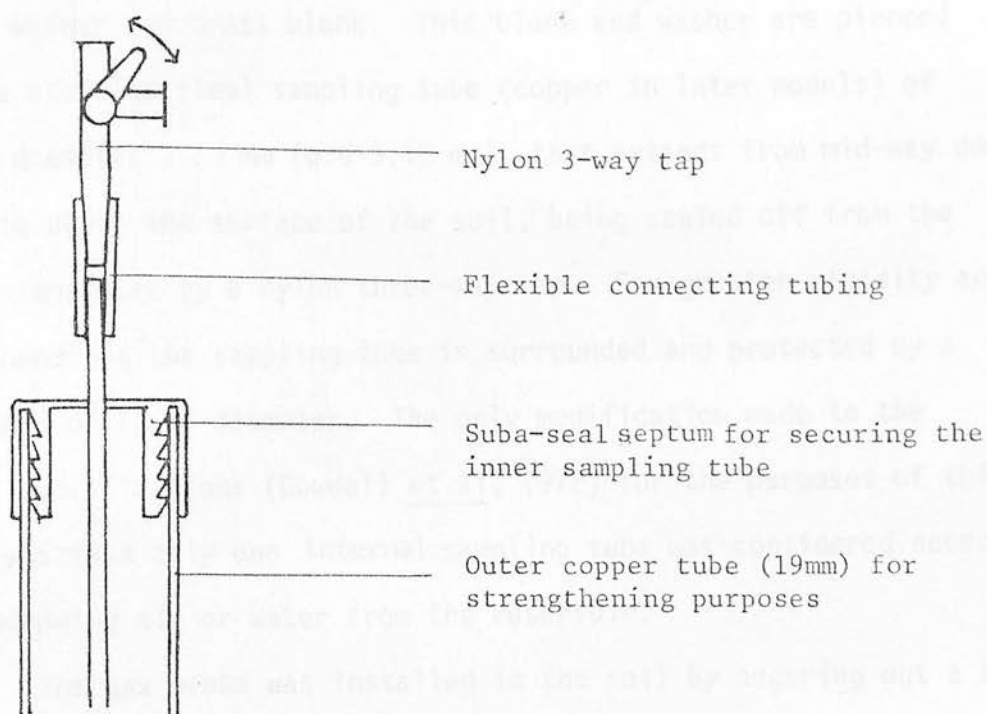
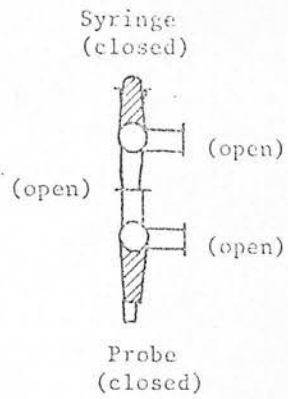


Fig.3.1 The "gas probe" used for sampling the soil pore space.
See text for description.

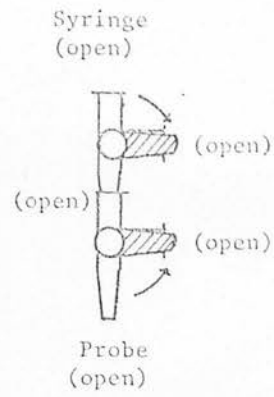
cup forms an enclosed reservoir in the soil when sealed off with a neoprene washer and brass blank. This blank and washer are pierced only by a stainless steel sampling tube (copper in later models) of internal diameter 1.63 mm (o.d 3.18 mm), that extends from mid-way down the cup to above the surface of the soil, being sealed off from the ambient atmosphere by a nylon three-way tap. For greater rigidity and ease of handling the sampling tube is surrounded and protected by a copper tube of 19 mm diameter. The only modification made to the original specifications (Dowdell et al, 1972) for the purposes of this project was that only one internal sampling tube was considered necessary for withdrawing air or water from the reservoir.

The gas probe was installed in the soil by augering out a hole a few centimetres greater in depth than the required depth of sampling, and which was only just wide enough to accommodate the brass blank. The tapered shape of the cup then ensures that it is surrounded by a cavity that is continuous and in equilibrium with the soil pore space. The augered hole above the blank was then backfilled with the excavated soil, which was puddled and tamped firmly down to provide a solid and impermeable plug above the blank, Plate 3.1. In the peaty gley soil this procedure was adequate, but in light soil it may be advisable to replace the excavated soil by clay from another source. In the deep peat the removed core (taken with a square corer described by Cuttle and Malcolm, 1979) was treated in the same way as the clay, but then "watered-in" to try and promote swelling to fill the hole tightly.

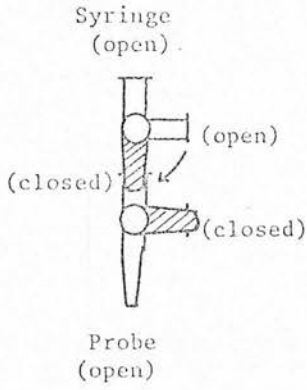
The procedure ensured that the sample obtained was in equilibrium with the soil pores at the required depth and that there was no preferential diffusion between the cup and the air above the soil through the interface between probe and auger hole.



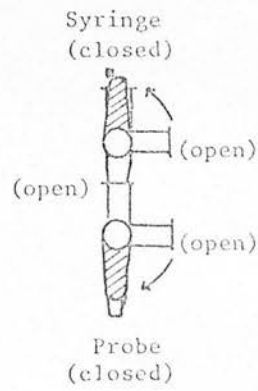
a



b



c



d

Fig.3.2 Sequence of tap positions on joined syringe and Gas probe taps when removing a sample. For details of operation, see text.



Plate 3.1 A gas sampling probe at 0.3m depth in an open site, showing the chamber surrounding the brass reservoir and the clay backfill above the flange. Note also, the bright copper surface due to being maintained in reducing conditions.

Samples were removed from the probe with a glass syringe fitted with a three-way nylon tap identical to that on the probe. By connecting the taps together, a sample may be withdrawn, sealed in the syringe and then stored until analysis. Other workers have stored samples in sealed ampoules (De Carmargo et al, 1974) or vials stoppered with Suba-seal septa (Sanderson, 1977). But the more re-connection and re-sampling steps there are between initial sampling and analysis, the more the chances increase of contamination, dilution and loss to the ambient atmosphere. The simple storage of samples in the glass syringes lubricated with silicone stopcock grease seems to be adequate for 2 or 3 days storage, and may even last longer (Appendix 2).

The procedure adopted for removing a sample from the probe was designed to prevent contamination of the sample by ambient air trapped in the Luer taps when they were joined together. It was as follows:-

- 1) Connect the taps, which are initially closed (Fig. 3.2a), then open both taps (Fig. 3.2b). This closes off the side ports.
- 2) Withdraw 5 ml gas/water into the syringe. Close the tap on the syringe to the gas probe (Fig. 3.2c).
- 3) Expel the sample through the side opening of the syringe tap. This vents the air contained in the sampling tube "dead space" and between the taps.
- 4) Open the tap on the syringe and withdraw a further 5 ml of gas/water into the syringe. Close both taps simultaneously (Fig. 3.2d). This is the sample to be analysed.

When sampling in the peaty gley soil this procedure was repeated for a second sample. The two samples taken were not necessarily both water or gas, and were very often a mixture of the two. This can be understood if one considers that the bronze cup has an internal volume of about 0.05 dm^3 , and it is conceivable that in the relatively

impermeable clay soil water movement between the probe and the surrounding soil may be relatively slow. If this is the case then it is possible to have either (a) water retained in the cup after the surrounding water table has fallen, giving an initial water sample and then a gas sample after the water level in the cup has fallen below the sampling tube due to removal of 2 x 5 ml in the first sampling; or (b) soil air trapped in the cup after a rapid rise in the surrounding water table (after a heavy rainfall), giving an initial gas sample and then, as water is drawn in by the partial vacuum formed, a second sample comprised partly or wholly of water. When this occurred both gas and water samples were analysed.

In the deep peat only one sample was taken, as previous studies had shown that successive gas samples from the same probe varied little in composition (Appendix 2).

The period of storage of gas samples before analysis was usually two days for samples from Falstone (one day in transit), and one day from Eddleston. Water samples were stored at 4°C (to limit microbial respiration) and usually analysed within a week. Occasionally they were stored for up to three weeks, when pressure of equipment use or, breakdown, or absence, prevented their analysis earlier.

Both gas and water samples were analysed by gas chromatography, using a Pye 104 gas chromatograph.

3.2.2 ANALYSIS OF GAS SAMPLES

The technique used was gas-solid chromatography, where the gaseous mobile phase (the "carrier gas") is passed directly over a stationary phase of some active solid. To maintain a constant flow of gas over the solid phase, a suitable inert carrier gas is needed. The solid phase is contained in columns of either glass or stainless steel, fitted into a constant temperature oven. The length and diameter of

these columns, the flow rate of the carrier gas, and the nature of the active solid can all be varied according to the particular separation of gases required. Even so, several alternative techniques are to be found in the literature, using different packing materials and multi-column combinations. This subject has been reviewed by Smith (1977) and only the system actually used in this project, which is essentially the same as that used by Goodlass (1978), is detailed here.

Samples of 2cm^3 volume were injected into a stream of helium carrier gas at a flow rate of approximately $1 \times 10^{-6} \text{m}^3 \text{s}^{-1}$, through an injection port mounted on a moisture trap (magnesium perchlorate ($\text{Mg}(\text{ClO}_4)_2$) in a 6mm diameter tube). This carrier stream was then split by a brass "T" piece and two pieces of stainless steel capillary tubing (o.d. 1.5mm) of lengths 270 mm and 195 mm. This (and column resistance) effectively gave a 32:1 ratio split of a sample between the carrier streams. These streams then passed through the chromatographic columns contained within the oven at 110°C (Fig.3.3).

The larger fraction of the gas sample was passed over a solid phase compound of 50-80 mesh "Porapak Q" (porous polymer beads), contained within a stainless steel column, $2\text{m} \times 6\text{mm}$, activated at 200°C . This separated carbon dioxide (also nitrous oxide) from a composite mixture of oxygen, nitrogen, argon and other minor possible components (Bell, 1968).

The smaller fraction was passed through a parallel column in the same oven (stainless steel $2\text{m} \times 3\text{mm}$), containing 60-80 mesh molecular seive 5A activated at 300°C . This separated oxygen and argon from nitrogen (Smith and Clark, 1960).

The separated gas streams were then recombined before passing through the hot-wire katharometer (thermal conductivity) detector (maintained in an oven at 160°C with a bridge current of 165mA), so that the component gases eluted in the sequence: oxygen plus nitrogen plus argon, carbon dioxide, oxygen plus argon, and finally nitrogen. The

(He FLOW RATE:- carrier gas 60 ml.min.⁻¹)

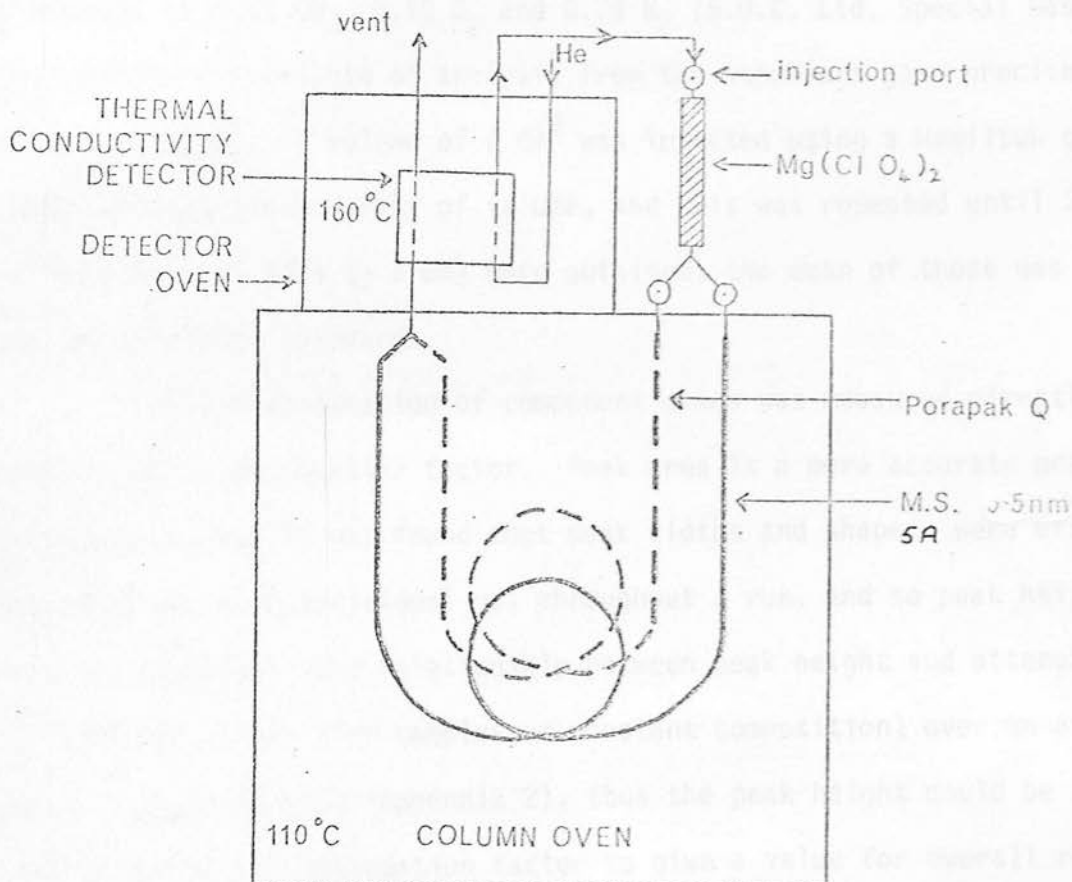


Fig.3.3- GAS CHROMATOGRAPHY SYSTEM FOR THE ANALYSIS OF GAS SAMPLES.

Source: Goodlass, 1978

chromatogram was recorded with a 1mV chart recorder. The use of helium as the carrier gas resulted in much greater sensitivity than would be achieved with nitrogen, because the response of the detector depends on differences in thermal conductivity between sample gases and the carrier gas.

To determine the concentration of a sample, the response of the detector was calibrated with a standard gas mixture containing volume fractions of 0.01 CO₂, 0.20 O₂ and 0.79 N₂ (B.O.C. Ltd. Special Gases Division)(a certificate of analysis from the suppliers gave precise concentrations). A volume of 2 cm³ was injected using a Hamilton gas-tight syringe for accuracy of volume, and this was repeated until 3 peaks of very similar size (± 3 mm) were obtained; the mean of these was used as the reference standard.

The concentration of component gases was measured directly as peak height x attenuation factor. Peak area is a more accurate measure of response, but it was found that peak widths and shapes were effectively constant for each individual gas throughout a run, and so peak height was just as accurate. The relationship between peak height and attenuator setting was linear (for samples of constant composition) over an attenuation range from x1 to x 20 (Appendix 2), thus the peak height could be routinely multiplied by the attenuation factor to give a value for overall response, from which the corresponding volume was calculated.

The calculated volumes of all the components in the sample were then added together to obtain the exact volume of sample injected, and then each component was divided into the total to obtain its fractional concentration by volume. These calculations were performed on a programmable calculator, according to the equations:-

Let A = response to CO_2 in the standard

B = " " N_2 " " "

C = " " O_2 " " "

a = fraction of CO_2 in the standard

b = " " N_2 " " "

c = " " O_2 " " "

V = volume of standard injected

x = response to CO_2 in the sample

y = " " N_2 " " "

z = " " O_2 " " "

T = total volume of sample

Ratio of N_2 to Ar in air = 83.3:1

Ar is present in the O_2 peak and, $\frac{\text{response to Ar}}{\text{response to } \text{N}_2} = 1.233$

$$\begin{aligned} \text{Therefore response to } \text{O}_2 &= (z - \frac{1}{83.3} 1.233 y) \quad \dots (38) \\ &= (z - 0.0148 y) \end{aligned}$$

The relationship between T and V is given by:

$$T = \left(\frac{yb}{83.3B} + \frac{xa}{A} + \frac{yb}{B} + \frac{(z-0.0148 y)c}{C} \right) V \quad \dots (39)$$

and therefore

$$\text{CO}_2 \text{ fraction (v/v)} = \frac{xa/A}{xa/A + yb/B + (z-0.0148 y) c/C} \quad \dots (40)$$

$$\text{N}_2 \text{ fraction (v/v)} = \frac{yb/B}{xa/A + yb/B + (z-0.0148 y) c/C} \quad \dots (41)$$

$$\text{O}_2 \text{ fraction (v/v)} = \frac{(z-0.0148y) c/C}{xa/A + yb/B + (z-0.0148 y) c/C} \quad \dots (42)$$

This assumes that the only significant component gases of the sample are O_2 , N_2 , CO_2 and Ar, other possible components (N_2O , CH_4 , C_2H_6 etc.) being present only in trace amounts, and water vapour having been removed in the magnesium perchlorate trap.

It was considered that this method of calculating component gas volumes and hence volume fractions was more accurate than the alternative, whereby the sample injected is assumed to be 2cm^3 and the peak height response compared directly to the standard concentrations. This was because the syringes used were fairly wide bodied, mass produced syringes, not calibrated to a high degree of accuracy.

3.2.3. ANALYSIS OF WATER SAMPLES

With water samples it is necessary to measure the concentration of dissolved oxygen and carbon dioxide, and then calculate the equivalent gas-phase concentrations according to Henry's Law. In this way they can be directly compared with measurements made on gas samples.

There are four possible ways of measuring the concentration of a dissolved gas, i.e. (1) stripping the dissolved gas out of solution by an inert gas such as helium, either by a stream of bubbles being passed through the solution (Swinerton, 1962), or by shaking with a volume of gas in a sealed container (Smith and Restall, 1971); (2) outgassing under reduced pressure (Ikels, 1965; Bjergbakke, 1976); (3) pumping an extractant gas continuously through the water sample in a closed circuit (Montgomery and Quarmby, 1966); (4) direct injection of the sample into the chromatograph followed by separation of dissolved gases and water vapour (Smith, et al 1976; Yamaguchi and Komatsu, 1977).

Of these methods Nos 2 and 3 involved the acquisition and setting up of extra equipment, and were considered far too complicated and time consuming for regular weekly analysis. This left Nos 1 and 4 as possible methods which were quick and only required simple apparatus in addition

to the existing chromatographic equipment.

Stripping of the dissolved gases in a fixed volume would be suitable for both oxygen and carbon dioxide if carried out using an inert gas such as nitrogen or helium. However, when measuring dissolved oxygen it is extremely difficult to prevent contamination by atmospheric oxygen. Thus a direct injection system was preferable as it was quick and avoided this problem. Such a system was that devised and operated by Smith et al (1976). In this system the water sample was vaporised, then the water vapour was separated from permanent gases in a short chromatographic column, fitted in the carrier stream before the main analytical column.

One drawback (or benefit, in some applications) of this is that only very small volumes of sample can be accommodated, about $10-20 \text{ mm}^3$, which means that a detector has to be used that is sensitive to only a fraction of a microlitre of gaseous oxygen. Smith et al (1976) used a helium ionisation detector, but it has subsequently been superseded by an electron capture detector (E.C.D.) (Hall and Burford, 1974). The latter type was used in this work.

The E.C.D. works on the principle that certain gases, such as oxygen, nitrous oxide and halogens, "capture" free electrons. In the E.C.D. a radioactive ^{63}Ni source (as anode) supplies electrons to a distant cathode, and the stream of carrier gas passes around and between the two. An electron capturing gas in this stream will have the effect of reducing the standing current between the electrodes in proportion to its concentration.

The details of the gas chromatography system used with this device are as follows and shown in Fig. 3.4.

The carrier gas was of oxygen-free nitrogen (supplied by Air Products Ltd. London) which had been purified by passing through

traps filled with an oxygen absorbing material ("Oxy-Trap" supplied by Phase Separations Ltd, Queensferry, Clwyd) and molecular sieve, respectively. Volumes of water up to 20 mm^3 were injected, via a standard injection port, into a copper tube filled with glass beads and heated to 160°C through which the carrier gas flowed. The vaporised sample plus carrier gas then passed through one of two parallel columns (100mm long packed with Porapak T) connected to an 8-way valve (Fig. 3.4) and maintained at 60°C . The Porapak T retarded the water vapour with respect to permanent gases. To remove this water vapour, after each sample had passed through, the column was backflushed by switching the 8-way valve, causing another stream of gas to flow in the reverse direction to, and at a higher flow rate ($0.75 \times 10^{-6} \text{ m}^3 \text{ s}^{-1}$) than, the normal flow ($0.5 \times 10^{-6} \text{ m}^3 \text{ s}^{-1}$). The switching of the valve also resulted in the carrier gas now passing through the second Porapak T column, which was used for the next separation. Thus the two columns were used alternately.

The gas stream passed from the Porapak T column to a stainless steel column (o.d. 6mm, length 2m) packed with Porapak Q in an oven at 110°C . From there it entered the E.C.D. maintained in its own oven at 120°C . This temperature was found to be that at which the greatest sensitivity to oxygen was obtained (Appendix 2), without falling below the column oven temperature and risking the condensation of any stray water vapour which had passed through the system.

The attenuation was kept constant for all water samples and standards, thus the oxygen concentrations were determined from a calibration curve of peak height versus volume of dissolved oxygen. A separate calibration curve was obtained for each position of the 8-way valve on each occasion analyses were made. This was done by injecting a range of volumes of distilled water through which had been bubbled gas mixtures containing known oxygen concentrations. From published solubility coefficients (Hodgman et al, 1956), the volume of dissolved

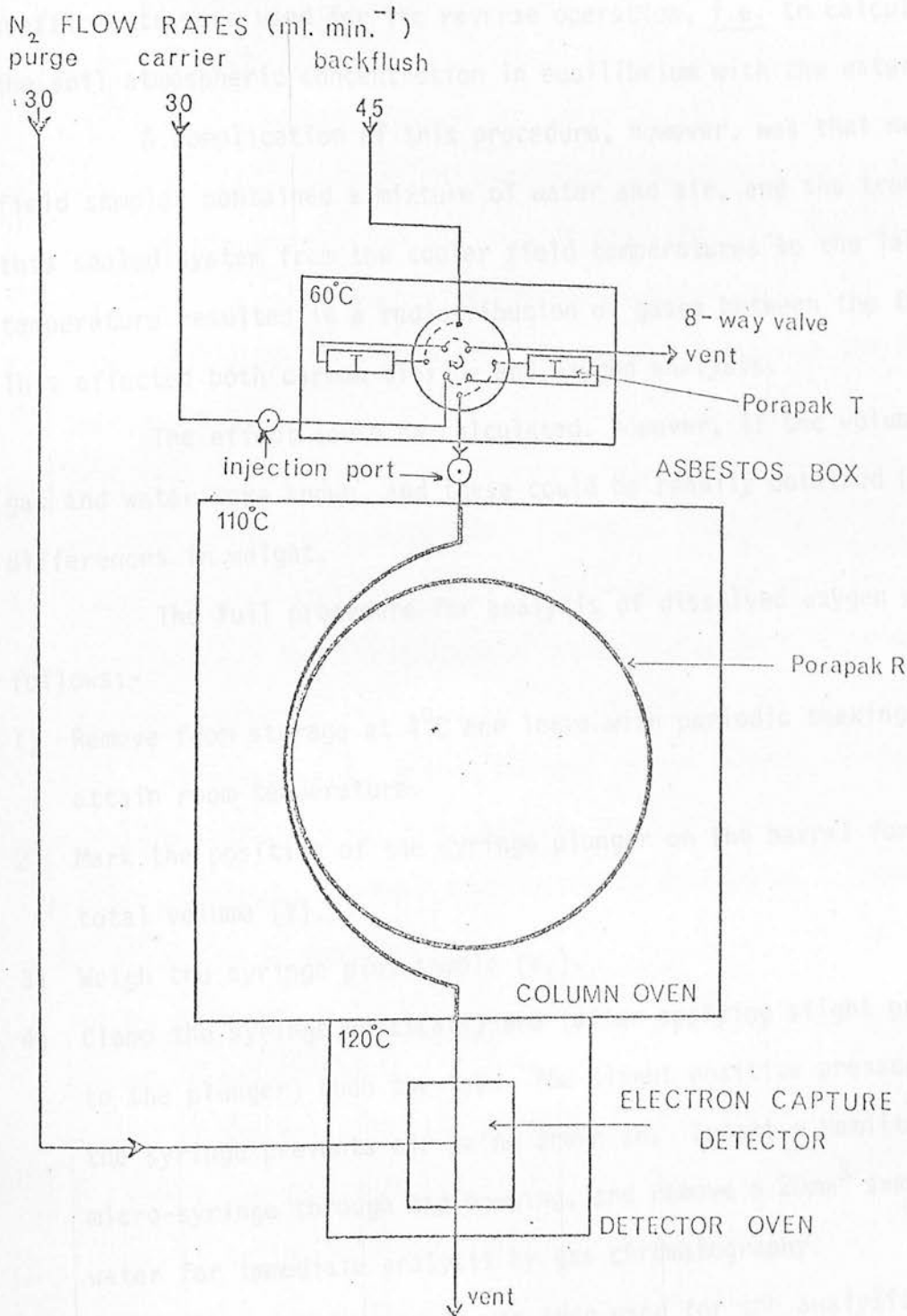


Fig.3.4 GAS CHROMATOGRAPHY SYSTEM FOR THE ANALYSIS OF WATER SAMPLES.

oxygen for unit volume of water could be calculated for any temperature.

When a sample from the field was analysed the solubility coefficients were used for the reverse operation, i.e. to calculate the soil atmospheric concentration in equilibrium with the water.

A complication of this procedure, however, was that numerous field samples contained a mixture of water and air, and the transfer of this sealed system from the cooler field temperatures to the laboratory temperature resulted in a redistribution of gases between the two phases. This affected both carbon dioxide and oxygen analysis.

The effect could be calculated, however, if the volumes of gas and water were known, and these could be readily obtained by differences in weight.

The full procedure for analysis of dissolved oxygen was as follows:-

- 1) Remove from storage at 4°C and leave with periodic shaking, to attain room temperature.
- 2) Mark the position of the syringe plunger on the barrel for the total volume (V).
- 3) Weigh the syringe plus sample (W_1).
- 4) Clamp the syringe vertically and (after applying slight pressure to the plunger) open the tap. The slight positive pressure in the syringe prevents air being drawn in. Insert a Hamilton micro-syringe through tap opening, and remove a 20mm³ sample of water for immediate analysis by gas chromatography.

The remaining sample was then used for the analysis of carbon dioxide. This could safely be accomplished by stripping the gas out of solution by air, as this only contains known small quantities of carbon dioxide that can be included in calculations, and do not constitute a contamination problem. The full procedure used was as follows:-

- 1) Inject about 1 ml of the remaining sample into an empty 5 ml

Vacutainer tube and immediately seal this with a gas tight stopper (observations had shown that outgassing at this stage was negligible).

- 2) Shake the Vacutainer for ten minutes to re-equilibrate the dissolved CO_2 between the gas and water phases.
- 3) Remove a 1 cm^3 sample of the Vacutainer gas phase using a syringe and Luer needle, through the self-sealing stopper. Analyse this for CO_2 , O_2 , and N_2 according to the procedure in Section 3.2.2.
- 4) Expel any remaining sample from the syringe and weigh the empty syringe (W_2).
- 5) Fill the syringe with water to the previously made mark for V. Weigh the full syringe (W_3).
- 6) Weigh the Vacutainer plus sub-sample (w_1), which can be used with known weights for the Vacutainer empty (w_2), and full of water (w_3), to obtain the sub-sample volume v_1 .

It was considered that changes in the density of water with temperature produced only minor errors, which could safely be ignored. Therefore, assuming the density of water to be 1 kg dm^{-3} , the following calculations could be made:

$$\text{Volume of water in sample} = W_1 - W_2 = V_s \quad \dots (43)$$

$$\text{Volume of gas in sample} = W_3 - W_1 = V_g \quad \dots (44)$$

$$\text{Volume of gas phase in Vacutainer} = w_3 - w_1 = v_g \quad \dots (45)$$

$$\text{Volume of sub-sample in Vacutainer} = w_1 - w_2 = v_s \quad \dots (46)$$

Using the volumes calculated in Equations (43) - (46), the field gas phase concentrations for oxygen and carbon dioxide could be calculated as follows overleaf.

Let T_F = field soil temperature (K)

T_R = room temperature (K)

α_F, α'_F = solubility coefficients of oxygen and carbon dioxide respectively at temperature T_F

α_R, α'_R = solubility coefficients of oxygen and carbon dioxide respectively at temperature T_R

Y, Y' = partial pressures of oxygen and carbon dioxide respectively in syringe gas phase (kPa)

X = concentration of dissolved oxygen

B = partial pressure of carbon dioxide measured in the Vacutainer gas phase (kPa)

A, A' = partial pressures of oxygen and carbon dioxide respectively in the field gas phase at temperature T_F (kPa)

Oxygen analysis

Field conditions

Laboratory conditions

(Aqueous phase) + (Gas phase) = (Aqueous phase) + (Gas phase)

$$\left[\left(\frac{A}{100} \alpha_F \frac{T_F}{273} V_s \right) + \left[\frac{A}{100} V_g \right] \right] = \left[\left(\frac{Y}{100} \alpha_R \frac{T_R}{273} V_s \right) + \left[\frac{Y}{100} V_g \right] \right] \quad \dots (47)$$

$$\text{But also } \left[\frac{Y}{100} \alpha_R \frac{T_R}{273} V_s \right] = X V_s \quad \dots (48)$$

$$\therefore X = \left[\frac{Y}{100} \alpha_R \frac{T_R}{273} \right]$$

$$\therefore Y = \frac{X \cdot 100 \cdot 273}{\alpha_R T_R} \quad \dots (49)$$

From (47)

$$A \left[\left(\alpha_F \frac{T_F}{273} v_s \right) + v_g \right] = Y \left[\left(\alpha_R \frac{T_R}{273} v_s \right) + v_g \right] \quad \dots (50)$$

$$\text{Let } \alpha_F \frac{T_F}{273} v_s = M_1$$

$$\text{and } \alpha_R \frac{T_R}{273} v_s = M_2$$

$$\therefore A = Y \frac{(M_2 + v_g)}{(M_1 + v_g)} \quad \dots (51)$$

Carbon dioxide analysis

Vacutainer conditions

(sub-sample from syringe) + (Air) = (Aqueous phase) + (Gas phase)

$$\left[\frac{Y'}{100} \alpha_R' \frac{T_R}{273} v_s \right] + \left[\frac{0.035}{100} v_g \right] = \left[\frac{B}{100} \alpha_R' \frac{T_R}{273} v_s \right] + \left[\frac{B}{100} v_g \right] \quad \dots (52)$$

where the partial pressure of carbon dioxide in normal air is assumed to be 0.035 kPa.

$$Y' \left[\alpha_R' \frac{T_R}{273} v_s \right] + (0.035 v_g) = B \left[\left(\alpha_R' \frac{T_R}{273} v_s \right) + v_g \right]$$

$$\text{Let } \alpha_R' \frac{T_R}{273} v_s = M_3$$

$$\text{and } 0.035 v_g = M_4$$

$$\therefore Y' (M_3) + M_4 = B (M_3 + v_g)$$

$$\therefore Y' = \frac{B (M_3 + v_g) - M_4}{M_3} \quad \dots (53)$$

By analogy with equation (51),

$$A' = Y' \frac{(M_2 + v_g)}{(M_1 + v_g)} \quad \dots (54)$$

4. SOIL PHYSICAL PROPERTIES - FALSTONE

4.1 METHODS

4.1.1 BULK DENSITY

During periods when the soil was at, or near, field capacity, the bulk density of each horizon was measured using a portable, hand-held gamma ray densitometer (Soane et al, 1971).

The gamma ray densitometer (Elcomatic Ltd. Kirktonfield Road, Glasgow) consists of two tubular stainless steel probes (o.d. 21.4 mm, length 0.4m) fixed parallel to each other 140 mm apart. The tubes contain a gamma ray source (^{137}Cs , 1mCi) and a detector, respectively, positioned 50mm from the free ends.

The detector is connected to a battery-operated scaler, so that the time required to receive a chosen number of pulses can be measured. When inserted in its carriage box the source is surrounded by a lead shield in which there is a small window facing the detector. This allows a beam of gamma rays to pass through a steel plate separating the two probes, to the detector. The time interval necessary to register a set number of counts (typically 10,000 or 15,000) (T_s) is recorded when the source is in its box, to obtain a reference standard. When the probe is inserted into materials of known density, the time interval (T) for the same number of counts varies with the material density according to Equation(49):

$$b_{\rho} = A \log_{10}(T/T_s) + B \quad \dots \quad (49)$$

where b_{ρ} is the wet bulk density of the material, and A and B are constants for each of the two probes used.

A calibration curve was obtained for each probe during 1980, using a range of soil materials packed into large bins, to known bulk densities. This curve was used to calculate A and B, so that values of T and Ts from field measurements could be inserted into Equation (49) and b_p obtained.

Pits 2 x 1 x 1m deep were dug in sites 2, 4, 5, 8, 9 and 11 of the Falstone experiment. Half of the pit was excavated to its full depth, and from the exposed surface of the other half, large bulk samples of each mineral soil horizon were taken from a defined area for analysis in the laboratory.

The densitometer probes were inserted into holes formed in the soil by inserting spikes through a steel jig, to ensure that the probes remained in alignment. For the Oh and Cg horizons insertion was vertical while for the other soil horizons the probe had to be inserted horizontally into the walls of the pit. The initial measurements from this procedure were of wet bulk density (b_p), so to obtain the dry bulk density (b_{p_s}) it was necessary to remove the soil from where the density measurement had been taken, and transport it back to the laboratory in sealed pots. The moisture content by weight, θ_m , was obtained gravimetrically by drying to constant weight at 105°C. The dry bulk density of the soil (b_{p_s}) could then be calculated from b_p and θ_m by Equation (50):

$$b_{p_s} = b_p \frac{1}{1 + \theta_m} \quad \dots (50)$$

Fifteen readings from each horizon in each pit were aimed for, though the stony nature of the soil sometimes prevented this, but never less than ten readings were taken.

When the densitometer is inserted in the soil the measurements made will be influenced by an approximately cylindrical region of soil (radius about 50mm) mainly between the source and detector, because of scattering of the gamma rays by soil particles. This means that horizons

thinner than about 0.1m cannot be measured with confidence. The Ag horizon was not measured for this reason, as it was usually less than 0.1m thick and adjacent to the less dense Oh horizon.

4.1.2 STONE CONTENT AND STONE DENSITY

The stone content of the soil was obtained from the bulk samples of each horizon removed from the pits described in Section 4.1.1. Each sample (≥ 30 kg) was spread out on trays in a drying cabinet at 30°C . When the soil was in a suitably friable condition, it was weighed (with stones) and then passed through revolving drum sieves of 2mm mesh. Care had to be taken to ensure that hard lumps of clay were not retained in the sieves with the stones, or conversely that soft sandstone was not unduly broken up by the pestle.

After separating the stones from the fine earth particles by this method, both were stored in plastic bags until required. The stones were weighed and expressed as the mass fraction of the whole soil (oven dry weight derived after the moisture content had been measured) (S_w).

A representative sample of the stones from each horizon was weighed (W_1) and then soaked in water overnight. The saturated stones were then weighed (W_2) in a gas-jar of known internal volume (V_j). The jar was then filled with water and weighed again (W_3). The bulk density of the stones ${}^b\rho_c$ was then calculated from V_j , W_1 , W_2 and W_3 using Equation (51):

$${}^b\rho_c = \frac{W_1}{V_j - (W_3 - W_2) \rho_w} \quad \dots (51)$$

where ρ_w is the density of water which was assumed to be 1 kg dm^{-3} .

From the stone content mass fraction (S_w), stone density

(ρ_c) and soil dry bulk density (ρ_s), the stone content volume fraction (S_v) could be calculated using Equation (52):

$$S_v = S_w \frac{\rho_s}{\rho_c} \quad \dots (52)$$

4.1.3 FINE EARTH DENSITY AND TRUE PARTICLE DENSITY

The portion of the soil that passes through the 2mm sieves, termed the fine earth component, makes up the general matrix of the soil around the stones. The bulk density of this component, i.e. the stone-free bulk density (ρ_f) of the soil, can be calculated from ρ_s , ρ_c and S_v using Equation (53):

$$\rho_f = \frac{\rho_s - S_v \rho_c}{1 - S_v} \quad \dots (53)$$

To be able to calculate the pore space of the soil it was necessary to know the true particle density (ρ_p) of the soil particles. The true particle density was measured on a sub-sample of the sieved fine earth component, that had been well riffled to ensure an even mixture and range of particle sizes.

This sub-sample (10-15g) was dried at 105°C to constant weight, and weighed in an oven dry density bottle (50 cm³ size) of known weight (W_1) to obtain W_2 . The soil was then immersed in filtered and de-aerated paraffin and placed under vacuum in a vacuum dessiccator. Paraffin was used in preference to water as it has a lower surface tension which facilitates entry into micro-pores and the complete wetting of the soil (Akroyd, 1969). Placing the samples under vacuum also helps the removal of trapped air. After all air had been removed from the soil, the samples were removed from the vacuum and placed in a water bath at a temperature slightly greater than room temperature (30°C was commonly used). After the samples had attained equilibrium, they were removed, dried, stoppered to the correct volume and weighed (W_3). The density of the de-aerated

paraffin at 30°C (ρ_1) had been measured previously by the use of a volumetric flask, calibrated for volume at 30°C with water (the density of water at 30°C was obtained from published tables). The density bottles had also been calibrated at this temperature, by filling with de-aerated paraffin only and weighed full (W_4) after equilibration at the temperature used in the soil tests. The density of the soil particles was then calculated according to equation (54):

$$t_{\rho} = \frac{(W_2 - W_1)}{(W_4 - W_1) - (W_3 - W_2)} \cdot \rho_1 \quad \dots (54)$$

The above was performed on duplicate sub-samples, t_{ρ} being taken as the mean of two readings.

4.1.4. PARTICLE SIZE DISTRIBUTION AND ORGANIC MATTER CONTENT

The fine earth component of the soil is composed of mineral particles of various sizes and organic material, sometimes adhering strongly in compound units or aggregates. To determine the relative amounts of primary particles of different size classes in the soil, it is necessary to disperse and separate the size fractions. The pipette method (Bascomb, 1974) with dry sieving, was used for this particle size analysis.

Each horizon sample of air dry fine earth was riffled, and four equal sized (15-20g) sub-samples were taken. Two duplicate sub-samples were used to determine the moisture content and organic matter content and the other two were used to determine the particle size distribution.

Moisture content and organic matter content determinations

To determine moisture and organic matter contents, duplicate samples were placed in porcelain crucibles of known weight (W_1), and weighed (W_2). They were then oven dried at 105°C to constant weight (W_3), placed in a muffle furnace and ignited at 375°C for 24h, and finally weighed again (W_4) after cooling in a desiccator. The moisture content mass fraction (θ_m) was calculated using Equation (55), and the weight

loss on ignition (L) as a mass fraction according to Equation (56).

$$e_m = \frac{W_2 - W_3}{W_3 - W_1} \quad \dots \quad (55)$$

$$L = \frac{W_3 - W_4}{W_3 - W_1} \quad \dots \quad (56)$$

Particle size analysis

The method used was the well known "pipette method" described by Bascomb (1974), but with a few modifications. (Only these modifications, but not the original procedure, are described here.)

The other two sub-samples (15-20g) from the procedure detailed above, were used in place of 10g samples advised by Bascomb. After pre-treatment with hydrogen peroxide the soil and solution were filtered using a Buchner funnel, instead of centrifuged. The filtered soil was washed through with distilled water whilst on the filter paper (Whatman No 50), to remove any organic liquids that may have formed from the oxidation of organic matter. These may affect the solution viscosity and hence settling times in the sedimentation stage (Day, 1965).

Dispersion of the soil water suspension with a solution of sodium hexametaphosphate and sodium carbonate was according to Bascomb, except that 25cm³ was mixed in with a high speed stirrer, rather than 10cm³ mixed by shaking overnight. This solution was made up to 1 dm³ rather than 500 cm³ and passed through a 200µm sieve on transference to the 1dm³ cylinder, not a 63µm sieve as in Bascomb. According to Bascomb, only two 25cm³ samples are removed from the solution representing the <63µm and <2µm size fractions at depths of 150 and 90mm respectively. In this analysis three samples were taken at a depth of 100mm from the surface, representing samples of <20µm, <6µm and <2µm.

After removing the <2µm sample the solution was left to stand

overnight, and the suspension fraction siphoned off. The fine sand sediment left was washed and siphoned several times until all traces of clay were removed, and finally evaporated to oven dryness. This was mixed with the $>200\mu\text{m}$ sand fraction sieved previously and also oven dried. This fraction was sieved through a nest of sieves with mesh sizes 600, 212, 106 and $63\mu\text{m}$ on an automatic shaker for 15 min.

Each size fraction is calculated and finally expressed as a mass fraction of the oven dried fine earth. The method of Bascomb results in 5 size classes being recognised, whereas the method used here results in 8 size classes (Appendix 3). This is probably more than is required for this analysis, but the fine sand fraction had to be divided to prevent overloading of one sieve as this is the largest fraction in these soils. The mesh sizes $63\mu\text{m}$ and $212\mu\text{m}$ were used in place of the standard limits for fine sand, $60\mu\text{m}$ and $200\mu\text{m}$, as the latter were unavailable and the difference considered insignificant.

4.1.5. MOISTURE RELEASE DATA

Undisturbed soil cores were taken using the coring device illustrated in Fig.4.1 (Soil Moisture Equipment Corp., Santa Barbara, California). The cores (measuring 30mm deep, 27mm radius) were contained in brass rings that fitted inside the main body of the corer. The cores were cut by the sharpened steel cutting edge as the corer was gently hammered into the soil using the device provided. Two core rings were accommodated in the body of the corer with a 10mm deep spacing ring at each end and a further spacing ring behind the cutting edge. The cores were removed by unscrewing the handle from the main body of the corer and pushing the cores out using a special tubular tool provided. The cores were then trimmed flush with the ends of their retaining rings with a sharp knife; most were covered with a plastic plate at one end and a porous ceramic plate at the other. When held together by an elastic

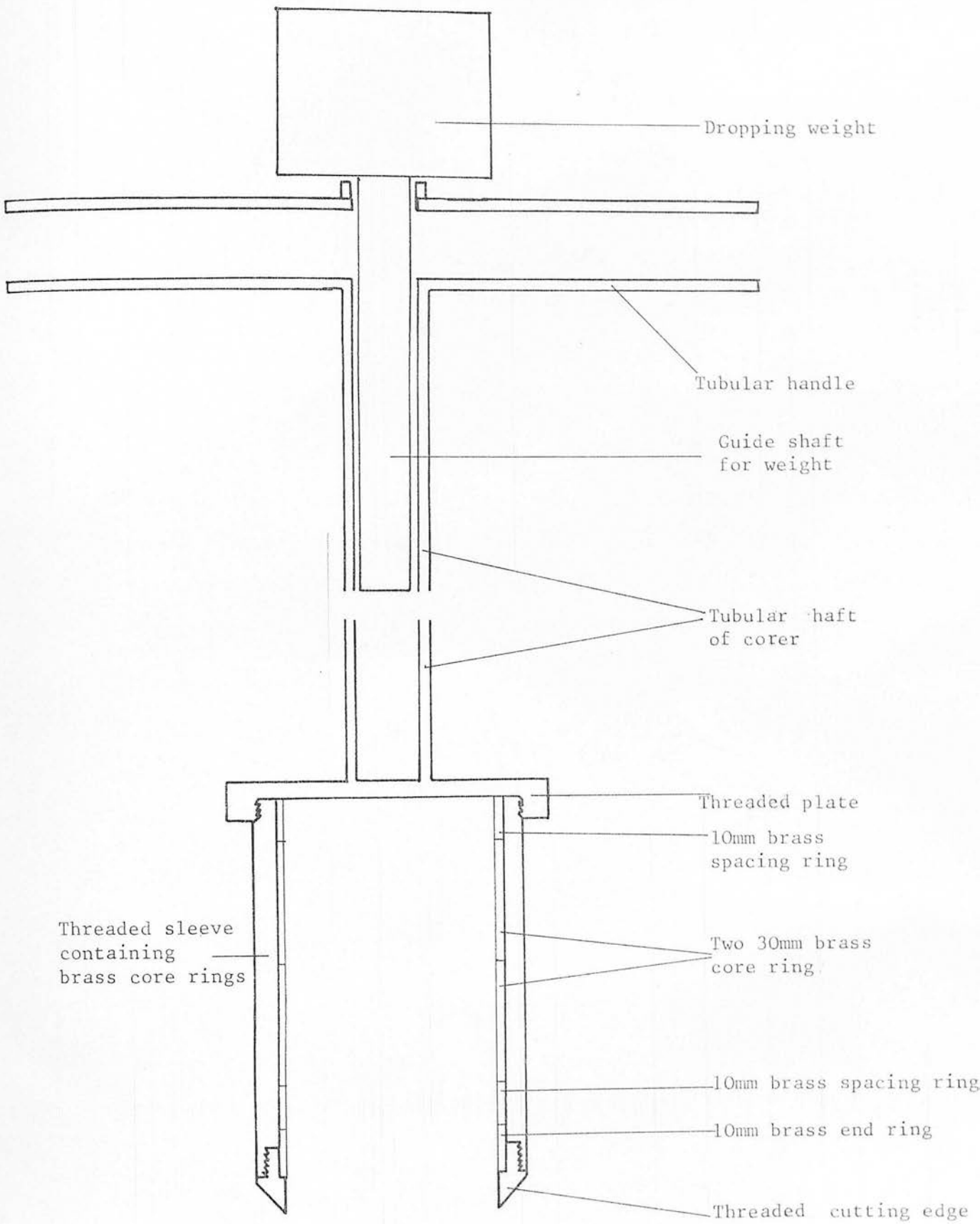


Fig.4.1 Schematic cross-section of the soil corer used (not to scale).

band this whole assembly could be transported back to the laboratory, stored, and finally saturated and placed on a suction table as a unit without further disturbance of the soil core.

Cores were taken at depths of 0.15, 0.30 and 0.60m (corresponding to the depths of gas probes), by digging a small pit and levelling off the soil at a depth 50mm shallower than the required depth of sampling. The corer was then hammered vertically into this prepared surface, the whole device dug out and the enclosed cores in their rings removed. At the same time smaller cores, measuring 20mm deep and 20mm radius, were taken by simply driving sharpened steel rings vertically into the soil. Five cores of each size were taken from each depth in sites 2, 4 and 5.

The cores were saturated by standing them in water on pieces of plastic foam. As the water did not cover their upper surfaces, they absorbed water by capillary action, which minimises the retention of air pockets. Evaporation from their upper surfaces was reduced by covering the whole tray of cores with aluminium foil.

As some of the cores were not contained in a porous plate assembly, pieces of fine nylon netting were placed over the end which would be in contact with the kaolin of the suction table. The large cores were then placed on a kaolin suction table similar to that described by Hall et al (1977), which was covered with aluminium foil to reduce evaporation, and contained a tray of open water to maintain humid conditions around the cores.

The cores were equilibrated to a series of moisture tensions (2.5, 5.0, 7.5 and 10 kPa) maintained by a negative head of water connected to the tank outflow. The equilibrium point was judged to be when a representative core from each group of 5 replicates, weighed every other day, had attained constant weight. Equilibration times varied according to the textural composition of the soils, but were of the order of 2 weeks

for peat at low tensions, but 4-5 weeks for clay soil at the highest tension. At this point the remaining cores were also removed and weighed. The cores were then returned to the suction table and the process repeated at the next higher tension. After being weighed at the final tension (10kPa), the cores were oven dried at 105°C and the weight of soil solids obtained (after accounting for the weight of the ring assembly).

The small cores were equilibrated to tensions of 50, 100, 300 and 1000 kPa in pressurised moisture extraction apparatus (Soil Moisture Equipment Corp., Santa Barbara, California). This apparatus is a series of pressurised vessels containing porous ceramic plates that are graded to retain water up to various moisture tensions (100, 300 and 1500 kPa). The cores are placed on these plates (saturated), and the vessel sealed and pressurised by air from a compressor. The pressure is maintained at set levels by diaphragm regulators so that the cores behave as if they were under moisture tension at these levels. The extracted water is removed from the vessel via outlet tubes connected to the ceramic plates and to a series of burettes (one for each plate). When the water level in these burettes was constant, then no more water was being removed from the cores, and they were considered to be in equilibrium at the set moisture tension. Equilibration time could be up to 7 weeks for clay samples at the highest tension (1000 kPa). When all cores were equilibrated to the desired tension the vessels were depressurised and the cores removed and weighed. The cores were then repressurised to the next tension and the process repeated until they had been weighed at the highest tension, after which they were oven-dried to obtain the oven-dried weight of soil solids.

The moisture content at each tension was calculated as the mass fraction of oven dried soil (θ_m) using Equation (57), and as a volume fraction (θ_v) using Equation (58).

$$\theta_m = \frac{(W_t - W_o)}{(W_o - W_c)} \quad \dots (57)$$

$$\theta_v = \frac{(W_t - W_o)}{\rho_w \cdot V_c} \quad \dots (58)$$

where W_t = weight of soil core and ^{ring} assembly at tension t .
 W_o = weight of soil core and ring assembly when oven dried.
 W_c = weight of ring assembly.
 V_c = volume of the soil core i.e. internal volume of ring.
 ρ_w = density of water (assumed to be 1 kg dm^{-3})

For the large cores $V_c = (\pi \cdot 27^2) \cdot 30 = 68707 \text{ mm}^3$, and for the small cores $V_c = (\pi \cdot 20^2) \cdot 20 = 25136 \text{ mm}^3$.

4.2 RESULTS

4.2.1. PROFILE DESCRIPTION

The soil of all sites was classified as a peaty gley (Pyatt 1970), which is a surface-water gley where an appreciably thick (up to 0.45m) layer of peat has developed at the surface. This soil type forms in relatively impermeable parent materials, in this case glacial till. Above the relatively unaltered till (C horizon) five other soil horizons can be recognised. These horizons are described below and illustrated in Plate 4.1 (Plate 4.1 is from site 8 but the colour data is from site 5). Colour codes are according to Munsell (1954).

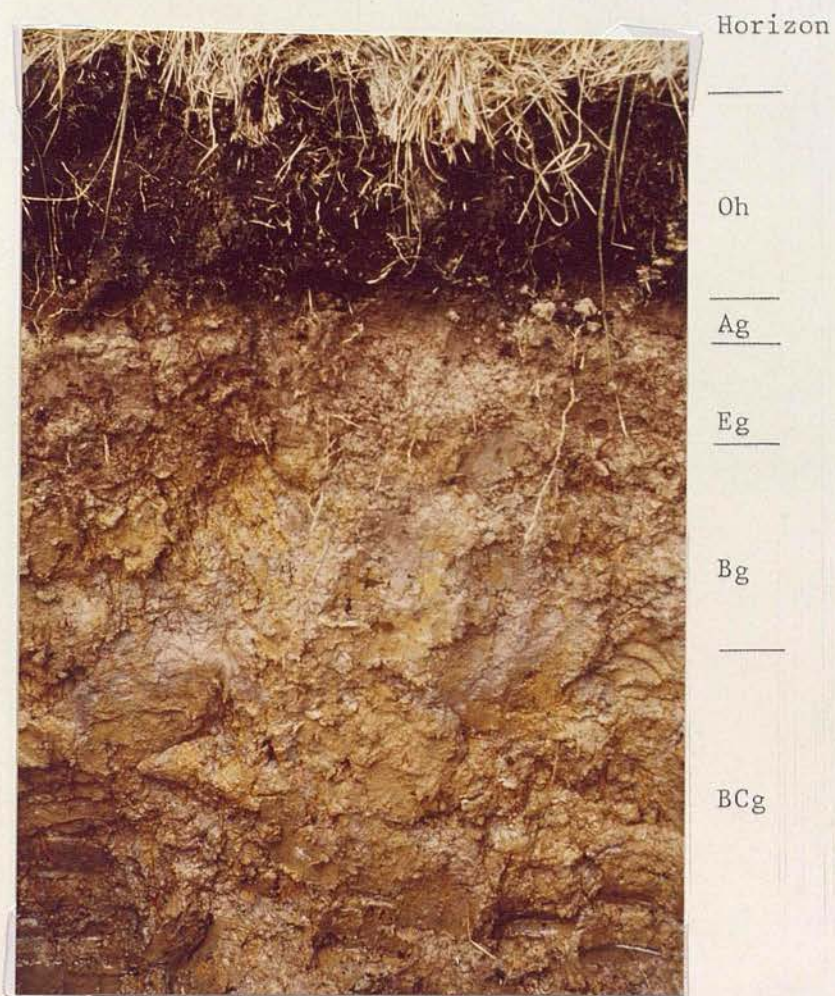


Plate 4.1 The peaty gley soil profile at Falstone to about 1m depth.

Generalised soil profile description (from surface downwards)

Horizon

Thickness (m)

Depth (m)

Description

LF

Litter, decomposing needles and moss

0.05m

0 - 0.05m

Oh

Black amorphous peat, many fine roots and occasional coarse woody roots.

0.2m

0.05 - 0.25m

Ag -

Mixed mineral and organic material;

0.06m

greyish brown (7.5 YR 4/2) with no mottling;

0.25 - 0.31m

sandy clay loam; weak sub-angular blocky structure; friable; common fine roots and occasional coarse woody roots.

Eg -

Greyish brown (7.5 YR 6/2), with a little

0.12 m

ochreous mottling in places; sandy loam;

0.31 - 0.43m

weak prismatic structure; slightly stony; moderately plastic; few fine roots.

Bg -

Bleached brownish grey (10YR 6/1) horizon

0.2m

with mottling of a bright yellowish brown

0.43 - 0.63m

colour (10YR 6/6), making up 30% of the surface clay loam; structureless; moderately stony with some rotting sandstone; slightly sticky; very few fine roots.

BCg -

Intergrade horizon; Grey (N6) with about 40%

0.4m

bright yellowish brown (2.5 Y 6/6) mottling

0.63 - 1.03m

in the upper half, and grey (N5) with about 50% olive (5Y 5/4) mottling in the lower half;

clay loam; structureless; sticky; stony with some rotting sandstone and large boulders;

<u>Horizon</u>	<u>Description (continued)</u>
<u>Thickness (m)</u>	
<u>Depth (m)</u>	
BCg -	(> 0.2m diameter); a few dead roots.
Cg-	Olive grey (5GY5/1) with some olive (5Y5/4)
-	mottling making up about 20% of the surface;
1.03m	clay loam; structureless; very sticky; stony with large boulders no roots.

The suffix 'g' indicates that gleying is present in all horizons. Gleying is the reduction of iron (III) and manganese (IV) compounds to iron (II) and manganese (II) compounds, respectively, which being more soluble are often leached down the profile, or out of the soil in drainage water. Gleying gives rise to the typical drab grey colouring, though deposits of rust coloured iron (III) material were observed around root channels in the B and BC horizons. This contributes partly to the ochreous mottling, as does the weathering of soft sandstone distributed throughout the mineral profile. Small pieces of coal were also found scattered sporadically in the lower horizons.

Of major importance to the experiment was the variation in thickness of the horizons, between sampling sites. Fig 4.2 illustrates the depths of horizons observed in the six sampling pits in sites 2, 4, 5, 8, 9, and 11, relative to the positions of installed gas probes. The importance of this will be discussed later.

4.2.2. BULK DENSITY

Table 4.1 shows the mean wet bulk density (ρ_b) and moisture contents by weight (θ_m) of each soil horizon at the time of sampling.

As the wet bulk density of the soil will vary with the moisture content, a more stable parameter is the dry bulk density (ρ_{d_s}).

Table 4.2 shows the mean dry bulk density (whole soil basis) of each horizon (derived using Equation (50)), together with the number (n) of

Turt-planted sites

Ploughed sites

Depth (m)	Turt-planted sites			Ploughed sites		
	8 (MC)	9 (SS)	11 (LP)	4 (SS)	5 (LP)	2 (MC)
	Oh	Oh	Oh	Oh	Oh	Oh
*						
0.2		Ag	Ag		Ag	Ag
	Ag			Ag	Eg	Eg
*	Eg	Eg	Eg	Eg	Bg	
0.4	Bg	Bg	Bg	Bg	BCg1	Bg
*			BCg1	BCg1	-----	BCg1
0.6	BCg1	BCg1	-----	-----	BCg2	-----
			BCg2	BCg2		BCg2
0.8	BCg2	BCg2				
*						
1.0			Cg	Cg	Cg	Cg
	Cg	Cg				

Fig. 4.2 Depths of soil horizons in each of the sites sampled
(compared with the depths of gas probes-*)

Table 4.1 Mean wet bulk densities (b_{ρ}) (kg dm^{-3}) and gravimetric moisture content (θ_m) of soil horizon in the indicated sites and horizons

Site		Wet bulk densities (kgdm^{-3})					
		Oh	Eg	Bg	BCg1	BCg2	Cg
2	b_{ρ}	1.09	1.69	1.64	1.66	1.74	1.80
	θ_m	3.36	0.344	0.398	0.400	0.339	0.268
4	b_{ρ}	0.97	1.44	1.64	1.78	1.89	1.95
	θ_m	5.02	0.914	0.485	0.300	0.289	0.299
5	b_{ρ}	1.11	1.68	1.68	1.65	1.73	1.96
	θ_m	1.39	0.313	0.393	0.308	0.273	0.227
8	b_{ρ}	1.11	1.68	1.73	1.79	1.85	1.90
	θ_m	3.51	0.535	0.496	0.515	0.460	0.367
9	b_{ρ}	1.13	1.60	1.78	1.78	1.76	1.80
	θ_m	2.14	0.327	0.234	0.262	0.278	0.252
11	b_{ρ}	1.14	1.70	1.71	1.74	1.84	1.82
	θ_m	4.26	0.335	0.338	0.346	0.303	0.305

Table 4.2 Mean dry bulk densities (ρ_s) (kgdm^{-3}) with the standard error of the mean (s.e.) and number of observations (n), for the sites and horizons indicated

Site		Dry bulk densities (kgdm^{-3})					
		Oh	Eg	Bg	BCg1	BCg2	Cg
2	ρ_s	0.26	1.25	1.18	1.19	1.30	1.30
	s.e.	0.016	0.036	0.018	0.033	0.012	0.043
	n	15	10	12	12	12	12
4	ρ_s	0.16	0.79	1.12	1.37	1.47	1.51
	s.e.	0.005	0.075	0.052	0.038	0.032	0.024
	n	15	12	10	13	12	14
5	ρ_s	0.49	1.28	1.21	1.27	1.36	1.60
	s.e.	0.029	0.027	0.035	0.022	0.015	0.032
	n	15	12	12	15	15	13
8	ρ_s	0.25	1.15	1.23	1.27	1.39	1.53
	s.e.	0.011	0.018	0.022	0.021	0.018	0.011
	n	15	15	15	15	15	15
9	ρ_s	0.38	1.23	1.47	1.42	1.38	1.44
	s.e.	0.030	0.059	0.026	0.036	0.027	0.027
	n	15	15	15	15	15	15
11	ρ_s	0.29	1.27	1.29	1.29	1.43	1.39
	s.e.	0.063	0.021	0.029	0.012	0.023	0.017
	n	15	15	15	15	15	15

readings taken to obtain the mean and the standard error of the mean (s.e).

Using Equation (53) values can be obtained for the fine earth bulk density (ρ_f^b). As this is the part of the soil exploitable by roots, it may give a better indication of any effects resulting from cultivation treatments or growth of trees. Fine earth bulk density figures are given in Table 4.3, and reproduced graphically in Fig. 4.3.

Apart from the noticeably lower values for dry and fine earth bulk densities in the ploughed Picea sitchensis site (site 4) above 0.5m depth, there are no obvious differences between sites.

Pyatt (1973) suggested that in some peaty gleys in the Borders Region, moisture removed by the crop had led to subsidence in the subsoil horizons, giving a slightly higher dry bulk density in the upper mineral horizons (E, B and BC) in forested sites compared with unplanted rides. This effect is also absent from the data presented here, except for a possible suggestion in the ploughed sites.

4.2.3. ORGANIC MATTER CONTENT

The organic matter content of the soil horizons, determined by the procedure described in Section 4.1.4, is given as a mass fraction of the whole soil (fine earth component) in Table 4.4.

Again site 4 stands out as different, having extremely high organic matter contents in the Ag and Eg horizons compared to the other sites. It is this high organic matter content that is the likely cause of the low bulk densities in these horizons (Table 4.2 and 4.3, and Fig. 4.3). The figure for the organic matter content in the Ag horizon of site 11 is suspiciously low, and the possibility that initial sampling did not cover the full thickness of the horizon must be considered.

The overall situation is one of very little incorporation of the organic matter into the mineral soil, except for the thin Ag horizon.

Table 4.3. Fine earth bulk densities (ρ_f) (kg dm⁻³), derived from dry bulk densities (ρ_b) and stone content (ρ_s), for the sites indicated.

Turfed area
(sites 8,9 and 11)

Ploughed area
(sites 2,4 and 5)

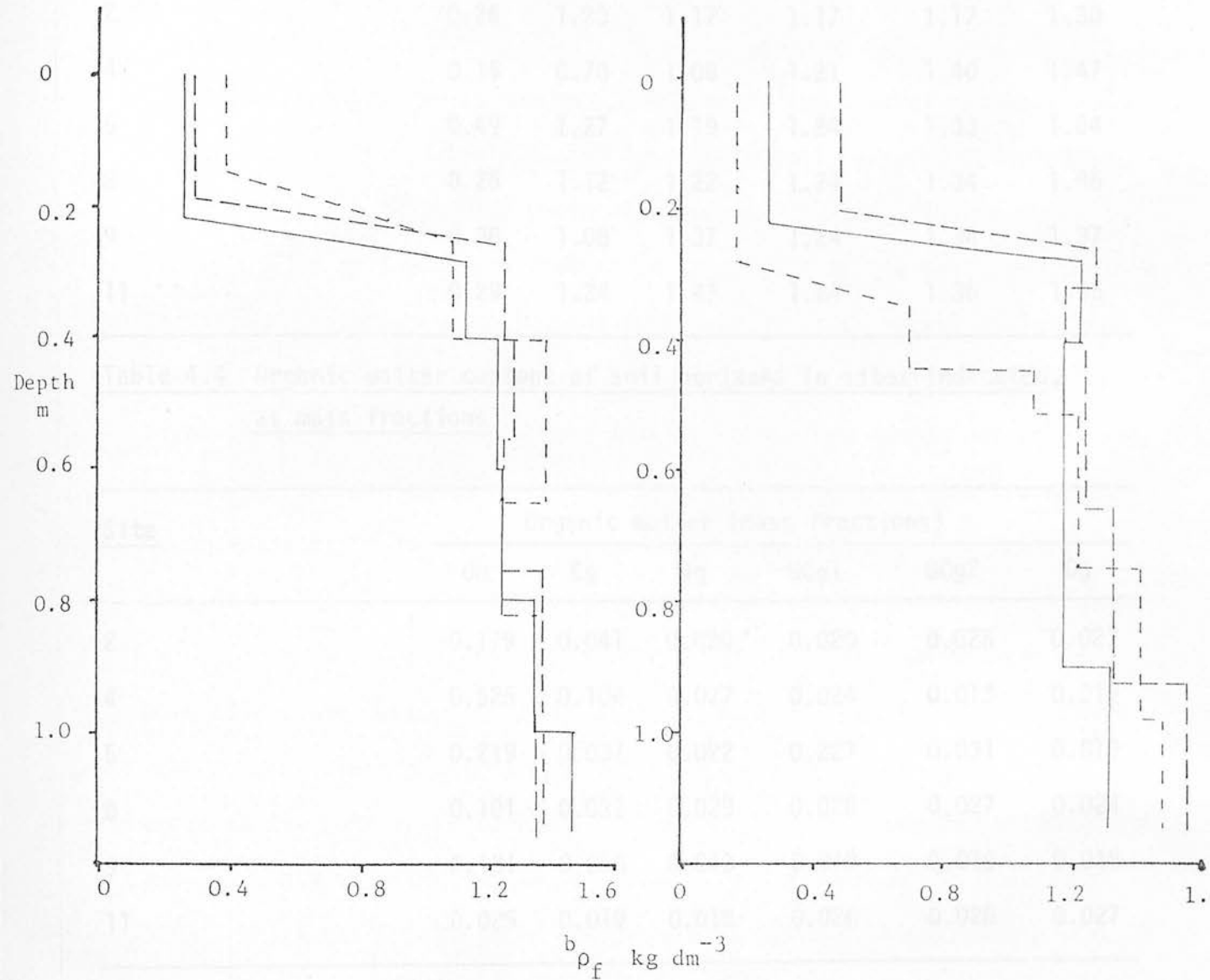


Fig.4.3 Variation of fine earth dry bulk density ρ_f (kg dm⁻³) with depth(m) in sites sampled. — *Molinia caerulea*, - - - *Picea sitchensis*, - · - · *Pinus contorta*.

Table 4.3 Fine earth bulk densities (ρ_f)(kg.dm⁻³), derived from dry bulk densities (ρ_s) and stone contents (s_v), for the sites indicated

Site	Fine earth bulk densities (kgdm ⁻³)					
	Oh	Eg	Bg	BCg1	BCg2	Cg
2	0.26	1.23	1.17	1.17	1.17	1.30
4	0.16	0.70	1.08	1.21	1.40	1.47
5	0.49	1.27	1.19	1.24	1.33	1.54
8	0.25	1.12	1.22	1.24	1.34	1.46
9	0.38	1.08	1.37	1.24	1.34	1.37
11	0.29	1.24	1.27	1.24	1.36	1.35

Table 4.4 Organic matter content of soil horizons in sites indicated, as mass fractions

Site	Organic matter (mass fractions)					
	Oh	Eg	Bg	BCg1	BCg2	Cg
2	0.179	0.041	0.020	0.020	0.025	0.027
4	0.525	0.104	0.027	0.024	0.013	0.019
5	0.219	0.037	0.022	0.227	0.031	0.019
8	0.101	0.032	0.029	0.028	0.027	0.024
9	0.131	0.056	0.013	0.019	0.016	0.018
11	0.025	0.019	0.018	0.026	0.026	0.027

Below this, only very small amounts were found, and again no distinct trends with cropping or cultivation treatments were apparent.

4.2.4 PARTICLE SIZE DISTRIBUTION

The particle size distribution data have been simplified from the 8 size classes measured (given in Appendix 3) to the 3 general classes of sand (63-2000 μm), silt (2-63 μm) and clay (<2 μm), and are presented in Table 4.5 as the mass fraction of the mineral component of the fine earth. Table 4.5 also includes a soil textural description, derived from the triangular coordinate diagram of Avery (1973).

The most constant feature of these data is the high clay content in the deeper subsoil, which apart from site 4, is uniformly a clay loam. The Ag, Eg and Bg horizons show quite considerable variation between the sites but with a general tendency for the Eg horizon (sometimes extending to the Bg) to have somewhat lower clay contents compared with the Ag and lower horizons. Site 4 again stands apart as having low clay contents throughout the profile and commensurately higher sand fractions.

As the soil particle size distribution partly determines the pore size distribution, it will therefore indirectly affect the moisture release characteristics and aeration. It is useful, therefore, to consider the data in Table 4.5 in relation to the problem of horizon depths and gas probe installation depths (Fig. 4.2). All probes at 0.15 and 0.9m depth can be considered as comparable between sites as they were placed in the same horizons throughout, and these horizons have consistent textures (except for site 4). The composition of the soil at 0.3 and 0.6m depth in the six profiles is compared in Table 4.6.

The data in Table 4.6 indicate that when probes were inserted at constant depth, in what was thought to be a reasonably uniform soil, textural variability between sites was large enough to make negligible any variability due to the probes being installed in adjacent horizons.

Table 4.5 Soil textural class and sand, silt and clay contents (mass fractions) of mineral fine earth, in sites and horizons indicated

Site	Horizon	Sand	Silt	Clay	Description
2	Ag	0.374	0.438	0.188	Clay loam
	Eg	0.490	0.345	0.165	Sandy silt loam
	Bg	0.504	0.320	0.176	Sandy loam
	BCg1	0.529	0.289	0.182	Sandy clay loam
	BCg2	0.461	0.287	0.251	Clay loam
	Cg	0.452	0.289	0.259	Clay loam
4	Ag	0.143	0.572	0.285	Silty clay loam
	Eg	0.468	0.385	0.147	Sandy silt loam
	Bg	0.706	0.208	0.092	Sandy loam
	BCg1	0.565	0.267	0.168	Sandy loam
	BCg2	0.603	0.239	0.158	Sandy loam
	Cg	0.503	0.324	0.173	Sandy loam
5	Ag	0.280	0.469	0.250	Clay loam
	Eg	0.455	0.344	0.202	Clay loam
	Bg	0.472	0.322	0.206	Clay loam
	BCg1	0.420	0.274	0.305	Clay loam
	BCg2	0.405	0.268	0.327	Clay loam
	Cg	0.354	0.361	0.285	Clay loam
8	Ag	0.470	0.397	0.134	Sandy silt loam
	Eg	0.529	0.356	0.115	Sandy loam
	Bg	0.469	0.300	0.230	Clay loam
	BCg1	0.396	0.323	0.281	Clay loam
	BCg2	0.384	0.340	0.277	Clay loam
	Cg	0.429	0.313	0.258	Clay loam
9	Ag	0.506	0.215	0.279	Sandy clay loam
	Eg	0.534	0.280	0.186	Sandy clay loam
	Bg	0.575	0.320	0.105	Sandy loam
	BCg1	0.531	0.247	0.222	Sandy clay loam
	BCg2	0.387	0.317	0.296	Clay loam
	Cg	0.247	0.402	0.351	Clay loam
11	Ag	0.555	0.303	0.142	Sandy loam
	Eg	0.607	0.264	0.129	Sandy loam
	Bg	0.662	0.219	0.119	Sandy loam
	BCg1	0.389	0.314	0.296	Clay loam
	BCg2	0.393	0.326	0.281	Clay loam
	Cg	0.350	0.369	0.281	Clay loam

This variability demonstrates the inherent spatial variability of the soil, for which no judicious positioning of equipment can compensate, and so must be accepted as a component of any variability observed in the data from the gas probes.

4.2.5 PORE SPACE AND MOISTURE RELEASE CHARACTERISTICS

To calculate the total pore space (ϵ_T) of the soil it is necessary to employ the particle densities (t_ρ) measured using the procedure in Section 4.1.3., in Equation (59) given below.

$$\epsilon_T = \frac{(t_\rho - b_{\rho_s})}{t_\rho} \quad \dots (59)$$

The pore volume fractions so calculated are given in Table 4.7 together with the true particle densities (the means of duplicate samples) for each soil profile horizon. For the Ag horizons where no dry bulk density was measured, it has been assumed to be the same as for the Eg horizon; the pore volume fraction is therefore only an estimate.

The true particle density of mineral soil is generally held to be in the range $2.5 - 2.8 \text{ kg dm}^{-3}$ (Marshall and Holmes, 1979), a commonly accepted value being 2.65 kg dm^{-3} , though this was considered too low by Pyatt (1978). The range of true particle densities for peat soils (the method of obtaining this is given in Section 5) is less certain but has generally been found in the range $1.4 - 1.5 \text{ kg dm}^{-3}$ (Pyatt, unpublished). The range of values displayed by the Ag horizons reflects their composition, having a varying amount of organic material mixed with the mineral, and thereby producing an overall particle density between the two above ranges. The Ag and Eg horizons in site 4 stand out as having exceptionally low particle densities compared with similar horizons in other sites, caused by their higher organic matter contents (see Table 4.4).

The high organic matter contents of the Ag and Eg horizons in site 4 also explain the high pore volume fractions observed, which

Table 4.6 Soil textures at 0.3 and 0.6m depth in the sites indicated

Depth (m)	Site and Horizon		Sand	Silt	Clay	Description
0.3	2	(Eg)	0.490	0.345	0.165	Sandy silt loam
	4	(Ag)	0.143	0.572	0.285	Silty clay loam
	5	(Eg)	0.454	0.344	0.202	Clay loam
	8	(Eg)	0.529	0.356	0.115	Sandy loam
	9	(Eg)	0.534	0.280	0.186	Sandy clay loam
	11	(Eg)	0.607	0.264	0.129	Sandy loam
0.6	2	(BCg1)	0.529	0.289	0.182	Sandy clay loam
	4	(BCg1)	0.565	0.267	0.168	Sandy loam
	5	(BCg1)	0.420	0.274	0.305	Clay loam
	8	(Bg)	0.469	0.300	0.230	Clay loam
	9	(Bg)	0.575	0.320	0.105	Sandy loam
	11	(BCg1)	0.390	0.314	0.296	Clay loam

Table 4.7 True particle density (t_p)(kgdm^{-3}) and pore volume fractions (ϵ_T) of each soil horizon

Site		Particle densities (kgdm^{-3}) and pore volume fractions						
		Oh	Ag	Eg	Bg	BCg1	BCg2	Cg
2	t_p	1.41	2.28	2.57	2.64	2.67	2.73	2.69
	ϵ_T	0.813	0.451	0.451	0.555	0.554	0.522	0.493
4	t_p	1.41	1.68	2.39	2.60	2.62	2.66	2.67
	ϵ_T	0.886	0.600	0.669	0.572	0.475	0.448	0.437
5	t_p	1.41	2.11	2.50	2.59	2.68	2.66	2.64
	ϵ_T	0.653	0.498	0.486	0.532	0.527	0.489	0.393
8	t_p	1.44	2.36	2.54	2.64	2.70	2.68	2.66
	ϵ_T	0.825	0.514	0.548	0.537	0.528	0.479	0.423
9	t_p	1.49	2.54	2.61	2.68	2.70	2.69	2.68
	ϵ_T	0.744	0.515	0.529	0.451	0.475	0.486	0.456
11	t_p	1.42	2.48	2.65	2.69	2.71	2.70	2.70
	ϵ_T	0.799	0.487	0.519	0.522	0.523	0.476	0.484

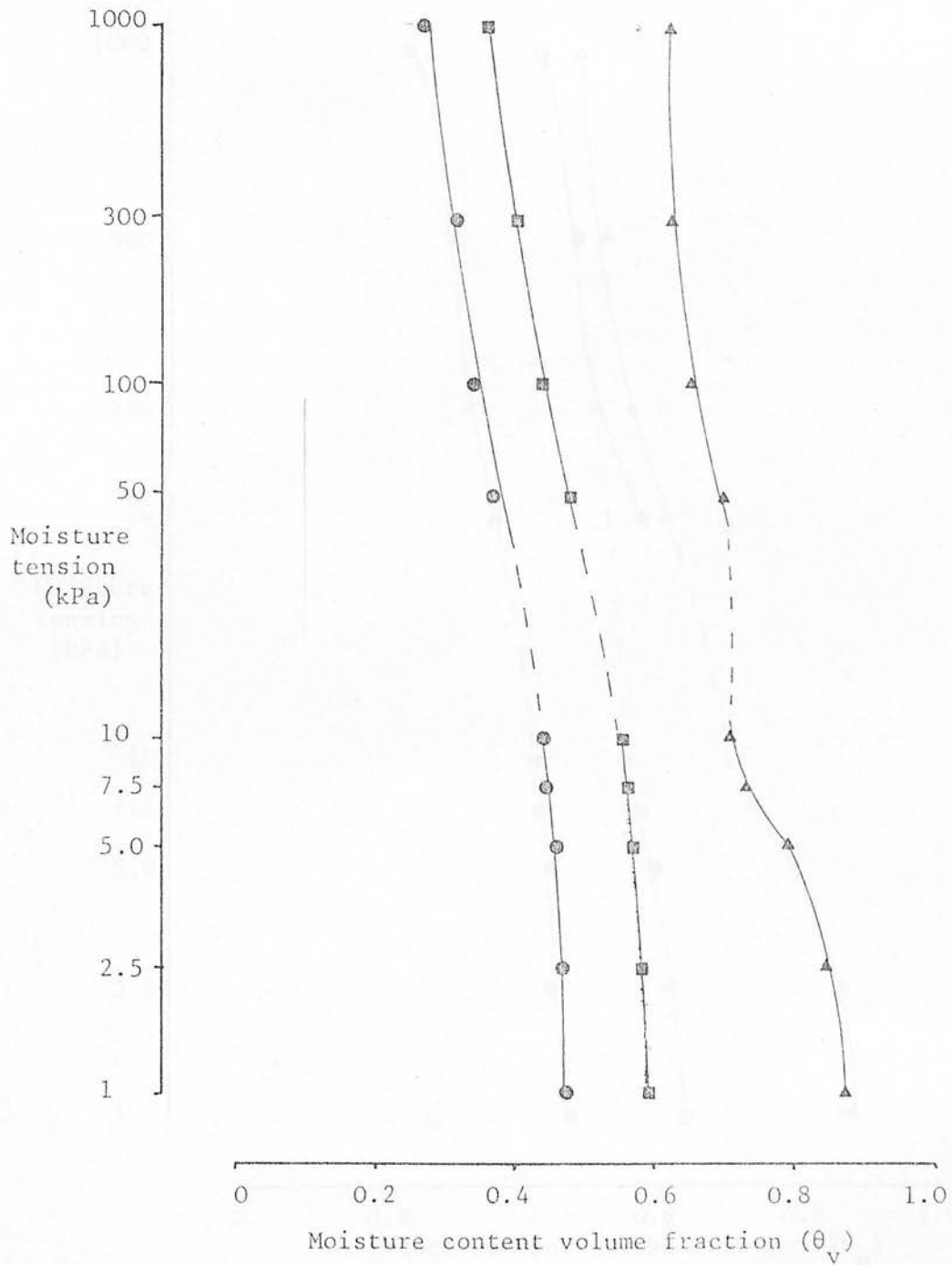


Fig. 4.4 Moisture release curves for site 2 (*Molinia caerulea*) at depths of: - ▲ - 0.15m, ● - 0.30m, and ■ - 0.60m.

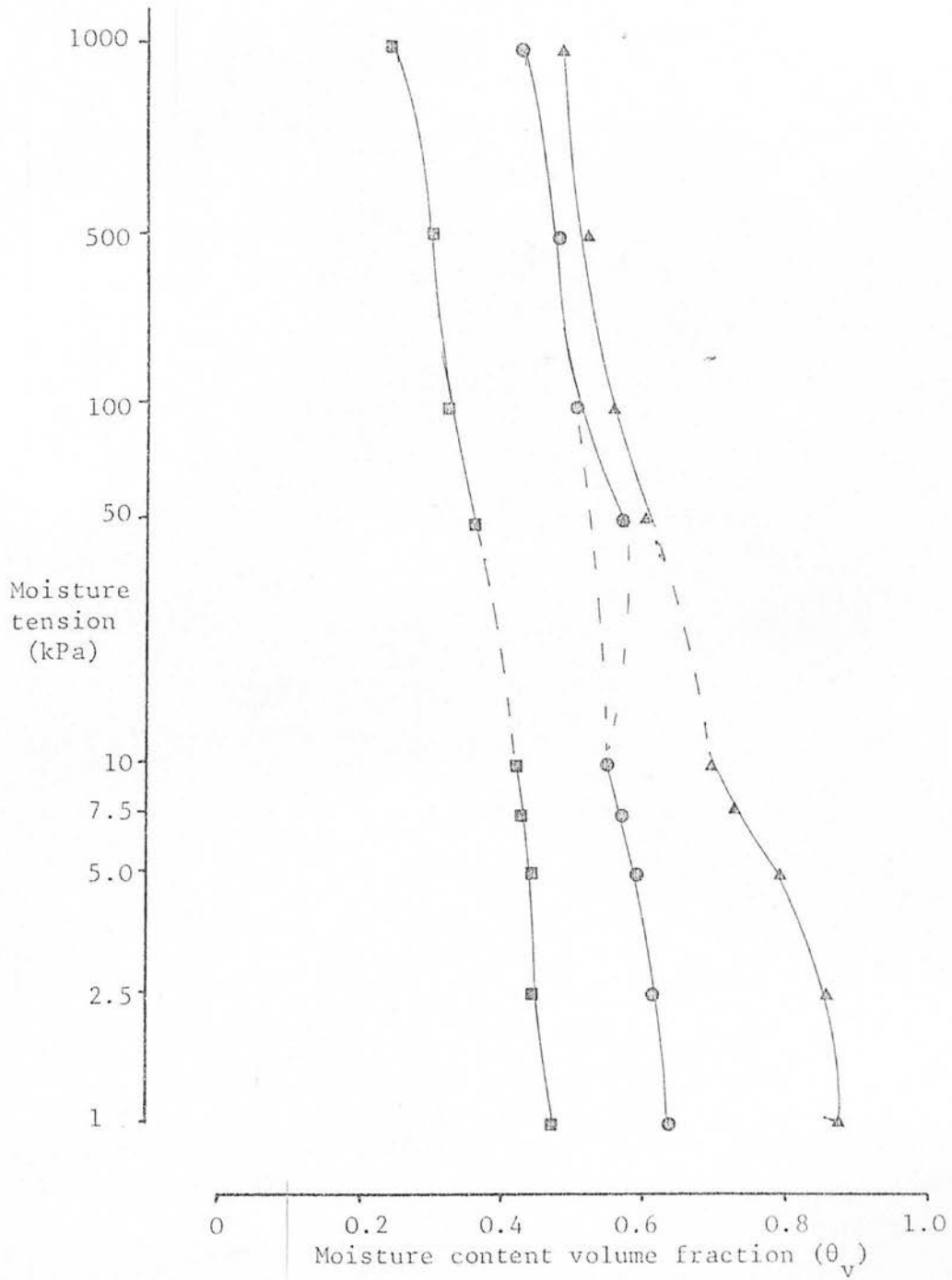


Fig.4.5 Moisture release curves for site 4 (*Picea sitchensis*) at depths of:- ▲ - 0.15m, ● - 0.30m, and ■ - 0.60m.

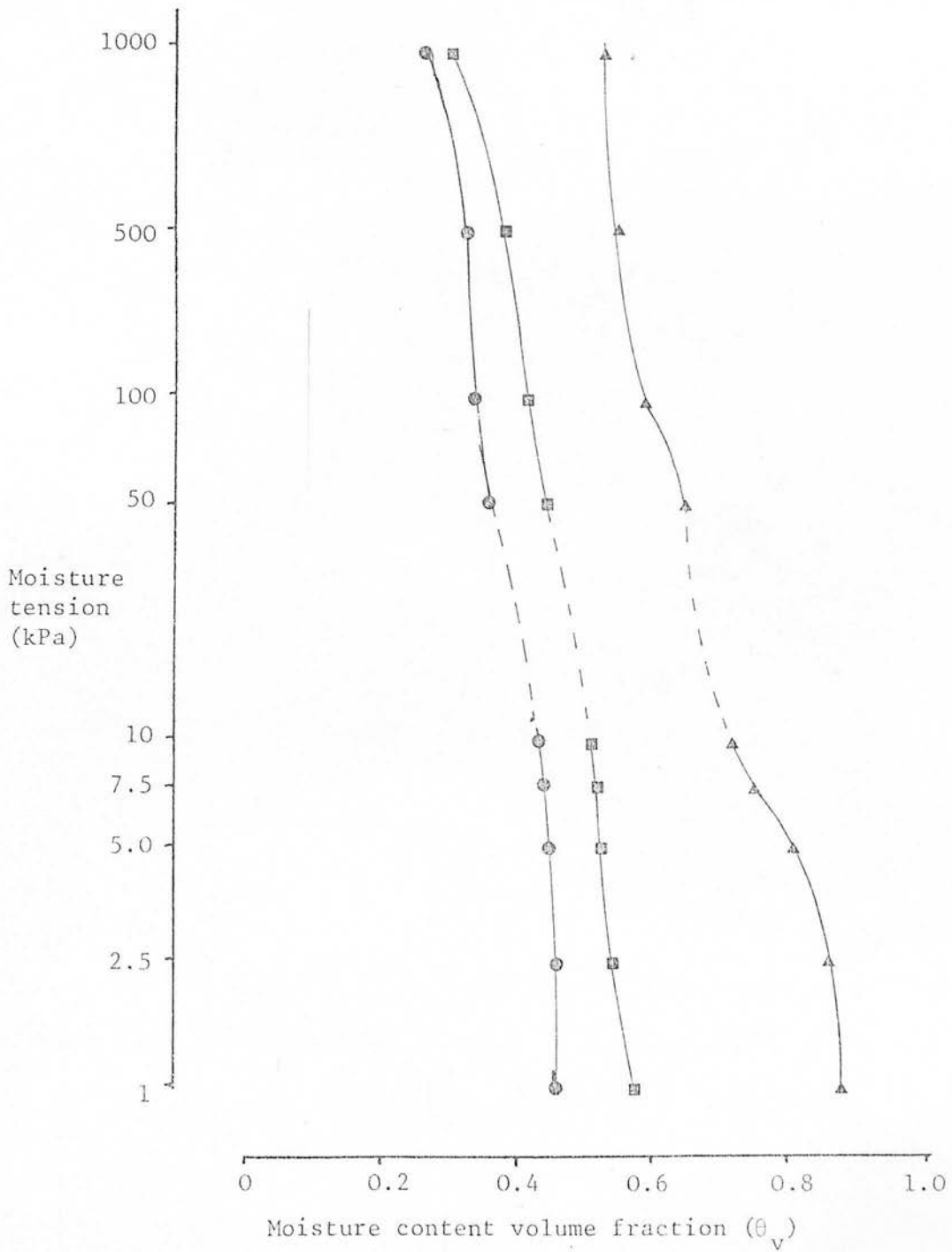


Fig.4.6 Moisture release curves for site 5 (*Pinus contorta*) at depths of:- ▲ - 0.15m, ● - 0.03m and ■ - 0.60m.

were intermediate between those of the mineral soil and overlying peat.

The total pore space of the soil is insufficient on its own to give any reliable insight into the potential for soil aeration. It is also necessary to look at the moisture release characteristics, to evaluate the pore size distribution and assess the relative amounts of pore space available for gaseous diffusion and blocked by soil water.

The moisture release curves for the three sites samples (2,4 and 5) at the three sampling depths (0.15, 0.3 and 0.6m) are expressed as the moisture content volume fraction of the total core volume (θ_v) for set moisture tensions, in Figs.4.4, 4.5 and 4.6. The means of five samples are plotted but it must be remembered that the values for tensions 1-10 kPa were taken from different cores to those at tensions 50-1000 kPa. The moisture tension is plotted on a logarithmic kPa scale (also known as a pF scale).

Comparing the three figures for each depth we can see that at 0.3 and 0.6m the curves for sites 2 and 5 are very similar indeed, and that although the positions of the curves for 0.3m are different from those for 0.6m, their shapes and gradients are similar. The curves for site 4 are quite different, the 0.3m curve being close to those for 0.15m. This is presumed to be due to its high organic matter content and low bulk density, giving it pore space characteristics intermediate between peat and mineral soil. The curve for 0.6m at site 4 agrees very closely with those for 0.3m at sites 2 and 5 in both shape and position. At 0.15m depth all sites are in close agreement at low tensions, but at high tensions site 2, the unplanted site, is divergent from the others, releasing less moisture. Possible explanations for this are that a greater degree of decomposition

has occurred under the tree crops, and/or a greater degree of irreversible drying has taken place, altering the pore size distribution. This problem will be discussed further in relation to the Eddleston peat site.

The fact that the curves for 0.3 and 0.6m depth have such similar gradients and shape suggests that they are releasing about the same quantity of water for a given applied tension (about 20-25% of soil volume over 1MPa), and that the volume of pores in any size class between 0.3 and 300 μ m diameter is also similar. The relative positions of the curves, with respect to the moisture content scale, indicate that they differ mainly in the volume of the pore space that is comprised of pores less than 0.3 μ m in diameter, releasing water at tensions greater than 1MPa and unavailable to plants (more usually taken as >1.5 MPa).

The remainder of the total soil volume is comprised of the soil solid matrix, and can be calculated from the core weight using the known true particle densities. The oven dried weight of soil in the cores can also provide an estimate of the soil fine earth bulk density (ρ_F) if divided by the core volume (V_C), and this is compared to the respective estimates from the gamma ray densitometer in Table 4.8.

The agreement between the two methods of assessing the fine earth dry bulk density is fairly good, on the whole. The consistently low estimates for the peat horizon from the core data are probably nearer the true value, as the gamma ray densitometer estimates for sites 2 and 5 could be coloured by woody root material or mineral matter near the base of the peat layer. The slightly higher values obtained by the core estimates at depths of 0.3 and 0.6m could possibly be due to compaction in the corer, but the diminutive size of any increase indicates that this is not a problem and probably within the bounds of natural variation.

Table 4.8 Fine earth dry bulk densities (ρ_f) (kg dm^{-3}) from gamma-ray densitometry compared with those from soil cores (mean of 10 cores), at the depths and sites shown

Method	Depth (m)	Fine earth dry bulk densities at each site (kg dm^{-3})		
		2	4	5
Cores	0.15	0.18	0.16	0.16
	0.30	1.28	0.67	1.30
	0.60	1.16	1.34	1.29
Densitometer	0.15	0.26	0.16	0.49
	0.30	1.23	0.70	1.27
	0.60	1.17	1.21	1.24

4.3 CONCLUSIONS

The information available for the textural and volumetric composition of the soil in the three sites 2, 4 and 5 is presented in graphical form in Figs. 4.7, 4.8 and 4.9, to give an overall appreciation of the changes occurring with depth.

For soil aeration the most important aspects to be revealed are the relative gas-filled pore volume fractions (ϵ_g) at low moisture tensions. In the peat layer, a relatively large volume fraction (about 0.1) of the soil is gas filled at only 5kPa tension, while at 0.6m depth very little water has been removed at this tension ($\epsilon_g = 0.02 - 0.03$). In site 4 at 0.6m depth this gas-filled volume is a little larger (about 0.05-0.06) and about the same as the intermediate values found at 0.3m depth. At 10kPa tension a further 0.1 of the soil volume becomes gas filled in the peat, but only another 0.01 or 0.02 in the clayey subsoil. As is typical of soils with high clay contents, a much larger volume of water is released at higher tensions (in the order of 100-1000kPa) at 0.3m and 0.6m depth.

Note must be made here that the above figures for ϵ_g in the peat layer have not taken into account peat shrinkage. As peat dries out with increasing moisture tension, then the whole peat block shrinks, at the expense of the gas filled pore space. This problem will be discussed in Section 5 when considering the Eddleston peat site, but as no shrinkage data was available for the peat layer at Falstone, no correction could be made for this phenomenon when calculating ϵ_g . The real gas filled pore volume fractions will therefore be somewhat lower than those quoted above.

Even allowing for peat shrinkage, the evidence presented here suggests that the peat layer will be generally well aerated, while there will be severe aeration problems at depth, even though the peat layer has a higher volumetric moisture content.

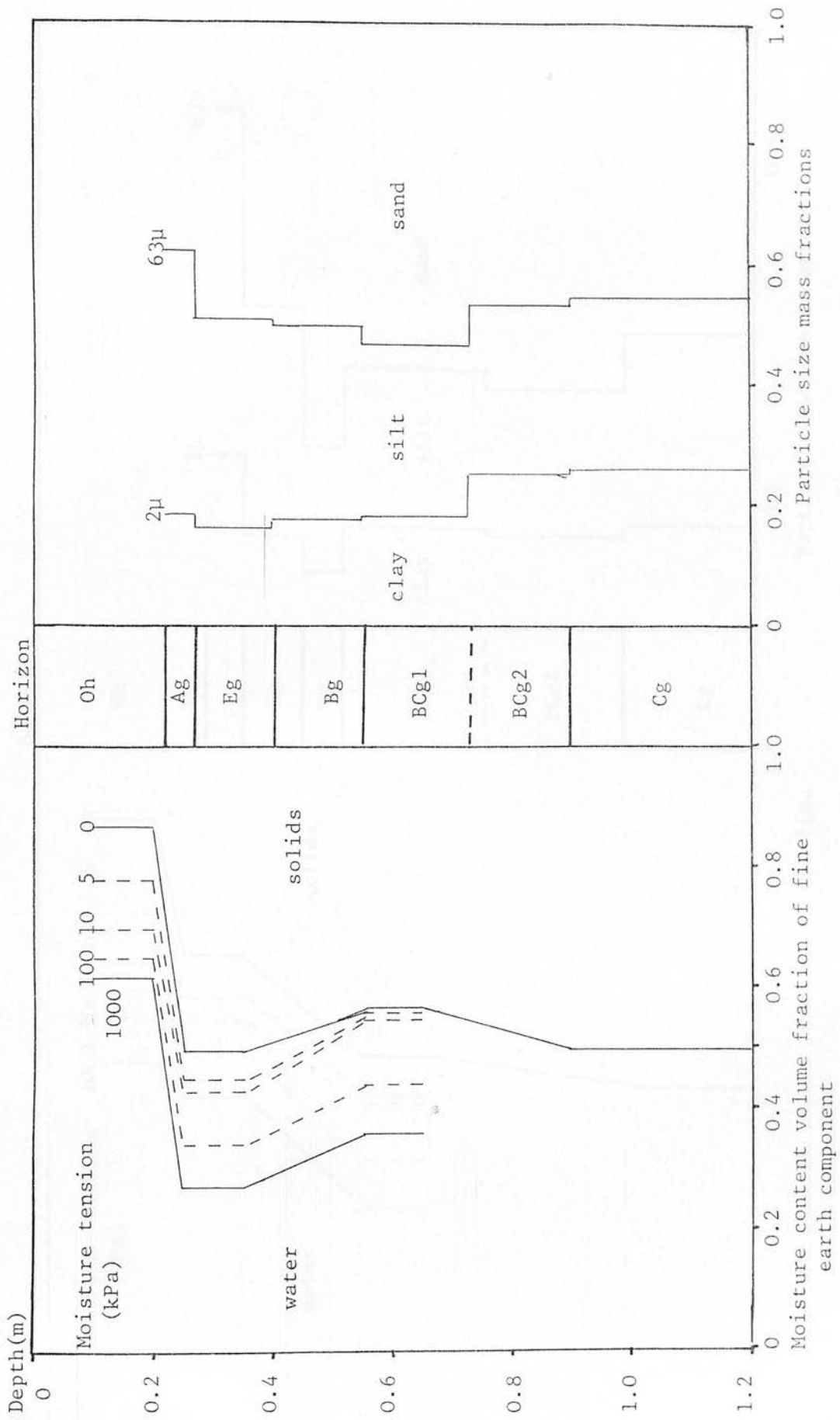


Fig.4.4.7 Moisture content and particle size distribution of fine earth in site 2 (*Molinia caerulea*).

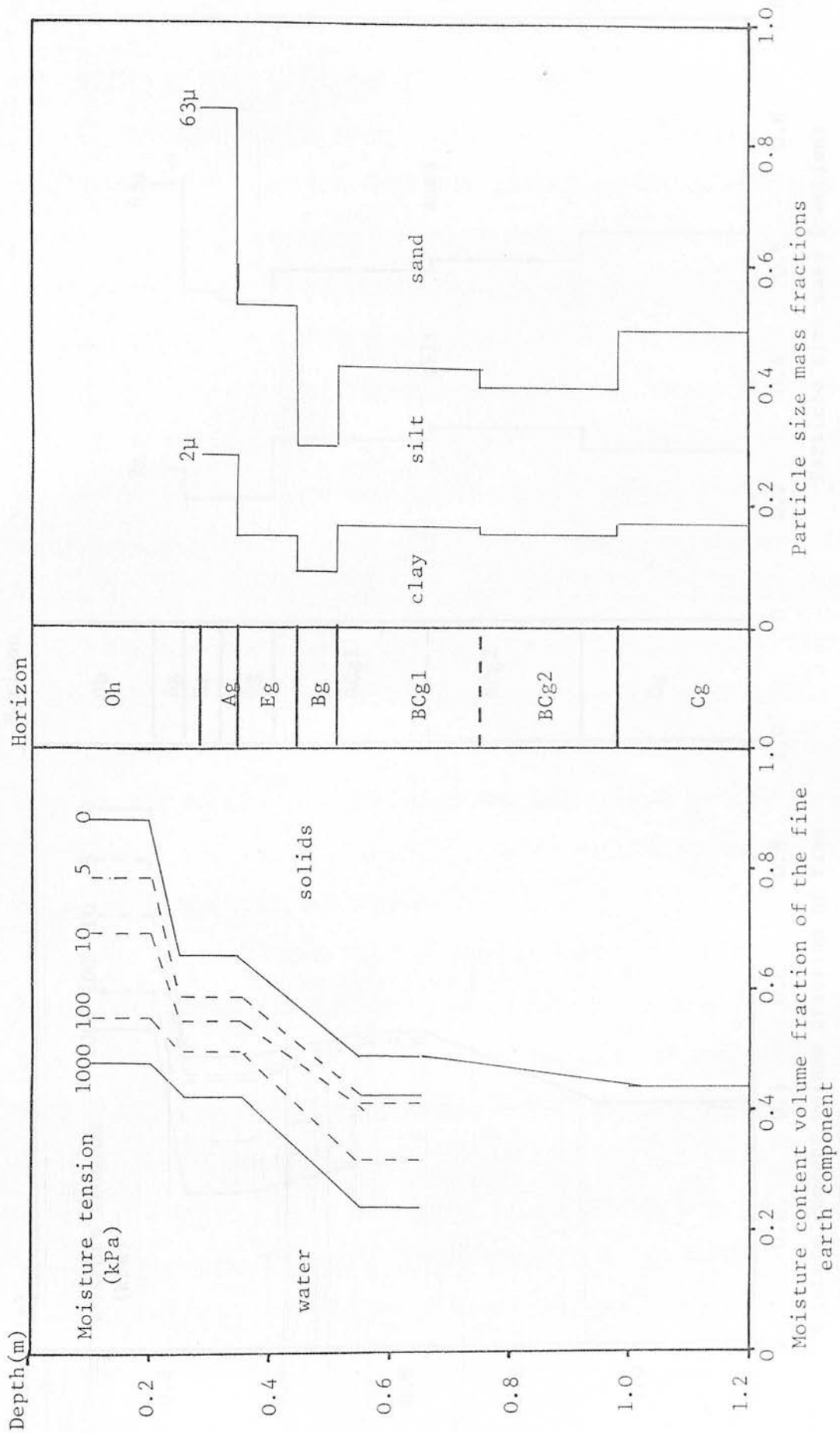


Fig.4.4.8 Moisture content and particle size distributions of fine earth in site 4 (*Picea sitchensis*).

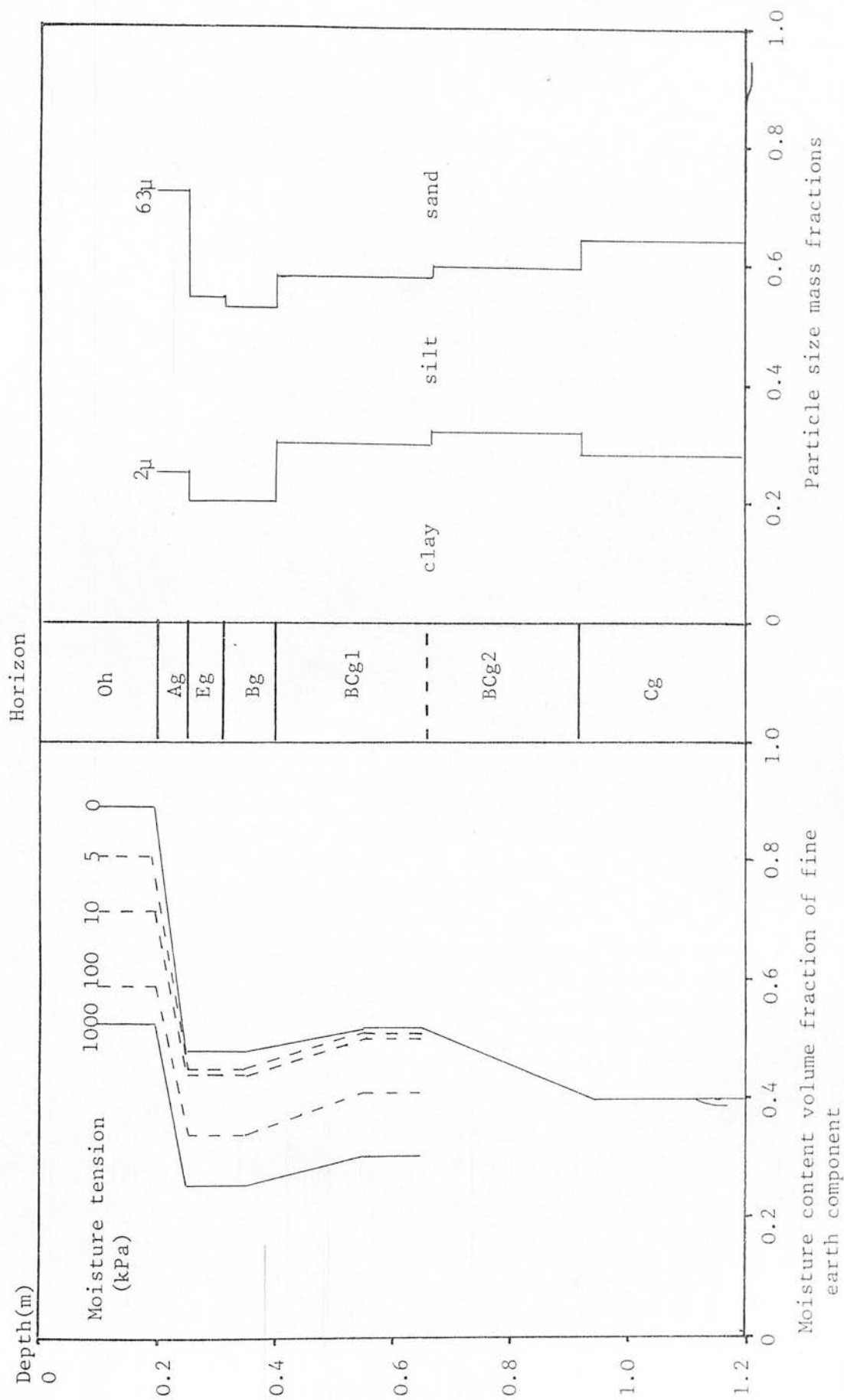


Fig.4.9 Moisture contents and particle size distributions of fine earth in site 5 (*Pinus contorta*).

Mention has already been made of the problems of the spatial variability of soil conditions between sites, emphasising the variation of soil horizons sampled^d at set depths from the soil surface. The conclusion reached earlier, that the textural variation within horizons outweighed that found between adjacent horizons, somewhat vindicates the decision to compare fixed depths from the soil surface rather than points in the soil profile dependent upon observed profile characteristics.

The similarity between moisture release curves from different sites is encouraging in this respect, in that they demonstrate that greater differences occur with depth down the profile than at the same depth between sites. Even at site 4 this trend is maintained, though the volume of pores drained at low tensions is greater than at the other sites at 0.3 and 0.6m depth. For installations of 0.9m depth the moisture release characteristics will be assumed to be closely similar to those at 0.6m. This is a reasonable assumption, as other influential soil properties such as bulk density and texture do not vary greatly between these depths. If anything, the problems for soil aeration will be worsened at 0.9m by higher bulk densities and clay contents.

Having noticed the inherent soil variation between the sampled sites, caution must be employed when extending the observations and conclusions from these sites to those that were not sampled (Sites 1, 3, 6, 7, 10 and 12). No information is available as to the distances over which soil conditions vary, so adjacent sites, such as 2 and 3, may be almost identical or as dissimilar as, say, sites 2 and 4. The most reasonable strategy in these circumstances is to apply the information from the sampled sites equally to their adjacent sites in the same crop and cultivation treatment.

5. PHYSICAL PROPERTIES OF PEAT AT EDDLESTON

5.1 METHODS

5.1.1 BULK DENSITY AND TRUE DENSITY

Bulk density measurements were made gravimetrically, using undisturbed cores obtained with the corer described in Section 4.1.5, during April 1980. These cores were also used to determine moisture release characteristics and for respiration experiments (see Sections 5.1.2 and 8). The dry bulk densities were obtained from the oven dried mass of peat after these experiments were finished.

Pits were dug in the four sites at Eddleston (OV, OP, LP and SS). One half of the pit was levelled off at 0.2m depth and cores (length 30 mm, radius 27mm) taken vertically, as described in Section 4.1.5. This process was repeated at depths of 0.4 and 0.6m. As no distinguishing features were visible at any point in the peat profile these depths were chosen arbitrarily, to provide samples representative of the whole of the possible rooting depth. The cores were trimmed flush with the ends of their containing rings and enclosed in the retaining units as in Section 4.1.5. As cores from the 0.2m depth were to be used for the respiration experiments (excepting those from the OV sites), 15 replicate cores were taken from this depth, while only 10 were taken from 0.4m and 0.6m depths. This enabled 5 cores to be used in the respiration experiment, while 10 were being used to determine the moisture release characteristics. The dry bulk density ($^b\rho_s$) of the peat at these depths in each site was calculated according to Equation (60) using the known internal volume of the cores (V_c) and the mass of oven dried peat (W_o).

$$^b\rho_s = \frac{W_o}{V_c} \quad \dots \quad (60)$$

After weighing to obtain W_0 , the dried peat cores were used to measure the true density of the peat ($^t\rho$), this being equivalent to that measured for mineral soil. The dried cores were bulked together for each site and depth, and then finely ground in a coffee-grinder. This ground peat was then treated in the same manner as the fine earth obtained from the Falstone experiment in Section 4.1.3. The experimental procedure was exactly the same as that for mineral soil, only greater care had to be taken to ensure that the peat was completely de-aerated when immersed in the paraffin. Duplicate samples were again measured, and the density calculated according to Equation (54).

5.1.2. FIBRE CONTENT OF PEAT

The determination of the fibre content of peat and relative amounts of fibre in different size classes, is an approximate equivalent to the particle size analysis carried out on mineral soils.

Cores were cut with a 50mm square corer (Cuttle and Malcolm, 1979) at the same time as those for moisture release measurements, and sectioned into 100mm long blocks, corresponding to depths of 0.1-0.2, 0.2-0.3, 0.4-0.5 and 0.7-0.8m depth. Five such cores were taken from each site providing 80 samples in total, which were transported back to the laboratory in sealed plastic pots, and stored at 4°C until required for analysis.

Each block was halved lengthwise, one half being used to determine the moisture content mass fraction (θ_m), the other being weighed to obtain W_w , and then immersed overnight in a solution of sodium hexametaphosphate and sodium carbonate (50 kg m^{-3}), to disperse the fibres. The dispersed peat was poured onto a stack of sieves with mesh sizes 1.0, 0.425, 0.25 and 0.18mm, and washed with a stream of water, whilst lumps were separated and rubbed gently between the fingers. When water leaving the stack ran clear, the sample retained on each sieve was carefully

washed off into a pot of known weight. These fractions were dried to constant weight at 105°C to obtain the dry weight of each fibre size class (w_f). This was used to calculate the mass fraction (F) of the total oven dried weight (W_d) that each size class constituted, using Equation (61).

$$F = \frac{w_f}{W_d} \quad \dots (61)$$

$$W_d = W_w \frac{1}{1 + \theta_m} \quad \dots (61a)$$

The material which passed through the 0.18mm sieve was found by difference ($W_d - \Sigma w_f$).

5.1.3. MOISTURE RELEASE CHARACTERISTICS

The cores previously described in Section 5.1.1. were used to obtain a moisture release curve in the same manner as those from the Falstone experiment (Section 4.1.5.). Ten cores from each site and depth were equilibrated at successive tensions of 2.5, 5.0, 10.0 and 15.0 kPa on the suction tables, being weighed at each tension and finally oven dried at 105°C and weighed again. The time to equilibration was typically about two weeks. The calculation to obtain the moisture content volume fraction was originally that of Equation (58), but later modified to account for shrinkage of the core, as explained below in Section 5.2.3.

For tensions of 50, 100, 300 and 1000 kPa, uncontained slices of peat were used, as no small core rings were available and this method had been found satisfactory in previous investigations by Pyatt (personal communication, 1980). Three undisturbed cores were cut from each site using the 50mm square corer, and sectioned into 100mm long blocks for depths of 0.15-0.25, 0.35-0.45 and 0.55-0.60m. These were transported to the laboratory undisturbed in sealed plastic pots. A 10 mm thick slice was cut from the mid-length section. The peat cut cleanly and

easily when still wet and the use of an electric carving knife minimised any distortion of the slice or smearing of the cut surface.

Each slice was placed on a numbered filter paper circle, and then stood on wetted pads of plastic foam, to saturate by capillary action. When fully saturated the slices were weighed and then placed (on their filter paper discs) on ceramic pressure plates used in the pressure vessels. Only three replicate cores were used as only this number (36 in total) could be accommodated in the pressure vessels at one time. The equilibration time for the cores was typically four to six weeks at these high tensions. At each tension the slices were weighed and replaced, the procedure being the same as described in Section 4.1.5. The cores were solid and consolidated enough for them to be handled directly without disintegration. At the higher tensions it was found that the slices tended to curl at the edges, and it was necessary to weight them down gently under a sheet of metal gauze, to maintain an adequate contact with the plate.

As the initial volume of the slices was unknown the moisture content volume fraction had to be calculated from the oven dried mass of the slice, and dry bulk density of the peat, as in Equation (62).

$$\theta_v = \frac{(W_t - W_o) \cdot \rho_s}{W_o \cdot \rho_w} \quad \dots \quad (62)$$

Where the notation is that given for Equation (58).

5.2 RESULTS

5.2.1 BULK DENSITY AND TRUE DENSITY

The mean dry bulk densities of the peat at each site and depth are given in Table 5.1, together with the number of observations (n) for the means and their standard errors (s.e.). The true densities of peat solids are given in Table 5.2, and are the means of duplicate samples.

It can be seen from Table 5.2 that only very slight differences

Table 5.1 Mean dry bulk densities of peat (b_{ρ_s})(kgdm^{-3}), with their standard errors (s.e.) and number of observations (n).

Depth (m)		Dry bulk densities at each site, (kgdm^{-3})			
		OV	OP	SS	LP
0.2	b_{ρ_s}	0.100	0.129	0.117	0.136
	s.e.	0.005	0.005	0.005	0.007
	n	10	15	15	15
0.4	b_{ρ_s}	0.077	0.084	0.090	0.090
	s.e.	0.003	0.003	0.004	0.003
	n	10	10	10	10
0.6	b_{ρ_s}	0.070	0.087	0.077	0.089
	s.e.	0.002	0.002	0.004	0.004
	n	10	10	10	10

Table 5.2 True densities of peat solids (t_{ρ})(kgdm^{-3}).

Depth (m)	True density, (kgdm^{-3})			
	OV	OP	SS	LP
0.2	1.40	1.41	1.42	1.43
0.4	1.38	1.41	1.42	1.41
0.6	1.38	1.39	1.41	1.42

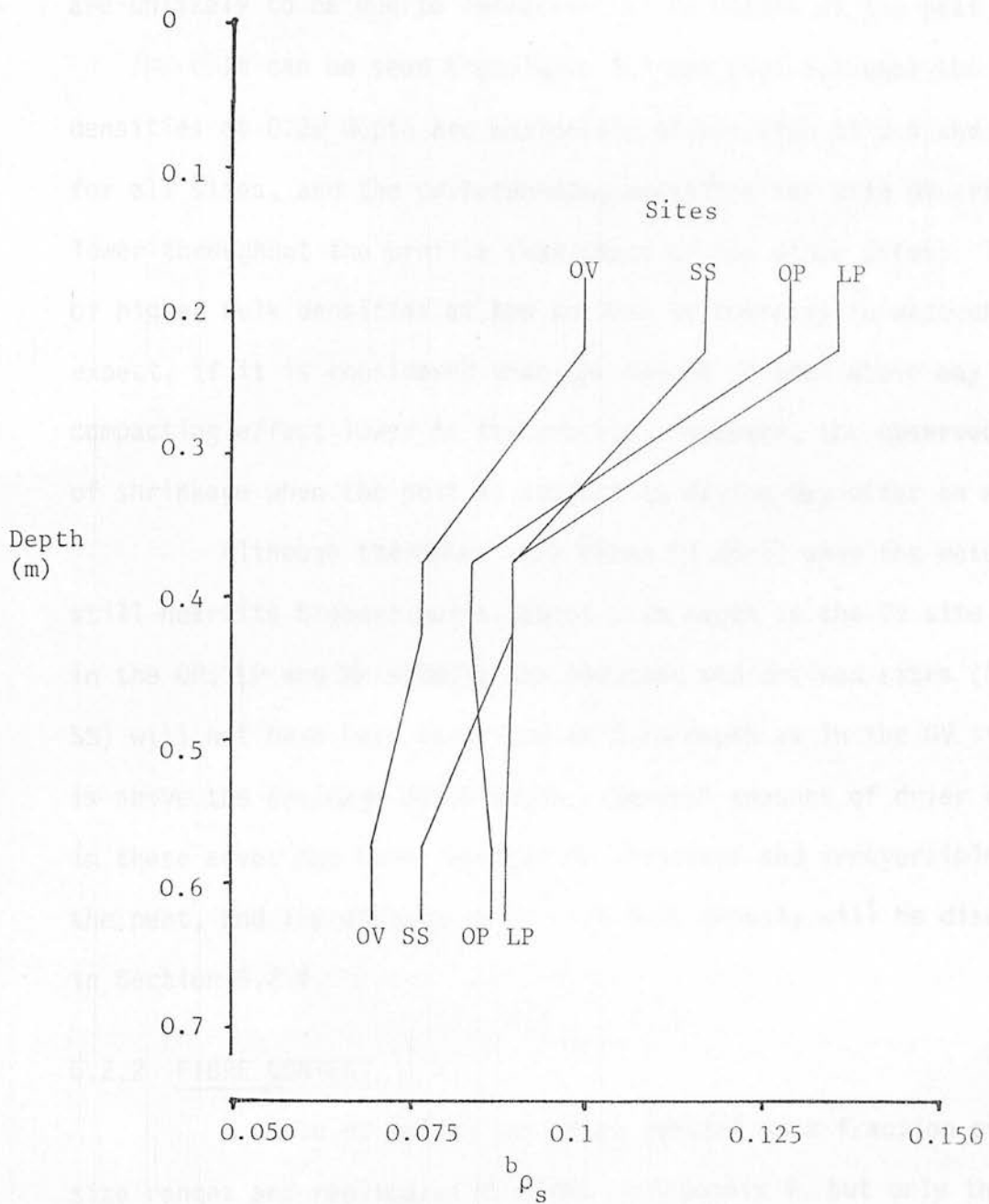


Fig.5.1 Dry bulk density ($b\rho_s$) (kg dm⁻³) of peat with depth (m) in the sites indicated (sloping lines indicate unknown values between measured depths).

exist between the true fibre densities for any particular depth or site, and so the differences in dry bulk density observed in Table 5.1 are unlikely to be due to variation in the nature of the peat solids.

It can be seen from Table 5.1 and Fig. 5.1 that the dry bulk densities at 0.2m depth are noticeably higher than at 0.4 and 0.6m depth for all sites, and the corresponding densities for site OV are noticeably lower throughout the profile than those of the other sites. This trend of higher bulk densities at the surface is contrary to what one may expect, if it is considered that the weight of peat above may have a compacting effect lower in the profile. However, the observed phenomenon of shrinkage when the peat is subject to drying may offer an explanation.

Although the cores were taken in April when the water table was still near its highest point (about 0.1m depth in the OV site and 0.35m in the OP, LP and SS sites), the ploughed and drained sites (OP, LP and SS) will not have been saturated at 0.2m depth as in the OV site, as this is above the drainage ditch depth. Several seasons of drier conditions in these areas may have resulted in shrinkage and irreversible drying of the peat, and the effects of this on bulk density will be discussed further in Section 5.2.4.

5.2.2 FIBRE CONTENT

A table of values for fibre content mass fraction over all size ranges and replicates is given in Appendix 4, but only the two extremes of $>1\text{mm}$ and $<0.18\text{mm}$ particle size were analysed further. A size of 1mm has been used to denote the transition between coarse fragments of undecomposed plant material and finer well comminuted fragments in various stages of decomposition. This size was chosen for the following reason: the gas-filled pore volume fraction of a porous solid at a moisture tension of 0.5 kPa increases sharply for composite particle sizes above 1mm (Puustjarvi and Robertson, 1975). The accepted transition from fibrous

to amorphous peat material is taken to be 0.1mm (Boelter, 1969), so for the purposes of this study the nearest mesh size of 0.18mm sufficed to indicate this point. Besides being another indication of how far advanced decomposition is, the <0.18mm fraction will have a large effect on the moisture retention properties at higher tensions, and may help to explain some of the variability observed in the moisture release curves.

A table of means of the coarse fibre fraction is presented in Table 5.3, and of the amorphous fraction in Table 5.4. These are represented graphically in Figs. 5.2 and 5.3.

The fact that lines cross in Figs. 5.2 and 5.3 and are not parallel, suggests that there may be an interaction between site and depth. Therefore the data were analysed as a factorial experiment with two treatments (sites and depths) and five replicate blocks. Tables 5.5 and 5.6 are the analysis of variance tables for the coarse fibre and amorphous solid fractions respectively.

The analysis reveals that only site effects gave rise to a significant amount of variation in coarse fibre content whereas for amorphous solids content significant variation is associated with site, depth and the replicates. There were no significant interactions between sites and depths.

For both fractions significant variation exists between sites, and an examination of Figs. 5.2 and 5.3 shows the OP site to be mainly responsible for this. The samples from all depths in the OP site tend to have a lower content of coarse fibres and a higher content of amorphous solids than the OV or planted sites. This tendency is less noticeable at depth, especially for the amorphous solids at 0.7 - 0.8m depth where very little variation is seen between any sites. Also of interest are the results for 0.1 - 0.2m depth for both fractions. At this depth considerable differences exist between the planted and unplanted sites;

Table 5.3 Content of fibres >1mm as a fraction of total weight of
peat solids

Depth(m)	Coarse fibre content (kgkg ⁻¹)				Mean
	OV	OP	SS	LP	
0.1 - 0.2	0.163	0.169	0.393	0.374	0.274
0.2 - 0.3	0.273	0.131	0.284	0.338	0.256
0.4 - 0.5	0.363	0.201	0.275	0.347	0.296
0.7 - 0.8	0.366	0.246	0.311	0.283	0.302
Mean	0.291	0.187	0.316	0.336	0.282

Table 5.4 Amorphous solids (<0.18mm) content as a fraction of total
weight of peat solids

Depth (m)	Amorphous solids content (kgkg ⁻¹)				Mean
	OV	OP	SS	LP	
0.1 - 0.2	0.536	0.585	0.367	0.355	0.461
0.2 - 0.3	0.380	0.511	0.385	0.362	0.410
0.4 - 0.5	0.280	0.461	0.285	0.341	0.342
0.7 - 0.8	0.333	0.343	0.341	0.344	0.340
Mean	0.383	0.475	0.345	0.351	0.388

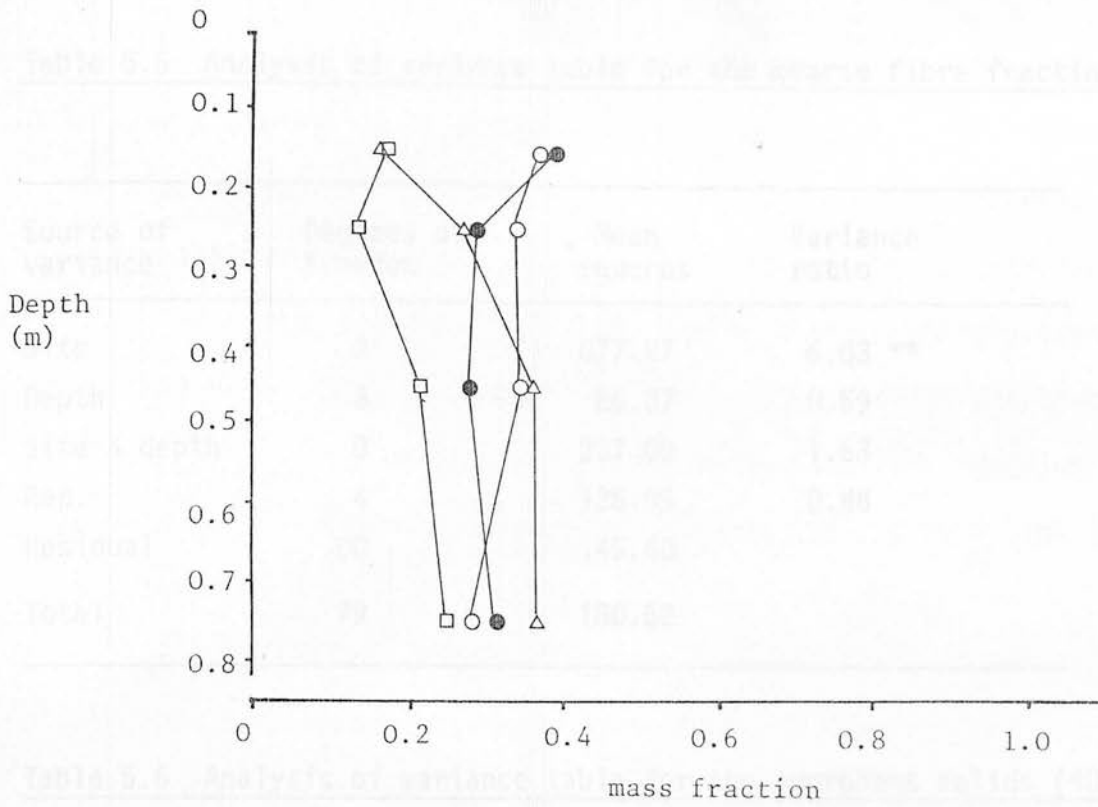


Fig.5.2 Mass fraction of oven dried peat solids comprised of fibres >1mm in sites, Δ -OV, □ -OP, ● -SS and ○ -LP.

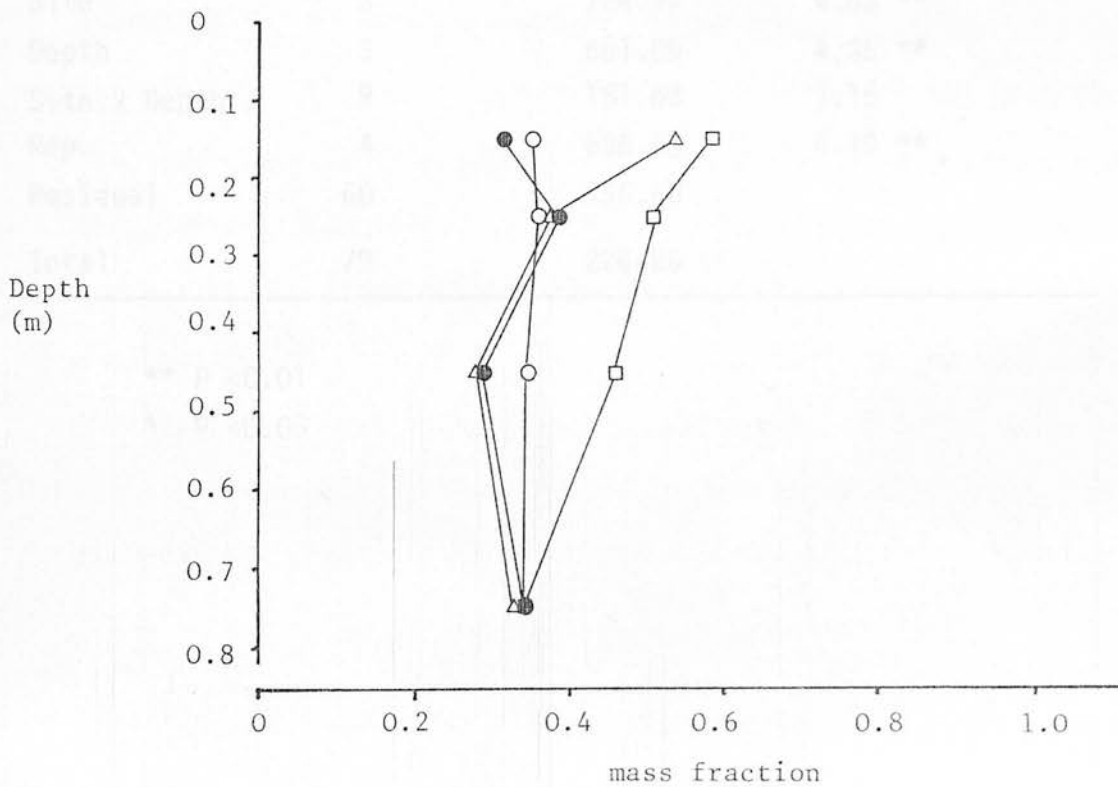


Fig.5.3 Mass fraction of oven dried peat solids comprised of fibres <0.18mm in sites, Δ -OV, □ -OP, ● -SS and ○ -LP

Table 5.5 Analysis of variance table for the coarse fibre fraction (>1mm)

Source of variance	Degrees of freedom	Mean squares	Variance ratio
Site	3	877.27	6.03 **
Depth	3	86.37	0.59
Site X depth	9	237.09	1.63
Rep.	4	128.09	0.88
Residual	60	145.40	
Total	79	180.52	

Table 5.6 Analysis of variance table for the amorphous solids (<0.1mm)

Source of variance	Degrees of freedom	Mean squares	Variance ratio
Site	3	724.97	4.63 **
Depth	3	681.89	4.35 **
Site x Depth	9	181.68	1.16
Rep.	4	655.68	4.19 **
Residual	60	156.60	
Total	79	226.26	

** P < 0.01

* P < 0.05

both OV and OP sites have much lower coarse fibre contents and much higher amorphous solid contents than the LP and SS sites. Here the OV site is more in agreement with the OP site than the planted sites, while at lower depths the OV sites agrees more closely with the LP and SS sites. Not too much should be read into the seemingly large overall differences with depth for the amorphous solid fraction, as the trend is inconsistent between the sites, and this fraction does show a significant variation between replicates, indicating a high inherent variability.

If reduced coarse fibre content and increased amorphous solid content is taken as indicative of increased decomposition, then the OP site shows a promotion of decomposition over the OV site at all depths above 0.7m. This is probably explained by a drier moisture regime, but this would mean that the even drier planted sites should also show these trends in fibre content. Paradoxically they show coarse fibre and amorphous solid contents nearer to those in the OV site. A possible explanation of this is that irreversible drying of the peat (or "ripening") has caused the amorphous solids to either adhere to coarse fibres, or conglomerate into larger units in the coarse fibre size range. This would mask any effects due to decomposition and is the most likely explanation of these data. The data also indicate that any surface treatments or planting effects are confined to the upper 0.7m of peat, there being greater uniformity of the peat below this depth over the experimental area.

5.2.3 MOISTURE RELEASE CHARACTERISTICS OF PEAT

The moisture content volume fraction (θ_v) is presented in Figs. 5.4 - 5.7, plotted against moisture tension (\log_{10} scale), for each site and depth. The values plotted over the tension range 2.5-15 kPa are means of 10 samples while those over

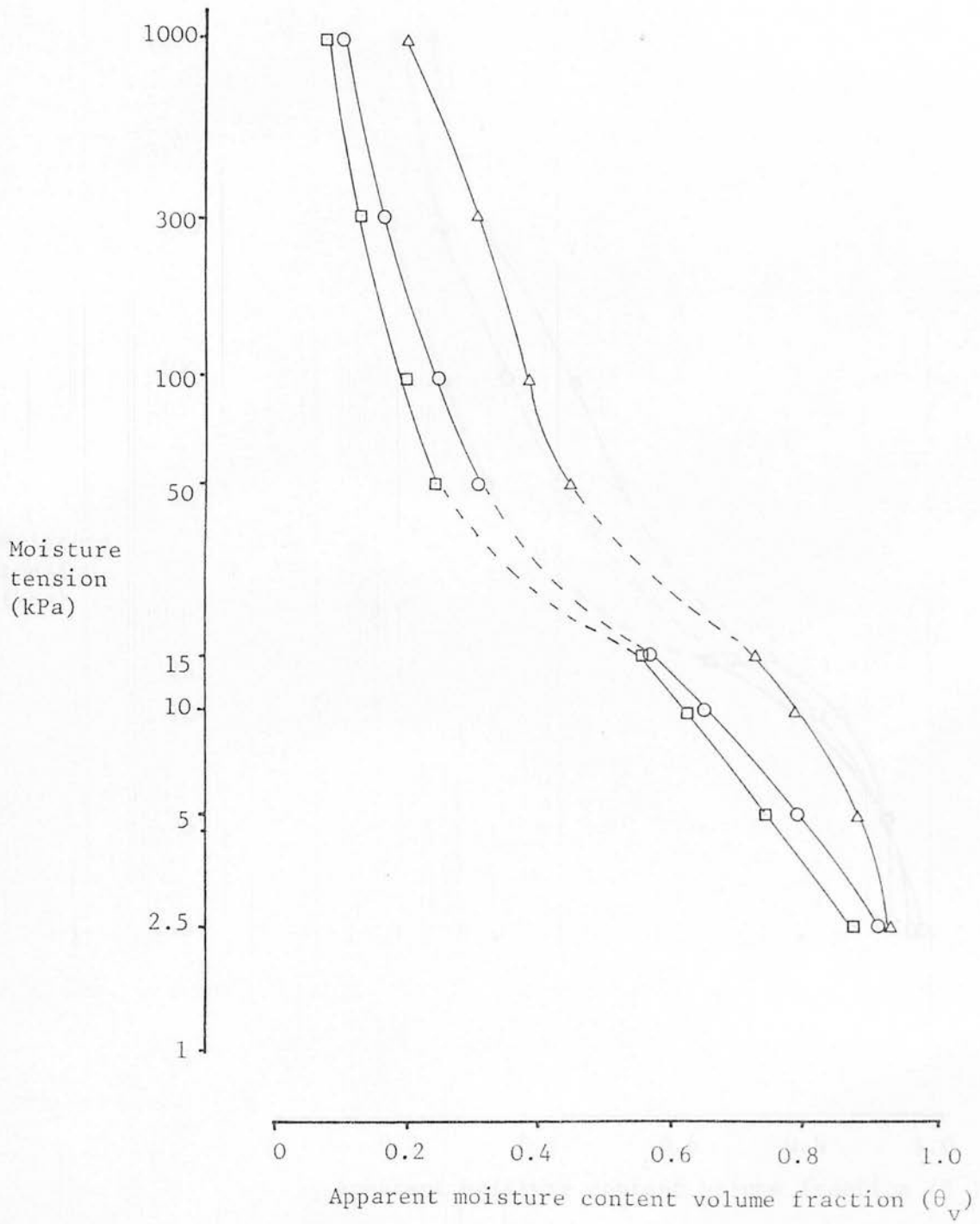


Fig.5.4 Moisture release curves for the OV site at depths of:
 Δ -0.2m, \circ -0.4m and \square -0.6m.

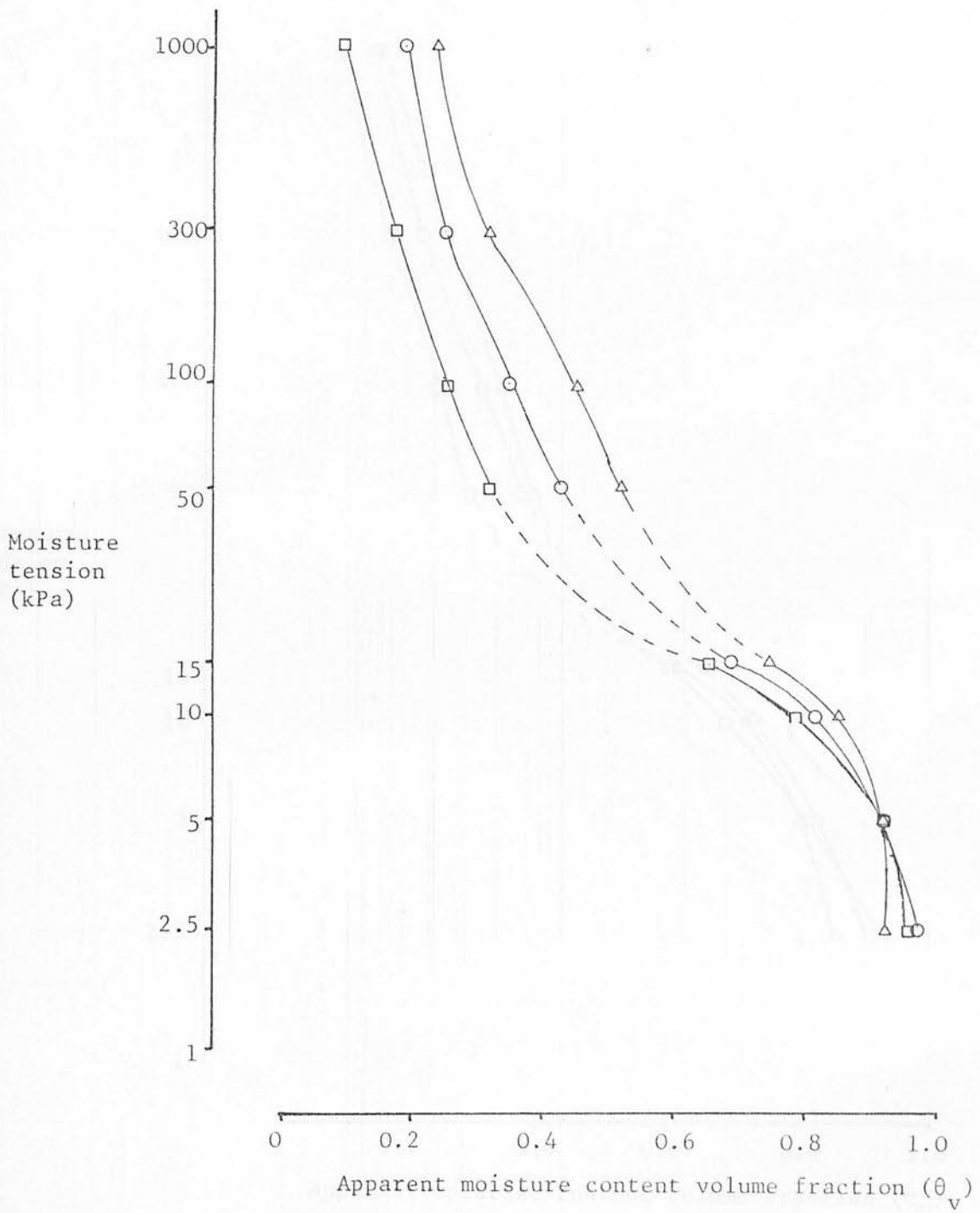


Fig.5.5 Moisture release curves for the OP site at depths of:-
 Δ - 0.2m, \circ -0.4m and \square -0.6m.

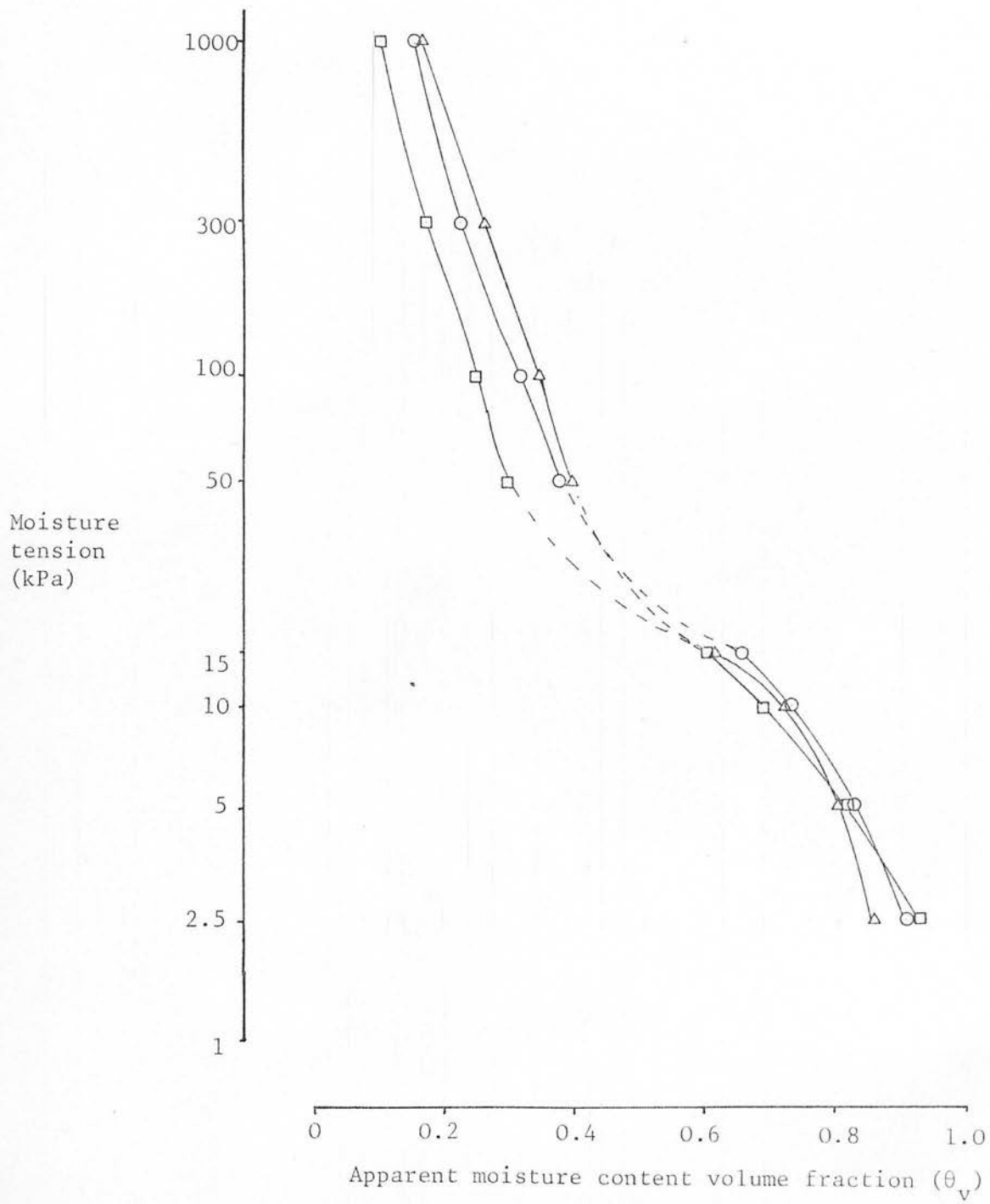


Fig.5.6 Moisture release curves for the SS site at depths of:-
 Δ - 0.2m, \circ -0.4m and \square -0.6m.

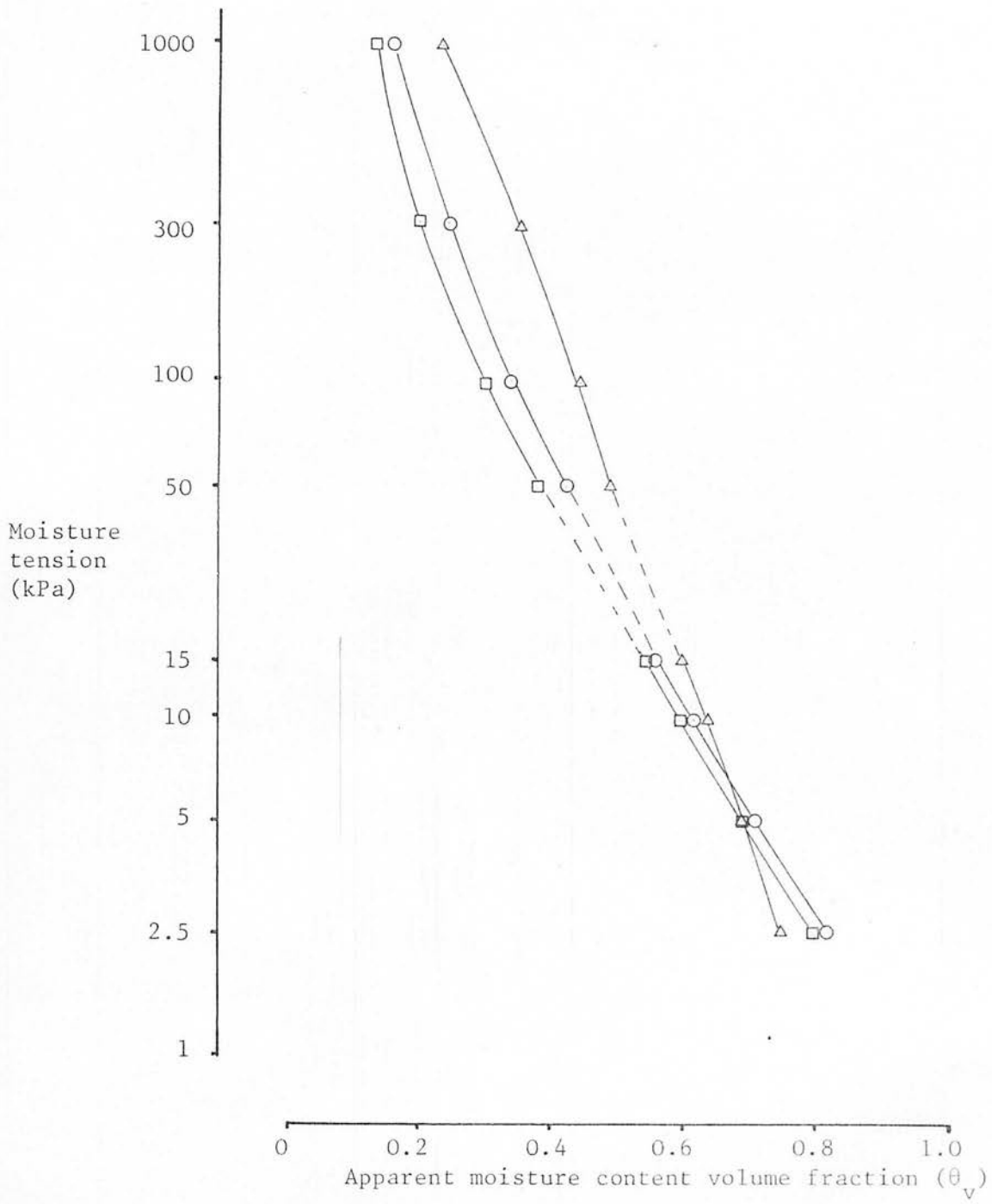


Fig.5.7 Moisture release curves for the LP site at depths:-
 Δ - 0.2m, \circ - 0.4m and \square - 0.6m.

the range 50-1000 kPa are the mean of 3 samples. The curves all display similar shapes and their positions over the moisture content range are also broadly similar. The LP site is possibly different here having lower moisture contents at low tensions than any of the other sites.

It would be unwise however, to draw any firm conclusions from these graphs because of the problem of shrinkage. For this reason it may prove valuable to look at the moisture content mass fractions (θ_m) as calculated by Equation (57), and how they vary with moisture tension. Figs 5.8 - 5.11 show the variation of θ_m with tension, and it becomes clear that the values obtained at low tensions for cores from 0.2m depth are considerably lower at each site than those from 0.4 and 0.6m depth. The values for θ_v did not show this, and it is most likely that this is a function of the higher dry bulk densities found at 0.2m depth, than at 0.4 and 0.6m depth. The bulk density, however, will also vary with the gravimetric moisture content, increasing as the peat shrinks with drying. To compensate for this and to calculate the true moisture content volume fraction, it is necessary to quantify the degree of shrinkage with moisture content (mass fraction).

Although no direct measurements of shrinkage were made as part of this study, unpublished data were obtained for Eddleston from Pyatt (personal communication, 1980). Fig. 5.12 is derived from these data and shows the volumes of three peat blocks as a fraction of their original volumes, at various moisture contents, obtained by allowing the blocks to dry at room temperature.

From Fig. 5.12 a mean volume fraction (V) can be read off for each moisture content mass fraction. This can be used to calculate the true moisture content volume fraction (θ_v') from the previously calculated θ_v , by the equation $\theta_v/V = \theta_v'$. A comparison between θ_v and θ_v' for a tension of 2.5 kPa is given in Table 5.7, for all sites and depths

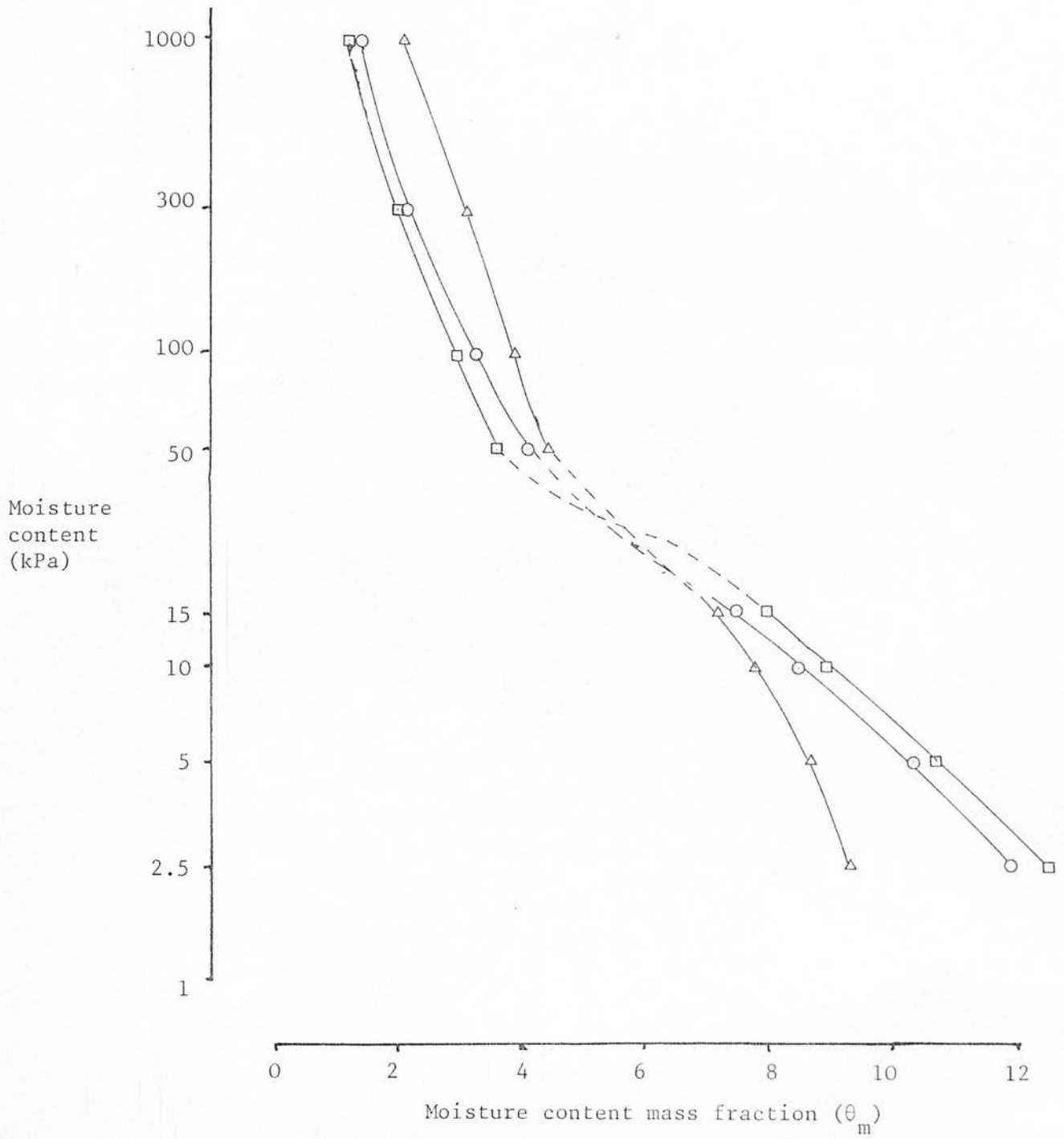


Fig.5.8 Moisture release curves (mass fractions) for the OV site at depths of:- Δ -0.2m, \circ -0.4m and \square -0.6m.

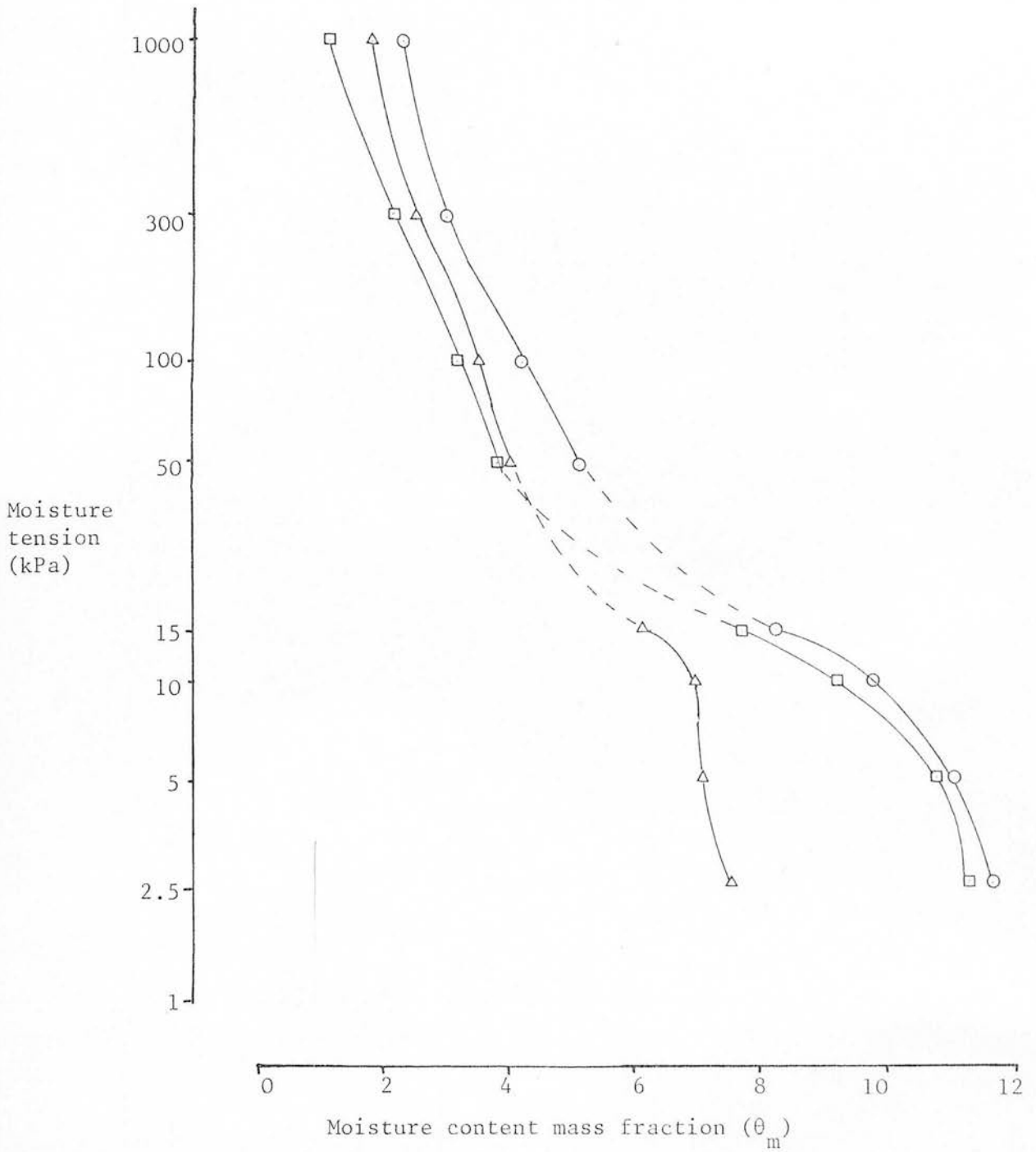


Fig.5.9 Moisture release curves (mass fractions) for the OP site at depths of: Δ -0.2m, O -0.4m and \square -0.6m.

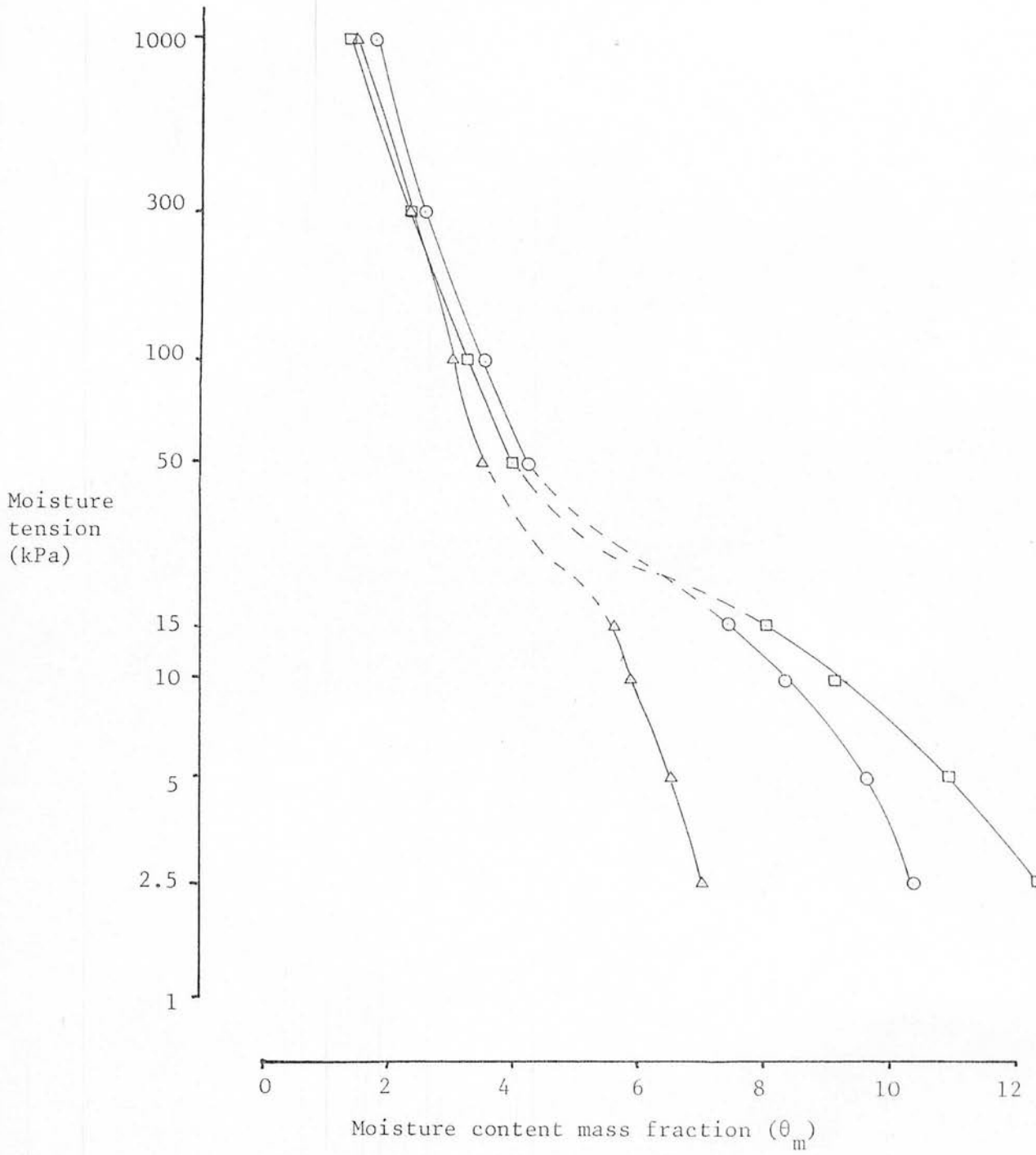


Fig.5.10 Moisture release curves (mass fractions) for the SS site at depths of: Δ -0.2m, \circ -0.4m and \square -0.6m.

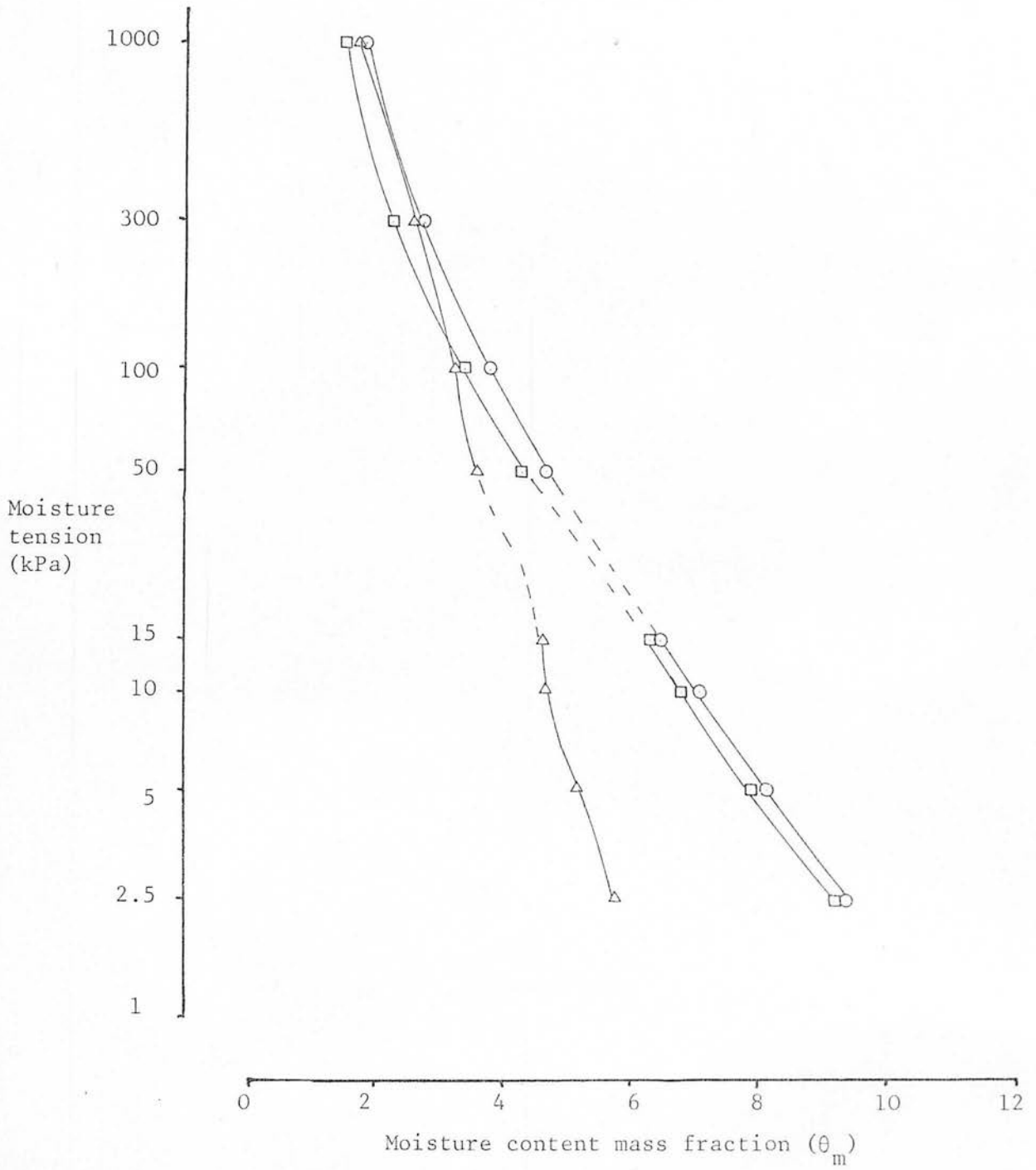


Fig.5.11 Moisture release curves (mass fractions) for the LP site at depths of : Δ -0.2m, \circ -0.4m and \square -0.6m.

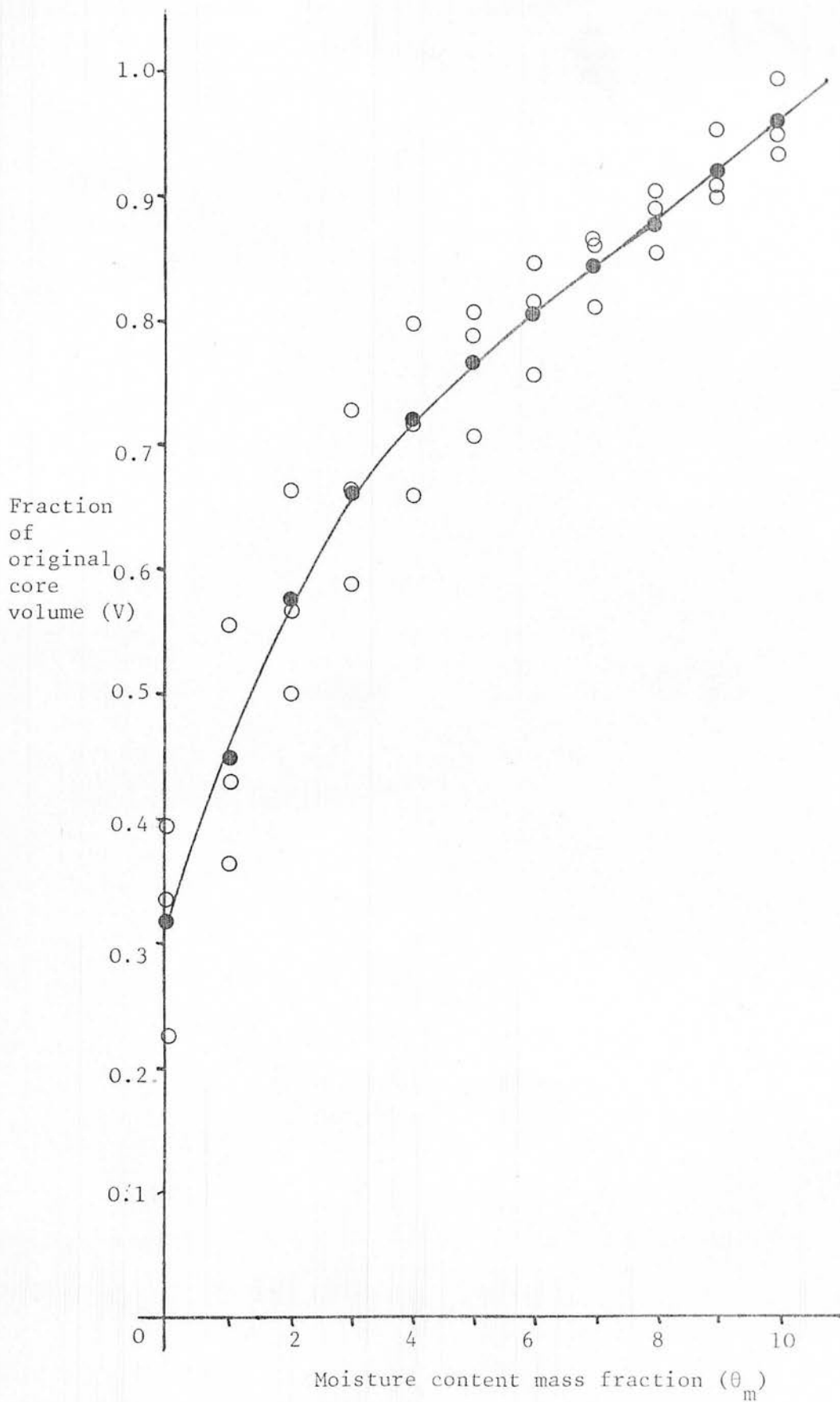


Fig.5.12 Volume of peat cores as a fraction of their original volume when naturated (V), for successive moisture contents (θ_m) on a drying cycle.

○ = values derived from the curves of actual cores,
 ● = means of derived values at set values of θ_m .

measured. It can be seen from this that fairly close agreement is obtained for all sites (except LP) at depths of 0.4 and 0.6m, indicating that the curve displayed in Fig. 5.12 is adequate to describe the moisture content/shrinkage characteristics for peat at these depths. The tension of 2.5 kPa was chosen as there should be little or no shrinkage at this tension and close agreement between θ_v and θ_v' expected. However, at 0.2m depth θ_v' proves to be a large overestimation, in some cases (OV, OP and SS) impossibly high. This error is caused by the dry bulk density at 0.2m depths being greater in all sites than the rather uniform density across the sites at lower depths (Table 5.1), which will alter θ_m for different values of V . To correct for this, new shrinkage curves need to be constructed for peat of different dry bulk density. To do this it was assumed that the general shape of the curve would remain the same. A transformation of the scales of Fig. 5.12 to \log_{10} , gives Fig. 5.13 for the mean data points, which is described by Equation (63):

$$\log_{10} V = -0.34 + 0.33 \log_{10} \theta_m \quad \dots (63)$$

This gives Equation (64) to describe the curve in Fig. 5.12.

$$V = 0.45 \theta_m^{0.33} \quad \dots (64)$$

This curve will only apply to peat of dry bulk density 0.09 kg dm^{-3} when fully saturated with $\theta_v' = 0.941$. θ_v' can be calculated as being equivalent to the total pore space from Equation (65), as both the dry bulk density (b_{ρ_s}) and true density (t_{ρ}) are known.

$$\theta_v' = 1 - \frac{b_{\rho_s}}{t_{\rho}} \quad \dots (65)$$

This can be done for the other dry bulk densities recorded in all sites at 0.2 depth (t_{ρ} is constant), and from θ_v' and b_{ρ_s} , θ_m can be calculated according to Equation (66).

$$\theta_m = \frac{\theta_v'}{b_{\rho_s}} \cdot \rho_w \quad \dots (66)$$

Table 5.7 Mean moisture content volume fraction (θ_v) as calculated for the original core volume, and re-calculated for taking into account peat shrinkage (θ_v'), for 2.5 kPa moisture tension.

Site	Depth (m)	θ_v	θ_v'
OV	0.2	0.93	0.99
	0.4	0.91	0.91
	0.6	0.88	0.88
OP	0.2	0.93	1.08
	0.4	0.97	0.97
	0.6	0.96	0.95
SS	0.2	0.86	1.00
	0.4	0.91	0.93
	0.6	0.93	0.93
LP	0.2	0.75	0.93
	0.4	0.82	0.86
	0.6	0.79	0.85

Table 5.8 The moisture content mass fraction (θ_m), total pore volume fraction (θ_v') and dry bulk density (ρ_s^b)(kg.dm⁻³), of peat cores when fully saturated

Site	Depth (m)	ρ_s^b (kg.dm ⁻³)	θ_v'	θ_m
OV	0.2	0.10	0.91	9.14
OP	0.2	0.13	0.91	7.00
SS	0.2	0.12	0.91	7.60
LP	0.2	0.14	0.91	6.49
All	0.4 & 0.6	0.09	0.94	10.45

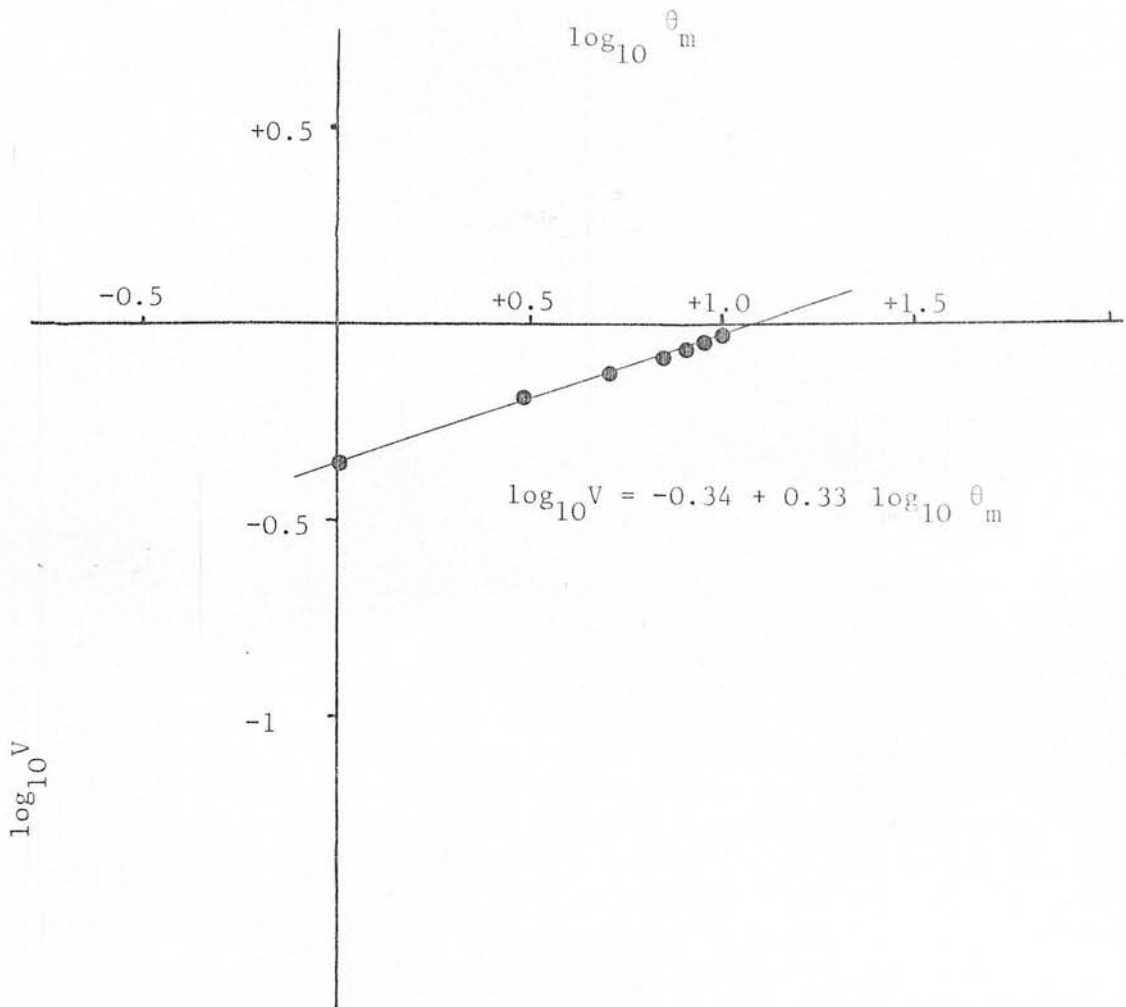


Fig.5.13 The relationship between the \log_{10} volume fraction (V) of shrinking peat core and \log_{10} of corresponding moisture content mass fraction (θ_m). The antilog of the above relationship, describes the curve in Fig.5.12, i.e.
 $V = 0.45 \theta_m^{0.33}$

Table 5.9 Shrinkage relationship of a peat core fraction of its original volume (V), when at moisture content mass fraction (θ_m) and dry bulk density (ρ_s)(kg dm⁻³).

Site	Depth (m)	ρ_s	Shrinkage equation
All	0.4 & 0.6	0.090	$V = 0.45 \theta_m^{0.33}$
OV	0.2	0.100	$V = 0.48 \theta_m^{0.33}$
OP	0.2	0.129	$V = 0.53 \theta_m^{0.33}$
SS	0.2	0.117	$V = 0.51 \theta_m^{0.33}$
LP	0.2	0.136	$V = 0.54 \theta_m^{0.33}$

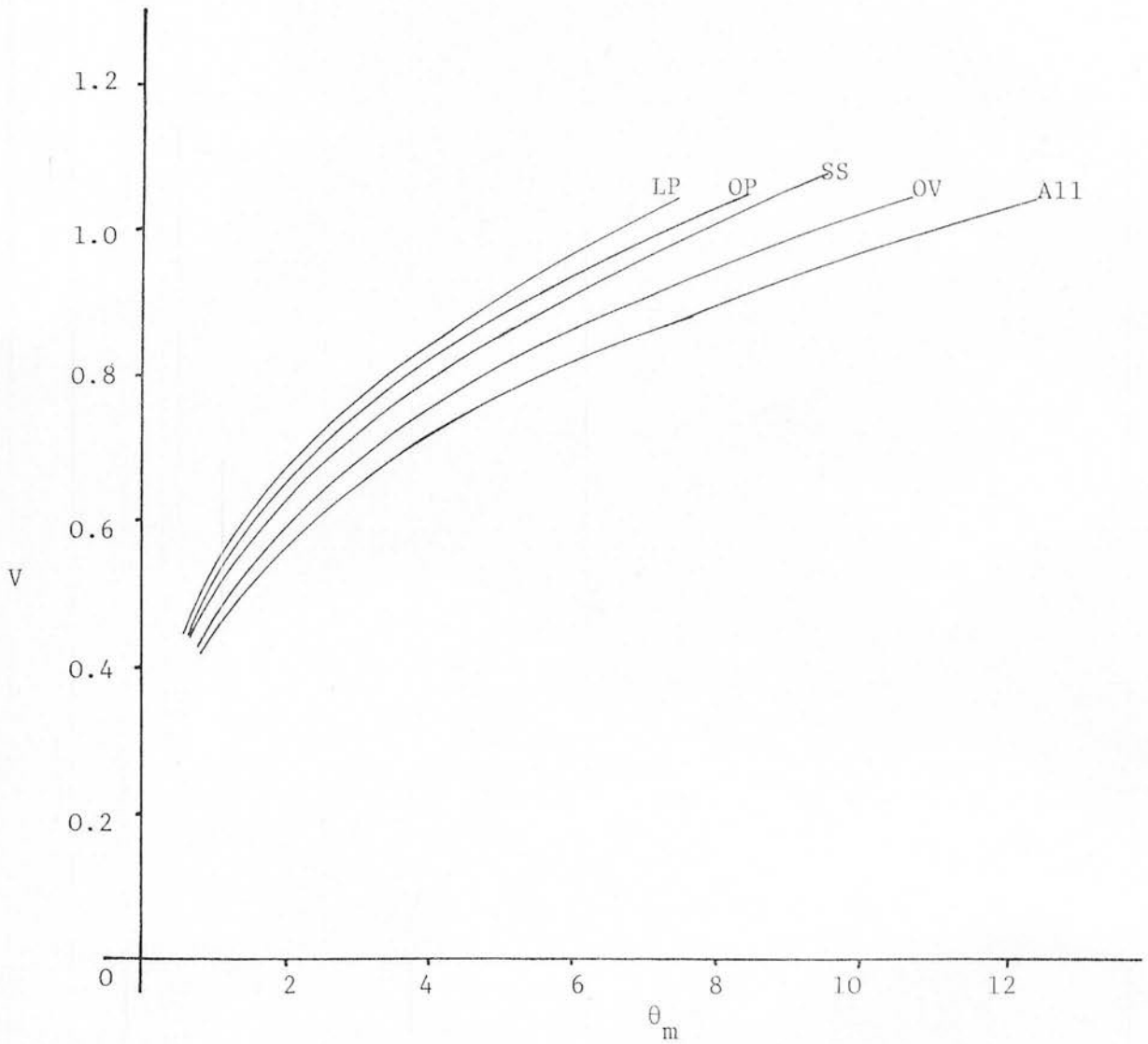


Fig.5.14 Shrinkage curves of fraction of saturated volume (V) against moisture content mass fraction (θ_m) for peat at 0.2m depth in the sites indicated, and for all sites at depths of 0.4 and 0.6m. The curves are those given in Table 5.9.

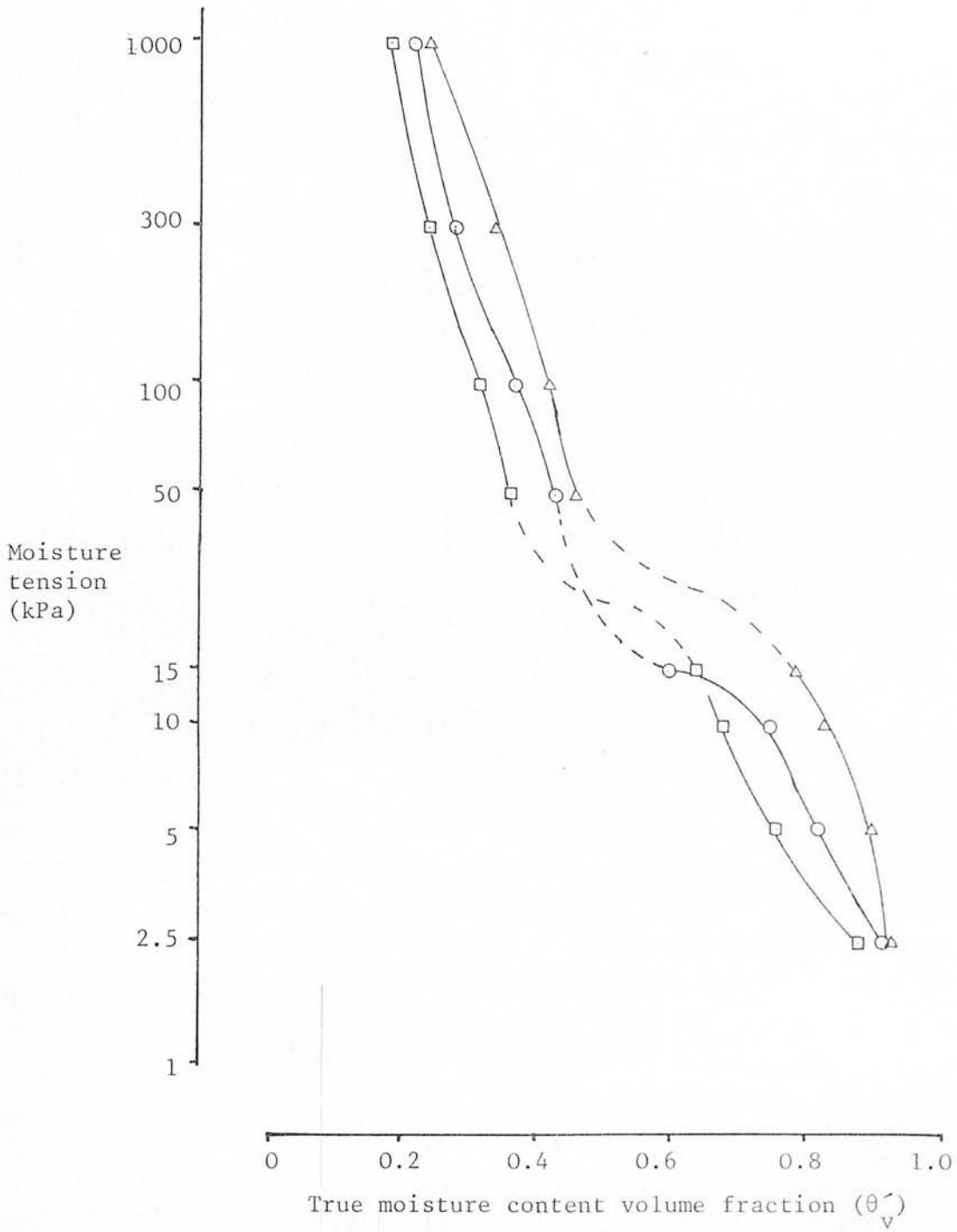


Fig.5.15 Amended moisture release curves for the OV site at depths of:- Δ -0.2m, \circ -0.4m and \square -0.6m.

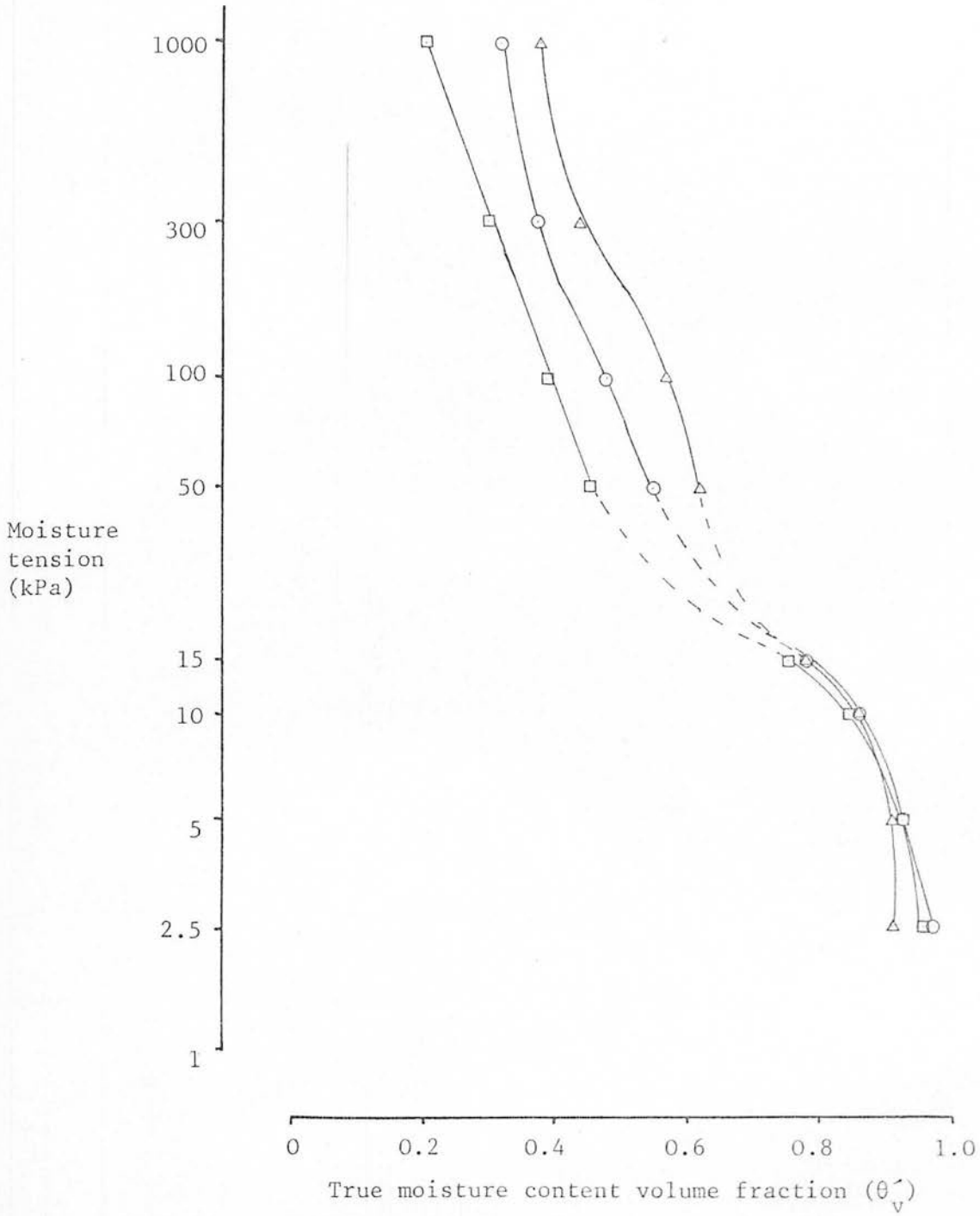


Fig.5.16 Amended moisture release curves for the OP site at depths of: Δ -0.2m, \circ -0.4m, and \square -0.6m.

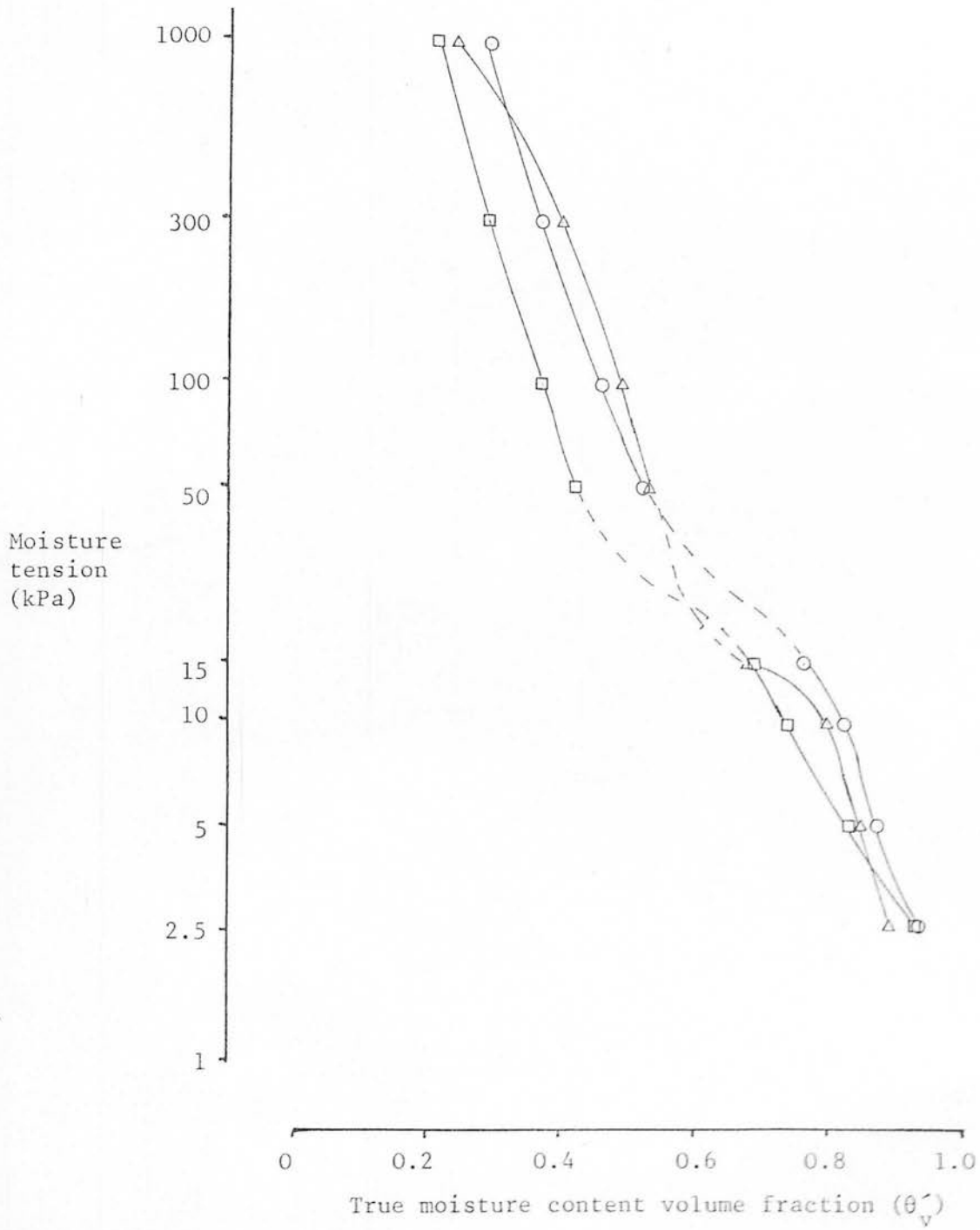


Fig. 5.17 Amended moisture release curves for the SS site at depths of:- Δ -0.2m, \circ -0.4m and \square -0.6m.

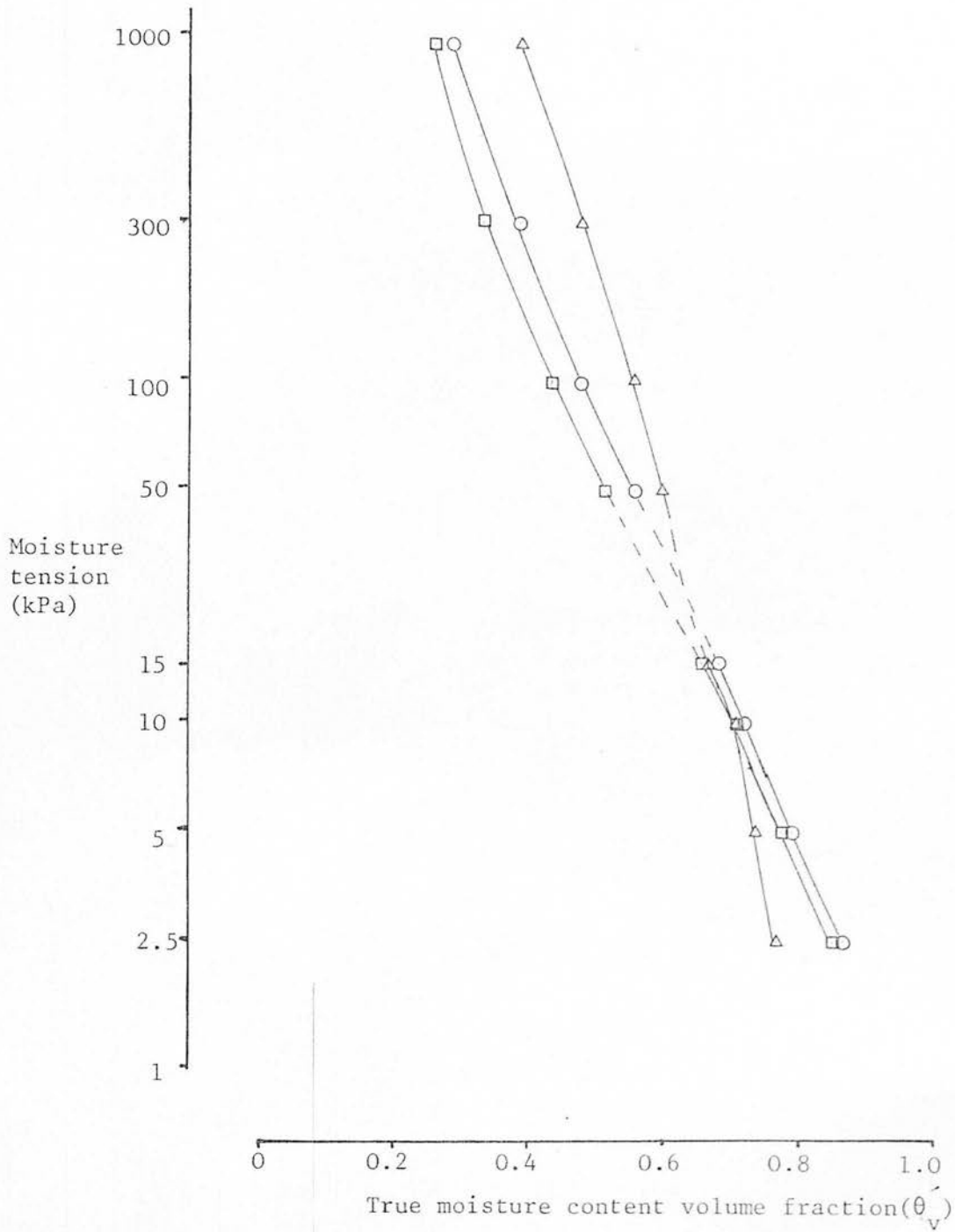


Fig.5.18 Amended moisture release curves for the LP site at depths of: Δ -0.2m, \circ -0.4m, and \square -0.6m.

θ_m in this case is the moisture content mass fraction when the peat is fully saturated, and is given in Table (5.8) together with the dry bulk density (ρ_s^b) and total pore space volume fraction (θ_v') that it was calculated from, for each site at 0.2m depth.

Using these figures as θ_m when $V = 1$, then assuming the shape of the curve remains constant (i.e. θ_m is always raised to the power 0.33), Equation (64) converts to those given in Table 5.9 for each new dry bulk density. This gives rise to the new shrinkage curves plotted with the original in Fig. 5.14.

Using these curves to obtain V , it is possible to calculate θ_v for the moisture release curves in Figs. 5.4 - 5.7 and these are given in Figs. 5.15-5.18. These moisture release curves must be considered the best estimate of the true moisture release characteristics, though some caution must be used in their interpretation as they are derived values from two other estimates.

The most noticeable feature of these curves is their general similarity in position and shape for all depths in the OP, LP and SS sites. The undisturbed OV site is different in that the curve for 0.2m depth is displaced relative to the others. A comparison of the 0.4m and 0.6m depth curves of the OV site with curves from the other sites, reveals that they are in a similar position. Therefore it must be concluded that at 0.2m depth less moisture is released for a given tension (more noticeable at higher tensions), rather than there being any variation of the peat at greater depths.

5.3 CONCLUSIONS

Peat bulk density has in the past been correlated with fibre content and degree of decomposition (Boelter, 1969) over different peat types. However, in the present data there is little suggestion of any relationship between the limited range of dry bulk density figures and

coarse fibre contents or amorphous solid contents within the same peat type. Bulk density is broadly similar at 0.4 and 0.6m depth over all sites, and at 0.2m depth where bulk densities were found to be higher, no trend was observed that reflects the lower coarse fibre contents found in the open sites compared with the planted sites. Nor were bulk densities noticeably different in the less fibrous OP site at any depth.

Another explanation for increased bulk density at 0.2m has therefore to be found. It was mentioned when discussing fibre content that irreversible drying can lead to the rearrangement of fibres that masks any increase in amorphous solids there may have been. The fact that this drying is irreversible means that, even on rewetting, more particles will occupy unit volume than originally. This itself would lead to higher dry bulk density and is the most likely explanation of the observed trends in bulk density and fibre content, in the data.

The alteration in the moisture release characteristic curves for samples from 0.2m depth at the drained sites, compared to that for the unaltered OV sites, is a function of this irreversible drying. The contention that the amorphous solid fraction has concreted into larger units in the planted sites, is supported by the moisture release curves. In the OV and OP sites at 0.2m depth there is slightly less moisture released at higher tensions than in the LP and SS, and it will be noticed in Table 5.4 that these have a higher amorphous solid fraction. This is as one would expect, as a higher proportion of fine particles gives a high volume of fine pores that do not drain readily. The fact that the LP and SS sites do not behave in the same manner suggests that the fine particles do not re-wet and that some irreversible shrinkage has indeed occurred.

It should not be assumed that this irreversible shrinkage is of the order displayed in the shrinkage curves given in Fig. 5.14, as

these are curves of an initial drying cycle for an unrestrained peat block and therefore to some extent reversible. Nor should shrinkage upon drying in the field be linked too closely with these curves, as they are derived from shrinkage occurring in three dimensions, whereas in the field only one (the vertical) is ^{initially} available. For this reason the moisture release characteristic curves (in Figs 5.15-5.18) are an overestimation of θ_v' for the same moisture tensions in the field.

The main point to come out of this survey is that the presence of a crop has sufficiently dried out the surface peat to cause permanent changes in the physical properties of the peat. The results are an increase in dry bulk density but at the same time a decrease in the moisture retention properties due to rearrangement of the fibre matrix and hence pore space. This should give an improved aeration regime and, in extreme cases of shrinkage, large cracks in the surface peat (Pyatt, 1976). Surface drainage of the peat has proved insufficient on its own to promote these changes to the same extent as planting, but evidence of increased humification is found in the fibre size analysis and the increase in dry bulk density. Fibre size analysis, however, has proved to be insufficient for monitoring the degree of humification in drying peat, as it is confounded by the effects of irreversible shrinkage.

6. FALSTONE FIELD EXPERIMENTS

6.1 MOISTURE REGIME

6.1.1. 1978 DATA

The weekly gross rainfall for 1978 is given in Fig.6.1, and the values shown are the mean of all the collectors in the unplanted sites (no significant differences were observed between sites). Some of the incident rainfall does not reach the ground under the tree canopy. This "interception loss" is due to moisture temporarily retained on the canopy evaporating back into the atmosphere. For a closed canopy the loss typically comprises about 30 percent of the total precipitation of the year, but for short periods of light rain the loss may be total. The rainfall that does reach the forest floor comprises both throughfall and stemflow. These have been combined in Table 6.1 to give a net rainfall under the forest canopy for each species on each cultivation type, for three month intervals. There is little difference in the interception loss between the two species (all sites had closed canopies), but that loss is a higher proportion of the rainfall during the drier summer months.

The effect of interception loss on the soil water regime is considerable. Figs. 6.2 and 6.3 show the mean depth to the water table under each species on the two cultivation types. The water table under the crop is always lower than in the unplanted sites (mean of all open sites) but the difference is greater during the summer months. This is mainly due to interception loss, but transpiration during the summer months may account for some of the difference, as the grassland sites are sheltered on all sides by the forest, and so transpiration may be less than from the tree canopy. The planted sites are slower to recover to their winter levels than the open sites, as evidenced by the lag of a week or two in the upward slope of the graphs during July, August and September. The depth to the water table is broadly similar under the

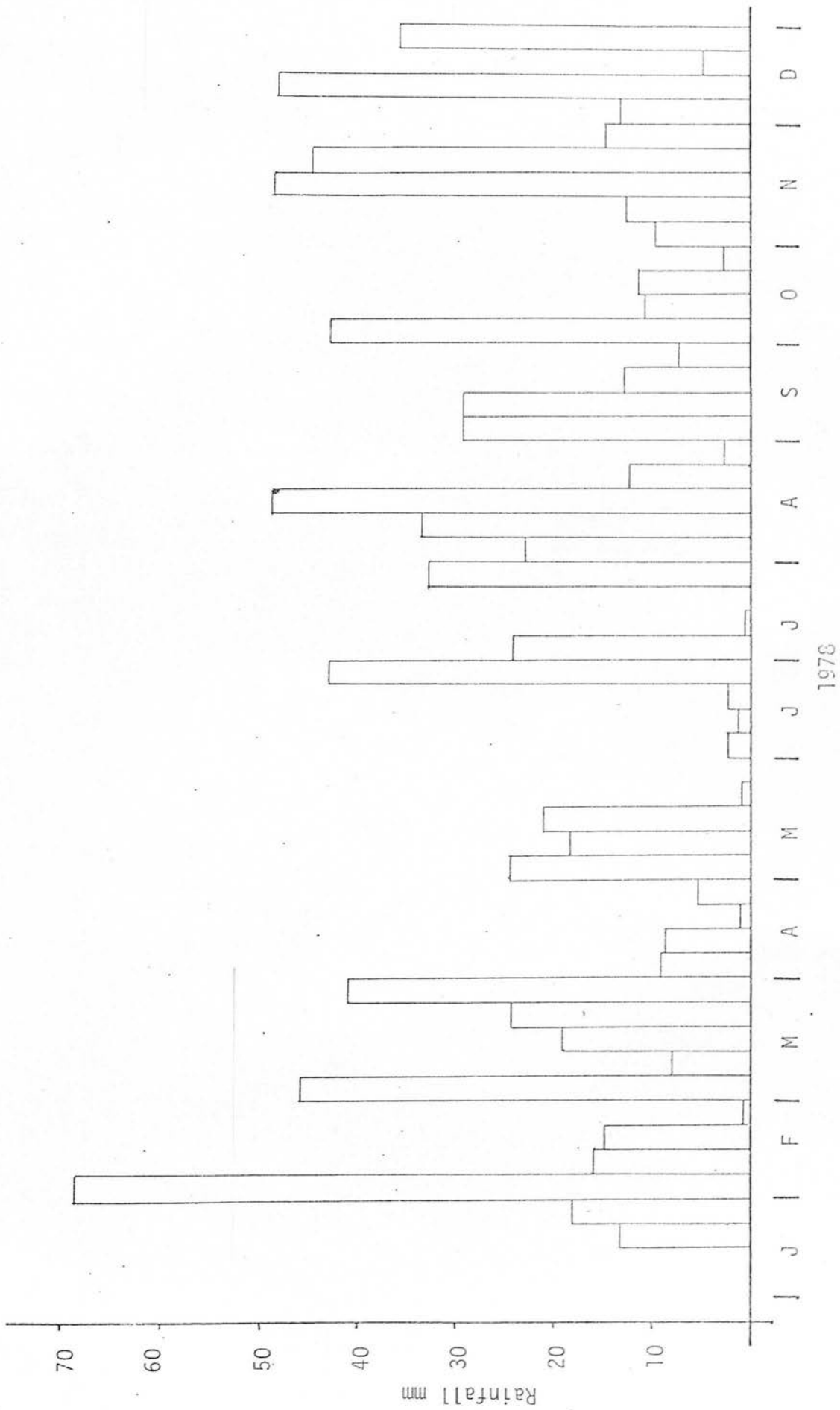


Fig.6.1 Weekly rainfall data for 1978 at Falstone sites.

Table 6.1 Total and net rainfall (mm), and interception loss (mm)
for the periods of the year (1978) shown, with the volume
fractions of total rainfall given in parenthesis

Period		Rainfall or Interception loss (mm)			
		<u>Turf-planted</u>		<u>Ploughed</u>	
		SS	LP	SS	LP
Jan	Total rainfall	301.80	301.80	301.80	301.80
-	Net rainfall	216.66(0.71)	225.25(0.75)	217.98(0.72)	230.73(0.76)
Mar.	Interception loss	85.14(0.28)	76.55(0.25)	83.82(0.28)	71.07(0.24)
Apr.	Total rainfall	137.90	137.90	137.90	137.90
-	Net rainfall	81.31(0.59)	78.74(0.57)	92.56(0.67)	80.91(0.58)
June	Interception loss	56.59(0.41)	59.16(0.43)	51.34(0.33)	56.99(0.41)
July	Total rainfall	258.30	258.30	258.30	258.30
-	Net rainfall	168.97(0.65)	166.75(0.65)	176.15(0.68)	162.66(0.63)
Sept	Interception loss	89.33(0.35)	91.55(0.35)	82.15(0.32)	95.64(0.37)
Oct.	Total rainfall	*	*	302.30	302.30
-	Net rainfall			239.01(0.79)	234.00(0.78)
Dec	Interception loss			63.29(0.21)	68.30(0.23)
Year	Total rainfall			1000.30	1000.30
1978	Net rainfall			725.72(0.73)	708.30(0.71)
	Interception loss			280.60(0.28)	292.00(0.29)

* - No data available for this period.

LP:- Pinus contorta

SS:- Picea sitchensis

1978

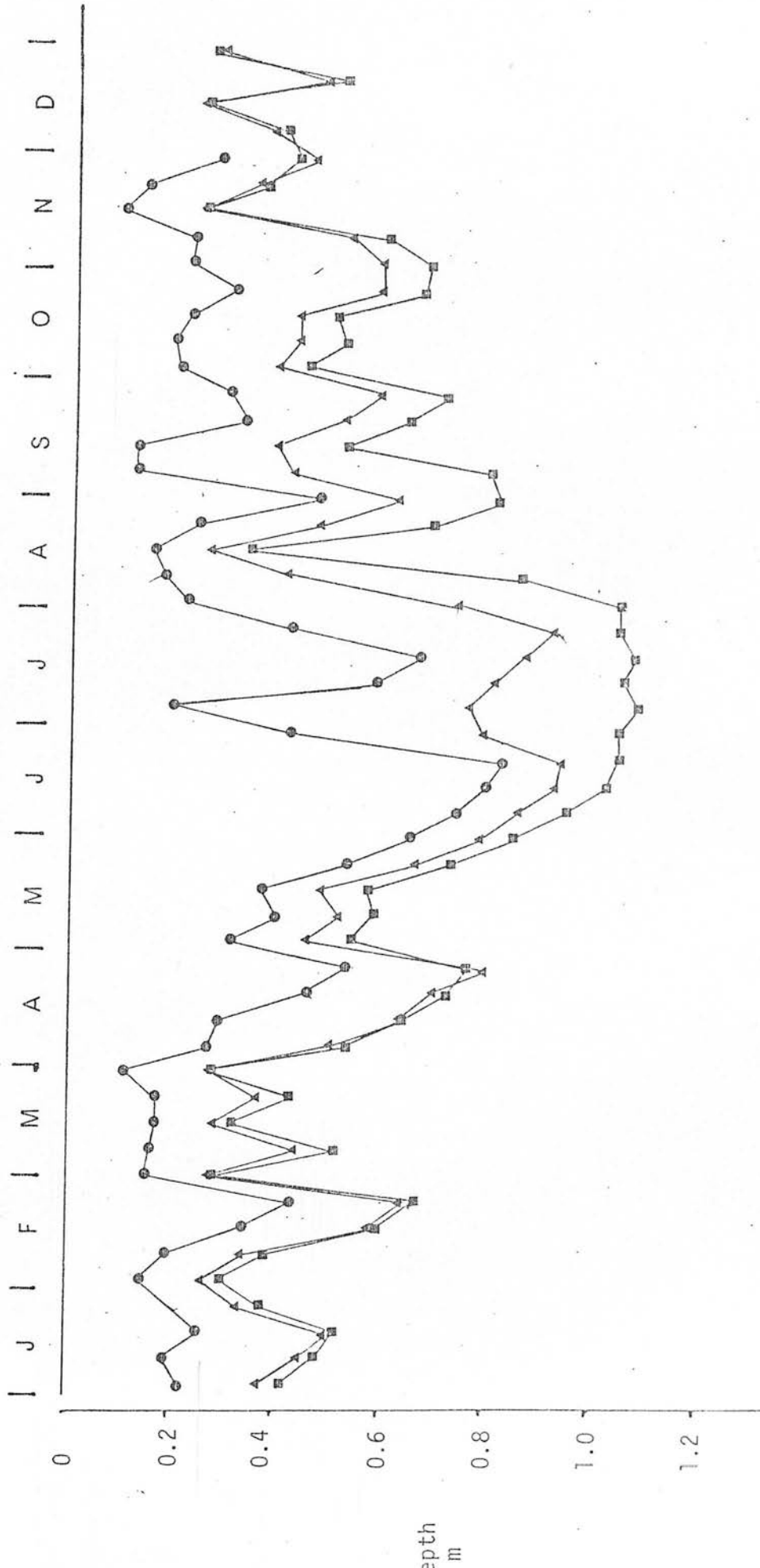


Fig.6.2 Mean depth to the water table for 1978 in sites:- ● - 1,2,7 and 8 (*Molinia caerulea*),
 ▲ - 3 and 4 (*Picea sitchensis*) and ■ - 5 and 6 (*Pinus contorta*).

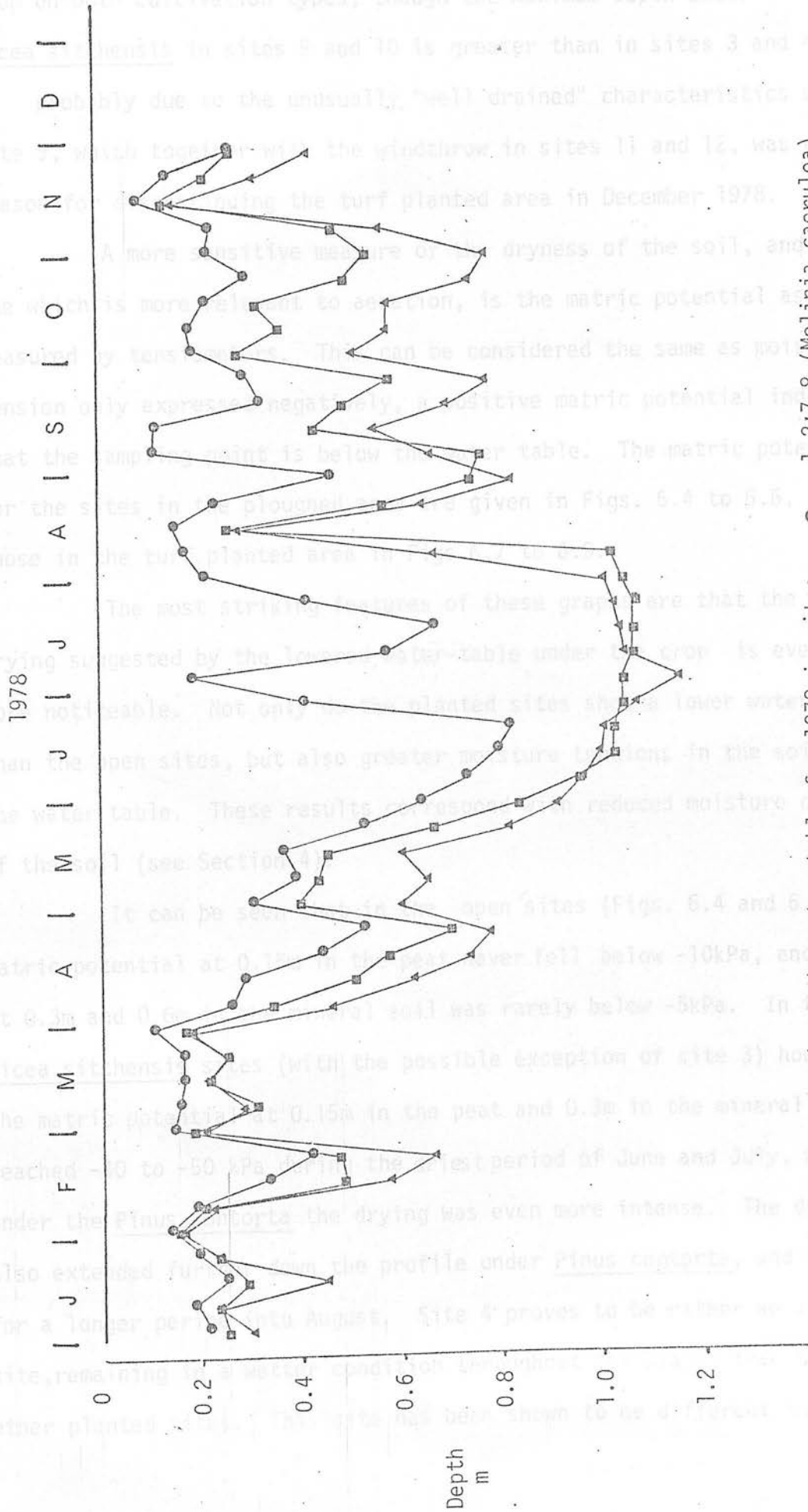


Fig.6.3 Mean depth to the water table for 1978 in sites:- ● - 1,2;7,8 (*Molinia caerulea*), ▲ - 9 and 10 (*Picea sitchensis*) and ■-11 and 12 (*Pinus contorta*)

crop on both cultivation types, though the maximum depth under Picea sitchensis in sites 9 and 10 is greater than in sites 3 and 4. This is probably due to the unusually "well drained" characteristics of site 9, which together with the windthrow in sites 11 and 12, was a reason for discontinuing the turf planted area in December 1978.

A more sensitive measure of the dryness of the soil, and one which is more relevant to aeration, is the matric potential as measured by tensiometers. This can be considered the same as moisture tension only expressed negatively, a positive matric potential indicating that the sampling point is below the water table. The matric potentials for the sites in the ploughed area are given in Figs. 6.4 to 6.6, and those in the turf planted area in Figs. 6.7 to 6.9.

The most striking features of these graphs are that the greater drying suggested by the lowered water-table under the crop is even more noticeable. Not only do the planted sites show a lower water-table than the open sites, but also greater moisture tensions in the soil above the water table. These results correspond with reduced moisture contents of the soil (see Section 4).

It can be seen that in the open sites (Figs. 6.4 and 6.7) the matric potential at 0.15m in the peat never fell below -10kPa, and at 0.3m and 0.6m in the mineral soil was rarely below -5kPa. In the Picea sitchensis sites (with the possible exception of site 3) however, the matric potential at 0.15m in the peat and 0.3m in the mineral soil reached -40 to -50 kPa during the driest period of June and July, while under the Pinus contorta the drying was even more intense. The drying also extended further down the profile under Pinus contorta, and lasted for a longer period into August. Site 4 proves to be rather an anomalous site, remaining in a wetter condition throughout the season than the other planted sites. This site has been shown to be different in other

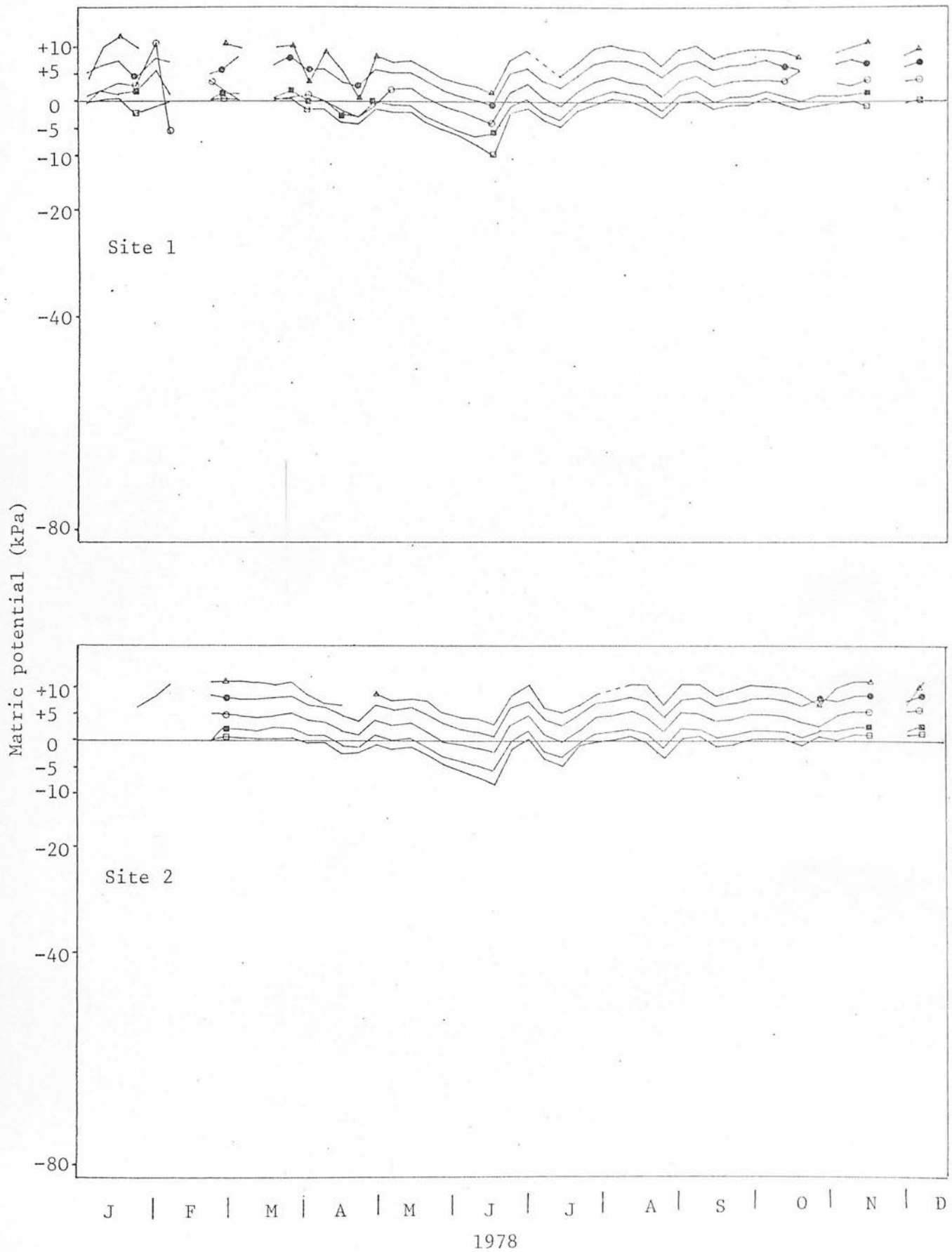


Fig.6.4 Matrix potentials for 1978 in the *Molinia caerulea* sites at depths of:- \square -0.15m, \blacksquare -0.30m, \circ -0.60m, \bullet -0.90m, \triangle -1.20m.

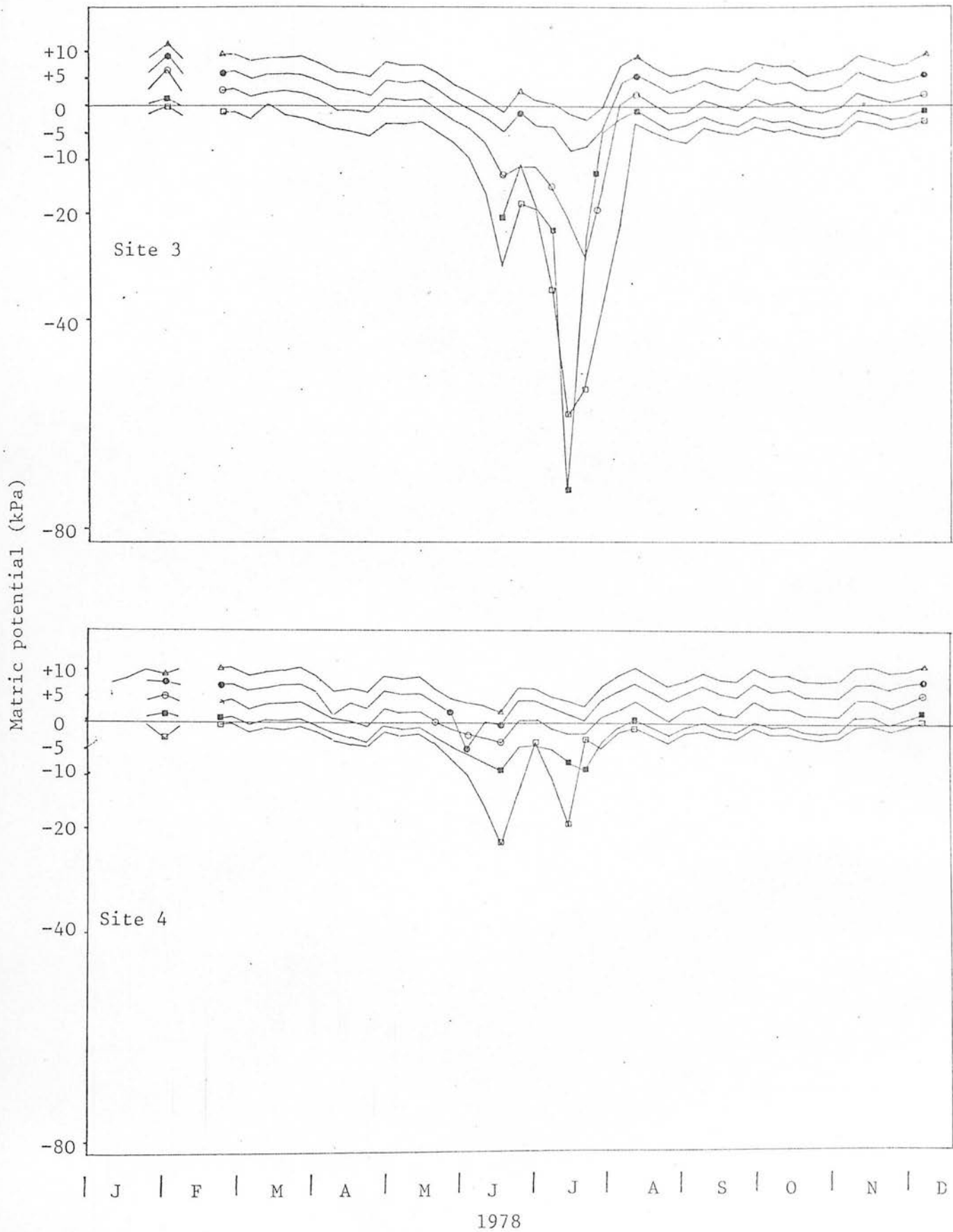


Fig.6.5 Matrix potentials for 1978 in the *Picea sitchensis* sites at depths of:- \square -0.15m, \blacksquare -0.30m, \circ -0.60m, \bullet -0.90m, \triangle -1.20m.

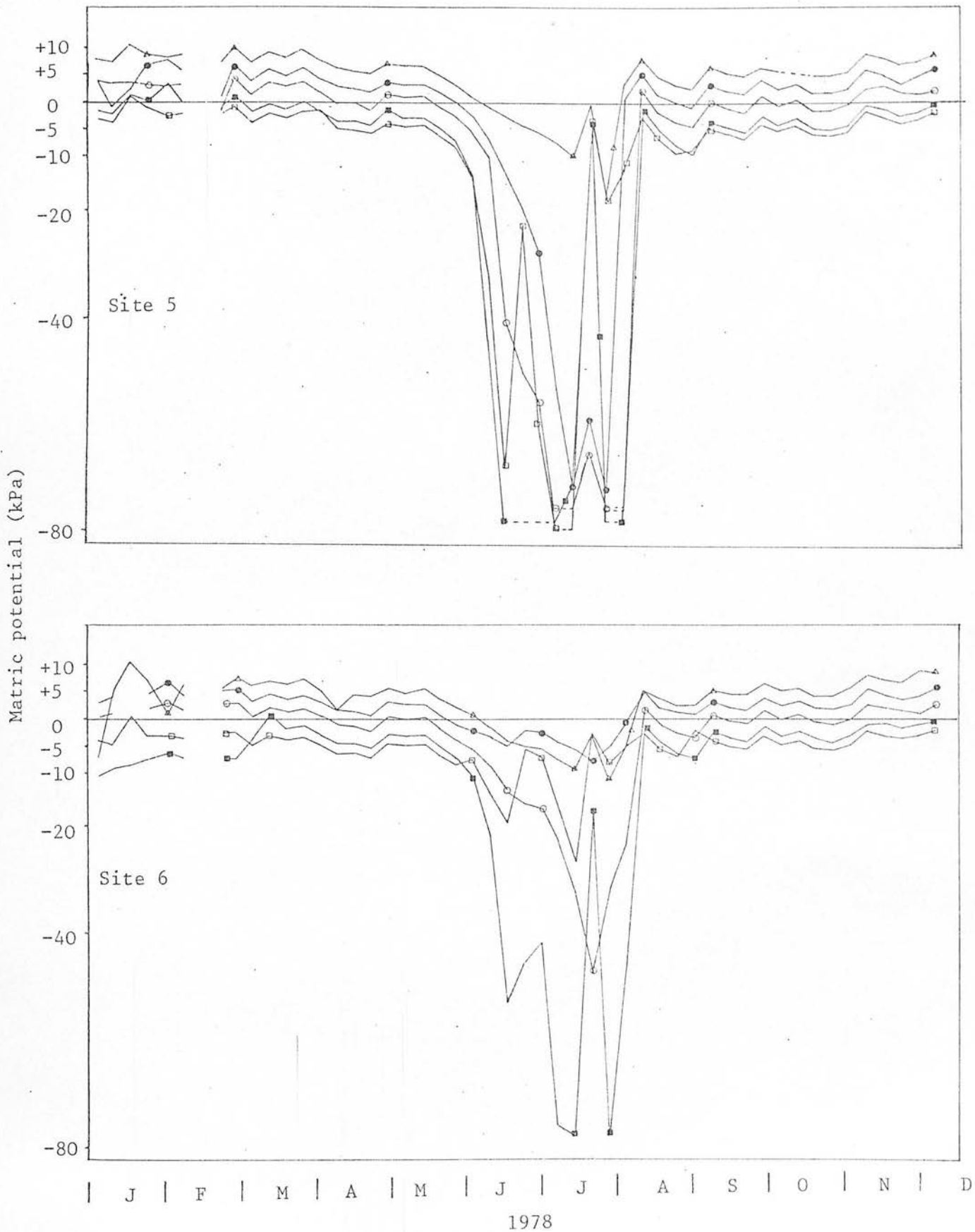


Fig.6.6 Matric potentials for 1978 in the *Pinus contorta* sites at depths of:- \square -0.15m, \blacksquare -0.30m, \circ -0.60m, \bullet -0.90m, \triangle -1.20m.

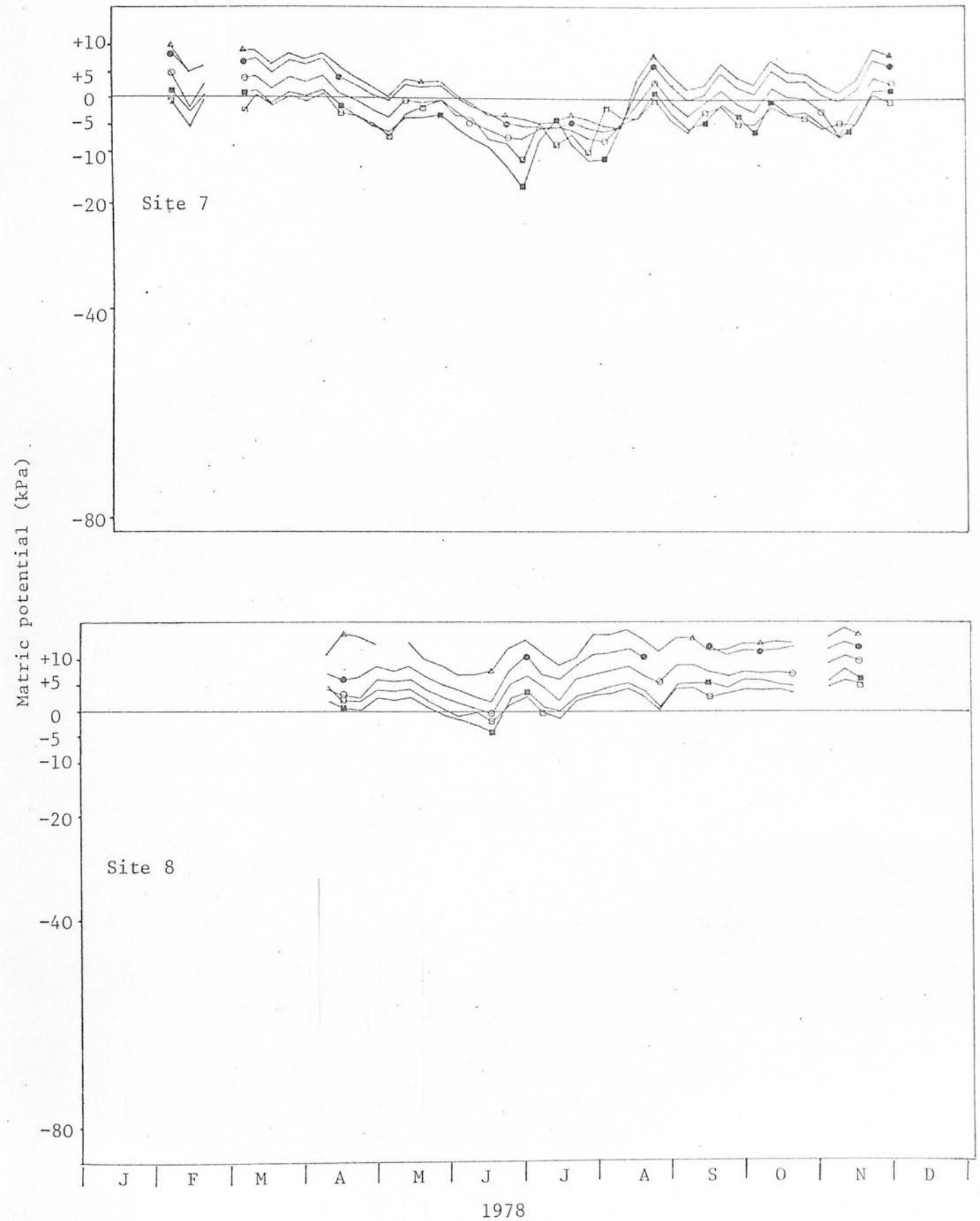


Fig.6.7 Matrix potentials for 1978 in the *Molinia caerulea* sites at depths of:- \square -0.15m, \blacksquare -0.30m, \circ -0.60m, \bullet -0.90m, \triangle -1.20m.

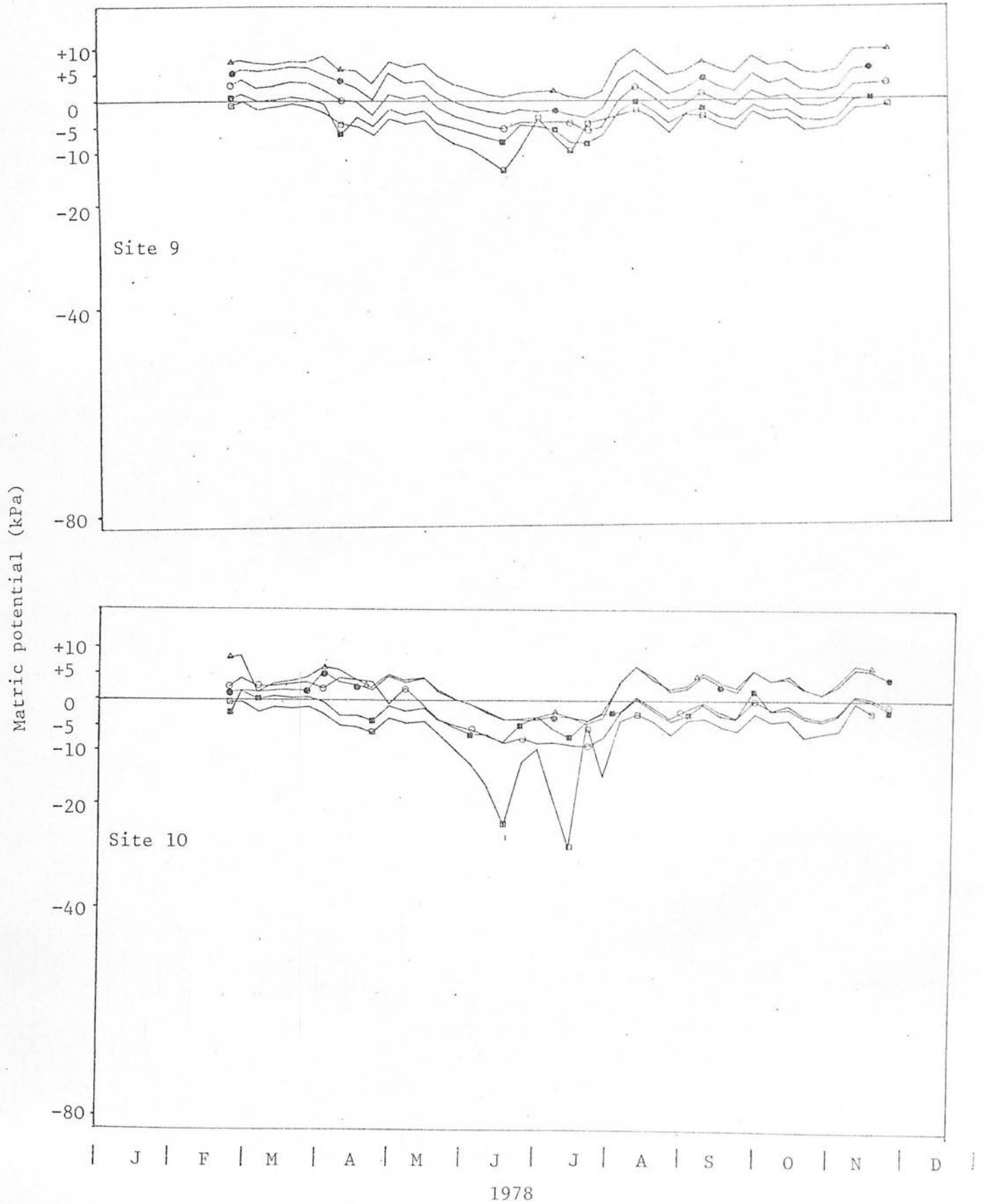


Fig.6.8 Matric potentials for 1978 in the *Picea sitchensis* sites at depths of:- \square -0.15m, \blacksquare -0.30m, \circ -0.60m, \bullet -0.90m, \triangle -1.20m.

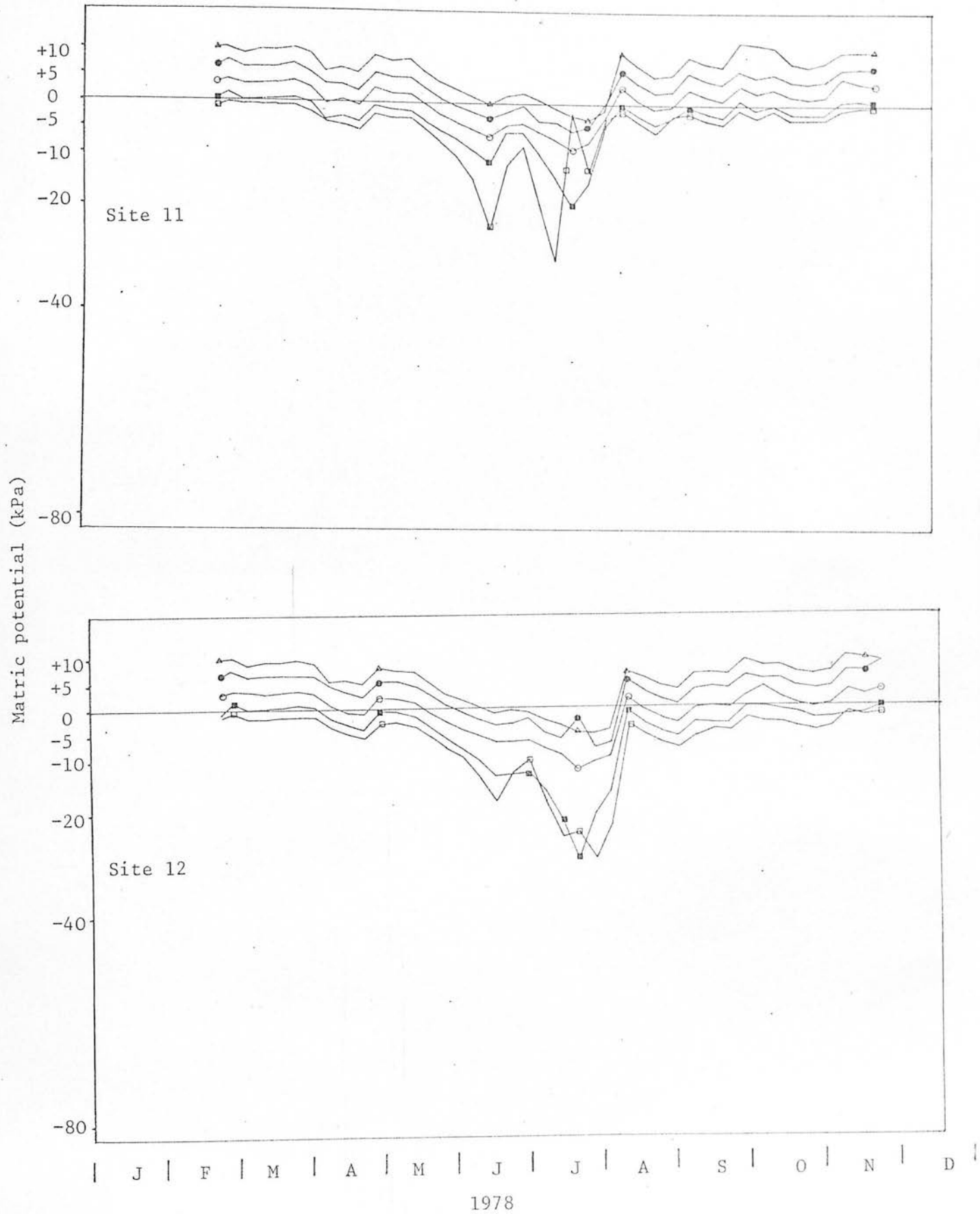


Fig.6.9 Matrix potentials for 1978 in the *Pinus contorta* sites at depths of:- \square -0.15m, \blacksquare -0.30m, \circ -0.60m, \bullet -0.90m, Δ -1.20m.

physical details, notably a deeper peat layer (see Section 4). Another noteworthy feature is that during dry periods in the summer, surface horizons in the soil can be in a wetter condition than deeper layers, as rain water drains down the profile (Fig. 6.9). It is this phenomenon that gives rise to the crossing of lines for different depths as the soil rewets at the end of the season.

The data for the turf-planted sites (Figs. 6.7 to 6.9) show that while conforming to the general trends between species displayed in the ploughed sites, all were generally wetter throughout the profile, even though the water-tables descended to similar depths. It is possible that these sites may have been receiving run-off water from an adjacent area (Pyatt, pers.comm.).

The matric potentials data corresponding to the period of aeration sampling (given in Section 2) were analysed statistically by an analysis of variance (Table 6.2). There are many significant variance ratios, partly due to the large number of degrees of freedom for the residual variance, and so only the highest ratios are examined further. Tables of means are presented (Tables 6.3 and 6.4) together with the standard errors of differences between means (s.e.d), to exhibit the nature of the variation between treatments indicated by the analysis as being most significant.

The most significant source of variance was seen to be that between species, and mainly due to the open sites being generally wetter than sites under either tree species. Species interaction with depth and cultivation type also gave significant variation, and it can be seen from Tables 6.3 and 6.4 that Pinus contorta sites had lower mean matric potentials than Picea sitchensis sites. Depth was the next largest single source of variance, showing not only an increase in matric potentials down the profile, but also the previous observation that the peat layer was often at a higher matric potential than the underlying

Table 6.2 Analysis of variance of Falstone Matrix potential data (m bar) for 1978

Source of Variation	DF	MS	VR
Cultivation	1	351659	120.58 **
Species	2	851959	292.13 **
Replicate	1	310877	106.59 **
Depth	3	548230	187.98 **
Time	26	163153	55.94 **
Cultivation Species	2	402412	137.98 **
Cultivation Replicate	1	141673	48.57 **
Species Replicate	2	3896	1.33
Cultivation Depth	3	50072	17.16 **
Species Depth	6	30776	10.55 **
Replicate Depth	3	1719	0.58
Cultivation Time	26	33742	11.57 **
Species Time	52	48708	16.70 **
Replicate Time	26	15314	5.25 **
Depth Time	78	6440	2.20 **
Cultivation Species Replicate	2	186765	64.04 **
Cultivation Species Depth	6	31354	10.75 **
Cultivation Replication Depth	3	3707	1.27
Species Replication Depth	6	8969	3.07 **
Cultivation Species Time	52	24031	8.24 **
Cultivation Replication Time	26	18561	6.36 **
Species Replication Time	52	5445	1.86 **
Cultivation Depth Time	78	5793	1.98 **
Species Depth Time	156	6208	2.12 **
Replication Depth Time	78	2584	0.88
Cultivation Species Rep.Depth	6	4539	1.55
Cultivation Species Rep.Time	52	9600	3.29 **
Cultivation Species Depth Time	156	6873	2.35 **
Cultivation Rep.Depth Time	78	2581	0.88
Species Replicate Depth Time	156	3618	1.24 **
Residual	144	2916	
Total	1283	16295	

* P < 0.05

** P < 0.01

Table 6.3 Means of 1978 Falstone matric potentials (kPa) (with their standard errors of differences given in parenthesis), for the sources of variance shown.

		Matric potential (kPa)		
		Turf planted	Ploughed	combined
All sites		-2.65	-5.94	(0.30)
Species	MC	-1.17	1.05 (0.52)	-0.06
	SS	-2.78	-5.04	-3.91
	LP	-3.99	-13.84	-8.92
				(0.37)
Replicate	1	-3.15	-8.54 (0.42)	-5.84
	2	-2.14	-3.35	-2.75
				(0.30)
Depth	0.15m	-6.13	-8.26 (0.60)	-7.19
	0.30m	-4.35	-11.07	-7.71
	0.60m	-1.78	-5.14	-3.46
	0.90m	-1.66	0.70	1.18
				(0.42)

Table 6.4 Means of 1978 Falstone matric potentials (kPa), for the depths and species shown, combined over both replicates and cultivation types.

Species	Matric potential (kPa)			
	0.15m	0.30m	0.60m	0.90m
MC	-2.67	-2.10	0.74	3.79
SS	-8.30	-6.32	-2.83	1.80
LP	-10.61	-14.72	-8.29	-2.04

mineral soil, as displayed by the means in Table 6.4 for the Pinus contorta sites.

The variance between replicates serves to emphasise the spatial variability inherent in the soil, when measuring such factors as matric potentials. It should not however, be seen as indicative of any bias between sites, as they were assigned to either replicate 1 or 2 at random, and another arrangement may either increase or decrease the disparity between replicates. It does however, provide a yardstick when assessing the reliability of conclusions drawn about differences between species and cultivation types.

Variance due to time was naturally large as the sampling period covered very nearly the full range of matric potentials observed. The fact that none of its interactions gave highly significant results (with the possible exception of species x time) justifies a comparison of the other treatments.

6.1.2. 1979 DATA

The weekly rainfall data for 1979 are given in Fig.6.10, and their net rainfall and interception loss components are given in Table 6.5. A comparison of Tables 6.1 and 6.5 shows that 1979 was a wetter year than 1978. An extra 160mm of rain fell over the whole year, but most of the extra rain (108mm of it) fell during the period April-June, a period when in 1978 the soil was beginning to dry out.

The wetter spring in 1979 had an effect on the depth to the water table. Whereas by mid-June in 1978 the water table had reached depths of 0.8, 0.93 and 1.03m in the Molinia caerulea, Picea sitchensis and Pinus contorta sites respectively (Fig.6.2), in 1979 it had only reached depths of 0.57, 0.74 and 0.76m in the same sites (Fig.6.11).

Because the soil rewetted during August in both years, the later date of maximum water table depth in 1979 meant a shorter summer moisture deficit period.

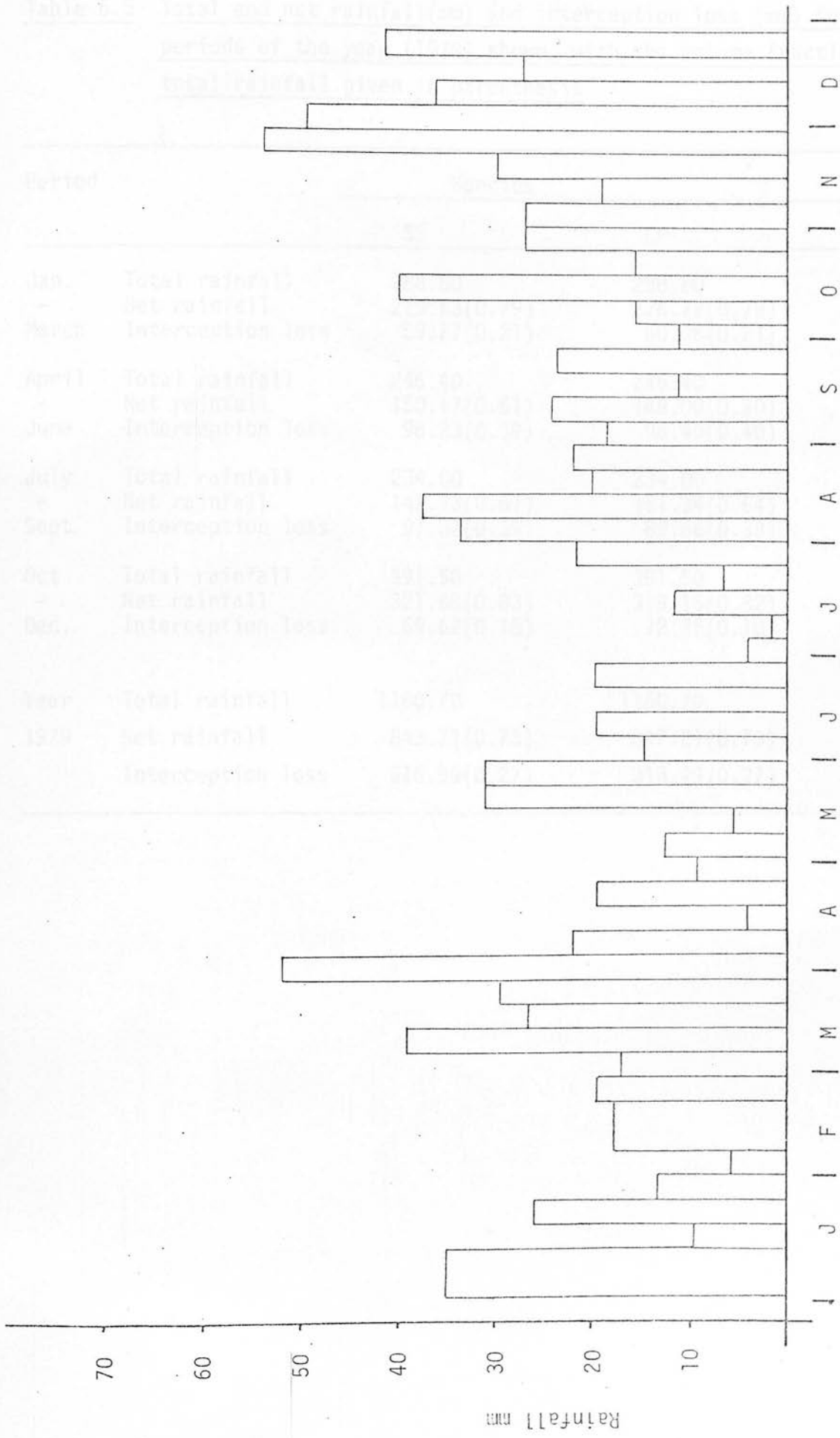


Fig.6.10 Weekly rainfall data for 1979 at Falstone sites.

Table 6.5 Total and net rainfall(mm) and interception loss (mm) for the periods of the year (1979) shown, with the volume fractions of total rainfall given in parenthesis

Period		Species	
		SS	LP
Jan.	Total rainfall	288.80	288.80
-	Net rainfall	229.53(0.79)	228.72(0.79)
March	Interception loss	59.27(0.21)	60.08(0.21)
April	Total rainfall	246.40	246.40
-	Net rainfall	150.17(0.61)	148.00(0.60)
June	Interception loss	96.23(0.39)	98.40(0.40)
July	Total rainfall	234.00	234.00
-	Net rainfall	142.13(0.61)	151.34(0.64)
Sept.	Interception loss	91.87(0.39)	82.66(0.35)
Oct.	Total rainfall	391.50	391.50
-	Net rainfall	321.88(0.83)	319.15(0.82)
Dec.	Interception loss	69.62(0.18)	72.35(0.18)
Year	Total rainfall	1160.70	1160.70
1979	Net rainfall	843.71(0.73)	847.21(0.73)
	Interception loss	316.99(0.27)	313.49(0.27)

1979

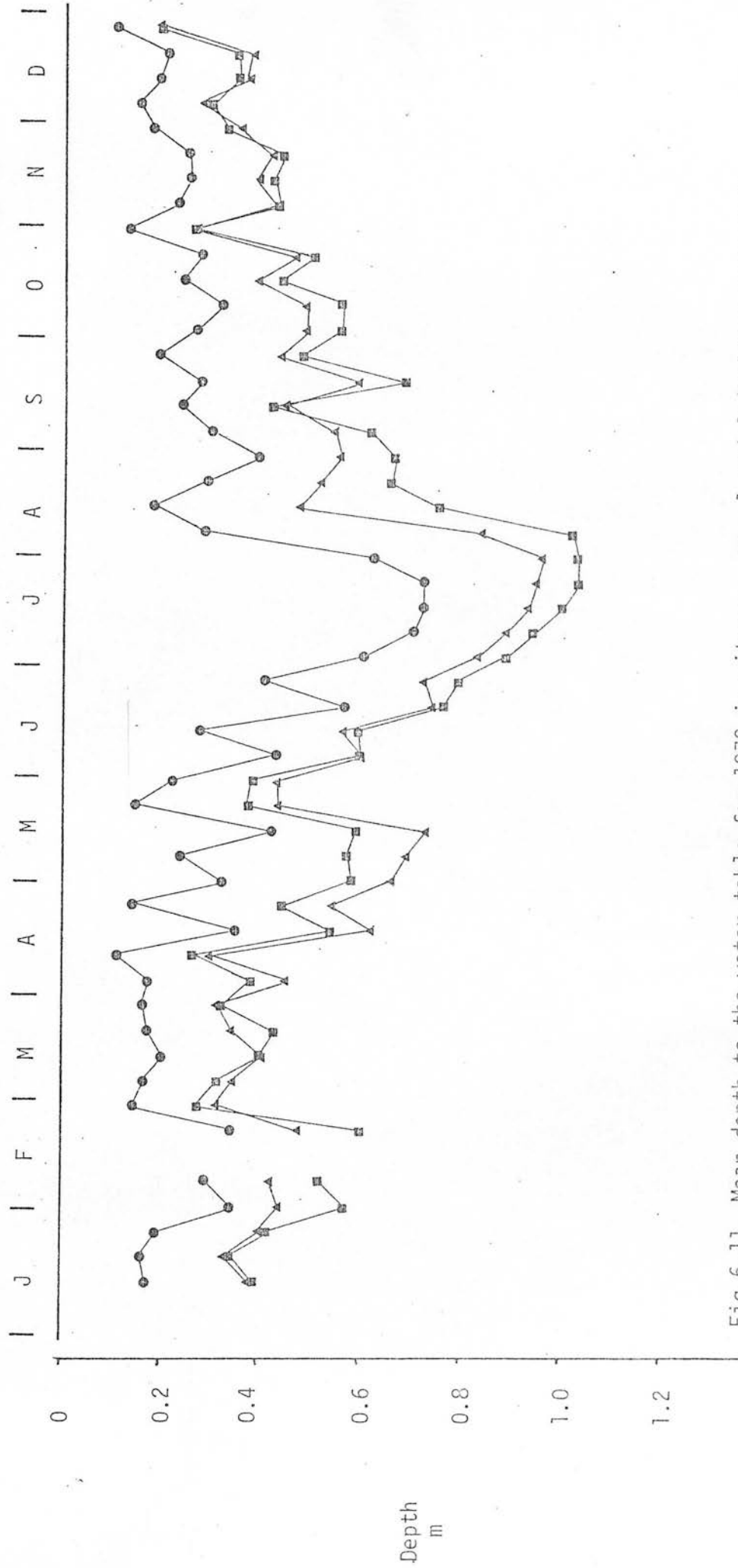


Fig.6.11 Mean depth to the water table for 1979 in sites:- ● - 1 and 2 (Molinia caerulea),

▲ - 3 and 4 (Picea sitchensis) and ■ - 5 and 6 (Pinus contorta).

The matric potentials for 1979 are given in Figs.6.12 to 6.14 and demonstrated the same trends as observed in the 1978 data (Fig.6.4 to 6.6) but at higher potentials. The soil at the grassland sites (Fig.6.12) again only dried below full saturation during June and July, and then only to a depth of about 0.3 to 0.6m. The peat layer during this period remained at higher potentials than 1978, and potentials below -5kPa were only of very short duration. In the Picea sitchensis sites the situation was little different from the open sites, the matric potentials being of the same order in site 4 (Fig. 6.13) as sites 1 and 2 (Fig.6.12). In site 3 (Fig.6.13) the matric potential dropped to about -30kPa at 0.15 and 0.3m depth, which was only about half the value attained in 1978. This pattern was repeated in the Pinus contorta sites, and though site 5 (Fig.6.14) again reached the lowest potential found in the survey it was only -66.9kPa compared with -88.6kPa in 1978.

Of more importance than minimum potentials reached, is the duration of periods when the soil is below a potential that allows adequate aeration. This diffusion experiment described in Section 9 suggests that -10kPa is a reasonable estimate for this potential in peat, and it is used here as a general guide for both peat and mineral soil, to provide a comparison between sites and years. On this basis, favourable conditions were found for longer periods under Pinus contorta than under Picea sitchensis, and 1978 was more favourable for aeration than 1979. How much of this difference between species is due to the original soil physical conditions at these sites, and how much is due to the species grown on them remains unresolved.

The matric potential data over the aeration sampling period were again subjected to analysis of variance similar to that for the 1978 data (Table 6.6). Again, only the most significant differences are examined in the tables of means given in Table 6.7 and 6.8.

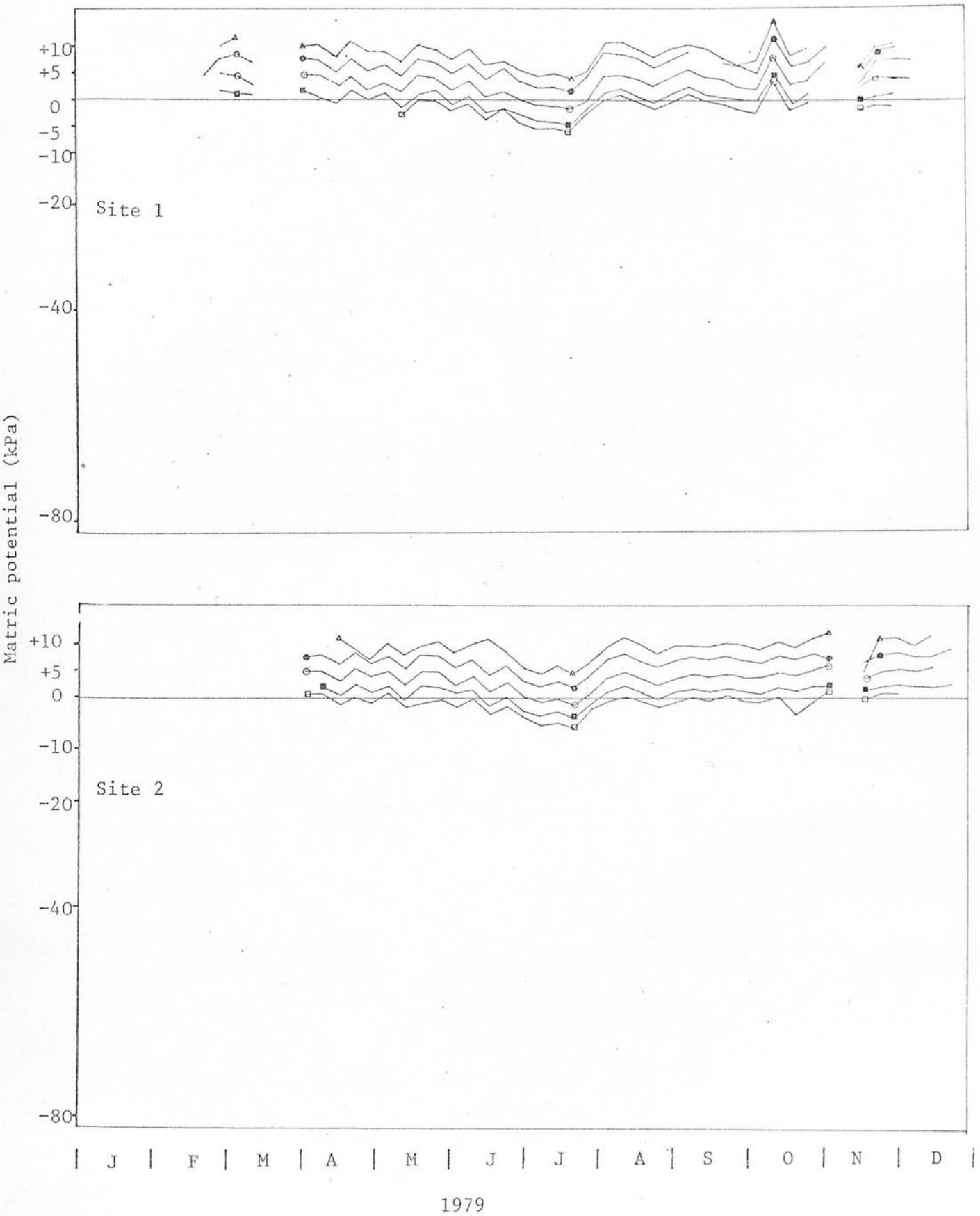


Fig.6.12 Matrix potentials for 1979 in the *Molinia caerulea* sites at depths of:- \square -0.15m, \blacksquare -0.30m, \circ -0.060m, \bullet -0.90m, Δ -1.20m.

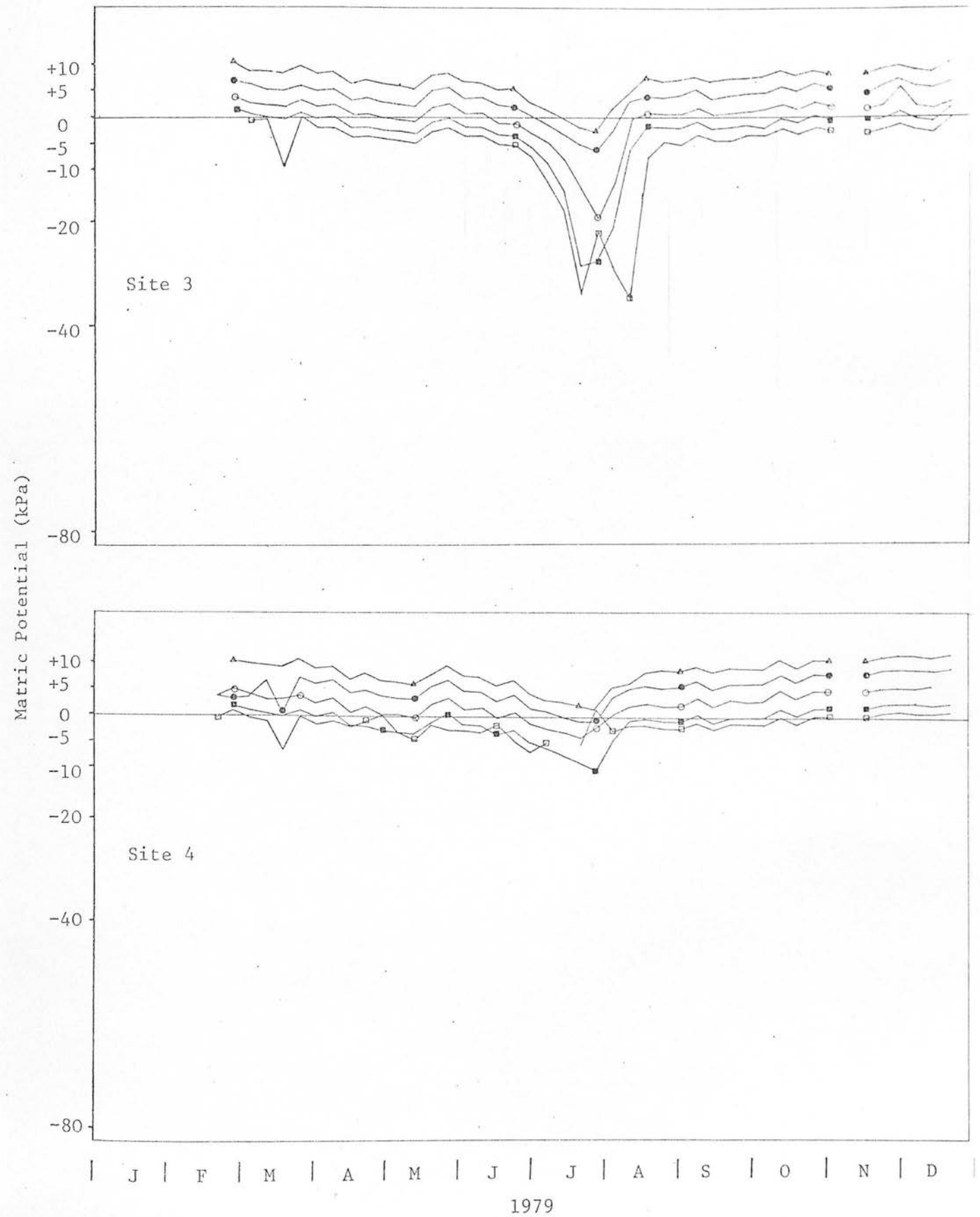


Fig.6.13 Matrix potentials for 1979 in the *Picea sitchensis* sites at depths of:- \square -0.15m, \blacksquare -0.30m, \circ -0.60m, \bullet -0.90m, Δ -1.20m.

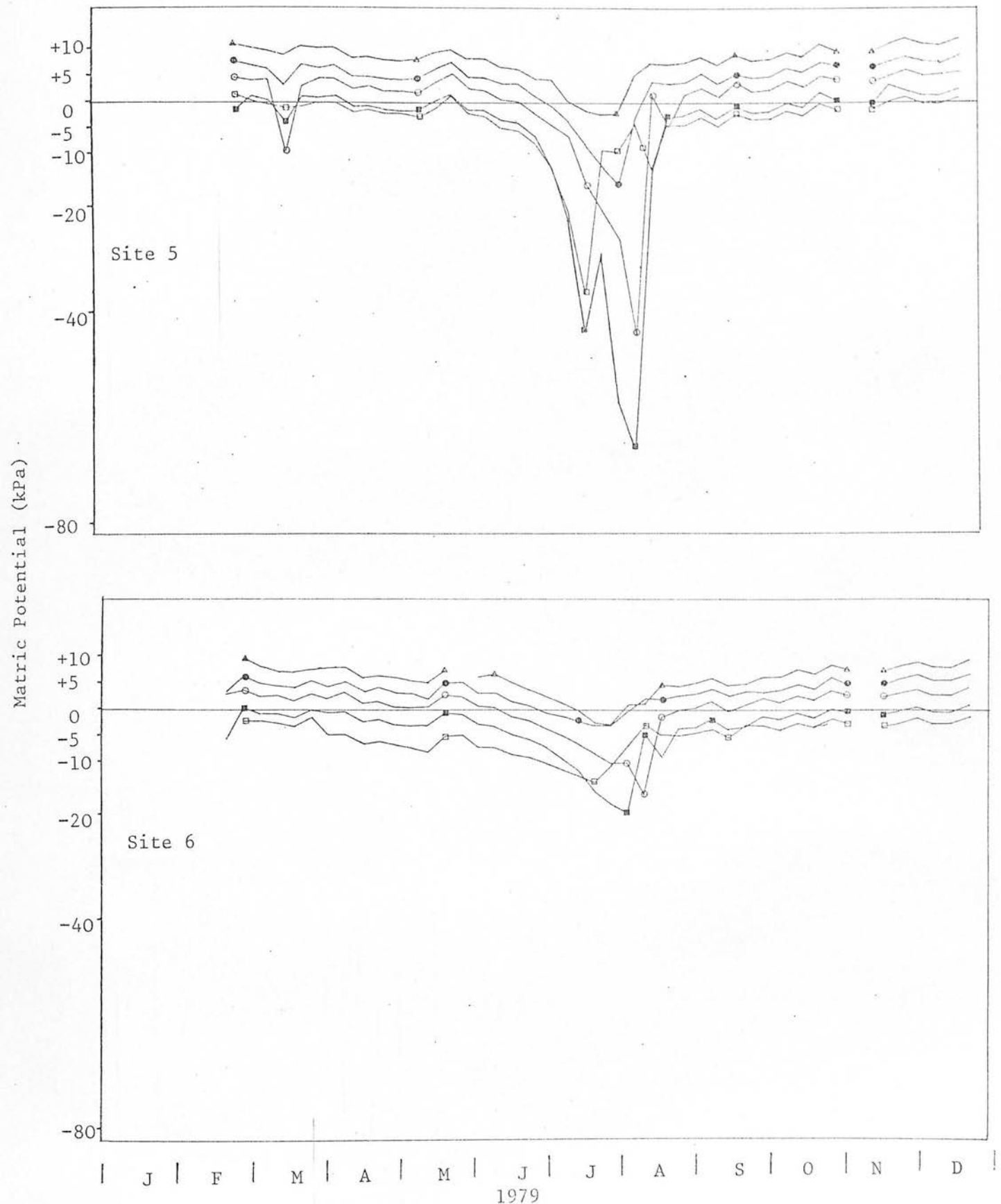


Fig.6.14 Matrix potentials for 1979 in the Pinus contorta sites at depths of:- \square -0.15m, \blacksquare -0.30m, \circ -0.60m, \bullet -0.90m, Δ -1.20m.

Table 6.6 Analysis of variance of Falstone matrix potential data (m bar) for 1979

Source of Variation	DF	MS	VR	
Species	2	177949	145.396	**
Replicate	1	49529	40.468	**
Depth	3	218489	178.519	**
Time	22	36138	29.527	**
Species Replicate	2	9980	8.155	**
Species Depth	6	5634	4.603	**
Replicate Depth	3	3369	2.753	*
Species Time	44	7783	6.359	**
Replicate Time	22	9763	7.977	**
Depth Time	66	1959	1.601	**
Species Replicate Depth	6	5567	4.549	**
Species Replicate Time	44	3449	2.818	**
Species Depth Time	132	2063	1.686	**
Replicate Depth Time	66	1002		
Residual	127	1224	0.819	
Total	546	6017		

* P < 0.05

** P < 0.01

Table 6.7 Means of 1979 Falstone matric potentials (kPa)(with their
standard errors of differences given in parenthesis) for species
and replicates

Replicate	Matric Potential (kPa)			
	MC	SS	LP	All
	1.14	-2.81	-5.00 (0.36)	
1	0.93	-4.49	-5.96 (0.52)	-3.17
2	1.34	-1.14	-4.03	-1.28
				(0.30)

Table 6.8 Means of 1979 Falstone matric potentials (kPa)(with their
standard errors of differences given in parenthesis) for
species and depth

Depth (m)	Matric Potential (kPa)			
	MC	SS	LP	ALL
0.15	-2.21	-6.94	-7.56 (0.73)	-5.57
0.30	-0.67	-5.25	-9.66	-5.19
0.60	2.05	-1.37	-3.73	-1.02
0.90	5.37	2.30	0.96	2.88
				(0.42)

Table 6.9 Means of matric potentials (kPa) for each site over the periods
of soil aeration sampling in 1978 and 1979, (with standard
errors of differences between means given in parenthesis)

Year	Depth	Matric Potential (kPa)					
		MC		SS		LP	
		1	2	3	Sites		6
					4	5	
1978	0.15	-2.27	-2.26	-13.57	-6.19	-17.60	-8.20 (1.47)
	0.30	-0.77	-0.95	-15.07	-3.51	-25.69	-20.43
	0.60	2.04	2.02	-6.31	0.17	-19.65	-9.11
	0.90	5.38	5.18	0.82	3.36	-10.33	-0.20
1979	0.15	-2.22	-2.20	-10.24	-3.64	-7.40	-7.70 (1.30)
	0.30	-1.00	-0.34	-6.71	-3.80	-12.57	-6.75
	0.60	1.82	2.29	-2.58	-0.16	-4.62	-2.85
	0.90	5.13	5.61	1.57	3.03	0.75	1.17

The most significant variance in these data is found between species, and the difference between species means (Table 6.7) is the same pattern as 1978 though the values are higher. Of the same order of significance is the variance due to depth, the overall means increasing down the profile. The interaction between species and depth again proved significant, and the pattern of means displayed in Table 6.7 and 6.8 is similar to that in Table 6.3 and 6.4. from 1978.

A direct comparison between the two years is confounded by the presence of the cultivation treatments in 1978. However, if the means for each depth in each site are taken, then a comparison of mean matric potentials throughout each year can be made for sites 1 to 6, between 1978 and 1979. These means are given in Table 6.9 and show how the variance due to replication is distributed between the sites (replicate 1 being sites 1, 3 and 5 and replicate 2 sites 2, 4 and 6). One feature to be noticed from Table 6.9 is that the mean matric potentials of the open sites for 1978 and 1979 are much closer than those in the planted sites for the two years. This is because a larger volume of water has to be removed at higher matric potentials to record a given difference in potential than at lower matric potential. For this reason moisture content differences between sites will not be so obvious as the differences in the matric potentials shown.

The differences between species and depths over time can be seen by comparing Figs. 6.4 to 6.9 and 6.12 to 6.14, and the interaction terms containing time in Tables 6.2 and 6.6 show that significant differences occur in the way each species and depth reacts at different periods.

6.2 TEMPERATURE REGIME

The temperatures recorded each week during 1978 and 1979 in sites 2, 4 and 6 are represented graphically in Figs. 6.15 and 6.16. These temperatures were spot recordings made between 9a.m. and 12 noon on the

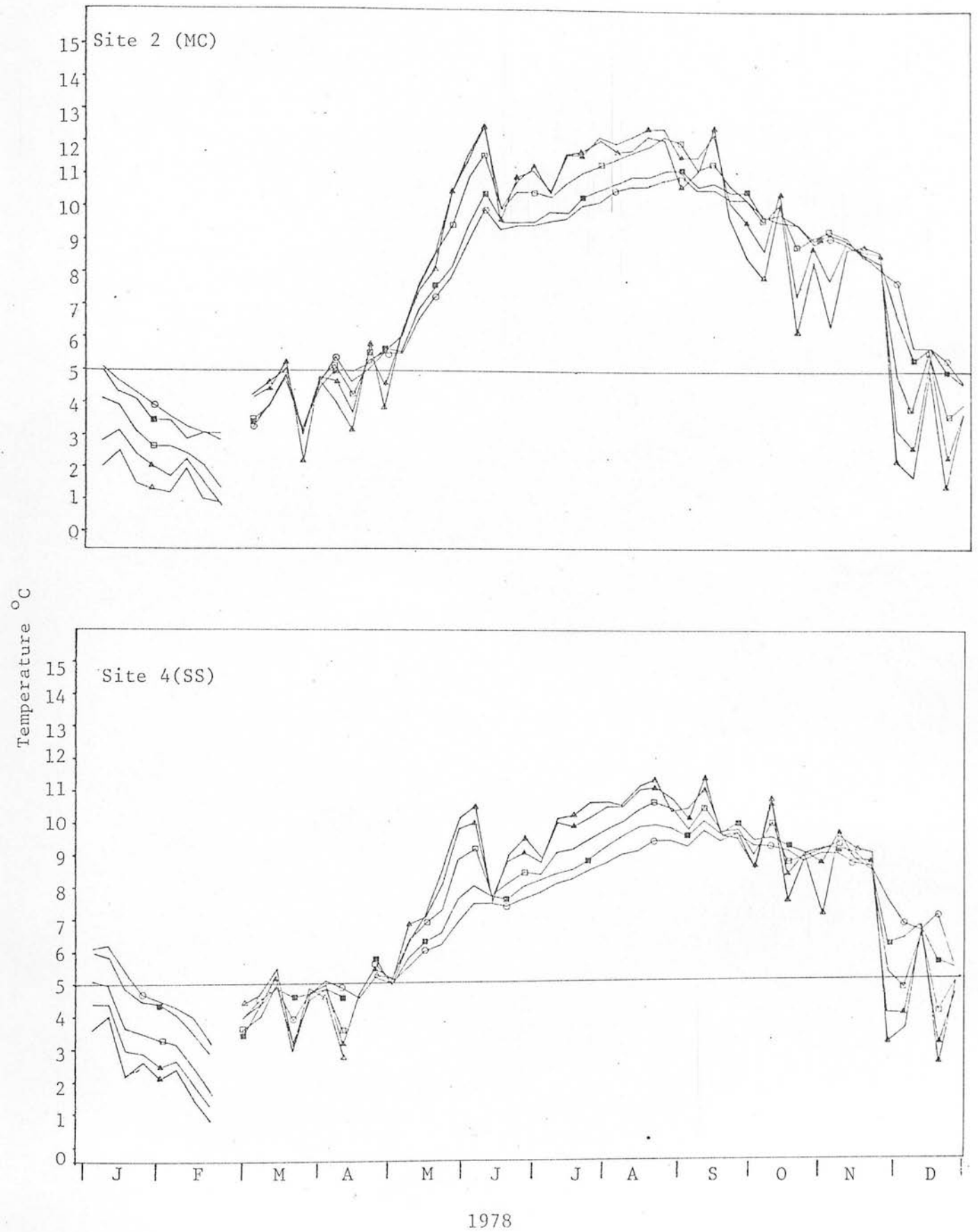


Fig.6.15 Soil temperatures in sites 2 (*Molinia caerulea*) and 4 (*Picea sitchensis*) for 1978, at depths of Δ -0.05m, \blacktriangle -0.10m, \square -0.20m, \blacksquare -0.40m and \circ -0.60m.

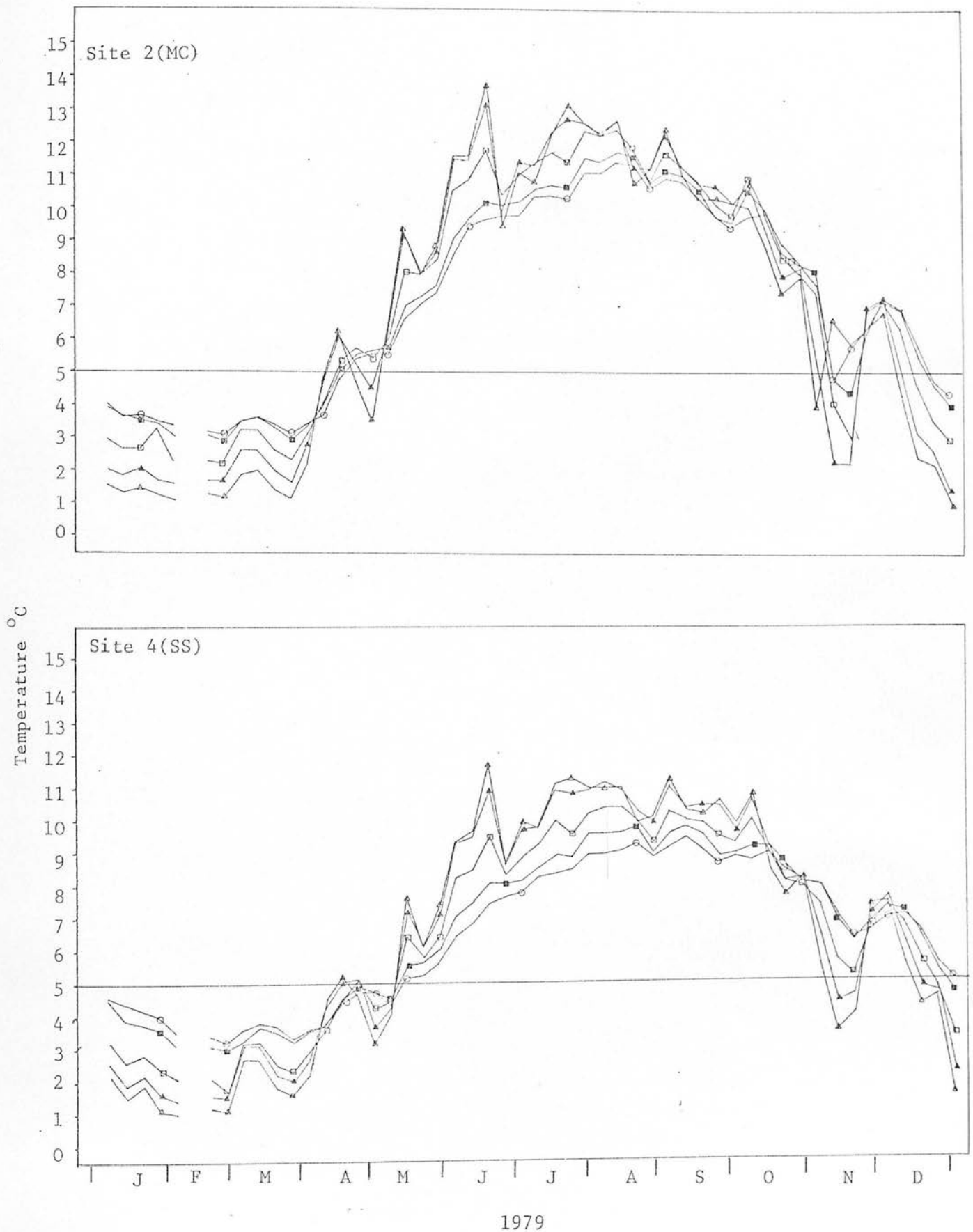


Fig.6.16 Soil temperatures in sites 2(*Molinia caerulea*) and 4(*Picea sitchensis*) for 1979, at depths of Δ -0.05m, \blacktriangle -0.10m, \square -0.20m \blacksquare -0.40m and \bigcirc -0.60m.

day of sampling, and do not indicate a daily mean, maximum or minimum temperature. Figs.6.15 and 6.16 show one complete cycle of the seasonal or yearly variation in soil temperatures. The soil temperature rose from early March until the end of August when the net flow of heat was into the soil, and fell from early September until late February when the heat flow was in the reverse direction.

The different effects of grassland and forest cover on soil temperatures can be seen by comparing (MC) with (LP) and (SS) on Figs.6.15 and 6.16. The chief difference was that higher temperatures were reached in the open sites during the summer months. This can be seen quite clearly in the graphs, but a general comparison can also be made by looking at the mean and maximum temperatures recorded during the period from May to November, given in Table 6.10 and 6.12 for 1978 and 1979 respectively. The mean temperatures during the summer were about the same under both tree species, and about 1°C lower than under the grassland. The maximum temperatures recorded showed a similar trend, though the maximum temperatures under grass could be 2°C or more above those under the forest, especially in the surface soil layers.

It is interesting to note from Table 6.11 that differences between the two vegetation types did not arise during winter. It may be thought that a forest canopy would provide a better insulating cover than grassland, limiting heat loss during the winter as it limits absorption during the summer. However, the data did not show any appreciable difference in mean or minimum winter temperatures (Table 6.11) between forest and grass cover. If any difference did occur then it must have been confined to the litter layer or surface 50mm of peat, and it will be noted that no temperature below 0°C was recorded.

Temperature also varied with depth as well as time, and the data here display the well known phenomenon of increased damping at depth, of the seasonal fluctuations. Soil temperatures follow air

Table 6.10 Mean and maximum temperatures ($^{\circ}\text{C}$) at indicated depths
in the sites shown for the period 1.5.78 to 30.10.78

Depth(m)		Temperature ($^{\circ}\text{C}$)					
		2(MC)	4(SS)	6(LP)	7(MC)	9(SS)	11(LP)
0.05	Max.	12.4	11.5	11.2	15.8	10.9	11.6
	Mean	10.1	9.0	9.4	11.8	9.0	8.7
0.10	Max.	12.4	10.6	11.4	13.4	10.8	11.1
	Mean	10.4	8.7	9.3	10.7	8.8	8.8
0.20	Max.	12.1	10.5	10.6	11.8	10.0	10.1
	Mean	10.3	8.6	8.9	10.0	8.5	8.4
0.40	Max.	11.4	10.1	9.6	11.1	10.1	10.0
	Mean	9.7	8.8	8.2	9.7	8.5	8.5
0.60	Max.	11.1	9.5	9.6	10.9	9.6	9.7
	Mean	9.6	8.2	7.9	9.4	8.2	8.2

Table 6.11 Mean and minimum temperatures ($^{\circ}\text{C}$) at indicated depths in
the sites shown for the period 1.11.78 to 30.4.79.

Depth(m)		Temperature ($^{\circ}\text{C}$)		
		2(MC)	4(SS)	6(LP)
0.05	Min.	1.0	1.0	1.2
	Mean	3.2	3.8	3.6
0.10	Min.	1.5	1.4	1.4
	Mean	3.7	4.2	3.7
0.20	Min.	2.1	2.1	2.1
	Mean	4.3	4.4	4.3
0.40	Min.	2.8	3.0	3.0
	Mean	4.8	5.1	5.0
0.60	Min.	3.0	3.2	3.1
	Mean	4.9	5.3	5.1

Table 6.12 Mean and maximum temperatures ($^{\circ}\text{C}$) at all depths in the
sites shown for the period 1.5.79 to 30.10.79

<u>Depth(m)</u>		<u>Temperature ($^{\circ}\text{C}$)</u>		
		2(MC)	4(SS)	6(LP)
0.05	Max.	13.6	11.6	11.4
	Mean	10.1	9.2	8.9
0.10	Max.	13.0	10.9	10.4
	Mean	10.2	9.1	8.6
0.20	Max.	12.2	10.3	10.1
	Mean	10.0	8.6	8.4
0.40	Max.	11.5	9.7	9.8
	Mean	9.5	8.1	8.2
0.60	Max.	11.2	9.4	9.5
	Mean	9.2	7.8	7.9

temperature changes, and so during spring there is an increasing temperature wave down the profile, which is reversed in autumn. The effect of this decreases with depth such that deeper layers will be cooler than the surface during the summer, but warmer in the winter. At two times in the year the soil temperature will be approximately the same at all depths, once during April or May and once again about October.

It has been shown that both root and shoot growth of Picea sitchensis seedlings are directly related to soil temperature (Coutts and Bowen, 1973); such that with a constant air temperature of 14°C , root growth increases considerably with increasing soil temperature from 6°C to 18°C . Below 5°C root growth ceases or is negligible, and so this temperature can be used as a lower limit for root activity. With this as a lower limit for root activity the period of potential root growth during the year was about 30 weeks from the end of April until November. This period covers the entire moisture deficit period during the summer and the aeration sampling period. It can therefore be assumed that temperature alone did not limit root growth during this period.

6.3 SOIL ATMOSPHERE

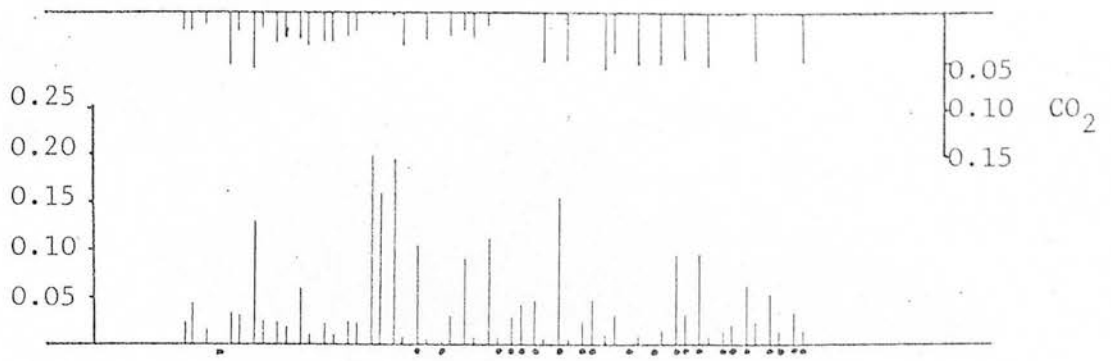
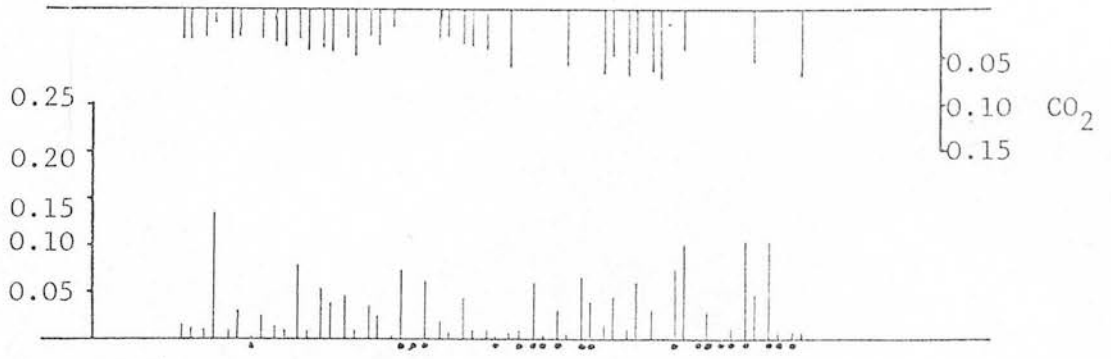
6.3.1 1978 DATA

The oxygen and carbon dioxide concentrations measured in the samples of the soil pore space taken each week during 1978, are given in Figs. 6.17 to 6.22. Both replicate sites are given on the same histogram for each depth in Figs. 6.17 to 6.22 and the concentrations are either the measured gas concentration or equivalent gas phase concentrations derived from water samples. The data from water samples are indicated by dots under the baseline, and missing samples by an asterisk under the baseline. It should be remembered that no carbon dioxide concentrations for water samples were measured in 1978, and should not be read as zero.

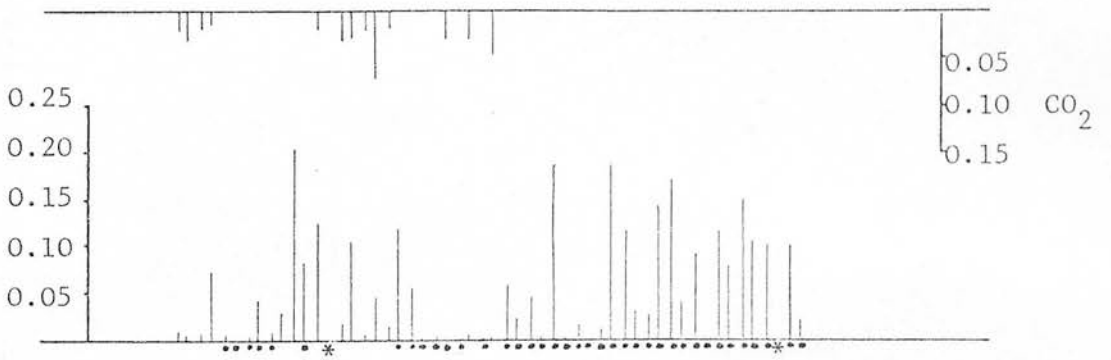
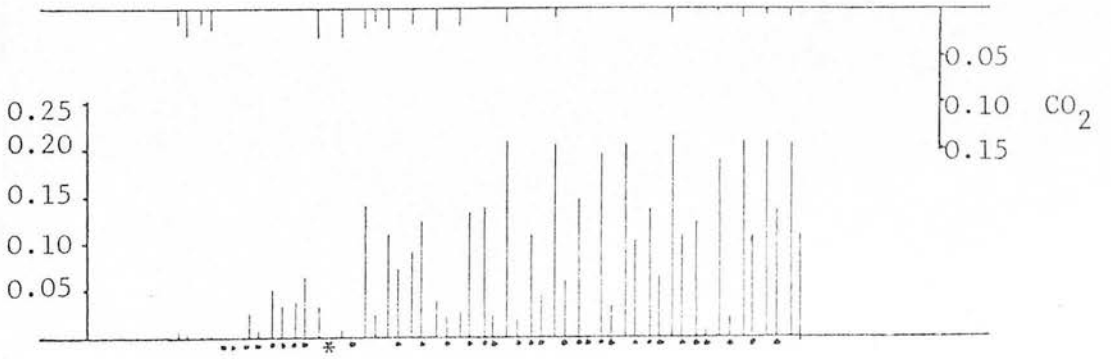
In the tree planted sites trends with depth and seasonal

Molinia caerulea (ploughed)

Depth

0.15m O₂0.30m O₂

1978

0.60m O₂0.90m O₂

1978

Fig.6.17 Soil oxygen and carbon dioxide concentration ($\text{m}^3 \text{m}^{-3}$) in sites 1 and 2 (left and right hand lines of a pair respectively), at the depths indicated. A dot under the baseline indicates a water sample and an asterisk missing data.

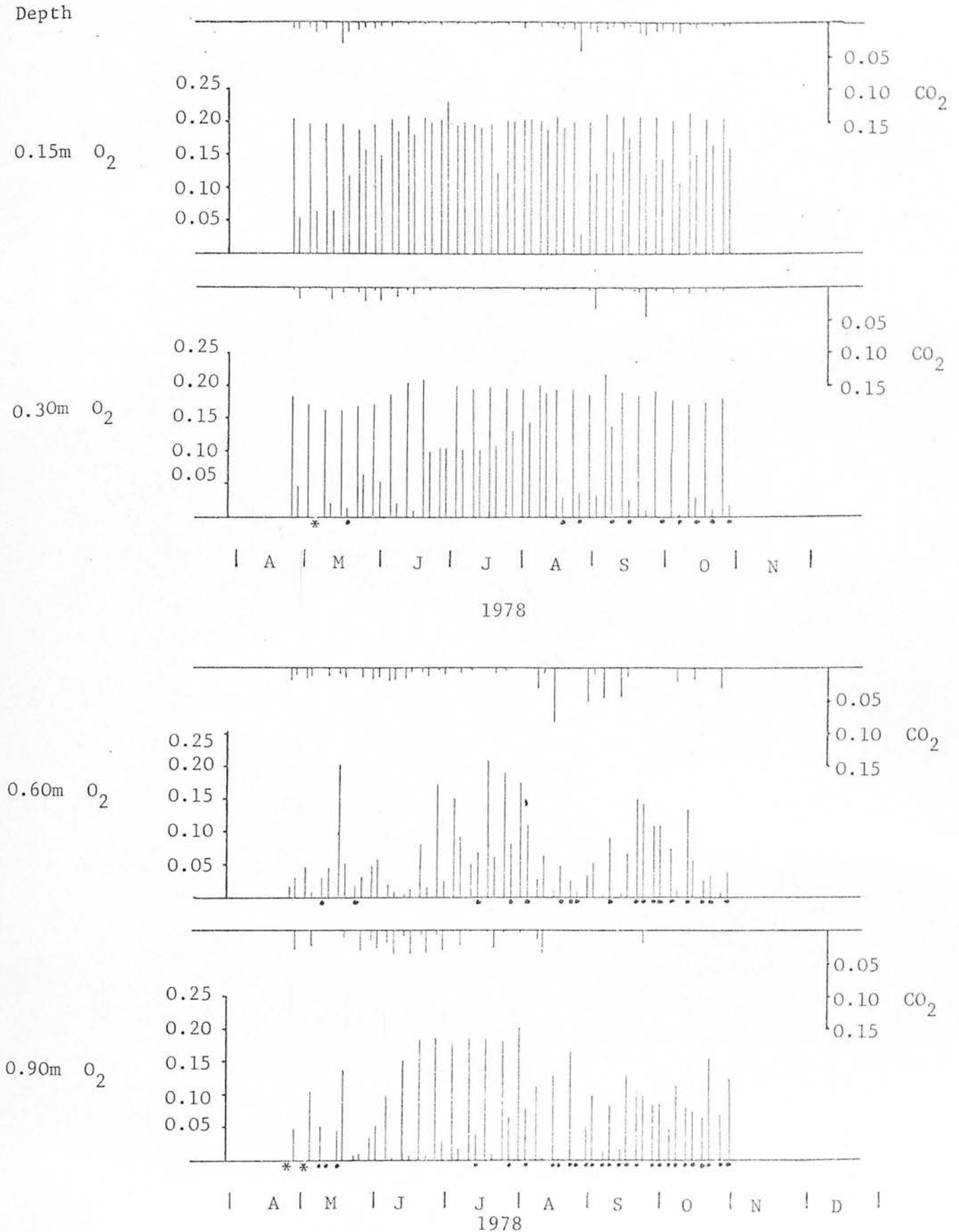
Picea sitchensis (ploughed)

Fig.6.18 Soil oxygen and carbon dioxide concentrations ($m^3 m^{-3}$) in sites 3 and 4 (left and right hand lines of a pair respectively), at the depths indicated. A dot under the baseline indicates a water sample and an asterisk missing data.

Pinus contorta (ploughed)

Depth

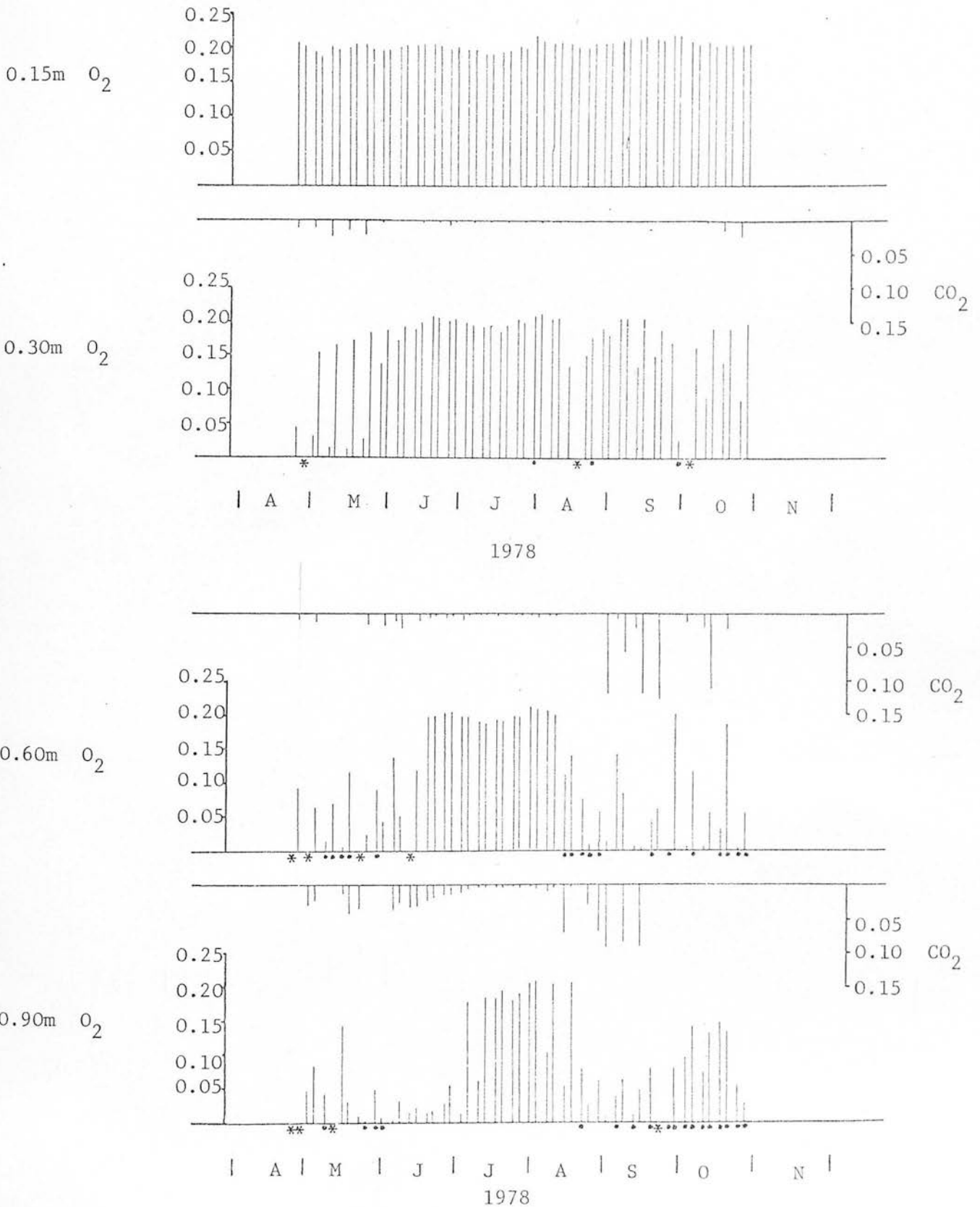


Fig.6.19 Soil oxygen and carbon dioxide concentrations ($m^3 m^{-3}$) in sites 5 and 6 (left and right hand lines of a pair respectively), at the depth indicated. A dot under the baseline indicates a water sample and an asterisk missing data. CO_2 concentrations at 0.15m depth were all below $0.01 m^3 m^{-3}$ and so have been omitted.

Molinia caerulea (turf-planted)

Depth

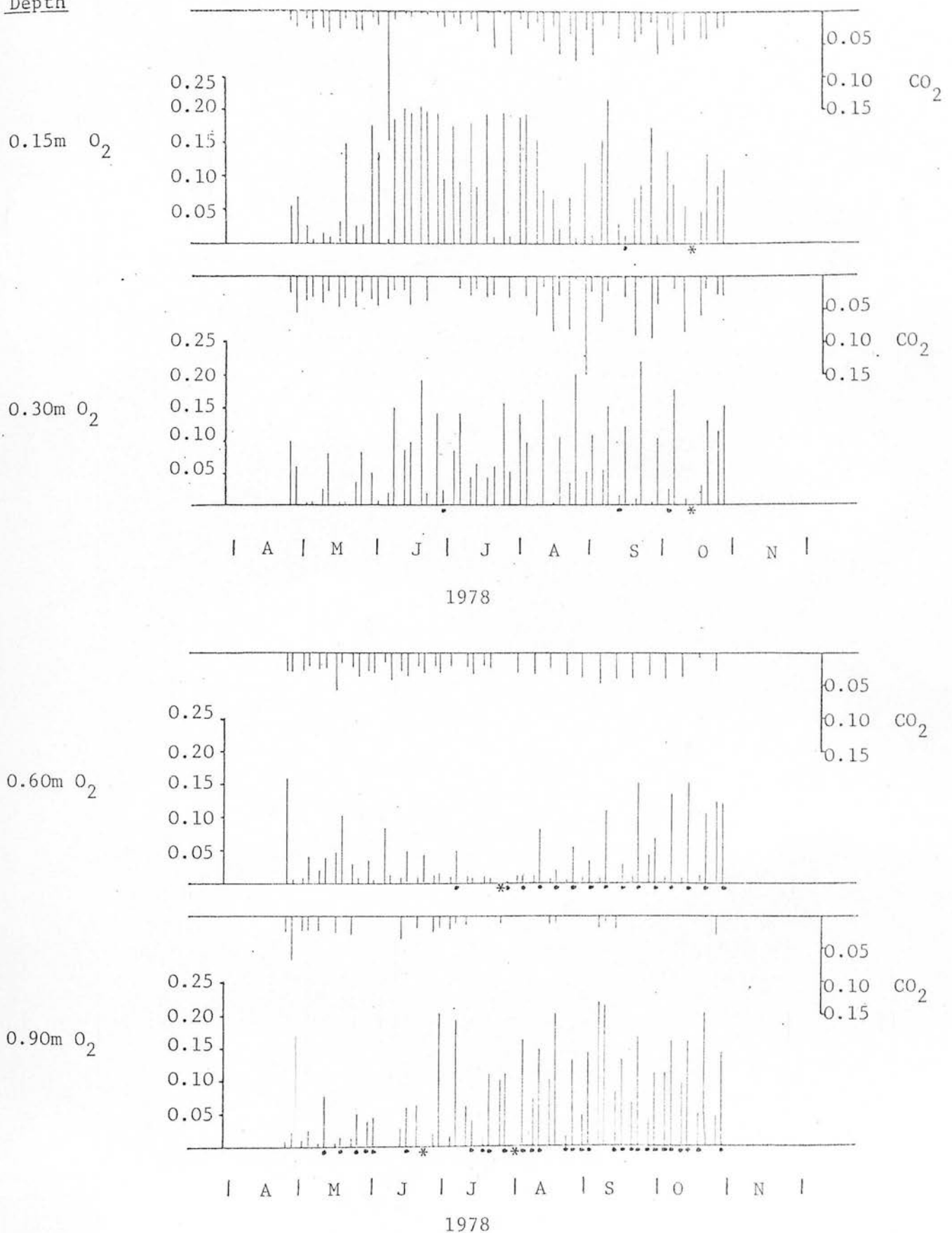
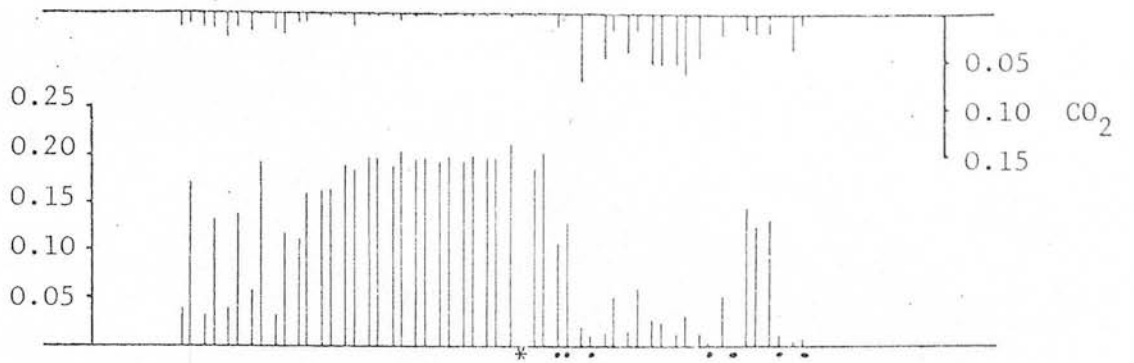
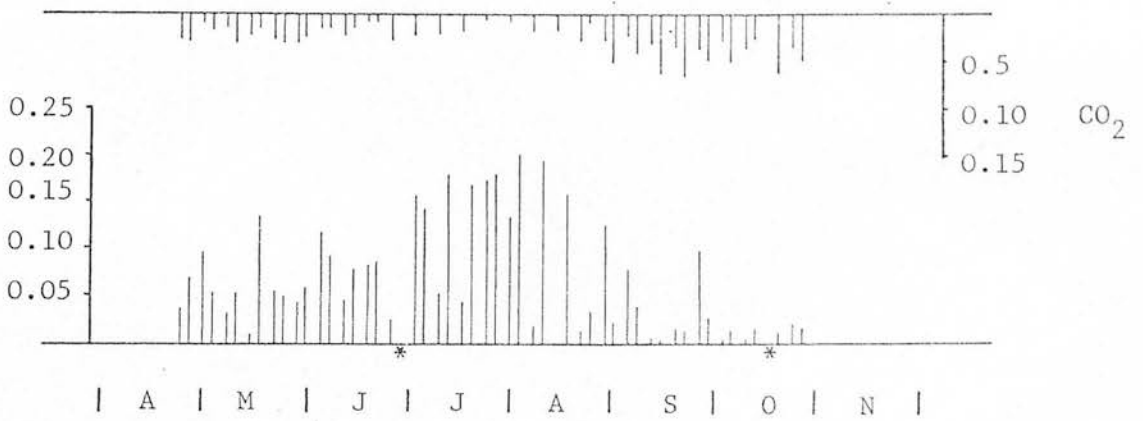
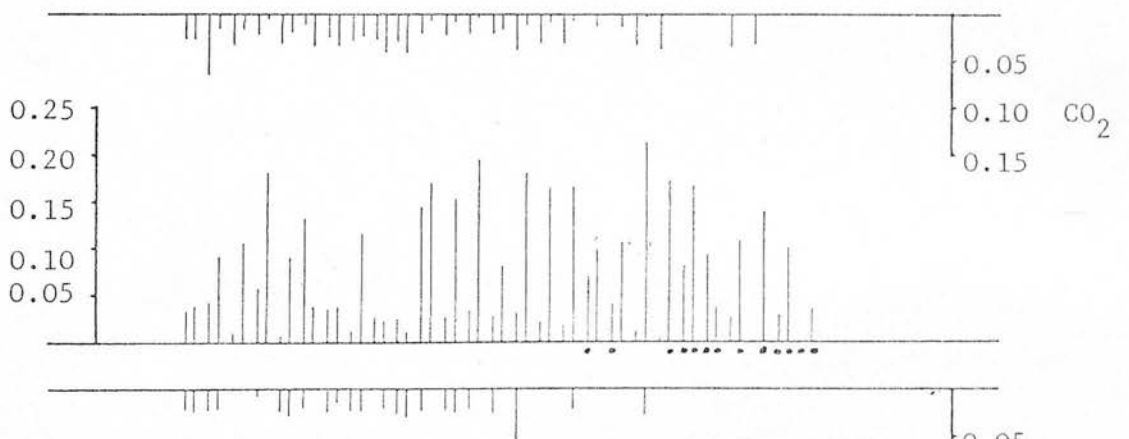
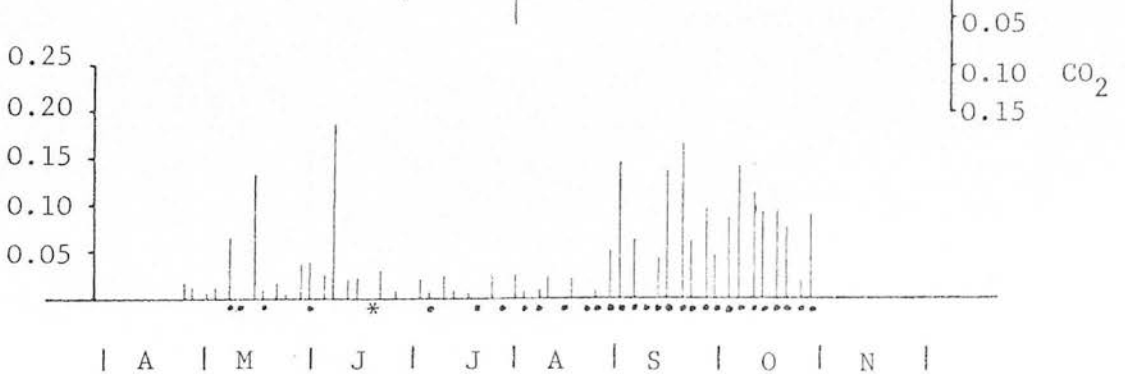


Fig.6.20 Soil oxygen and carbon dioxide concentrations (mm^{-3}) in sites 7 and 8 (left and right hand lines of a pair respectively), at the depths indicated. A dot under the baseline indicates a water sample and an asterisk missing data.

Picea sitchensis (turf-planted)

Depth

0.15m O₂0.30m O₂0.60m O₂0.90m O₂

1978

Fig.6.21 Soil oxygen and carbon dioxide concentrations ($\text{m}^3 \text{m}^{-3}$) in sites 9 and 10 (left and right hand lines of a pair respectively), at the depth indicated. A dot under the baseline indicates a water sample and an asterisk missing data.

Pinus contorta (turf-planted)

Depth

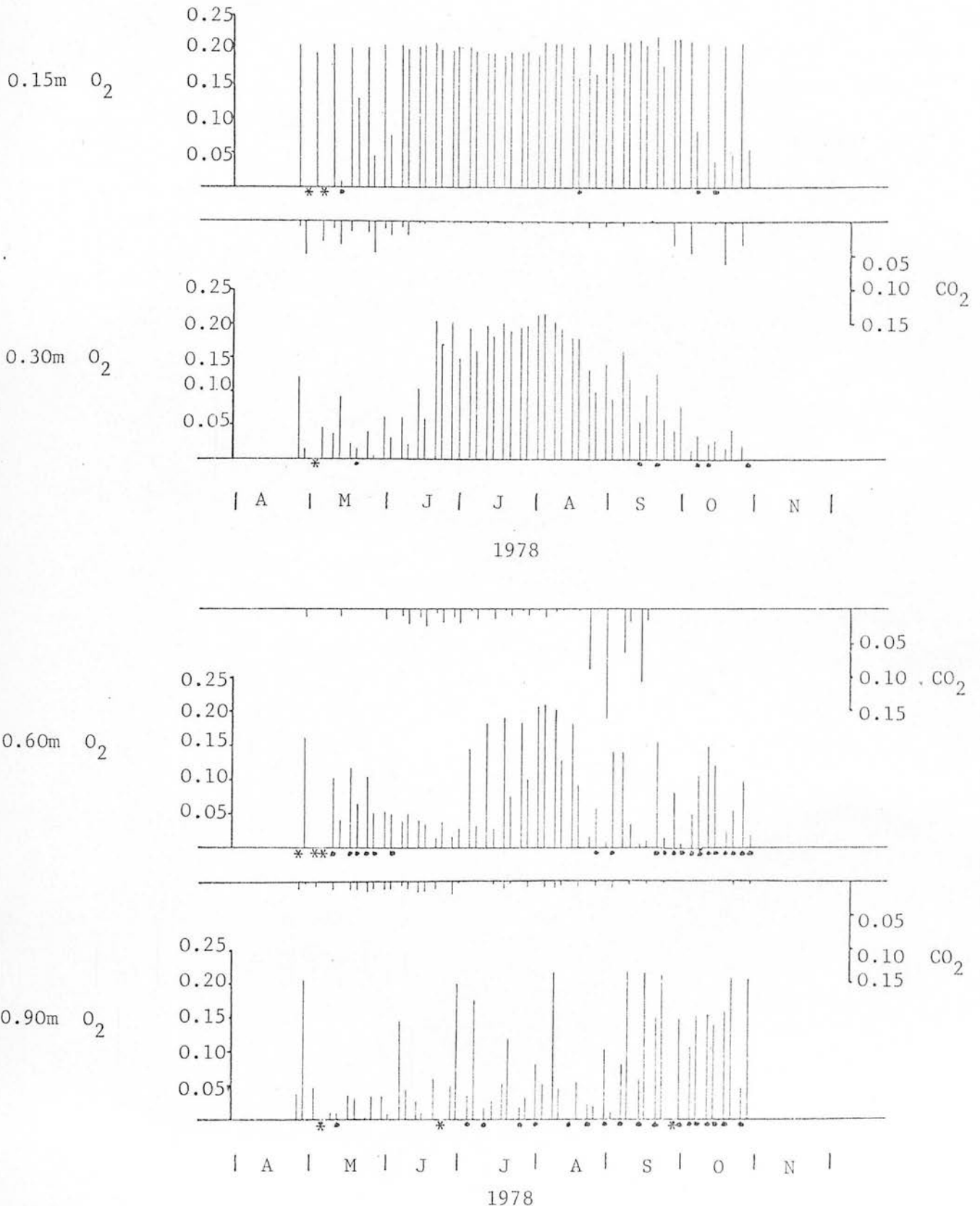


Fig.6.22 Soil oxygen and carbon dioxide concentrations ($m^3 m^{-3}$) in sites 11 and 12 (left and right hand lines of a pair respectively), at the depths indicated. A dot under the baseline indicates a water sample and an asterisk missing data. CO_2 concentrations at 0.15m depth were all below $0.01m^3 m^{-3}$ and so have been omitted.

variation are easily visible in the oxygen concentration data. A slight difference between the turf-planted and ploughed sites is also shown.

At 0.15m depth in the forested sites the soil was well aerated throughout the season, and in sites 3,5,6,9 and 11 rarely fell much below the ambient atmospheric concentration of $0.21 \text{ m}^3 \text{ m}^{-3}$, at any time. However, in sites 4,10 and 12 the oxygen concentrations were markedly lower (0.05 to $0.15 \text{ m}^3 \text{ m}^{-3}$) at the start and end of the sampling period, only sustaining atmospheric concentrations from June until August. If these data (Figs.6.18, 6.19, 6.21, and 6.22) are compared with the matric potentials in these sites at 0.15m depth (Figs.6.5, 6.8 and 6.9) then it is seen that the periods of best aeration commenced when the matric potential fell below about -5kPa , and lasted over the moisture deficit period.

A general trend with depth was most obviously displayed by the data from Pinus contorta sites, and that was a progressive shortening of the period when oxygen concentrations were near atmospheric, with increasing depth. In sites 11 and 12 (turf-planted) the period of best aeration was only from mid-June to mid-August at 0.3m depth (Fig.6.22) and only from July until mid-August at 0.6m depth (Fig.6.22). There was less agreement between sites in the oxygen concentrations recorded at these depths, with site 12 generally having lower concentrations at 0.6m depth than site 11. At 0.9m depth (Fig.6.22) little evidence existed for the mid-summer peak of oxygen concentrations, which were generally low (about $0.05 \text{ m}^3 \text{ m}^{-3}$) until mid-September, except for occasional weeks. This trend of shortening periods of high oxygen concentrations with increasing depth was observed right down the profile to 0.9m in the ploughed Pinus contorta sites (5 and 6). At 0.3m depth site 6 (Fig.6.19) was well aerated throughout the sampling period, while maximum oxygen concentrations in site 5 lasted from the start of June until September. At 0.6m depth (Fig.6.19) oxygen concentrations were near atmospheric from mid-June until mid-August in

both sites, and at 0.9m depth (Fig.6.19) from July until mid-August.

A comparison with the relevant matric potentials (Fig 6.6) show that these trends reflect the enhanced drying found in the ploughed sites, the periods of maximum aeration again following the moisture deficit period when matric potentials were lower than about -5kPa.

The same trends were seen in the Picea sitchensis sites (3, 4, 9 and 10) though less clearly, with more frequent lower oxygen concentrations being recorded mid-season compared with the Pinus contorta sites. In the turf-planted sites, site 9 was generally well aerated throughout the season at 0.3m depth (Fig.6.21), but in site 10 very low oxygen concentrations ($<0.05\text{m}^3\text{m}^{-3}$) were recorded at the start and end of the sampling period. Little trend was discernible at 0.6m and 0.9m depth (Fig.6.21), generally low oxygen concentrations being recorded in both sites with occasional weeks when concentrations appear to be high. A look at the matric potentials recorded in these sites (Fig 6.8) will show that potentials rarely fell below -5kPa at these depths.

In the ploughed Picea sitchensis sites (3 and 4) a mid-season trend was discernible at 0.3m in site 4 (Fig.6.18), while site 3 was generally well aerated at this depth. Site 3 also showed a short period of high oxygen concentrations in July at 0.6m depth (Fig.6.18), while site 4 yielded lower oxygen concentrations throughout the season, reflecting the more intense drying observed in site 3 compared with site 4 (Fig.6.5).

Carbon dioxide concentrations showed some indication of a trend the mirror image of that of oxygen, but the evidence is inconclusive. At many points on the graphs carbon dioxide concentrations are insignificant when oxygen concentrations were near atmospheric, and are absent for water samples. This absence for water samples often leads to a lack of information as to carbon dioxide levels at the end of the season when rewetting of the soil had occurred, especially at depths of 0.6 and 0.9m.

However at depths of 0.3, 0.6 and 0.9m in all planted sites (Figs.6.18, 6.19, 6.21 and 6.22) minimum levels of carbon dioxide were observed when oxygen concentrations were maximal, with higher levels during periods of oxygen depletion. In all cases the carbon dioxide concentrations were higher than atmospheric ($3.5 \times 10^{-4} \text{ m}^3 \text{ m}^{-3}$), and could reach very high levels (0.10 to $0.15 \text{ m}^3 \text{ m}^{-3}$) when oxygen concentrations were near zero.

At depths of 0.6 and 0.9m in all sites there seemed to be a few weeks at the end of August when oxygen concentrations were extremely low (0 to $0.05 \text{ m}^3 \text{ m}^{-3}$). This period followed that of the best aeration during the moisture deficit period, and was when the soil was re-wetting to positive matric potentials. It was followed in turn by a period of higher oxygen concentrations, but recorded from water samples. Soil temperatures at this time were at their highest levels for those depths, at about 9 to 10°C . The implication of this will be discussed in Section 6.4.

When considering the Molinia caerulea sites (1,2,7 and 8) the extent and duration of well aerated periods was visibly much less than in the forested sites. In site 7 there were frequent recordings of atmospheric oxygen concentrations at 0.15m depth (Fig.6.20) but in site 8 at this depth they were often very much lower. It is only at this depth in these sites that any trend of higher oxygen concentrations during mid-summer was visible, but even then it was ill defined. At 0.3m depth in the turf planted sites (7 and 8) oxygen concentrations were generally lower (0.05 to $0.1 \text{ m}^3 \text{ m}^{-3}$) with individual weeks showing either near atmospheric or near zero concentrations (Fig.6.20). At 0.15m and 0.3m depth in the ploughed sites (1 and 2, Fig.6.17) oxygen concentrations were very low (below $0.05 \text{ m}^3 \text{ m}^{-3}$) throughout the sampling period and often approached zero, with many samples being water. At 0.6m depth in all grassland sites a seasonal trend, was observed (Figs.6.17 and 6.20) though the reverse of that occurring in the planted sites. This trend was one

of ^{high} reasonable oxygen concentrations being recorded at the beginning and end of the sampling period but with concentrations approaching zero during July and early August. This was also seen at 0.3m depth in sites 1 and 2 (Fig.6.17). Inspection of Figs.6.4 and 6.7 of the matric potentials in these sites show that they never fell below -5kPa at these depths, and indeed most of the samples taken were water. At 0.9m depth in all open sites the oxygen concentrations were paradoxically higher than at shallower depths, especially towards the end of the season, and most of these concentrations were derived from water samples. Note must now be made of the agreement or lack of it, between oxygen concentrations in replicate sites. In many instances, great differences existed between concentrations recorded in the two replicates, especially during periods of soil drying or re-wetting. It must be remembered that the replicates are many metres distant (about 30m) and the moisture conditions cannot be expected to be exactly those recorded over all the site area. But, as the seasonal trends displayed by each probe largely coincide with their replicate with respect to timing and duration, then the preceding deductions as to the nature of soil aeration in these sites are justified.

An analysis of variance similar to that carried out on the matric potential data was attempted on the oxygen concentration data expressed as volume percentages of the total gas sample. However, it was clear from the plot of residual variance against fitted values, that this was inadequate to describe the total variance. To fit an analysis of variance test the data have to conform to three precepts; (1) that the components of the mathematical model are additive, (2) that the experimental errors all come from the same frequency distribution, and (3) that the frequency distribution for the residual error is Normal. The plot of residuals against fitted values for the

raw data showed clearly a non-Normal distribution, with two groupings of values at the ends of the fitted values range (near 0 and $0.21 \text{ m}^3 \text{ m}^{-3}$). These groupings were displaced either side of the zero residual line and indicated a bi-modal distribution, evidence for which has also been found in soil of oxygen concentration data by Dowdell et al (1979). The data had therefore, to be transformed to give a single Normal distribution about the zero residual variance line. Such a transformation was found to be that in Equation (67).

$$\text{Transformed value} = \text{Log}(\{O_2\} + 0.01)/(23.99 - \{O_2\}) \dots (67)$$

In this transformation the oxygen concentrations were expressed as volume percentages and the inserted value of 23.99 was chosen as being just greater than the highest recorded values (the highest theoretical value is 21% V/v but due to small detection errors some values of 22% V/v were calculated). The inserted values (0.01 and 23.99) are necessary to avoid dividing by zero or trying to read the logarithm of zero or a negative number.

The resulting analysis of variance table is Table 6.13 and the significant results are indicated. As with the matric potential data, only the most significant sources of variance are examined further by tables of means. The means used in these tables (Tables 6.14 and 6.15) are those from the untransformed data with the corresponding means of transformed data in parenthesis. The back-transformation means are not used to compare treatments, as they are somewhat exaggerated due to biasing introduced in the transformed analysis, and of little real meaning (Finney, 1973). Fortunately the order or ranking of means remained unchanged by the transformation, so this approach is validated.

The most significant source of variance indicated in Table 6.13, is species, and the overall mean oxygen concentrations for each species are given in Table 6.14. These show an enhancement of aeration under

Table 6.13 Analysis of variance of Falstone soil oxygen concentrations ($\%V/V$) for 1978

Source of Variation	DF	MS	VR
Cultivation	1	7.02	3.42
Species	2	296.62	144.75 **
Replicate	1	6.65	3.24
Depth	3	177.18	86.46 **
Time	26	15.59	7.61 **
Cultivation Species	2	95.01	46.37 **
Cultivation Replicate	1	64.63	31.54 **
Species Replicate	2	11.40	5.56 **
Cultivation Depth	3	3.14	1.53
Species Depth	6	42.35	20.66 **
Replicate Depth	3	11.75	5.73 **
Cultivation Time	26	2.55	1.24
Species Time	52	4.85	2.37 **
Replicate Time	26	1.97	0.96
Depth Time	78	4.76	2.32 **
Cultivation Species Replicate	2	76.13	37.15 **
Cultivation Species Depth	6	16.95	8.27 **
Cultivation Replicate Depth	3	6.04	2.95 *
Species Replicate Depth	6	17.88	8.72 **
Cultivation Species Time	52	2.04	0.99
Cultivation Replicate Time	26	3.24	1.58 *
Species Replicate Time	52	2.01	0.98
Cultivation Depth Time	78	3.22	1.57 **
Species Depth Time	156	3.45	1.68 **
Replicate Depth Time	78	2.48	1.21
Cultivation Species Rep.Depth	6	10.38	5.06 **
Cultivation Species Rep.Time	52	2.41	1.18 **
Cultivation Species Depth Time	153	2.50	1.22 **
Cultivation Replicate Depth Time	78	1.92	0.93
Species Replicate Depth Time	153	2.64	1.29 **
Residual	123	2.04	
Total	1256	4.69	

* P < 0.05

** P < 0.01

Table 6.14 Means of 1978 Falstone oxygen concentrations ($\text{m}^3 \text{m}^{-3}$) for the source of variance shown with their transformation means given in parenthesis, and standard errors of differences s.e.d.

Species	Oxygen concentration ($\text{m}^3 \text{m}^{-3}$)					
	Turf-planted		Ploughed		Combined	
MC	0.077(-1.22)		0.051(-2.12)		0.064(-1.67)	
SS	0.077(-1.31)		0.111(-0.41)		0.094(-0.86)	
LP	0.115(-0.24)		0.138(0.21)		0.126(-0.02)	
		s.e.d. 0.004		s.e.d. 0.003		
Replicate	1	2	1	2	1	2
All	0.083(-1.07)	0.090(-0.77)	0.111(-0.48)	0.088(-1.07)		
		s.e.d. 0.004				
MC	0.064(-1.58)	0.090(-0.86)	0.067(-1.65)	0.034(-2.60)	0.065(-1.62)	0.062(-1.73)
SS	0.063(-1.58)	0.091(-1.04)	0.141(0.34)	0.080(-1.16)	0.102(-0.62)	0.085(-1.10)
LP	0.123(-0.06)	0.106(-0.41)	0.124(-0.13)	0.151(0.55)	0.124(-0.10)	0.129(0.07)
		s.e.d. 0.006				s.e.d. 0.004

Table 6.15 Means of 1978 Falstone oxygen concentrations (m^3m^{-3}) for the source of variance shown with their transformation means given in parenthesis, and standard errors of differences s.e.d.

Species and cultivation type	Oxygen concentration (m^3m^{-3})			
	0.15m	0.30m	0.60m	0.90m
All sites	0.137(0.20)	0.093(-0.90)	0.070(-1.47)	0.079(-1.23)
		s.e.d. 0.004		
MC	0.071(-1.31)	0.054(-1.91)	0.046(-2.39)	0.085(-1.08)
SS	0.145(0.36)	0.095(-0.85)	0.071(-1.24)	0.065(-1.71)
LP	0.195(1.56)	0.131(0.05)	0.093(-0.77)	0.086(-0.91)
		s.e.d. 0.006		
Turf planted	0.099(-0.63)	0.077(-1.16)	0.042(-2.35)	0.090(-0.73)
MC Ploughed	0.042(-1.98)	0.031(-2.66)	0.049(-2.44)	0.080(-1.42)
Turf planted	0.115(-0.44)	0.068(-1.46)	0.078(-1.10)	0.047(-2.25)
SS Ploughed	0.175(1.15)	0.121(-0.24)	0.063(-1.39)	0.082(-1.16)
Turf planted	0.182(1.28)	0.104(-0.51)	0.087(-0.75)	0.085(-0.97)
LP Ploughed	0.207(1.85)	0.159(0.616)	0.098(-0.79)	0.088(-0.86)
		s.e.d. 0.009		

the tree species compared with the grassland sites, and a higher mean oxygen concentration under Pinus contorta than under Picea sitchensis. This ranking of mean oxygen concentration with species is also seen in Tables 6.14 and 6.15, where interactions with replication, cultivation regime and depth are examined.

Depth is the second most significant source of variance in the data (Table 6.13), and in Table 6.15 the overall means show a trend of decreasing oxygen concentration from 0.15m to 0.6m, but then a slight increase at 0.9m depth. If Table 6.15 is examined, then this increase can be seen to be caused by the Molinia caerulea sites in particular, and partly by Picea sitchensis sites in the ploughed area. In the Molinia caerulea sites the highest overall mean oxygen concentration is found at 0.9m depth not at 0.15m depth as generally found in the planted sites.

When examining the interaction between species and depth in Table 6.15, the ranking of mean oxygen concentrations being higher under Pinus contorta than Picea sitchensis and both higher than Molinia caerulea, is true at depths of 0.15 to 0.6m but at 0.9m depth little difference exists between any sites. It must be remembered that the gas probes are not vertically above one another, and that the increase at 0.9m may only be due to spatial differences in the soil.

The third largest source of variance is the interaction between cultivation regimes and species (Table 6.13), which takes the form of higher mean oxygen concentrations in the ploughed sites than the turf-planted sites (Table 6.14) under the tree species, but the reverse under Molinia caerulea. However, too much emphasis should not be placed upon this as evidence of enhanced aeration in the ploughed sites, as an examination of Table 6.14 shows that as great a difference can exist between replicates in one cultivation regime, as between the two regimes. Replication does not prove to be a significant single source of variance,

but its interactions with cultivation regimes, and cultivation regimes and species, prove to be of high significance. An examination of Table 6.14 shows again that differences between replicate means within a species are no greater than between cultivation regimes in one replicate within a species. Indeed the agreement of means for each species between replicates, when the cultivation regimes have been bulked together, is fairly close (Table 6.14). These observations, together with the fact that the two cultivation regimes do not constitute a significant single source of variance, lead to the conclusion that the differences in mean oxygen concentrations observed between them are no more than those found due to inherent soil spatial variability.

Unfortunately, the lack of carbon dioxide concentrations for water samples meant that a very large number of data points were missing for an analysis of variance test (385/1296 were missing, compared with 39/1296 missing oxygen concentrations). Because the computer program used for these tests (Genstat V) creates an estimate for missing values with zero residual variance, then the resulting analysis of variance is highly unreliable. For this reason no further analysis was conducted on carbon dioxide concentrations for 1978.

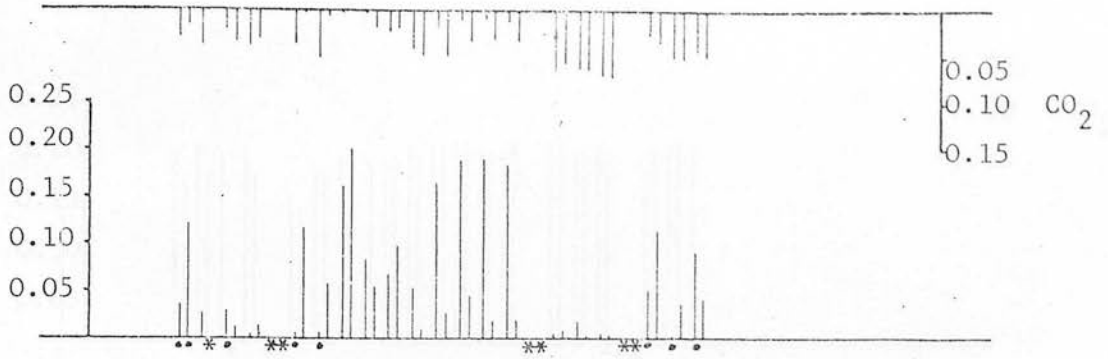
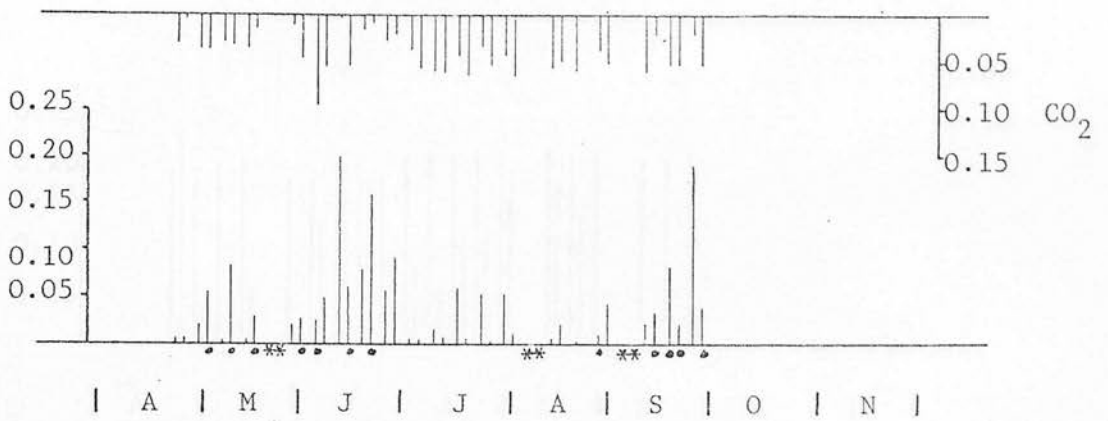
6.3.2. 1979 DATA

The oxygen and carbon dioxide concentrations for 1979 in sites 1 to 6, are shown in Figs. 6.23 to 6.25 in a similar manner to those for 1978.

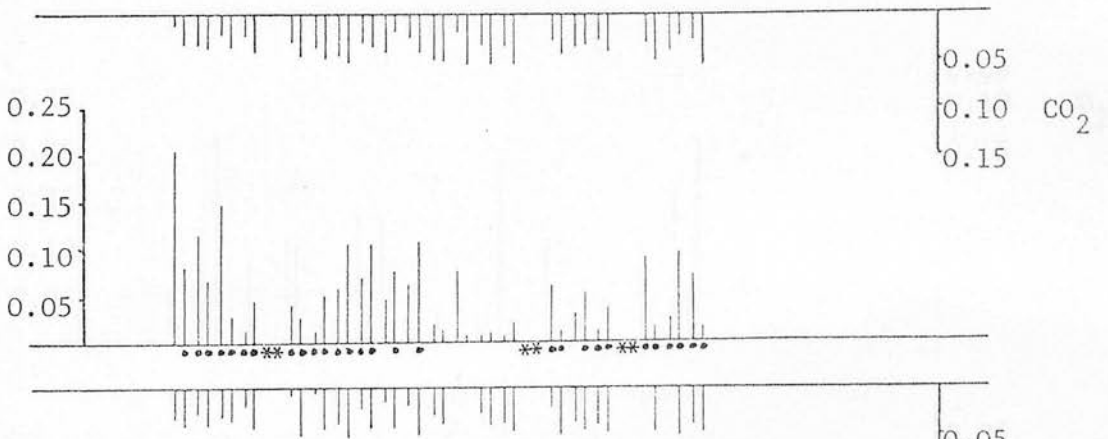
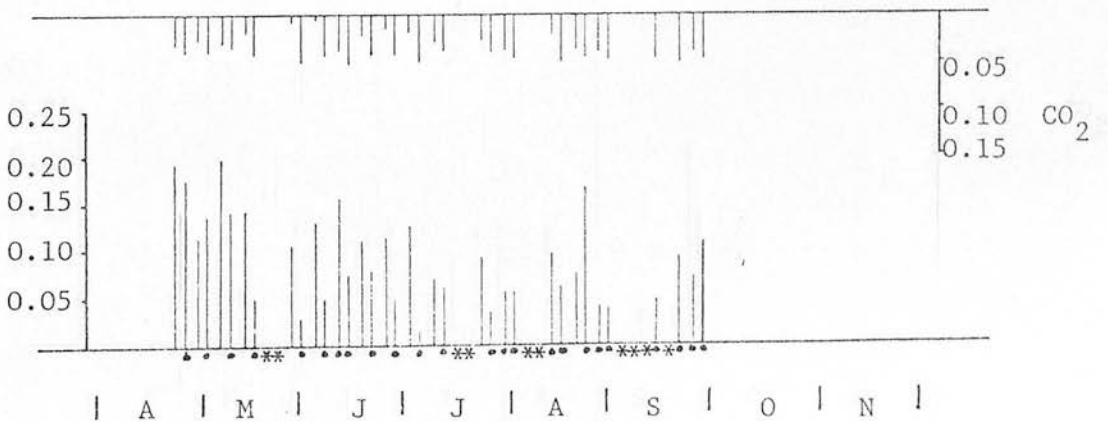
The main trends observed in 1978 are again apparent. The forested sites were well aerated throughout the season at 0.15m depth, with oxygen concentrations near $0.21 \text{ m}^3 \text{ m}^{-3}$, and carbon dioxide concentrations below $0.01 \text{ m}^3 \text{ m}^{-3}$ (though this is greater than atmospheric concentrations). At 0.3m depth sites 3 and 6 showed a similar maintenance of near atmospheric oxygen concentrations throughout the

Molinia caerulea (ploughed)

Depth

0.15m O₂0.30m O₂

1979

0.60m O₂0.90m O₂

1979

Fig.6.23 Soil oxygen and carbon dioxide concentrations ($\text{m}^3 \text{m}^{-3}$) in sites 1 and 2 (left and right hand lines of a pair respectively), at the depth indicated. A dot under the baseline indicates a water sample and an asterisk missing data.

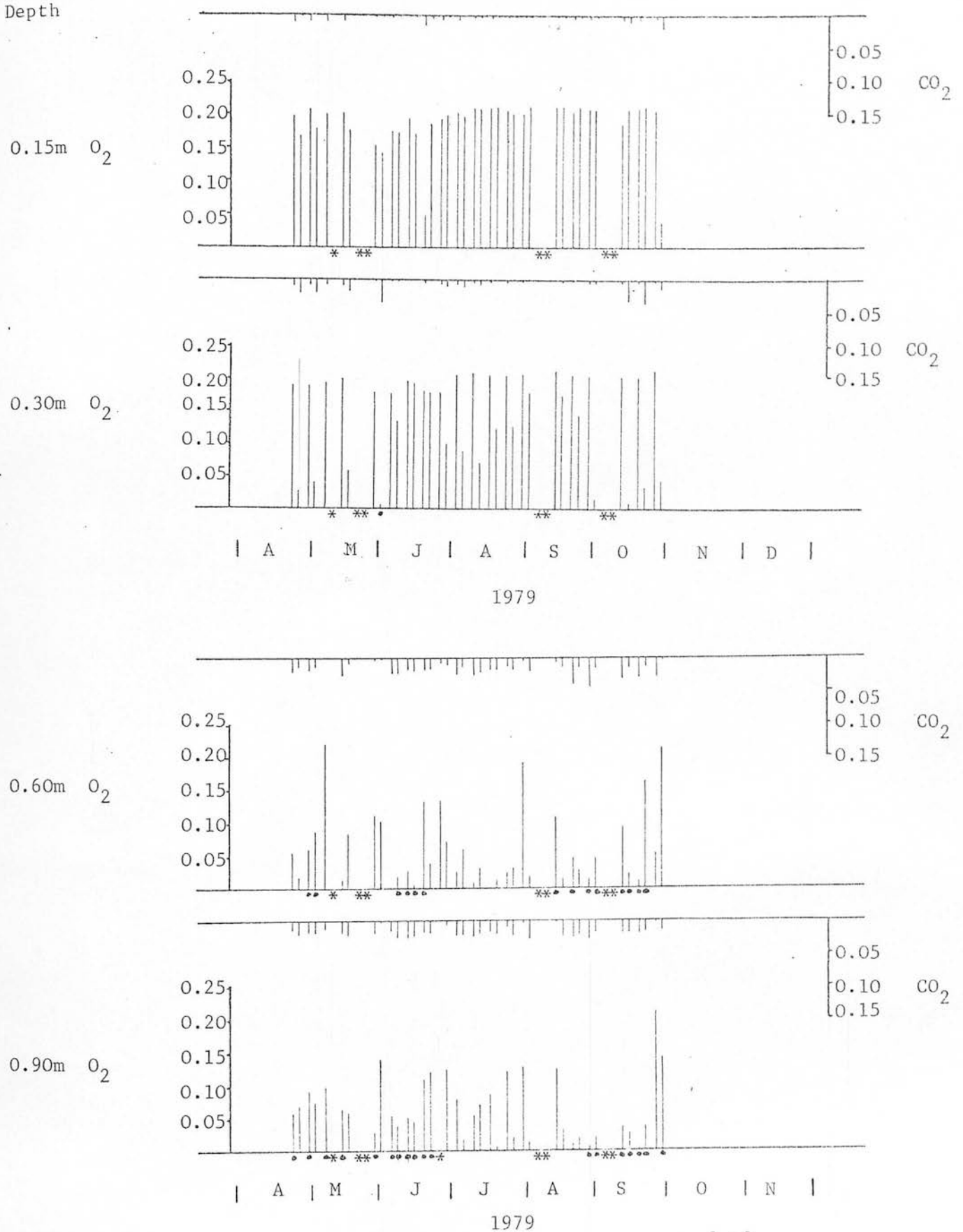
Picea sitchensis (ploughed)

Fig.6.24 Soil oxygen and carbon dioxide concentrations ($m^3 m^{-3}$) in sites 3 and 4 (left and right hand lines of a pair respectively), at the depth indicated. A dot under the baseline indicates a water sample and an asterisk missing data.

Pinus contorta (ploughed)

Depth

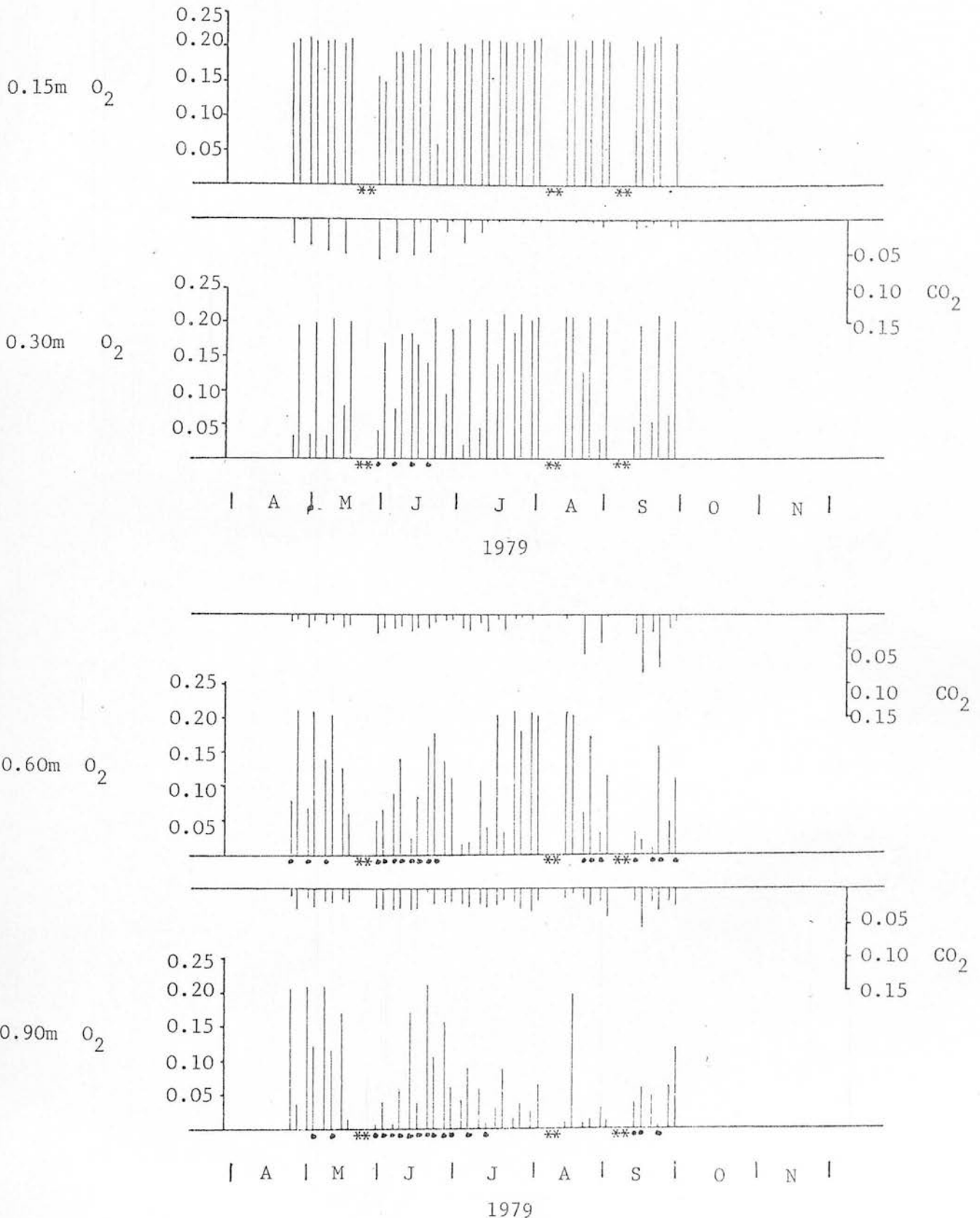


Fig.6.25 Soil oxygen and carbon dioxide concentrations ($m^3 m^{-3}$) in sites 5 and 6 (left and right hand lines of a pair respectively), at the depth indicated. A dot under the baseline indicates a water sample and an asterisk missing data. CO_2 concentrations at 0.15m depth were all below 0.01 $m^3 m^{-3}$ and so have been omitted.

season, but sites 4 and 5 indicated periods of poor aeration until mid-June, at the start of July, and from mid-August onwards (Figs.6.24 and 6.25). If the matric potentials for these sites are examined (Figs.6.12 to 6.14) then it will be seen that sites 4 and 5 were generally wetter than their replicates (sites 3 and 6). In site 5 under Pinus contorta carbon dioxide concentrations frequently reached 0.03 to 0.05 $\text{m}^3 \text{m}^{-3}$ during the initial period of poor aeration until July, and in site 4 under Picea sitchensis concentrations were often above 0.01 $\text{m}^3 \text{m}^{-3}$.

The trend of shorter periods of enhanced aeration with depth observed in the 1978 data was also present in the 1979 data for sites 5 and 6 under Pinus contorta (Fig.6.25) but is indistinct for Picea sitchensis sites (Fig.6.24). At 0.6m depth under Pinus contorta this period corresponded roughly to the period when matric potentials were less than -5kPa, but coincided less exactly than in the 1978 data. At 0.6m depth in the Picea sitchensis sites (Fig.6.24) the oxygen concentrations were generally very low ($<0.05 \text{m}^3 \text{m}^{-3}$) throughout the season. Carbon dioxide concentrations were generally 0.02 to 0.03 $\text{m}^3 \text{m}^{-3}$ and the pattern resembled that found at 0.9m depth in sites of both tree species. At 0.9m depth in all these forested sites oxygen concentrations were generally low, reaching almost zero during early August. This period corresponded to that of maximum moisture deficit at shallower depths, but at 0.9m the soil did not fall much below -5kPa matric potential, and the temperature was at its highest (about 9°C). This trend is also mentioned with regard to the 1978 data, but carbon dioxide values from water samples were missing from much of this period. The carbon dioxide data for 1979 at 0.9m depth in these forested sites showed reasonably constant values at about 0.02 to 0.025 $\text{m}^3 \text{m}^{-3}$, irrespective of what the oxygen concentration was and whether it was obtained from a water or gas sample.

Carbon dioxide concentrations in the open sites proved to be generally higher than the forested sites for all depths and were of the order of 0.02 to 0.06 m^3m^{-3} throughout the season. There was little evidence in these sites of marked periods when high carbon dioxide concentrations coincided with low oxygen concentrations, though some trend of this type was shown at a depth of 0.15m (Fig.6.23). The oxygen concentrations in the grassland sites at all depths (Fig.6.23) showed the trend observed in 1978 and also at 0.9m depth in the forested sites, of very low oxygen concentrations (0 to 0.02 m^3m^{-3}) during August. Higher oxygen concentrations were observed before and after this period but they were much lower than those found at similar depths in the forested sites. At 0.9m depth practically all the samples removed were water samples and showed consistently higher oxygen concentrations than at shallower depths, while carbon dioxide concentrations remained of the same order at depths from 0.3 to 0.9m.

To examine the differences between species and depths further, an analysis of variance test was conducted as for the 1978 data. The oxygen concentration data were again transformed according to Equation (67) and a transformation was also found necessary for the carbon dioxide data. A simple logarithmic transformation was all that was required to produce a random scatter in the carbon dioxide data residuals.

The analysis of variance table for oxygen concentrations is given in Table 6.16, and that for carbon dioxide concentrations in Table 6.19. As for the 1978 data, the tables of means that follow (Tables 6.17 and 6.18) are the means of untransformed data with the means from the transformed analysis in parenthesis.

The most significant source of variance in the oxygen concentration data is again species and the overall means for 1979 are given in Table 6.17. The comparison between species indicates the same trend as 1978 i.e. that higher oxygen concentrations are maintained

Table 6.16 Analysis of variance of Falstone soil oxygen concentrations (%^v/v) for 1979

Source of Variation	DF	MS	VR	
Species	2	147.99	82.79	**
Replicate	1	3.24	1.81	
Depth	3	76.50	42.80	**
Time	19	5.50	3.07	**
Species Replicate	2	18.83	10.53	**
Species Depth	6	53.31	29.82	**
Replicate Depth	3	4.42	2.47	
Species Time	38	2.05	1.15	*
Replicate Time	19	1.95	1.09	
Depth Time	57	2.37	1.33	*
Species Replicate Depth	6	12.83	7.18	**
Species Replicate Time	37	1.01	0.56	
Species Depth Time	113	1.91	1.06	**
Replicate Depth Time	57	1.29	0.72	
Residual	104	1.78		
Total	467	3.95		

* P<0.05
** P<0.01

Table 6.17 Means of 1979 Falstone oxygen concentrations (m^3m^{-3}) for the source of variance shown with their transformation means given in parenthesis, and standard errors of differences s.e.d.

Depth(m)	Oxygen concentration (m^3m^{-3})			
	MC	SS	LP	All
0.15	0.059(-1.66)	0.188(1.39)	0.201(1.71)	0.015(0.48)
0.30	0.042(-2.20)	0.147(0.48)	0.145(0.50)	0.111(-0.41)
0.60	0.052(-1.63)	0.062(-1.65)	0.113(-0.20)	0.076(-1.16)
0.90	0.090(-0.60)	0.066(-1.27)	0.074(-1.16)	0.077(-1.01)
			s.e.d.	s.e.d.
			0.005	0.006
All	0.061(-1.52)	0.116(-0.26)	0.133(0.21)	
		s.e.d.		
		0.005		

Table 6.18 Means of 1979 Falstone oxygen concentrations (m^3m^{-3}) for the sources of variance shown with their transformation means given in parenthesis, and standard errors of difference s.e.d.

Replicate	Species	Oxygen concentration (m^3m^{-3})			
		0.15	0.30	0.60	0.90
1	MC	0.068(-1.53)	0.045(-2.13)	0.057(-1.53)	0.106(-0.19)
	SS	0.191(1.46)	0.198(1.56)	0.065(-1.80)	0.081(-0.96)
	LP	0.206(1.80)	0.091(-0.60)	0.099(-0.53)	0.085(-0.96)
2	MC	0.050(-1.79)	0.038(-2.28)	0.047(-1.74)	0.074(-1.07)
	SS	0.185(1.31)	0.096(-0.61)	0.060(-1.51)	0.052(-1.58)
	LP	0.196(1.62)	0.198(1.59)	0.127(0.13)	0.063(-1.36)

under Pinus contorta than under Picea sitchensis, which in turn is higher than under Molinia caerulea. This ranking is seen again in Table 6.17 for species interaction with depth, but the exception noticed in the 1978 data, that at 0.9m depth little difference existed, is even more marked as the mean oxygen concentration in the open sites is significantly higher than the forested sites.

Depth is the next most significant source of variance and Table 6.17 shows that the same trend as 1978 is maintained, i.e. that the mean oxygen concentration tends to decrease with depth down to 0.6m and then there is a slight increase at 0.9m depth. Once again this is shown to be caused by a major increase at this depth in the open sites compared with shallower depths (Table 6.17). Table 6.18 shows this to occur in both replicates, and also shows that it occurred in site 3 under Picea sitchensis. The mean oxygen concentration was shown to be at its lowest in the open sites at 0.3m depth (Table 6.18), and it is also interesting to note that at this depth the mean oxygen concentrations in sites 4 and 5 were somewhat lower than their replicates (3 and 6). This is another indication of the nature of spatial variability affecting aeration and the sampling method, but it is encouraging to note that replication does not seem a major source of variance overall.

The analysis of variance on the carbon dioxide concentrations (Table 6.19) largely mirrors that for oxygen concentrations in that the largest source of variance is again species, with depth the next largest. Table 6.20 shows the mean carbon dioxide concentrations for each species and demonstrates the generally higher concentrations found under Molinia caerulea than under either tree species (Table 6.20). Overall, ~~oxygen~~ ^{carbon dioxide} concentrations ~~declined~~ ^{increased} with increasing depth (Table 6.20), but Tables 6.20 and 6.21 show that this trend varied between species. In the grassland sites mean carbon dioxide concentrations proved to be about

Table 6.19 Analysis of variance of Falstone soil carbon dioxide concentrations (%^v/v) for 1979

Source of Variation	DF	MS	VR
Species	2	136.52	172.83 **
Replicate	1	4.70	5.95 *
Depth	3	59.76	75.65 **
Time	19	1.35	1.71 *
Species Replicate	2	8.66	10.97 **
Species Depth	6	11.89	15.05 **
Replicate Depth	3	5.34	6.76 **
Species Time	38	0.99	1.26
Replicate Time	19	0.89	1.13
Depth Time	57	0.82	1.04
Species Replicate Depth	6	8.45	10.70 **
Species Replicate Time	37	0.37	0.47
Species Depth Time	113	0.77	0.98
Replicate Depth Time	57	0.74	0.94
Residual	104	0.78	
Total	467	2.07	

* P<0.05

** P<0.01

Table 6.20 Means of 1979 Falstone carbon dioxide concentrations ($\text{m}^3 \text{m}^{-3}$)
for the sources of variance shown with their transformation
means given in parenthesis and standard errors of differences
s.e.d.

		Carbon dioxide concentration ($\text{m}^3 \text{m}^{-3}$)			
		MC	SS	LP	All
Depth(m)	0.15	0.035(0.95)	0.005(-1.16)	0.003(-1.42)	0.014(-0.54)
	0.30	0.042(1.28)	0.008(-0.76)	0.014(-1.03)	0.021(-0.17)
	0.60	0.037(1.27)	0.019(0.37)	0.020(0.29)	0.025(0.64)
	0.90	0.037(1.25)	0.018(0.44)	0.025(0.83)	0.027(0.84)
				s.e.d. 0.002	s.e.d 0.001
	All	0.038(1.19)	0.015(-0.33)	0.013(-0.28)	s.e.d. 0.001

Table 6.21 Means of 1979 Falstone carbon dioxide concentrations ($\text{m}^3 \text{m}^{-3}$)
for the sources of variance shown with their transformation
means given in parenthesis and standard errors of differences
s.e.d.

Replicate	Species	Carbon dioxide concentration ($\text{m}^3 \text{m}^{-3}$)			
		0.15	0.30	0.60	0.90
1	MC	0.035(1.00)	0.039(1.15)	0.032(1.118)	0.029(0.99)
	SS	0.007(-0.52)	0.005(-1.02)	0.022(0.50)	0.017(0.28)
	LP	0.002(-1.42)	0.025(0.06)	0.021(0.57)	0.022(0.70)
2	MC	0.036(0.90)	0.044(1.41)	0.042(1.41)	0.046(1.51)
	SS	0.003(-1.81)	0.012(-0.50)	0.015(0.24)	0.020(0.60)
	LP	0.003(-1.42)	0.002(-2.13)	0.020(0.02)	0.028(0.96)
		s.e.d. 0.003			

50 percent higher than in the forested sites at depths 0.6 and 0.9m, but up to 10 x higher at 0.15m depth.

In the grassland sites, the highest mean carbon dioxide concentrations were found at 0.3m depth (Table 6.20), though this is mainly due to site 1 and there was no significant difference between 0.3, 0.6 and 0.9m depth in site 2. The only significant differences between sites 1 and 2 occurred at depths of 0.6 and 0.9m where site 1 yielded lower carbon dioxide concentrations than site 2. In the forested sites there was no significant differences between depths of 0.6 and 0.9m in any site (Table 6.20) nor between 0.15 and 0.3m depths in sites 3 and 6, but in sites 4 and 5 concentrations at 0.3m depth were closer to those lower down the profile, than to 0.15m. In all forested sites at 0.15m depths mean concentrations were of the order of 5 to 10 times lower than at greater depths, at about $0.003\text{m}^3\text{m}^{-3}$, though this is about 10 times higher than ambient atmospheric concentrations.

It is interesting to note that for carbon dioxide concentrations, "Time" is only just significant as a source of variance at the 5 percent probability level, and that none of its interactions are significant (Table 6.19). Although not a major single source of variance in the oxygen concentration analysis, it is significant at the 1 percent probability level in both 1978 and 1979 (Table 6.13 and 6.16).

6.4 CONCLUSIONS

The improvements in soil aeration under the tree cover, compared with the grassland, are partly caused by the reduction in the rain input to the soil by canopy interception loss. This loss causes a permanent lowering of the water table and subsequently lower matric potentials in the soil above the water table during the moisture deficit period during the summer. The effect on the aeration-status is that a zone of almost permanently well aerated soil exists in the top 0.2 to

0.3m under the trees, whereas in the open sites at the same depths there were frequent periods of very low oxygen concentrations. At greater depths well aerated periods were firmly correlated with periods of moisture deficit, when the soil moisture potentials fell below a value of about -5kPa. Oxygen concentrations rose to near atmospheric levels rapidly after the matric potential had fallen below this value, and if it continued to fall. When the soil was above or at -5kPa matric potential, the oxygen concentrations were very variable, but usually showed some depletion of oxygen and enhanced carbon dioxide levels. In the grassland site where the matric potential rarely fell below -5kPa even at 0.15 and 0.30m depth, oxygen concentrations rarely reached atmospheric levels, and varied greatly from week to week. In the grassland sites it was seen that the highest oxygen concentrations were very often at the lowest depth of 0.9m, and measured in water samples removed from far below the water table.

Two possible explanations for this are; (1) that the roots of Molinia caerulea, which are known to have an extensive aerenchyma system (Armstrong, 1964) are providing a preferential pathway for oxygen diffusion which is being released to the soil pore space at depth, and (2) that freshly aerated rainwater is moving down the profile (and possibly laterally into the site), and the oxygen is not being removed at depth as there are no aerobically respiring roots or microorganisms.

If (1) were the case then one would expect more oxygen to be released or respired at the surface, and progressively less down the root as its internal concentration fell with distance. The oxygen concentration recorded nearer the surface in these sites was very low indeed, nearing zero in mid-season when temperatures were high (10°C) at 0.30 and 0.60m depth. This suggests that the mass of respiring roots is at depths down to 0.6m. It is difficult to see how oxygen diffusion through this actively respiring region could provide sufficient oxygen

to be released from fewer roots to give equivalent gas phase concentrations of 0.05 to 0.10 m^3m^{-3} in the general soil pore water. Conversely if (2) were the case, the aerated rainwater would have to percolate through the rooting zone without releasing all of its dissolved oxygen to respiration. If this were the case, then once the water was below this active rooting zone then there would be little respiratory drain on the dissolved oxygen. A third possibility also exists, and that is that the higher oxygen concentrations at 0.9m compared with shallower depths in the grassland sites, is a statistical effect due to soil spatial variability. A comparison of the data from replicate probes show that very large spatial differences can occur. However, the mean oxygen concentrations given in Table 6.18 suggest that the difference in mean oxygen concentration between 0.9m and shallower depths in each grassland site is greater than between replicates and greater than the standard error of differences between means. It is difficult therefore, to come to any firm conclusions as to aeration at this depth under Molinia caerulea.

Whichever of the above cases is correct, there can be little doubt that under both grassland and tree species in regions of the soil where matric potentials are about or above -5kPa, oxygen concentrations can approach zero if aerobic respiration is occurring. It has already been mentioned that under the tree species, following a period of higher oxygen concentrations during the driest period at 0.6 and 0.9m depth, there was a period of low oxygen concentrations, followed in turn by a period of higher concentrations again (from water samples). The most likely explanation of this is that gaseous diffusion is sufficient to supply oxygen to respiring roots during the moisture deficit period, but when the water table rises again diffusion is limited and oxygen rapidly depleted. The subsequent rise in concentrations again, suggests the

cessation of aerobic respiration even though the soil temperature is still favourable. The implications of this are that actively respiring root tips are killed off by the onset of anaerobicity. It is at this time of year (about September) that the internal air space system in Pinus contorta may confer an advantage to this species over Picea sitchensis (Coutts and Philipson, 1978b).

The use of an analysis of variance test to identify major causes of variance in the measured concentrations of oxygen and carbon dioxide, is one method of enabling us to compare the effectiveness of species and depths on the soil aeration status. The fact that the major trends observed (i.e. that oxygen concentrations decrease with depth and are generally higher under Pinus contorta, than under Picea sitchensis and lower still under Molinia caerulea), are similar for both years, even though 1979 was a much wetter year than 1978, lends credence to the deduction made. However, the necessary transformation of the data may cause some doubt as to conclusions, drawn from the untransformed means. The transformation was necessary because the distribution of residual errors was not normal and this condition arises from the bi-modal frequency distribution of the oxygen concentration data themselves. The overall distribution of oxygen concentrations for 1979 is given in Fig.6.26, and it can be seen that there is a large number of measurements where the concentration is either near atmospheric or near zero, with fewer observations at intermediate concentrations. This is caused by the skewed distributions found for individual species/depth treatments in Figs.6.27 to 6.29 (replicates have been bulked together). The shifts in the maxima of these distributions with depth for each species, are themselves a clear indication of the effectiveness of each species on the aeration status of the soil. Under Molinia caerulea (Fig. 6.27) the soil is nearly anaerobic for most of the time at depths down to 0.6m, but at 0.9m an almost equal number of instances were recorded for discrete intervals

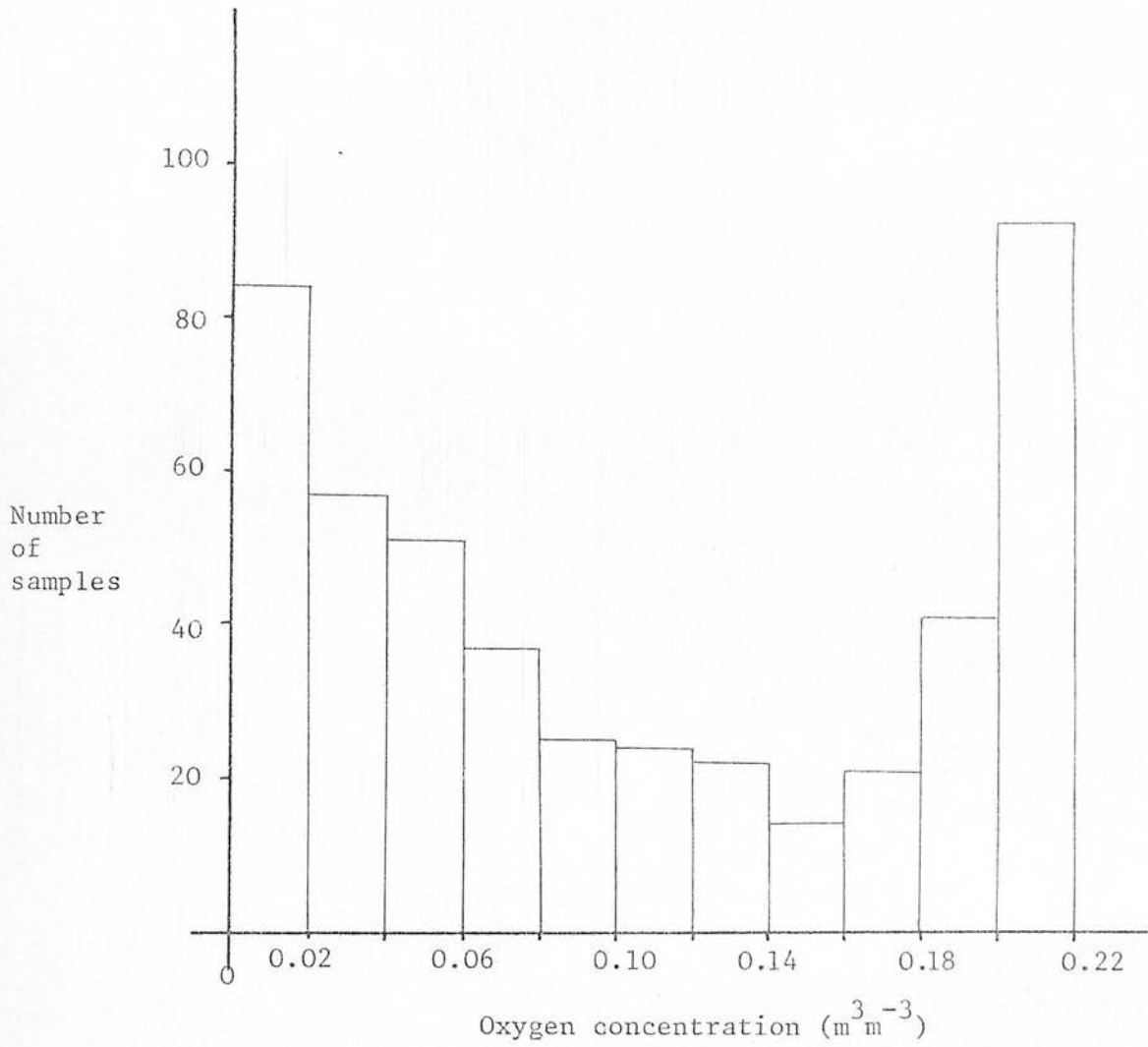


Fig.6.26 Frequency distribution of 1979 oxygen concentration data, for all sites and depths.

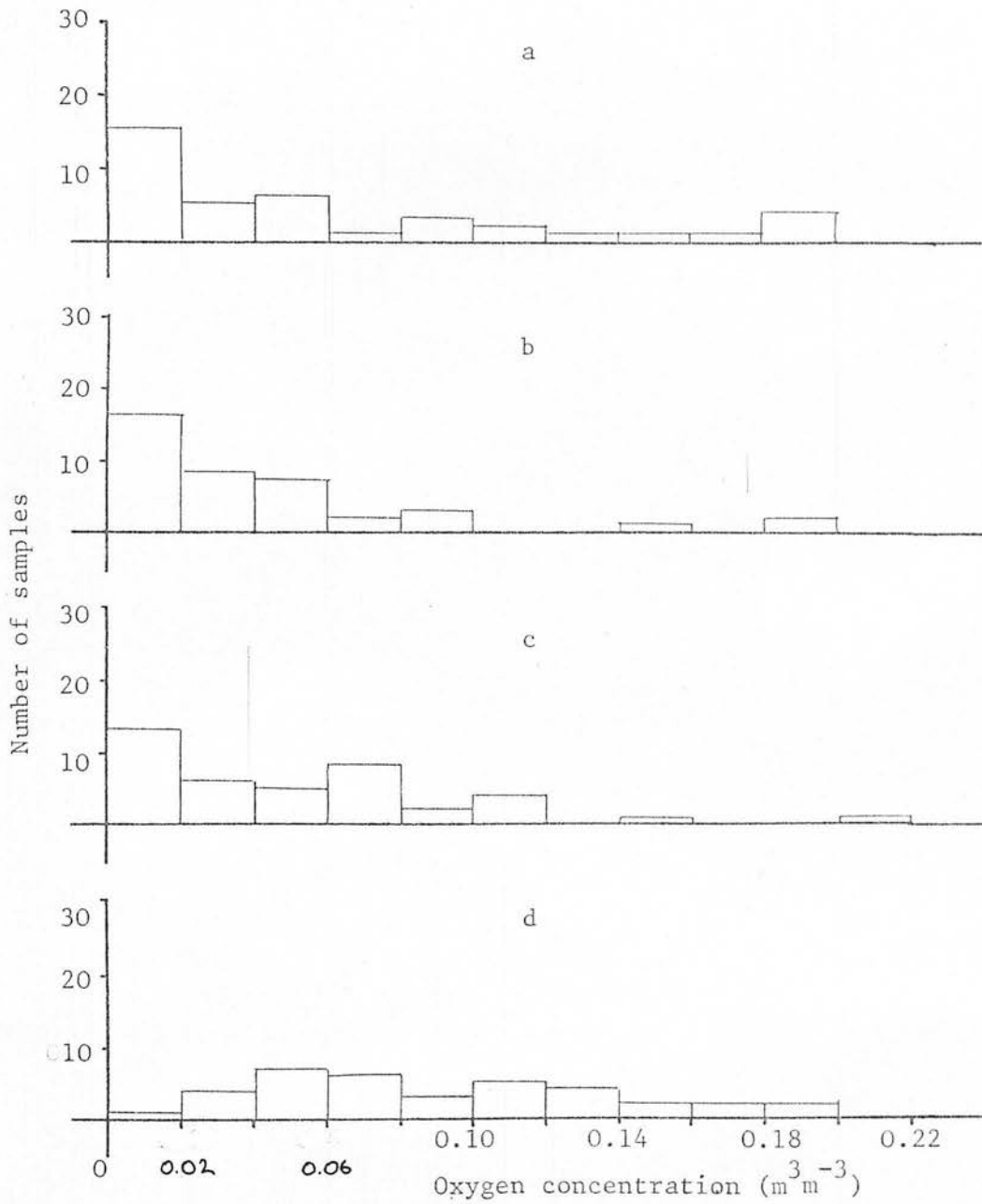


Fig.6.27 Frequency distribution of 1979 oxygen concentration data for sites 1 and 2 (*Molinia caerulea*) at depths of:-
a -0.15m, b-0.30m, c-0.60m, d-0.90m.

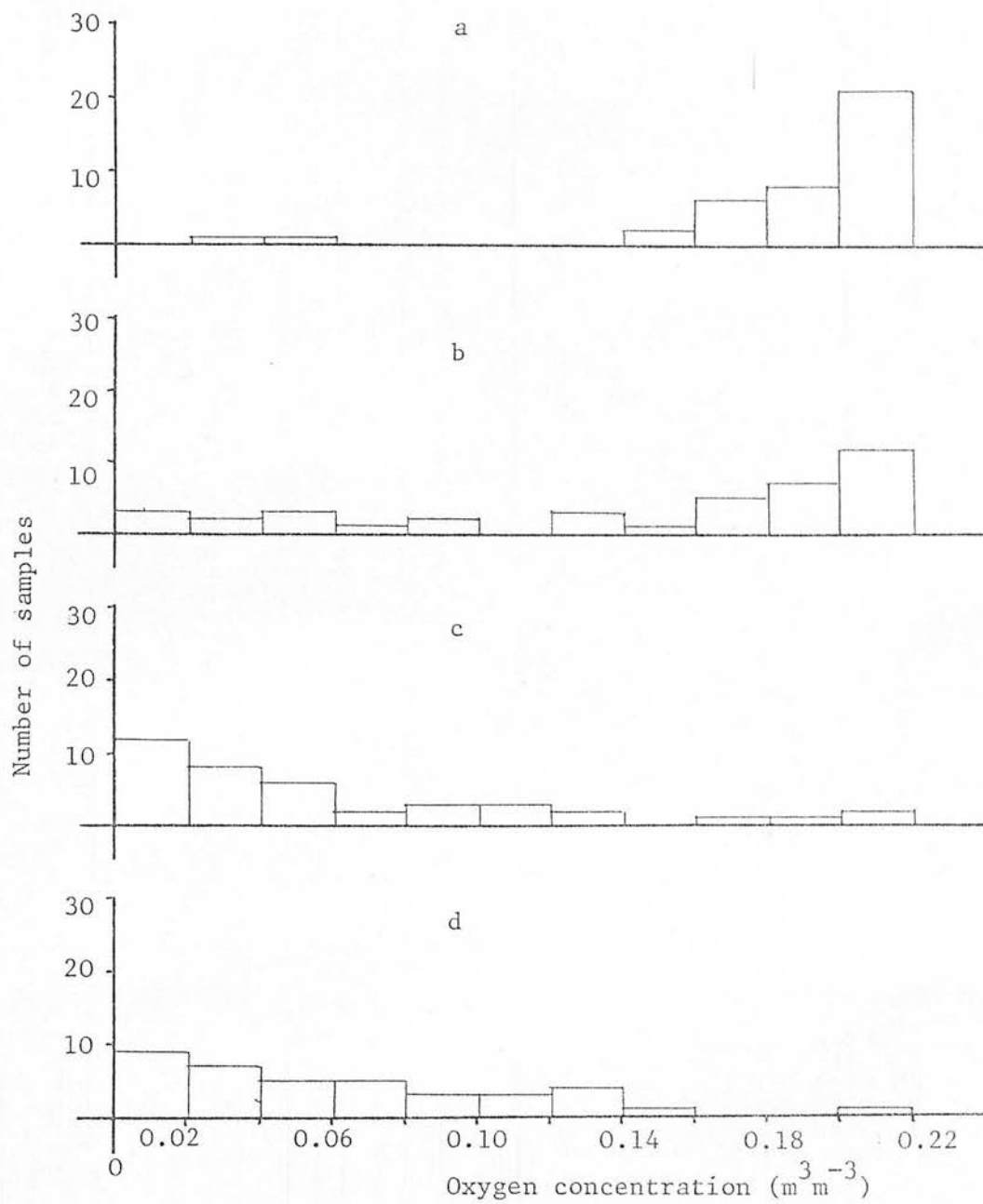


Fig.6.28 Frequency distributions of 1979 oxygen concentration data for sites 3 and 4 (*Picea sitchensis*) at depths of:-
a -0.15m, b-0.30, c-0.60m and d-0.90m.

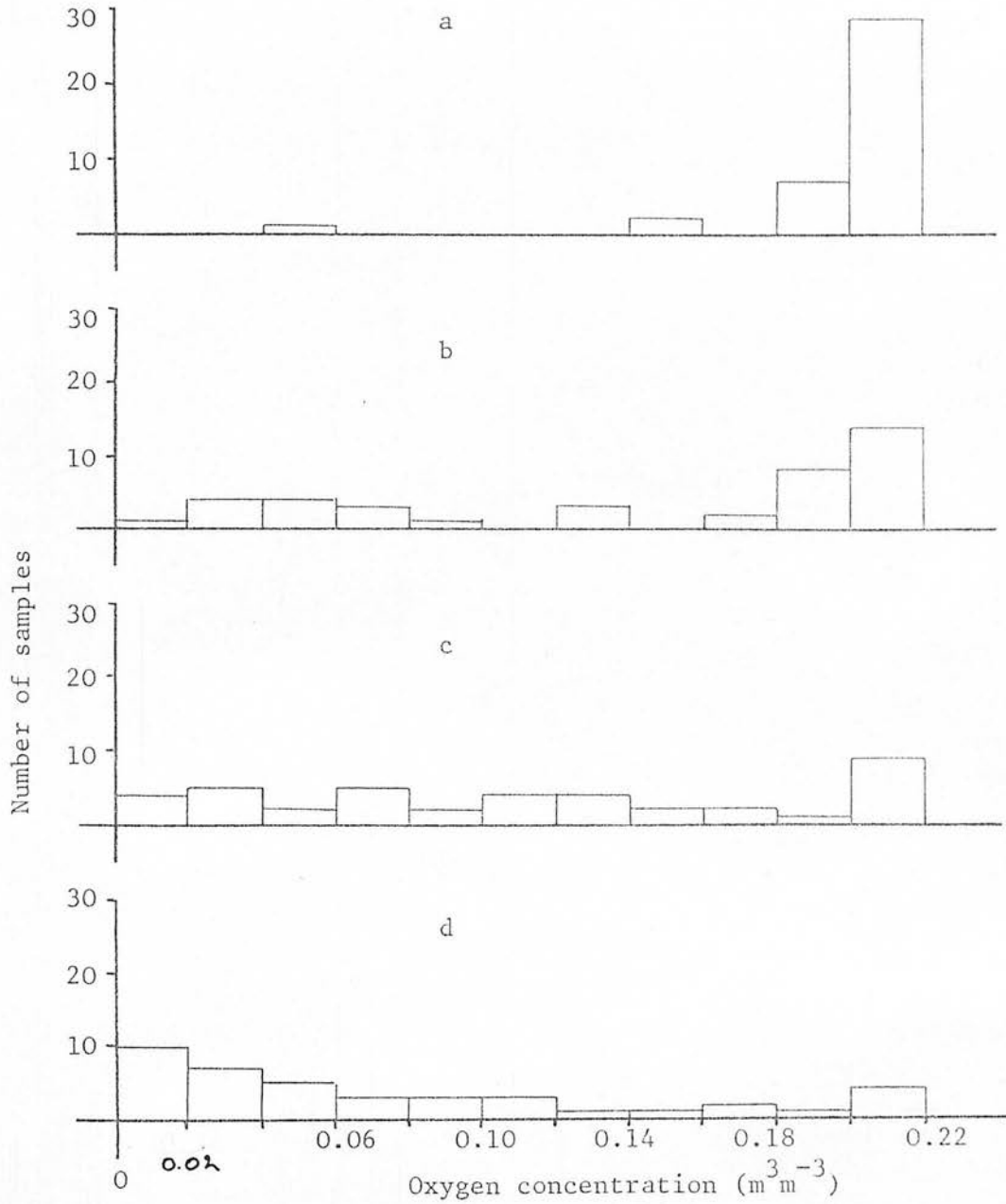


Fig.6.29 Frequency distribution of 1979 oxygen concentration data sites 5 and 6 (*Pinus contorta*) at depths of:-
a - 0.15m, b-0.30m, c-0.60m, d-0.90m.

of $0.02\text{m}^3\text{m}^{-3}$ over the whole range of oxygen concentrations. The Pinus contorta sites (Fig.6.29) show a very different picture, with a gradual shift in the number of observations from near atmospheric at 0.15m depth to near zero at 0.9m depth. The Picea sitchensis data (Fig.6.28) show a similar shift, but are different from the Pinus contorta sites, in that there is already a maximum number of observations near zero at 0.6m depth while under Pinus contorta at this depth there is a more even distribution with a slight maximum at atmospheric levels.

This method of using frequency distributions to observe soil aeration patterns was used by Dowdell et al (1979), who went further and used a χ^2 test to compare treatments. To do this the oxygen concentration of $0.10\text{m}^3\text{m}^{-3}$ was taken to represent the difference between "well aerated" and "poorly aerated" conditions (Grable, 1966). On this basis a χ^2 test has been performed across all three species at each depth (Table 6.22), and similarly just across the two tree species at each depth (Table 6.23).

This analysis corroborates the differences between species observed in the analysis of variance test, but highlights depths at which significant differences exist. Table 6.22 shows that no significant differences existed between open and forested sites at 0.9m depth in 1979, and Table 6.23 shows that the only significant difference between the two tree species occurred at 0.6m depth. The overall conclusion is that there is convincing evidence that Pinus contorta have higher oxygen concentrations than Picea sitchensis at depths between the water table and a well aerated surface zone.

The carbon dioxide concentration data for 1979 could not be used as a variable to show seasonal fluctuations in the soil aeration status. Although significant differences in concentrations were recorded between species and depth, only small changes over time were recorded. According to theory, one molecule of carbon dioxide should be released for every molecule of oxygen respired, and so gaseous carbon dioxide

Table 6.22 Fraction of samples in 1979 with oxygen concentrations greater than $0.10 \text{ m}^3 \text{ m}^{-3}$, in all sites at depths shown

Depth(m)	Fraction			χ^2
	MC	SS	LP	
0.15	0.07	0.32	0.32	72.24 ***
0.30	0.03	0.24	0.23	40.22 ***
0.60	0.05	0.08	0.18	16.96 ***
0.90	0.13	0.08	0.11	2.93

Table 6.23 Fraction of samples in 1979 with oxygen concentrations greater than $0.10 \text{ m}^3 \text{ m}^{-3}$, in the forested sites only at depths shown

Depth(m)	Fraction		χ^2
	SS	LP	
0.15	0.47	0.49	0.36
0.30	0.35	0.34	0.20
0.60	0.11	0.28	8.90 **
0.90	0.12	0.15	0.39

N.B. * $P < 0.05$
 ** $P < 0.01$
 *** $P < 0.001$

concentration ρ should equal the oxygen deficit from $0.21 \text{ m}^3 \text{ m}^{-3}$. The presence of water alters this relationship in the gas phase, as carbon dioxide is much more soluble in water than oxygen (Appendix 2), and this dissolved carbon dioxide must be taken into account to assess the RQ of a field soil. This problem will be discussed in Section 10, when the nature of oxygen and carbon dioxide concentration ρ changes with matric potentials and gas filled pore space are considered.

7. EDDLESTON FIELD EXPERIMENT

7.1 MOISTURE REGIME

The weekly rainfall figures at Eddleston from May onwards are given in Fig.7.1. No data are available for interception loss or throughfall at this site, but the resulting depths to the water table in each site are given in Fig.7.2.

The most obvious feature of the water table data is that in the untouched open site (OV) the depth to the water table was less than 0.1m, from October onwards, while in the open ploughed site (OP) it was about 0.35m (Fig.7.2). As both these sites have very similar vegetation cover, the most likely reason for this major difference is that the OP site is drained by sub-surface run-off to this depth, into a ditch surrounding the plot. At the end of the season, when the peat under the crop had returned to field capacity, the water table was at this same depth in the LP and SS sites, which are also surrounded by a drainage ditch.

The water table depths in Fig.7.2 suggest that the peat had already started to dry out when the experiment was started, and from then until August a steady increase in depth was observed. This corresponds to a period of low rainfall, as seen in Fig.7.1. The depths reached at the end of July were the maximum recorded in the OV (0.35m), OP (0.60m) and SS (0.75m) sites, before a sharp rise in the water table due to a period of high rainfall in August. The depth to the water table in the LP site, however, did not show a similar increase and continued to increase to a maximum depth of 0.9m in October.

The matric potential data from these sites are given in Figs. 7.3 and 7.4 in a similar manner to those for Falstone (where more than one tensiometer was installed at any depth a mean is given). The general

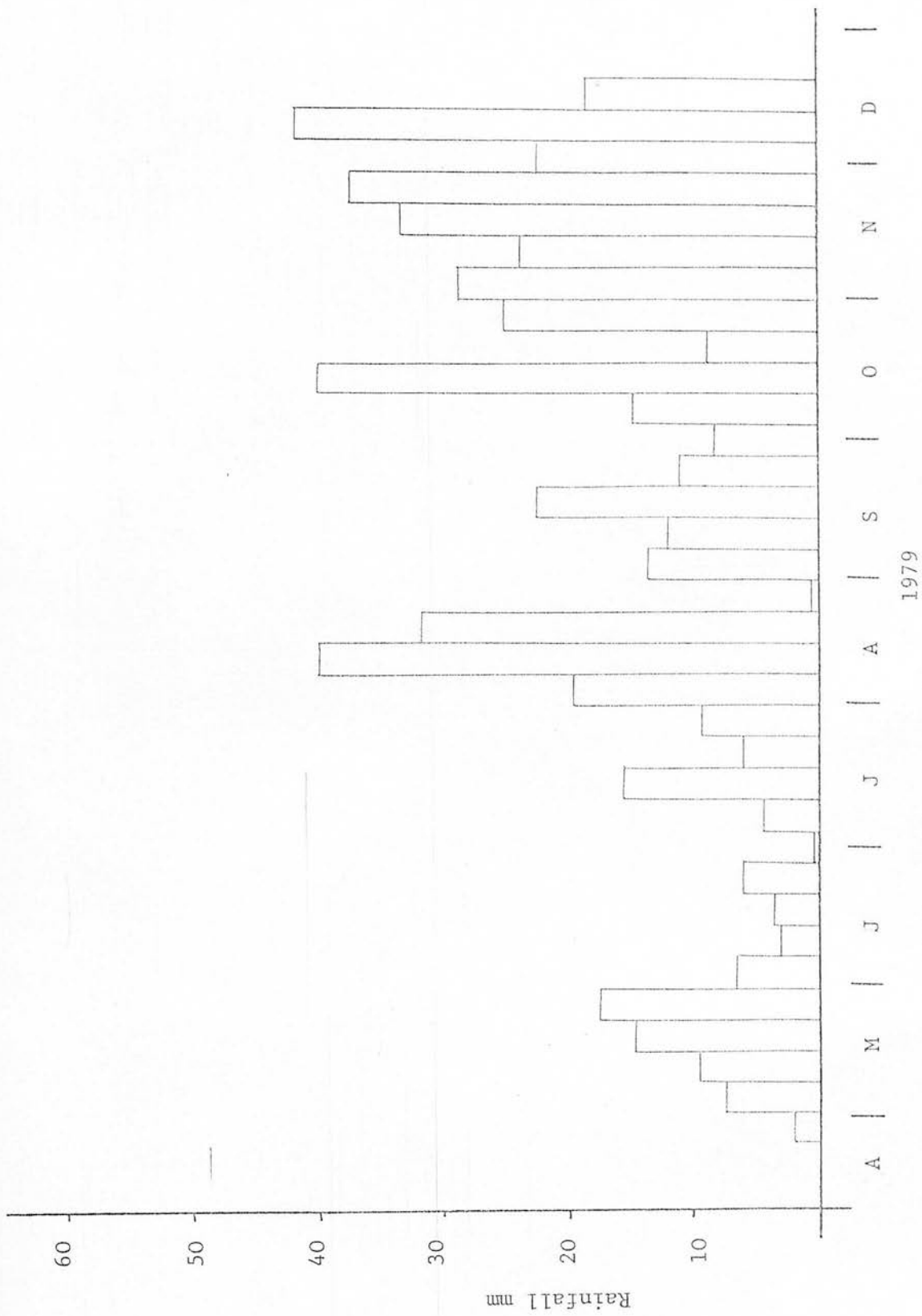


Fig.7.1 Weekly rainfall data for 1979 at Eddleston site.

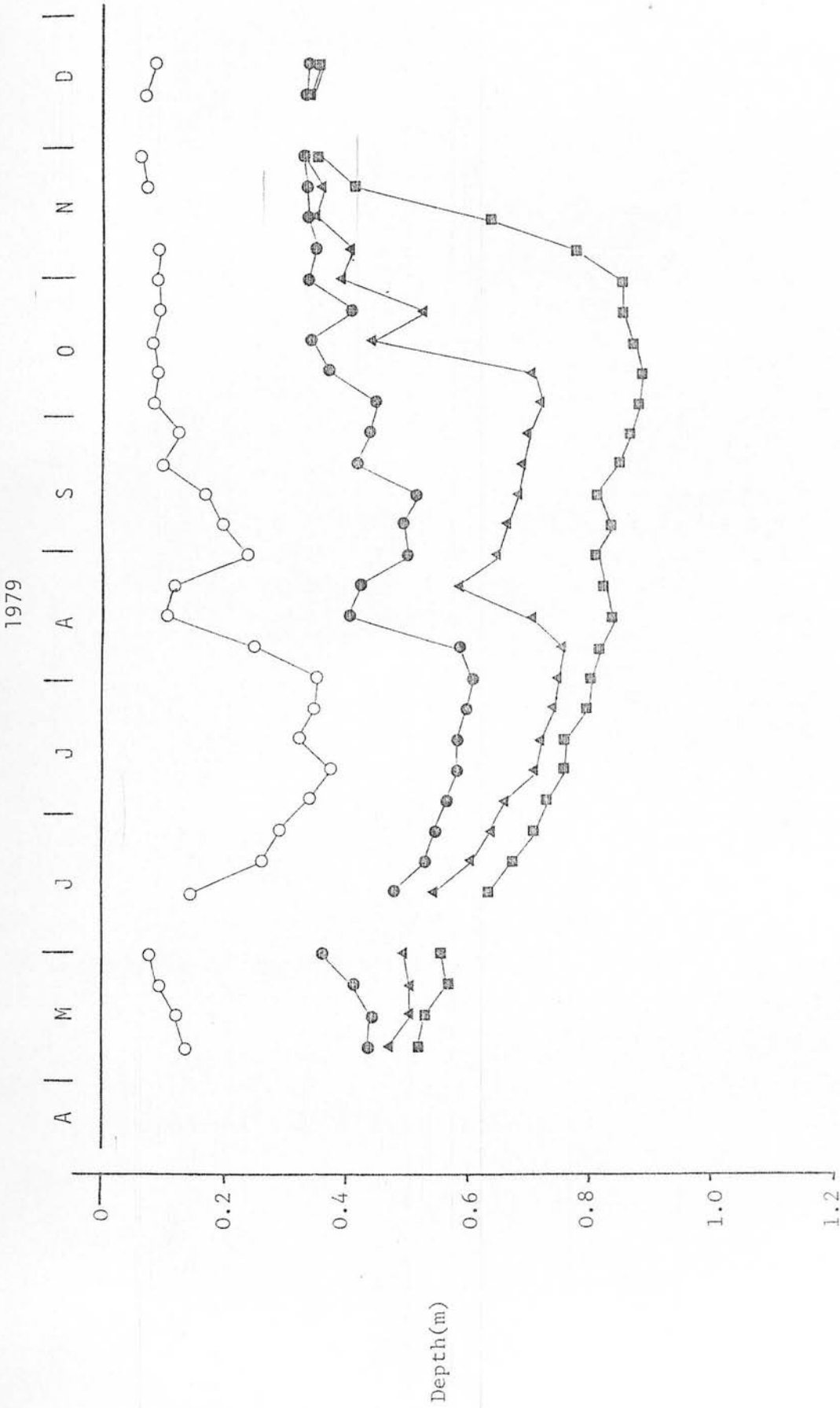


Fig.7.2 Mean depth to the water table for 1979 in the Eddleston site:-
O - 0V, ● - 0P, ▲ - SS, and ■ - LP.

differences between sites seen in Fig.7.2 for the depths to the water table are supported by these data. In the OV site negative potentials were only found at depths of 0.1 and 0.2m from mid-June to mid-August, when the water table had fallen below 0.2m. These potentials were still greater than -5kPa, and even in July when the water table was below 0.3m in depth the matric potential at this depth was about zero. In the OP site negative potentials were recorded at depths above the water table, but even during the driest period in July the matric potential at 0.2m depth was only -6kPa, and below this depth greater than -5kPa. The greater depths to the water table found in the SS site allowed much lower matric potentials to develop, reaching -25 kPa at 0.2m depth during the driest period in early August. The subsequent rise in the water table in mid-August (Fig.7.2) was clearly seen in the matric potentials for all depths rising to -4kPa at 0.2m depth, before falling again during September. At 0.3m depth the matric potential fell to -8kPa in the driest period and was generally about -5kPa from July to mid-October. Figs.7.3 and 7.4 show that drying in the LP site was much more intense than in the SS site and matric potentials were much lower than at similar depths in the SS site. From July to mid-October all depths gave negative potentials and significant periods when potentials of less than -5kPa occurred to depths of 0.6m. At 0.2m depth the lowest matric potential was -71kPa in early August followed by a rise to only -8kPa. This corresponded to the similar rises in matric potential and water table depth seen in sites SS, OP and OV, caused by the rainfall peak seen in Fig.7.1. However, this was not seen in the depth to water table data for the LP site (Fig.7.2), and it seems from this evidence that all of the throughfall in this site entered the gas filled pore space without draining to the ground water level. The large rise in the matric potential at 0.2m depth compared to a smaller rise at 0.3m depth also suggests that

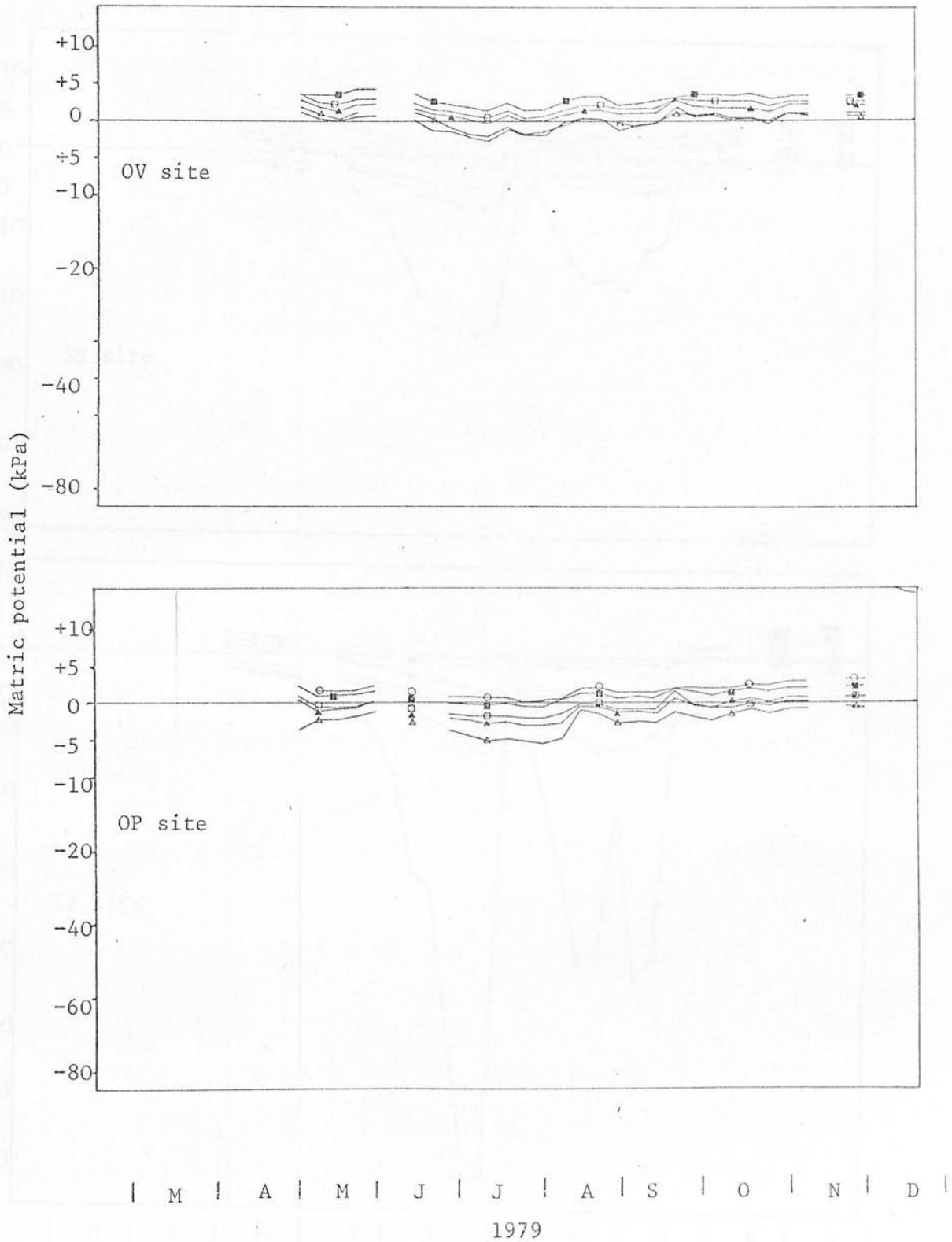


Fig.7.3 Matric potential for 1979 in the Open virgin and Open ploughed sites at depths of:- — -0.1m, Δ -0.2m, ▲ -0.3m, □ -0.4m, ■ -0.5m and ○ -0.6m.

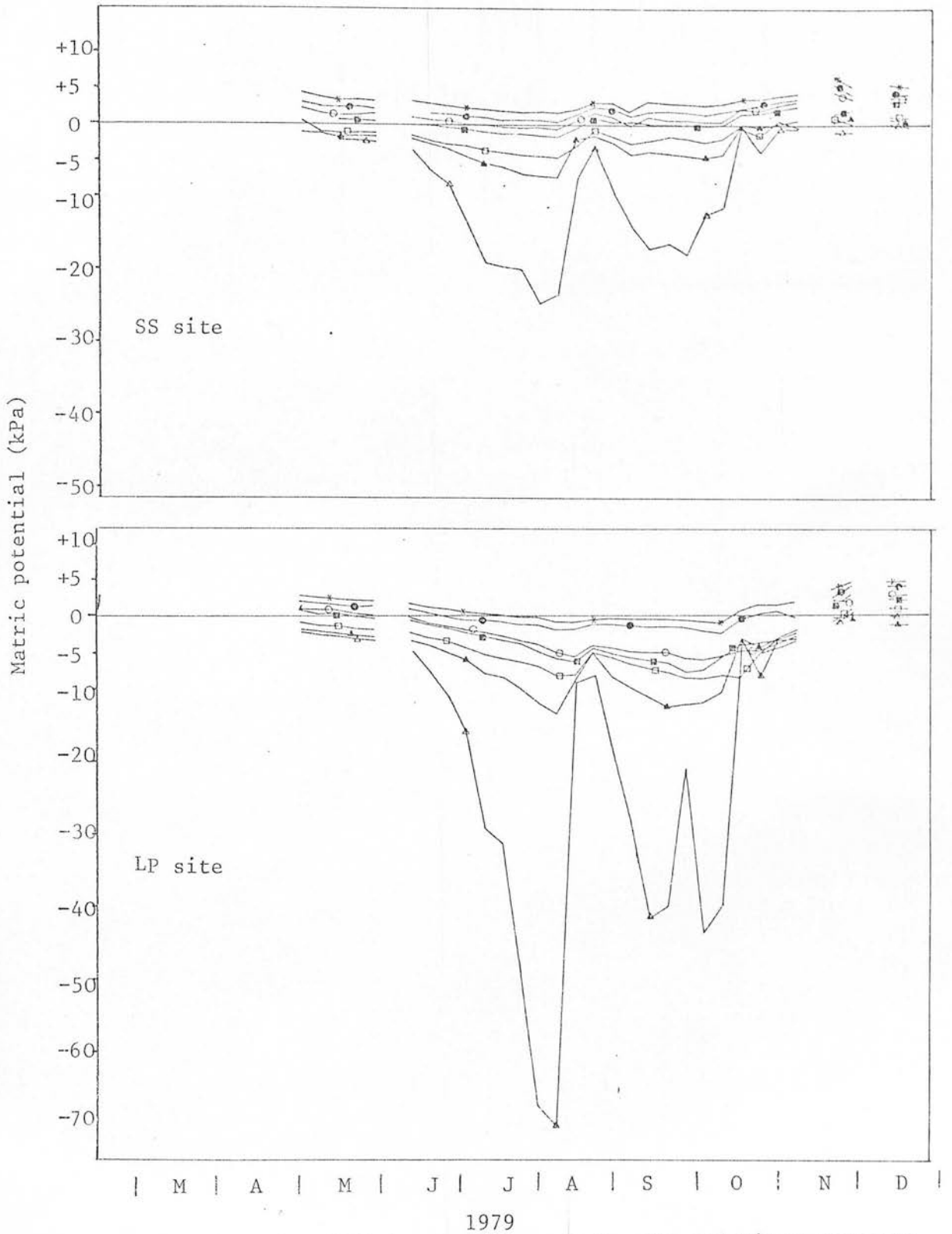


Fig.7.4. Matric potentials for 1979 in the *Picea sitchensis* and *Pinus contorta* sites at depths of:- Δ -0.2m, \blacktriangle -0.3m, \square -0.4m, \blacksquare -0.5m, \circ -0.6m, \bullet -0.7m, and $*$ -0.8m.

most of this water was held at depths of less than 0.3m, according to the greater volume of gas-filled pore space available (see moisture release curves Fig.5.18). The greater drying in the LP site relative to the SS site continued after the heavy rain in August until the end of October when the matric potentials at both sites increased sharply to about -5kPa. During the winter months from mid-November onwards the matric potentials and depths to water table were about the same for the OP, SS and LP sites, corresponding to the depth of the surrounding drainage ditches.

No statistical analysis was performed on these data, as tensiometers were not replicated at most depths and Figs.7.3 and 7.4 give an adequate comparison of variation between species and depths.

The greater difference between the moisture regimes under Picea sitchensis and Pinus contorta seen in this experiment, compared with the Falstone experiment, were probably caused by the age difference of the trees and differences in canopy closure. At Falstone the trees were approximately 25 years old and both species have a complete canopy cover. At Eddleston however, the trees were only about 15 years old, and it is noticeable that the Pinus contorta trees were larger and had formed a completely closed canopy over the LP site, whereas the Picea sitchensis showed a wider range of tree size with many small poorly developed individuals and hence large gaps in the covering canopy.

7.2 TEMPERATURE REGIME

The weekly temperature data from Eddleston during 1979 are given in Figs.7.5 and 7.6, and like those at Falstone are spot readings taken between 9 a.m. and 12 noon on the day of sampling. The data represent part of the seasonal cyclic fluctuation evident in soil temperature changes, and show a warming phase from early March until August when maximum temperatures were reached followed by a cooling phase.

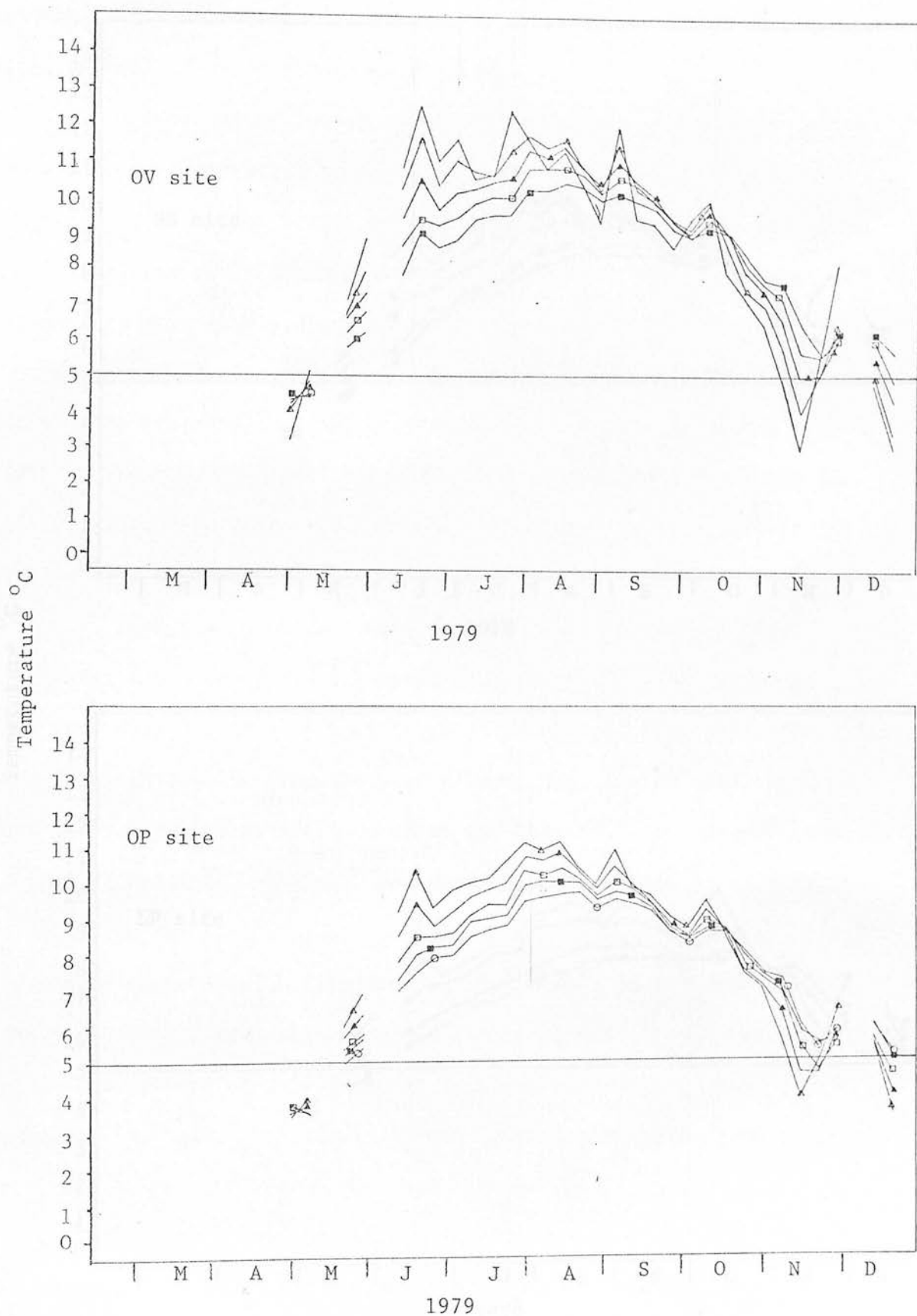


Fig.7.5 Soil temperatures in the OV and OP sites for 1979, at depths of:
 — 0m, Δ - 0.2m, \blacktriangle - 0.3m, \square - 0.4m, \blacksquare - 0.5m. and \circ - 0.6m.

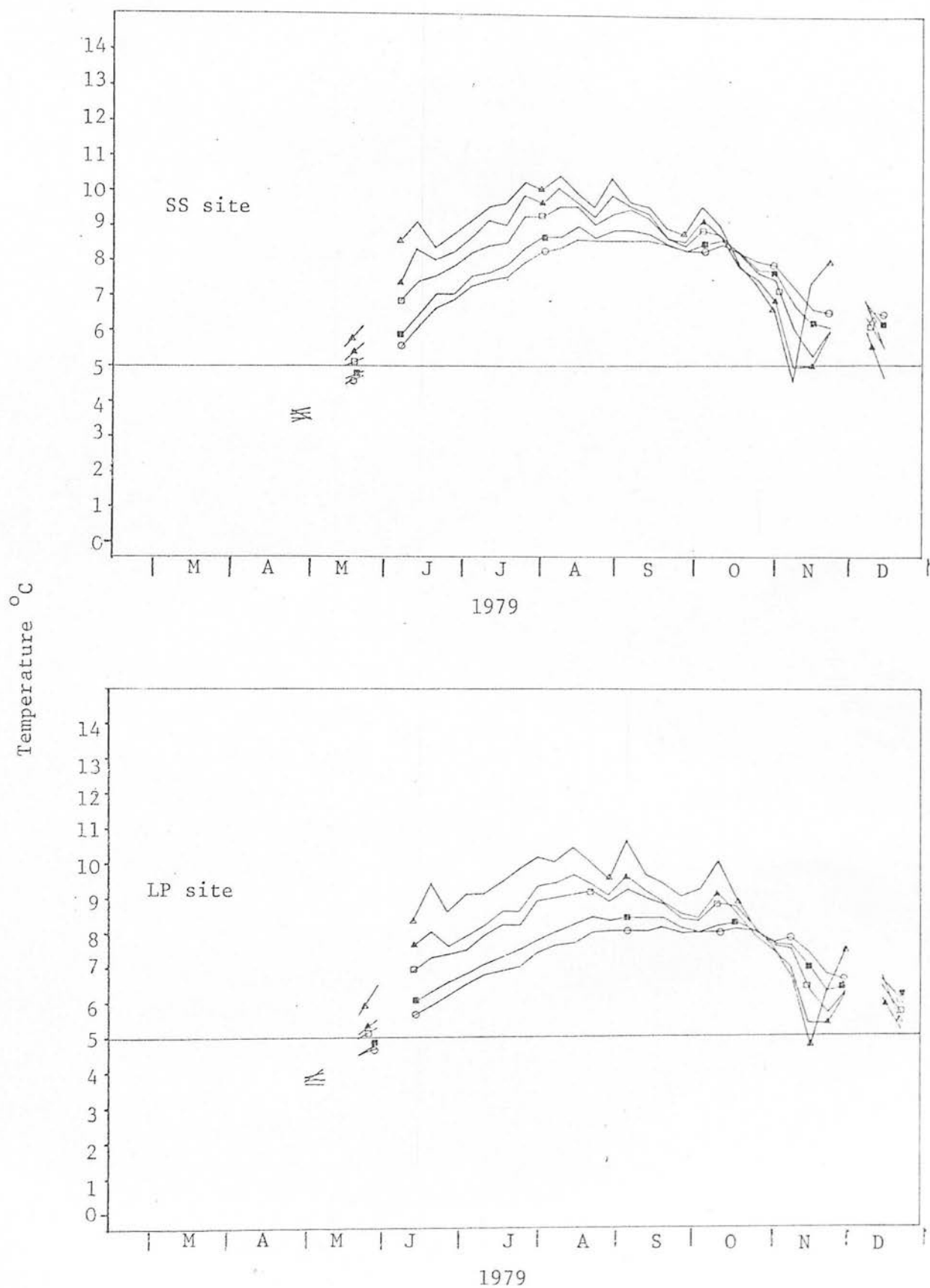


Fig.7.6 Soil temperatures in the SS and LP sites for 1979, at depths of:
 Δ -0.2m, \blacktriangle -0.3m, \square -0.5m, \blacksquare -0.7m and \circ -0.8m.

The higher temperatures recorded in the open sites compared with the forested sites in the Falstone experiment (Section 6), are again evident, with temperatures at 0.2m depth reaching 11.5°C in the open sites and only 10°C in the forested sites.

The trends of increasing soil temperature with depths during the winter and decreasing during the summer were present in peat as they were in the mineral soil at Falstone. The times of the year when these gradients reverse themselves giving constant temperatures at all depths were more easily discernible in these data than those from Falstone, and were the first week in May and mid-October for all the sites. The increased damping of fluctuations at greater depths are again apparent, being especially noticeable at 0.7 and 0.8m in the SS and LP sites; the thermistor placed in the loose surface peat in the OV site gave much wider fluctuations than at even 0.2m depth.

It was suggested in Section 6 that root growth of Picea sitchensis proceeded only at temperatures above 5°C , and it can be seen from Figs. 7.5 and 7.6 that temperatures at all depths, in each site were above this value from the last week in May onwards until November. This gives a period of about 30 weeks for potential root growth, similar to that at Falstone. The mean and maximum temperatures at each depth in each site during the period 1.5.79 to 30.10.79 are given in Table 7.1, and can be compared with data from similar depths at Falstone for the same period. The temperatures under the crops seem broadly comparable, though the temperatures in the open sites were generally about 1°C higher at Falstone. This could be due to Eddleston being a more exposed area, and it must be remembered that the open plots at Falstone were better sheltered by the surrounding forest than at Eddleston. The discrepancy of about 0.5°C between the OV and OP sites is hard to explain as they were both under similar vegetation (Calluna dominated heath)

Table 7.1 Mean and maximum temperatures ($^{\circ}\text{C}$) at all depths in the
sites shown for the period 1.5.79 to 30.10.79, at Eddleston

Depth(m)		Temperature ($^{\circ}\text{C}$)			
		OV	OP	SS	LP
0.2	Max	11.7	11.1	10.4	10.4
	Mean	9.6	9.0	8.5	8.7
0.3	Max	11.4	10.8	10.0	9.6
	Mean	9.4	8.7	8.2	8.0
0.5	Max	10.4	10.0	9.5	9.2
	Mean	8.7	8.2	7.9	7.7
0.7	Max	*	*	8.9	8.4
	Mean	*	*	7.4	7.1
0.8	Max	*	*	8.5	8.1
	Mean	*	*	7.2	6.9

* No data taken at these depths in these sites.

and in similarly exposed sites. The Calluna cover on the OP site was however, more dense than on the OV site and it seems likely that it acts in the same way as the tree cover. Indeed during May when temperatures in the OV site are about 1°C higher the temperatures under the OP, SS and LP sites are very similar.

7.3 SOIL ATMOSPHERE

The oxygen and carbon dioxide concentrations in the soil pore space samples are given in Figs.7.7 to 7.14. Data from the two replicate probes are given on the same histogram for each depth, and where four replicates were installed two histograms are given. Where gas concentrations are the equivalent gas phase concentrations derived from water samples, these are indicated by a dot under the baseline. Missing weeks data are indicated by an asterisk under the baseline.

At 0.2m depth all samples from the SS and LP sites were gas samples with oxygen concentrations at or near atmospheric conditions. The carbon dioxide concentrations in these samples were higher than in the ambient atmosphere, but less than $0.01\text{m}^3\text{m}^{-3}$ (Figs.7.11 and 7.13). The OP site was also generally well aerated at this depth though lower oxygen concentrations of about $0.15\text{m}^3\text{m}^{-3}$ were recorded from one probe at the start of the season and in early September (Fig.7.9). Carbon dioxide concentrations were slightly higher than in the planted sites at about 0.01 to $0.02\text{m}^3\text{m}^{-3}$. In the OV site at 0.2m depth very low oxygen concentrations were recorded at the end of May and mid-August from both probes, and concentrations between these dates varied between 0.01 and $0.10\text{m}^3\text{m}^{-3}$ in one probe, and 0.05 and $0.17\text{m}^3\text{m}^{-3}$ in the other (Fig.7.7). Carbon dioxide concentrations were much higher than any of the other sites reaching 0.05 to $0.10\text{m}^3\text{m}^{-3}$ at the start of the sampling period. This site showed something of a seasonal trend, with maximum oxygen and minimum carbon dioxide concentrations being measured

Open virgin site

Depth

0.2m

 O_2 0.25
0.20
0.15
0.10
0.050.05
0.10
0.15 CO_2

0.2m

 O_2 0.25
0.20
0.15
0.10
0.050.05
0.10
0.15 CO_2 I A | M | J | J | A | S | O | N |
1979

0.3m

 O_2 0.25
0.20
0.15
0.10
0.050.05
0.10
0.15 CO_2

0.4m

 O_2 0.25
0.20
0.15
0.10
0.050.05
0.10
0.15 CO_2 I A | M | J | J | A | S | O | N |
1979

Fig.7.7 Soil oxygen and carbon dioxide concentrations (mm^{-3}) in site OV (left and right hand lines of a pair are two replicates), at the depth indicated. A dot under the baseline indicates a water sample and an asterisk missing data.

Open virgin site

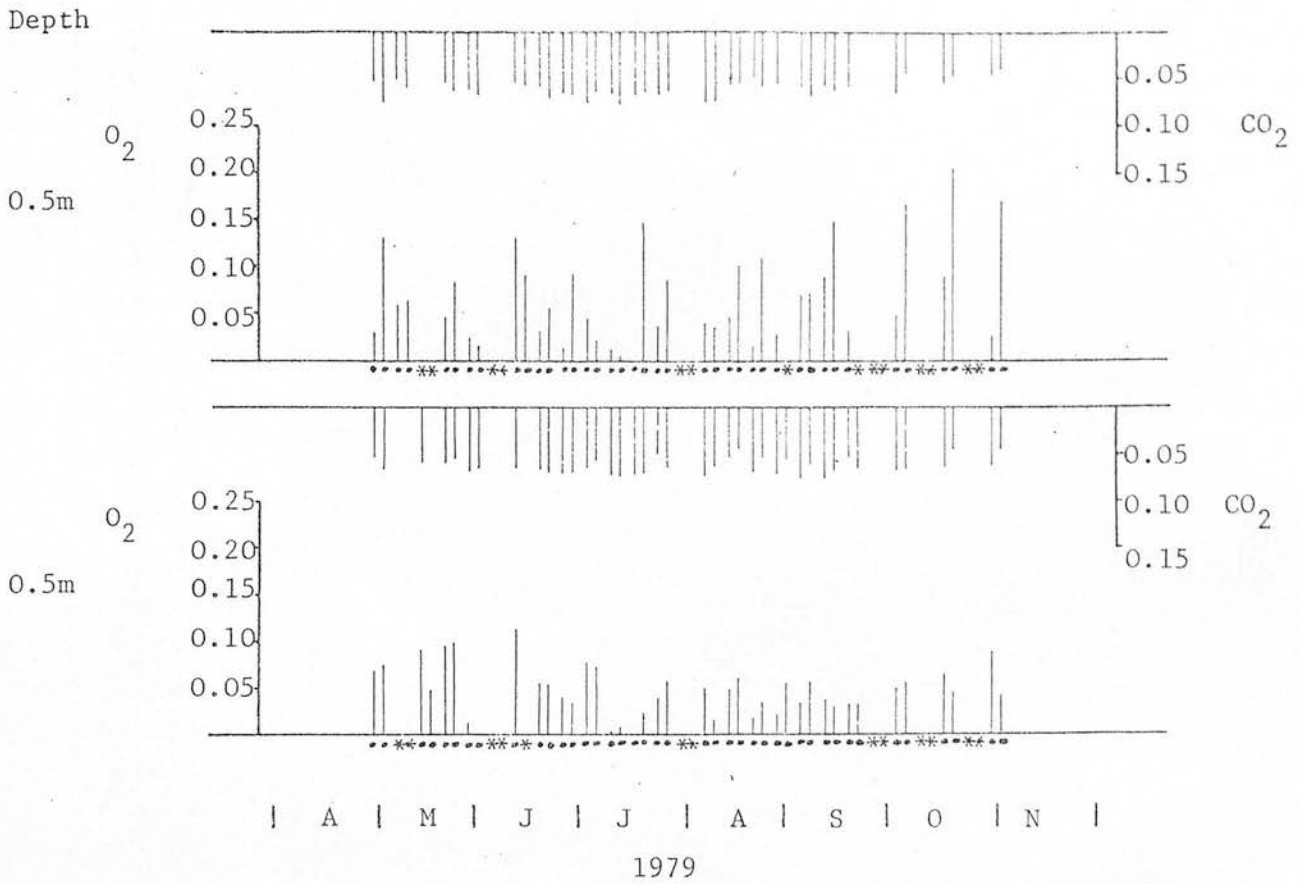


Fig.7.8 Soil oxygen and carbon dioxide concentrations ($m^3 m^{-3}$) at site OV (left and right hand lines of a pair are two replicates), at the depth indicated. A dot under the baseline indicates a water sample and an asterisk missing data.

Open ploughed sites

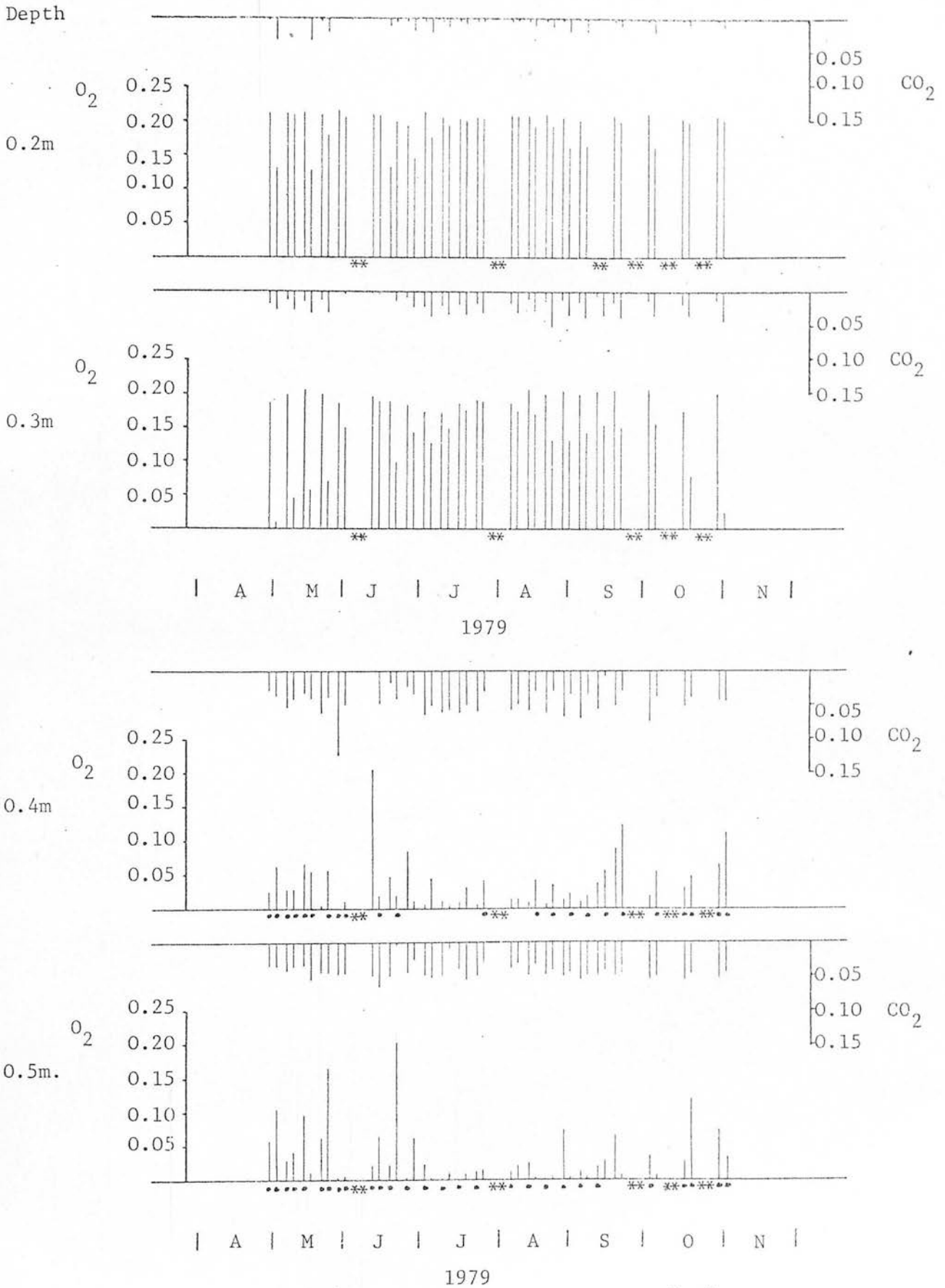


Fig.7.9 Soil oxygen and carbon dioxide concentrations ($m^3 m^{-3}$) in site OP (left and right hand lines of a pair are two replicates), at the depth indicated. A dot under the baseline indicates a water sample and an asterisk missing data.

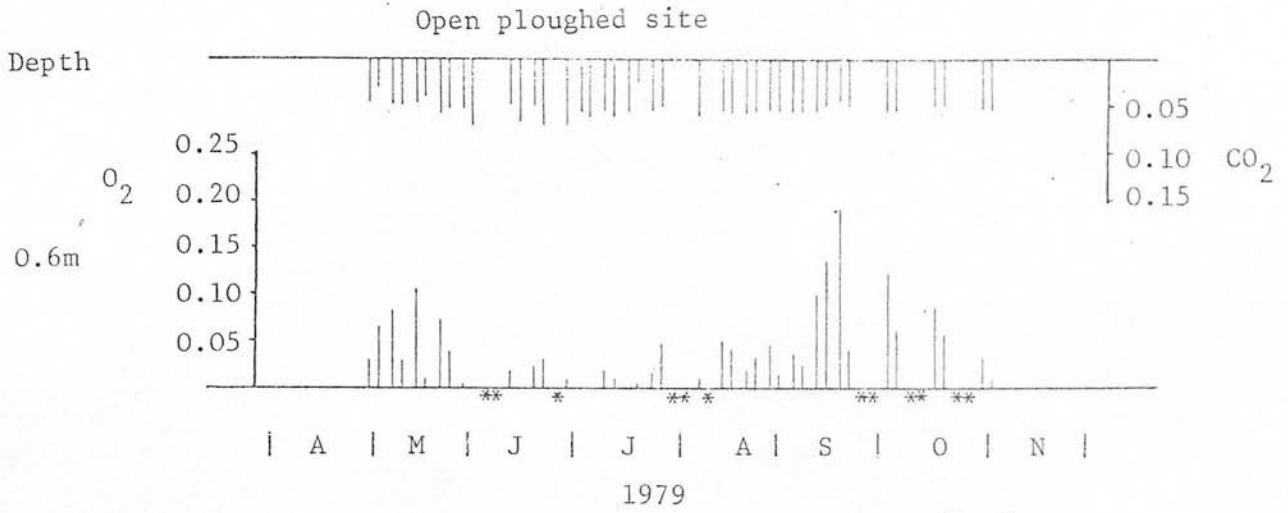


Fig.7.10 Soil oxygen and carbon dioxide concentrations ($m^3 m^{-3}$) at site OP (left and right hand lines of a pair are two replicates), at the depth indicated. A dot under the baseline indicates a water sample and an asterisk missing data.

Piceasitchensis site

Depth

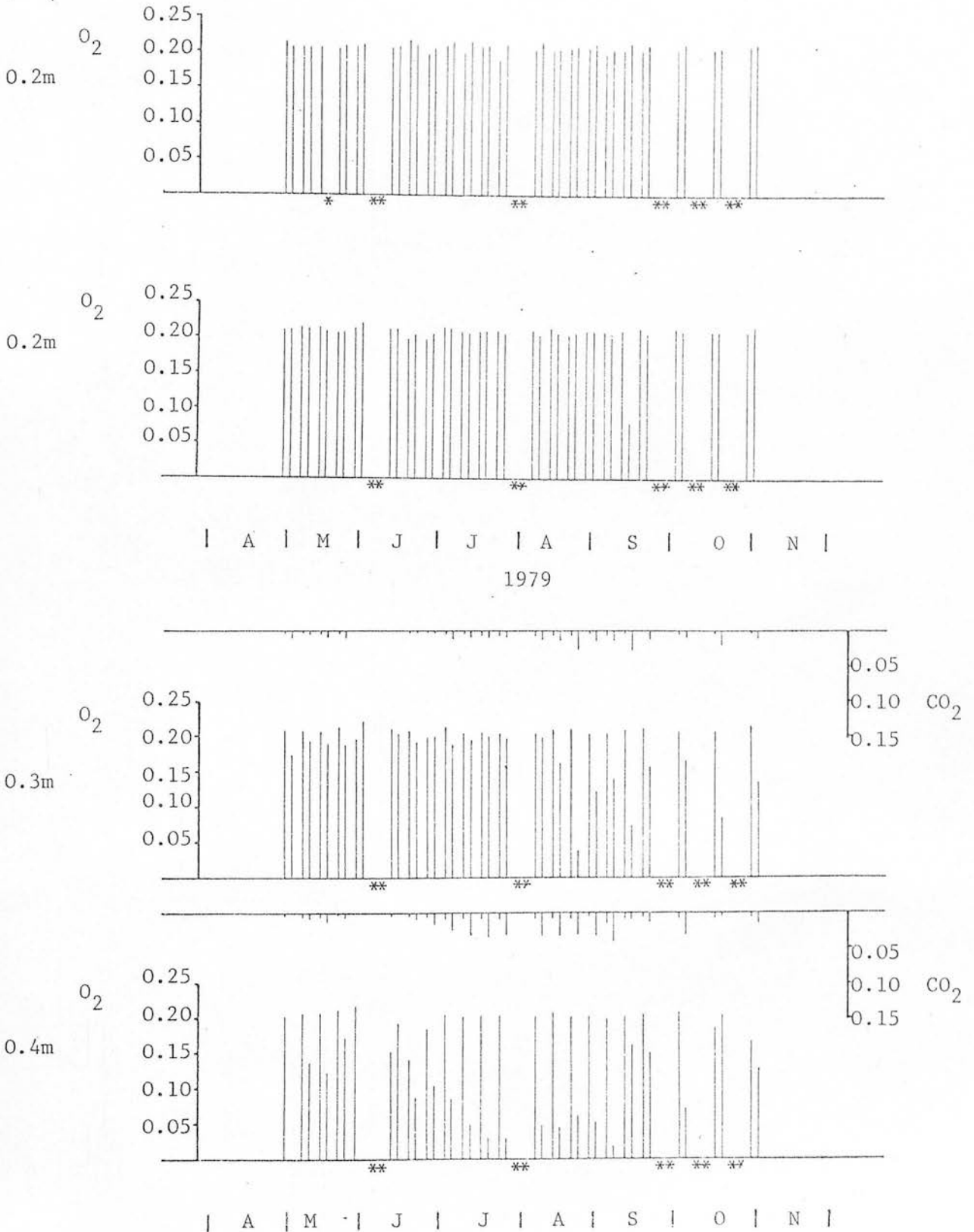


Fig.7.11 Soil oxygen and carbon dioxide concentrations ($m^3 m^{-3}$) in site SS (left and right hand lines are a pair of replicates) at the depth indicated. A dot under the baseline indicates a water sample and an asterisk missing data. CO_2 concentrations at 0.2m depth were all less than $0.01 m^3 m^{-3}$ and so have been omitted.

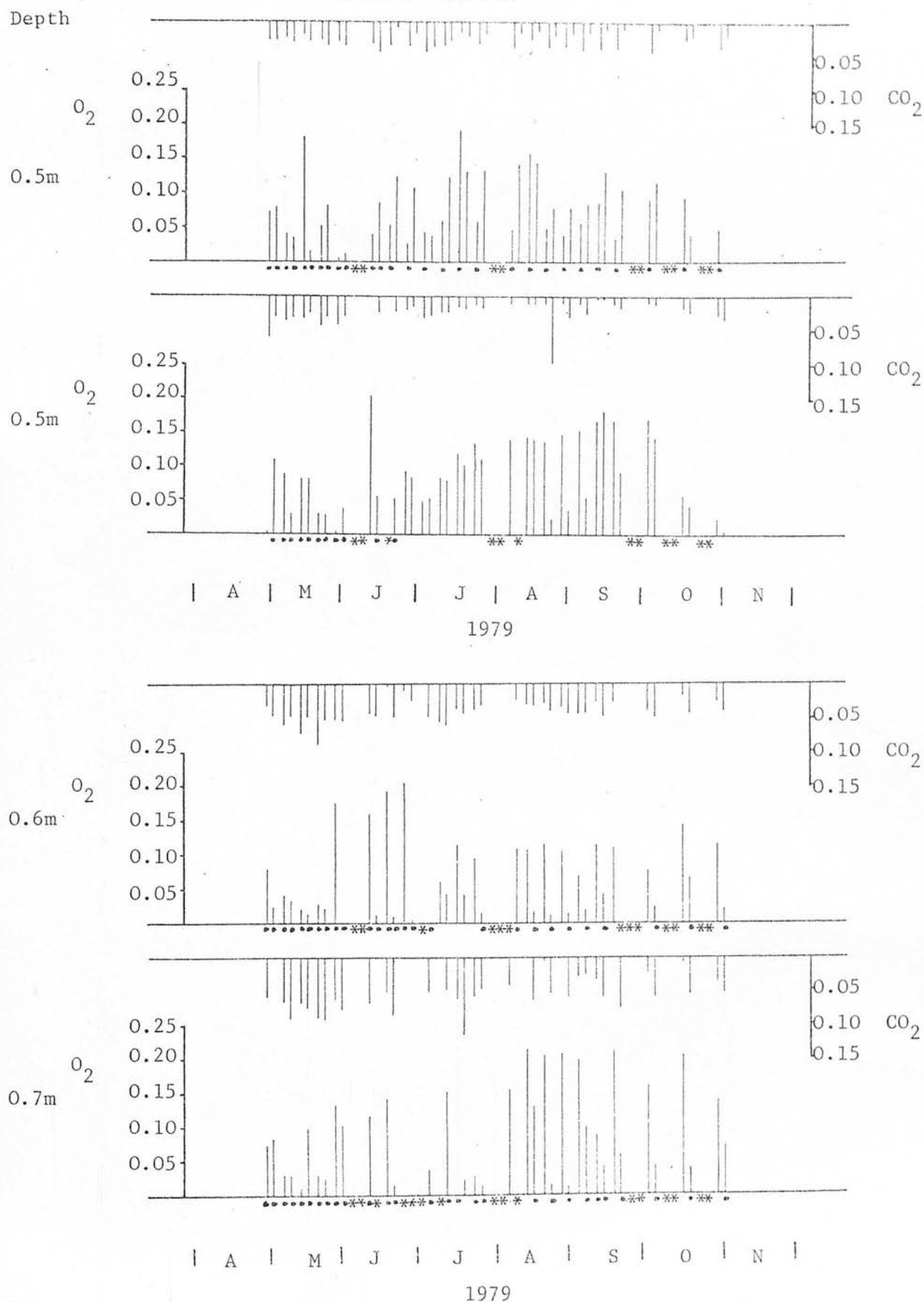


Fig.7.12 Soil oxygen and carbon dioxide concentrations ($\text{m}^3 \text{m}^{-3}$) in site SS (left and right hand lines of a pair are two replicates), at the depth indicated. A dot under the baseline indicates a water sample and an asterisk missing data.

Pinus contorta site

Depth

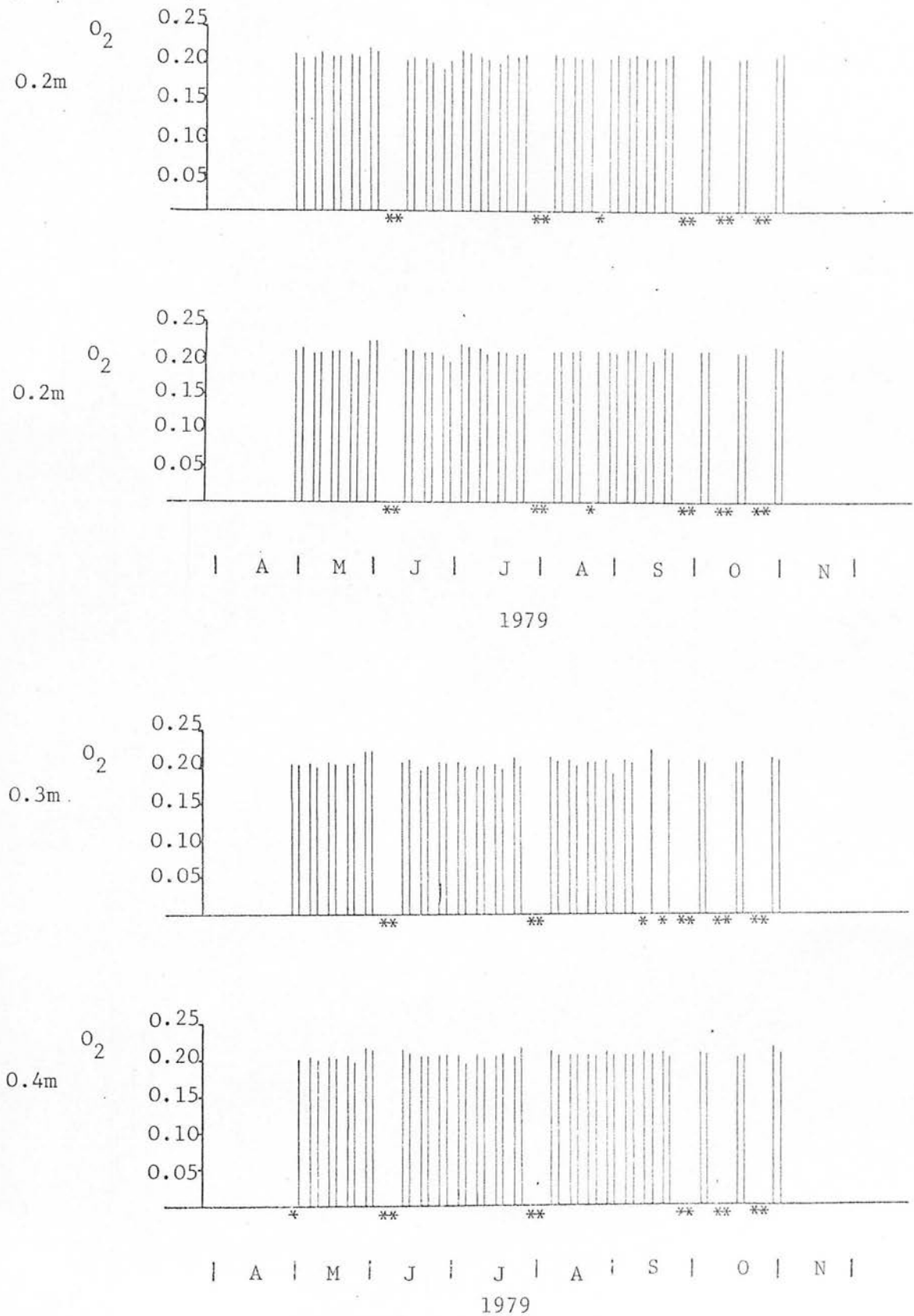


Fig.7.13 Soil oxygen and carbon dioxide concentrations ($\text{m}^3 \text{m}^{-3}$) in the LP site (left and right hand lines of a pair are two replicates), at the depth indicated. A dot under the baseline indicates a water sample and an asterisk missing data. CO_2 concentrations at 0.2m, 0.3 and 0.4 were all less than $0.01 \text{m}^3 \text{m}^{-3}$ and so have been omitted.

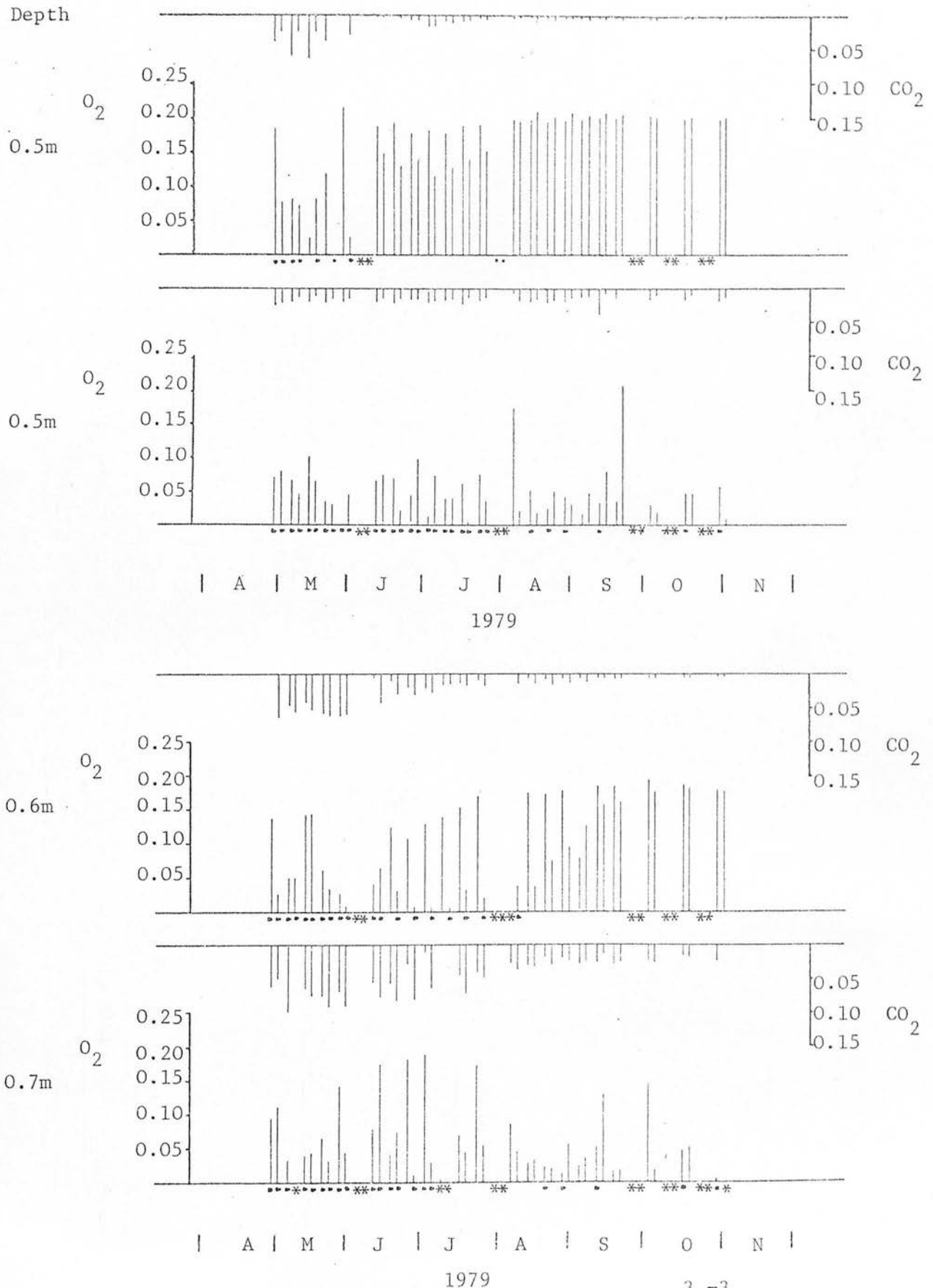
Pinus contorta site

Fig.7.14 Soil oxygen and carbon dioxide concentrations ($\text{m}^3 \text{m}^{-3}$) in the LP site (left and right hand lines of a pair are two replicates), at the depth indicated. A dot under the baseline indicates a water sample and an asterisk missing data.

during July.

At 0.3m depth the planted SS and LP sites were again generally well aerated, giving atmospheric oxygen concentrations from both probes, except for lower oxygen concentrations in August for one of the SS probes (Figs. 7.11 and 7.13). The carbon dioxide concentrations were typically $0.01 \text{ m}^3 \text{ m}^{-3}$ with a peak of about $0.025 \text{ m}^3 \text{ m}^{-3}$ for the samples with lower oxygen concentrations in the SS sites. In the OP site at 0.3m depth, one probe gave near atmospheric oxygen concentrations throughout the sampling period, but the other showed a distinct seasonal trend of concentrations rising from less than $0.05 \text{ m}^3 \text{ m}^{-3}$ in May to about $0.18 \text{ m}^3 \text{ m}^{-3}$ in July and then falling slightly again at the end of August. The carbon dioxide concentrations from this probe were generally higher than the other throughout the season and were the mirror image of the seasonal trend in oxygen concentrations. Samples from the OV site at 0.3m depth were mostly water, and low oxygen concentrations of less than $0.05 \text{ m}^3 \text{ m}^{-3}$ were recorded throughout the season, but minimum levels were reached in both probes during August (Fig.7.7). One probe consistently gave higher oxygen concentrations than the other, and lower carbon dioxide concentrations. Carbon dioxide levels showed a maximum when oxygen was at a minimum.

The LP sites at 0.4m depth were again well aerated throughout the period giving oxygen concentrations of about $0.20 \text{ m}^3 \text{ m}^{-3}$ and very low carbon dioxide concentrations (Fig.7.13). Only one probe in the SS site however, gave consistently high oxygen concentrations, the other gave minimal values of less than $0.05 \text{ m}^3 \text{ m}^{-3}$ during July and August, with higher values of about 0.1 to $0.15 \text{ m}^3 \text{ m}^{-3}$ earlier and later in the season (Figs.7.11). The carbon dioxide concentrations from this probe also showed a peak of about $0.03 \text{ m}^3 \text{ m}^{-3}$ during the July-August period. Both probes in the OP site gave extremely low oxygen concentrations throughout the sampling period, whether from water or gas samples (Fig.7.9). The

lowest values of about $0.01 \text{ m}^3 \text{ m}^{-3}$ were reached during July, when carbon dioxide concentrations of about $0.05 \text{ m}^3 \text{ m}^{-3}$ were recorded. The trend was the same in the OV site, though all the samples taken were water samples and even higher carbon dioxide concentrations of about $0.07 \text{ m}^3 \text{ m}^{-3}$ were reached (Fig.7.7).

If Figs. 7.3 and 7.4 are compared with the relevant aeration data, then it will become apparent that matric potentials in peat need not necessarily fall below -5 kPa , to give well oxygenated samples. This is most noticeable in the OV and OP sites at depths of 0.3 m and 0.4 m , at which depths matric potentials did not fall below -5 kPa , but high oxygen concentrations were still being measured. The low oxygen concentrations often found during August agree broadly with the rise in matric potentials found at this time, to values of about -2 or -3 kPa .

At 0.5 m depth there was a marked difference between the probes in the LP site. Two probes gave generally high oxygen concentrations, except at the start of the sampling period in May, whilst the other two gave concentrations of about $0.05 \text{ m}^3 \text{ m}^{-3}$ (Fig.7.14). Most of the samples for these two low reading probes were water samples, and carbon dioxide levels were also higher than the high reading probes over most of the season. In the SS site at 0.5 m depth all four probes gave oxygen concentrations about 0.05 to $0.10 \text{ m}^3 \text{ m}^{-3}$, and the carbon dioxide concentrations were marginally higher than in the LP site. Seasonal trends were not obvious at either site though some probes did show a decrease in oxygen concentrations in early June and mid-August. In the OP site one probe consistently gave gas samples whilst the other gave water samples, but extremely low oxygen concentrations were recorded from both (about $0.02 \text{ m}^3 \text{ m}^{-3}$) especially during July and August. The carbon dioxide concentrations from these probes were higher than at the SS and LP sites, at about $0.05 \text{ m}^3 \text{ m}^{-3}$ throughout the season. All four probes at 0.5 m depth in the OV site gave water samples throughout

the sampling period, and oxygen concentrations fluctuated at about $0.05 \text{ m}^3 \text{ m}^{-3}$ with little seasonal trend obvious. The carbon dioxide concentrations remained at about $0.06 \text{ m}^3 \text{ m}^{-3}$ throughout the season.

In the LP site at 0.6m depth oxygen concentrations rose steadily from low levels in May to about $0.15 \text{ m}^3 \text{ m}^{-3}$ in July in one probe, and reached this level in September in the other. Samples from both probes in May were water samples and carbon dioxide concentrations from these samples were higher (about $0.05 \text{ m}^3 \text{ m}^{-3}$) than the concentrations measured in gas samples later in the season (less than $0.01 \text{ m}^3 \text{ m}^{-3}$). In the SS site at this depth one probe gave consistently low oxygen concentrations (about $0.01 \text{ m}^3 \text{ m}^{-3}$) measured in water samples throughout the sampling period, whilst the other gave somewhat higher concentrations of about $0.1 \text{ m}^3 \text{ m}^{-3}$ (Fig.7.12). Carbon dioxide concentrations fluctuated about $0.03 \text{ m}^3 \text{ m}^{-3}$ throughout the sampling period. The probes at this depth in the OP site consistently gave water samples with extremely low oxygen concentrations during June and July, often being zero. Slightly higher oxygen concentrations were recorded in May and September, though carbon dioxide concentrations remained about $0.05 \text{ m}^3 \text{ m}^{-3}$ throughout the season.

At 0.7m depth in the LP and SS sites oxygen and carbon dioxide concentrations were more erratic than at shallower depths, though a trend in the LP site was discernible (Figs. 7.12 and 7.14). Carbon dioxide concentrations in the LP site started off very high at about $0.07 \text{ m}^3 \text{ m}^{-3}$ but steadily decreased to about $0.02 \text{ m}^3 \text{ m}^{-3}$ at the end of the sampling period, as for 0.6m depth. The oxygen concentration, however, did not increase throughout the season, but fell from about $0.05 \text{ m}^3 \text{ m}^{-3}$ to about $0.02 \text{ m}^3 \text{ m}^{-3}$, with occasional higher values. In the SS sites both oxygen and carbon dioxide concentrations were highly erratic throughout the season, but one probe gave near atmospheric oxygen concentrations from August onwards. As the depth to the water table at this time was also about 0.7m in the SS site, it makes such high oxygen concentrations doubtful, and it may be

that leakage had occurred in these samples possibly due to a faulty tap or connection.

A comparison of the aeration data from these deeper probes with the relevant matric potentials confirms the suggestion made earlier that potentials need not fall below -5kPa to enable high oxygen concentrations to be reached. In the LP and SS sites, matric potentials at 0.5m depth and deeper rarely fell much below -5kPa (Fig. 7.3 and 7.4), and in the SS site remained around 0 to -2kPa . When the matric potential did fall below -5kPa , as at 0.5m depth in the LP site, the spatial differences in the peat gave rise to either well aerated or very poorly aerated conditions (Fig. 7.14). No conclusions can be drawn therefore, as to the matric potential at which gaseous diffusion is sufficient to ensure well aerated conditions, except to say that it lies between 0 and -5kPa .

An analysis of variance similar to that carried out on the data from Falstone, was again performed for both oxygen and carbon dioxide concentrations. This was performed on transformed data (according to Equation 67) from two replicate probes at depths of: 0.3 , 0.4 and 0.5m in each site to maintain a balanced design. The two probes used for the readings from 0.5m depth in the LP site were the two giving higher oxygen concentrations, and this must be borne in mind when interpreting the results of the analysis. The analyses of variance are given in Table 7.2 for oxygen and 7.4 for carbon dioxide readings; both analyses unavoidably contain a high proportion of estimated values (210/928).

Table 7.2 shows that the most significant source of variance for oxygen is species, followed by depth, confirming the evidence found at Falstone. Species (sites) and depths can be compared in Table 7.3, as table of means from the untransformed data (with means from the transformed data in parenthesis) for sites and depths in the experiment.

Table 7.2 Analysis of variance of Eddleston soil oxygen concentration (% V/V)

Source of Variation	DF	MS	VR
Species	3	412.956	402.843 **
Replicate	1	6.059	5.905 *
Depth	3	208.660	203.368 **
Time	22	3.750	3.655 **
Species Rep.	3	13.879	13.527 **
Species Depth	9	45.223	44.076 **
Rep.Depth	3	13.612	13.267 **
Species Time	66	1.879	1.832 **
Rep.Time	22	1.146	1.116
Depth Time	66	1.373	1.338 **
Species. Rep.Depth	9	7.923	7.722 **
Species. Rep.Time	66	1.697	1.654 **
Species. Depth. Time	196	1.324	1.291 **
Rep.Depth. Time	66	1.087	1.060 **
Residual	182	1.026	
Total	717	4.720	

Table 7.3 Means of 1979 Eddlestone oxygen concentrations (m^3m^{-3}) for the source of variance shown with their transformation means given in parenthesis, and standard errors of differences (s.e.d.)

Site	Oxygen concentration (m^3m^{-3})			
	0.2m	0.3m	0.4m	0.5m
OV	0.103(-0.63)	0.062(-1.33)	0.042(-2.17)	0.069(-1.202)
OP	0.193(1.51)	0.155(0.62)	0.041(-2.07)	0.038(-2.37)
SS	0.206(1.83)	0.183(1.31)	0.152(0.68)	0.076(-1.04)
LP	0.209(1.91)	0.210(1.94)	0.208(1.89)	0.168(0.95)
				s.e.d. 0.006
All sites	0.178(1.16)	0.152(0.63)	0.111(-0.42)	0.088(-0.92)
				s.e.d. 0.003

The overall trends for species and depth found at Falstone are also present in these data, with mean oxygen concentrations being higher under Pinus contorta than Picea sitchensis, and the means for both species higher than under the natural heath vegetation. The mean oxygen concentrations are also greater at shallower depths, both generally and under each species. A comparison of sites OV and OP shows that the higher overall mean oxygen concentration in the OP site is due to much higher means at depths of less than 0.3m, whilst at 0.4m depth means are not significantly different, and are actually higher in the OV site at 0.5m depth. The mean of 0.5m depth in the OV site is also greater than that at 0.4m depth in the same site, a similar phenomenon to open sites in the Falstone experiment, where concentrations at 0.9m depth were often higher than those at shallower depths (Table 6.15 and 6.17). The improvement at 0.2m and 0.3m depth in the SS sites compared with the OP site was not as marked as at 0.4 and 0.5m depth. This must reflect the fact that both sites were drained to about 0.35m depth, but the water table did not fall as much in the OP site as in the planted sites during the summer. Mean oxygen concentrations were higher under Pinus contorta than Picea sitchensis for all depths, except at 0.2m depth where they were essentially the same.

The analysis of variance for the carbon dioxide concentrations (Table 7.4) shows that once again the most significant source of variance is species (sites) followed by depth. The mean carbon dioxide concentrations for each site and depth are given in Table 7.5 and show the inverse trend to the oxygen concentration data. Mean carbon dioxide concentrations were significantly higher under Picea sitchensis than Pinus contorta at all depths, but neither were as high as those found in the Calluna dominated areas. The mean carbon dioxide concentration increased with greater depth in all sites, but not appreciably so from 0.4 to 0.5m in the OV and OP sites. The mean concentrations at all depths in the OV site were much

Table 7.4 Analysis of variance of Eddleston soil carbon dioxide concentrations (% V/V)

Source of Variation	DF	MS	VR
Species	3	256.2905	788.292 **
Rep.	1	4.7905	14.735 **
Depth	3	112.7644	346.838 **
Time	22	5.8802	18.086 **
Species.Rep.	3	4.1998	12.918 **
Species.Depth	9	5.5995	17.223 **
Rep.Depth	3	6.2057	19.087 **
Species.Time	66	1.1385	3.502 **
Rep.Time	22	0.2172	0.668 **
Depth.Time	66	0.8655	2.662 **
Species.Rep.Depth	9	5.2378	16.110 **
Species.Rep.Time	66	0.2442	0.751 **
Species.Depth.Time	195	0.5089	1.565 **
Rep.Depth.Time	66	0.3425	1.053 *
Residual	181	0.3251	
Total	715	2.3831	

Table 7.5 Means of 1979 Eddleston carbon dioxide concentrations (m^3m^{-3}) for the source of variance shown, with their transformation means given in parenthesis, and standard errors of differences (s.e.d.)

Site	Carbon dioxide concentrations (m^3m^{-3})				All depths
	0.2m	0.3m	0.4m	0.5m	
OV	0.028(0.62)	0.043(1.30)	0.062(1.77)	0.062(1.80)	0.049(1.37)
OP	0.009(-0.52)	0.022(0.50)	0.047(1.38)	0.044(1.41)	0.031(0.69)
SS	0.004(-1.22)	0.009(-0.60)	0.013(-0.22)	0.028(0.93)	0.013(-0.27)
LP	0.003(-1.54)	0.003(-1.24)	0.005(-0.96)	0.013(-0.30)	0.006(-1.01)
				s.e.d. 0.002	s.e.d. 0.001
All sites	0.011(-0.67)	0.019(-0.07)	0.032(0.49)	0.037(0.96)	s.e.d. 0.001

higher than at equivalent depths in the OP site, and in both sites the mean carbon dioxide concentrations at 0.4 and 0.5m depth were about the same as the mean oxygen concentrations.

Time is naturally a large source of variance in both the oxygen and carbon dioxide analyses, but the histograms in Figs. 7.7 to 7.14 show the seasonal fluctuations adequately. Replication is a more significant source of variance in the carbon dioxide data (Table 7.4) than in the oxygen data (Table 7.2). Though statistically significant both generally and in its interactions with species and depth, the significance was not as large as species or depth on their own. The high proportion of estimated values in these analyses of variance make them somewhat less reliable than the similar analyses carried out on the Falstone data, and this fact together with the significance of replication, mean that the interpretation of the tables of means should not be too rigid. However, the differences between species and depths are so great in most cases that they make the comparison and conclusions drawn valid, and the data usefully confirm trends observed in the Falstone experiment.

7.4 CONCLUSIONS

The drainage ditches surrounding the three sites, OP, SS and LP have obviously had a major effect on the moisture regime and hence aeration of the peat. Due to run-off into these ditches the water-table was maintained at a depth of 0.35m during the wettest part of the year, when the water table was less than 0.1m below the surface of the virgin peat. This resulted in almost permanently well aerated peat down to about 0.3m in all three drained sites with oxygen concentrations being at or near atmospheric, whilst much lower concentrations were experienced in the OV site. High oxygen concentrations were maintained in this region even though the matric potential was often in the region of 0 to -5kPa.

Although no throughfall data were collected in this experiment, it was evident from the greater depth to the water table under Pinus contorta that soil conditions were drier under this species. The better canopy closure of Pinus contorta was considered to be a major factor. Both the SS and LP sites had a lower water table and more intensive drying above this than the OP site, but in the LP site these conditions continued until November, whilst the SS site returned to saturation during October. However, no evidence for enhanced aeration in the LP site compared with the SS site at this time is shown by the data, and temperatures were also declining from the end of September onwards. Whether this prolonged period of peat drying confers any advantage to root growth of Pinus contorta remains in doubt, but it may allow time for suberization to occur before anaerobic conditions return.

The main trends of decreasing oxygen concentration with depths and better aeration under Pinus contorta than under Picea sitchensis (and both an improvement over unplanted sites), are observed in this experiment on peat as well as on the mineral soil at Falstone (Section 6). The converse trends for carbon dioxide concentrations are perhaps better illustrated in this experiment, and the main sources of variance in both oxygen and carbon dioxide concentrations are shown to be species and depth (Tables 7.2 and 7.4), as in the Falstone experiment (Tables 6.13 6.16 and 6.19).

The spatial variability of individual probes, however (clearly seen in Figs. 7.7 to 7.14), and the large proportion of missing values in the analysis of variance (Tables 7.2 and 7.4), make an examination of the frequency distribution for oxygen concentrations helpful.

The overall frequency distribution is given in Fig. 7.15 and for each site at each depth in Figs. 7.16 to 7.19. Fig. 7.16 clearly shows that in the uncultivated peat poorly aerated conditions existed for most of the season at depths greater than 0.3m, and even at 0.2m depth

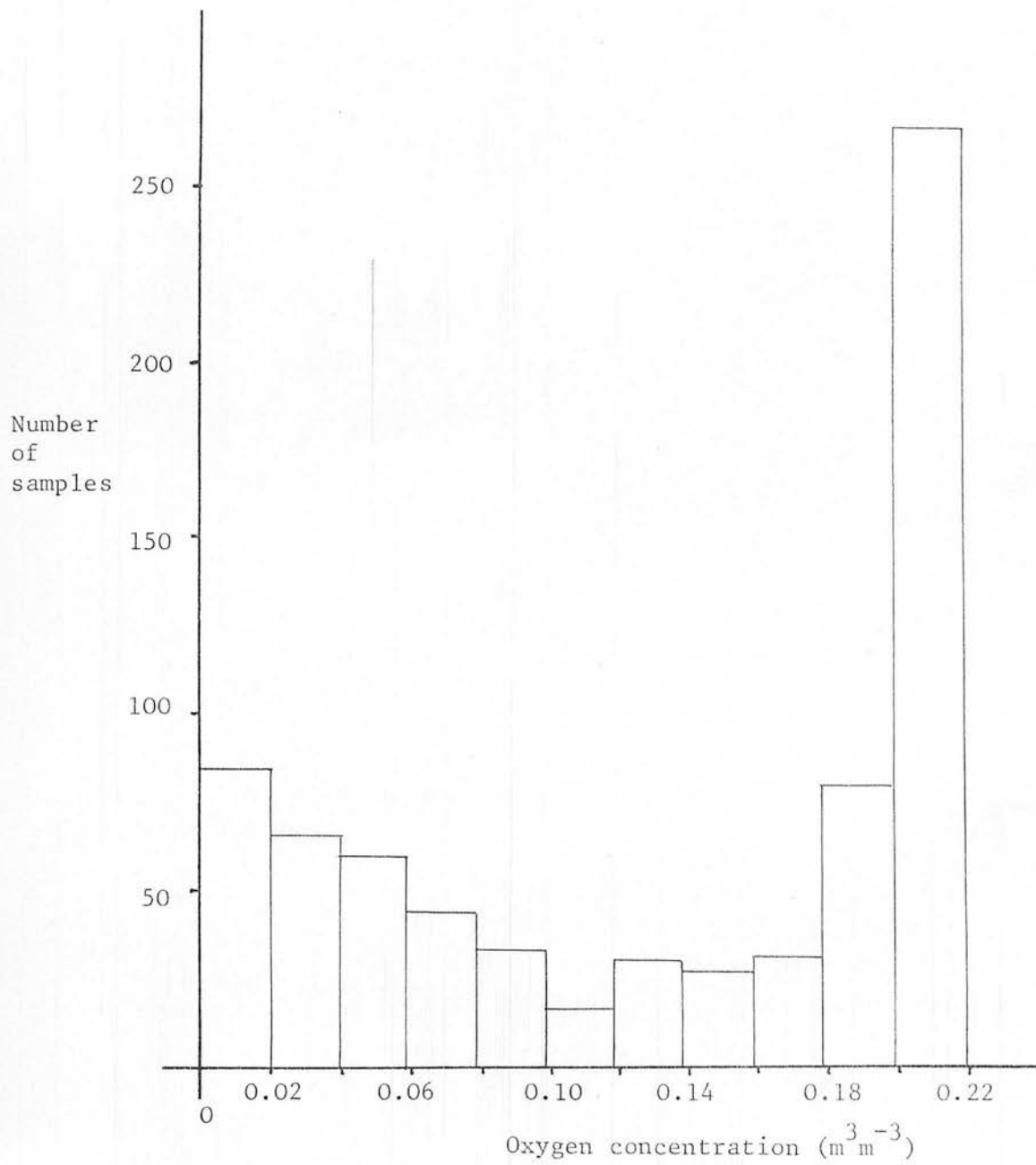


Fig.7.15 Frequency distribution of Eddleston oxygen concentration data for all sites and depths.

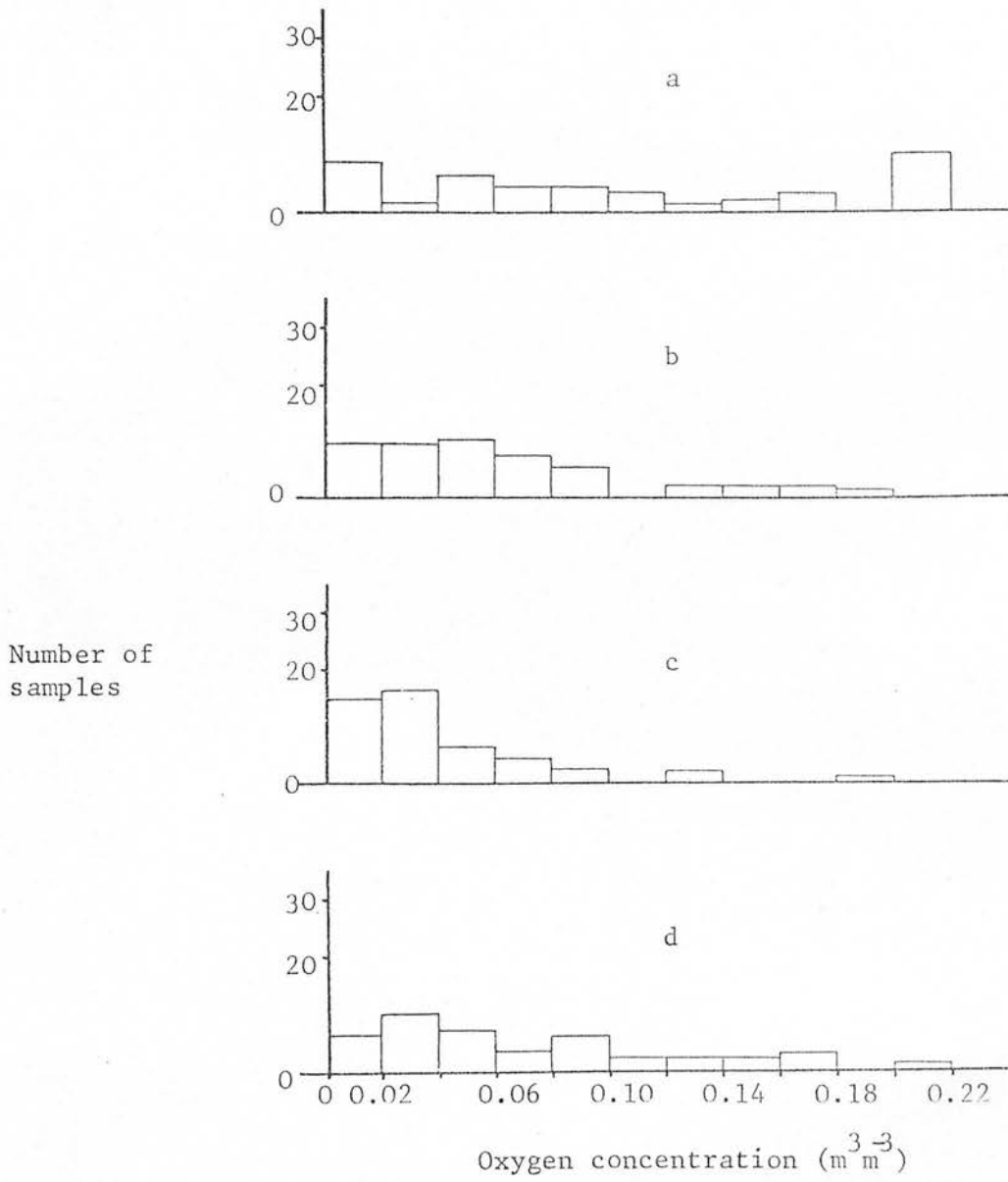


Fig.7.16 Frequency distribution of Eddleston oxygen concentration data for the OV site at depths of:- a - 0.2m, b - 0.3m, c - 0.4m, d- 0.5m.

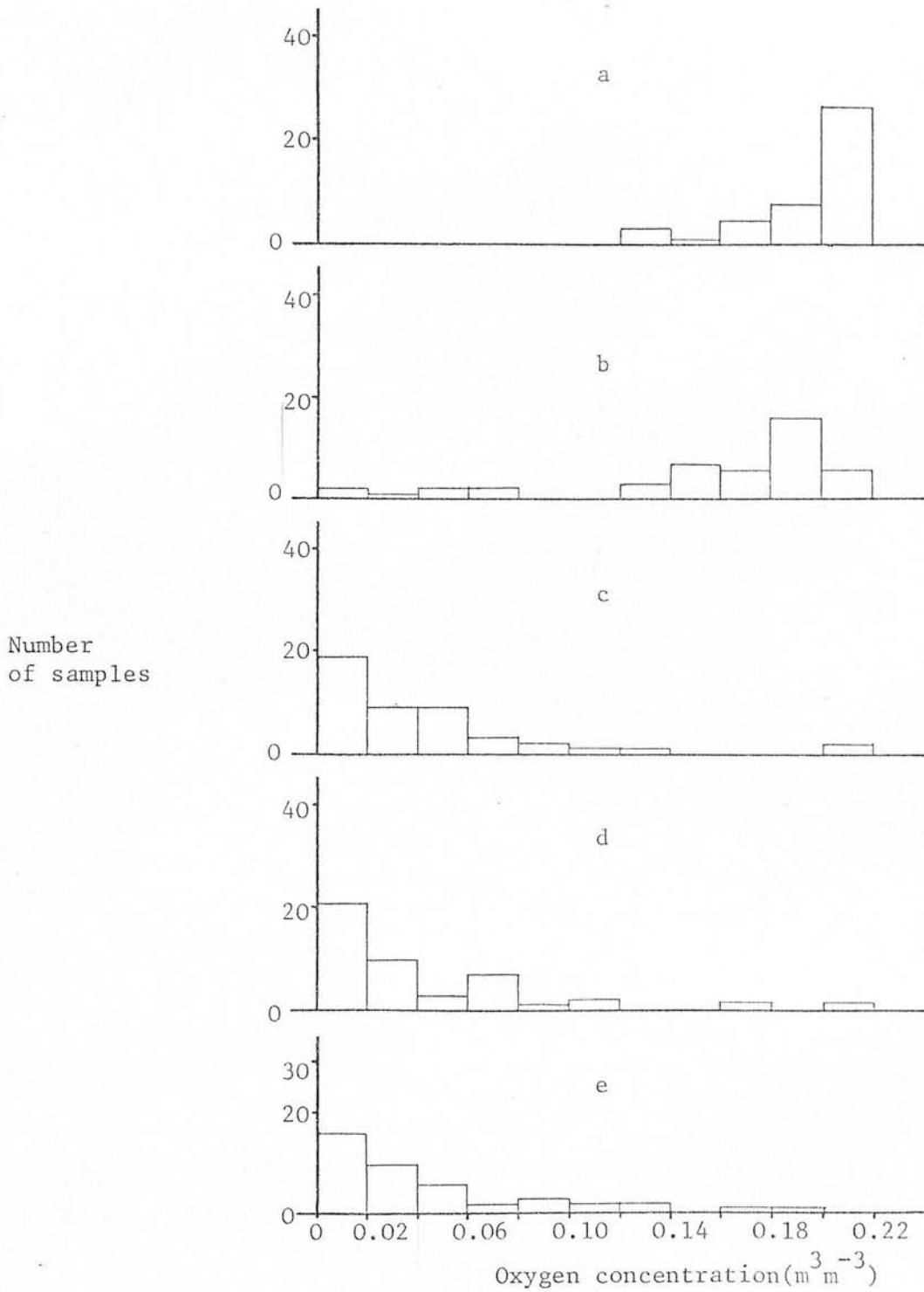


Fig.7.17 Frequency distribution of Eddleston oxygen concentration for the OP site at depths of:- a- 0.2m, b- 0.3m, c-0.4m, d- 0.5m, e- 0.6m.

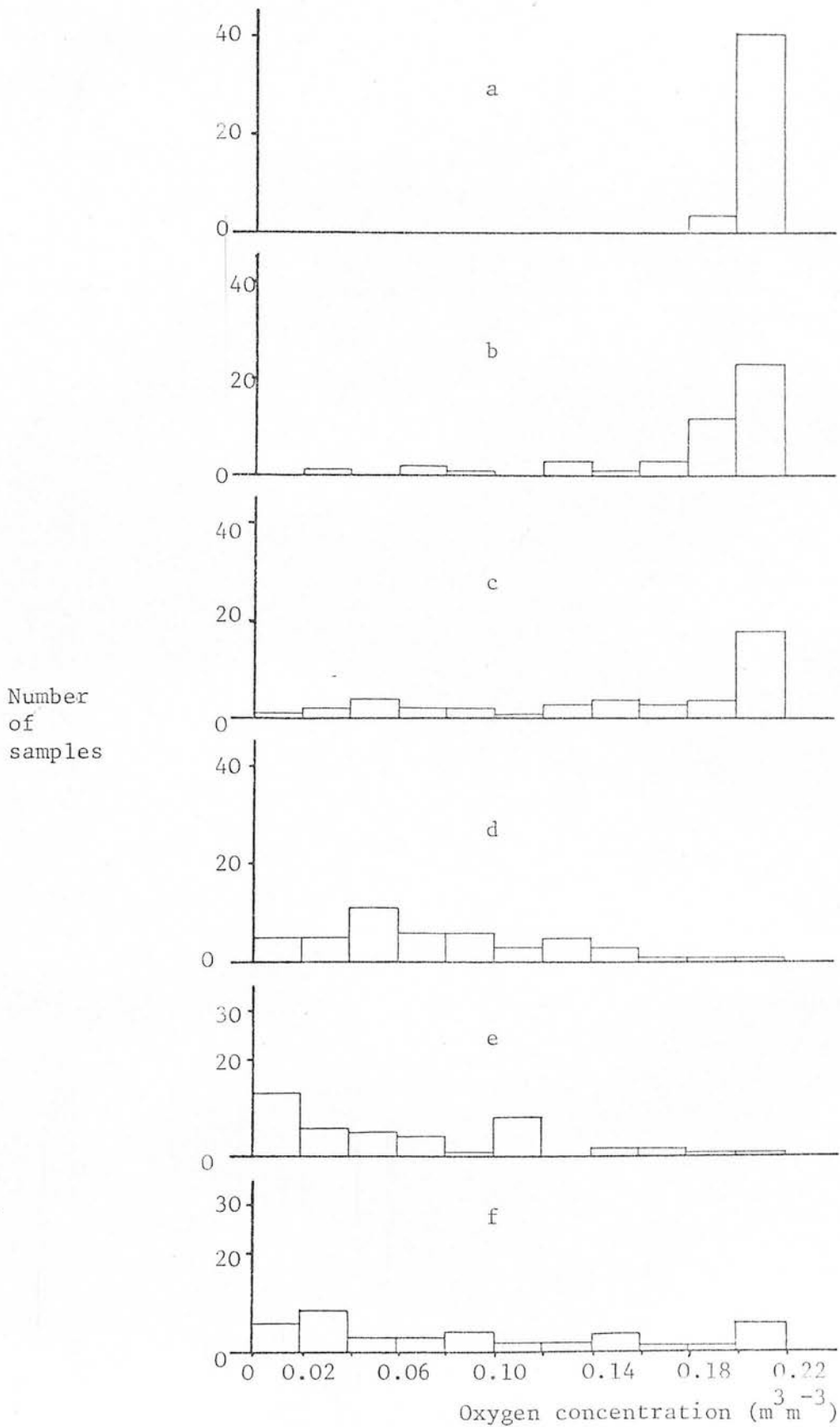


Fig.7.18 Frequency distribution of Eddleston oxygen concentration for the SS site at depths of:- a - 0.2m, b- 0.3m, c-0.4m, d - 0.5m, e- 0.6m and f - 0.7m.

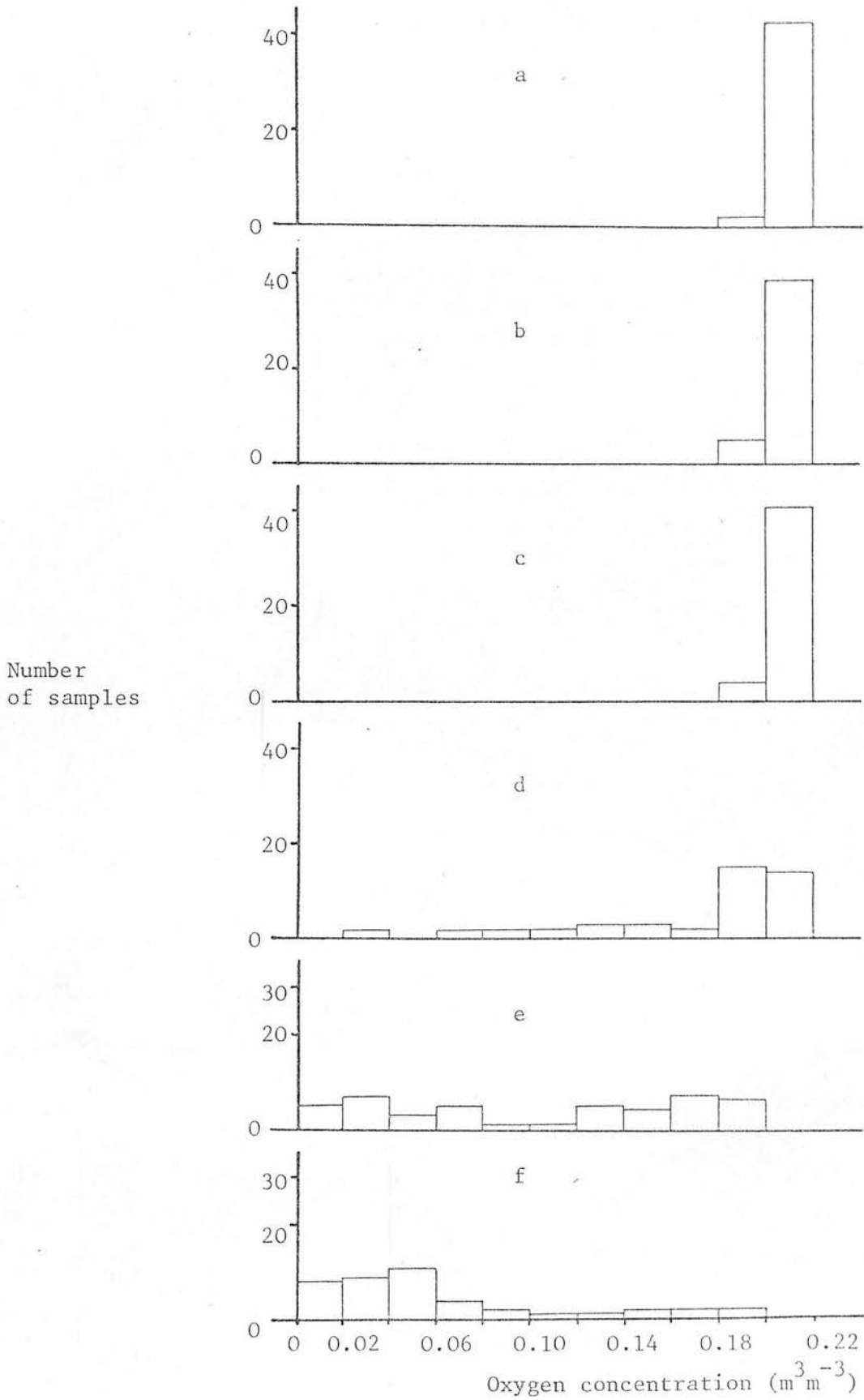


Fig.7.19 Frequency distribution of Eddleston oxygen concentration for the LP site at depths of:- a - 0.2m, b-0.3m, c-0.4m, d-0.5m, e-0.6m and f-0.7m.

the number of samples taken were fairly evenly distributed over the oxygen concentration range. This compares with the ploughed open site (Fig.7.17) where the majority of samples were found to be well aerated at depths of 0.2 and 0.3m, but at 0.4, 0.5 and 0.6m were found to be near anaerobic. In the SS site (Fig.7.18), the majority of samples were near atmospheric at depths down to 0.4m, but with a gradually increasing number at lower concentrations. At 0.5m depth they were fairly evenly distributed across the 0 to $0.16 \text{ m}^3 \text{ m}^{-3}$ range, while at 0.6m depth the majority were near zero.

Under Pinus contorta (Fig.7.19) the atmospheric conditions were even more obvious down to 0.4m depth, with no samples having an oxygen concentration lower than $0.18 \text{ m}^3 \text{ m}^{-3}$. At 0.5m depth the majority of samples were still above $0.18 \text{ m}^3 \text{ m}^{-3}$, and it was not until 0.6m depth that an even number of samples at both ends of the range was encountered. At 0.7m depth most samples were at very low oxygen concentrations in the LP site, whereas the situation was unclear at this depth in the SS site.

A χ^2 test was again performed on the oxygen data, as for the Falstone data, and the value of $0.1 \text{ m}^3 \text{ m}^{-3}$ was again used as the critical concentration above which conditions were said to be well aerated. The results of the χ^2 test across all sites at depths to 0.5m are given in Table 7.6, and for depths to 0.7m between the forested sites in Table 7.7. As can be seen from Table 7.6 highly significant differences exist when both open sites are compared with the forested sites. An examination of the proportions however, suggests that it is really only the OV site that was radically different at 0.2 and 0.3m depth, while at 0.5m depth this site was in fairly close agreement with the SS site. Table 7.7 indicates that better aerated conditions existed under Pinus contorta compared with Picea sitchensis at all depths except 0.2m and 0.6m (and possibly 0.3m).

Table 7.6 Fraction of samples from 1979 Eddleston oxygen concentration data greater than $0.10 \text{ m}^3 \text{ m}^{-3}$, in sites and depths shown

Depth(m)	Fraction				χ^2
	OV	OP	SS	LP	
0.2	0.47	1.00	1.00	1.00	76.77***
0.3	0.15	0.84	0.91	1.00	106.60***
0.4	0.07	0.09	0.75	1.00	121.70***
0.5	0.24	0.09	0.30	0.87	65.99***

Table 7.7 Fraction of samples from 1979 Eddleston oxygen concentration data greater than $0.10 \text{ m}^3 \text{ m}^{-3}$, in the forested sites only at depths shown

Depth(m)	Fraction		χ^2
	SS	LP	
0.2	1.00	1.00	0
0.3	0.91	1.00	4.14*
0.4	0.75	1.00	15.05***
0.5	0.30	0.87	31.44***
0.6	0.33	0.52	3.01
0.7	0.40	0.19	5.52*

* $P < 0.05$
 ** $P < 0.01$
 *** $P < 0.001$

The reversal of this trend at 0.7m depth is interesting, but could be a function of a possibly leaking probe or a fortuitous location of the SS probes in a well aerated position.

8. RESPIRATION IN PEAT CORES

8.1. AIMS

Work done on mineral soils has shown that oxygen uptake by undisturbed soil cores is maximal when the gas filled pore volume fraction (ϵ_g) of the soil is approximately 0.1-0.15 (Bridge and Rixon, 1976). The RQ values from the data of these workers also showed a transition, from being greater than 1 above this gas filled pore volume fraction to less than 1 below. An experiment was therefore set up to investigate whether a similar relationship held in peat, and whether a gas filled pore volume fraction could be deduced, below which anaerobic conditions predominated.

The experiment was also designed so that the change in respiration rate with temperature could be ascertained, and a Q_{10} for aerobic peat respiration evaluated. Possible variation in respiration rate between sites OP, LP and SS was investigated, but not variation with depth, as only peat from 0.2m depth was used.

8.2. METHODS

Fifteen preserving jars (Kilner jars, Ravenhead glass Ltd.) were available to use as re-sealable, air-tight incubation jars, with internal volumes of about 0.45dm^3 . Each jar provided a wide enough mouth (75mm diameter) and internal volume to accommodate one of the undisturbed cores in its retaining sleeve (54mm diameter and 30mm deep). It was sealed with a metal lid which had an inbuilt silicone rubber ring that abutted onto the lip of the jar, which was held securely in place with a threaded brass retaining ring. A hole was drilled through the metal lid, and a short (60mm) piece of copper tubing (o.d. 3mm) cemented in place through this hole with epoxy resin. A nylon three-way tap was affixed to the external end of this tubing by a short piece of flexible

polythene tubing, also cemented in place. The jars were tested for air tightness by forcing air into the sealed jars, via the open nylon tap using a syringe with a similar nylon tap. The nylon tap was then closed, so sealing the jar at a higher than atmospheric pressure (after injecting $0.03\text{--}0.05\text{ dm}^3$ of air), and then the whole jar was submerged under water. Escaping air bubbles would indicate a leak. All jars were successfully sealed against pressure gradients in excess of anything they were likely to experience in the experiment. The jars were then labelled, and their internal volumes measured by finding the weight of water they held when completely full, with no air bubbles present.

When taking cores for moisture release characteristics from the Eddleston sites, 15 cores were taken from 0.2m depth in the OP, LP and SS sites. This enabled 5 cores to be used for respiration measurements, while maintaining 10 replicates for the moisture release work. To make the best use of available time the two experiments were run simultaneously, in the following manner.

All cores were equilibrated to 2.5 kPa tension for one week, at the end of which 5 from each site were taken and enclosed in the respiration jars. The remaining cores were replaced on the suction tables which were re-set at 5kPa. After a further week these cores were weighed again and a further 5 from each site taken and exchanged for those in the respiration jars. The cores formerly in the jars were replaced on the re-set suction tables at 10kPa together with the remaining 5, after standing in water overnight, to replace any water lost as vapour. In this way 5 replicate cores of known moisture contents were used in each respiration run, for set tensions of 2.5, 5.0, 10.0 and 15.0kPa, but not the same five cores each time.

Before being placed in the respiration jars the cores' surfaces had only a single cover of nylon netting, to allow free gaseous exchange

across both open surfaces. The cores were then sealed in the jars and a 1cm^3 gas sample removed from each to ascertain the initial concentrations of oxygen and carbon dioxide in the jar. The jars were incubated at 30°C for one week, being sampled at daily intervals (or the same time on the next day if daily sampling could not be maintained throughout). Samples were removed using a 1cm^3 glass syringe fitted with a three-way nylon tap, in the same manner as samples were removed from gas probes (Fig.3.2 Section 3.2.1.), including the venting of 1cm^3 to remove the tap dead-space. The samples were analysed using the gas chromatography system described in Section 3.2.2.

From the concentrations of oxygen and carbon dioxide obtained, the total volumes of oxygen and carbon dioxide in the jars could be calculated according to Equation 68. The gas volume V_g was calculated as the equivalent gas volume had the pressure remained at atmospheric, after allowing for the removal of samples and the volume of gases dissolved in water.

$$\text{Volume of } O_2 \text{ or } CO_2 = \left(V_w \cdot \alpha_R \cdot \frac{Y}{100} \cdot \frac{T_R}{273} \right) + \left(V_g \cdot \frac{Y}{100} \right) \dots (68)$$

where

- V_w = volume of soil moisture in the core (m^3)
- Y = partial pressure of oxygen/carbon dioxide
in jar air space (kPa)
- α_R = solubility coefficient of oxygen/carbon dioxide
at temperature (T_R)
- T_R = temperature of incubation (K)
- V_g = total gas volume in the jar (m^3)

When the volumes of oxygen and carbon dioxide had been calculated for every sampling day, then the changes in volume from the previous day were calculated and hence the oxygen absorption and carbon dioxide evolution rates. This could not be done until the oven dried

Table 8.1 Respiration rates of individual cores, as expressed by oxygen consumption, and carbon dioxide evolution rates ($10^{-9} \text{ m}^3 \text{ kg}^{-1} \text{ s}^{-1}$) at set moisture tensions (kPa)

Tension (kPa)	Respiration rate ($10^{-9} \text{ m}^3 \text{ kg}^{-1} \text{ s}^{-1}$)						
	OP		LP		SS		
	O_2	CO_2	O_2	CO_2	O_2	CO_2	
2.5		5.75	4.48	1.90	1.88	5.71	4.38
		4.03	1.57	3.25	2.00	3.55	1.71
		7.26	5.23	2.84	1.97	3.00	1.76
		5.05	3.25	4.26	2.56	1.70	1.77
		5.85	4.22	3.07	2.06	2.86	1.88
	Mean	5.59	3.75	3.06	2.09	3.36	2.30
	s.e.	0.47	0.56	0.34	0.11	0.59	0.46
5.0		5.20	2.92	2.77	2.01	3.39	3.38
		4.92	2.65	2.44	1.91	3.29	1.48
		3.85	2.08	2.81	1.04	2.48	1.31
		4.39	1.89	4.26	1.32	1.72	1.13
		3.75	1.32	2.88	0.51	1.27	1.16
	Mean	4.42	2.17	3.03	1.36	2.43	1.69
	s.e.	0.26	0.25	0.20	0.25	0.37	0.38
10.0		2.35	2.03	2.80	1.75	6.04	5.27
		2.71	1.81	2.15	2.08	3.68	2.30
		2.20	1.93	2.71	2.05	2.37	2.72
		2.45	2.23	1.46	2.00	3.47	2.09
		2.97	1.62	3.34	2.25	2.23	2.26
	Mean	2.54	1.92	2.49	2.03	3.56	2.93
	s.e.	0.12	0.09	0.29	0.07	0.61	0.53
15.0		7.48	3.84	0.89	1.31	1.11	2.55
		1.97	0.88	2.86	1.54	1.01	1.27
		4.46	3.36	0.47	1.64	2.49	2.12
		3.46	2.42	1.01	1.62	1.69	1.62
		3.00	2.78	1.61	1.60	1.27	1.34
	Mean	4.07	2.66	1.37	1.54	1.51	1.78
	s.e.	0.84	0.45	0.37	0.05	0.24	0.22

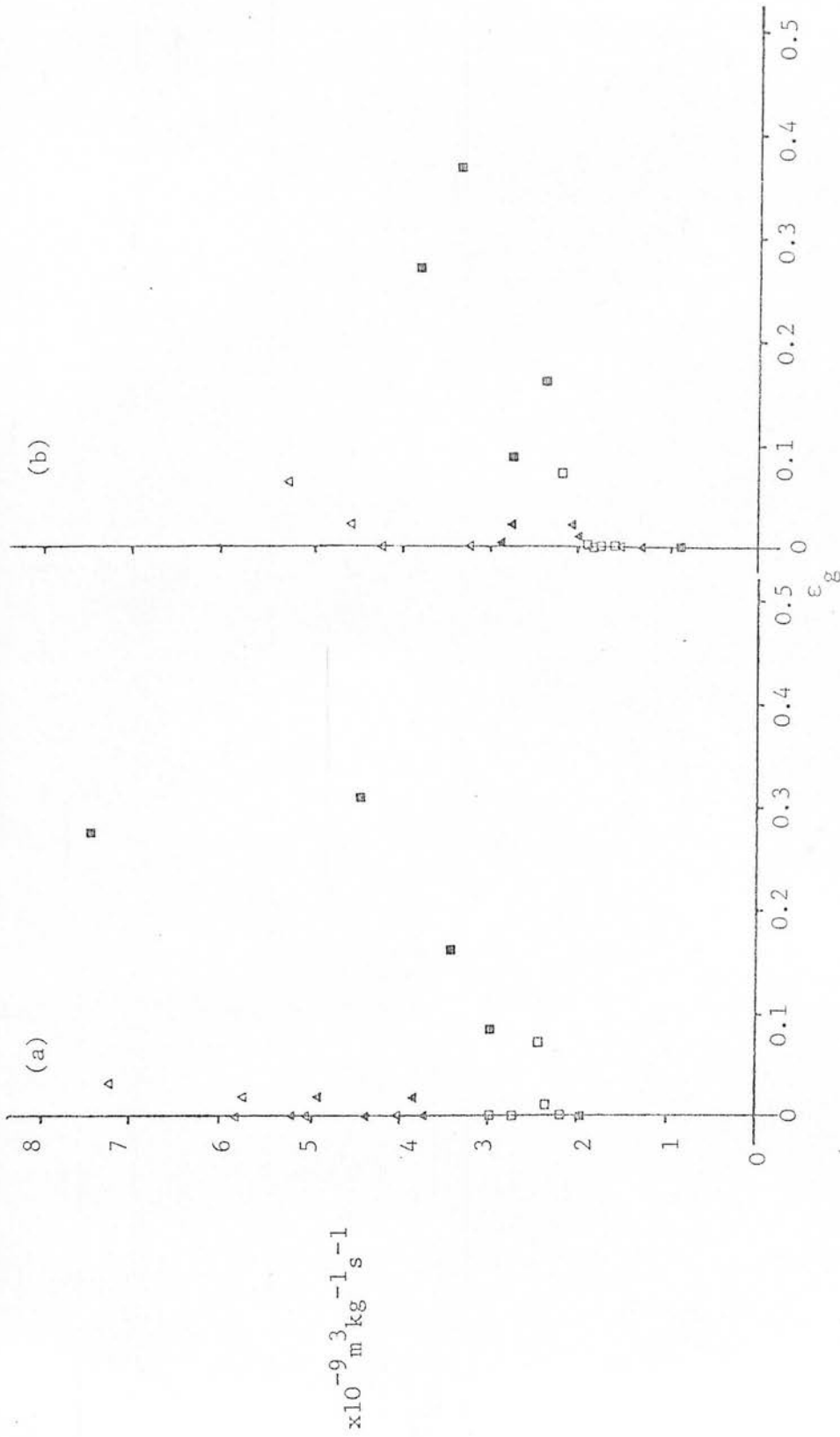


Fig.8.1 Oxygen consumption rates (a) and carbon dioxide evolution rates (b) ($10^{-9} \text{ m}^3 \text{ kg}^{-1} \text{ s}^{-1}$) for peat cores from the OP site at the gas filled pore volume fractions (ϵ_g) shown (equilibrated to moisture tensions of: Δ -2.5 kPa, \blacksquare -10.0 kPa, and \blacksquare -15.0 kPa).

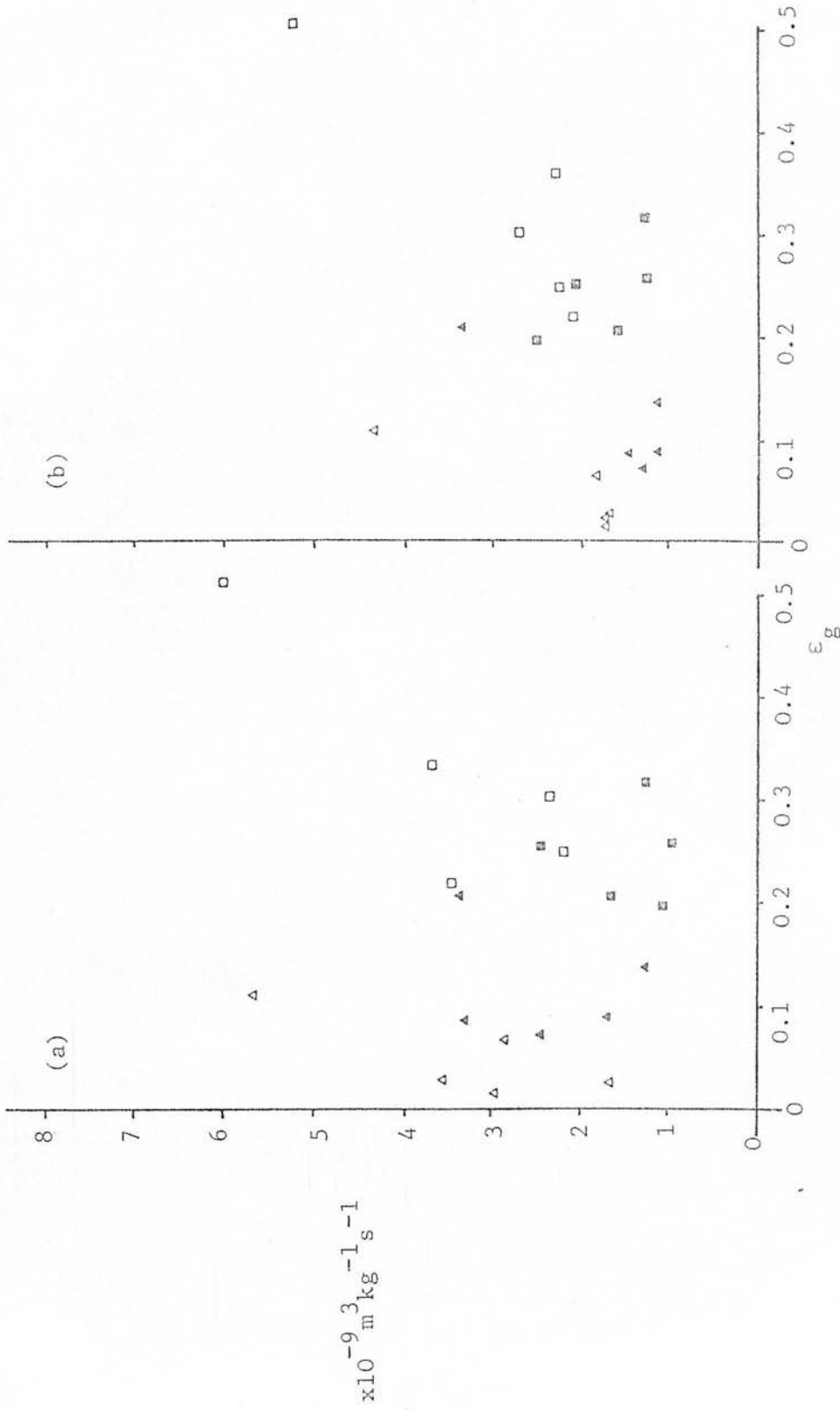


Fig.8.2 Oxygen consumption rates (a) and carbon dioxide evolution rates (b) ($10^{-9} \text{ m kg}^{-1} \text{ s}^{-1}$) for peat cores from the SS site at the gas filled pore volume fractions (ϵ_g) shown (equilibrated to moisture tensions of: Δ -2.5 kPa, ▲ -5.0 kPa, □ -10.0 kPa and ■ -15.0 kPa.)

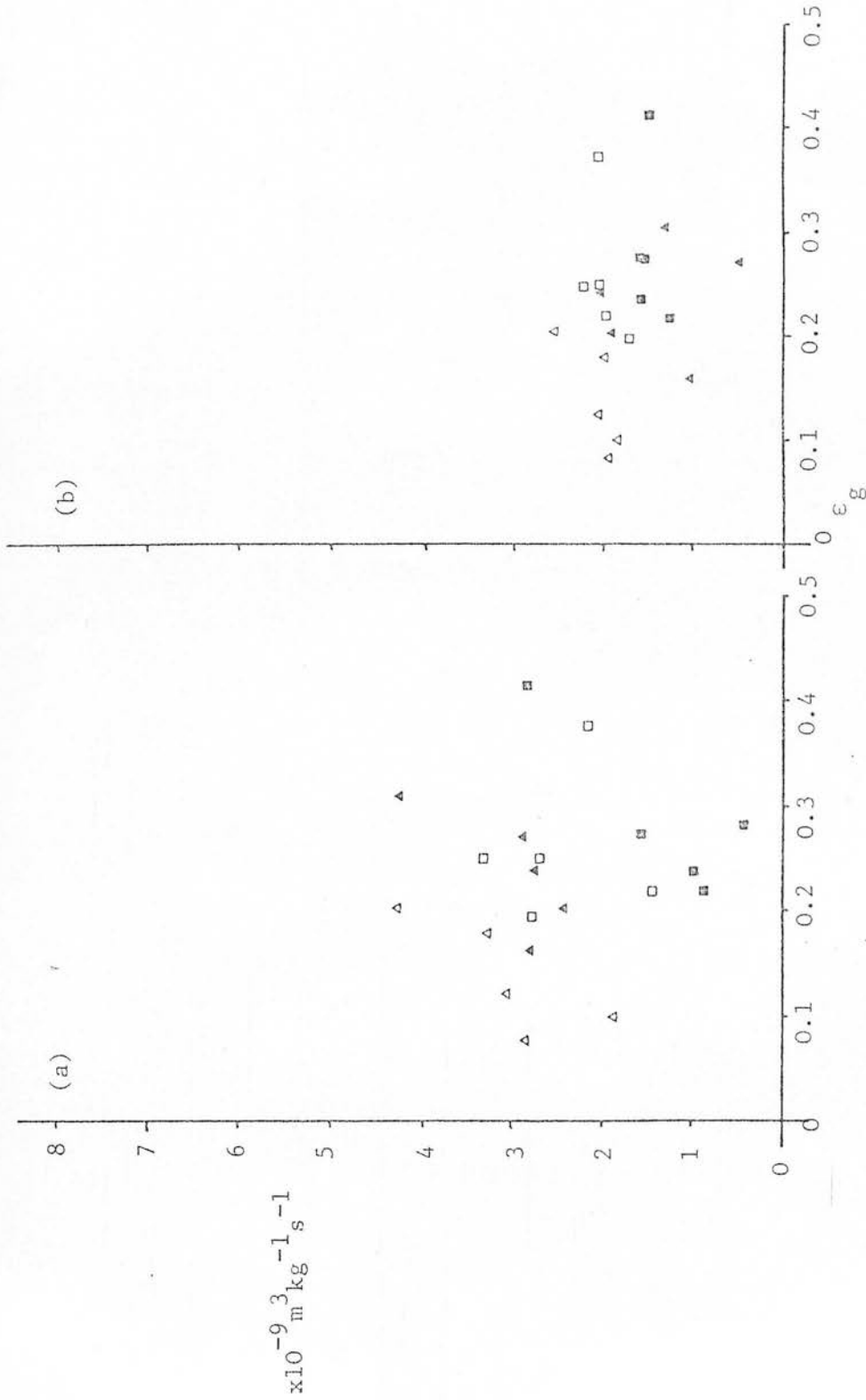


Fig. 8.3 Oxygen consumption rates (a) and carbon dioxide evolution rates (b) ($10^{-9} \text{ m}^3 \text{ kg}^{-1} \text{ s}^{-1}$) for peat cores from the LP site at the gas filled pore volume fractions (ϵ_g) shown (equilibrated to moisture tensions of: - Δ -2.5 kPa, □ -5.0 kPa, Δ -10.0 kPa and □ -15.0 kPa).

weight of peat (W_o) was known so that V_g could be calculated from the total internal volume of the jars (V), volume of the brass retaining ring ($7.85 \times 10^{-6} \text{ m}^3$) and peat moisture content, according to Equation 69.

$$V_g = V - \left(7.85 \times 10^{-6} + \frac{W_o}{t_p} + V_w \right) \quad \dots (69)$$

where t_p = particle density of peat (kg m^3). Finally the respiration rate per kilogram of peat could be calculated.

After the moisture release work and the above respiration experiment had been completed, 5 cores from each site were retained and resaturated. They were then re-equilibrated to 10kPa tension for one week, before being sealed in the respiration jars. These were then incubated for one week at temperatures of 5, 10 and 20°C, being opened to the atmosphere between different temperature runs. The sampling and calculation procedures were the same as those used in the above moisture tension experiment.

8.3. RESULTS

8.3.1. VARIATION OF RESPIRATION RATE WITH MOISTURE POTENTIAL

The oxygen consumption and carbon dioxide evolution rates for each core, are given in Table 8.1. together with the means for each tension and site. These values are the means of the rates calculated for each day, there being no differences or trends with time, other than random variation, observed during the experimental period (Appendix 5).

These rates are plotted against the calculated gas filled pore volume fraction of each core over all tensions in Figs.8.1-8.3. No observable trends for variation of respiration rate with gas filled pore volume fraction can be found in any of the sites whether judged by carbon dioxide evolution or oxygen consumption. It was not considered profitable to attempt a polynomial regression analysis as performed by Bridge and Rixon (1976), as not even a hint of a curvilinear relationship can be

observed in Figs.8.1-8.3, unlike their data in Fig.8.4. A visual comparison of the data from each site reveals a slightly higher mean respiration rate for peat from the OP site than in the planted sites (Table 8.1). Paradoxically this site has extremely low gas filled pore volume fractions, even at 10kPa tension, but the RQ's for this site (Table 8.2) are all less than 1, showing the overall respiration to be aerobic rather than anaerobic.

Fig.8.5. is a plot of the RQ's (as calculated by dividing the total oxygen consumption by the total carbon dioxide evolution), against the gas filled pore volume fraction for all cores. Again no trend is discernible, the values being generally lower than 1, at all values of V_g unlike the results obtained by Bridge and Rixon (1976) shown in Fig.1.8. The few values greater than 1 are found at gas filled pore volume fractions too high to be consistent with the results of Bridge and Rixon, and are thought to be due to the inaccuracies inherent in the measurement of oxygen depletion.

Smith (1978) has explained these inaccuracies by using an example, where a measured decrease in gas phase oxygen concentration of $0.02 \text{ m}^3 \text{ m}^{-3}$ has an error limit of say $\pm 0.002 \text{ m}^3 \text{ m}^{-3}$, which is only an error of 1% of the oxygen concentration of $0.19 \text{ m}^3 \text{ m}^{-3}$ but an error of 10% of the $0.02 \text{ m}^3 \text{ m}^{-3}$ depletion. Carbon dioxide determinations do not suffer from this problem as levels start from very low concentrations. These errors will of course be multiplied up when expressed as oxygen consumed per unit of material.

An explanation for the absence of obviously anaerobic RQ's may be an effect discussed by Bridge and Rixon (1976). They considered that the surface of a core would always support aerobic respiration which would swamp the effects of anaerobic respiration occurring at lower rates in central zones of the core. This is a distinct possibility in this experiment, and with a relatively large

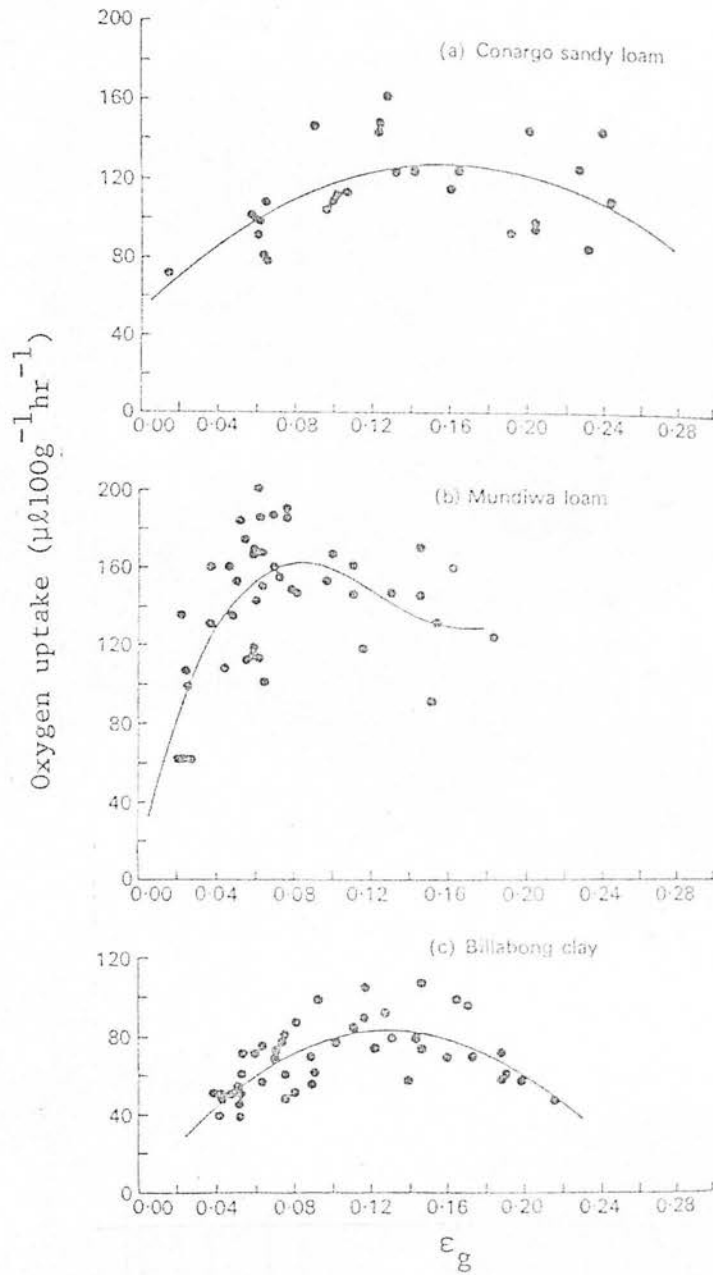


Fig.8.4 Relationship between oxygen uptake and gas filled pore volume fraction (ϵ_g) for three Australian soils with polynomial regression lines fitted. From Bridge and Rixon, 1976.

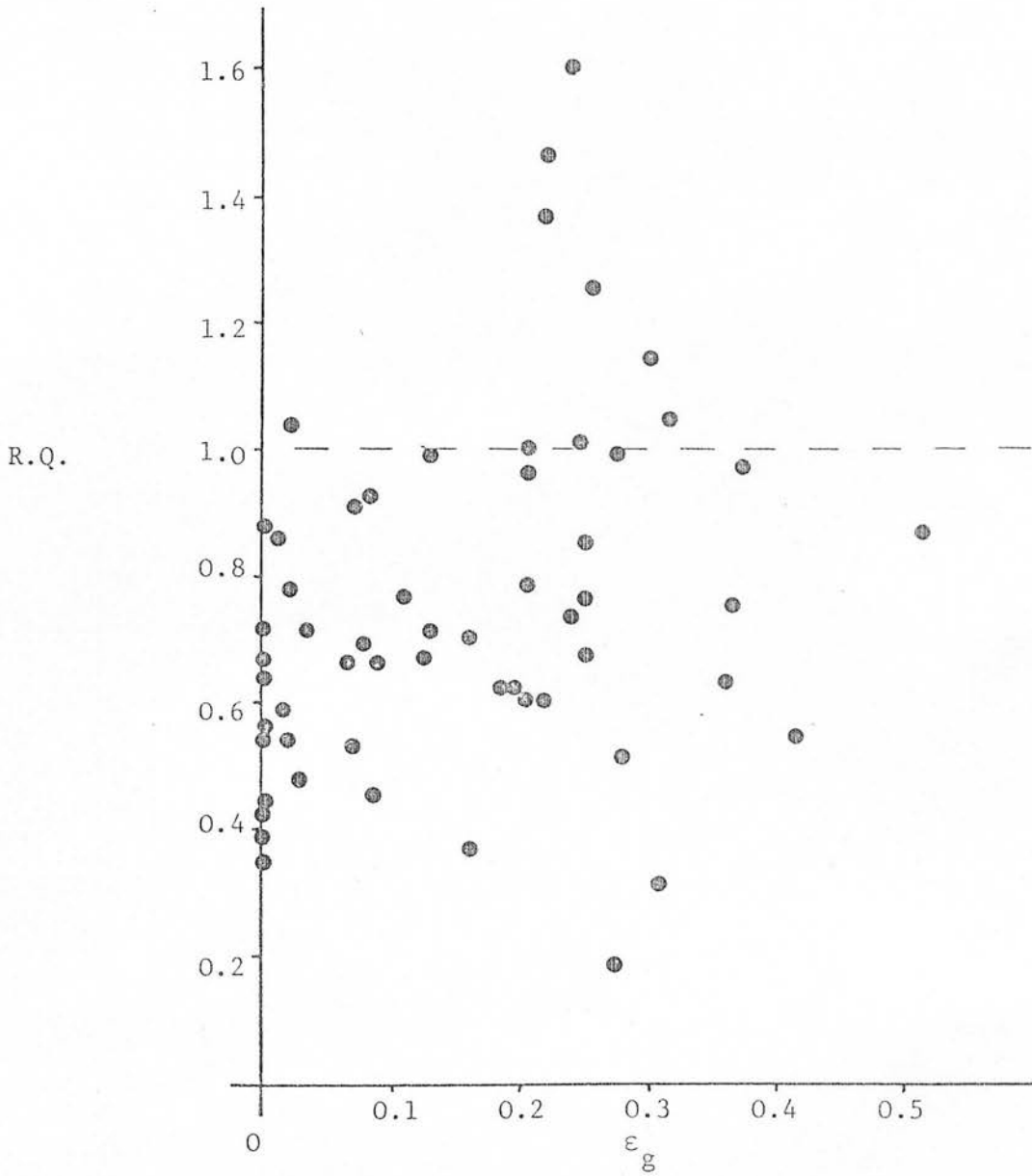


Fig.8.5 The respiratory quotient (R.Q.) at various gas filled pore volume fractions (ϵ_g) of peat cores incubated at 30°C.

Table 8.2 Gas filled pore volume fractions (ϵ_g) and RQ's for individual cores at set moisture tensions (kPa)

Tension (kPa)	Site					
	OP		LP		SS	
	ϵ_g	RQ	ϵ_g	RQ	ϵ_g	RQ
2.5	0.02	0.78	0.10	0.99	0.11	0.77
	0.00	0.39	0.18	0.62	0.03	0.48
	0.03	0.72	0.08	0.69	0.01	0.59
	0.00	0.64	0.20	0.60	0.02	1.04
	0.00	0.72	0.12	0.67	0.07	0.66
Mean		0.65		0.71		0.71
5.0	0	0.56	0.24	0.73	0.21	1.00
	0.02	0.54	0.21	0.78	0.09	0.45
	0.02	0.54	0.16	0.37	0.07	0.53
	0	0.43	0.31	0.31	0.09	0.66
	0	0.35	0.27	0.18	0.13	0.91
Mean		0.48		0.47		0.71
10.0	0.01	0.86	0.20	0.62	0.51	0.87
	0	0.67	0.38	0.97	0.36	0.63
	0	0.88	0.25	0.76	0.30	1.15
	0.07	0.91	0.22	1.37	0.22	0.60
	0	0.54	0.25	0.67	0.25	1.01
Mean		0.77		0.88		0.85
15.0	0.28	0.51	0.22	1.47	0.19	2.29
	0	0.45	0.42	0.54	0.26	1.26
	0.31	0.75	0.28	3.46	0.25	0.85
	0.16	0.70	0.25	1.61	0.21	0.96
	0.09	0.93	0.28	0.99	0.32	1.05
Mean		0.67		1.61		1.28

reservoir of air surrounding the core, the concentration of oxygen would not fall much from atmospheric ($0.21\text{m}^3\text{m}^{-3}$), so maintaining a high concentration gradient between this reservoir and the respiring sites. The likelihood and extent of any anaerobic zone in the centre of the core has been estimated here using the aerobic oxygen consumption rate from this experiment and diffusion coefficients from Section 9.

Because of the variable nature of respiration rates and diffusion coefficients, a mean of each was calculated for all values measured at tensions of less than 5kPa (at which capillary pores should be water filled). The oxygen consumption rate had to be converted to the rate per unit volume, before it could be incorporated into Equation (15) ($r = \sqrt{6DSP/M}$) to obtain the maximum radius r at which a peat sphere will be wholly aerobic. This was simply done by multiplying the rate per kg by the dry bulk density (from Section 5) of peat at 0.2m depth in the OP site. Only data for the OP site were used, as the diffusion coefficients were measured on peat from this site, and the mean oxygen consumption rates were higher than the LP or SS sites. The calculations are shown below, where the solubility of oxygen in water at 30°C is taken as 0.026 and the partial pressure of oxygen P as 0.2.

$$\text{Mean diffusion coefficient } D = 1.53 \times 10^{-7} \text{ m}^2 \text{ s}^{-1}$$

$$\begin{aligned} \text{Mean oxygen consumption rate } M &= 5.003 \times 10^{-9} \text{ m}^3 \text{ kg}^{-1} \text{ s}^{-1} \\ &= 6.5 \times 10^{-7} \text{ m}^3 \text{ m}^{-3} \text{ s}^{-1} \end{aligned}$$

$$\begin{aligned} \therefore r &= \sqrt{\left[\frac{6 \times 1.53 \times 10^{-7} \times 0.026 \times 0.2}{6.5 \times 10^{-7}} \right]} \\ &= 8.6 \times 10^{-2} \text{ m} = 86 \text{ mm} \end{aligned}$$

N.B. The spherical diffusion model was used because (a) sufficient air penetration was considered to occur between core and ring to allow diffusion into all surfaces, (b) as the geometry was therefore that of a right cylinder, this was the best available theoretical model.

If a diffusion coefficient D , typical of near saturated conditions is used ($1 \times 10^{-8} \text{ m}^2 \text{ s}^{-1}$), the maximum radius for a wholly aerobic sphere now becomes:

$$r = \sqrt{\left[\frac{6 \times 10^{-8} \times 0.026 \times 0.2}{6.5 \times 10^{-7}} \right]}$$

$$= 2 \times 10^{-2} \text{ m} = 20 \text{ mm}$$

The results show that at typical respiration rates and diffusion coefficients found at gas filled pore volume fractions around 0.1, a peat sphere would have to be greater than about 80mm radius to contain an anaerobic zone. Even near total saturation the radius would have to be greater than 20mm. As the cores were only 30mm in depth, this explains why anaerobic zones were not created, as even in totally saturated cores only small zones of anaerobic activity would occur.

8.3.2. VARIATION OF RESPIRATION RATE WITH TEMPERATURE

The oxygen consumption and carbon dioxide evolution rates for each core are given in Table 8.3, together with the means and their standard errors for each site at each temperature. The means of the oxygen consumption rates are plotted against temperature in Fig.8.6, and the means for carbon dioxide evolution rates in Fig.8.7. Both graphs demonstrate the expected increase with temperature, though the oxygen consumption rates for sites OP and LP show a decrease in the mean rate at some point (from 10-20°C and 5-10°C respectively). The already stated susceptibility of oxygen depletion measurement to error makes Fig.8.9 less likely to indicate the true respiration rate than the carbon dioxide evolution rate (Fig. 8.10). Therefore the carbon dioxide evolution rates were taken as the respiration rate when calculating the Q_{10} and basal respiration rate (R_0) for these cores. The Q_{10} , or thermal coefficient, is the factor by which the respiration rate increases over a 10°C rise in temperature e.g. rate at 20°C/rate at 10°C. The Q_{10}

N.B. The value of D/D_0 of $1 \times 10^{-8} \text{ m}^2 \text{ s}^{-1}$ was used to represent the relative diffusivity at tensions of the order of 0-2 kPa.

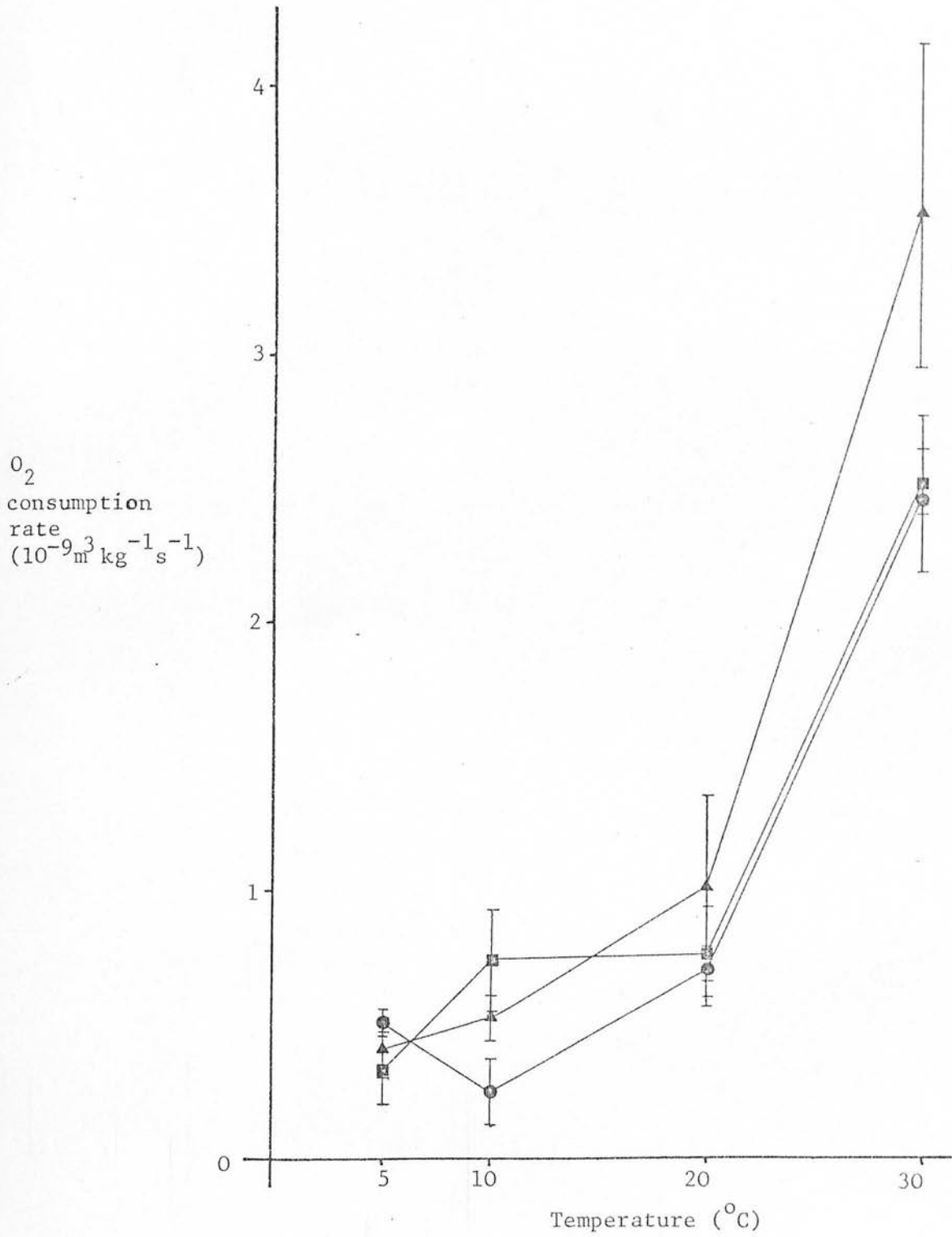


Fig.8.6

Mean oxygen consumption rate of peat cores from the sites
 ■ -OP, ▲ -SS and ● -LP, incubated at the temperatures
 shown.

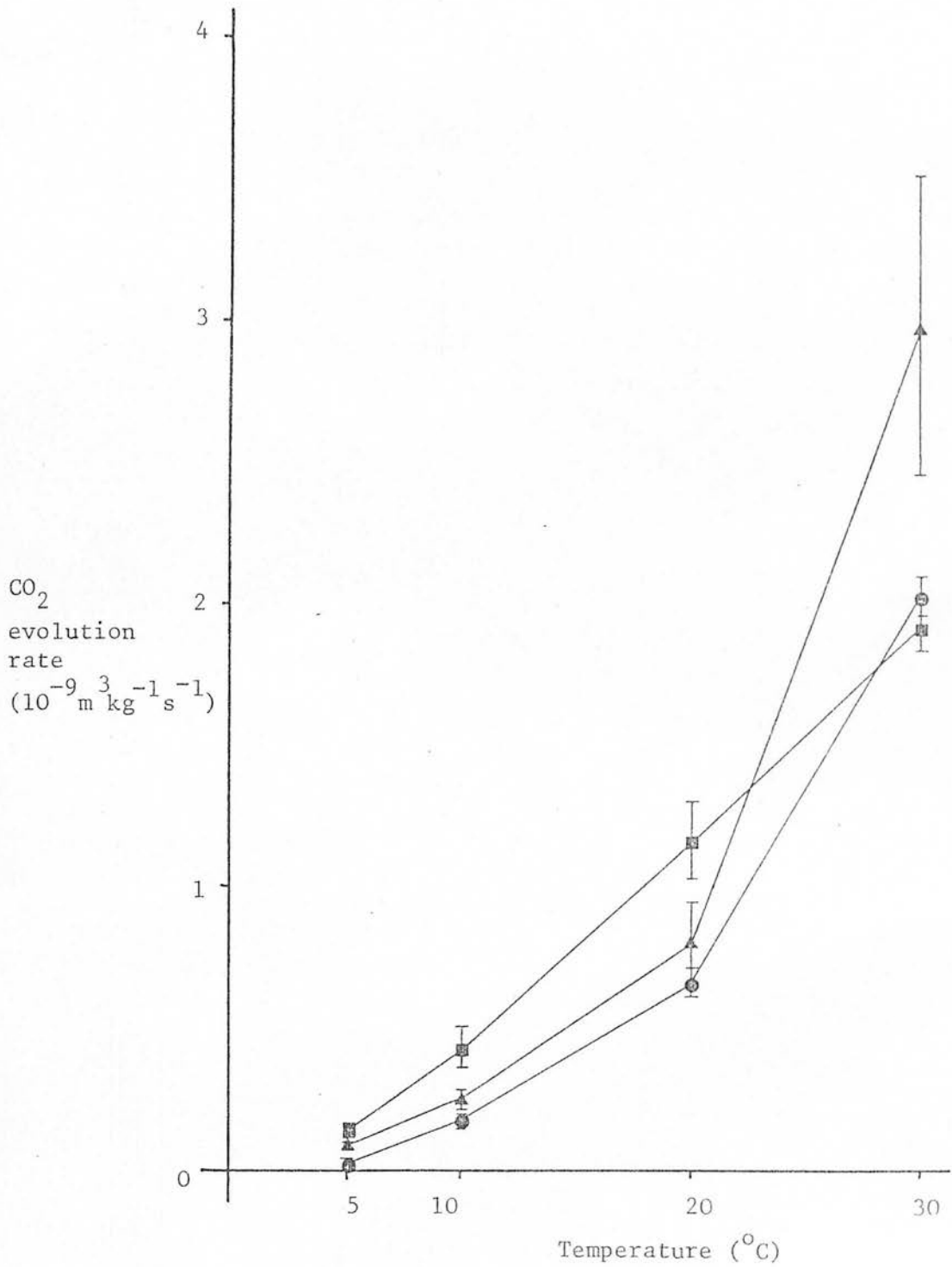


Fig.8.7 Mean carbon dioxide evolution rates of peat cores from the sites, ■ - OP, ▲ - SS and ● - LP, incubated at the temperatures shown.

Table 8.3 Respiration rates of individual cores as expressed by oxygen consumption and carbon dioxide evolution rates ($10^{-9} \text{ m}^3 \text{ kg}^{-1} \text{ s}^{-1}$) at successive incubation temperatures.

Temperature (°C)	Gas consumption/evolution ($10^{-9} \text{ m}^3 \text{ kg}^{-1} \text{ s}^{-1}$)						
	OP		LP		SS		
	O ₂	CO ₂	O ₂	CO ₂	O ₂	CO ₂	
5		0.04	0.20	0.50	0.06	0.04	0.09
		0.58	0.08	0.45	0.06	0.40	0.14
		0.14	0.12	0.66	0.07	0.72	0.07
		0.13	0.16	0.49	0.04	0.65	0.09
		0.80	0.12	0.45	0.04	0.35	0.06
	Mean	0.34	0.14	0.51	0.05	0.43	0.09
	s.e.	0.13	0.02	0.04	0.01	0.11	0.01
10		0.16	0.66	0.10	0.16	0.22	0.34
		1.12	0.13	0.82	0.15	0.73	0.36
		0.96	0.45	0.04	0.27	0.49	0.18
		1.18	0.47	0.24	0.15	0.72	0.21
		0.36	0.44	0.29	0.22	0.50	0.18
	Mean	0.76	0.43	0.30	0.19	0.53	0.25
	s.e.	0.19	0.08	0.12	0.02	0.08	0.04
20		1.46	1.40	0.44	0.70	2.37	1.39
		0.68	0.54	1.13	0.84	1.25	0.97
		0.50	1.39	0.51	0.67	0.65	0.58
		1.23	1.30	0.68	0.50	0.23	0.54
		1.32	1.18	0.68	0.57	0.53	0.51
	Mean	1.04	1.16	0.69	0.66	1.01	0.80
	s.e.	0.17	0.14	0.11	0.05	0.34	0.15
30		2.35	2.02	2.80	1.75	6.04	5.27
		2.71	1.81	2.15	2.08	3.68	2.30
		2.20	1.93	2.71	2.05	2.37	2.72
		2.45	2.24	1.46	2.00	3.47	2.09
		2.97	1.62	3.34	2.24	2.23	2.26
	Mean	2.54	1.92	2.49	2.03	3.56	2.93
	s.e.	0.12	0.09	0.29	0.07	0.61	0.53

was calculated for both rises in temperature from 10 to 20°C (case 'A') and also 20-30°C (case 'B') even though rates at 30°C were measured on a different set of cores to those at the other temperatures. The resulting values for Q are listed in Table 8.4, together with the basal respiration rates R_0 (respiration at 0°C). R_0 was calculated using Equation (22), the calculated values for Q and T as 20 and 30°C. From this we have two different sets of Q and R_0 , which although similar for the LP and SS sites are quite different for the OP site. To test which set was a better estimation of the true values, the figures in Table 8.4 were applied back into Equation (22) at values of T corresponding to the temperatures used in the experiment. The resulting carbon dioxide evolution rates are given in Table 8.5, together with an indication as to whether they came within one standard error of the measured means in Table 8.3. Naturally the figures for the temperatures from which Q was estimated are about the same as the originals (those at 10 and 20°C in case 'A', and those at 20 and 30°C in case 'B'). However outside this expected correlation the calculated figures for case A are in close agreement with the originals measured only at 30°C, except for site OP. In neither case is a close agreement found at 5°C, but if the values for R_0 are compared with the original measured rates, then it is found that those from case 'A' are within one standard error for each site. It is therefore suggested that respiration does not increase appreciably until a temperature of about 5°C has been reached, remaining fairly static at a minimal rate below this temperature.

Ideally both case 'A' and case 'B' should give identical values for Q_{10} and R_0 , and the difference is most likely caused by the use of different cores at 30°C. In the LP and SS sites this difference is not too great and both sets of data are probably reasonable estimates of the true mean value for peat from these sites. The larger difference in peat from the OP site could be caused by an underestimation of the

Table 8.4 Basal respiration rates R_o ($10^{-9} \text{ m}^3 \text{ kg}^{-1} \text{ s}^{-1} \text{ CO}_2$ evolution rate) and Q_{10} factors from the mean respiration rates of peat cores

Temperature ($^{\circ}\text{C}$)		Site		
		OP	LP	SS
"A" 10-20	Q_{10}	2.70	3.47	3.20
	R_o	0.16	0.05	0.08
"B" 20-30	Q_{10}	1.66	3.08	3.66
	R_o	0.42	0.07	0.06

Table 8.5 Calculated respiration rates ($\times 10^{-9} \text{ m}^3 \text{ kg}^{-1} \text{ s}^{-1}$) at experiment temperature values, using Q_{10} and R_o values from Table 8.4 (*- within one standard error of measured rates)

Temperature category from Table 8.4	Site	Respiration rate ($10^{-9} \text{ m}^3 \text{ kg}^{-1} \text{ s}^{-1}$)			
		5°C	10°C	20°C	30°C
"A"	OP	0.26	0.43*	1.17*	3.15
	LP	0.09	0.17*	0.60*	2.09*
	SS	0.14	0.26*	0.82*	2.62*
"B"	OP	0.54	0.70	1.16*	1.92*
	LP	0.12	0.22	0.66*	2.05*
	SS	0.11	0.22*	0.80*	2.94*

respiration rate at 30°C. Fig. 8.7 shows a marked difference in the shape of the curve for the OP site, compared with the other sites and curves for oxygen consumption in Fig. 8.6, due to what looks like a low value for carbon dioxide evolution at 30°C. The value for Q_{10} in case B excepted, all the Q_{10} values are comparable to the values of about 3 found by Monteith *et al* (1964) working on field estimates from a mineral soil, and other workers' data (see Section 1.2).

8.4. CONCLUSIONS

The lack of any obvious relationship between respiration rate and gas filled pore volume fractions in Fig. 8.1-8.3, rather suggests that, unlike mineral soil, the peat from this site does not develop localised anaerobic zones before becoming wholly anaerobic when totally saturated. For this to be the case then a larger proportion of the pores must be of a non-capillary size and therefore drained at very low tensions. Sections 4 and 5 demonstrate that indeed a larger volume of soil is drained at -5kPa in peat than in the clayey subsoil at Falstone. The data of Bridge and Rixon (1976) (Fig. 1.8), however, indicates that the critical gas filled pore volume fraction is within a range of 0.05-0.15 for sandy and loamy soil types as well as clay, and hence the size and overall volume of pores drained may not be so important as their spatial distribution. The soils used by Bridge and Rixon were all surface samples of pasture soils and therefore likely to be aggregated to some degree. The anaerobic zones formed below gas filled pore volume fractions of about 0.1 are probably those described by Currie (1961b) in saturated soil aggregates containing only capillary pores. The fibrous nature of the peat at Eddleston with a high proportion of large fibres (>1mm), may act to prevent formation of clods of finely comminuted particles, by maintaining an even distribution of non-capillary pores due to the looser packing associated with larger particles.

It does not necessarily follow that in the field the peat will be either waterlogged and anaerobic, or partly drained and aerobic. Although respiration rates from the above experiment were derived at 30°C, which is much higher than would be experienced in the field, plant root respiration would be added to that of soil microorganisms, plus the probability that the oxygen concentration in gas filled pores would be lower than $0.2 \text{ m}^3 \text{ m}^{-3}$. These factors would increase the likelihood of anaerobic zones and their extent (by minimising r in Equation (15)). Countering this effect, it must be remembered that at typical summer field soil temperatures, about 10°C, the peat respiration rate will be less than half those measured near saturation in this experiment, so increasing r in Equation (15).

9. GASEOUS DIFFUSION THROUGH PEAT CORES

9.1 AIMS

Previous measurements of gaseous diffusion through soil samples, either reconstituted (Grable and Siemer, 1968) or undisturbed cores (Gradwell, 1960), have been conducted on mineral soils, often with a well defined crumb structure or composed of selected soil crumbs (Currie, 1979). Little is known however of the diffusion coefficients and relative diffusivity for peat which is rather more porous and structureless. The relationship between moisture content and gas filled pore space is difficult to define in peat (see Section 5), and so it was necessary to find out whether accepted ideas about gaseous diffusion through mineral soil held for peat. An experiment was therefore set up to measure the relative diffusivity through peat over a range of gas filled pore volume fractions near saturation, where a change from overall aerobic to anaerobic conditions may occur.

9.2 METHODS

Thirty undisturbed cores were taken from the OP site at Eddleston from a depth of 0.45m. The cores (radius 38mm and length 50mm) were taken by gently hammering a sharpened steel ring into a levelled surface of the peat at the required depth. The rings containing the cores were then sealed at both ends to prevent moisture loss, during transport back to the laboratory. The rings were then saturated by standing them on a plastic foam mat in a tray of water, keeping them covered to reduce evaporation. Twenty-five cores were then equilibrated on the suction tables previously mentioned (Section 4), to tensions of 2,4,6,8 and 10kPa (five at each tension), while the remaining five were left saturated. The cores were then re-sealed (with tinsplate caps and plastic tape) at either end to prevent moisture loss and stored at 4°C.

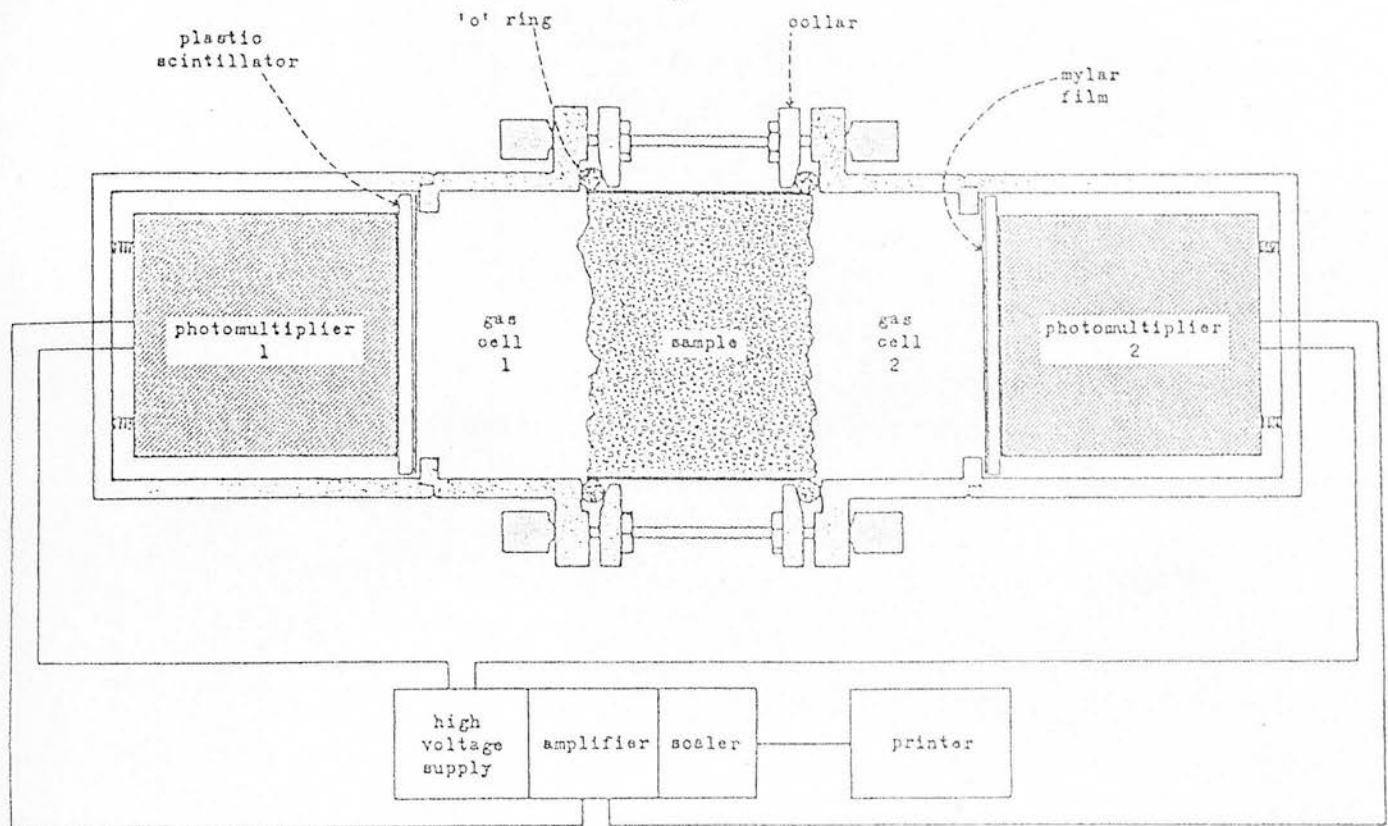


Fig.9.1 Apparatus for measurement of gas diffusion through soil cores. From Ball, 1980.

The measurement of gaseous diffusion through the cores was carried out on equipment at the Agricultural Research Council Letcombe Laboratory, where it had been designed and constructed. The equipment measures the diffusion rate of the radioactive gas ^{85}Kr through a core of porous material of the dimensions given above. The device is illustrated in Fig.9.1 and fully described by Ball *et al* (1981), who used it to measure relative diffusion rates and air permeabilities in ploughed and direct-drilled mineral soils (Ball, 1980).

The soil core is held in its retaining ring between two gas chambers of known volume (171 cm³), and sealed by rubber O rings. These gas chambers are adjacent to two photomultiplier tubes covered by a disc of plastic scintillator and Mylar film. Each gas cell has an inlet/outlet port, which is stoppered by a rubber self sealing septum during use. To measure gaseous diffusion, 1 cm³ of ^{85}Kr in air ($\sim 1 \mu\text{Ci cm}^{-3}$) is injected into one gas chamber through the rubber septum, using a Luer needle and syringe. The ^{85}Kr gradually diffuses through the soil core into the other chamber until an equilibrium is reached. The rate of decrease of beta activity in the injection chamber, and the rate of increase in activity in the distal chamber, are measured by taking the number of counts registered in a fixed time period (usually 60s) by each photomultiplier tube at suitable time intervals (usually 5 min), until equilibrium is reached. The pressure difference between the two gas chambers is small (less than 500 Pa) due to the volume of ^{85}Kr /air mixture injected being small compared to the total volume of the apparatus (1.576 cm³), and rapid pressure equilibrium via the soil pores. The temperature of the ambient air around the apparatus is taken during the experiment, so that the measured diffusion coefficient (D_a) of ^{85}Kr in the soil sample can be compared with that in free air (D_o) at the same

temperature.

The diffusion coefficient of the sample is calculated by solving Fick's First Law of Diffusion (Equation 1) using Equations 70 and 71.

$$C_I - C_R = 2C_e^{-kt} \quad \dots (70)$$

$$k = \frac{2 D_a A_s}{v L_s} \quad \dots (71)$$

where C_I = Concentration (counts s^{-1}) of ^{85}Kr in the injection chamber

C_R = Concentration (counts s^{-1}) of ^{85}Kr in the receiving chamber

C_e = Equilibrium concentrations of ^{85}Kr

A_s = Cross sectional area of core

L_s = Length of sample core

v = Volume of gas chamber (171 cm^3)

t = Time

To obviate the need to wait until equilibrium of the ^{85}Kr concentrations, C_e and k were calculated from values of C_I , C_R and t fed into a "Maximum Likelihood" computer programme for Equation 70. D_a was then calculated from a re-arrangement of Equation 71, which simplifies down to Equation 72 when the known values for A_s , L_s and V are inserted.

$$D_a = 0.15928 k \text{ cm}^2 \text{ s}^{-1} \quad \dots (72)$$

The computer analysis to obtain values of k was performed by staff at the Department of Statistics at Rothamsted Experimental Station, and final values of D_a and D_a/D_0 were calculated by the author.

To compensate for shrinkage of the peat at the higher tensions, the space between the shrunken peat core and the retaining ring was filled with molten paraffin wax. No correction was made for the reduction in A_s , as this was very small and not considered a major source of error.

Table 9.1 The weight of oven dried peat solids (W_s)(g), contained water (W_w)(g) derived moisture content mass fraction (θ_m), diffusion coefficient (D) and temperature (t) for peat cores equilibrated at different moisture tensions.

Core No.	Moisture tension(kPa)	W_s	W_w	θ_m	$D(10^{-6} m^2 s^{-1})$	$t(^{\circ}C)$
1	0	17.4	210.1	12.07	0.002	20
2		19.0	216.8	11.41	0.008	20
3		17.0	221.7	13.04	0.001	20
4		17.4	216.3	12.43	0.005	22
5		15.7	219.5	13.98	0.001	20
6	2	16.7	206.1	12.34	0.121	21
7		22.2	181.8	8.19	0.145	20
8		18.6	196.7	10.58	0.130	22
9		17.7	194.4	10.98	0.182	19
10		22.5	200.3	8.90	0.021	20
11	4	25.3	165.0	6.52	0.189	18
12		26.0	158.1	6.08	0.189	18
13		22.6	167.6	7.42	0.433	18
14		20.1	155.3	7.73	0.383	20
15		19.9	148.1	7.44	0.493	20
16	6	22.8	171.5	7.52	0.339	19
17		20.0	176.3	8.82	0.415	17
18		25.7	144.7	5.63	0.349	18
19		16.9	159.1	9.41	0.393	16
20		27.3	166.7	6.11	0.286	18
21	8	28.3	154.2	5.45	0.434	20
22		30.1	136.8	4.54	0.403	20
23		30.6	142.5	4.66	0.481	20
24		34.6	141.9	4.10	0.270	20
25		34.0	139.1	4.09	0.219	20
26	10	26.3	157.1	5.97	0.536	20
27		28.2	142.1	5.04	0.529	20
28		27.2	128.0	4.71	0.530	20
29		28.7	125.0	4.36	0.527	20
30		34.6	115.2	3.33	0.451	19

Table 9.2 Diffusion coefficients of ^{85}Kr in free air (D_0)
at different temperatures (t)

$t(^{\circ}\text{C})$	$D_0(10^{-6}\text{m}^2\text{s}^{-1})$
15	14.60
16	14.70
17	14.80
18	14.90
19	15.00
20	15.10
21	15.15
22	15.20
23	15.30
24	15.40
25	15.50

Table 9.3 The fraction of original volume (v), moisture content
volume fraction (θ_v), gas-filled pore volume fraction (ϵ_g)
and relative diffusivity (D/D_o) of each peat core

Core No.	v	θ_v	ϵ_g	D/D_o
1	1.04	0.886	0.064	0.00013
2	1.02	0.932	0.012	0.00053
3	1.07	0.909	0.044	0.00007
4	1.05	0.904	0.047	0.00033
5	1.09	0.883	0.074	0.00007
6	1.05	0.861	0.092	0.00799
7	0.91	0.876	0.051	0.00960
8	1.00	0.863	0.082	0.00855
9	1.01	0.844	0.104	0.01213
10	0.94	0.935	-0.006	0.00139
11	0.85	0.851	0.060	0.01268
12	0.83	0.835	0.077	0.01268
13	0.89	0.826	0.098	0.02906
14	0.90	0.757	0.177	0.02536
15	0.89	0.730	0.194	0.03265
16	0.89	0.845	0.078	0.02260
17	0.94	0.823	0.114	0.02804
18	0.81	0.784	0.122	0.02342
19	0.96	0.727	0.221	0.02673
20	0.83	0.881	0.021	0.01919
21	0.80	0.845	0.049	0.02874
22	0.75	0.800	0.080	0.02669
23	0.76	0.822	0.057	0.03185
24	0.73	0.853	0.006	0.01788
25	0.73	0.836	0.025	0.01450
26	0.82	0.840	0.064	0.03550
27	0.78	0.799	0.093	0.03503
28	0.76	0.739	0.155	0.03510
29	0.74	0.741	0.143	0.03490
30	0.68	0.743	0.105	0.03007

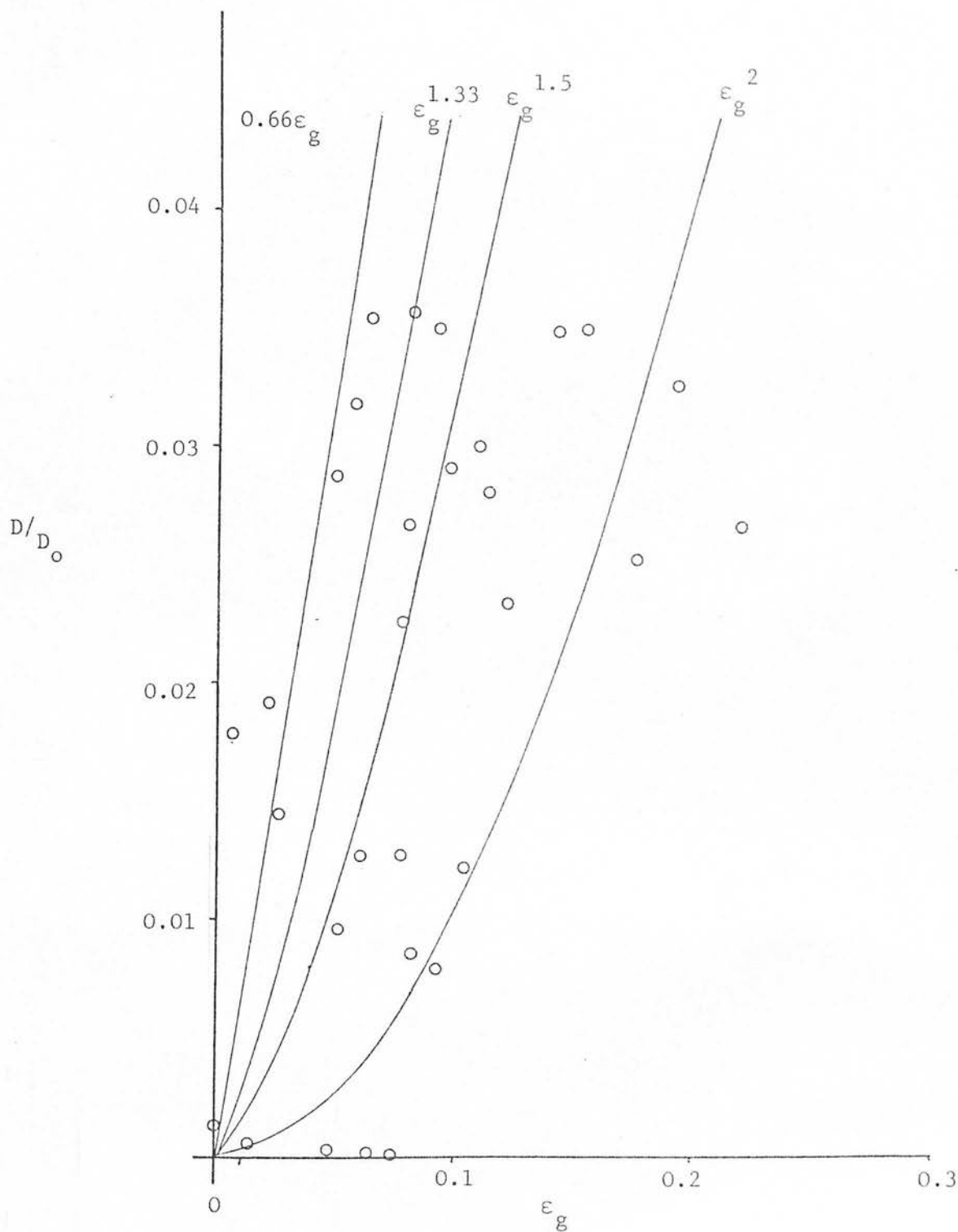


Fig.9.2 Variation of relative diffusivity (D/D_0) with gas filled pore volume fraction (ϵ_g) of the peat cores, with relationships from the literature superimposed.

Cores were stored at 4°C between sampling runs and allowed to equilibrate (whilst sealed) to room temperature before analysis. After the diffusion measurements had been made the cores were oven dried to 105°C to obtain the amount of peat solids. The cores that had had paraffin wax injected round their edges had the accessible pieces of this removed, but that which could not be removed easily was left to run out upon heating. The moisture contents and gas filled pore volume fractions were calculated as in Section 5. A correction to the gas filled pore space to compensate for shrinkage was made using the equation $V = 0.45 \theta_m^{0.33}$, from Table 5.9.

9.3 RESULTS

The mass of oven dried peat solids (W_s) and volume of water in the core (W_w) are given, together with the derived moisture content mass fractions (θ_m), in Table 9.1. The measured diffusion coefficients (D) for each core are also given in Table 9.1, together with the ambient temperature around the apparatus. The diffusion coefficients of ^{85}Kr in free air (D_0) over the range of temperatures encountered are given in Table 9.2.

The relative diffusivity (D/D_0) is given in Table 9.3, together with the core volume as a percentage of the original (V) (calculated using the θ_m quoted in Table 9.1), and the resulting moisture content volume fraction (θ_v) and gas-filled pore volume fraction (ϵ_g). The relationship between D/D_0 and ϵ_g is shown in Fig. 9.2, where theoretical relationships from the literature are super-imposed over the scatter diagram.

By visual inspection it does not seem that the scatter in Fig. 9.2 favours any particular relationship, but a possible error noticed during calculation of θ_m may have produced ϵ_g values that were too small in some cores.

It can be seen in Table 9.1 that the mass of peat solids is larger in cores equilibrated to higher tensions than those at lower tensions. For most cores equilibrated to 6, 8 and 10 kPa tension the oven dried weights are greater than that predicted by the bulk density measurements from other cores ($\rho_s^b = 0.084 \text{ kg dm}^{-3}$, $W_s = 0.019 \text{ kg}$) (see Section 5). As cores were taken from the same area and assigned to each tension at random, it is highly unlikely that this is a genuine effect, especially as it involves effectively doubling the dry bulk density in some cases. It is precisely for those cores that had paraffin injected that the increase in solids weight is most noticeable, and it must be concluded that this is the cause of the error. Although attempts were made to remove most of this wax, not all of it was readily accessible without breaking the core and risking the loss of material. It was considered that this remaining wax would melt and run out of the space between the core and retaining ring upon heating, but the evidence suggests that instead it was absorbed into the peat pore space, increasing the weight of the dried core.

A correction for this effect can be made by assuming the cores had the previously measured dry bulk density of 0.084 kg dm^{-3} , and recalculating θ_m , V , θ_v and ϵ_g according to the predicted mass of peat solids of 0.0191 kg . This was considered reasonable as the standard error of the bulk density was previously found to be low (0.003), giving a range of peat solids masses from 0.01847 kg to 0.01984 kg .

It will be noticed from Table 9.1 that, at tensions of 0 and 2 kPa, the mass of peat solids is often outside the range of one standard error either side of the mean predicted by the mean bulk density. As both sets of cores were taken from different areas then this could be an area of genuinely lower bulk density. For this reason it was decided not to apply the correction for cores with less than 0.02 kg of peat solids, as the figures are likely to be genuine, and not contaminated with paraffin

wax. The assumption of the peat solids mass being 0.0191 kg, however, is a much closer approximation to the true values than the grossly inflated values at 8 and 10 kPa tension.

The new estimated values of θ_m' , V' , θ_v' and ϵ_g' are given in Table 9.4, and the scatter shown in Fig.9.3. To find the closest approximation of the theoretical relationship from the literature (shown in Fig.9.2), a regression analysis was carried out on this data to ascertain the best fitting curve. This was done by transforming the data, by taking the logarithm₁₀ of D/D_0 and ϵ_g' , and conducting a linear regression analysis on this scatter (Fig.9.4). The resulting curve is described by Equation 73:

$$D/D_0 = 0.653 \times \epsilon_g'^{-2.16} \quad \dots (73)$$

and plotted on Fig.9.3, as is a linear regression line derived from the untransformed data, and described by Equation 74:-

$$D/D_0 = -0.0015 + 0.126(\epsilon_g') \quad \dots (74)$$

The analysis of variance tables for these regressions are given in Tables 9.5 and 9.6, together with the correlation coefficients (r). It can be seen from these tables that both relationships are significantly different from the horizontal for a probability level of 1%, and both have a high correlation coefficient.

Although the correlation is slightly better for the linear relationship, theory indicates that the true relationship should be curvilinear. Therefore the relationship indicated in Equation 7.3 is favoured, as it is of the same form as that proposed by Currie (1960b): $D/D_0 = \gamma \epsilon_g'^{\mu}$ (Equation 8). Bakker and Hidding (1970), however, suggested that over a short range of ϵ_g' values the relationship could be described as $D/D_0 = a(\epsilon_g' - b)$, and a rearrangement of Equation 74 gives such a relationship (Equation 75).

$$D/D_0 = 0.126 (\epsilon_g' - 0.012) \quad \dots (75)$$

Table 9.4 The moisture content mass fraction (θ'_m) and volume fraction (θ'_v), of peat cores with a fractional volume v' of their original volume and gas filled pore volume fraction ϵ'_g , assuming the mean mass of oven dry peat to be 0.019kg and not greater than 0.02kg.

Core No.		θ'_m	v'	θ'_v	ϵ'_g	D/D _o
1		12.10	1.04	0.886	0.064	0.00013
2		11.40	1.02	0.932	0.012	0.00053
3		13.00	1.07	0.909	0.044	0.00007
4		12.40	1.05	0.904	0.047	0.00033
5		14.00	1.09	0.883	0.074	0.00007
6		12.30	1.05	0.861	0.092	0.00799
7	*	9.52	0.96	0.831	0.107	0.00960
8		10.60	1.00	0.863	0.082	0.00855
9		11.00	1.01	0.844	0.104	0.01213
10	*	10.50	0.99	0.887	0.053	0.00139
11	*	8.64	0.93	0.778	0.158	0.01268
12	*	8.28	0.92	0.754	0.182	0.01268
13	*	8.77	0.94	0.782	0.155	0.02906
14		7.73	0.90	0.757	0.177	0.02536
15		7.44	0.89	0.730	0.194	0.03265
16	*	8.98	0.94	0.800	0.137	0.02260
17		8.82	0.94	0.823	0.114	0.02804
18	*	7.58	0.89	0.713	0.220	0.02342
19		9.41	0.96	0.727	0.221	0.02673
20	*	8.73	0.93	0.786	0.150	0.01919
21	*	8.07	0.91	0.743	0.192	0.02874
22	*	7.16	0.88	0.682	0.251	0.02669
23	*	7.46	0.89	0.702	0.231	0.03185
24	*	7.43	0.89	0.699	0.234	0.01788
25	*	7.28	0.88	0.693	0.240	0.01450
26	*	8.23	0.92	0.749	0.187	0.03550
27	*	7.44	0.89	0.700	0.233	0.03503
28	*	6.70	0.8.6	0.653	0.278	0.03510
29	*	6.54	0.85	0.645	0.285	0.03490
30	*	6.03	0.83	0.609	0.320	0.03007

* indicates that a peat solid mass of 0.019kg has been used.

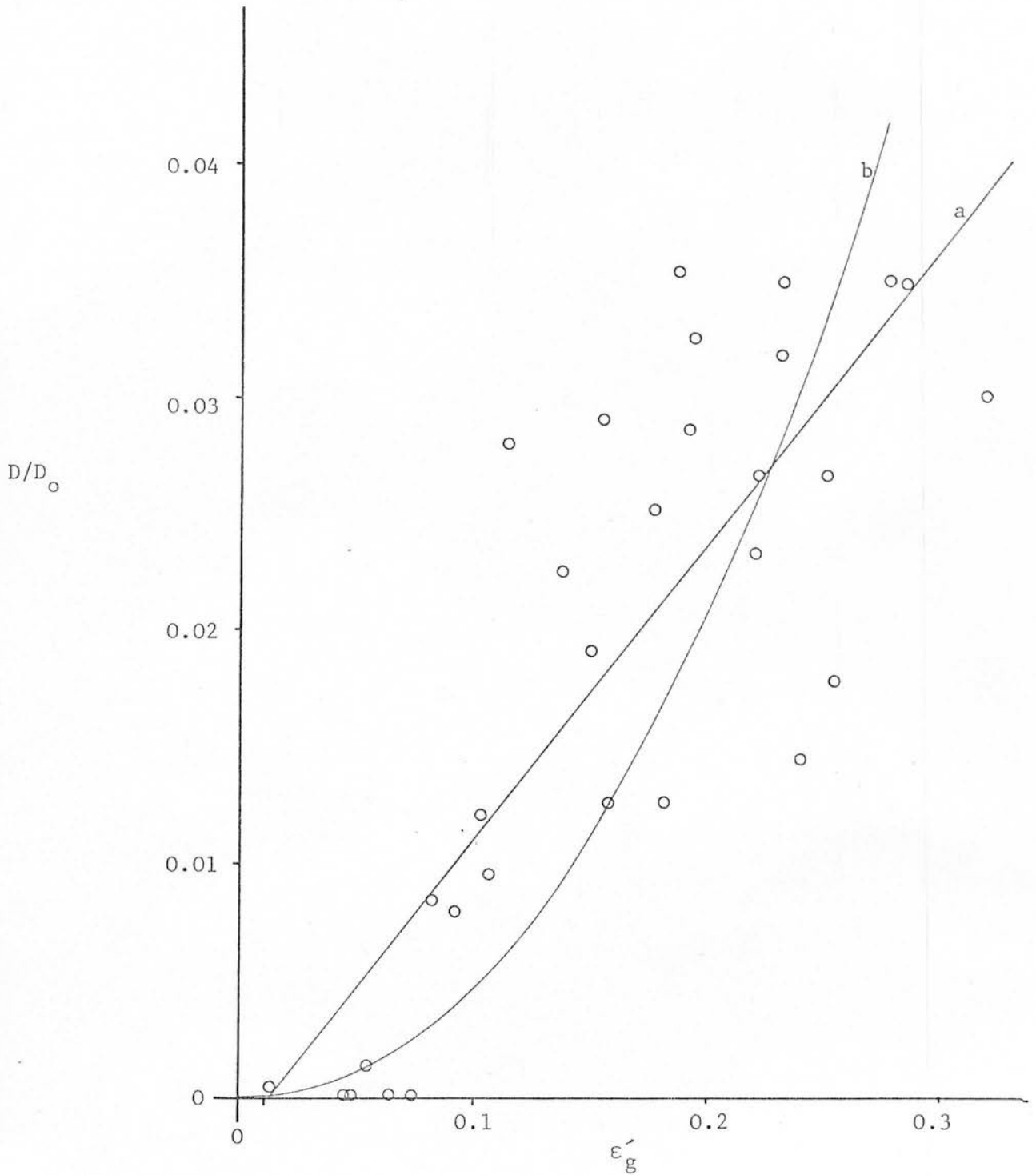


Fig.9.3 Relationship between relative diffusivity (D/D_o) and recalculated values of gas filled pore volumes fraction (ϵ'_g) with the calculated regression lines; a, $-D/D_o = 0.0015 + 0.126 \epsilon'_g$, b, $D/D_o = 0.653 \epsilon'^{2.16}_g$ superimposed.

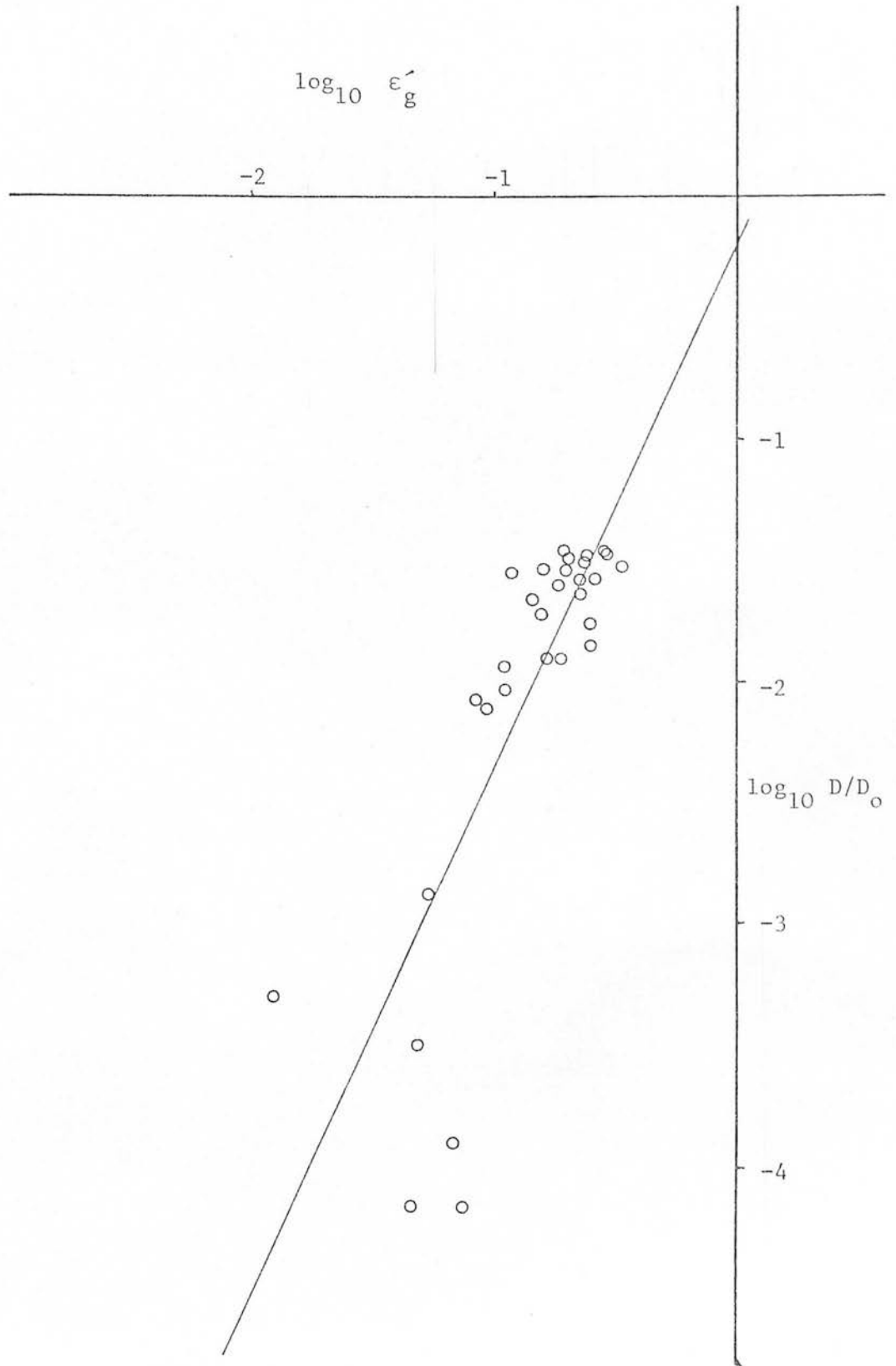


Fig.9.4 Regression of $\log_{10} D/D_0$ on $\log_{10} \epsilon'_g$ to derive the curvilinear relationship $D/D_0 = 0.653 \epsilon_g^{-2.16}$ given in Fig.9.3

Table 9.5 Analysis of variance for the linear regression analysis of \log_{10} transformed data (Fig.9.4). The curve $D/D_0 = 0.653\epsilon_g^{-2.16}$

Source of variance	Degrees of freedom	Mean Squares	Variance ratio	Correlation coefficient
Regression	1	13.12	47.90**	+ 0.79
Residual	28	0.27		
Total	29			

Table 9.6 Analysis of variance for the linear regression analysis of untransformed data (Fig.9.3). The line $D/D_0 = 0.0015 + 0.126\epsilon_g$

Source of variance	Degrees of freedom	Mean Squares	Variance ratio	Correlation coefficient
Regression	1	0.00305	57.83**	+ 0.82
Residual	28	0.0000527		
Total	29			

* $P < 0.05$

** $P < 0.01$

9.4 CONCLUSIONS

The constants in Equation 74 and 75 can be compared with those found in the literature, tabulated by Bakker and Hidding (1970) and reproduced in Table 9.7. No close agreement is found with any of the published data, but as the latter are all derived from mineral soils and usually involving disturbed soil samples rather than intact cores, none should really be expected. Of the earlier less sophisticated models, that of Penman (1940) ($D/D_0 = 0.66 \epsilon_g$) and those of Millington (1959) ($D/D_0 = \epsilon_g^{1.33}$ and $\epsilon_g^{1.5}$), do not fit the data for the peat. However, the earliest published relationship suggested by Buckingham (1904) ($D/D_0 = \epsilon_g^2$) is a reasonably close approximation to the regression curve obtained in the present study. The fact that D/D_0 varies more closely with ϵ_g^2 than $\epsilon_g^{1.33}$ may suggest that factors such as increasing pore continuity with increasing gas filled pore space, are of less importance in peat than mineral soils. This may be an effect of shrinkage in peat acting to negate the effects of increased continuity by closing or narrowing drained pores.

Possible measures of pore complexity and effectiveness for gaseous diffusion were examined by Currie (1979), who proposed that the effectiveness α was given by Equation 76, and complexity k by Equation 77.

$$\alpha = \frac{D/D_0}{\epsilon_g} \quad \dots (76)$$

$$k = \frac{\epsilon_g}{1 - \epsilon_g} \cdot \frac{1 - (D/D_0)}{D/D_0} \quad \dots (77)$$

Calculated values of these constants from both the linear (Equation 74) and curvilinear (Equations 73) relationships derived here, are given in Table 9.8 for successive values of ϵ_g .

Table 9.7 Relationships found between gas-filled pore volume fractions (ϵ_g) and relative gas diffusivity (D/D_0), by previous workers on the soil types indicated. From Bakker and Hidding, 1970

Author	Year	Material	ϵ_g	D/D_0
Penman	1940	Dry sand, soil and glass spheres	0.18-0.50	$0.66\epsilon_g$
			>0.50	$1(\epsilon_g - 0.25)$
		Rothamsted subsoil	0.15-0.5	$0.66\epsilon_g$
Blake and Page	1948	In situ clay soils		
		blocky structure	0.05-0.3	$0.67\epsilon_g$
		fine aggregates	0.15-0.3	$1.3(\epsilon_g - 0.1)$
Taylor	1949	Wet sand	0.15-0.45	$1.0(\epsilon_g - 0.09)$
		Wet loam	0.10-0.49	$0.67\epsilon_g$
Currie	1960	Dry sand, glass spheres	0.20-0.55	$0.9\epsilon_g^{1.4}$
	1961	wet sand	0.05-0.18	$0.25\epsilon_g$
			0.18-0.30	$0.8(\epsilon_g - 0.15)$
			>0.16	$6.0\epsilon_g^{3.4}$
Gradwell	1961	undisturbed pasture topsoil	0.02-0.4	$0.27\epsilon_g$
	1965	clay loam	0.02-0.09	$0.06(\epsilon_g - 0.02)$
			0.09-0.16	$0.3(\epsilon_g - 0.07)$
Grable and Siemer	1968	silty clay loam	0.2-0.4	$5.25\epsilon_g^{3.36}$
Bakker and Hidding	1970	non-puddled topsoil	0.02-0.4	$0.85\epsilon_g^2$
		puddled topsoil	0.02-0.4	$2.00\epsilon_g^3$

Table 9.8 Pore effectiveness for gaseous diffusion (α) and pore complexity (k), for a given range of gas filled pore volume fractions(ϵ_g), for both linear and curvilinear models derived (Equations 73 and 74.)

ϵ_g	Linear		Curvilinear	
	α	k	α	k
0.05	0.096	10.9	0.020	52.6
0.10	0.110	10.0	0.045	24.6
0.15	0.116	10.0	0.073	15.8
0.20	0.118	10.4	0.101	12.1
0.25	0.120	10.8	0.132	9.9

The figures in Table 9.8 confirm the adoption of a curvilinear model to describe D/D_0 with increasing ϵ_g . If a linear relationship exists, then the effectiveness of pores for diffusion only increases slightly with increasing gas filled pore volume fractions, and the pore complexity remains much the same. The curvilinear model assumes a much greater pore complexity at low gas filled pore volume fractions, and hence a much reduced effectiveness for diffusion, as demonstrated by the figures in Table 9.8.

The possibility stated earlier, that shrinkage might reduce the importance of increased pore continuity with increased gas filled pore space, would favour the maintenance of pore complexity, as it occurs mainly at the expense of the larger pores and the collapse of the core may distort drained pores further. It may be, therefore, that a linear relationship between D/D_0 and ϵ_g fits better (as in this study) for peat cores showing unrestrained shrinkage in three dimensions. In the field situation, however, shrinkage over the range of moisture contents at the wet end of the scale can only occur in one dimension. This would have the effect of maintaining pore continuity and reducing complexity with increasing gas filled pore space, once again indicating a curvilinear relationship.

10. THE VARIATION OF FIELD OXYGEN AND CARBON DIOXIDE

CONCENTRATIONS WITH MOISTURE CONTENT AND TEMPERATURE

Some broad suggestions were made in Sections 6 and 7 that variations in the observed oxygen and carbon dioxide concentrations in the soil were due to coinciding changes in temperature and matric potential. The first stage in checking these suggestions is to plot the data variables against each other. This has been done for oxygen deficits, i.e. the difference between measured and ambient oxygen concentrations, against matric potentials (Figs.10.1) oxygen deficits against temperature (Figs.10.3); and carbon dioxide concentrations against matric potentials and temperature (Figs.10.2 and 10.4, respectively).

The scatter of points in Fig 10.1 is approximately the same shape for all three experiments. This shows that, irrespective of depth or species, large oxygen deficits are only associated with matric potentials above a value between -10 and -5kPa, whilst at potentials below -10kPa only small oxygen deficits are recorded. The vast majority of points lie above this value and the full range of oxygen deficits are found within a range from about -5 to +1kPa. There is, however, a slight tendency for more numerous large oxygen deficits at positive or zero matric potentials, and more numerous small deficits at potentials near -5kPa.

The scatter of carbon dioxide concentrations with matric potentials in Figs.10.2, is also of similar shape for all three experiments. The carbon dioxide data are also similar to the oxygen deficit data in that high carbon dioxide concentrations are only found at matric potentials above about -5kPa, whilst the few points below -10kPa are only very low concentrations. All three (Fig.10.2 a,b and c) show that the highest

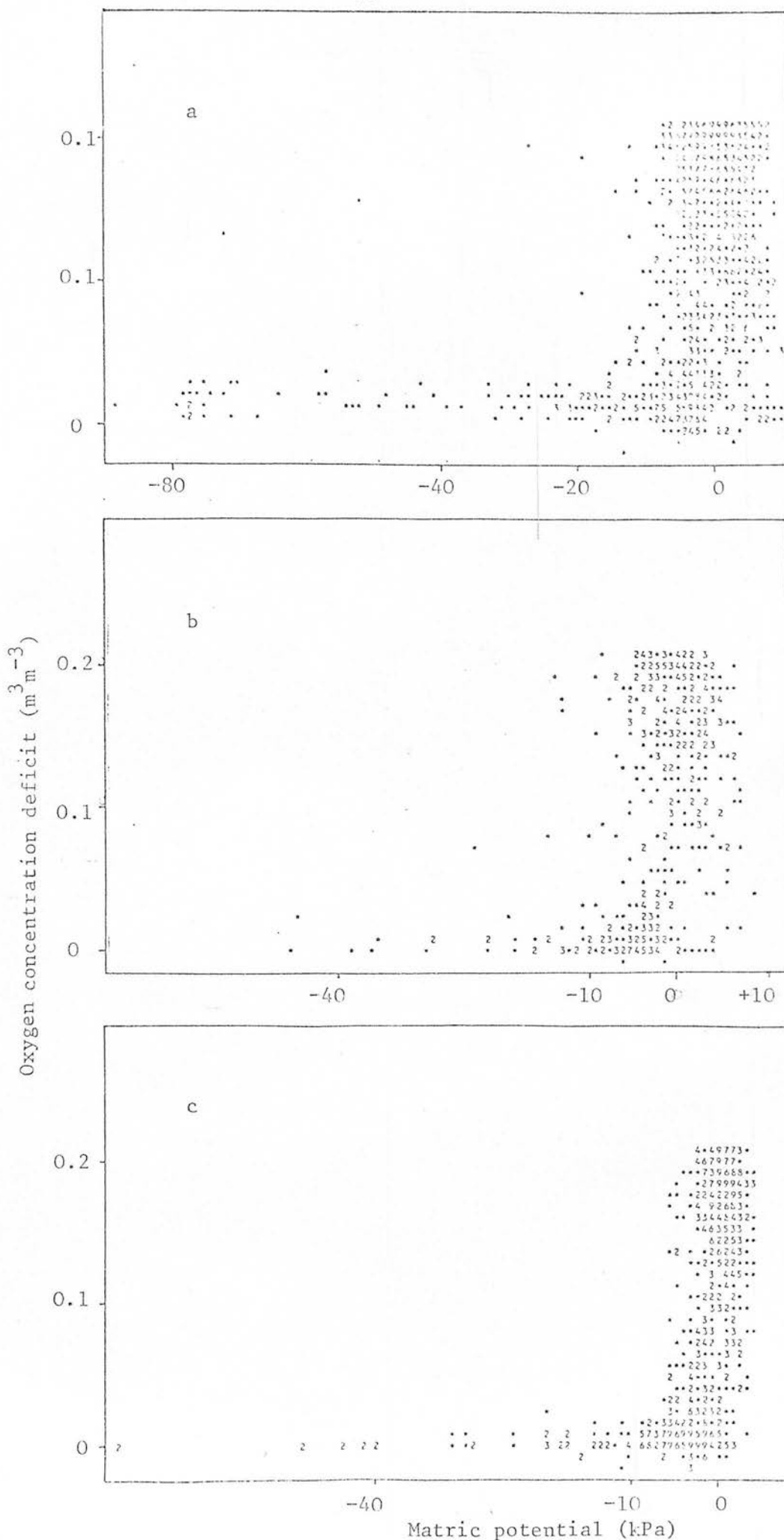


Fig.10.1 The scatter of oxygen concentration deficits against matric potential for Falstone 1978(a), 1979(b) and Eddleston(c).

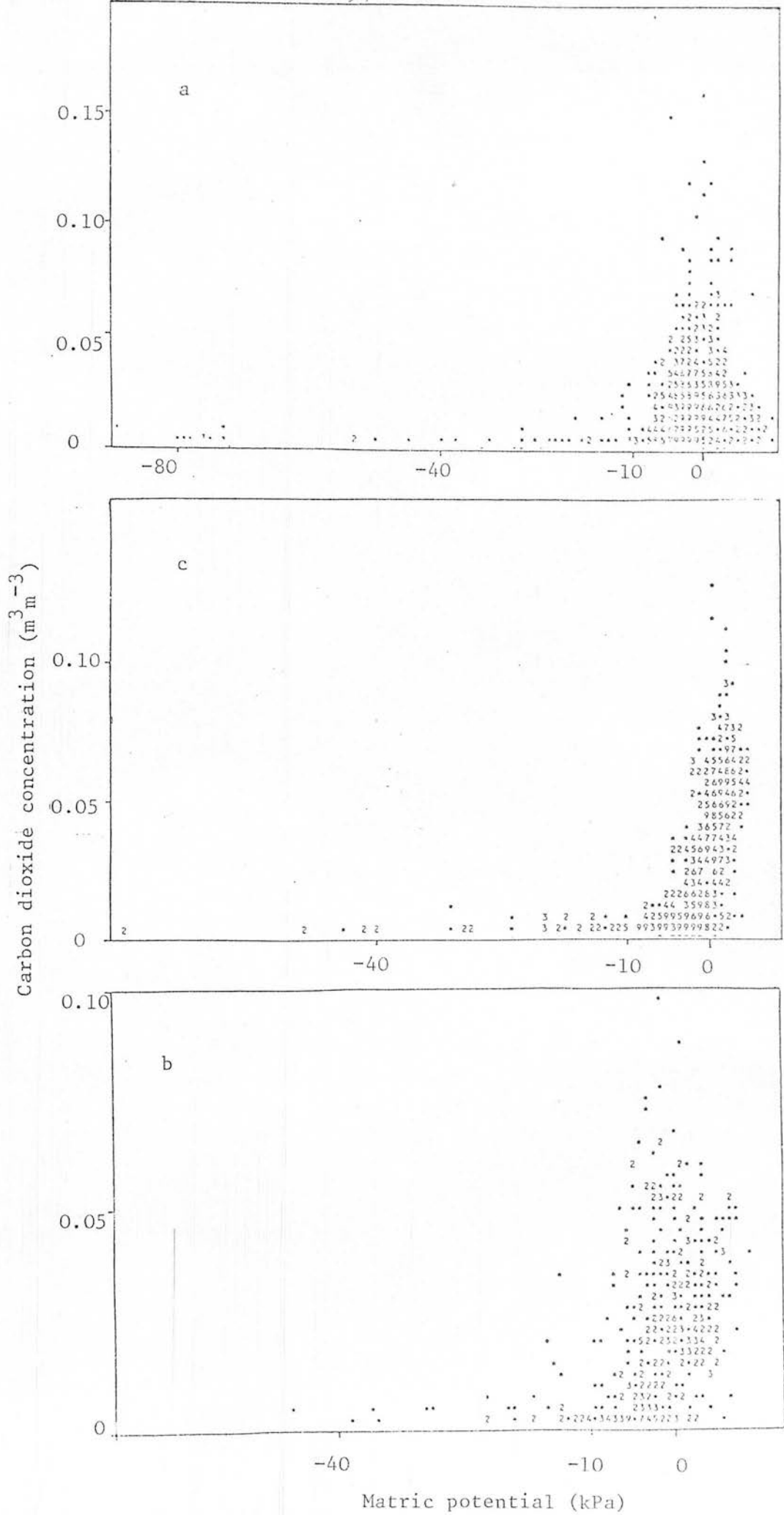


Fig.10.2 The scatter of carbon dioxide concentrations against matric potentials for Falstone 1978 (a), 1979 (b) and Eddleston (c).

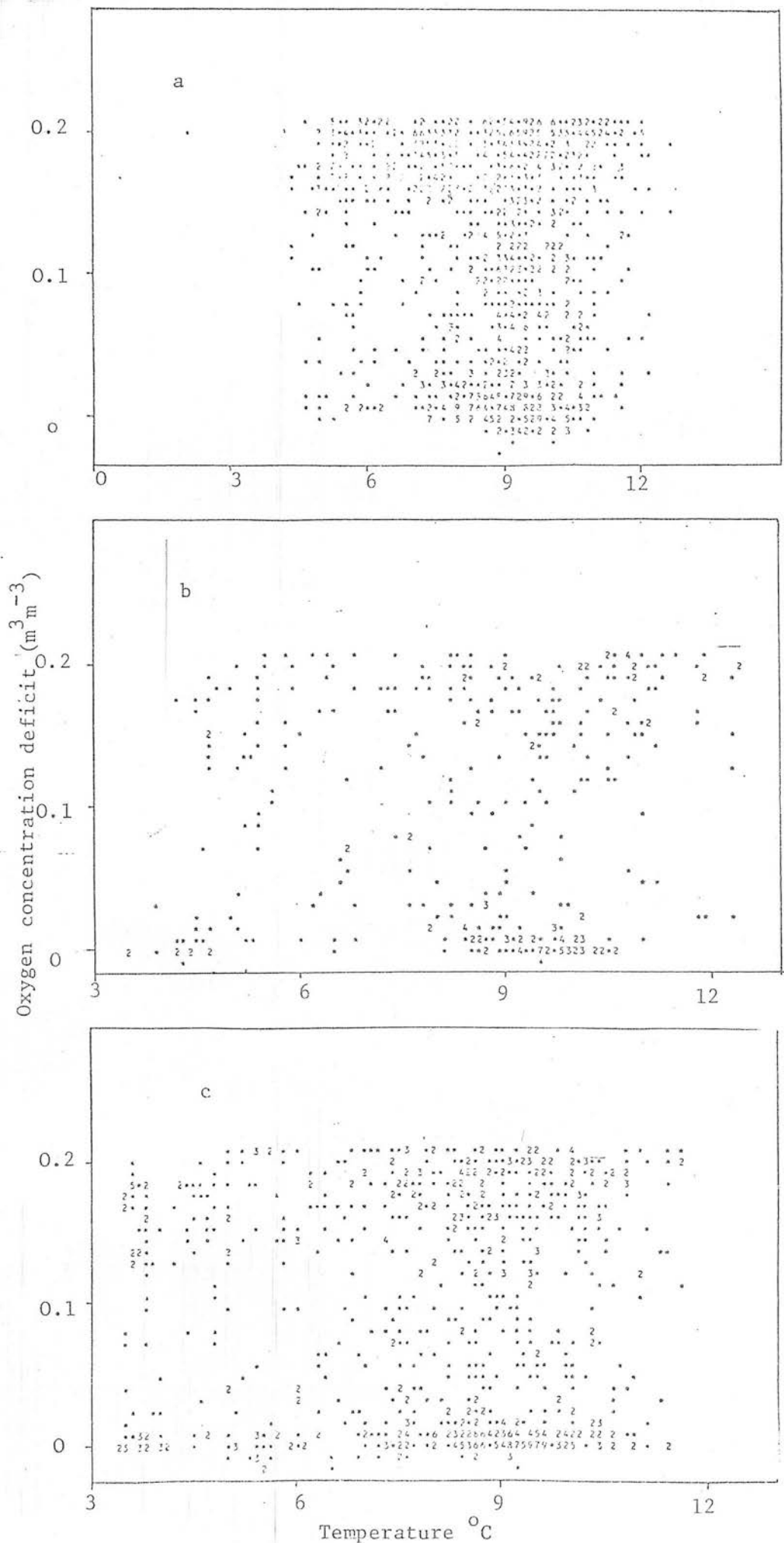


Fig.10.3 The scatter of oxygen concentration deficits against field temperature for Falstone 1978(a), 1979(b) and Eddleston (c).

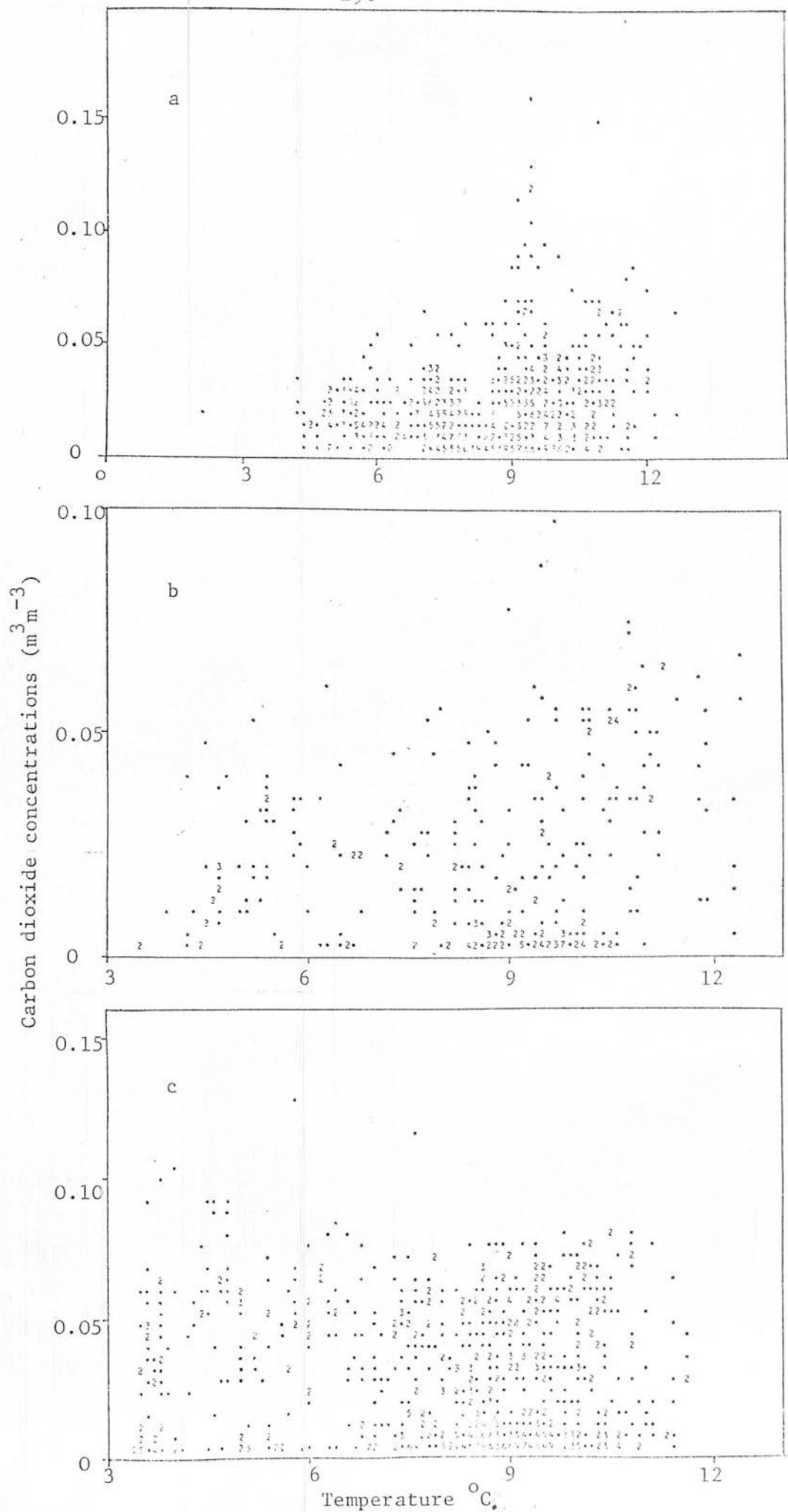


Fig.10.4 The scatter of carbon dioxide concentrations against field temperature for Falstone 1978(a), 1979(b) and Eddleston (c).

carbon dioxide concentrations occur at about zero matric potential.

For both oxygen deficits and carbon dioxide concentrations there seems no obvious relationship with temperature (Figs.10.3 and 10.4).

A simple linear regression analysis was performed on the oxygen deficit and carbon dioxide concentration data from Falstone, regressing them on matric potential. This was done only for the data associated with matric potentials between +1 and -5kPa, as this was considered the most critical range for changes in oxygen and carbon dioxide concentrations. The regressions for the 1978 and 1979 oxygen deficit data are shown in Figs.10.5 and the analysis of variance and correlation coefficients are given in Table 10.1. The regressions for the carbon dioxide concentrations are shown in Figs.10.6 and, their analysis of variance and correlation coefficients in Table 10.2. There are significant relationships for both oxygen deficits and carbon dioxide concentrations when plotted against matric potentials, but the correlation coefficients are very low, showing a large amount of variance unaccounted for by the model fitted. This can be seen in the wide scatter of points in Figs.10.5 and 10.6.

The matric potential of the soil only affects the oxygen and carbon dioxide concentrations indirectly, via the relative diffusivity determined by the gas filled pore volume fraction. The matric potentials were therefore used to obtain gas filled pore volume fractions from the moisture release curves (only data from the ploughed sites was used from the 1978 Falstone experiment). Linear regression analyses were performed, regressing oxygen deficits and carbon dioxide concentrations on their associated gas filled pore volume fractions. Temperature also affects the oxygen and carbon dioxide concentrations via the soil respiration rate. Therefore, temperature was used as a co-variable with gas filled pore volume fractions in a multiple linear regression analysis.

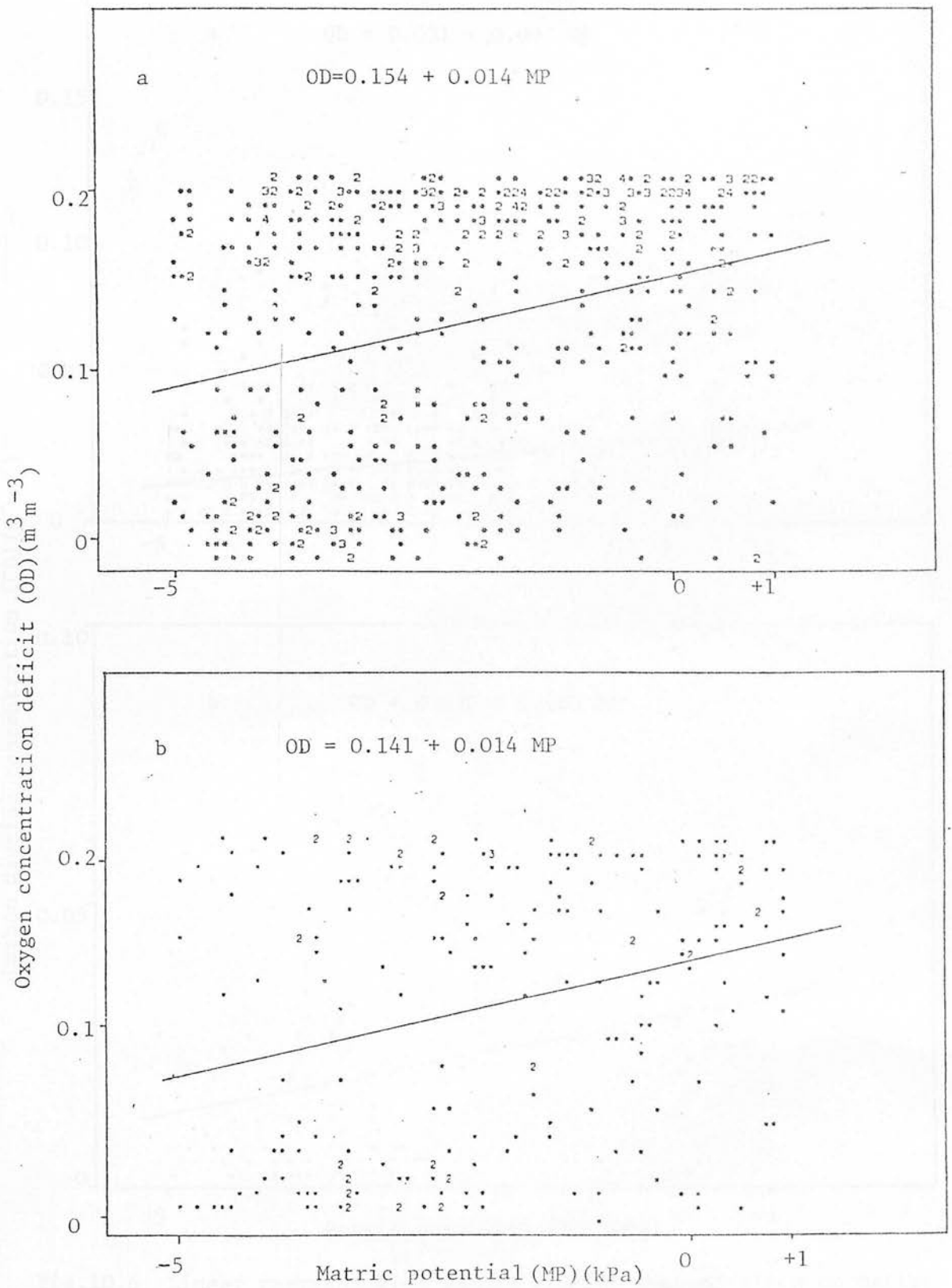


Fig.10.5 Linear regression of oxygen concentration deficits on matric potential between -5 and +1kPa for Falston 1978(a) and 1979(b) data

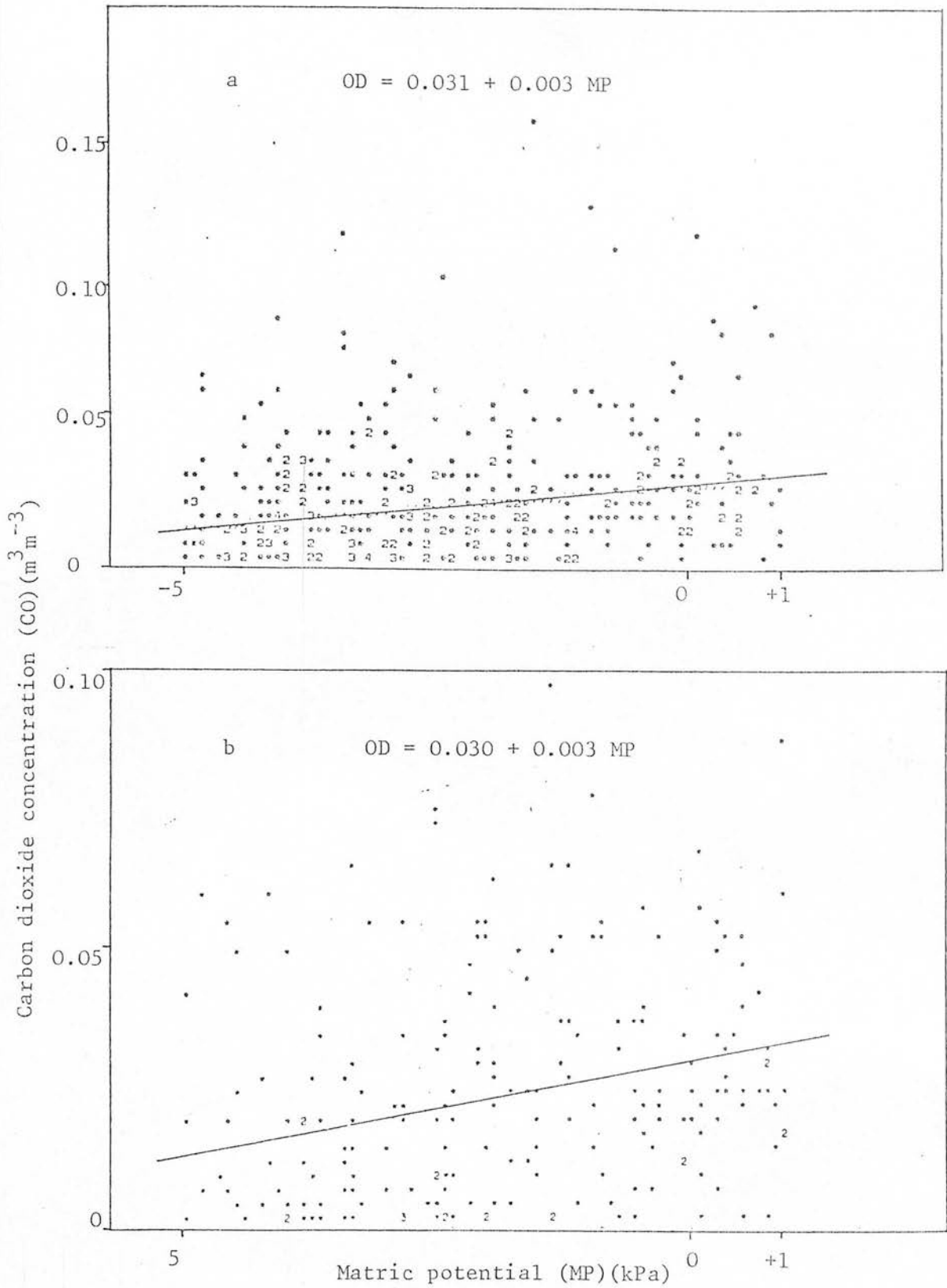


Fig.10.6 Linear regression of carbon dioxide concentration on matric potentials between -5 and +1kPa for Falstone 1978(a) and 1979(b) data.

Table 10.1 Analysis of variance for linear regression of oxygen deficit ($\%V/v$) on soil matric potential (m bar), from the Falstone experiments

Year	Source of variance	d.f.	M.S.	V.R.	Variance accounted for	Correlation coefficient (r)
1978	regression	1	2032.28	38.50**	0.08	+0.28
	residual	458	52.78			
	Total	459	57.08			
1979	regression	1	883.58	16.67**	0.08	+0.28
	residual	187	53.19			
	Total	188	57.60			

Table 10.2 Analysis of variance for linear regression of carbon dioxide concentrations ($\%V/v$) on soil matric potentials (m bar), from the Falstone experiments

Year	Source of variance	d.f.	M.S.	V.R.	Variance accounted for	Correlation coefficient (r)
1978	regression	1	118.23	24.78**	0.05	+0.22
	residual	458	4.77			
	Total	459	5.02			
1979	regression	1	52.43	12.41**	0.06	+0.24
	residual	187	4.23			
	Total	188	4.48			

* P < 0.05

** P < 0.01

The regressions of oxygen deficits on gas filled pore volume fractions are shown in Fig.10.7 for 1978 and 1979 and their analysis of variance and correlation coefficients in Table 10.3. Table 10.4 shows the analysis of variance of the multiple regression analysis including temperature. The similar regressions for carbon dioxide concentrations are shown in Fig.10.8 and their analysis of variance in Tables 10.5 and 10.6.

All the regressions are significant and the use of gas filled pore volume fractions gave some improvement of the correlation coefficients compared with the use of matric potentials. However, the variance accounted for is still very low, and the inclusion of temperature in a multiple regression analysis only increased this slightly (compare Tables 10.4 and 10.6 with 10.3 and 10.5), but more so for the carbon dioxide concentrations than the oxygen deficits.

To detect whether there was a better correlation for the data at each depth, masked in the above bulked data analysis, similar regressions were performed on the data from 0.15, 0.30 and 0.60m depths separately. The full analysis of variance are not given here, but the variance ratios, variance accounted for and correlation coefficients, are given in Table 10.7 for the oxygen deficit data, and Table 10.8 for the carbon dioxide concentrations. Both tables show almost the same pattern, that the best correlations in both years were obtained from 0.15m depth (in the peat layer). At greater depths practically no significant linear relationships were detected for either oxygen deficits or carbon dioxide concentrations, though the inclusion of temperature often produced a significant fit and improved correlation in the multiple regression analysis.

The same analyses were also performed on the Eddleston peat data for the (restricted to 0.3, 0.4 and 0.5m depths): OP, LP and SS sites, to maximise the number of samples with matric potentials

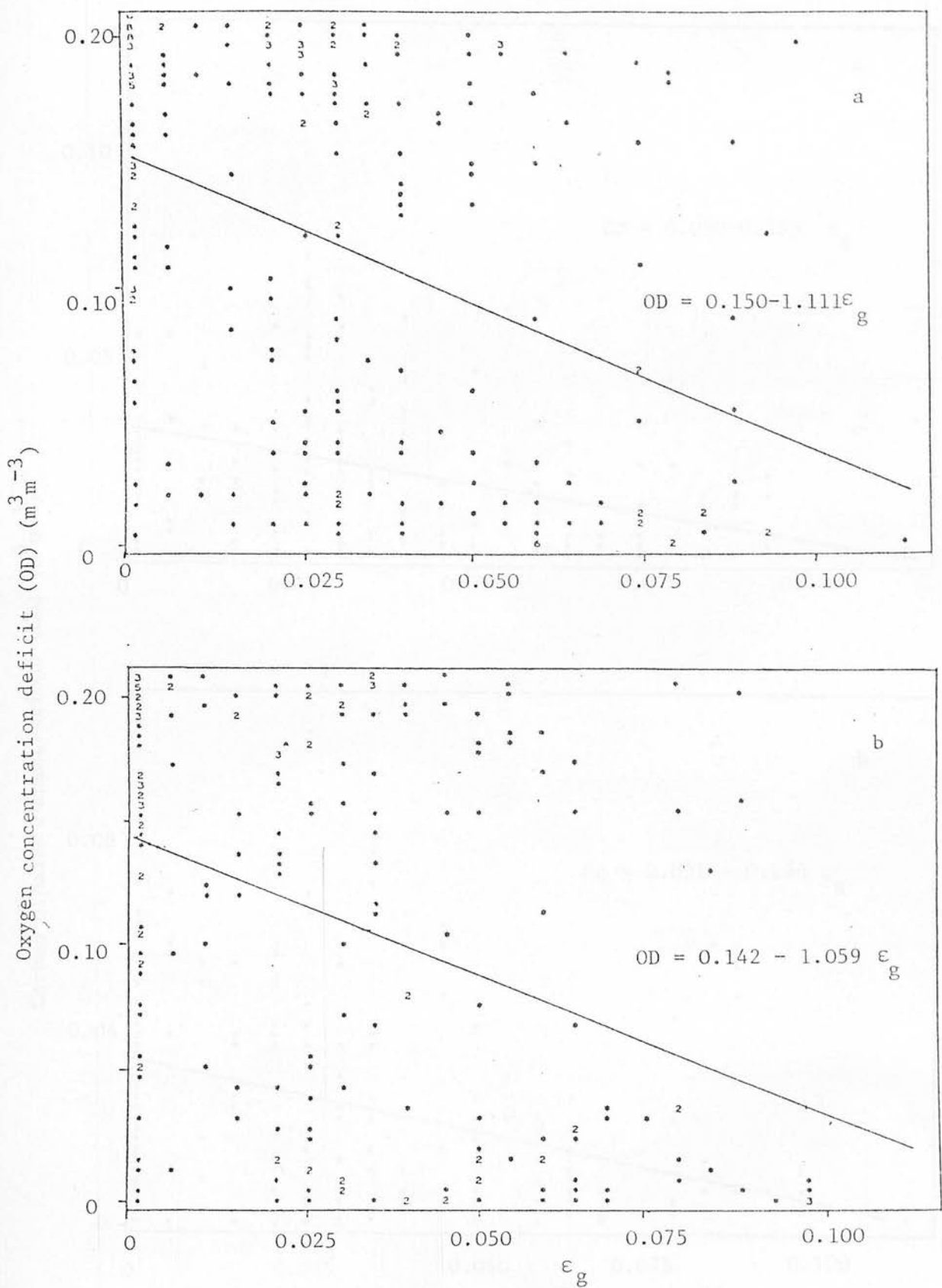


Fig.10.7 Linear regression of oxygen concentration deficits on gas filled pore volume fractions (ϵ_g) for Falstone 1978(a) and 1979(b) data.

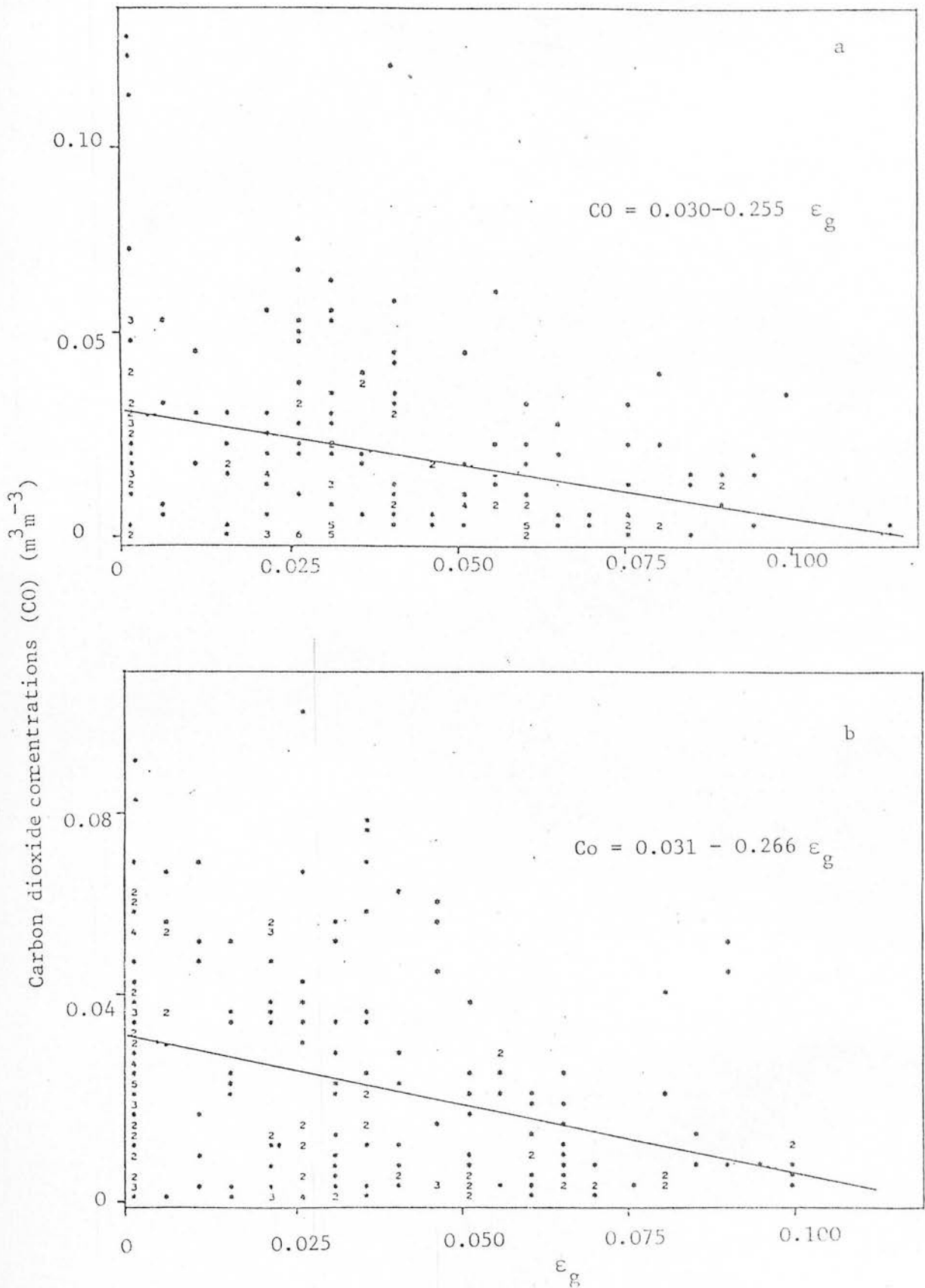


Fig.10.8 Linear regression of carbon dioxide concentrations on gas-filled pore volume fractions (ϵ_g) for Falstone 1978(a) and 1979(b) data.

Table 10.3 Analysis of variance for linear regression of oxygen deficits
(% V/V) on gas filled pore volume fraction, from the Falstone
experiments.

Year	Source of variance	d.f.	M.S.	V.R.	Variance accounted for	Correlation coefficient (r)
1978	regression	1	1673.78	31.09**	0.14	-0.38
	residual	180	53.83			
	Total	181	62.78			
1979	regression	1	1763.05	33.66**	0.14	-0.37
	residual	205	52.37			
	Total	206	60.68			

Table 10.4 Analysis of variance for linear regression of oxygen deficits
(% V/V) on gas filled pore volume fraction including temperature
($^{\circ}\text{C}$), from the Falstone experiment

Year	Source of variance	d.f.	M.S.	V.R.	Variance accounted for	Correlation coefficient (r)
1978	regression	2	895.11	16.75**	0.15	-0.38
	residual	179	53.48			
	Total	181	62.78			
1979	regression	2	1184.65	23.86**	0.18	-0.43
	residual	204	49.66			
	Total	206	60.68			

* $P < 0.05$

** $P < 0.01$

Table 10.5 Analysis of variance for linear regression of carbon dioxide concentration (% V/V) on gas filled pore volume fractions from the Falstone experiments

Year	Source of variance	d.f.	M.S.	V.R.	Variance accounted for	Correlation coefficient (r)
1978	regression	1	87.90	18.72**	0.09	-0.30
	residual	180	4.69			
	Total	181	5.16			
1979	regression	1	111.41	28.29**	0.12	-0.34
	residual	205	3.94			
	Total	206	4.46			

Table 10.6 Analysis of variance for multiple linear regression of carbon dioxide concentrations (% V/V) on gas filled pore volume fractions including temperature ($^{\circ}\text{C}$), from the Falstone experiments.

Year	Source of variance	d.f.	M.S.	V.R.	Variance accounted for	Correlation coefficient (r)
1978	regression	2	63.30	14.05**	0.13	-0.35
	residual	179	4.51			
	Total	181	5.16			
1979	regression	2	105.03	30.24**	0.22	-0.47
	residual	204	3.47			
	Total	206	4.46			

* $P < 0.05$

** $P < 0.01$

Table 10.7 Correlation coefficients (r) and significance of oxygen
concentration deficits ($\% \text{ }^v/\text{ }^v$) regressed on ϵ_g , and
including temperature ($^{\circ}\text{C}$) for each depth in the
Falstone experiment

Year	Depth(m)	Oxygen deficit regressed on ϵ_g		Oxygen deficit regressed on ϵ_g including temperature	
		VR	r	VR	r
1978	0.15	17.86**	-0.44	9.17**	-0.43
	0.30	2.24	-0.13	2.04	-0.17
	0.60	0.50	-0.11	1.52	-0.16
1979	0.15	13.33**	-0.40	14.58**	-0.54
	0.30	8.97**	-0.30	5.83**	-0.33
	0.60	0.85	-0.05	3.28*	-0.27

* $P < 0.05$

** $P < 0.01$

Table 10.8 Correlation coefficients (r) and significance of carbon dioxide concentrations ($\% \text{ }^v/v$) regressed on gas filled pore volume fractions (ϵ_g) and including temperature ($^{\circ}\text{C}$) for each depth in the Falstone experiment

Year	Depth (m)	regressed on ϵ_g		regressed on ϵ_g including temperature	
		VR	r	VR	r
1978	0.15	16.18**	-0.42	10.68**	-0.46
	0.30	2.57	-0.15	2.26	-0.19
	0.60	0.97	-0.03	3.24*	-0.31
1979	0.15	10.42**	-0.36	12.88*	-0.52
	0.30	11.44**	-0.34	8.09**	-0.39
	0.60	2.83	-0.17	11.64**	-0.51

* $P < 0.05$

** $P < 0.01$

between +1 and -5kPa). The linear regression of oxygen deficits on gas filled pore volume fractions is shown in Fig.10.9 and its analysis of variance in Table 10.9, together with that for the multiple regression including temperature. The results for the regressions of the carbon dioxide concentrations are given in Fig.10.10 and Table 10.10.

Like the Falstone data the relationships are significant but not highly correlated. The correlation coefficients are slightly higher than the overall Falstone results and of the same order as the correlation coefficients from the Falstone peat layer. The scatter of points in Figs.10.9 and 10.10 show that a very large proportion are for gas filled pore volume fractions of zero. This is because of the difficulty in matching up accurately matric potentials measured in the field, and gas filled pore volume fractions measured in cores that may have shrunk slightly at low tensions.

The data were again split into those from each depth and the same analysis performed. The variance ratios and correlation coefficients are given in Table 10.11, and are significant in all cases. The correlation coefficients are generally better than those from the Falstone experiments, and increase with depth for the oxygen deficit data.

Whether aerobic or anerobic respiration was predominant in the soil should be shown by the RQ values, and these were calculated for the ~~Falstone~~ ^{Edderton} data used above. To calculate the RQ's the oxygen deficit volume (VOD) and volume of carbon dioxide (VCO) in unit volume of peat were calculated using Equations 78 and 79, and then these values inserted into Equation 80.

$$VOD = ((\epsilon_T - \epsilon_g) \cdot \alpha \cdot \frac{(273+T)}{273} \cdot (OD + 0.0001)) + (\epsilon_g \cdot OD) \quad (78)$$

$$VCO = ((\epsilon_T - \epsilon_g) \cdot \alpha' \cdot \frac{(273+T)}{273} \cdot (CO - 0.00035)) + \epsilon_g (CO - 0.00035) \quad (79)$$

where ϵ_T = total pore volume fraction

ϵ_g = gas filled pore volume fraction

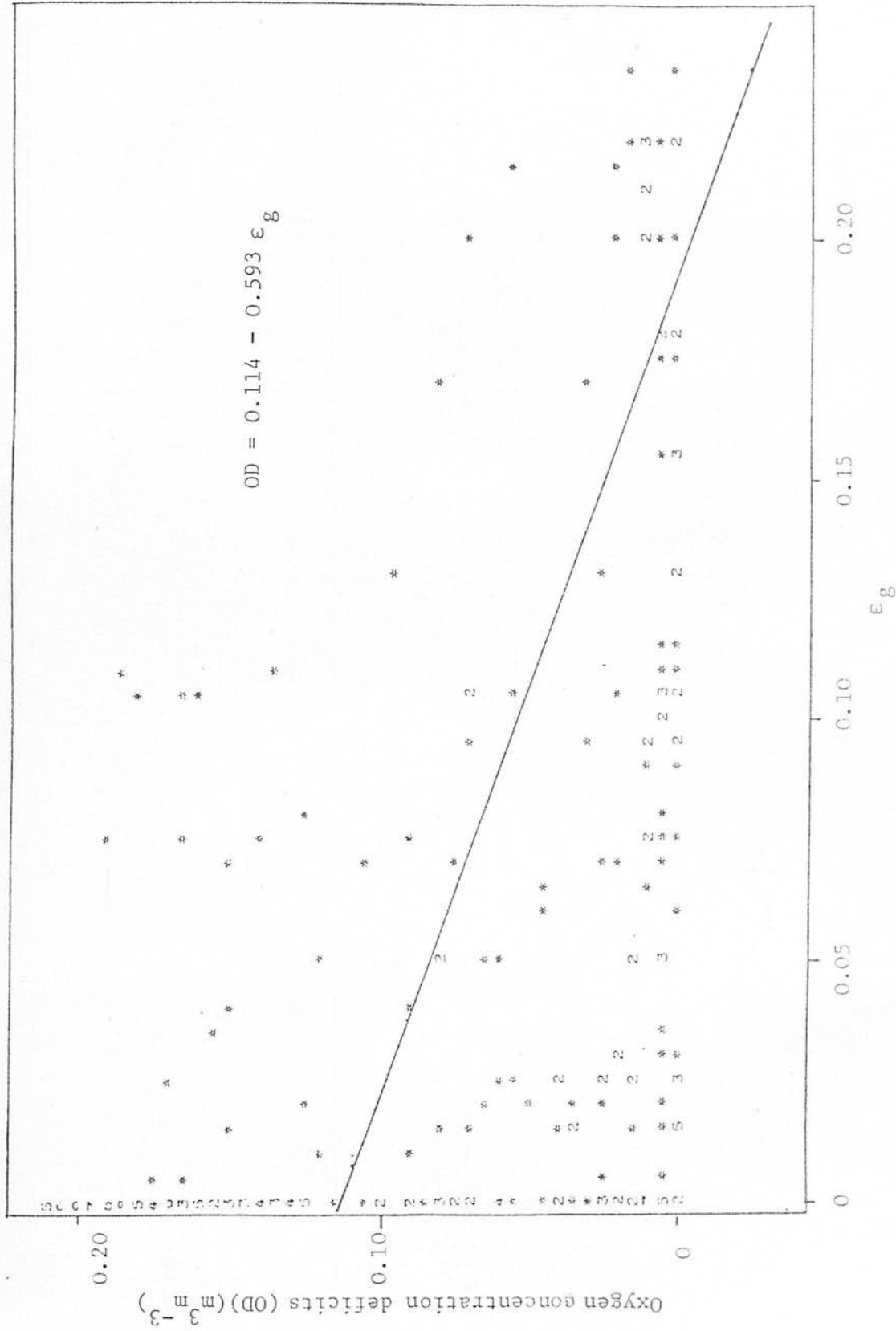


Figure 10.9 Linear regression of oxygen concentration deficits on gas-filled pore volume fractions (ϵ_g) for the Eddleston data.

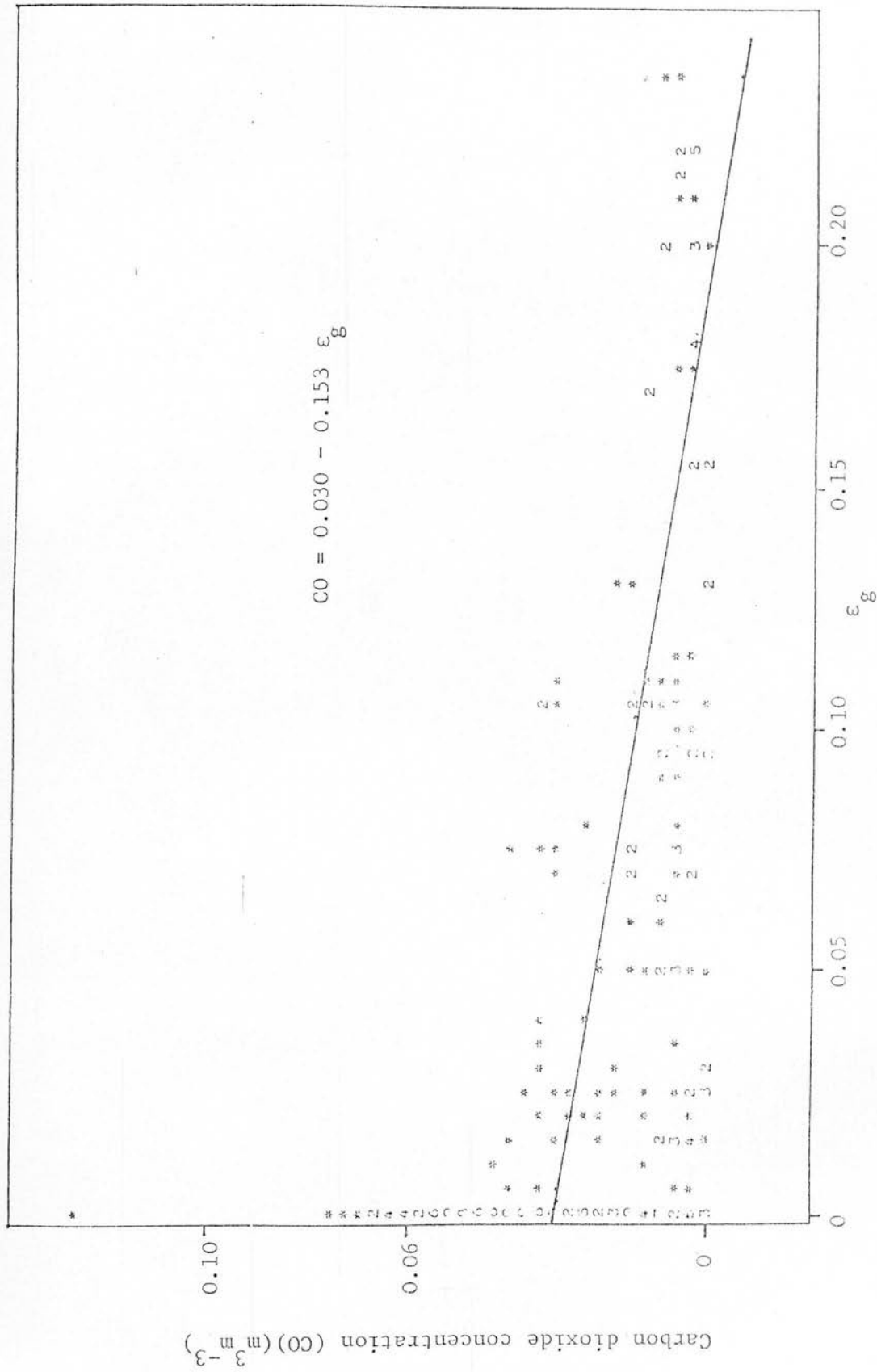


Figure 10.10 Linear regression of carbon dioxide concentrations on gas-filled pore volume fractions (ϵ_g) for Eddleston data.

Table 10.9 Analysis of variance for oxygen deficits ($\% V/V$) regressed on gas filled pore volume fractions, and the multiple regression including temperature ($^{\circ}\text{C}$) for the Eddleston data.

Regression	Source of variance	d.f.	M.S.	V.R.	Variance accounted for	Correlation coefficient (r)
Single	regression	1	4164.00	93.95**	0.25	-0.50
	residual	277	44.32			
	Total	278	59.14			
Multiple	regression	2	2290.59	53.31**	0.27	-0.53
	residual	276	42.97			
	Total	278	59.14			

Table 10.10 Analysis of variance for carbon dioxide concentrations ($\% V/V$) regressed on gas filled pore volume fractions, and the multiple regression including temperature ($^{\circ}\text{C}$) for the Eddleston data

Regression	Source of variance	d.f.	M.S.	V.R.	Variance accounted for	Correlation coefficient (r)
Single	regression	1	277.89	95.89**	0.25	-0.50
	residual	277	2.90			
	Total	278	3.89			
Multiple	regression	2	156.11	56.07**	0.28	-0.53
	residual	276	2.78			
	Total	278	3.89			

* $P < 0.05$

** $P < 0.01$

Table 10.11 Correlation coefficient (r) and significance of oxygen deficit ($\% \text{ }^v/v$) and carbon dioxide concentrations ($\% \text{ }^v/v$) regressed on gas filled pore volume fractions (ϵ_g), and including temperature ($^{\circ}\text{C}$) for each depth in the Eddleston experiment.

	Depth(m)	regressed on ϵ_g		regressed on ϵ_g including temperature	
		V.R.	r	V.R.	v
oxygen	0.3	11.06**	-0.32	5.49**	-0.31
deficit	0.4	39.89**	-0.54	29.53**	-0.61
	0.5	70.60**	-0.65	42.72**	-0.68
carbon dioxide	0.3	27.61**	-0.48	22.39**	-0.57
	0.4	32.71**	-0.50	20.76**	-0.54
	0.5	46.92**	-0.57	23.66**	-0.57

* $P < 0.5$

** $P < 0.1$

OD = oxygen deficit in concentration ($\text{m}^3 \text{m}^{-3}$)

CO = carbon dioxide concentration ($\text{m}^3 \text{m}^{-3}$)

T = temperature ($^{\circ}\text{C}.$)

α = solubility coefficient of oxygen at $T^{\circ}\text{C}$

α' = solubility coefficient of carbon dioxide at $T^{\circ}\text{C}.$

$$\text{RQ} = \text{VCO}/\text{VOD} \quad (80)$$

Linear regression analyses were performed, regressing RQ on gas filled pore volume fractions and on temperature separately, as well as combined in a multiple regression. The analyses of variance are presented in Table 10.12 and the regression of RQ on gas filled pore volume fractions in Fig.10.11. Although the regression on gas filled pore volume fractions is significant the correlation is poor and there is no significant relationship between RQ's and temperature. It can be seen from Fig.10.11 that the RQ's are nearly all above 1 irrespective of the gas filled pore volume fraction, so it would be advantageous to examine the relationship between VCO and VOD calculated in Equation 78 and 79. A linear regression analysis was performed, regressing the volume of carbon dioxide on the oxygen deficit volume shown in Fig.10.12 (its analysis of variance is shown in Table 10.13). The regression is significant and suggests that the overall conditions are anaerobic, with approximately 2.5 times the volume of carbon dioxide evolved for the volume of oxygen consumed.

Many of the results that gave RQ's greater than 1 have only small oxygen deficits, and the oxygen and carbon dioxide concentrations would be considered favourable for root growth. This seeming paradox is no doubt due to the very high water content of peat, even when gas filled pore volume fractions are 0.1 or more. Because the solubility of carbon dioxide is so much greater than that of oxygen (Appendix 2), then for a given gas phase carbon dioxide concentration there is a much larger volume of dissolved carbon dioxide in the soil than there is

Table 10.12 Analysis of variance for R.Q. regressed on gas filled pore volume fractions (ϵ_g) temperature (T) and on gas filled pore volume fractions including temperature for Eddleston data

R.Q.regressed on	Source of variance	d.f.	M.S.	V.R.	Variance accounted for	r
ϵ_g	regression	1	128.24	17.57**	0.05	-0.24
	residual	277	7.30			
	Total	278	7.73			
T	regression	1	17.38	2.26	0	-0.07
	residual	277	7.70			
	Total	278	7.73			
ϵ_g including T	regression	2	73.24	10.09**	0.06	-0.25
	residual	276	7.26			
	Total	278	7.73			

Table 10.13 Analysis of variance for volume of carbon dioxide on oxygen deficit volume from Eddleston data

Source of variance	d.f.	M.S.	V.R.	Variance accounted for	r
regression	1	0.037416	79.13**	0.22	+0.47
residual	277	0.0004728			
Total	278	0.0006058			

* $P < 0.05$

** $P < 0.01$

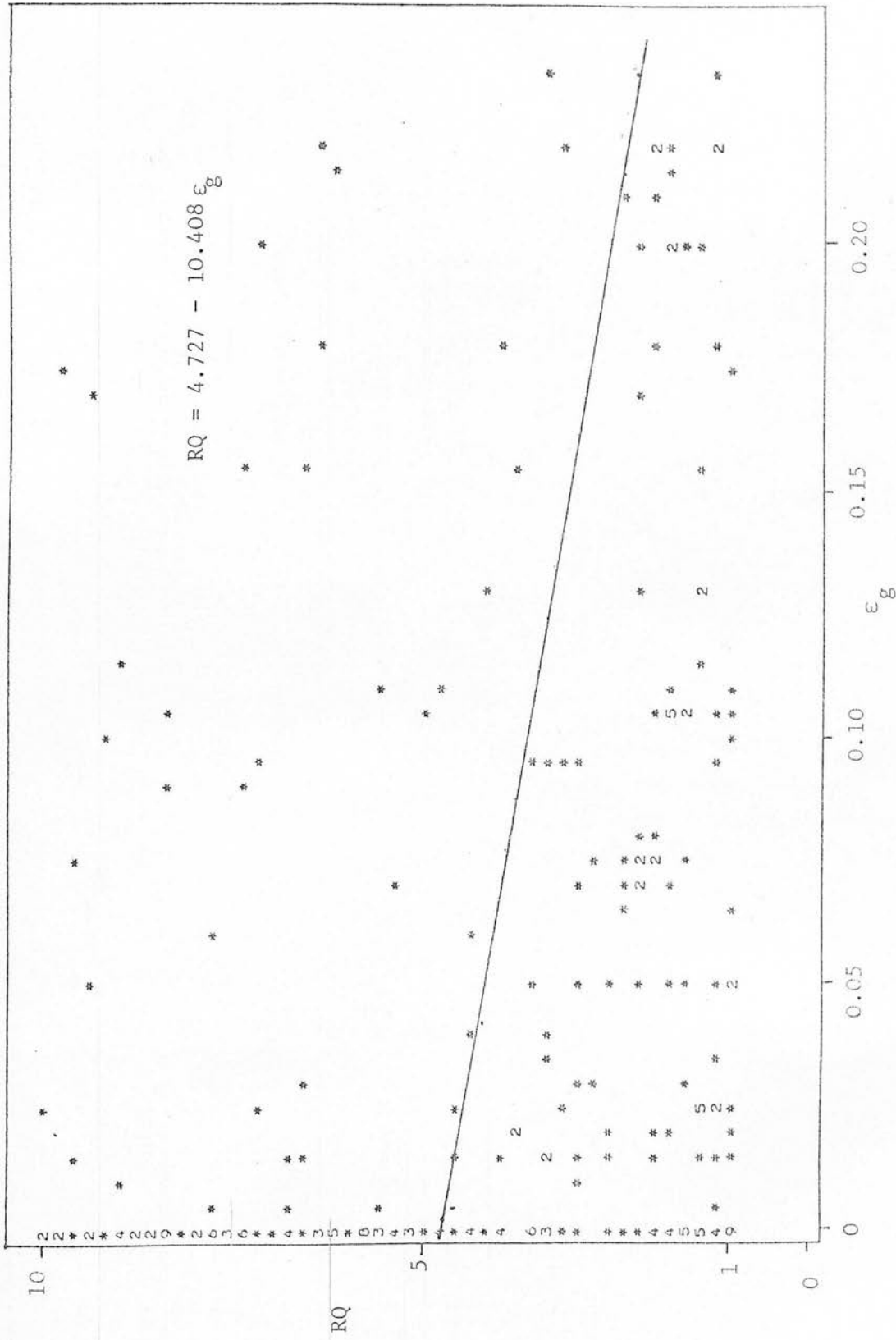


Fig. 10.11 Linear regression of the calculated field respiratory quotient (R.Q.) on gas-filled pore volume fractions (ϵ_g) for the Eddleston data.

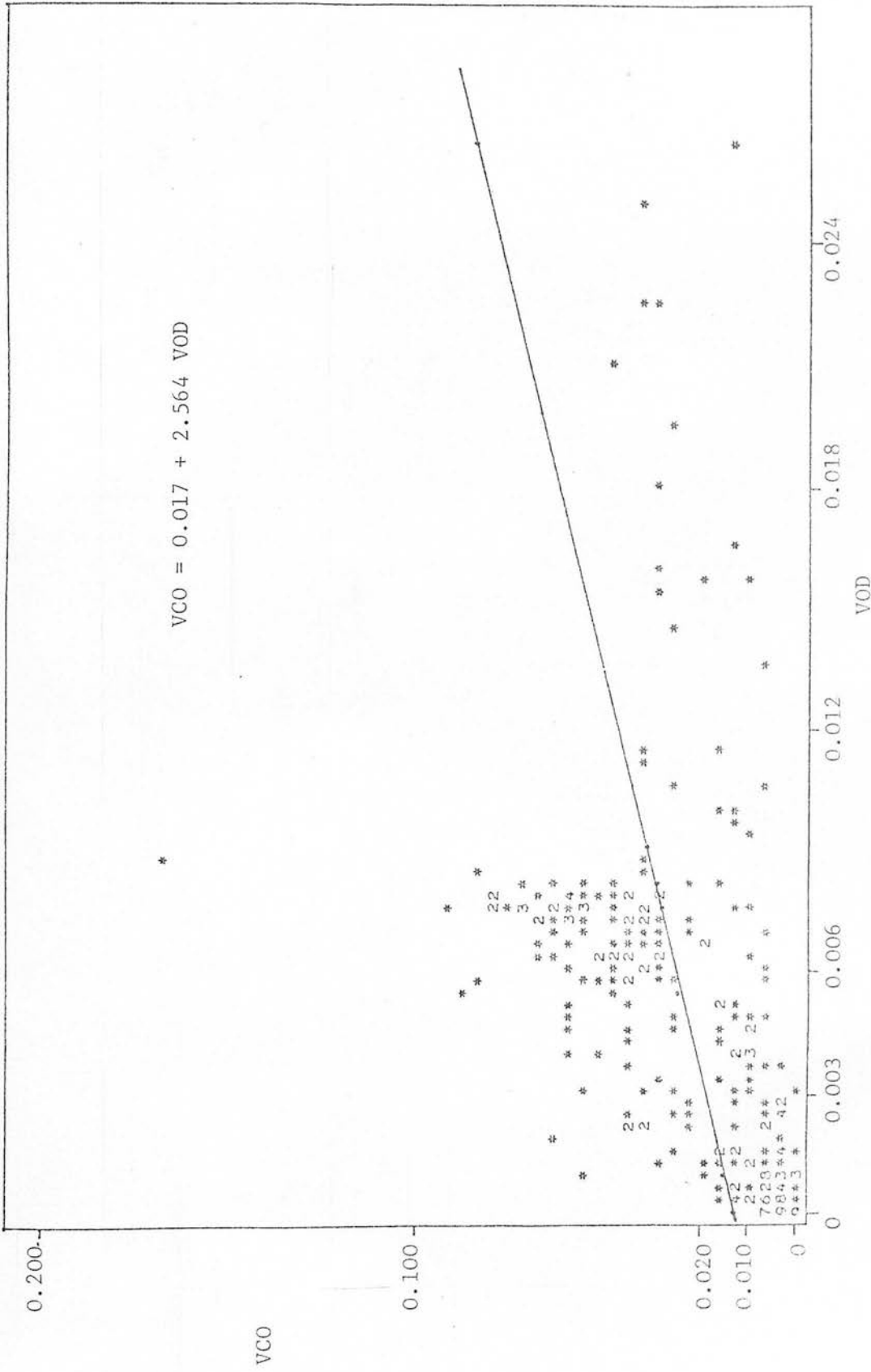


Fig. 10.12 Linear regression of volume of carbon dioxide evolved (VCO) on the volume of oxygen absorbed (VOD) by unit volume of respiring peat in the field at Eddleston.

volume deficit of oxygen, for even greater gas phase oxygen deficit concentration. This explains why high RQs exist for fairly low carbon dioxide concentrations and oxygen deficits, which do not immediately suggest anaerobic conditions. However, even if large regions of the peat are respiring anaerobically, this does not necessarily mean that other regions have not sufficient oxygen for aerobic respiration and root growth. This situation can exist because there can be a large gradient of oxygen concentration through a saturated zone, whilst the gradient of carbon dioxide concentration is much less, due to the difference in solubility (Greenwood, 1972).

11. GROWTH OF CONIFER ROOTS UNDER VARIOUS CARBON DIOXIDE CONCENTRATIONS

11.1 AIMS

It has been discussed in Section 1.4 how root growth of various species is reduced by lowered oxygen concentrations around the roots. What has not been studied so extensively however, is the possible effects of high carbon dioxide concentrations on conifer roots.

It was seen in Sections 6 and 7 how high carbon dioxide concentrations can occur in the soil while oxygen is still at non-limiting concentrations. It was therefore considered worthwhile to conduct experiments to examine the effect of a range of carbon dioxide concentrations on the root growth of Pinus contorta and Picea sitchensis cuttings, when oxygen concentrations were both high ($0.21 \text{ m}^3 \text{ m}^{-3}$) and low ($0.01 \text{ m}^3 \text{ m}^{-3}$).

11.2 METHODS

Two experiments were carried out, at different times. Oxygen concentrations around the roots were maintained in the first experiment at $0.21 \text{ m}^3 \text{ m}^{-3}$, and in the second at $0.01 \text{ m}^3 \text{ m}^{-3}$. In each experiment four concentrations of carbon dioxide (0.01 , 0.06 , 0.12 and $0.18 \text{ m}^3 \text{ m}^{-3}$) were applied, and two other treatments were also included: nitrogen only (i.e. no oxygen or carbon dioxide present), and air (i.e. $0.21 \text{ m}^3 \text{ m}^{-3}$ and $0.00035 \text{ m}^3 \text{ m}^{-3}$ carbon dioxide). All gas mixtures were obtained as compressed gases in cylinders (B.O.C. Ltd, Special Gases Division.)

Nitrogen and compressed air were similarly obtained from B.O.C. Ltd.

The treatments were applied to one year old cuttings of Pinus contorta and Picea sitchensis (to avoid genetic variation found using seedlings), which had already formed root systems in loose peat and sand compost. It was found necessary to use equal numbers of cuttings

from two plants of each species, two replicates of each being used for each treatment, making four replicates of each species in total.

Each cutting was grown in moist peat packed loosely (to facilitate the movement of gas) into a perspex tube of 33mm internal diameter and 670mm long, fitted with a rubber bung at the top with two holes in it, and another bung at the bottom with a single hole. The stem of the cutting was placed in one hole in the rubber bung through a slit cut into the side, and sealed in with an inert silicone rubber compound. The second hole was used as a gas outlet, and the single hole of the bottom bung as the inlet. The perspex tube was then wrapped in aluminium foil to prevent light entry and reduce temperature extremes due to direct sunlight.

The tubes were then clipped vertically on a stand and the cuttings were allowed to grow for two weeks, with both gas inlets and outlets open to the atmosphere. This ensured that the root systems had time to readjust to their new environment and active root tips were visible through the perspex tube at the onset of the experiment. The plants were watered every day by injecting 20ml of water into the gas outlet hole.

The gas supply system consisted of the compressed gas cylinders with pressure regulators fitted, each of which was connected via a needle valve to a large P.V.C. manifold via flexible rubber tubing. The P.V.C. manifolds were constructed out of 120mm diameter drainpipe cut into sections, and sealed at both ends with P.V.C. sheet welded on. The manifolds had a single gas inlet from the cylinder and eight outlets, one for each of the four replicates of each species. The manifold outlets were connected to the plant tubes via flexible P.V.C. tubing (Portex Ltd, Hythe, Kent) and a short length of steel tubing (i.d. 2mm) inserted into the rubber bungs at the bottom. The flow rate of gases from the plant tubes were roughly

equalised to a bare trickle (about $1\text{cm}^3\text{min}^{-1}$) by passing them through plastic tubes into a cylinder of water, and adjusting the depths of the tubes in the water until the bubbling rates were similar.

The experiment was carried out in a glasshouse during June and July 1980, in natural daylight and at temperatures below 25°C . The experimental system is shown schematically in Fig.11.1 and as it actually appeared, in Plate 11.1.

After the initial two-week equilibration period, the plant tubes were unwrapped, and pieces of tape were placed on the perspex tube on the same horizontal level as any visible root tips growing down the sides of the tube. The roots were numbered on each tube, as in Plates 11.2 and 11.3. For a further 7 days of experiment with 21% O_2 , 8 days for the one with 1% O_2 , whilst the tubes were still open to the atmosphere, the tubes were unwrapped each day and extension beyond the tape was measured. Then the tubes were connected to the gas flow system and measurements of root extension were made daily as before. Watering was carried out by injecting 20ml daily when the gas tubing was temporarily disconnected for root measurements.

11.3 RESULTS

The number and size of roots visible in each tube varied a great deal, ranging from none in some tubes, up to seven suitable for measurements in others. Although each individual root was measured, only the mean root lengths for each plant are given in Appendix 5, as it was the change in overall elongation rates that was of interest. The mean root lengths on each day are represented graphically in Figs.11.2 and 11.3 for the 'high' and 'low' oxygen experiments, respectively.

The first point to be noticed from these figures is that all root growth stopped when pure nitrogen was passed over them (Figs.11.2(a) and 11.3(a)). In the low oxygen experiment, in which fully aerobic

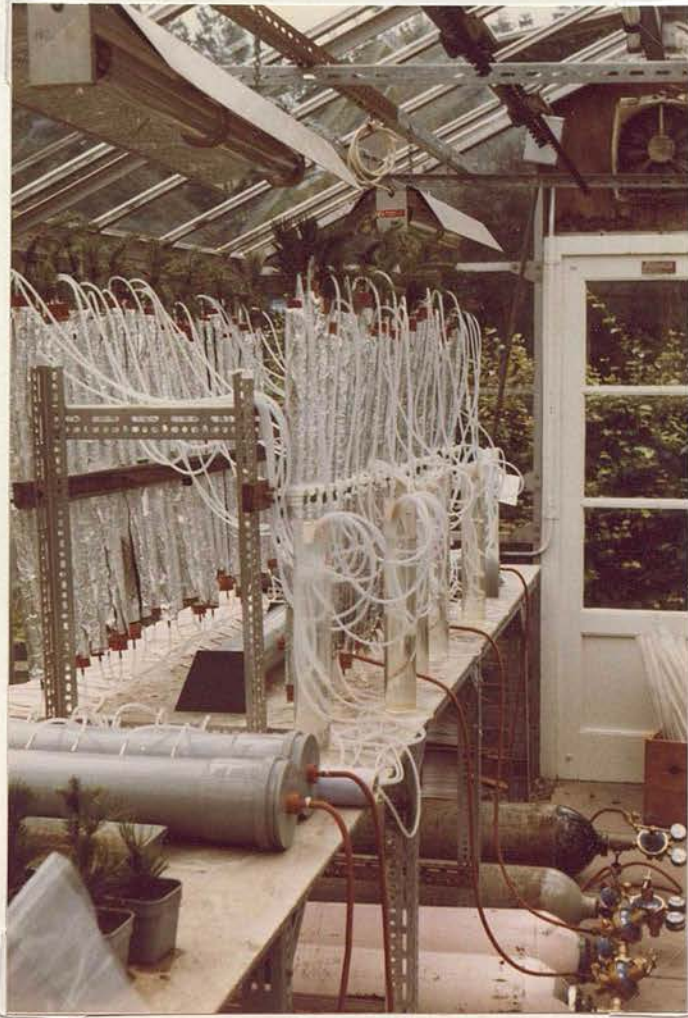


Plate 11.1 The operating gas flow system for the root growth experiment, showing the gas cylinders, P.V.C. manifolds and plant tubes.

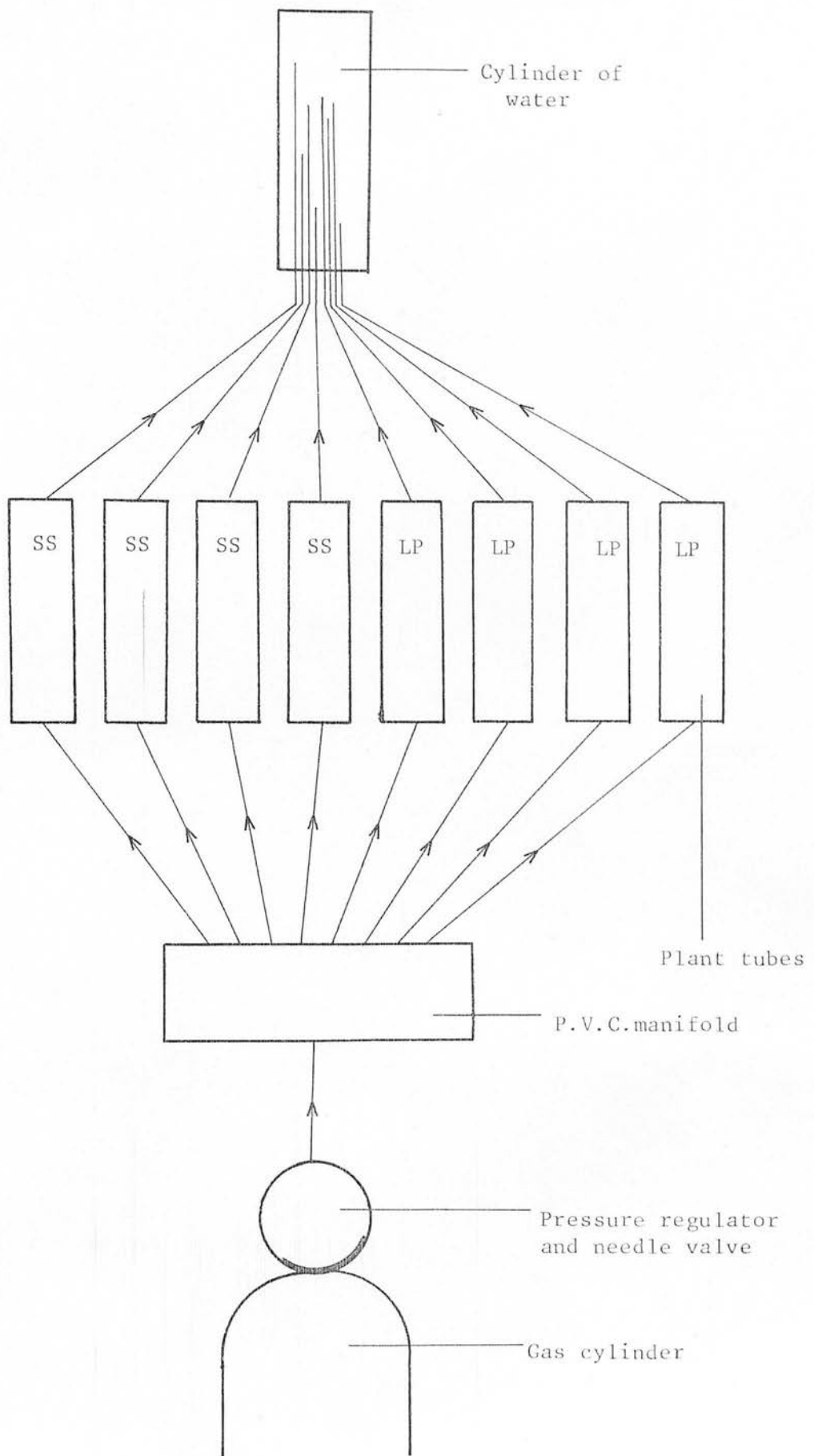


Fig.11.1 Schematic representation of gas flow (arrowed lines) for one of the six gas mixture treatments.



Plate 11.2 Picea sitchensis roots after treatment with nitrogen only.
Note the brown and shrivelled appearance behind the root tip,
compared with the root illustrated in Plate 11.3.

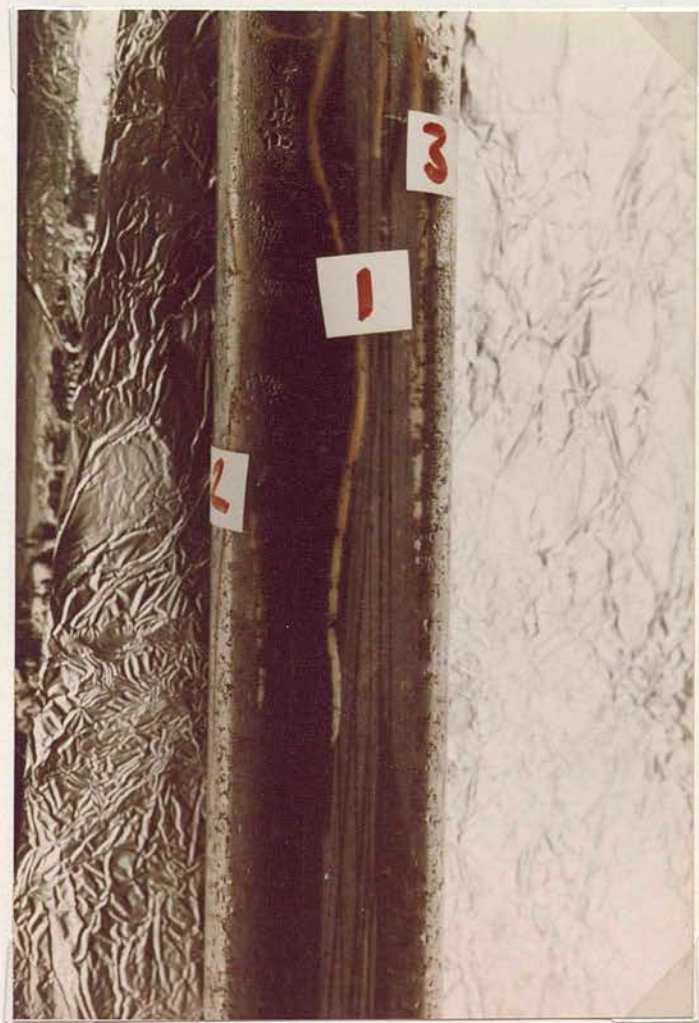


Plate 11.3 Healthy Picea sitchensis roots, after being treated with air.

conditions were re-established on day 13, the roots that had been in nitrogen failed to respond and were presumed dead. Plate 11.2 shows some of these roots from the nitrogen treatment, in contrast to healthy roots in Plate 11.3. It can be seen that the roots in Plate 11.2 are somewhat shrivelled in appearance about 10mm behind the tip, and have a brown colour for this distance immediately behind the tip. The healthy roots, on the other hand, are white from the tip for several centimetres.

In both experiments the roots maintained in air (Figs.11.2b and 11.3b) showed a steady elongation rate throughout the experiment, suggesting that no external factor was responsible for changes in the elongation rate in the other gas treatments. At $0.21 \text{ m}^3 \text{ m}^{-3}$ of oxygen (Fig.11.2) the gas treatments show little alteration of the elongation rate from the onset of treatment except for a possible slight decrease in $0.18 \text{ m}^3 \text{ m}^{-3}$ of carbon dioxide. Conversely, at $0.01 \text{ m}^3 \text{ m}^{-3}$ of oxygen, elongation practically ceased at the onset of treatment, except for the $0.01 \text{ m}^3 \text{ m}^{-3}$ of carbon dioxide treatment in which it continued at a much reduced rate. However, signs of recovery with the return to fully aerobic conditions, were present in most cases for each treatment.

A better understanding of changes in growth rate under each gas treatment can be gained by looking at the mean elongation rate for each species. No greater differences were noticed between the two clones of each species, than between the two plants of each clone.

The mean elongation rates (mm day^{-1}) for each species during each stage of the experiment are given in Table 11.1. Table 11.2 shows the elongation rates during the treatments (and the return to atmospheric conditions for low oxygen experiment) expressed as a fraction of the elongation rate measured during the initial period at atmospheric concentrations. The values in Table 11.2 are presented graphically in Fig. 11.4.

Table 11.1 Mean root elongation rates, before, during and after exposure to the gas mixtures.

Experiment	Gas concentrations ($\text{m}^3 \text{ m}^{-3}$)			Root elongation rate(mm day^{-1})					
				Before exposure		During exposure		After exposure	
	O_2	CO_2	N_2	SS	LP	SS	LP	SS	LP
1	0.21	0.00035	Balance	2.84	3.64	3.59	2.58	-	-
	0.21	0.01	"	2.87	4.65	4.65	3.40	-	-
	0.21	0.06	"	2.94	3.85	3.09	2.73	-	-
	0.21	0.12	"	2.96	3.06	2.43	1.72	-	-
	0.21	0.18	"	2.71	2.97	1.40	0.88	-	-
	0	0	1.0	2.95	3.02	0.18	0.16	-	-
2	0.21	0.00035	Balance	4.29	4.14	3.85	3.62	3.95	3.07
	0.01	0.01	"	4.41	5.58	0.78	0.71	1.90	2.21
	0.01	0.06	"	3.82	4.71	0.50	0.03	1.97	1.63
	0.01	0.12	"	4.35	5.98	0.48	0.09	0.98	5.28
	0.01	0.18	"	3.58	5.58	0.50	0.97	0.91	3.18
	0	0	1.0	3.97	3.64	0.12	0.07	0	0.17

LP - Lodgepole pine (Pinus contorta)

SS - Sitka spruce (Picea sitchensis)

Table 11.2 Relative root elongation during gas treatments and recovery,
periods, as a fraction of the elongation rate during the
initial atmospheric period

Experiment	Gas concentrations ($\text{m}^3 \text{m}^{-3}$)			Ratio of root elongation rate to the rate during the initial period at atmospheric concentrations			
	O_2	CO_2	N_2	During treatment		After return to atmospheric conditions	
				SS	LP	SS	LP
1	0.21	0.00035	Balance	1.26	0.71	-	-
	0.21	0.01	"	1.62	0.73	-	-
	0.21	0.06	"	1.05	0.71	-	-
	0.21	0.12	"	0.82	0.56	-	-
	0.21	0.18	"	0.52	0.30	-	-
	0	0	1.0	0.06	0.05	-	-
2	0.21	0.00035	Balance	0.90	0.87	0.92	0.74
	0.01	0.01	"	0.18	0.13	0.43	0.40
	0.01	0.06	"	0.13	0.01	0.52	0.35
	0.01	0.12	"	0.11	0.02	0.23	0.88
	0.01	0.18	"	0.14	0.17	0.25	0.57
	0	0	1.0	0.03	0.02	0	0.05

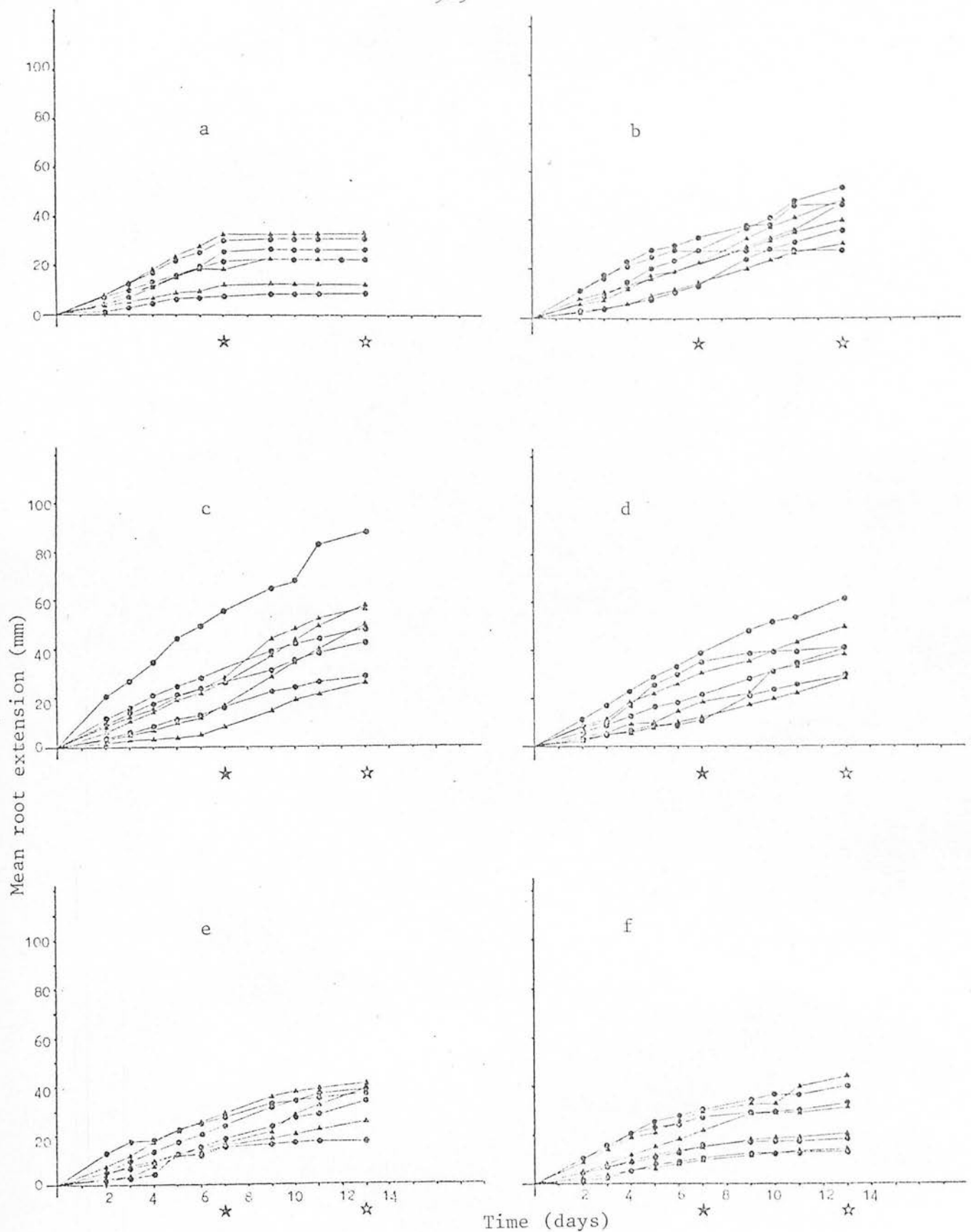


Fig.11.2 Mean root lengths for each plant of *pinus contorta* (●) and *picea sitchensis* (▲) in each gas treatment:- a, Nitrogen, b, Air, c, 0.01 m³m⁻³ CO₂, d, 0.06 m³m⁻³ CO₂, e, 0.12 m³m⁻³ CO₂ and f, 0.18 m³m⁻³ CO₂, in the "high" oxygen experiment. (☆ - start of gas treatment, ☆ - end of gas treatment).

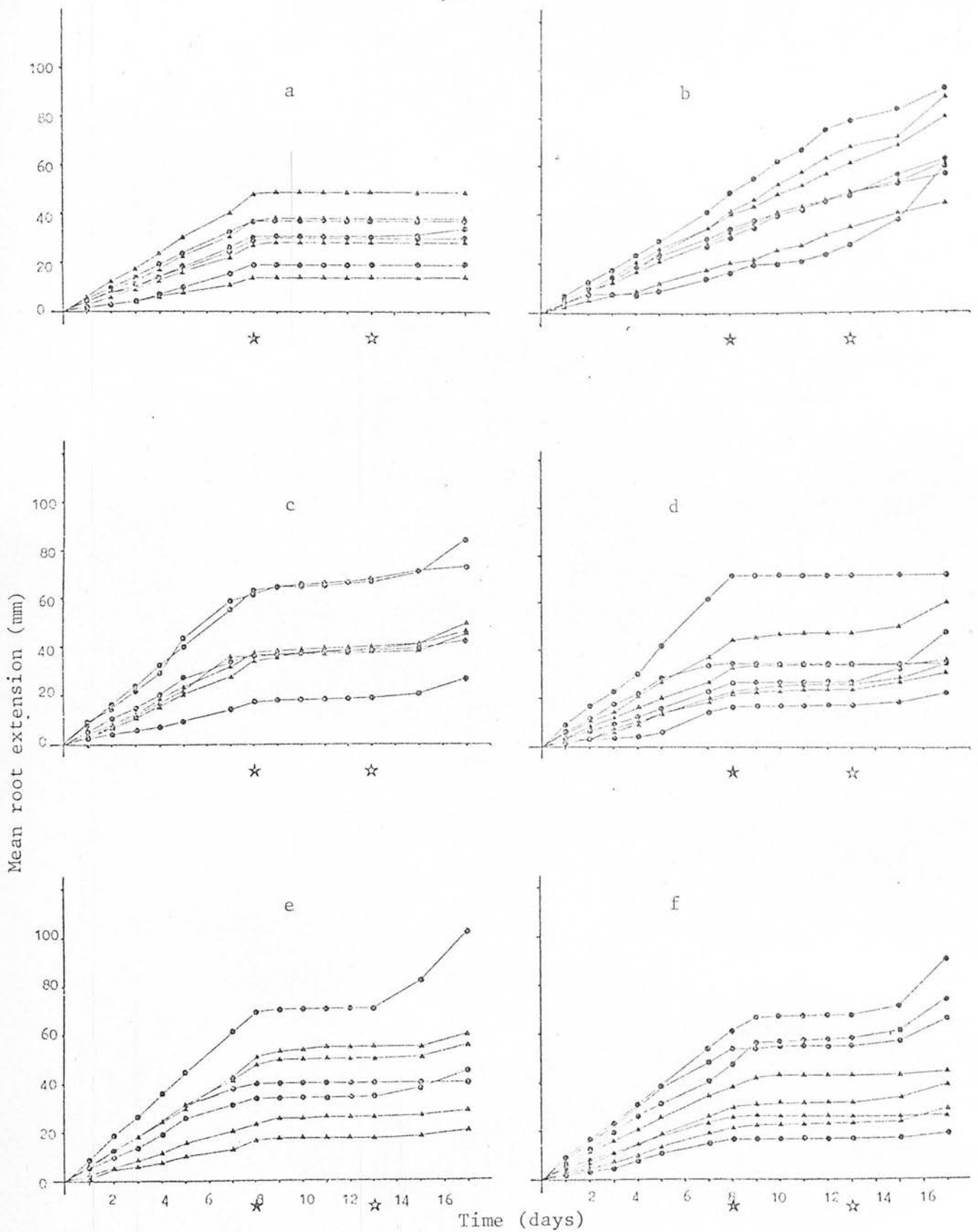


Fig.11.3 Mean root lengths for each plant of *pinus contorta* (●) and *picea sitchensis* (▲) in each gas treatment: a, nitrogen, b, air, c, $0.01 \text{ m}^3\text{m}^{-3} \text{ CO}_2$, d, $0.06 \text{ m}^3\text{m}^{-3} \text{ CO}_2$, e, $0.12 \text{ m}^3\text{m}^{-3} \text{ CO}_2$ and f, $0.018 \text{ m}^3\text{m}^{-3}$, in the "low" oxygen experiment. (☆- start of gas treatment, ☆-end of gas treatment).

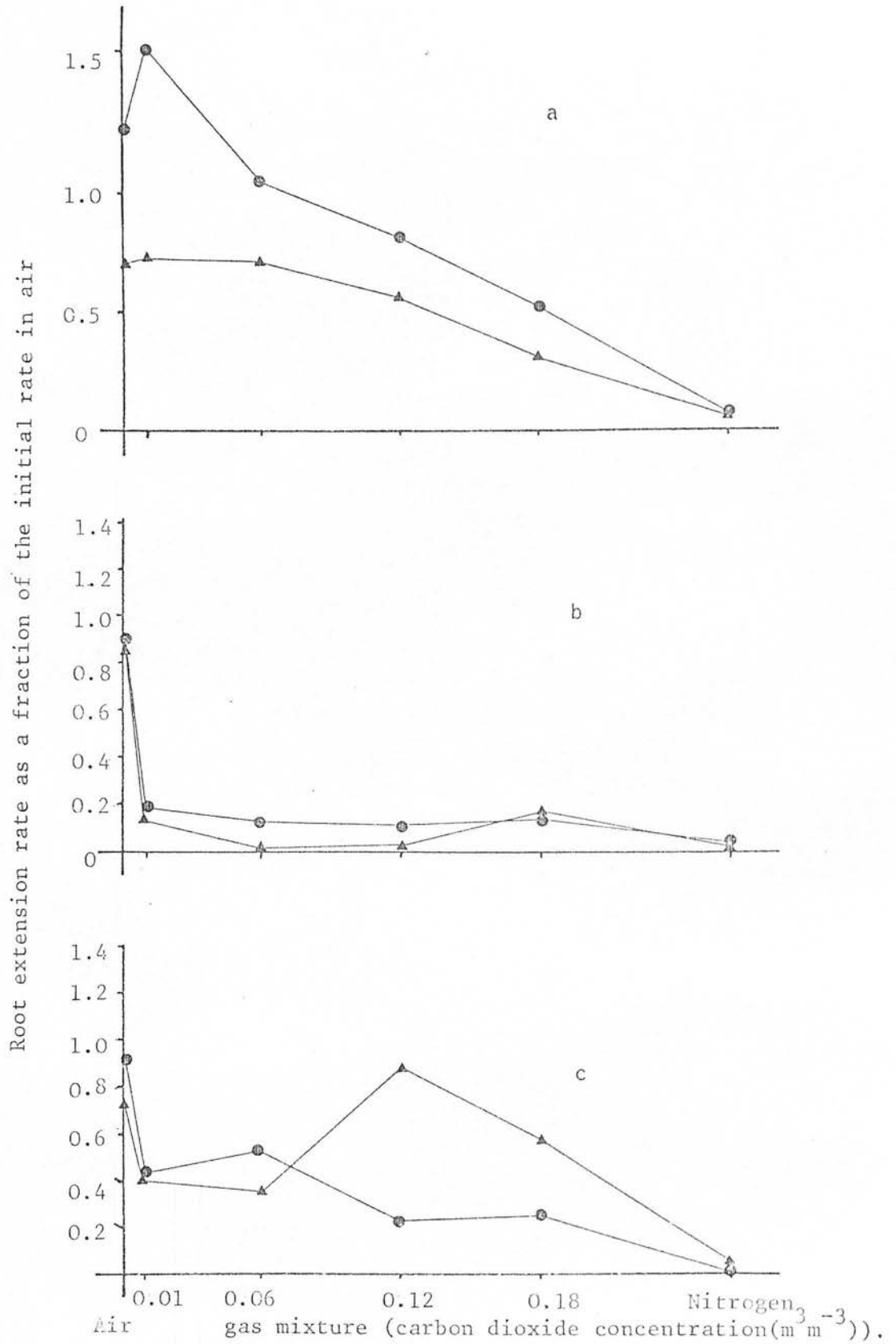


Fig.11.4 Mean extension rates of root elongation for *Picea sitchensis* (●) and *Pinus contorta* (▲) as expressed as a fraction of their original rate under atmospheric conditions; a-during treatments with 0.21 m³ m⁻³ of oxygen; b-during treatment with 0.01 m³ m⁻³ of oxygen and c - during atmospheric recover from treatment with 0.01 m³ m⁻³ of oxygen.

Fig.11.4(a) suggests that there was a decrease in elongation rate at high carbon dioxide concentrations (0.12 and $0.18 \text{ m}^3 \text{ m}^{-3}$) for both species, when the oxygen concentration was $0.21 \text{ m}^3 \text{ m}^{-3}$. When the oxygen concentration was only $0.01 \text{ m}^3 \text{ m}^{-3}$ in the low oxygen experiment (Fig.11.4(b)) the elongation rate was minimal (less than 0.2 of the former rate) at all carbon dioxide concentrations, but increased considerably on return to atmospheric oxygen concentrations (Fig.11.4(c)). This indicates that the majority of root tips were not killed as in the nitrogen treatment. The fraction of the elongation rate for the air treatment is given as well as for the carbon dioxide treatments, to give some idea of the variation from the previous rates under atmospheric conditions due to influences other than exposure to carbon dioxide.

11.4 CONCLUSIONS

Many workers have shown that low oxygen concentrations reduce or prevent root elongation. An investigation of available data by Greenwood (1971) showed that this occurred at oxygen concentrations of about 0.02 to $0.06 \text{ m}^3 \text{ m}^{-3}$ according to species. Boggie (1974) has shown that root growth of Pinus contorta and Picea sitchensis seedlings was impaired by gas phase oxygen concentrations of 0.05 and $0.10 \text{ m}^3 \text{ m}^{-3}$ respectively, when grown in nutrient solution. It is no surprise, therefore, that in the present work the root elongation rates were uniformly reduced to less than 0.2 of their aerobic rate, when the oxygen concentration was only $0.01 \text{ m}^3 \text{ m}^{-3}$, irrespective of the carbon dioxide concentration. The present experiment, however, was designed to show the possible effect of high carbon dioxide concentrations at low oxygen levels, and the conclusion must be that at the levels chosen, the effect of reduced oxygen outweighed or masked any effects due to the carbon dioxide.

Harris and Van Bavel (1957) came to the general conclusion that carbon dioxide concentrations did not have a toxic effect until they were

higher than the oxygen concentration, for tobacco. Data from other workers, however (see Section 1.4), showed toxic effects over a wide range of concentrations below the oxygen concentration, for various species. The results from the experiment at atmospheric oxygen concentration show that high carbon dioxide concentrations ($0.18 \text{ m}^3 \text{ m}^{-3}$) may well have a detrimental effect even though they are below the oxygen concentration ($0.21 \text{ m}^3 \text{ m}^{-3}$). Although the plot in Fig.11.4(a) may at first suggest a gradual effect with increasing carbon dioxide concentration, it is suggested that the reduction observed for 0.01, 0.06 and $0.12 \text{ m}^3 \text{ m}^{-3}$ carbon dioxide concentrations are probably not significant, taking into account the variation from 1 shown by the plants in the air treatment. Likewise, no real conclusions about the relative effects on the two species can be deduced from these data.

It is interesting to note from Fig.11.4 that both species survived, and recovered from, the low oxygen treatment at all carbon dioxide concentrations. This agrees with the accepted view that very low oxygen concentrations are necessary before respiration itself is affected and permanent damage done (see Section 1.2). It also corresponds with the observations by Coutts and Philipson (1978) that root growth of both Pinus contorta and Picea sitchensis could resume, after ceasing during a period of waterlogging. They also noticed a higher incidence of regrowth for Pinus contorta roots than for Picea sitchensis. The data presented here suggest a slightly nearer return to initial growth rates in Pinus contorta than Picea sitchensis after 0.12 and $0.18 \text{ m}^3 \text{ m}^{-3}$ carbon dioxide treatments, though this difference should be viewed with caution.

No statistical analysis was carried out on this experiment, as it was thought that due to the uneven number and size of roots examined for each plant, and the low replication, further conclusions beyond the trends already observed would not be particularly valid. With hindsight it may have been better to have used a slightly higher oxygen concentration than $0.01 \text{ m}^3 \text{ m}^{-3}$ in the second experiment, as effects due to carbon dioxide

concentrations may then have been observed.

12. GENERAL SUMMARY

The overall aims of this set of experiments, was to elucidate some of the ways the water regime on two problem soil types causes shallow rooting of the trees planted on them, and their subsequent instability.

In the peaty gley soil waterlogged conditions were seen to be caused by a very dense structureless subsoil, impeding drainage in a high rainfall area. The low pore volume fraction and predominantly fine particle size of this clay subsoil (Section 4), meant that it was saturated for most of the year, with only a very small gas-filled pore volume fraction ($\epsilon_g = 0.03-0.05$) at matric potentials of about -10kPa . Above this the peat layer had a much larger gas-filled pore volume fraction ($\epsilon_g = 0.2$ at about -10kPa) at low tensions, but only extended for 0.2 to 0.3m in depth. The presence of a closed canopy on this soil gave a permanent lowering of the water table and lower matric potentials at greater depth compared with unplanted areas.

This resulted in improved aeration generally, with a permanently well aerated zone in the peat layer under the trees, compared with frequent periods of low oxygen in the peat in the open sites. At greater depths periods of good aeration occurred when the matric potential fell below about -5kPa (Section 6). At or above this potential, oxygen depletion and increased carbon dioxide concentrations often occurred. In the grassland sites matric potentials rarely fell below -5kPa .

At the end of the moisture deficit period in the summer, low oxygen and high carbon dioxide concentrations were recorded under the crop, when the water table rose again. This was followed later by high dissolved oxygen concentrations. This suggests that this may be a critical period when aerobic respiration is still active but the soil is returning to a waterlogged condition and new root tips may be killed

off (see Section 6.4). The subsequent removal of many aerobically respiring sites, allowed dissolved oxygen levels to remain high. There is evidence to suggest that the general level of aeration, especially during this critical period, is better under Pinus contorta than under Picea sitchensis, and both are better than in the soil beneath the natural Molinia caerulea grass cover. Both Pinus contorta and Picea sitchensis were well aerated to 0.3m depth for most of the year, but the soil at 0.6m depth had more frequent periods of high oxygen concentrations under Pinus contorta. There was also a trend of decreasing oxygen concentrations with greater depth in the soil. Both the trends with depth and between species were consistent over both years of study.

In the deep peat a permanent lowering of the water table was achieved by surrounding plots with a drainage ditch, causing a permanently well aerated zone down to about 0.35m even without a crop present. The water table and matric potentials were lower under the Pinus contorta than the Picea sitchensis, and this was thought to be caused by greater rainfall interception by a more completely closed canopy. The drier conditions under the crop had led to a change in the fibre size distribution of the upper peat layers, in favour of more coarse fibres, less amorphous material and a higher bulk density (Section 5.4). The greater drying under Pinus contorta lasted longer, until November, at the end of the moisture deficit period than under Picea sitchensis, this was more noticeable under the younger trees at Eddleston than at Falstone, and may confer an advantage for deeper rooting of Pinus contorta, even though the aeration data did not show enhanced aeration over the Picea sitchensis site at this time (Section 7.4). The trends of decreasing oxygen and increasing carbon dioxide concentrations with greater depth seen in the peaty gley soil, were also evident in the deep peat at Eddleston. The trend of more frequent periods of good

aeration under Pinus contorta than under Picea sitchensis found at Falstone was again seen, and generally good aeration occurred to a depth of 0.5m under the Pinus contorta compared with 0.4m under Picea sitchensis. Well aerated conditions in the open ploughed site only really occurred in the surface 0.2m of peat, and hardly at all in the undisturbed virgin peat. The periods of high oxygen concentrations in the peat occurred once the matric potential fell below about -3kPa. This is probably due to the larger gas-filled pore volume fractions at low tensions in peat compared with the mineral soil.

The trend of higher carbon dioxide concentrations at greater depth and under the unplanted areas compared with forested areas, were better illustrated in the deep peat than the mineral soil. It is difficult, however, to use the oxygen and carbon dioxide concentrations to establish the R.Q. of peat in the field, due to the greater solubility of carbon dioxide and high moisture content of peat, even at relatively high gas-filled pore volume fractions. However, the fact that calculated R.Q's tended to be above unity in a majority of cases (Secton 10) is evidence that areas of anaerobic respiration occur in peat, even though the gas-filled pore space may have a high oxygen concentration.

The lack of any obvious relationship between gas-filled pore volume fraction and respiration rate of removed peat cores suggests that there are sufficient large pores evenly distributed in the peat to maintain overall aerobic conditions, even at low moisture tensions (Secton 8). The diffusion experiment suggests that in removed cores of peat, three dimensional shrinkage of the block may cause large drained pores to collapse as finer pores drain. This has the effect of maintaining the effectiveness of the pore space for gaseous diffusion rather than increasing it with increasing gas-filled pore volume. This may explain why a linear model for relative diffusivity with gas-filled

pore volume fraction fits the data better than the traditional exponential model. In the field though, where only one dimension is allowed for shrinkage, the curvilinear model found in mineral soils may fit better (Section 9.4). The experiment on root growth rate showed that both species were affected by low oxygen concentrations, but no conclusions as to the effectiveness of high carbon dioxide concentrations could be drawn (Section 11). It could be a profitable line of investigation in the future to examine the effect of high carbon dioxide concentrations at intermediate oxygen concentrations, as these sometimes occur in the field.

BIBLIOGRAPHY

- AKROYD, T.N.W. 1969. Laboratory testing in soil engineering. Publ. Soil Mechanics Ltd. London.
- ARMSTRONG, W. 1964. Oxygen diffusion from the roots of some British bog plants. *Nature* 204 801-802
- ARMSTRONG, W. 1967. The relationship between oxidation-reduction potentials and oxygen diffusion levels in some waterlogged organic soils. *J. Soil Sci.* 18 27-34
- ARMSTRONG, W. 1968. Oxygen diffusion from the roots of woody species. *Physiol. Pl.* 21 539-543
- ARMSTRONG, W. 1971a. Oxygen diffusion from the roots of rice grown under non-waterlogged conditions. *Physiol. Pl.* 24 242-241
- ARMSTRONG, W. 1971b. Radial losses from intact rice roots as affected by distance from the apex, respiration and waterlogging. *Physiol. Pl.* 25 192-197
- ARMSTRONG, W., BOOTH, T.C., PRIESTLEY, P. AND READ, D.J. 1976. The relationship between soil aeration stability and growth of sitka spruce on upland peaty gleys. *J. appl. Ecol.* 13 585-589
- ARMSTRONG, W. AND READ, D.J. 1972. Some observations on oxygen transport in conifer seedlings. *New Phytol.* 71 55-62
- AVERY, B.W. 1973. Soil classification in the Soil Survey of England and Wales. *J. Soil Sci.* 24 324-338
- BAKKER, J.W. AND HIDDING, A.P. 1970. The influence of soil structure and air content on gas diffusion in soils. *Neth. J. agric. Sci.* 18 37-48
- BALL, B.C. 1980. Characterisation of soil pores by gas flow and diffusion. Ph.D. Thesis Reading Univ. 1980.
- BALL, B.C., the late HARRIS, W. AND BURFORD, J.R. 1981. A laboratory method to measure gas diffusion and flow in soil and other porous materials. *J. Soil. Sci.* 32 323-333
- BARBER, D.A., EBERT, M. AND EVANS, N.T.S. 1962. The movement of $^{15}\text{O}_2$ through barley and rice plants. *J. exp. Bot.* 13 397-403
- BASCOMB, C.L. 1974. Physical and chemical analyses of <2mm samples. In, Soil survey laboratory methods. Soil survey Tech. Mono. 6.
- BELL, R.G. 1968. Separation of gases likely to be evolved from flooded soils by gas chromatography. *Soil Sci.* 105 78-80
- BERGMAN, H.F. 1959. Oxygen deficiency as a cause of disease in plants. *Bot. Rev.* 25 417-485

- BINNS, W.O. 1959. The physical and chemical properties of deep peat in *relation* to afforestation. Ph.D. Thesis, Aberdeen, Univ. 1959.
- BIRKLE, D.E., LETEY, J., STOLZY, L.H. AND SUSZKIEWICZ, T.E. 1964. Factors influencing the measurement of oxygen diffusion rates with the Platinum micro-electrode. *Hilgardia*. 35 20 p555-566
- BJERGBAKKE, E. 1976. Measurement of oxygen. Ed. Degn, H., Balsler, I and Brook, R. Proc. symposium, Odense, Denmark. 1974. Elsevier, Amsterdam 1-10
- BLAKE, G.R. AND PAGE, J.B. 1948. Direct measurement of gaseous diffusion in soils. *Soil Sci. Soc. Amer. Proc.* 13 37-42
- BLINKS, L.R. AND SKOW, R.K. 1938. The time course of photosynthesis as shown by the glass electrode, with anomalies in the acidity changes. *Proc. Nat. Acad. Sci. U.S.A.* 24 413-420
- BOELTER, D.H. 1969. Physical properties of peats as related to degree of decomposition. *Soil Sci. Soc. Amer. Proc.* 33 606-609
- BOGGIE, R. 1972. Effect of water-table height on root development of Pinus contorta on deep peat in Scotland. *Oikos*. 23 304-312
- BOGGIE, R. 1974. Response of seedlings of Pinus contorta and Picea sitchensis to oxygen concentration in culture solution. *New Phytol.* 73 467-473
- BOGGIE, R. 1977. Water-table depth and oxygen content of deep peat in relation to root growth of Pinus contorta *Pl. Soil.* 48 447-454
- BREMNER, J.M. AND SHAW, K. 1958. Denitrification in soil. II Factors affecting denitrification. *J. agric. Sci.* 51 40-52
- BRIDGE, B.J. AND RIXON, A.J. 1976. Respiratory quotient arising from microbial activity in relation to matric suction and air-filled pore space of soil. *Nature* 218 961-962
- BROCK, T.D. 1970. Biology of microorganisms. Pentice-Hall, Englewood Cliffs, New Jersey. U.S.A.
- BRUCE, R.R. AND WEBBER, L.R. 1953. The use of a diffusion chamber as a measure of the rate of oxygen supplied by a soil. *Can. J. agric. Sci.* 33 430-436
- BUCKINGHAM, E. 1904. Contributions to our knowledge of the aeration of soils. U.S.D.A. Bureau of Soils. Bulletin 25
- BURFORD, J.R. AND MILLINGTON, R.J. 1968. Nitrous oxide in the atmosphere of a red-brown earth. *Trans. 9th Int. Congr. Soil Sci.* 505-511
- BURFORD, J.R., STEFANSON, R.C. AND MILLINGTON, R.J. 1973. Measurement of gaseous losses of nitrogen from soils. *Soil Biol. Biochem.* 5 133-141
- BUNNELL, F.L., TAIT, D.E.N., FLANAGAN, P.W. AND VAN CLEEVE, K. 1977. Microbial respiration and substrate weight loss. I. A general model of the influences of abiotic variables. *Soil Biol. Biochem.* 9 23-40

- CANNELL, R.Q. 1977. Soil aeration and compaction in relation to root growth and soil management. *J.appl.Biol.* 2 1-86
- CHILDERS, N.F. AND WHITE, D.G. 1942. Influence of submersion of the roots on transpiration, apparent photosynthesis and respiration of young apple trees. *Pl.Physiol.* 17 603-618
- CHO, D.Y. AND PONNAMPERUMA, F.N. 1971. Influence of soil temperature on the chemical kinetics of flooded soils and the growth of rice. *Soil Sci.* 112 184-194
- CONNELL, W.E. AND PATRICK, W.H. 1968. Sulphate reduction in soil. Effects of redox potential and pH. *Science* 159 86-87
- COOPER, P.J.M. 1975. Studies on the soil atmosphere composition under maize, grass and bare fallow in western Kenya. *E.Afr.agric.For.* 40 313-331
- COUTTS, M.P. AND ARMSTRONG, W. 1976. Role of oxygen transport in the tolerance of trees to waterlogging. In Tree Physiology and yield improvement. Ed.Cannell, M.G.R. and Last F.T. Academic Press, New York, and London.
- COUTTS, M.P. AND BOWEN, M.R. 1973. Physiology of tree roots. *Rep.Forest Res.* 1973 92-93 HMSO, London.
- COUTTS, M.P. AND PHILIPSON, J.J. 1978a. Tolerance of tree roots to waterlogging. I. Survival of Sitka spruce and lodgepole pine. *New Phytol.* 80 63-69
- COUTTS, M.P. AND PHILIPSON, J.J. 1978b. Tolerance of tree roots to waterlogging. II. Adaptation of Sitka spruce and lodgepole pine to waterlogged soil. *New Phytol.* 80 71-77
- CRAWFORD, R.M.M. 1977. Tolerance of anoxia and ethanol metabolism in germinating seeds. *New Phytol.* 79 511-517
- CRAWFORD, R.M.M. AND BAINES, M.A. 1977. Tolerance of anoxia and the metabolism of ethanol in tree roots. *New Phytol.* 79 519-526
- CURRIE, J.A. 1960a. Gaseous diffusion in porous media. I. A non-steady state method. *Brit.J.appl.Phys.* 11 314-317
- CURRIE, J.A. 1960b. Gaseous diffusion in porous media. II. Dry granular materials. *Brit.J.appl.Phys.* 11 318-324
- CURRIE, J.A. 1961a. Gaseous diffusion in porous media. III. Wet granular materials. *Brit.J.appl.Phys.* 12 275-281
- CURRIE, J.A. 1961b. Gaseous diffusion in the aeration of aggregated soils. *Soil Sci.* 92 40-45
- CUTTLE, S.P. AND MALCOLM, D.C. 1979. A corer for taking undisturbed peat samples. *Pl.Soil.* 51 297-300
- CURRIE, J.A. 1979 Rothamsted studies of soil structure IV. Porosity, gas diffusion and pore complexity in dry soil crumbs. *J. Soil Sci.* 30, 441-452

- DAY, W.R. 1949. The soil conditions which determine wind-throw in forests. *Forestry* 23 30-95
- DAY, W.R. 1953. The growth of Sitka spruce on shallow soils in relation to root-disease and wind-throw. *Forestry* 26 81-95
- DAY, W.R. 1963. The development of Sitka spruce on shallow peat. Scot. *Forestry* 17 219-236
- DAY, P.R. 1965. Particle fractionation and particle-size analysis. In, *Methods of soil analysis. Pt.1.* Ed.Black, C.A. Am.Soc.Agron.Madison.
- De CAMARGO, O.A., GROHMANN, F., SALATI, E. AND MATSUI, E. 1974. A technique for sampling the soil atmosphere. *Soil Sci.* 117 173-174
- De VRIES, D.A. 1950. Some remarks on gaseous diffusion in soils. *Trans. 4th Intr.Congr. of Soil Sci.* II 41-43
- DOWDELL, R.J., SMITH, K.A., CREES, R. AND RESTALL, S.W.F. 1972. Field studies of ethylene in the soil atmosphere - equipment and preliminary results. *Soil Biol. Biochem.* 4 325-331
- DOWDELL, R.J. AND SMITH, K.A. 1974. Field studies of the soil atmosphere II. Occurrence of nitrous oxide. *J.Soil Sci.* 25 231-238
- DOWDELL, R.J., CREES, R., BURFORD, J.R. AND CANNELL, R.Q. 1979. Oxygen concentrations in a clay soil after ploughing or direct drilling. *J.Soil.Sci.* 30 239-245
- EAVIS, B.W. AND PAYNE, D. 1969. Soil physical conditions and root growth. In *Root growth. Proc. 15th Easter School. Univ. of Nottingham 1968* 315-338 Ed. Whittington, N.J.
- FINNEY, D.J. 1973. Transformation of observations for statistical analysis. *Cott.Grow.Rev.* 50 1-15
- FLÜHLER, J. 1973. Sauerstoffdiffusion in Boden. Schweizerische anstalt fur das Forstliche versuchswesen. Bd.49.
- FRASER, A.I. 1965. The uncertainty of wind damage in forest management. *Irish Forestry* 22 23-30
- FRASER, A.I. AND GARDINER, J.B.H. 1967. Rooting and stability in Sitka spruce. *For.Comm.Bull.* 40 H.M.S.O. London.
- GARDNER, W.R. 1956. Representation of soil aggregate-size distribution by a logarithmic-normal distribution. *Soil Sci.Soc.Amer.Proc.* 20 151-153
- GOODLASS, G. 1978. Studies on the occurrence of ethylene in soil and its effects on root growth. Ph.D.Thesis Edinburgh Univ. 1978.
- GOODLASS, G. AND SMITH, K.A. 1978a. Effects of organic amendments on evolution of ethylene and other hydrocarbons from soil. *Soil Biol.Biochem.* 10 201-205

- GOODLASS, G. AND SMITH, K.A. 1978b. Effect of pH, organic, matter content and nitrate on the evolution of ethylene from soils. *Soil Biol.Biochem.* 10 193-200.
- GRABLE, A.R. 1966. Soil aeration and plant growth. *Adv.Agron.* 18 57-106
- GRABLE, A.R. AND SIEMER, E.G. 1968. Effects of bulk density, aggregate size, and soil water suction on oxygen diffusion, redox potentials and elongation of corn roots. *Soil Sci.Soc.Amer. Proc.* 32 180-186
- GRADWELL, M.W. 1960. A laboratory study of the diffusion of oxygen through pasture topsoils. *N.Z. J. Sci.* 4 250-270
- GREENE, H. 1963. Prospects in soil science. *J.Soil Sci.* 14 1-11
- GREENWOOD, D.J. 1961. The effect of oxygen concentration on the decomposition of organic materials in soils. *Pl.Soil* 14 360-376
- GREENWOOD, D.J. 1962. Nitrification and nitrate dissimilation in soil. *Pl.Soil.* 17 378-391
- GREENWOOD, D.J. 1963. Nitrogen transformations and the distribution of oxygen in soil. *Chemistry and Industry* p 799
- GREENWOOD, D.J. 1970. Distribution of carbon dioxide in the aqueous phase of aerobic soils. *J. Soil Sci.* 21 314-329
- GREENWOOD, D.J. 1971. Soil aeration and plant growth. *Rep.Prog.appl. Chem.* 55 423-431
- GREENWOOD, D.J. 1975. Measurement of soil respiration. In *Soil Physical Conditions and Crop production*. Tech.Bull. 29 M.A.F.F. 261-272
- GREENWOOD, D.J. AND GOODMAN, D. 1964. Oxygen diffusion and aerobic respiration in soil spheres. *J.Sci.Fd.Agric.* 15 579-588
- GREENWOOD, D.J. AND GOODMAN, D. 1967. Direct measurement of the distribution of oxygen in soil aggregates and in columns of fine soil crumbs. *J.Soil Sci.* 18 182-196
- HALL, K.C. AND BURFORD, J.R. 1975. Gas chromatographic measurement of dissolved oxygen using an electron capture detector. *Rep.Agric. Res.Coun.Letcombe Lab.* 1974 53-54
- HALL, D.G.M., REEVE, M.J., THOMASSON, A.J. AND WRIGHT, V.F. 1977. Water retention, porosity and density of field soils. *Soil Survey Tech.Mono.* 9
- HAMMOND, L.C., ALLOWAY, W.H. AND LOOMIS, W.E. 1955. Effects of oxygen and carbon dioxide levels upon absorption of potassium by plants. *Pl.Physiol.* 30 155-161
- HARRIS, D.G. AND VAN BAVEL, C.H.M. 1957. Growth, yield and water absorption of tobacco plants as affected by the composition of the root atmosphere. *Agron.J.* 49 11-14

- HODGMAN, C.D., WEEST, R.C., AND SELBY, S.M. 1956 Handbook of Chemistry and Physics. 37th Ed., Chemical Rubber Publishing Co. Cleveland, Ohio, U.S.A.
- HOOK, D.D., BROWN, C.L. AND KORMANIK, P.P. 1971. Inductive flood tolerance in swamp tupelo. *J.exp.Bot.* 22 73-79
- HOWELER, R.H. AND BOULDIN, D.R. 1971. The diffusion and consumption of oxygen in submerged soils. *Soil Sci.Soc.Amer.Proc.* 35 203-208
- HU, S.C. AND LINNARTZ, N.E. 1972. Variations in oxygen content of forest soils under mature loblolly pine stands. Louisiana State University Bull.668
- IKELS, K.G. 1965. Gas chromatographic determination of small volumes of Nitrogen dissolved in blood. *J.Gas Chromatography* 3 359-362
- JACKSON, M.B. AND CAMPBELL, D.J. 1975a. Hormones and the responses of plants to waterlogged soil. Rep.Agric.Res.Coun.Letcombe Lab. 1974 45-48
- JACKSON, M.B. AND CAMPBELL, D.J. 1975b. Movement of ethylene from roots to shoots, a factor in the response of tomato plants to waterlogged soil conditions. *New Phytol.* 74 397-406
- JENKINSON D.S. 1977. Studies on the decomposition of plant material in soil. IV. The effect of rate of addition. *J.Soil Sci.* 28 417-423
- JONES, H.E. 1971. Comparative studies of plant growth and distribution in relation to waterlogging. *J.Ecol.* 59 583-591
- JONES, H.E. AND ETHERINGTON, J.R. 1970. Comparative studies of plant growth and distribution in relation to waterlogging. *J.Ecol.* 58 487-496
- KELLER, T. 1972. Gaseous exchange of forest trees in relation to some edaphic factors. *Photosynthetica* 6 197-206
- KOLTHOFF, I.M. AND LINGANE, J.J. 1952. Polarography I and II. Wiley, New York.
- KRAMER, P.J. 1951. Causes of injury to plants resulting from flooding of the soil. *Plant Physiol.* 26 722-736
- LEES, J.C. 1972. Soil aeration and Sitka spruce seedling growth in peat. *J.Ecol.* 60 343-349
- LEMON, E.R. 1962. Soil aeration and plant root relations. I Theory. *Agron.J.* 54 167-170
- LEMON, E.R. AND ERICKSON, A.E. 1952. The measurement of oxygen diffusion in the soil with a platinum microelectrode. *Soil Sci.Soc.Amer. Proc.* 16 160-163
- LEMON, E.R. AND WIEGAND, C.L. 1962. Soil aeration and plant root relations. II. Root respiration. *Agron J.* 54 171-175
- LETEY, J. AND STOLZY, L.H. 1967. Limiting distances between root and gas phase for adequate oxygen supply. *Soil Sci.* 103 404-409

- LETEY, J., STOLZY, L.H. AND BLANK, G.B. 1962. Effect of duration and timing of low soil oxygen content on shoot and root growth. *Agron.J.* 54 34-37
- LEYTON, L. AND ROUSEAU, L.Z. 1958. Root growth of tree seedlings in relation to aeration. In The physiology of forest trees. symp. at Harvard forest 1957. Ed.Thiman, K.V. The Ronald Press Co. New York.
- LONGMUIR, I.S. 1954. Respiration rate of bacteria as a function of oxygen concentration. *Biochem.J.* 57 81-87
- LUXMOORE, R.J., STOLZY, L.H. AND LETEY, J. 1970a. Oxygen diffusion in the soil plant system. I.A model.*Agron.J.* 62 317-321
- LUXMOORE, R.J., STOLZY, L.H. AND LETEY, J. 1970b. Oxygen diffusion in the soil plant system. II.Respiration rate, permeability and porosity of consecutive excised segrements of maize and rice roots. *Agron.J.* 62 322-324
- LUXMOORE, R.J., STOLZY, L.H. AND LETEY, 1970c. Oxygen diffusion in the soil plant system. III. Oxygen concentration profiles, respiration rates and the significance of plant aeration predicted for maize roots. *Agron.J.* 62 325-329
- LUXMOORE, R.J., STOLZY, L.H. AND LETEY, J. 1970d. Oxygen diffusion in the soil plant system. IV. Oxygen concentration profiles, respiration rates and radial oxygen losses predicted for rice roots. *Agron.J.* 62 329-332
- MacCAULLY, B.J. AND GRIFFIN, D.M. 1969. Effects of carbon dioxide and oxygen on activity of some soil fungi. *Trans.Br.mycol.Soc.* 53 53-62
- MARSHALL, T.J. 1959. The diffusion of gases through porous media. *J.Soil Sci.* 10 79-82
- MARSHALL, T.J. AND HOLMES, J.W. 1979. Soil Physics. Cambridge University Press, Cambridge
- McINTYRE, D.J. 1970. The platinum microelectrode method of soil aeration measurement. *Adv.Agron.* 22 235-283
- McMANMON, M. AND CRAWFORD, R.M.M. 1971. A metabolic theory of flooding tolerance, the significance of enzyme distribution and behaviour. *New Phytol.* 79 519-526
- MILLER, R.D. AND JOHNSON, D.D. 1964. The effect of soil moisture tension on carbon dioixde evolution nitrification and nitrogen mineralisation. *Soil Sci.Soc. Amer.Proc.* 28 544-646
- MILLINGTON, R.J. 1959. Gas diffusion in porous media. *Science* 130 100-102

- MILLINGTON, R.J. AND SHEARER, R.C. 1971. Diffusion in aggregated porous media. *Soil Sci.* 111 372-378
- MONTEITH, J.L., SZIECZ, G. AND YABUKI, K. 1964. Crop photosynthesis and the flux of carbon dioxide below the canopy. *J.appl.Ecol.* 1 321-337
- MONTGOMERY, H.A.C. AND QUARMBY, C. 1966. The extraction of gases dissolved in water for analysis by Gas chromatography. *Lab. Practice* 15 538-543
- MUNSELL, COLOUR COMPANY INC. 1954(ed) Munsell soil colour charts.
- NICHOLAS, D.J.D. 1963. The metabolism of inorganic nitrogen and its compounds in microorganisms. *Biol.Rev.* 38 530-568
- PARR, J.F. AND REUSZER, H.W. 1959. Organic matter decomposition as influenced by oxygen level and method of application to soil. *Soil Sci.Soc.Amer.Proc.* 23 214-216
- PENMAN, H.L. 1940a. Gas and vapour movement in the soil. I The diffusion of vapours through porous solids. *J.agric.Sci.* 30 437-462
- PENMAN, H.L. 1940b. Gas and vapour movement in the soil. II. The diffusion of carbon dioxide through porous solids. *J.agric.Sci.* 30 570-581
- PHILIPSON, J.J. AND COUTTS, M.P. 1978. Tolerance of tree roots to waterlogging. III. Oxygen transport in lodgepole pine and Sitka spruce roots of primary structure. *New Phytol.* 80 341-349
- POEL, L.W. 1960a. The estimation of oxygen diffusion rates in soil. *J.Ecol.* 48 165-173
- POEL, L.W. 1960b. A preliminary survey of soil aeration conditions in a Scottish hill grazing. *J.Ecol.* 48 733-736
- PONNAMPERUMA, F.N. 1972. The chemistry of submerged soils. *Adv.Agron.* 24 29-95
- PONNAMPERUMA, F.N., MARTINEZ, E. AND LOY, T. 1966. Influence of redox potentials and partial pressures of carbon dioxide on the pH values and the suspension effects of flooded soils. *Soil Sci.* 101 421-431
- PUUSTJARVI, V. AND ROBERTSON, R.A. 1975. Physical and chemical properties In. *Peat in Horticulture* Ed. Robinson, D.W. and Lamb J.G.D. Academic Press, London.
- PYATT, D.G. 1966. The soil and windthrow surveys of Newcastleton forest, Roxburghshire. *Scot. Forestry* 20 175-183
- PYATT, D.G. 1968. Forest management surveys in forests affected by winds. In *Wind effects on the forest* supplement to *Forestry* 1968, 67-76
- PYATT, D.G. 1970. Soil groups of upland forests. *For.Comm.Forest Record.* 71 HMSO, London.
- PYATT, D.G. 1973. Physical and mechanical properties of soil types. *Rep.Forest.Res.* 1973 62-66 HMSO, London.

- PYATT, D.G. 1976. Classification and improvement of upland soils. Rep.Forest Res.1976 p25 HMSO, London.
- PYATT, D.G. 1978. Physical properties of soils with indurated material. Ph.D. Thesis. Aberdeen University 1978.
- PYATT, D.G., McLAREN, D.T. AND CRAVEN, M.M. 1979. Physical properties of four soils at Newcastleton forest, south Scotland. North of England Soils Disc. Group Proc. 15 35-63
- RIXON, A.J. AND BRIDGE, B.J. 1968. Respiratory quotient arising from microbial activity in relation to matric suction and air-filled pore space of soil. *Nature* 218 961-962
- RUSSELL, E.W. 1973. Soil conditions and plant growth. 10th Ed. Longmans, London.
- RUSSELL, R.S. 1977. Plant root systems. Their function and interaction with the soil. McGraw-Hill Ltd, London.
- RUSSELL, E.J. AND APPLEYARD, A. 1915. The atmosphere of the soil: Its composition and the causes of variation. *J.agric.Sci.* 7 1-48
- RUSSELL, E.W. AND TAMHANE, R.V. 1940. The determination of the size distribution of soil clods and crumbs. *J.agric.Sci.* 30 210-234
- SANDERSON, P.L. 1977. The response of Sitka spruce and lodgepole pine to conditions associated with waterlogged soil. Ph.D. Thesis, Hull University.
- SANDERSON, P.L. AND ARMSTRONG, W. 1978. Soil waterlogging, root rot and conifer wind-throw; oxygen deficiency or phytotoxicity. *Pl.Soil* 49 185-190
- SCOTT, A.D. AND EVANS, D.D. 1955. Dissolved oxygen in saturated soil. *Soil Sci.Soc.Amer.Proc.* 19 7-11
- SMITH, D. H. AND CLARK, F.E. 1960. Volatile losses of nitrogen from acid or neutral soils or solutions containing nitrite and ammonium ions. *Soil Sci.* 90 86-92
- SMITH, K.A. 1976. Aeration status of upland soils. Rep.For.Res.Lond. 1976 56-57
- SMITH, K.A. 1977a. Gas-chromatographic analysis of the soil atmosphere. In *Advances in Chromatography* Vol.15 Ed.Giddings et al Dekker, New York, p197-231
- SMITH, K.A. 1977b. Aeration status of upland soils. Rep.For Res.Lond.
- SMITH, K.A. 1980. A model of the extent of anaerobic zones in aggregated soils, and its potential application to estimates of denitrification. *J.Soil Sci.* 31 263-277

- SMITH, K.A. AND RESTALL, S.W.F. 1971. The occurrence of ethylene in anaerobic soil J.Soil Sci. 22 430-443
- SMITH, K.A. AND ROBERTSON, P.D. 1971. Effect of ethylene on root extension of cereals. Nature 234 148-149
- SMITH, K.A. AND DOWDELL, R.J. 1974. Relationships between ethylene, oxygen, soil moisture content and temperature. J.Soil Sci. 25 217-230
- SMITH, K.A., DOWDELL, R.J. AND HALL, K.C. 1976. Measurement of oxygen in the soil atmosphere and in aqueous solution by gas chromatography. In Measurement of oxygen Proc.Symp. Odense, Denmark 1974. Ed.Degn.H. et al Elsevier, Amsterdam, 226-242
- SOANE, B.D., CAMPBELL, D.J. AND HERKES, S.M. 1971. Hand held gamma ray transmission equipment for the measurement of bulk density of field soils. J.agric.eng.Res. 16 146-156
- SWINNERTON, J.W., LINNENBOM, V.J. AND CHEEK, C.H. 1962. Determination of dissolved gases in aqueous solutions by gas chromatography Anal.Chem. 34 483-485
- TACKETT, J.L. 1968. Theory and application of gas chromatography in soil aeration research. Soil Sci.Soc.Amer.Proc. 32 346-350
- TACKETT, J.L. AND PEARSON, R.W. 1964. Effect of carbon dioxide on cotton seedling root penetration of compacted soil cores. Soil Sci.Soc.Amer.Proc. 28 741-743
- TAYLOR, S.A. 1949. Oxygen diffusion in porous media as a measure of soil aeration. Soil Sci.Soc.Amer.Proc. 14 55-61
- TEAL, J.M. AND KANWISHER, J.W. 1966. Gas transport in marsh grass, Spartina alterniflora J.exp.Bot. 17 355-361
- THOMASSON, A.J. AND BULLOCK, P. 1975. Pedology and hydrology of some surface-water gley soils. Soil Sci. 119 339-348
- VAN BAVEL, C.H.M. 1951. A soil aeration theory based on diffusion. Soil Sci. 72 33-46
- VAN BAVEL, C.H.M. 1952a. Gaseous diffusion and porosity in porous media. Soil Sci. 73 91-104
- VAN BAVEL, C.H.M. 1952b. A theory on the soil atmosphere in and around a hemisphere in which soil gases are used or released. Soil Sci.Soc.Amer.Proc. 16 150-153
- WANG, T.S.C., CHENG, S.Y. AND TUNG, H. 1967. Dynamics of soil organic acids. Soil Sci. 104 138-144
- WIANT, H.V. 1967a. Influence of temperature on the rate of soil respiration. J.Forestry 65 489-490
- WIANT, H.V. 1967b. Influence of moisture content on soil respiration. J.Forestry 65 902-903

- WIERSUM, L.K. 1960. Some experiments in soil aeration measurements and relationships to depth of rooting. *Neth.J.agric.Sci.* 8 245-252
- WILDUNG, R.E., GARLAND, T.R. AND BUSCHBOM, R.L. 1975. The interdependant effects of soil temperature and water content on soil respiration rate and plant root decomposition in arid grassland soils. *Soil Biol.Biochem.* 7 373-378
- WILLIAMSON, R.E. AND SPLINTER, W.E. 1969. Effects of light intensity temperature and root gaseous environment on growth of *Nicotiana tabacum* L. *Agron.J.* 62 224-229
- WITKAMP, M. 1966. Rates of carbon dioxide evolution from the forest floor. *Ecology* 47 492-494
- WITKAMP, M. 1969. Cycles of temperature and carbon dioxide evolution from litter and soil. *Ecology* 59 922-924
- WITKAMP, M. AND FRANK, M.L. 1969. Evolution of CO₂ from litter, humus and subsoil of a pine stand. *Pedobiologia* 9 358-365
- YAMAGUCHI, M. AND KOMATSU, Y. 1977. Direct determination of dissolved oxygen in soil water by gas chromatography. *Pl.Soil* 47 265-268
- YAMAGUCHI, M. FLOCKER, W.J. AND HOWARD, F.D. 1967. Soil atmosphere as influenced by temperature and moisture. *Soil Sci.Soc.Amer.Proc.* 31 164-167.

APPENDIX 1

Below are given brief descriptions of five soil types mentioned in the text. The descriptions are only general and soils may differ in various respects at various geographical locations. The descriptions are taken from Pyatt (1970) and are typical for upland areas open to afforestation. This reference should be consulted for further details and a discussion of the soil types in relation to forestry.

BROWN EARTHS

Soils having brownish or reddish colours, freely drained with moderate or strong acidity. Organic matter is humified readily and incorporated into a dark brown A horizon. The B horizon (there is no E horizon) is a richer brown than the underlying C horizon due to weathering. A and B horizons are friable with a crumb or small blocky structure, and with textures ranging from coarse loamy to fine loamy. The C horizon can be either unconsolidated material, indurated material or stony merging into bedrock.

IRONPAN SOILS

Also termed Stagnopodzols (Avery, 1973). Essential features of these soils are a waterlogged Eg horizon, resting on top of a thin ironpan. There may be a thick Oh horizon of up to 45cm and the B horizon is usually reddish brown and well aerated. Strongly acidic throughout the profile, ironpan soils form on permeable sandy or loamy materials in regions of high rainfall, sometimes over an indurated layer.

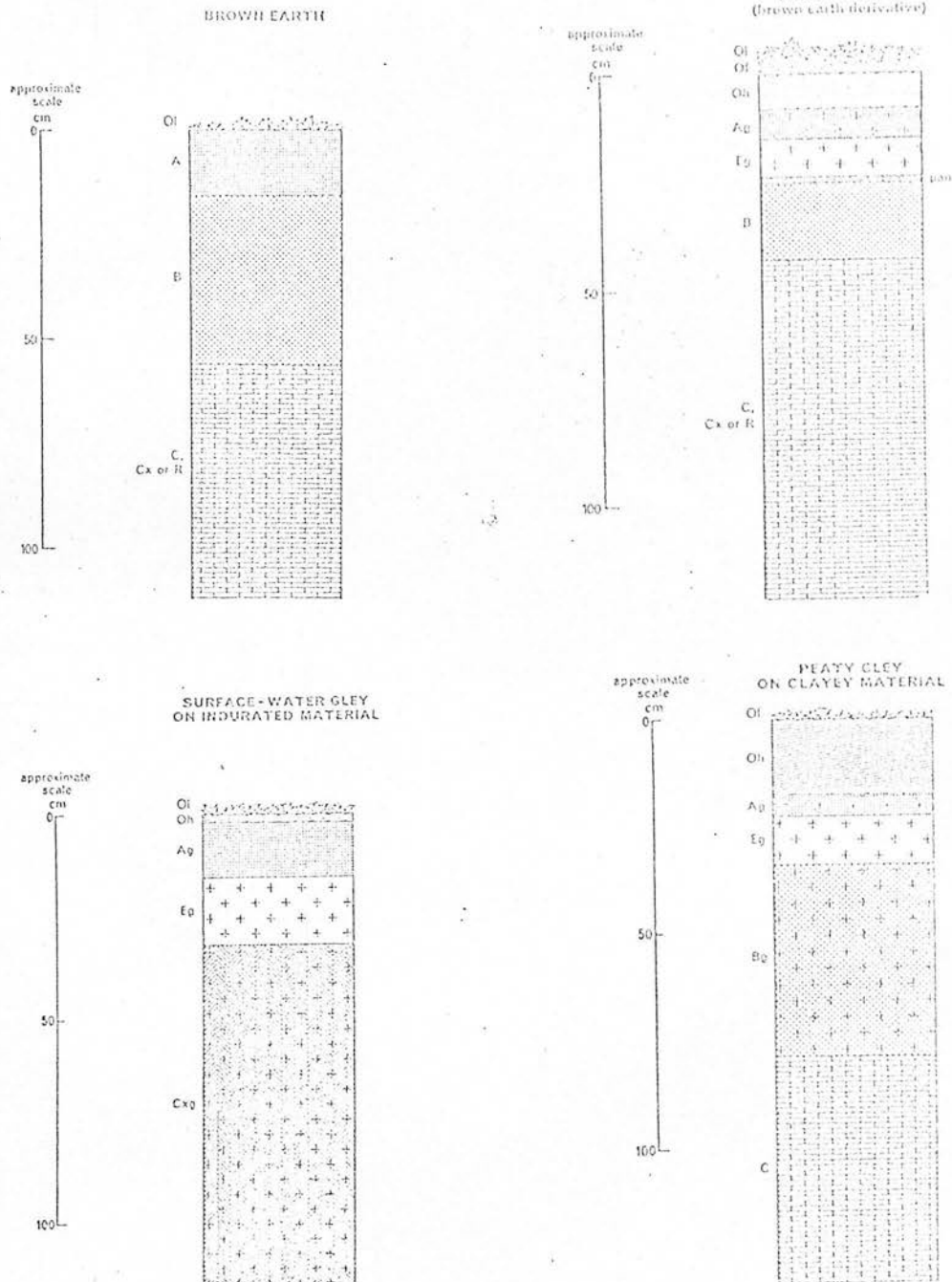


Fig.A1.1 Profiles of four soil types described in the text.
From Pyatt, 1970.

SURFACE-WATER GLEYS

Also termed cambic stagnogleys (Avery, 1973), these are formed on a C horizon of dense and structureless material that impedes vertical drainage. Below an Ag horizon of mixed mineral and humus materials there is usually a gleyed E horizon (Eg) of a drab greyish colour with ochreous mottling. The Bg horizon is typically clayey and has prismatic structure, with a greyish colour and ochreous mottling. The C horizon is usually less gleyed and reflects the colour of the parent material more than the above horizons.

PEATY GLEYS

Also termed stagnohumic gleys (Avery, 1973). A sub-group of surface-water gleys, which differ from the rest of the group by having a layer of black amorphous peat (Oh) overlying the Ag horizon, which is less prominent in these soils than the Eg. Peaty gleys are moderately or strongly acid at the surface but the pH rises with depth.

DEEP PEATS

Organic soils greater than 0.45m depth. Physical properties vary greatly and the fibrous or amorphous nature of the peat reflects the parent vegetation materials. Various degrees of humification and acidity exist, according to climatic conditions and topographical siting.

APPENDIX 2

Illustrated in Fig.A2.1 is a typical trace from the gas chromatograph used for the analysis of gas samples. This trace is from a sample of B.O.C. gas mixture comprising volume fractions of 0.20 oxygen, 0.01 carbon dioxide and 0.79 nitrogen; the response due to each gas is indicated in the Figure, along with other points of interest.

Reproducibility of gas standards

Table A2.1 gives the peak heights (mm) for component gases in successive 2cm^3 injections of the standard gas mixture (comprised of volume fractions 0.20 oxygen, 0.01 carbon dioxide and 0.79 nitrogen) at an attenuation factor of x5.

Linearity of peak height response over attenuator range

Table A2.2 and Fig.A2.2 give the peak heights (mm) for component gases in five successive 0.5cm^3 injections of the standard gas mixture (as in Fig.A2.1), one at each setting of the chromatograph attenuator over the range from x1 to x20.

Table A2.2 also shows the overall "response", as defined in the main text, for each gas, found by multiplying the observed peak height by the attenuation factor. The data show only random variation, and no significant trend to higher or lower values at high or low attenuation, indicating that the attenuator was linear over the range used.

Linearity of peak height response for samples of different volumes

Fig.A2.3 gives the peak heights (mm) for component gases in five successive gas mixture samples of volume 0.5, 1, 1.5, 2.0 and 2.5cm^3 . Oxygen and carbon dioxide prove to be linear over this range with only slight scattering probably due to measurement errors. Nitrogen has a slight curvilinear response for peak height. This is due to an increase in peak width at larger volumes, and it has been shown

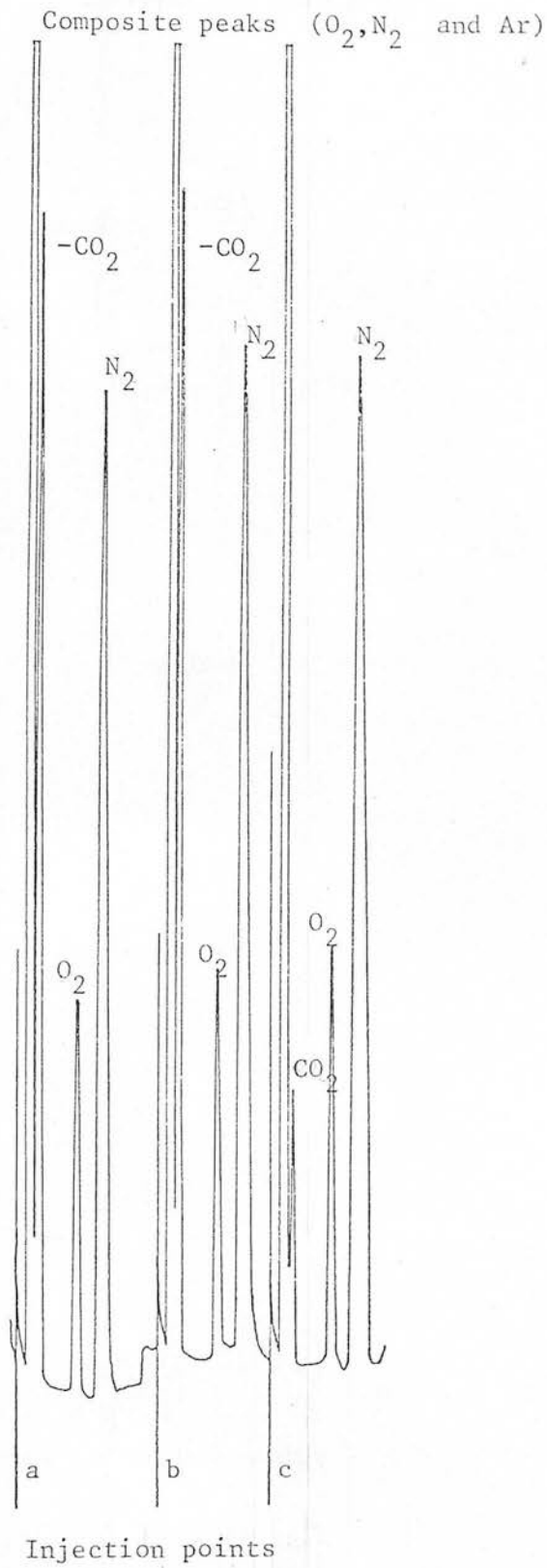


Fig.A2.1 Sample of gas chromatograph trace for injections of 2cm^3 standard gas mixture ($0.2\text{m}^3\text{m}^{-3}\text{O}_2$, $0.01\text{m}^3\text{m}^{-3}\text{CO}_2$ and $0.79\text{m}^3\text{m}^{-3}\text{N}_2$) (a and b), and laboratory air (c).

Table A2.1 Peak heights (mm) for successive standard gas mixture injections, at an attenuation factors of x5.

Injection No.	Peak height (mm)		
	CO ₂	O ₂	N ₂
1	89	62	150
2	85	63	155
3	91	62	153
4	90	61	150
5	90	63	154
6	85	64	156
Mean	88.3	62.5	153
s.e.	0.99	0.39	0.94

Table A2.2 Peak height (mm) for successive standard gas mixture injections at attenuation factors shown, together with their response (peak height x attenuation factor)

Attenuation factor	Peak height (mm)					
	CO ₂		O ₂		N ₂	
x1	117	117	78	78	225	225
x2	55	110	39	78	112	224
x5	21	105	15	75	45	225
x10	11	110	8	80	22	220
x20	5	100	4	80	11	220

Table A2.3 Estimated errors in gas concentrations ($\text{m}^3 \text{m}^{-3}$) due to assuming a linear response for peak heights

Gas	Peak height (mm)	Estimated Gas Concentration	
		linear	
CO ₂	430	5.057	4.958
O ₂	16	5.057	4.958
N	174	89.760	90.084
Total volume cm^3		1.978	2.017

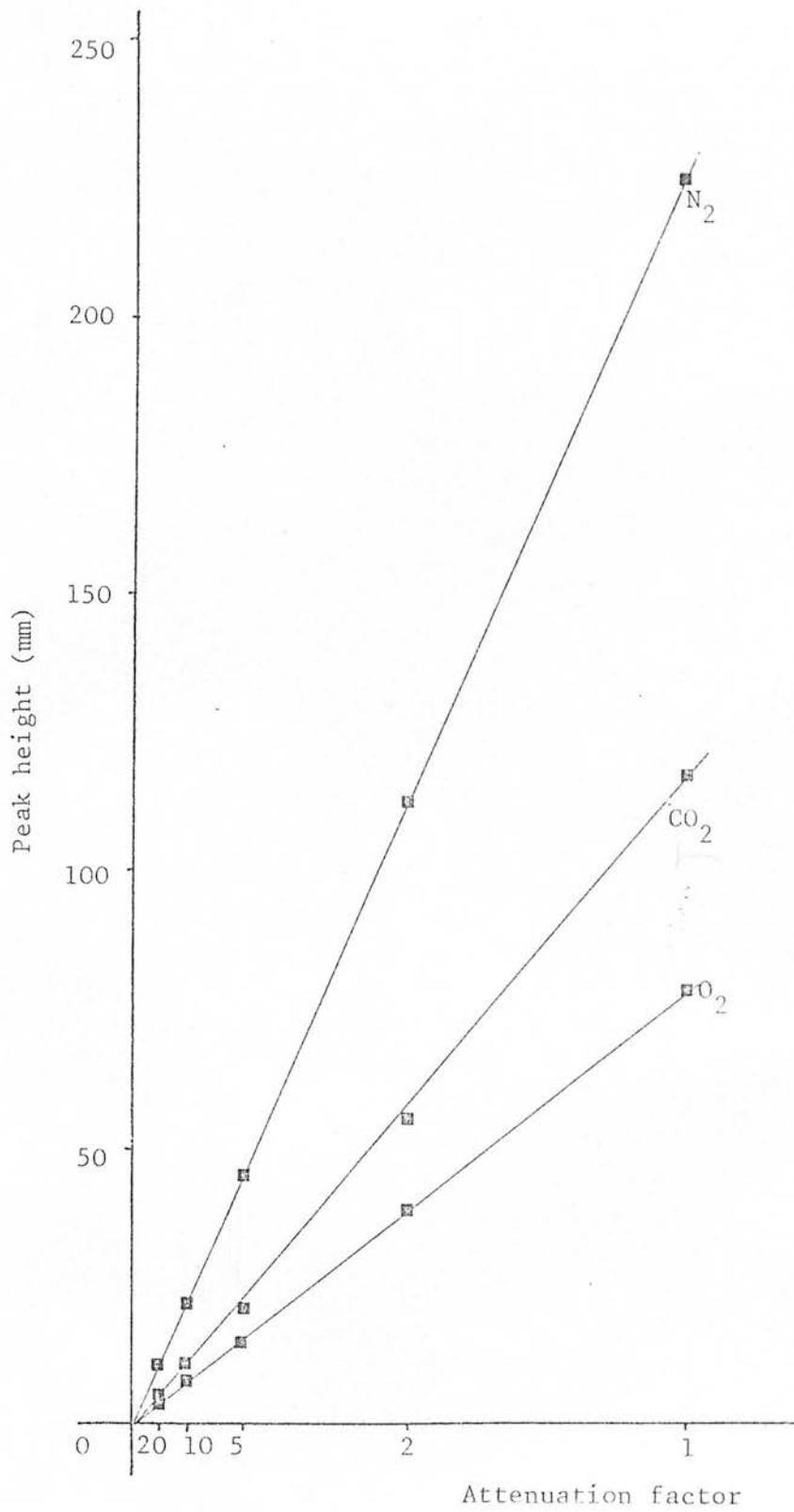


Fig.A2.2 Linearity of peak height over attenuation range.

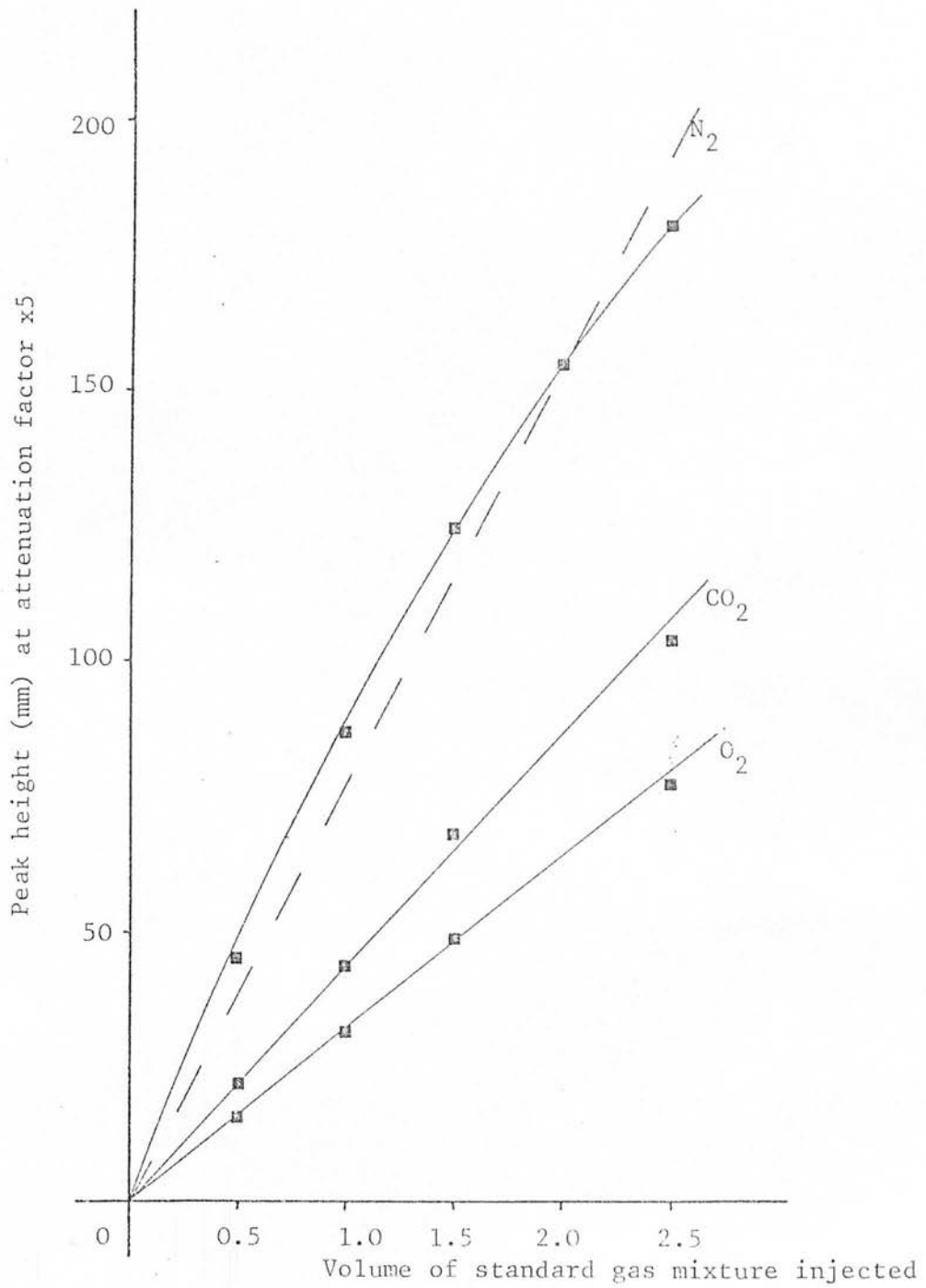


Fig A2.3 Linearity of peak height over a range of volume of standard gas mixture ($0.79 \text{ m}^3 \text{ m}^{-3} \text{ N}_2$, $0.20 \text{ m}^3 \text{ m}^{-3} \text{ O}_2$ and $0.01 \text{ m}^3 \text{ m}^{-3} \text{ CO}_2$) volume injected

that the peak area-volume relationship remains linear over this range (Goodlass, 1978).

Peak area measurements are laborious unless a digital integrator is available. Therefore all measurements were based on peak height and it was assumed that the peak height response was linear over the range of possible nitrogen component volumes (0.8 -0.9 of a 2cm^3 sample) when compared to the standard gas mixture (0.79 of a 2cm^3 sample). This assumed linear response is represented by the broken line in Fig. A2.3.

At nitrogen concentrations approaching the normal atmospheric level of $0.79\text{ m}^3\text{m}^{-3}$, the error is almost non-existent as this is also the reference standard and the two lines converge at this point. For a hypothetical sample where the peak was measured at 174mm, the calculations assuming a linear relationship would give a volume of $2.25 \times 0.79 = 1.777\text{ cm}^3$ (broken line), but the true volume would be $2.3 \times 0.79 = 1.817\text{ cm}^3$ (curve in Fig. A2.3). In a 2cm^3 sample these would represent concentrations of 0.8887 and $0.9085\text{ m}^3\text{m}^{-3}$ respectively, leading to a slight underestimation of the nitrogen component and an overestimation of the oxygen and carbon dioxide components. As the total volume of the sample is calculated from these calculated component volumes, there will also be an underestimation of this volume.

When nitrogen is such a large component of a sample, oxygen concentrations will be low with high carbon dioxide levels. A typical set of figures, for a sample such as this, is given in Table A2.3, together with the percentage concentrations of the component gases and final sample volume, as calculated by assuming a linear response and also the true curvilinear response.

It was considered that this degree of error was acceptable, and less than that associated with the variability of stored samples.

Storage of gas samples in glass syringes

Table A2.4 shows the concentration of component gases in 15 glass syringes, picked at random from those used in the field experiments, filled with 5 cm³ of a gas mixture comprising by volume fractions 0.8 nitrogen 0.1 oxygen and 0.1 carbon dioxide. The concentration of the component gases was measured using the same procedure as that used for the field samples, on the day of filling and after 3 and 7 days' storage in the laboratory.

As no certificate of analysis was available for this standard mixture, then the exact concentrations may have been only approximately 0.1m³m⁻³ for carbon dioxide and oxygen. The analysis of the gas mixture carried out on the day the syringes were filled indicates that the true concentrations are of the order of 0.09 for both gases, but this could also be caused by a small systematic error in the calculating procedure. The change in concentration over 3 and 7 days in the syringes was not significant, being of the order of 2% of the original measured concentrations.

The implications of these results for field gas samples is that storage in the syringes used for sampling does not constitute a major source of error. Any source of error in the data will therefore be due to contamination by air upon sampling or small systematic errors in the analysis. As transference of the sample from one container to another would only increase the chances of contamination, then storage in the original sampling syringe is probably the safest strategy.

Successive sampling of the gas probe

Table A2.5 shows the concentrations of component gases in successive 5cm³ samples removed from a probe at 0.4m depth in the OP peat site during August 1980. The samples were analysed in the normal way, and represent a total removal from the buried cup of 30cm³(including the "waste" sample).

Table A2.4 Gas concentrations (m^3m^{-3}) after storage in glass syringes of B.O.C. gas mixture comprising $0.1 \text{ m}^3\text{m}^{-3} \text{CO}_2$, $0.1 \text{ m}^3\text{m}^{-3} \text{O}_2$ and $0.8 \text{ m}^3\text{m}^{-3} \text{N}_2$.

Storage Time (days)	Gas concentration		
	CO_2	O_2	N_2
0	0.0951	0.0916	0.8037
	0.0892	0.0922	0.8089
	0.0938	0.0917	0.8048
	0.0938	0.0917	0.8048
	0.0943	0.0922	0.8038
	mean	0.0932	0.0919
	s.e.	0.0010	0.0001
3	0.0899	0.0914	0.8089
	0.0954	0.0850	0.8099
	0.0840	0.0953	0.8110
	0.0904	0.0920	0.8079
	0.0886	0.0871	0.8146
	mean	0.0900	0.0902
	s.e.	0.0018	0.0018
7	0.0920	0.0977	0.8007
	0.0979	0.0922	0.8003
	0.0954	0.0924	0.8026
	*	*	*
	0.0959	0.0936	0.8008
	mean	0.0953	0.0940
	s.e.	0.0012	0.0013

* Indicates a lost sample due to syringe breakage.

Table A2.5 Gas concentrations measured in five successive 5cm² samples removed from a gas probe at Eddleston.

Sample No.	Gas concentration (m ³ m ⁻³)		
	CO ₂	O ₂	N ₂
1	0.076	0.014	0.899
2	0.089	0.020	0.881
3	0.083	0.047	0.859
4	0.085	0.019	0.886
5	0.085	0.017	0.887

Table A2.6 Peak heights (mm) for dissolved oxygen measured in different volumes of water (equilibrated with the standard gas mixture) injected. Results shown are for 4 successive sample runs.

Volume of water (mm ³)	Volume of O ₂ (mm ³)	Peak height (mm)							
		1		2		3		4	
		Valve position							
		1	2	1	2	1	2	1	2
25	0.144	155	152	154	157	159	166	154	146
20	0.115	134	131	132	132	122	126	128	125
15	0.086	102	95	106	102	94	95	103	96
10	0.058	78	71	76	72	68	66	64	67
5	0.029	29	34	29	31	43	33	27	31
2.5	0.014	16	11	25	13	17	15	15	17

Again it is uncertain whether the high oxygen concentrations in samples 2 and 3 are due to contamination at sampling or are in fact genuine. However as samples 4 and 5 are so similar to sample 1, then contamination seems more likely, and the belief that the first sample removed is an accurate indication of the general pore space is strengthened. Another possibility is that individual syringes, may not be as gas tight as indicated in the previous experiment. But even if errors of this nature do occur occasionally, they will only represent small periodic deviations from the general trends observed in the field data.

Temperature-dependence of electron capture detector response to oxygen

Fig. A2.4 shows the peak height response (multiplied by the attenuation factor) of the electron capture detector over a range of detector oven temperatures. The data points indicated are the means of several 10 mm^3 injections of air.

Sample calibration curves of electron capture detector response over a range of dissolved oxygen volumes

Table A2.6 gives the peak heights for dissolved oxygen in distilled water over a range of volumes injected from 2.5 to 25 mm^3 . The water was equilibrated with the standard gas mixture ($0.01 \text{ m}^3 \text{ m}^{-3} \text{ CO}_2$, $0.20 \text{ m}^3 \text{ m}^{-3} \text{ O}_2$ and $0.79 \text{ m}^3 \text{ m}^{-3} \text{ N}_2$), by bubbling a stream of gas through the distilled water kept at laboratory temperature (297°K). The volume of oxygen as calculated by Henry's Law is also given.

Four sample runs were made and the means of these are plotted in Fig. A2.5 and A2.6, corresponding to the two positions of the 8-way switching valve mounted upstream of the analytical column. These are typical calibration curves similar to those calculated for each sample run, and against which dissolved oxygen concentrations in field samples were measured. Although there was usually no observable difference

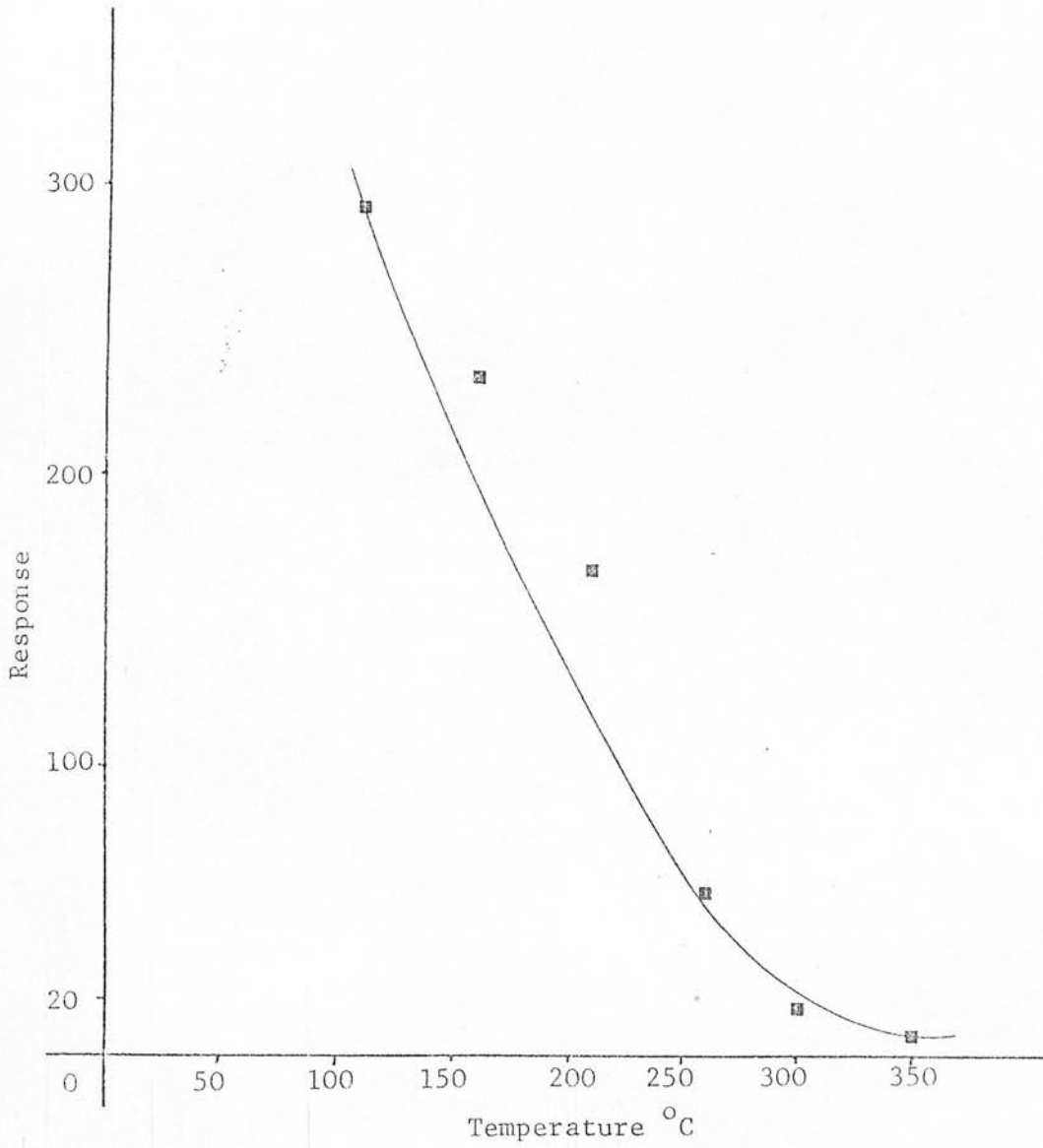


Fig. A2.4 Response (peak height \times attenuation factor) of the electron capture detector to 10 μ l of air injected over a range of detector oven temperatures.

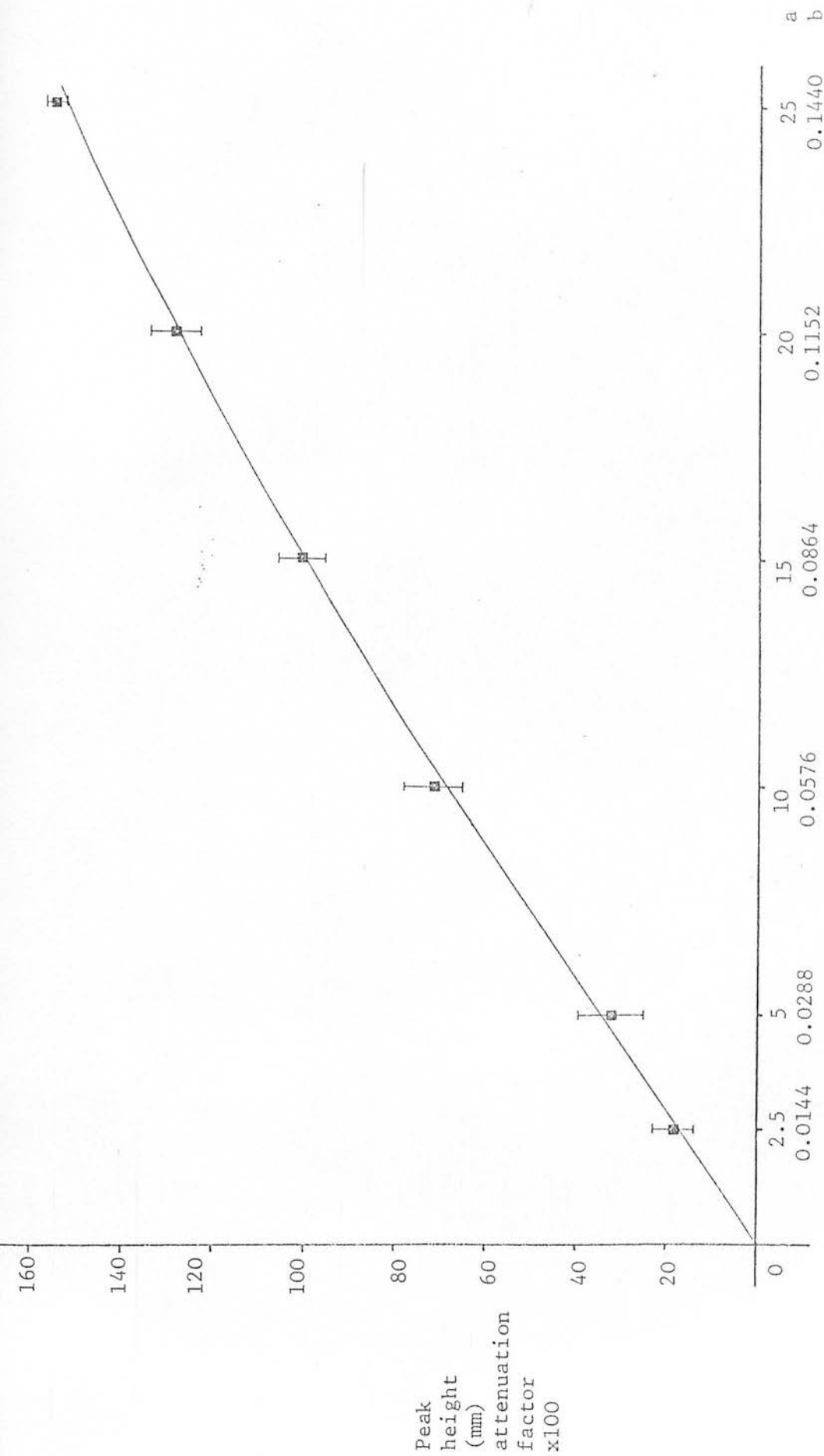


Fig.A2.5 Peak heights over a range of dissolved oxygen volumes injected through position 1 of the E.C.D. chromatography system.

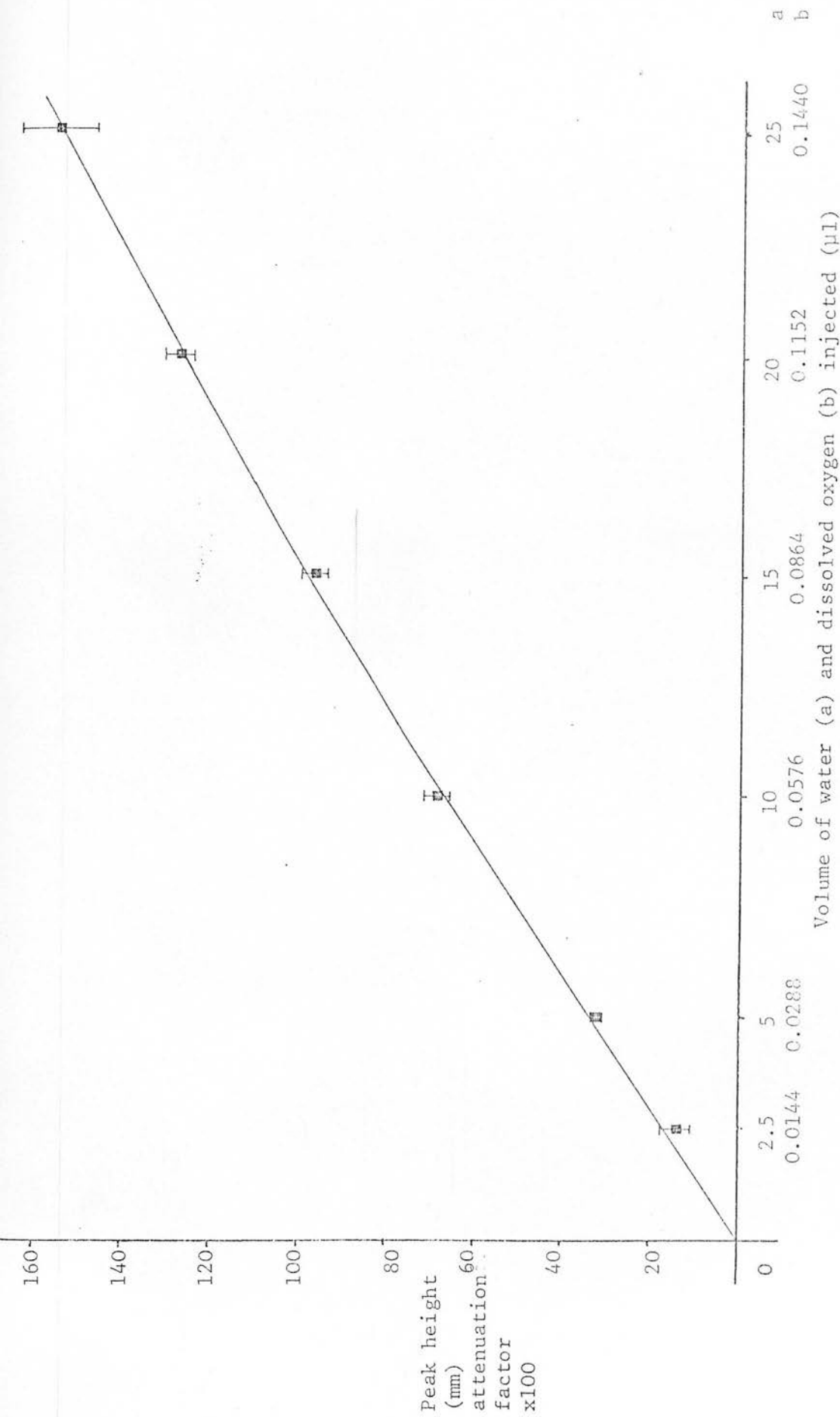


Fig.A2.6 Peak heights over a range of dissolved oxygen volumes injected through position 2 of the E.C.D. chromatography system.

between the curves obtained for both position of the valve, slight divergence sometimes occurred at the higher end of the scale, and both curves were calculated for each run as a precautionary measure.

Test of accuracy of calculations of field gas phase concentrations (of oxygen and carbon dioxide from dissolved gas concentrations)

As a general test of the accuracy of the method of calculating oxygen and carbon dioxide concentrations in water samples, described in the text, an experiment was conducted using gas mixtures of various oxygen and carbon dioxide concentrations. Three gas mixtures (B.O.C. Ltd, Special Gases Division) were used comprising by volume: (a) 0.0100 CO_2 , 0.2079 O_2 and 0.7821 N_2 , (b) 0.0496 CO_2 , 0.1470 O_2 and 0.8034 N_2 , (c) 0.0971 CO_2 , 0.1000 O_2 and 0.8029 N_2 . These were bubbled through distilled water at 286°K. Five 5cm³ samples of the equilibrated water (after bubbling for 30 min) were taken from each gas mixture treatment. The samples were taken using the same syringes as used in the field experiments. The closed syringes were then stored at 277°K for 2 weeks.

After storage the samples were analysed using exactly the same procedure and calculations as used for field samples, described in the text. Table A2.7 gives the oxygen and carbon dioxide concentrations derived from this procedure with the original "gas phase" concentrations.

The carbon dioxide figures show a consistent underestimation of the original gas phase concentrations, which could be due to either systematic errors in the measurement and/or calculation of concentration or a slow leakage and re-equilibration towards atmospheric concentrations, or a combination of both. The oxygen concentrations show a similar error, but as any re-equilibration towards atmospheric levels would increase the concentrations, then the errors must be systematic in origin. It is possible that the water sampled was not fully saturated during the 30 min equilibration time, which would give an underestimation of both

Table A2.7 Comparison of equivalent gas phase concentrations ($\text{m}^3 \text{m}^{-3}$)
derived from stored water samples, with the original gas
phase concentrations with which the water was originally
equilibrated

Sample No.	<u>Original concentration</u>		<u>Derived concentration</u>	
	O_2	CO_2	O_2	CO_2
1	0.208	0.010	0.178	0.006
2	0.208	0.010	0.178	0.008
3	0.208	0.010	0.195	0.008
4	0.208	0.010	0.175	0.006
5	0.208	0.010	0.173	0.007
Mean			0.180	0.007
1	0.150	0.050	0.157	0.043
2	0.150	0.050	0.118	0.045
3	0.150	0.050	0.168	0.049
4	0.150	0.050	0.108	0.046
5	0.150	0.050	0.156	0.046
Mean			0.142	0.046
1	0.100	0.100	0.080	0.074
2	0.100	0.100	0.115	0.093
3	0.100	0.100	0.101	0.100
4	0.100	0.100	0.122	0.090
5	0.100	0.100	0.160	0.096
Mean			0.116	0.090

oxygen and carbon dioxide values, but as the variation about the original values occur in both directions for oxygen, then there is clearly some error inherent in the method.

A larger degree of error for water samples compared to gas samples must therefore be accepted, but the difference is not so great as to invalidate their comparison against each other. As the main aim of the field measurements is to observe trends in soil gas concentrations relative to each other and to other sites in the soil, a high degree of precision is not so important as obtaining reasonably reliable measurements at regular intervals to follow the fluctuations which occur with environmental factors such as rainfall. It was felt that the accuracy of this method was sufficient to enable a more detailed examination to be made of soil aeration under fluctuating moisture regimes than has been possible before.

Table A2.8 Solubility coefficients (α) of oxygen and carbon dioxide
in water at temperature within the range shown, α represents
the volume of gas absorbed by unit volume of water at S.T.P.
when in equilibrium with that gas

Temperature ($^{\circ}\text{C}$)	$\alpha(\text{O}_2)$	$\alpha(\text{CO}_2)$
10	0.03801	1.194
11	0.03718	1.154
12	0.03637	1.117
13	0.03559	1.083
14	0.03486	1.050
15	0.03415	1.019
16	0.03348	0.985
17	0.03283	0.956
18	0.03220	0.928
19	0.03161	0.902
20	0.03102	0.878
21	0.03044	0.854
22	0.02988	0.829
23	0.02934	0.804
24	0.02881	0.781
25	0.02831	0.759

APPENDIX 3

Table A3.1 Mass fraction of the eight particle size classes measured for each horizon in the six sites sampled at Falstone.

Site No.	Horizon	Mass fraction in each particle size range(μm)							
		2000-600	600-212	212-106	106-63	63-20	20-6	6-2	< 2
1 , 2	Ag	0.003	0.056	0.178	0.137	0.190	0.130	0.118	0.188
	Eg	0.012	0.111	0.238	0.139	0.180	0.093	0.072	0.165
	Bg	0.011	0.122	0.246	0.126	0.174	0.099	0.046	0.176
	BCg1	0.020	0.134	0.243	0.132	0.163	0.081	0.045	0.182
	BCg2	0.018	0.104	0.211	0.128	0.152	0.081	0.055	0.251
	Cg	0.033	0.105	0.200	0.114	0.155	0.084	0.051	0.259
3 , 4	Ag	0.004	0.067	0.039	0.033	0.098	0.228	0.246	0.285
	Eg	0.005	0.123	0.206	0.136	0.203	0.102	0.080	0.147
	Bg	0.017	0.230	0.337	0.117	0.114	0.049	0.045	0.092
	BCg1	0.018	0.170	0.260	0.117	0.146	0.077	0.044	0.168
	BCg2	0.025	0.162	0.291	0.126	0.130	0.073	0.036	0.158
	Cg	0.031	0.133	0.227	0.112	0.186	0.092	0.046	0.173
5 , 6	Ag	0.002	0.061	0.116	0.100	0.187	0.235	0.047	0.250
	Eg	0.009	0.115	0.211	0.120	0.177	0.138	0.028	0.202
	BC	0.016	0.110	0.221	0.126	0.181	0.093	0.048	0.206
	BCg1	0.016	0.102	0.188	0.115	0.152	0.078	0.044	0.305
	BCg2	0.017	0.089	0.177	0.121	0.145	0.062	0.061	0.327
	Cg	0.018	0.077	0.157	0.102	0.183	0.106	0.072	0.285
7 , 8	Ag	0.006	0.119	0.209	0.136	0.157	0.092	0.148	0.134
	Eg	0.013	0.140	0.255	0.132	0.168	0.092	0.096	0.115
	Bg	0.019	0.112	0.220	0.118	0.133	0.075	0.093	0.230
	BCg1	0.018	0.115	0.162	0.101	0.150	0.080	0.092	0.281
	BCg2	0.016	0.092	0.169	0.106	0.164	0.087	0.088	0.277
	Cg	0.029	0.116	0.185	0.100	0.156	0.068	0.089	0.258
9 , 10	Ag	0.205	0.114	0.121	0.067	0.103	0.071	0.041	0.279
	Eg	0.072	0.139	0.215	0.108	0.161	0.096	0.023	0.186
	BC	0.047	0.156	0.248	0.124	0.189	0.084	0.047	0.105
	BCg1	0.068	0.143	0.199	0.121	0.147	0.060	0.040	0.222
	BCg2	0.029	0.096	0.158	0.103	0.164	0.088	0.065	0.296
	Cg	0.034	0.044	0.078	0.091	0.191	0.113	0.098	0.351
11 , 12	Ag	0.010	0.161	0.240	0.145	0.159	0.077	0.067	0.142
	Eg	0.006	0.155	0.301	0.138	0.127	0.078	0.059	0.129
	Bg	0.014	0.170	0.349	0.129	0.103	0.049	0.067	0.119
	BCg1	0.013	0.092	0.176	0.108	0.150	0.090	0.074	0.296
	BCg2	0.019	0.093	0.172	0.108	0.155	0.091	0.080	0.281
	Cg	0.022	0.080	0.140	0.106	0.198	0.098	0.073	0.281

APPENDIX 4

Table A4.1 Peat fibre contents (mass fractions) in the OV site

Depth (m)	Fibre size class (mm)	Replicate				
		1	2	3	4	5
0.1-0.2	>1	0.151	0.120	0.329	0.088	0.120
	0.425-1	0.130	0.148	0.157	0.222	0.119
	0.250-0.425	0.108	0.109	0.045	0.117	0.077
	0.180-0.250	0.030	0.070	0.053	0.080	0.047
	<0.180	0.581	0.553	0.416	0.493	0.637
0.2-0.3	>1	0.412	0.210	0.306	0.200	0.235
	0.425-1	0.195	0.211	0.142	0.300	0.141
	0.250-0.425	0.091	0.094	0.073	0.120	0.107
	0.180-0.250	0.047	0.046	0.049	0.050	0.066
	<0.180	0.255	0.439	0.430	0.330	0.448
0.4-0.5	>1	0.428	0.348	0.308	0.219	0.512
	0.425-1	0.206	0.286	0.202	0.255	0.149
	0.250-0.425	0.098	0.094	0.086	0.114	0.073
	0.180-0.250	0.046	0.036	0.046	0.055	0.037
	<0.180	0.222	0.236	0.358	0.357	0.229
0.7-0.8	>1	0.479	0.358	0.315	0.241	0.435
	0.425-1	0.212	0.147	0.177	0.147	0.166
	0.250-0.425	0.096	0.070	0.081	0.091	0.093
	0.180-0.250	0.046	0.038	0.045	0.059	0.039
	<0.180	0.167	0.387	0.382	0.462	0.267

Table A4.2 Peat fibre contents (mass fractions) in the OP site

Depth (m)	Fibre size class (mm)	Replicate				
		1	2	3	4	5
0.1-0.2	>1	0.250	0.125	0.122	0.148	0.197
	0.425-1	0.065	0.119	0.211	0.110	0.101
	0.250-0.425	0.049	0.072	0.096	0.073	0.067
	0.180-0.250	0.041	0.052	0.068	0.058	0.046
	<0.180	0.591	0.632	0.503	0.611	0.589
0.2-0.3	>1	0.125	0.193	0.105	0.169	0.063
	0.425-1	0.157	0.222	0.223	0.161	0.188
	0.250-0.425	0.087	0.107	0.109	0.118	0.098
	0.180-0.250	0.057	0.058	0.076	0.054	0.074
	<0.180	0.574	0.420	0.487	0.498	0.597
0.4-0.5	>1	0.290	0.222	0.267	0.128	0.098
	0.425-1	0.145	0.142	0.215	0.160	0.234
	0.250-0.425	0.093	0.082	0.106	0.108	0.111
	0.180-0.250	0.058	0.039	0.049	0.074	0.075
	<0.180	0.414	0.515	0.363	0.530	0.482
0.7-0.8	>1	0.197	0.175	0.170	0.467	0.219
	0.425-1	0.225	0.265	0.232	0.160	0.228
	0.250-0.425	0.158	0.147	0.107	0.100	0.154
	0.180-0.250	0.061	0.050	0.064	0.048	0.059
	<0.180	0.359	0.363	0.427	0.225	0.340

Table A4.3 Peat fibre contents(mass fractions) in the SS site

Depth (m)	Fibre size class (mm)	Replicate				
		1	2	3	4	5
0.1-0.2	>1	0.294	0.265	0.601	0.467	0.337
	0.425-1	0.105	0.094	0.240	0.183	0.053
	0.250-0.425	0.048	0.072	0.108	0.066	0.034
	0.180-0.250	0.042	0.034	0.064	0.043	0.026
	<0.180	0.511	0.535	0	0.241	0.550
0.2-0.3	>1	0.325	0.127	0.312	0.556	0.101
	0.425-1	0.066	0.120	0.257	0.194	0.356
	0.250-0.425	0.035	0.046	0.199	0.103	0.052
	0.180-0.250	0.018	0.036	0.101	0.034	0.035
	<0.180	0.556	0.671	0.131	0.113	0.456
0.4-0.5	>1	0.241	0.176	0.355	0.270	0.331
	0.425-1	0.258	0.288	0.363	0.315	0.109
	0.250-0.425	0.103	0.077	0.154	0.140	0.083
	0.180-0.250	0.056	0.060	0.087	0.074	0.035
	<0.180	0.342	0.399	0.041	0.201	0.442
0.7-0.8	>1	0.285	0.252	0.260	0.532	0.228
	0.425-1	0.193	0.175	0.299	0.172	0.161
	0.250-0.425	0.091	0.075	0.132	0.083	0.087
	0.180-0.250	0.050	0.060	0.079	0.041	0.042
	<0.180	0.381	0.438	0.230	0.172	0.482

Table A4.4 Peat fibre contents (mass fractions) in the LP site

Depth (m)	Fibre size class (mm)	Replicates				
		1	2	3	4	5
0.1-0.2	>1	0.328	0.428	0.558	0.434	0.120
	0.425-1	0.098	0.150	0.087	0.248	0.161
	0.250-0.425	0.060	0.071	0.059	0.086	0.105
	0.180-0.250	0.034	0.029	0.041	0.064	0.062
	<0.180	0.480	0.322	0.255	0.168	0.552
0.2-0.3	>1	0.200	0.437	0.598	0.188	0.268
	0.425-1	0.144	0.100	0.117	0.295	0.199
	0.250-0.425	0.061	0.048	0.071	0.121	0.112
	0.180-0.250	0.039	0.028	0.037	0.075	0.051
	<0.180	0.556	0.387	0.177	0.321	0.370
0.4-0.5	>1	0.387	0.337	0.191	0.350	0.469
	0.425-1	0.200	0.174	0.188	0.195	0.129
	0.250-0.425	0.079	0.068	0.098	0.090	0.109
	0.180-0.250	0.034	0.039	0.059	0.050	0.048
	<0.180	0.300	0.382	0.464	0.315	0.245
0.7-0.8	>1	0.093	0.209	0.251	0.424	0.440
	0.425-1	0.198	0.245	0.204	0.294	0.167
	0.250-0.425	0.093	0.088	0.096	0.156	0.101
	0.180-0.250	0.043	0.049	0.054	0.036	0.039
	<0.180	0.573	0.409	0.395	0.090	0.253

APPENDIX 5

Table A5.1 Gas mixture concentrations corresponding to the
numbers used in Tables A5.2-A5.5

No.	Concentration (m^3m^{-3})		
	O_2	CO_2	N_2
1	0.21	0.00035	Bal.
2	0.20	0.01	"
3	0.20	0.06	"
4	0.20	0.12	"
5	0.20	0.18	"
6	0	0	1.0
7	0.21	0.00035	Bal.
8	0.01	0.01	"
9	0.01	0.06	"
10	0.01	0.12	"
11	0.01	0.18	"
12	0	0	1.0

Table A5.2 Mean root lengths(mm) for the *Picea sitchensis* plants in the
high oxygen experiment.

Gas conc. No.	Clone	Rep.	Mean root length(mm) on each day													
			1	2	3	4	5	6	7	8	9	10	11	12	13	14
1	1	1	-	7	10	12	16	18	22	-	23	32	35	-	48	-
		2	-	6	7	12	16	18	22	-	33	37	41	-	48	-
2		1	-	1	3	3	4	5	8	-	15	19	22	-	26	-
		2	-	6	10	14	19	22	26	-	37	43	49	-	58	-
3		1	-	-	-	-	-	-	-	-	-	-	-	-	-	-
		2	-	3	5	6	9	11	12	-	18	20	23	-	29	-
4		1	-	4	8	10	13	14	17	-	21	28	32	-	39	-
		2	-	-	-	-	-	-	-	-	-	-	-	-	-	-
5		1	-	2	4	5	7	8	10	-	12	13	13	-	15	-
		2	-	5	7	9	12	13	15	-	18	18	19	-	21	-
6		1	-	5	8	12	15	18	19	-	22	22	22	-	22	-
		2	-	4	5	7	9	9	12	-	12	12	12	-	12	-
1	2	1	-	2	4	6	9	11	14	-	20	24	27	-	30	-
		2	-	5	9	13	17	19	22	-	29	33	36	-	40	-
2		1	-	8	12	15	20	23	28	-	44	49	53	-	58	-
		2	-	3	5	7	10	12	17	-	29	35	40	-	50	-
3		1	-	4	6	10	10	15	19	-	22	32	34	-	39	-
		2	-	9	11	18	22	26	31	-	35	40	43	-	50	-
4		1	-	2	3	8	12	13	16	-	18	20	22	-	25	-
		2	-	7	12	18	22	25	29	-	36	38	39	-	41	-
5		1	-	5	8	12	15	18	21	-	29	27	29	-	31	-
		2	-	9	14	19	20	26	30	-	32	32	40	-	43	-
6		1	-	8	12	18	24	27	33	-	33	33	33	-	33	-
		2	-	4	7	11	15	18	21	-	22	22	22	-	22	-

Table A5.3 Mean root lengths (mm) of the *Pinus contorta* plants in the "high" oxygen experiment.

Gas conc. No.	Clone	Rep.	Mean root length (mm) on each day													
			1	2	3	4	5	6	7	8	9	10	11	12	13	14
1	1	1	-	11	17	21	25	28	28	-	28	28	28	-	28	-
		2	-	11	16	23	27	29	33	-	38	38	46	-	47	-
2		1	-	20	27	34	44	49	55	-	65	67	83	-	88	-
		2	-	9	14	18	21	23	26	-	31	36	39	-	43	-
3		1	-	8	10	17	26	30	35	-	39	39	40	-	41	-
		2	-	11	17	23	29	33	39	-	48	52	54	-	61	-
4		1	-	2	3	4	12	15	18	-	24	27	28	-	34	-
		2	-	13	17	18	22	25	27	-	33	34	35	-	37	-
5		1	-	10	15	20	23	25	27	-	29	29	30	-	33	-
		2	-	10	15	21	25	27	30	-	34	36	36	-	40	-
6		1	-	5	7	12	15	19	25	-	26	26	26	-	26	-
		2	-	8	13	17	22	25	30	-	31	31	31	-	31	-
1	2	1	-	3	4	5	8	10	13	-	24	28	31	-	36	-
		2	-	6	9	14	20	23	28	-	37	40	48	-	53	-
2		1	-	11	16	21	25	28	32	-	40	42	44	-	48	-
		2	-	3	6	8	12	13	16	-	23	24	26	-	29	-
3		1	-	3	4	7	9	9	11	-	21	24	26	-	30	-
		2	-	7	9	13	17	19	22	-	29	32	35	-	41	-
4		1	-	5	7	9	12	13	15	-	16	17	17	-	17	-
		2	-	7	10	14	17	20	24	-	32	34	37	-	39	-
5		1	-	5	7	9	11	13	15	-	17	17	17	-	18	-
		2	-	1	2	5	7	9	10	-	12	12	13	-	13	-
6		1	-	7	10	13	16	18	21	-	22	23	23	-	23	-
		2	-	1	2	4	6	7	8	-	8	8	8	-	8	-

Table A5.4 Mean root lengths(mm) for the *Picea sitchensis* plants in the
"low"oxygen experiment

Gas conc. No	Clone	Rep.	Mean root length (mm) on each day																
			1	2	3	4	5	6	7	8	9	10	11	12	13	14	15	16	17
7	1	1	6	10	15	20	26	-	35	41	44	49	52	57	62	-	69	-	81
		2	2	5	7	9	12	-	17	20	22	26	27	32	35	-	40	-	45
8		1	3	7	11	16	21	-	29	34	36	37	38	39	40	-	41	-	50
		2	3	8	12	17	22	-	29	36	37	38	39	39	39	-	41	-	46
9		1	2	4	7	10	13	-	19	22	23	24	24	24	24	-	27	-	31
		2	2	4	6	9	14	-	19	23	24	26	26	26	26	-	29	-	35
10		1	2	5	8	11	16	-	20	23	25	25	26	26	26	-	27	-	29
		2	7	13	18	25	32	-	42	48	50	50	50	50	50	-	50	-	50
11		1	3	5	7	10	13	-	19	21	22	23	23	23	23	-	24	-	28
		2	3	7	10	14	18	-	26	30	31	32	32	32	32	-	34	-	39
12		1	3	6	9	13	16	-	22	28	28	28	28	28	28	-	28	-	28
		2	2	3	4	6	8	-	11	14	14	14	14	14	14	-	14	-	14
7	2	1	5	9	12	17	21	-	28	32	37	41	43	47	49	-	54	-	62
		2	5	9	13	18	25	-	34	42	46	53	58	64	68	-	73	-	89
8		1	4	9	13	19	24	-	32	37	39	39	39	39	39	-	41	-	47
		2	3	7	11	15	20	-	28	34	37	38	38	38	38	-	39	-	45
9		1	4	8	12	16	20	-	27	33	34	34	34	34	34	-	34	-	36
		2	6	11	14	20	27	-	37	44	46	47	48	48	48	-	51	-	61
10		1	6	13	18	24	31	-	43	52	53	54	55	55	55	-	55	-	60
		2	1	5	6	7	10	-	12	16	17	17	17	17	17	-	18	-	20
11		1	5	8	11	15	18	-	23	25	26	26	26	26	26	-	26	-	27
		2	5	11	16	20	25	-	34	38	42	43	43	43	43	-	43	-	45
12		1	7	12	17	23	30	-	41	48	49	49	49	49	49	-	49	-	49
		2	4	8	12	17	22	-	30	37	38	38	38	38	38	-	38	-	38

Table A5.5 Mean rootlength (mm) for the *Pinus contorta* plants in the "low" oxygen experiment

Gas core No.	Clone	Rep.	Mean root lengths(mm) on each day																
			1	2	3	4	5	6	7	8	9	10	11	12	13	14	15	16	17
7	1	1	5	10	13	19	23	-	30	35	38	41	43	46	49	-	57	-	63
		2	2	7	8	8	9	-	14	17	20	20	21	24	28	-	38	-	41
8	1	1	2	4	6	7	10	-	14	17	18	18	19	19	19	-	21	-	27
		2	5	10	15	20	27	-	34	36	37	37	38	39	39	-	40	-	43
9	1	1	3	4	4	5	6	-	14	18	18	18	18	18	18	-	19	-	22
		2	9	17	23	30	42	-	62	72	72	72	72	72	72	-	72	-	72
10	1	1	-	-	-	-	-	-	-	-	-	-	-	-	-	-	-	-	-
		2	5	10	14	19	26	-	31	34	34	34	34	34	34	-	38	-	45
11	1	1	8	16	22	30	38	-	48	54	55	55	55	55	55	-	57	-	66
		2	2	4	5	8	10	-	14	17	17	17	17	17	17	-	17	-	19
12	1	1	2	3	4	7	10	-	15	19	19	19	19	19	19	-	19	-	19
		2	5	8	10	14	18	-	26	31	31	31	31	31	31	-	32	-	34
7	2	1	7	13	18	24	30	-	41	49	55	62	67	75	79	-	83	-	93
		2	7	10	15	19	23	-	28	31	35	40	42	46	49	-	53	-	57
8	2	1	9	17	23	32	40	-	55	63	65	66	67	67	68	-	72	-	73
		2	9	15	22	29	44	-	59	62	65	65	65	66	67	-	71	-	85
9	2	1	6	11	18	22	29	-	34	35	35	35	35	35	35	-	35	-	35
		2	3	7	9	12	16	-	23	29	27	27	27	27	27	-	33	-	48
10	2	1	9	19	26	36	45	-	61	69	70	70	70	70	70	-	82	-	102
		2	7	12	17	24	31	-	38	40	40	40	40	40	40	-	40	-	-
11	2	1	7	12	19	26	31	-	40	47	57	57	57	58	58	-	61	-	74
		2	9	16	23	31	38	-	54	61	67	67	68	68	68	-	71	-	90
12	2	1	4	7	10	14	17	-	24	29	30	30	30	30	30	-	30	-	30
		2	5	10	14	19	24	-	33	37	38	38	38	38	38	-	38	-	38